TOOLS FOR EFFICIENT ASYMMETRIC SYNTHESIS: DESIGN, SYNTHESIS AND APPLICATION OF FLUOROUS OXAZOLIDINONE CHIRAL AUXILIARIES

by

Jason Ellis Hein

A thesis

submitted to the Faculty of Graduate Studies

in partial fulfillment of the requirements

for the degree of

Doctor of Philosophy

Department of Chemistry

University of Manitoba

Winnipeg, MB, Canada

R3T 2N2

ABSTRACT

A new class of oxazolidinone chiral auxiliary has been synthesized from various α-amino acids, incorporating a perfluoroalkyl functional chain as a soluble support. This feature allows the chiral auxiliaries to be employed under standard solution-phase reaction conditions, and rapidly purified from crude mixtures using fluorous solid phase extraction (FSPE). Our investigation of these new materials has been divided into two main sections.

To obtain the chiral auxiliaries in multi-gram quantities a synthetic protocol was designed, where efficiency and reproducibility were the primary objectives. Meeting these goals required an extensive study of the reactivity of perfluoroalkyl nucleophiles. This study identified a versatile and scalable protocol for the perfluoroalkylation of the required amino acid starting materials. These results have allowed us to design a general, five-step synthetic pathway to create the fluorous chiral auxiliaries quickly and effectively.

The new auxiliaries were then applied in several model reactions, specifically chosen to examine the reactivity and behavior of these compounds. In particular, the auxiliaries were tested for their stereoselectivity, recyclability, and ease of purification, in a series of Aldol reactions, 1,3 dipolar cycloadditions, and radical conjugate additions. This set of model reactions, combined with the facile and efficient synthesis clearly demonstrates that these new chiral auxiliaries are useful alternatives to the non-fluorous oxazolidinone chiral auxiliaries currently employed in stoichiometric asymmetric syntheses.

ACKNOWLEDGEMENTS

This work would not be possible without the help of many individuals. First and foremost I would like to thank my supervisor and mentor Dr. Phil Hultin for his wisdom, guidance, patience and assistance. He has pushed me to exceed my boundaries, while stressing the need for focus in my work, and for that I am very grateful. Thank you to my examining committee Dr. Norm Hunter, Dr. Frank Schweizer, Dr. Alan McIntosh, and Dr. Dennis Curran for their comments and guidance during this project.

I would like to thank my colleagues Pedro Aguiar, Richard Dawes, Marion Earle, Laina Geary, Ashley Jaworski, and Xianghui Wen for their help over the years in the many endeavors we have taken on together. Thanks to the graduate and undergraduate members of the Hultin group for making the lab a pleasant and energetic place to study. I also wish to thank the faculty and staff of the Department of Chemistry for their support.

I would like to acknowledge the assistance of our collaborators Dr. Mukund Sibi at North Dakota State University, Dr. Phil Yeske at Fluorous Technologies Incorporated, and Melanie Drouin from Silicycle Inc.. Thanks to Dr. Kirk Marat, Mr. Terry Wolowiec, Mr. Wayne Buchannon, and Mr. Gilles Roy for their technical expertise and assistance. Also, I would like to thank Dr. Jim Britton and Dr. Laura Harrington at the McMaster Analytical Xray diffraction facility and Dr. Bob McDonald at the Alberta Xray diffraction facility for analysis and structure solutions.

I would like to thank the Natural Sciences and Engineering Research Council of Canada for the graduate scholarships and research funding that made this project possible.

Last but not least, I thank my family and friends for their support and caring over the last five years. I know I could not have done it without them.

DEDICATION

This work is dedicated to the two people that have helped me the most over the last few years; my wife Sylvia and my sister Melissa. They have been my source of endless strength, creativity and, determination.

"It is a capital mistake to theorize before one has data. Insensibly one begins to twist fact to suit theory instead of theory to suit fact" – Sir Arthur Conan Doyle.

TABLE OF CONTENTS

Abstract i

Acknowledgements ii

Dedication iii

List of Figures and Tables xvii

List of Abbreviations xxv

Chapter 1: Introduction and Background 1

1.1 Introduction 1

1.2 Asymmetric Synthesis 2

1.2.1 Stereochemistry and Chirality 2

1.2.2 The Importance of Stereochemistry 5

1.2.3 Isolation of Individual Stereoisomers 8

1.2.4 Oxazolidinone Chiral Auxiliaries 14

1.3 Supported Synthesis 21

1.3.1 Background 21

1.3.2 History of Supported Organic Synthesis 23

1.3.3 Polymer-Supported Chiral Auxiliaries 26

1.4 Fluorous Organic Synthesis 39

1.4.1 Introduction 39

1.4.2 History and Development of Fluorous Supported Synthesis 41

1.4.3 Fluorous Solid Phase Extraction 50

1.4.4 Light Fluorous Synthesis *56*

1.5 Applications of Oxazolidinone Chiral Auxiliaries 59

1.5.1 Asymmetric Aldol Reactions *59*

1.5.2 Stereoselective Radical Conjugate Additions *66*

1.5.3 Stereoselective 1,3 Dipolar Cycloadditions *71*

Chapter 2: Thesis Objectives 77

2.1.1 Design and Synthesis of a Fluorous Oxazolidinone *77*

2.1.2 Asymmetric Reactions using the Fluorous Auxiliary *80*

Chapter 3: Results and Discussion 83

3.1 Introduction 83

3.2 Synthesis of the Fluorous Oxazolidinone Auxiliary 83

3.2.1 First Generation Fluorous Oxazolidinone Chiral Auxiliaries *84*

3.2.2 Second Generation Fluorous Oxazolidinone Chiral Auxiliaries *98*

3.2.3 Extension of the General Synthetic Route *117*

3.3 Application of the New Auxiliaries to Asymmetric Synthesis 124

3.3.1 Asymmetric Aldol Reactions using Titanium Enolates *125*

3.3.2 Lewis Acid Mediated Radical Conjugate Additions *131*

3.3.3 Stereoselective 1,3 Dipolar Cycloadditions with Diphenylnitrone *141*

Chapter 4: Conclusions and Future Work 160

4.1 Conclusions 160

4.2 Future Studies 163

4.2.1 Large-Scale Production of Fluorous Oxazolidinone 163

4.2.2 Application of the Auxiliary to Multi-Step Synthesis 164

Chapter 5: Experimental Procedures 168

General Procedures 168

General procedures for purification using FSPE 169

*Method A: Purification of fluorous material using a liquid loading protocol; Isolation of (E)-(4S,5R)-4-benzyl-3-(2'-butenoyl)-5-(1'H,-1'H,2'H,2'H-perfluorooctyl)-2-oxazolidinone (**290a**): 169*

*Method B: Purification of fluorous material using adsorption protocol; Isolation of (E)-(4S,5R)-4-benzyl-3-(3'-phenyl-2'-propenoyl)-5-(1'H,-1'H,2'H,-2'H-perfluorooctyl)-2-oxazolidinone (**290b**): 170*

*Method C: Removal of alkyltin from fluorous material; Isolation of (3'R,4S,5R)-4-benzyl-3-(3',4'-dimethyl-pentanoyl)-5-(1'H,1'H,-2'H,2'H-perfluorooctyl)-2-oxazolidinone (**291a**): 170*

Synthesis of Amino Acid Electrophiles 171

General Procedure for the Synthesis of Amino Ester Hydrochlorides; Preparation of Methyl phenylalaninate hydrochloride: 171

Methyl phenylalaninate hydrochloride: 172

Ethyl phenylalaninate hydrochloride: 172

Methyl phenylglycinate hydrochloride: 172

*Methyl (S)-N-(benzyloxycarbonyl)-phenylalaninate (**208a**): 173*

*Methyl (S)-N-(ethoxycarbonyl)-phenylalaninate (**208b**): 173*

*Ethyl (S)-N-(benzyloxycarbonyl)-phenylalaninate (**208c**): 174*

*Ethyl (S)-N-(ethoxycarbonyl)-phenylalaninate (**208d**):..... 175*

*Methyl (S)-N-(iso-propoxycarbonyl)-phenylalaninate (**232b**): 175*

*Methyl (S)-N-(ethoxycarbonyl)-phenylglycinate (**252**): 176*

*General Procedure for the Synthesis of N-Carbamoyl Amino Acids via Modified Schotten-Baumann Conditions; Preparation of 2(S)-N-(ethoxycarbonyl) phenylalanine (**237a**):..... 177*

*2(S)-N-(Ethoxycarbonyl)-phenylalaninate (**237a**): 177*

*2(S)-N-(iso-Propoxycarbonyl)-phenylalaninate (**237b**):..... 178*

*N-(Benzyloxycarbonyl)-phenylalaninate (**237c**):..... 178*

(S)-N-(tert-Butoxycarbonyl)-valaninate:..... 179

(R)-N-(tert-Butoxycarbonyl)-phenylglycinate:..... 179

*General Procedure for the Synthesis of N-Carbamoyl Weinreb Amides Using Isobutyl Chloroformate; 2(S)-N-(Ethoxycarbonyl)-N'-methoxy-N'-methyl-phenylalaninamide (**240a**):..... 179*

*General Procedure for the Synthesis of N-Carbamoyl Weinreb Amides Using 3-Chloro-methylpyridinium iodide; 2(S)-N-(Benzyloxycarbon-yl)-N'-methoxy-N'-methyl-phenylalaninamide (**240c**):..... 180*

*General Procedure for the Synthesis of N-Carbamoyl Weinreb Amides Using 2-chloro-4,6-dimethoxy-[1,3,5]triazine; 2(S)-N-(Benzyloxy-carbonyl)-N'-methoxy-N'-methyl-phenylalaninamide (**240c**):..... 181*

*General Procedure for the Synthesis of N-Carbamoyl Weinreb Amides Using TBTU; 2(S)-N-(tert-Butoxycarbonyl)-N'-methoxy-N'-methyl-valinamide (**251**):.. 181*

*2(S)-N-(Ethoxycarbonyl)-N'-methoxy-N'-methyl-phenylalaninamide (**240a**):..... 182*

*2(S)-N-(iso-Propoxycarbonyl)-N'-methoxy-N'-methyl-phenylalanin-amide (**240b**): 183*

*2(S)-N-(Benzyloxycarbonyl)-N'-methoxy-N'-methyl-phenylalaninamide (**240c**): . 184*

*2(S)-N-(tert-Butoxycarbonyl)-N'-methoxy-N'-methyl-valaninamide (**257**): 184*

*2(R)-N-(tert-Butoxycarbonyl)-N'-methoxy-N'-methyl-phenylglycin-amide (**261**): 185*

Nucleophilic Perfluoroalkyl Additions Using Perfluoroalkyl Grignard and Perfluoroalkyllithium Reagents 185

*General Procedure for Perfluoroalkylation of N-Carbamoyl Amino Esters using Perfluoroalkyllithium Reagents Derived from $C_8F_{17}I$: 2(S)-(Ethoxycarbonylamino)-4,4,5,5,6,6,7,7,8,8,9,9,10,10,11,-11,11-heptadecafluoro-1-phenyl-undecan-3-one (**209b**):..... 185*

*2(S)-(Benzyloxycarbonylamino)-4,4,5,5,6,6,7,7,8,8,9,9,10,10,11,11,11-heptadecafluoro-1-phenyl-undecan-3-one (**209a**):..... 186*

*2(S)-(Ethoxycarbonylamino)-4,4,5,5,6,6,7,7,8,8,9,9,10,10,11,11,11-heptadecafluoro-1-phenyl-undecan-3-one (**209b**):..... 187*

*2(S)-(Benzyloxycarbonylamino)-4,4,5,5,6,6,7,7,8,8,9,9,10,10,11,11,11-heptadecafluoro-3-methly-1-phenyl-undecan-3-ol (**211a**): 187*

*2(S)-(Ethoxycarbonylamino)-4,4,5,5,6,6,7,7,8,8,9,9,10,10,11,11,11-heptadecafluoro-3-methyl-1-phenyl-undecan-3-ol (**211b**): 188*

*General Procedure for Perfluoroalkylation of N-Carbamoyl Amino Esters using Perfluoroalkyl Grignard Reagents Derived from $C_6F_{13}(CH_2)_2I$; 2(S)-(Benzyloxycarbonylamino)-6,6,7,7,8,8,9,9,10,10,-11,11,11-tridecafluoro-1-phenyl-undecan-3-one (**233c**):..... 189*

General Procedure for Perfluoroalkylation of N-Carbamoyl Amino Esters or N-Carbamoyl Weinreb Amides using Perfluoroalkyllithium Reagents Derived from

*$C_6F_{13}(CH_2)_2I$; 3(S)-(tert-Butoxycarbony-lamino)-7,7,8,8,9,9,10,10,11,11,12,12,12-tridecafluoro-2-methyl-dodec-an-4-one (**250**): 190*

*General Procedure for the Application of a Sacrificial Base in the Perfluoroalkylation of N-Carbamoyl Weinreb Amides; 2(S)-(Ethoxycarbonylamino)-6,6,7,7,8,8,9,9,10,10,11,11,11-tridecafluoro-1-phenyl-undecan-3-one (**233a**):..... 190*

*2(S)-(Ethoxycarbonylamino)-6,6,7,7,8,8,9,9,10,10,11,11,11-tridecafluoro-1-phenyl-undecan-3-one (**233a**):..... 191*

*2(S)-(iso-Propoxycarbonylamino)-6,6,7,7,8,8,9,9,10,10,11,11,11-trideca-fluoro-1-phenyl-undecan-3-one (**233b**):..... 192*

*2(S)-(Benzyloxycarbonylamino)-6,6,7,7,8,8,9,9,10,10,11,11,11-trideca-fluoro-1-phenyl-undecan-3-one (**233c**):..... 193*

*3(S)-(tert-Butoxycarbonylamino)-7,7,8,8,9,9,10,10,11,11,12,12,12-tridecafluoro-2-methyl-dodecan-4-one (**250**):..... 194*

*1(R)-(Ethoxycarbonylamino)-5,5,6,6,7,7,8,8,9,9,10,10,10-tridecafluoro-1-phenyl-decan-2-one (**253**):..... 195*

*1(R)-(tert-Butoxycarbonylamino)-5,5,6,6,7,7,8,8,9,9,10,10,10-trideca-fluoro-1-phenyl-decan-2-one (**262**):..... 196*

*2(S)-(Ethoxycarbonylamino)-3,3-bis(1'H,1'H,2'H,2'H-perfluorooctyl)-1-phenyl-propan-3-ol (**234a**): 196*

*2(S)-(iso-Propoxycarbonylamino)-3,3-bis(1'H,1'H,2'H,2'H-perfluoro-octyl)-1-phenyl-propan-3-ol (**234b**): 197*

*2(S)-(Benzyloxycarbonylamino)-3,3-bis(1'H,1'H,2'H,2'H-perfluoro-octyl)-1-phenyl-propan-3-ol (**234c**): 198*

*3(S)-(tert-Butoxycarbonylamino)-4,4-bis(1'H,1'H,2'H,2'H-perfluoro-octyl)-2-methyl-butan-4-ol (**251**):..... 199*

*1(R)-(Ethoxycarbonylamino)-2,2-bis(1'H,1'H,2'H,2'H-perfluorooctyl)-1-phenyl-ethan-2-ol (**254**):* *200*

Reduction of the Perfluoroalkyl Ketones 201

*General Procedure for Reductions of Perfluoroalkylketone; syn and anti 2-(Ethoxycarbonylamino)-4,4,5,5,6,6,7,7,8,8,9,9,10,10,11,11,11-heptadec-afluoro-1-phenyl-undecan-3-ol (**224b**, **225b**):* *201*

*General Procedure for Diastereoselective Reductions of Perfluoro-alkylketones Using Chelation Control; (2S,3R)-2-(Ethoxy-carbonylamino)-6,6,7,7,8,8,9,9,10,10,11,11,11-tridecafluoro-1-phenyl-undecan-3-ol (**243a**):* *201*

*(2S,3R)-2-(Benzyloxycarbonylamino)-4,4,5,5,6,6,7,7,8,8,9,9,10,10,11,11,-11-heptadecafluoro-1-phenyl-undecan-3-ol (**224a**):* *202*

*(2S,3R)-2-(Ethoxycarbonylamino)-4,4,5,5,6,6,7,7,8,8,9,9,10,10,11,11,11-heptadecafluoro-1-phenyl-undecan-3-ol (**224b**):* *203*

*(2S,3S)-2-(Benzyloxycarbonylamino)-4,4,5,5,6,6,7,7,8,8,9,9,10,10,11,11,-11-heptadecafluoro-1-phenyl-undecan-3-ol (**225a**):* *203*

(2S,3S)-2-(Ethoxycarbonylamino)-4,4,5,5,6,6,7,7,8,8,9,9,10,10,11,11,11-heptadecafluoro-1-phenyl-undecan-3-ol (225b): *204*

*(2S,3R)-2-(Ethoxycarbonylamino)-6,6,7,7,8,8,9,9,10,10,11,11,11-tridecafluoro-1-phenyl-undecan-3-ol (**243a**):* *205*

*(2S,3R)-2-(iso-Propoxycarbonylamino)-6,6,7,7,8,8,9,9,10,10,11,11,11-tridecafluoro-1-phenyl-undecan-3-ol (**243b**):* *206*

*(2S,3R)-2-(Benzyloxycarbonylamino)-6,6,7,7,8,8,9,9,10,10,11,11,11-tridecafluoro-1-phenyl-undecan-3-ol (**243c**):* *207*

*(3S,4R)-3-(tert-Butoxycarbonylamino)-7,7,8,8,9,9,10,10,11,11,12,12,12-tridecafluoro-2-methyl-dodecan-4-ol (**258**):* *208*

*(1R,2S)-1-(tert-Butoxycarbonylamino)-5,5,6,6,7,7,8,8,9,9,10,10,10-tri-decafluoro-1-phenyl-decan-2-ol (**263**):* *209*

Synthesis of MTPA Derivatives for Determination of Enantiomeric Excess..... 210

*General procedure for synthesis of MTPA esters from (perfluoroalkyl)alcohols; (2S,2'R,3R)-2-(Ethoxycarbonylamino)-3-(2'-methoxy-2'-trifluoromethyl-phenylacetyl)-6,6,7,7,8,8,9,9,10,10,11,11,-11-tridecafluoro-1-phenyl-undecan-3-ol (**248**):* *210*

*(2S,2'S,3R)-2-(Ethoxycarbonylamino)-3-(2'-methoxy-2'-trifluoromethyl-phenylacetyl)-6,6,7,7,8,8,9,9,10,10,11,11,11-tridecafluoro-1-phenyl-undecan-3-ol (**247**):* *211*

*(2S,2'R,3R)-2-(Ethoxycarbonylamino)-3-(2'-methoxy-2'-trifluorometh-yl-phenylacetyl)-6,6,7,7,8,8,9,9,10,10,11,11,11-tridecafluoro-1-phenyl-undecan-3-ol (**248**):* *212*

*(2'S,3S,4R)-3-(tert-Butoxycarbonylamino)-4-(2'-methoxy-2'-trifluoro-methyl-phenylacetyl)-7,7,8,8,9,9,10,10,11,11,12,12,12-tridecafluoro-2-methyl-dodecan-4-ol (**260a**):* *213*

*(2'R,3S,4R)-3-(tert-Butoxycarbonylamino)-4-(2'-methoxy-2'-trifluoro-methyl-phenylacetyl)-7,7,8,8,9,9,10,10,11,11,12,12,12-tridecafluoro-2-methyl-dodecan-4-ol (**260b**):* *214*

*(1R,2S,2'S)-1-(tert-Butoxycarbonylamino)-2-(2'-methoxy-2'-trifluoro-methyl-phenylacetyl)-5,5,6,6,7,7,8,8,9,9,10,10,10-tridecafluoro-1-phenyl-decan-2-ol (**264a**):* *215*

*(1R,2S,2'R)-1-(tert-Butoxycarbonylamino)-2-(2'-methoxy-2'-trifluoro-methyl-phenylacetyl)-5,5,6,6,7,7,8,8,9,9,10,10,10-tridecafluoro-1-phenyl-decan-2-ol (**264b**):* *216*

Cyclization of Perfluoroalkyl Alcohols to Oxazolidinones 217

*General Procedure for Cyclization of Mono and Bis(perfluoroalkyl)-alcohols; (4S,5R)-4-Benzyl-5-(1'H,1'H,2'H,2'H-perfluorooctyl)-2-oxa-zolidinone (**245**):* ... 217

*Alternate Cyclization Protocol Employing Refluxing THF; (4S,5S)-4-Benzyl-5-heptadecafluorooctyl-oxazolidin-2-one (**231**):* 217

*(4S,5R)-4-Benzyl-5-heptadecafluorooctyl-oxazolidin-2-one (**230**):* 218

*(4S,5S)-4-Benzyl-5-heptadecafluorooctyl-oxazolidin-2-one (**231**):* 218

*(4S,5R)-4-Benzyl-5-(1'H,1'H,2'H,2'H-perfluorooctyl)-2-oxazolidinone (**245**):* 219

*4(S)-Benzyl-5,5-bis(1'H,1'H,2'H,2'H-perfluorooctyl)-2-oxazolidinone (**246**):*..... 220

*4(S)-iso-Propyl-5,5-bis(1'H,1'H,2'H,2'H-perfluorooctyl)-2-oxazolidinone (**255**):* 220

*4(R)-Phenyl-5,5-bis(1'H,1'H,2'H,2'H-perfluorooctyl)-2-oxazolidinone (**256**):*..... 221

*(4S,5R)-4-iso-Propyl-5-(1'H,1'H,2'H,2'H-perfluorooctyl)-2-oxazolidin-one (**259**):* 222

Titanium-Mediated Aldol Reactions..... 223

*General Acylation Protocol for Fluorous Oxazolidinones; (4S,5R)-4-Benzyl-5-heptadecafluorooctyl-3-propionyl-oxazolidin-2-one (**269**):* 223

*(4S,5R)-4-Benzyl-5-heptadecafluorooctyl-3-propionyl-oxazolidin-2-one (**269**):* .. 223

*(4S,5S)-4-Benzyl-5-heptadecafluorooctyl-3-propionyl-oxazolidin-2-one (**270**):* .. 224

*General Procedure for Titanium-Mediated Aldol Reactions: (4S,5S,2'S,3'S)-4-Benzyl-5-heptadecafluorooctyl-3-(3'-hydroxy-2'-methyl-3'-phenyl-propionyl)-oxazolidin-2-one (**280a**):* 225

*(4S,5S,2'S,3'S)-4-Benzyl-5-heptadecafluorooctyl-3-(3'-hydroxy-2'-methyl-3'-phenyl-propionyl)-oxazolidin-2-one (**280a**):* 225

*(4S,5S,2'S,3'R)-Benzyl-5-heptadecafluorooctyl-3-(3'-hydroxy-2',4'-dimethyl-pentanoyl)-oxazolidin-2-one (**280b**):* *226*

*(4S,5S,2'S,3'R)-4-Benzyl-5-heptadecafluorooctyl-3-(3'-hydroxy-2'-methyl-nonanoyl)-oxazolidin-2-one (**280c**):* *227*

*(E)-(4S,5S,2'S,3'R)-4-Benzyl-5-heptadecafluorooctyl-3-(3'-hydroxy-2'-methyl-hex-4'-enoyl)-oxazolidin-2-one (**280d**):* *227*

*General Procedure for LiOOH Hydrolysis of Aldol Products; (2S,3S)-3-Hydroxy-2-methyl-3-phenylpropanoic acid (**288a**):* *228*

*(2S,3S)-3-Hydroxy-2-methyl-3-phenylpropanoic acid (**288a**):* *229*

*(2S,3R)-3-Hydroxy-2,4-dimethylpentanoic acid (**288b**):* *229*

*(2S,3R)-3-Hydroxy-2-methylnonanoic acid (**288c**):* *229*

*(E)-(2S,3R)-2-Methyl-4-hexene-1,3-diol (**289**):* *230*

Radical Conjugate Additions 230

*(E)-(4S,5R)-4-Benzyl-3-(2'-butenoyl)-5-(1'H,1'H,2'H,2'H-perfluorooct-yl)-2-oxazolidinone (**290a**):* *230*

*(E)-(4S,5R)-4-Benzyl-3-(3'-phenyl-2'-propenoyl)-5-(1'H,1'H,2'H,2'H-perfluorooctyl)-2-oxazolidinone (**290b**):* *232*

*(E)-(4S,5R)-4-Benzyl-3-(3'-ethoxycarbonyl-2'-propenoyl)-5-(1'H,1'H,-2'H,2'H-perfluorooctyl)-2-oxazolidinone (**290c**):* *233*

*Synthesis of the Norephedrine Oxazolidinone Auxiliary; (4S,5R)-4-methyl-5-phenyl-2-oxazolidinone (**301**):* *234*

*(E)-(4S,5R)-4-Methyl-3-(3'-phenyl-2'-propenoyl)-5-phenyl-2-oxazolidinone (**302a**):* *235*

*(E)-(4S,5R)-3-(3'-Ethoxycarbonyl-2'-propenoyl)-4-methyl-5-phenyl-2-oxazolidinone (**302b**):* *236*

*General Experimental Procedure for Lewis Acid-Mediated Conjugate Radical Addition to Enoates; (3'R,4S,5R)-4-benzyl-3-(3',4'-dimethyl-pentanoyl)-5-(1'H,1'H,2'H,2'H-perfluorooctyl)-2-oxazolidinone (**291a**):* *237*

*(3'R,4S,5R)-4-Benzyl-3-(3',4'-dimethyl-pentanoyl)-5-(1'H,1'H,2'H,2'H-perfluorooctyl)-2-oxazolidinone (**291a**):* *237*

*(3'R,4S,5R)-4-Benzyl-3-(4'-methyl-3'-phenyl-pentanoyl)-5-(1'H,1'H,-2'H,2'H-perfluorooctyl)-2-oxazolidinone (**291b**):* *238*

*(3'R,4S,5R)-4-Benzyl-3-(3'-ethoxycarbonyl-4'-methyl-pentanoyl)-5-(1'H,1'H,2'H,2'H-perfluorooctyl)-2-oxazolidinone (**291c**):* *239*

*(4S,5R)-4-Benzyl-3-(butanoyl)-5-(1'H,1'H,2'H,2'H-perfluorooctyl)-2-oxazolidinone (**293a**):* *240*

*(3'R,4S,5R)-4-Methyl-3-(4'-methyl-3'-phenyl-pentanoyl)-5-phenyl-2-oxazolidinone (**303a**):* *241*

*(3'R,4S,5R)-4-Methyl-3-(3'-ethoxycarbonyl-4'-methyl-pentanoyl)-5-phenyl-2-oxazolidinone (**303b**):* *242*

*General Procedure for LiOOH Hydrolysis of Radical Products; (R)-3,4-dimethylpentanoic acid (**229a**):* *242*

*(R)-3,4-Dimethylpentanoic acid (**299a**):* *243*

*(3R)-3-Methyl-4-phenylpentanoic acid (**299b**):* *243*

*(R)-2-iso-Propylfumaric acid (**299c**):* *244*

Procedure for the Measurement of Tin Following Various Purification Protocols: 244

1,3-Dipolar Cycloadditions Using Diphenylnitrone 245

*General Procedure for 1,3-Dipolar Cycloaddition; (3'R,4S,4'S,5R,5'R)-4-benzyl-3-((5'-methyl-2',3'-diphenylisoxazolidin-4'-yl)carbonyl)-5-(1'H,1'H,2'H,-2'H-perfluorooctyl)-2-oxazolidinone (**308**):* *245*

*(3'R,4S,4'S,5R,5'R)-4-Benzyl-3-((5'-methyl-2',3'-diphenylisoxazolidin-4'-yl)carbonyl)-5-(1'H,1'H,2'H,-2'H-perfluorooctyl)-2-oxazolidinone (**308**):* *246*

*(3'S,4S,4'R,5R,5'S)-4-Benzyl-3-((5'-methyl-2',3'-diphenylisoxazolidin-4'-yl)carbonyl)-5-(1'H,1'H,2'H,-2'H-perfluorooctyl)-2-oxazolidinone (**309**):* *246*

*(3'S,4S,4'S,5R,5'R)-4-Benzyl-3-((5'-methyl-2',3'-diphenylisoxazolidin-4'-yl)carbonyl)-5-(1'H,1'H,2'H,-2'H-perfluorooctyl)-2-oxazolidinone (**310**):* *247*

*(3'R,4S,4'R,5R,5'S)-4-Benzyl-3-((5'-methyl-2',3'-diphenylisoxazolidin-4'-yl)carbonyl)-5-(1'H,1'H,2'H,-2'H-perfluorooctyl)-2-oxazolidinone (**311**):* *248*

*(3R,4S,5R)-4-Isoxazolidinecarboxylic acid, 5-methyl-2,3-diphenyl-, isopropyl ester (**314**)* *249*

Reductive Cleavage Applied in Recyclability Study *249*

*(3S,4S,5R)-5-Methyl-2,3-diphenyl-isoxazolidine-4-methanol (**320**):* *250*

*(3R,4R,5S)-5-Methyl-2,3-diphenyl-isoxazolidine-4-methanol (**321**):* *250*

*2-((5'-Methyl-2',3'-diphenylisoxazolidin-4'-yl)carbonylamino)-6,6,7,7,8,8,9,9,10,10,11,11,11-trideafluoro-1-phenyl-undecan-3-ol (**340**):* *251*

Appendices 252

X-Ray Structure Report for Oxazolidinone 245 252

X-ray Crystal Structure Report for Dipolar Cycloaddition Product **310** 268

References 284

NMR Section 302

LIST OF FIGURES AND TABLES

Figure 1.2.1.1: Geometric isomers of dibromobenzene..... 2

Figure 1.2.1.2: Examples of chiral and achiral compounds..... 3

Figure 1.2.1.3: Enantiomers and diastereomers of 2-chloro-3-hydroxy-propanoic acid.... 4

Figure 1.2.1.4: Enantiotopic and diasterotopic atoms..... 5

Figure 1.2.2.1: Bioavailability of the stereoisomers in synthetic vitamin E..... 6

Figure 1.2.2.2: Enantiomers of omeprazole..... 7

Scheme 1.2.3.1: Dynamic kinetic resolution of *N*-phthalylamino acids..... 9

Figure 1.2.3.1: Kinetically and thermodynamically controlled transformations..... 11

Figure 1.2.3.2: Reaction via enantiomeric and diastereomeric transition states..... 12

Scheme 1.2.3.2: Application of pseudoephedrine as a chiral auxiliary..... 13

Figure 1.2.4.1: General structure of oxazolidinones..... 14

Figure 1.2.4.2: Methods for the synthesis of chiral α-amino alcohols. 15

Scheme 1.2.4.1: Methods for the synthesis of oxazolidinones from amino alcohols..... 16

Scheme 1.2.4.2: Methods for the synthesis of *N*-acyloxazolidinones. 17

Scheme 1.2.4.3: Asymmetric aldol reactions using *N*-acyloxazolidinones..... 17

Scheme 1.2.4.4: Examples of asymmetric reactions using oxazolidinones..... 18

Scheme 1.2.4.5: Hydrolysis of *N*-acyloxazolidinones..... 19

Scheme 1.2.4.6: Examples for the deacylation of oxazolidinones. 20

Figure 1.3.1.1: Schematic representation of a combinatorial synthesis..... 21

Figure 1.3.1.2: Supported organic synthesis. 22

Scheme 1.3.2.1: Merrifield's protocol for solid-phase peptide synthesis. 24

Scheme 1.3.2.2: Synthesis of *Z* and *E* insect pheromones using solid phase methods. 25

Scheme 1.3.3.1: Asymmetric synthesis using a polymer-bound carbohydrate auxiliary. 26

Scheme 1.3.3.2: Examples of polymer-supported chiral auxiliaries. 27

Scheme 1.3.3.3: Asymmetric allylation using a polymer bound chiral imine. 28

Scheme 1.3.3.4: Solid and solution phase alkylation using pseudoephedrine. 29

Figure 1.3.3.1: Polymer-supported oxazolidinone chiral auxiliaries. 30

Scheme 1.3.3.5: Asymmetric alkylation using polymer supported oxazolidinones. 31

Scheme 1.3.3.6: Dipolar cycloaddition using a non-crosslinked polystyrene support. 32

Scheme 1.3.3.7: Asymmetric alkylation using a supported oxazolidinone derived from L-serine. 33

Scheme 1.3.3.8: Rearrangement to give *O*- and *N*-linked oxazolidinones. 34

Scheme 1.3.3.9: Epimerization of the *N*-linked oxazolidinone. 35

Scheme 1.3.3.10: Recycling study using supported oxazolidinones in 1,3 dipolar cycloadditions. 37

Scheme 1.3.3.11: Recycling study using asymmetric alkylation of a supported oxazolidinone chiral auxiliary 38

Figure 1.4.1.1: Schematic of polymer-supported and fluorous-supported methods. 40

Table 1.4.2.1: Selected examples of fluorous/hydrocarbon liquid/liquid partitioning. 42

Scheme 1.4.2.1: Hydroformylation using fluorous biphasic catalysis 44

Scheme 1.4.2.2: Preparation of isoxazolidine libraries using fluorous synthesis. 45

Scheme 1.4.2.3: Examples of fluorous synthetic protocols employing liquid/liquid separation. 46

Figure 1.4.2.1: Balance between fluorous and organic solubility..... 47

Table 1.4.2.2: Effect of fluorine content on liquid/liquid partitioning. 48

Scheme 1.4.2.4: Radical allylation using fluorous allyl stannane **123**. 49

Figure 1.4.3.1: Comparison of chromatography and solid phase extraction. 51

Scheme 1.4.3.1: Formation of fluorous reverse phase silica gel. 52

Figure 1.4.3.2: Comparison of retention times for fluorinated and non-fluorinated benzenes on alkyl (RP-10, A) and fluorocarbon (RPF-10, B) bonded phases. 53

Figure 1.4.3.3: Separation of materials by fluorine content using fluorous silica gel 54

Figure 1.4.3.4: Schematic of liquid-surface contact angles. 55

Scheme 1.4.4.1: Synthesis of amides using the ^{F}Boc protection group. 57

Scheme 1.4.4.2: Generation of a library of amides using the ^{F}Boc protection group. 58

Scheme 1.5.1.1: Formation of *erythro* and *threo* isomers via the aldol reaction. 59

Scheme 1.5.1.2: Mechanism for the formation of the *Z* and *E* enolate of **142**. 60

Figure 1.5.1.1: Chair and boat transition structures for aldol reactions. 61

Figure 1.5.1.2: Orientation of the aldehyde and syn-axial interactions in aldol transition structures. 61

Figure 1.5.1.3: Generation of the four potential aldol addition diastereomers. 62

Scheme 1.5.1.3: Stereoselective aldol reactions using *N*-acyl oxazolidinones. 63

Scheme 1.5.1.4: Coordinated intermediates for aldol reactions with octahedral metals. . 64

Scheme 1.5.2.1: Radical chain mechanism for conjugate addition to *N*-acyl oxazolidinones. 67

Scheme 1.5.2.2: Rotamers available for α,β-unsaturated *N*-acyloxazolidinones. 68

Scheme 1.5.2.3: Radical addition to α,β-unsaturated *N*-acyloxazolidinones. 69

Scheme 1.5.3.1: 1,3-Dipolar cycloaddition forming chiral isoxazolidines..... 71

Figure 1.5.3.1: Conversion of isoxazolidines to important precursors. 71

Figure 1.5.3.2: Molecular orbital interpretation of Lewis acid catalysis in 1,3 dipolar cycloadditions. 72

Scheme 1.5.3.2: Regioisomers resulting from 1,3 dipolar cycloaddition to *N*-acyloxazolidinones..... 73

Scheme 1.5.3.3: 1,3-Dipolar cycloaddition between diphenylnitrone and *N*-acyloxazolidinones..... 74

Scheme 1.5.3.4: Open and chelated intermediates for dipolar cycloaddition..... 75

Figure 1.5.3.3: *Endo* and *exo* transition states in cycloaddition reactions. 75

Scheme 1.5.3.5: Steric repulsion in *exo* dipolar cycloaddition transition state structure. 76

Scheme 2.1.1.1: Synthesis of a mono-functionalized oxazolidinone. 78

Scheme 2.1.1.2: Synthesis of a 4,5 disubstituted oxazolidinone. 78

Scheme 2.1.1.3: General pathway for the synthesis of 4,5 disubstituted fluorous oxazolidinones. 80

Scheme 3.2.1.1: Perfluoroalkyl Grignard and lithium additions to ester **208a**..... 84

Table 3.2.1.1: Perfluoroalkyllithium addition to *N*-CBz phenylalanine methyl ester. 86

Scheme 3.2.1.2: Proposed mechanism for the stabilization of perfluoroalkyllithium reagents. 87

Scheme 3.2.1.3: Competitive reactions present during the perfluoroalkylation of **208a**. 88

Table 3.2.1.2: Addition of perfluorooctyl lithium to *N*-carbamoyl amino esters. 90

Figure 3.2.1.1: Homo-aggregates of *n*-butyllithium. 91

Scheme 3.2.1.4: Improvement of the perfluoroalkylation of ester **217** using $BF_3{\cdot}EtO_2$.[217] 92

Scheme 3.2.1.5: Reduction of amino ketones via steric or chelation control. 93

Table 3.2.1.3: Attempted diastereoselective reduction of perfluoroketones. 94

Figure 3.2.1.2: Possible chelated intermediates for the reduction of *N*-carbamoyl amino ketones. 95

Scheme 3.2.1.6: Mechanism for chelate formation in alcoholic solvents. 96

Scheme 3.2.1.7: Cyclization to form *syn* and *anti* oxazolidinones. 97

Figure 3.2.1.3: NOE results for *syn* and *anti* fluorous oxazolidinones. 98

Table 3.2.2.1: Perfluoroalkyl Grignard addition to *N*-carbamoyl amino esters..... 100

Scheme 3.2.2.1: Mechanism for mono- and bis-perfluoroalkylation of *N*-carbamoyl esters. 101

Table 3.2.2.2: Effect of solvent composition on perfluoroalkyllithium addition. 103

Figure 3.2.2.1: Solvated aggregates of organolithium reagents..... 105

Table 3.2.2.3: Perfluoroalkyllithium addition to *N*-carbamoyl amino esters. 106

Scheme 3.2.2.2: Epimerization during the formation of Weinreb amides..... 107

Table 3.2.2.4: Formation of *N*-carbamoyl Weinreb amides. 109

Table 3.2.2.5: Perfluoroalkyl addition to *N*-carbamoyl Weinreb amides. 111

Scheme 3.2.2.3: Perfluoroalkyllithium addition using predeprotonation. 112

Table 3.2.2.6: Diastereoselective reduction of perfluoroalkyl ketones. 113

Scheme 3.2.2.4: Cyclization of perfluoroalkyl alcohols to oxazolidinones 114

Figure 3.2.2.2: NOE results for *syn* and *anti* 4,5 disubstituted oxazolidinones..... 115

Figure 3.2.2.3: X-ray structure of oxazolidinone **245**..... 116

Scheme 3.2.2.5: Esterification of alcohol **243a** with (*R*) and (*S*) MTPA. 116

Scheme 3.2.3.1: Optimized synthesis of oxazolidinone **245** 117

Scheme 3.2.3.2: General synthetic pathway for the synthesis of fluorous oxazolidinones 117

Scheme 3.2.3.3: Perfluoroalkylation of *N*-carbamoyl amino esters **249** and **252**..... 118

Scheme 3.2.3.4: Cyclization of bis(perfluoroalkyl) alcohols. 118

Scheme 3.2.3.5: Synthesis of fluorous oxazolidinone from L-valine. 119

Scheme 3.2.3.6: Esterification of alcohol **258** with (*R*) and (*S*) MTPA. 120

Scheme 3.2.3.7: Perfluoroalkylation of amide **261** derived from D-phenylglycine. 120

Scheme 3.2.3.8: Esterification of alcohol **263** with (*R*) and (*S*) MTPA. 121

Scheme 3.2.3.9: Cyclization of alcohol **263** derived from L-phenylglycine. 122

Figure 3.2.3.1: Coupling constants and NOE results from oxazolidinones **265** and **266**. 122

Scheme 3.2.3.10: Epimerization of perfluoroalcohol **263**. 123

Table 3.3.1.1: Titanium mediated aldol reactions using the *anti* oxazolidinone **269**. 126

Scheme 3.3.1.1: Aldol transition structures for reaction supported on *anti* 4,5 disubstituted oxazolidinone **269**. 127

Table 3.3.1.2: Titanium mediated aldol reactions using the *syn* oxazolidinone **270**. 128

Scheme 3.3.1.2: Aldol transition structure for *syn* 4,5 disubstituted oxazolidinone. 129

Scheme 3.3.1.3: Mechanism for LiOOH hydrolysis of *N*-acyl oxazolidinones. 129

Scheme 3.3.1.4: Reductive cleavage of crotyl aldol product. 130

Scheme 3.3.2.1: Synthesis of *N*-crotyl fluorous oxazolidinone **290a**. 131

Table 3.3.2.1: Effect of Lewis acids on radical conjugate additions. 132

Scheme 3.3.2.2: Radical addition to *N*-crotyl fluorous oxazolidinone. 133

Scheme 3.3.2.3: Chelated and open intermediates in radical conjugate addition. 134

Scheme 3.3.2.4: Synthesis of cinnamoyl and monoethyl fumaroyl derivatives. 135

Table 3.3.2.2: Examination of substrate variability 135

Scheme 3.3.2.5: Hydrolysis of radical addition products using LiOOH. 136

Scheme 3.3.2.6: Facial selectivity for the Lewis acid-mediated radical conjugate addition. 137

Scheme 3.3.2.7: Steric volume of benzyl group in mono and disubstituted oxazolidinones. 137

Scheme 3.3.2.8: Synthesis and radical conjugate addition using norephedrine derivatives. 138

Table 3.3.2.3: Residual tin in samples following purification by various methods..... 139

Scheme 3.3.3.1: Synthesis of *N*-crotyl fluorous oxazolidinone **290a**. 141

Scheme 3.3.3.2: Synthesis of diphenylnitrone. 142

Scheme 3.3.3.3: 1,3 Dipolar cycloaddition of diphenylnitrone and **290a**. 142

Scheme 3.3.3.4: *Endo* and *exo* cycloaddition pathways. 144

Scheme 3.3.3.5: Lewis acid mediated transesterification. 144

Scheme 3.3.3.6: Dipolar cycloaddition using non-fluorous dipolarophile **315**. 145

Scheme 3.3.3.7: Reductive cleavage of *exo* isoxazolidine products..... 146

Figure 3.3.3.1: X-ray structure of dipolar cycloaddition product **310**. 147

Table 3.3.3.1: 1,3-Dipolar cycloaddition using Lewis acid catalysts. 149

Scheme 3.3.3.8: Open and chelated intermediates for dipolar cycloaddition. 151

Scheme 3.3.3.9: Steric repulsion in *exo* dipolar cycloaddition transition structure..... 152

Table 3.3.3.2: 1,3-Dipolar cycloadditions using **290a** and *o*-phenanthroline. 153

Table 3.3.3.3: 1,3-Dipolar cycloadditions using **290a** and 4Å molecular sieves. 154

Scheme 3.3.3.10: Switching facial selectivity of catalyzed dipolar cycloaddition..... 155

Scheme 3.3.3.11: Recycling of **290a** in 1,3-dipolar cycloadditions with diphenylnitrone. 156

Table 3.3.3.4: Recovery and recycling of **290a** in 1,3-dipolar cycloadditions. 157

Figure 3.3.3.2: Comparison of polymer-supported, fluorous-supported, and unsupported oxazolidinones in 1,3-dipolar cycloadditions. 158

Figure 4.2.2.1: Stereoisomers of methylphenidate. 165

Scheme 4.2.2.1: General synthesis of methylphenidate analogues using a fluorous chiral auxiliary. 166

LIST OF ABBREVIATIONS

[α]	Specific Rotation
Ac	Acetyl
aq	aqueous
Ar	aryl
Bu	butyl
t-Bu	*tert*-butyl
Boc	*tert*-butoxycarbonyl
Bn	Benzyl
Bz	Benzoyl
c	concentration in g/100 mL
Cbz	benzyloxycarbonyl
CDMT	chlorodimethoxytriazine
CMPI	2-chloro-1-methylpyridinium iodide
δ	chemical shift in ppm
DCC	1,3-dicyclohexylcarbodiimide
de	diastereomeric excess
DMAP	4-dimethylaminopyridine
DMF	*N*,*N*-dimethylformamide
DIPEA	diisopropylethylamine
ee	enantiomeric excess
Et	ethyl
EtOH	ethanol

FSPE	fluorous solid phase extraction
h	hour
J	coupling constant (in NMR)
LDA	lithium diisopropylamide
Me	methyl
MeOH	methanol
MTPA	α -methoxy-α-trifluoromethylphenylacetic acid (Mosher's acid)
NMR	nuclear magnetic resonance
NOE	Nuclear Overhauser Effect
Ph	phenyl
*i*Pr	*iso*-propyl
PrOH	propanol
TBDMS	*tert*-butyldimethylsilyl
TBTU	*O*-(Benzotriazol-1-yl)-*N*,*N*,*N*',*N*'-tetramethyluronium tetrafluoroborate
TEA	triethylamine
TFA	trifluoroacetic acid
THF	tetrahydrofuran
TMEDA	*N*,*N*,*N'*,*N'*-tetramethyl-1,2-ethylenediamine
TMS	trimethylsilyl

Chapter 1: INTRODUCTION AND BACKGROUND

1.1 Introduction

The focus of this thesis is to create new methods and compounds to carry out efficient stoichiometric asymmetric synthesis. This project has two primary goals: the first involves the design and optimization of an oxazolidinone chiral auxiliary containing a fluorocarbon or *fluorous* domain (Section 3.2); the second details the application of this new compound in asymmetric transformations (Section 3.3). The background and history of asymmetric synthesis employing chiral auxiliaries will be discussed, along with a review of synthetic methods using polymeric materials as supports for the construction of small molecules. Some of the advantages and disadvantages of polymer-supported protocols will be discussed, with particular focus on the application of polymer and supported methods to stoichiometric asymmetric synthesis. Finally, the concept of fluorous organic synthesis will be introduced, highlighting the superiority of this method. Several asymmetric transformations have been accomplished using the new oxazolidinone chiral auxiliary, including aldol reactions, radical conjugate additions, and 1,3 dipolar cycloadditions of nitrones. Background information pertinent to these reactions will be discussed, including the models describing how oxazolidinone chiral auxiliaries participate to give high stereoselectivity.

1.2 Asymmetric Synthesis

1.2.1 Stereochemistry and Chirality

The macroscopic properties of all matter ultimately have their roots in the microscopic world. The physical and chemical properties of a molecular species are defined by three parameters: the type and number of atoms present, the connectivity among these atoms, and the three-dimensional configuration of the molecule. Variation in this third property gives rise to differences in the chemical and physical properties of molecules, and is referred to as the stereochemistry. Chemical compounds having identical atomic composition but different structures are termed isomers. Geometric isomers arise from differences in the bonding arrangement of the atoms within a molecule, as seen in compounds such as *ortho*- and *para*-dibromobenzene (Figure 1.2.1.1). Stereoisomers are isomeric molecules that have identical connectivity but differ in the spatial arrangement of the constituent atoms. The category of stereoisomers can be separated further into enantiomers and diastereomers.

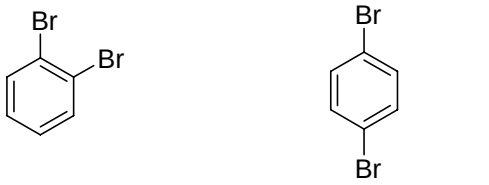

o-dibromobenzene *p*-dibromobenzene

Figure 1.2.1.1: Geometric isomers of dibromobenzene.

Any object that is not superimposable on its own mirror image is said to be "chiral".[1] Therefore, the symmetry of a compound is the defining characteristic of molecular chirality. A molecule that contains a plane (σ), centre (*i*) or alternating axis (S_n) of symmetry is achiral.[2] A compound which contains one asymmetric carbon,

referred to as a stereogenic centre, is always chiral due to the lack of these symmetry elements, as seen in *S*-serine (Figure 1.2.1.2). A molecule can have multiple stereogenic centres without being chiral overall.[2] These compounds are referred to as *meso*, and have a symmetry element, such as a mirror plane or inversion centre which relates the stereogenic centres (Figure 1.2.1.2). A molecule may also be chiral without any specific stereogenic centres present, allowing the compound to exist as individual enantiomers due to hindered rotation about a single bond.[2] This phenomenon is referred to as atropisomerism, and is seen in compounds like 1,1'-bi-2-naphthol (BINOL) (Figure 1.2.1.2).

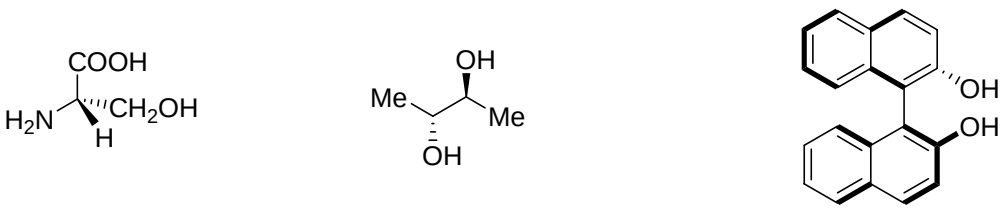

S-serine *meso*-butane-2,3-diol *S*-BINOL

Figure 1.2.1.2: Examples of chiral and achiral compounds.

Pairs of non-superimposable mirror-image stereoisomers are termed enantiomers and are indistinguishable chemically and physically in non-chiral environments. Stereoisomers that are not mirror images of one another are referred to as diastereomers, and display different physical and chemical properties, regardless of the chirality of the environment.

The relationship among enantiomers and diastereomers is illustrated by the stereoisomers of 2-chloro-3-hydroxypropanoic acid (Figure 1.2.1.3). The 2*R*,3*R* and 2*S*,3*S* compounds are mirror images are one another and thus form a pair of enantiomers. A second pair of enantiomers is defined by the 2*R*,3*S* and 2*S*,3*R* compounds. While the

2*R*,3*R* and 2*R*,3*S* compounds have the same connectivity they are not mirror images of each other. The same relationship exists for the 2*S*,3*S,* 2*S*,3*R* pair. These pairs are, therefore, diastereomers, and the set of four compounds may be described as two diastereomeric pairs of enantiomers.

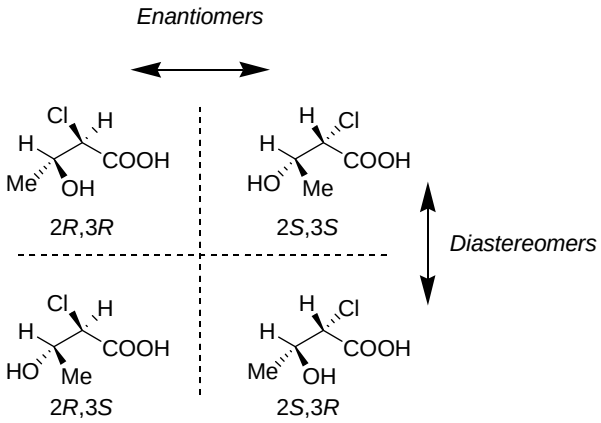

Figure 1.2.1.3: Enantiomers and diastereomers of 2-chloro-3-hydroxy-propanoic acid.

A related topic to molecular chirality is the designation of prochirality. This can be illustrated with chloroethane (Figure 1.2.1.4, A) and *S*-1-chloro-1-propanol (Figure 1.2.1.4, B). In compounds **1** and **4** the carbon bearing the protons Ha and Hb is not stereogenic. However, substitution of one of these atoms gives rise to a stereogenic centre. In chloroethane, the resulting compounds **2** and **3** are enantiomers, and thus Ha and Hb are termed enantiotopic. Compounds **5** and **6**, generated from *S*-1-chloro-1-propanol are diastereomers, and thus Ha and Hb are termed diastereotopic. Due to this relationship protons Ha and Hb are termed heterotopic.[2]

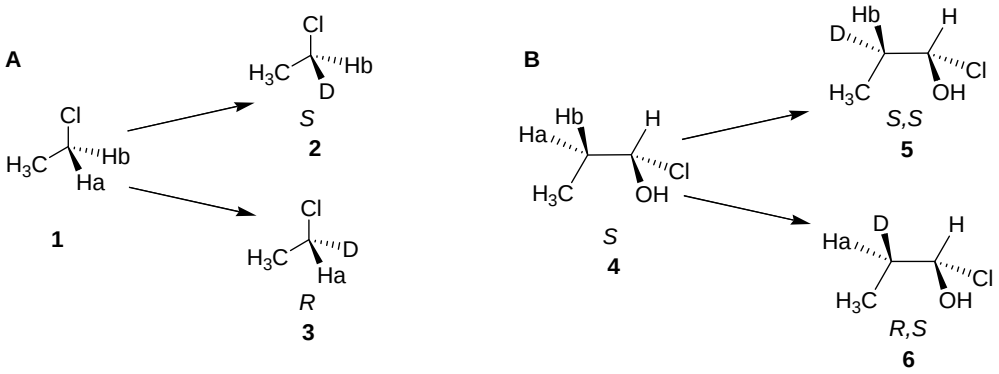

Figure 1.2.1.4: Enantiotopic and diasterotopic atoms.

1.2.2 The Importance of Stereochemistry

For many years functional group transformation and manipulation was the mainstay of organic synthesis, illustrating the focus of the researchers on molecular bonding, and not necessarily spatial arrangement. The entire face of organic synthesis began to change with the recognition of the importance of the three-dimensional nature of molecules.[3,4] Even a quick survey of the literature over the last thirty years clearly reveals a shift in the perception of synthetic chemists, demonstrating that molecular geometry has become as important to the creation of a compound as the atomic connectivity.

The desire to control the stereochemistry of a system during organic synthesis is stronger than ever. Research into the selective synthesis of single enantiomers and diastereomers has yielded a great deal of fundamental knowledge about many aspects of molecular theory. While these advances are of critical importance the major driving force behind this development is the pharmaceutical industry.[5,6] Biological systems are made up of a vast array of chiral species including metabolic enzymes, cellular receptors,

and membrane transport systems.[7] It is therefore obvious that each enantiomer of a chiral molecule may interact differently with this chiral environment.

Many examples exist where stereoisomeric molecules have very different pharmacological activities.[8-10] In certain cases one stereoisomer simply displays a much higher biological activity than the others, as is observed with natural versus synthetic vitamin E. The naturally sourced compound, d-α-tocopherol, is a single stereoisomer and is derived primarily from soybean, sunflower and corn oils.[11] Synthetic vitamin E is produced commercially by reacting trimethylhydroquinone with isophytol, resulting in a mixture of eight stereoisomers in varying amounts (Figure 1.2.2.1).[12] As a result, the biologically active enantiomer, d-α-tocopherol, makes up less than 12% of the total mixture. The other seven stereoisomers have biological activities that range from 21-90% of the activity of natural vitamin E based on rat fetal resorption tests.[13]

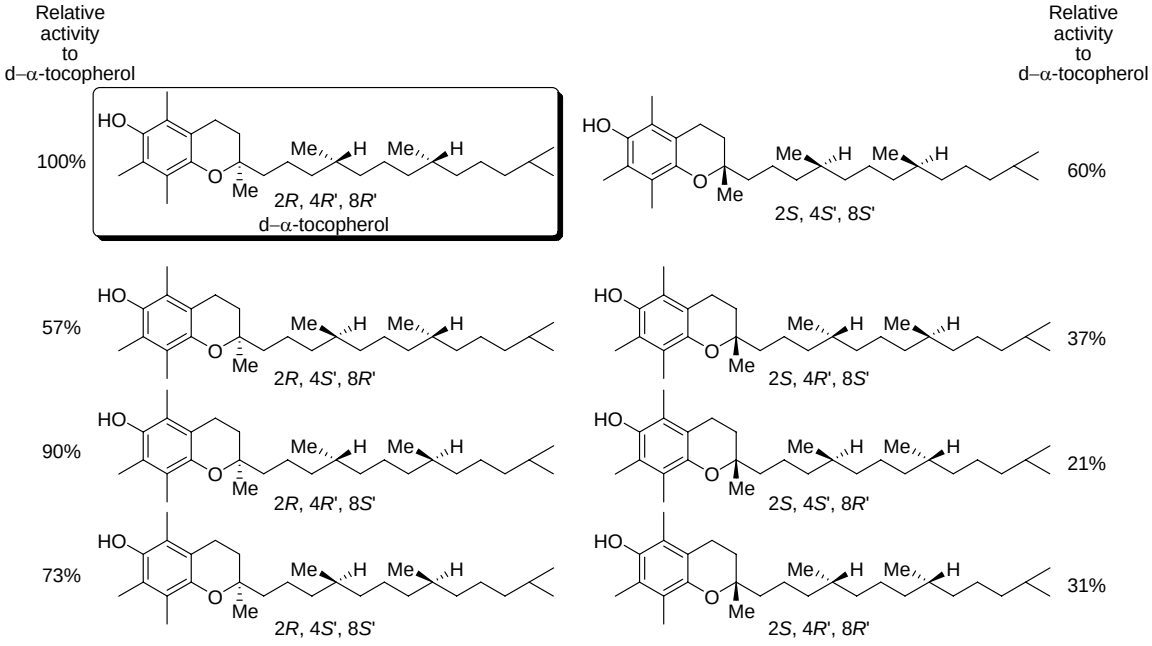

Figure 1.2.2.1: Bioavailability of the stereoisomers in synthetic vitamin E.[13]

While the presence of these other stereoisomers in synthetic vitamin E is not detrimental, synthesizing and delivering inactive materials is inefficient. To address this issue, some pharmaceutical companies have redeveloped racemic drugs and released single isomer replacements. This process of redeveloping existing racemic pharmaceuticals as the single enantiomer is known as a "chiral switch".[3,6] One example of this redesign process was seen with the proton pump inhibitor esomeprazole (Nexium®), which is the (*S*)-enantiomer of racemic (*S*,*R*)-omeprazole (Losec®) (Figure 1.2.2.2). While both *S*- and *R*-omeprazole share the same mechanism of action, *S*-omeprazole is less susceptible to small intestinal and hepatic metabolism than the (*R*)-form, resulting in 70% – 90% higher steady-state serum concentrations than racemic omeprazole using an equal dosage.[14]

Figure 1.2.2.2: Enantiomers of omeprazole.

The main rationale for redeveloping drugs in single enantiomer forms stems from the ability to extend the life of a patent on a pharmaceutical. Once the original patent on the racemic compound expires the new single enantiomer can be marketed as an "improved" version of the original.[15] Aside from this purely financial motivation, a number of medical benefits seem apparent. The differences in bioavailability and bioactivity observed between stereoisomers combined have made the redevelopment of racemic drugs very attractive to both the pharmaceutical industry and medical community. This has led to the promise of more cost effective and safer pharmaceuticals by delivering

only the active single enantiomer; however, this has not been sufficiently demonstrated to date.[15] While *S*-omeprazole has a higher bioavailability the clinical benefit appears to be minimal, and at present the effective daily dosage is more expensive than the corresponding dosage of the racemic drug (*S*-omeprazole [Nexium®]; $4.03 per day, *S,R*-omeprazole [Losec®]; $ 3.87).[15]

Presently, nine of the ten highest revenues-generating pharmaceuticals employ chiral species, and four of them (Lipitor®, Zocor®, Plavix®, and Nexium®) are sold as a single enantiomer.[16] This does illustrate a trend towards the production of single isomers of chiral drugs. However, the lack of clinically significant benefits in many cases highlights the need for innovation in the field of chiral pharmaceuticals. Developing new chiral species is restricted by the methods available, necessitating new technologies capable of preparing single stereoisomers in the high-throughput paradigm employed in modern drug discovery.

1.2.3 Isolation of Individual Stereoisomers

If a material already exists as a racemate, then the individual enantiomers may be resolved or separated. To accomplish this, one of four basic techniques can be used: selective crystallization,[17,18] chiral chromatography,[18,19] temporary conversion to diastereomers followed by separation,[18] and kinetic resolution.[20] Each of these techniques permits the isolation of single enantiomers from a mixture of stereoisomers; however, they all suffer form one major drawback. Half of the material exists as the undesired enantiomer, making the synthesis of a compound as a racemate followed by resolution very inefficient, and undesirable in industrial practice.

Under certain circumstances stereoisomers can be interconverted by using dynamic kinetic resolution.[21] This process allows the undesired geometry to be transformed into that of the target molecule. In principle, this method functions by converting the racemic compound to some species that can rapidly convert between two different stereoisomers, followed by reaction to some final compound. One example of this process is the resolution of *N*-phthalylamino acids such as **7** (Scheme 1.2.3.1).[22] Reaction of amino acid **7** with DCC and DMAP gives the two rapidly interconverting *N*-acyl pyridinium ions **9** and **10**. Subsequent reaction with chiral alcohol **8** shows a difference in rate, depending on the geometry of the intermediate. Reaction of **9** is significantly faster than that of **10** leading to the selective formation of ester **11**.

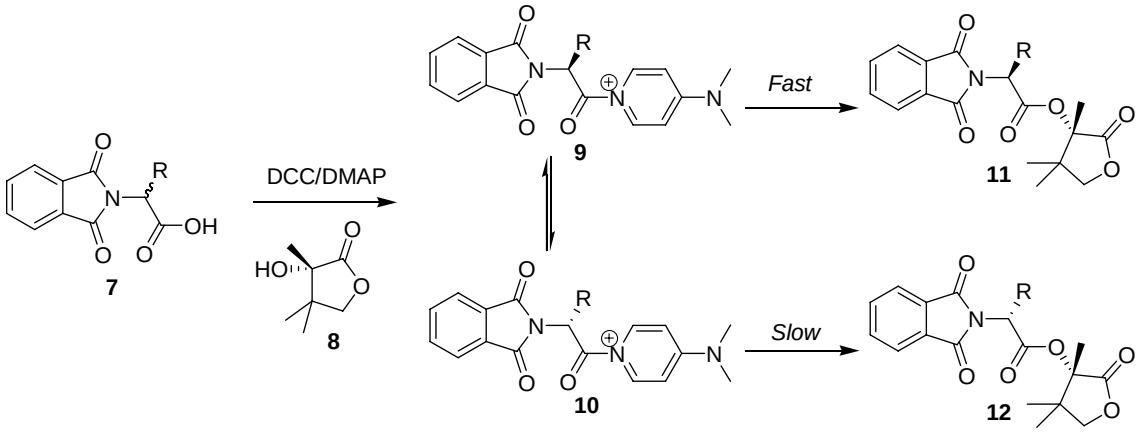

Scheme 1.2.3.1: Dynamic kinetic resolution of *N*-phthalylamino acids.[22]

While these separation methods yield individual stereoisomers, it is far more efficient to synthesize a single molecular geometry selectively. One method of accomplishing this goal is to employ starting materials drawn from the so-called "chiral pool". These compounds are chiral molecules found in nature as single isomers, such as amino acids or carbohydrates. Provided the desired geometry can be obtained from some available starting material, the stereochemistry of the product is installed using the chiral

pool compound. Numerous strategies employ this method to generate the appropriate isomer of some desired compound.[23,24] However, the breadth of synthetic targets is limited to the array of molecules readily available from natural sources.

A more general approach to creating chiral compounds is known as stereoselective or asymmetric synthesis. In general, this technique involves the creation of one or more stereogenic centres giving rise to the creation of a specific stereoisomer preferentially over all other possible geometries.[1] These transformations can be either enantioselective or diastereoselective. In an enantioselective synthesis, one enantiomer of the possible product stereoisomers is generated preferentially from some prochiral reactant. Diastereoselective processes generate one diastereomer in preference to the other possible geometries.

This selection of molecular geometry arises from the presence of diastereomeric intermediates or transition states during the formation of the stereogenic centres. These reactions can be either kinetically or thermodynamically controlled, as illustrated by the reaction coordinates for some set of hypothetical transformations in Figure 1.2.3.1. In Figure 1.2.3.1A the competing transformations of the starting material **s.m.** are both irreversible. As a result the process **s.m.→P2** will be favoured over **s.m.→P1** due to a difference between the energies of the transition states ($\Delta\Delta G^{\ddagger}$). Therefore, this process is kinetically controlled as the distribution between product **P1** and **P2** is ultimately governed by differences in the two rates of reaction.

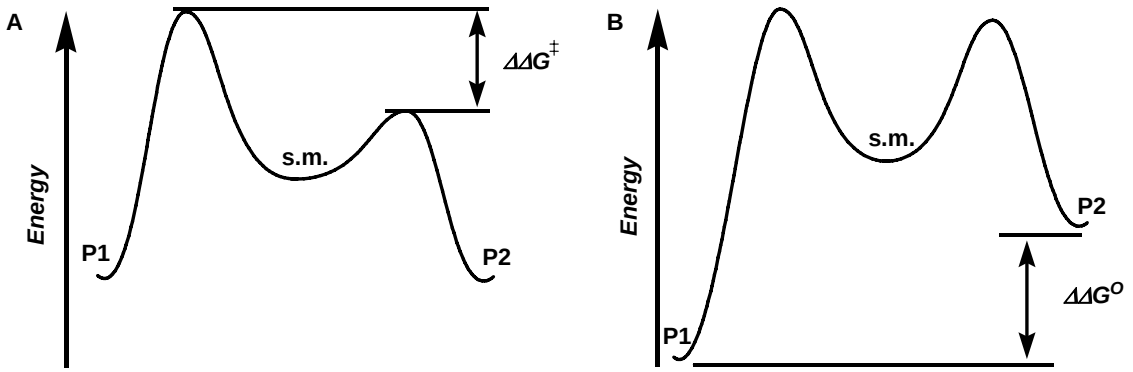

Figure 1.2.3.1: Kinetically and thermodynamically controlled transformations.

In Figure 1.2.3.1B the transformations from starting material **s.m.** occur reversibly, allowing the products to equilibrate. Therefore, **s.m.→P1** will be favoured over **s.m.→P2** due to the difference between the free energies of the two products (ΔΔG°). This process is thermodynamically controlled as the final distribution between **P1** and **P2** is governed by the relative stability of the two products. In either case, the key controlling factor is some energetic dissimilarity between molecules or complexes with different spatial arrangements. The degree of selection between potential stereoisomers is therefore determined by the magnitude of these energy differences.

In order to carry out a kinetically-controlled reaction stereoselectively, the reaction must pass through competing diastereomeric transition states or intermediates. Reactions of achiral molecules at enantiotopic faces or groups are not selective because the transition states or intermediates are enantiomers and thus have the same energy, as illustrated in Figure 1.2.3.2. Reduction of the achiral ketone **13** with an achiral reducing agent, such as sodium borohydride, proceeds through two enantiomeric transition states (Figure 1.2.3.2, A). These two transition states have the same energy, resulting in no selectivity in the production of enantiomers **14** and **15**.

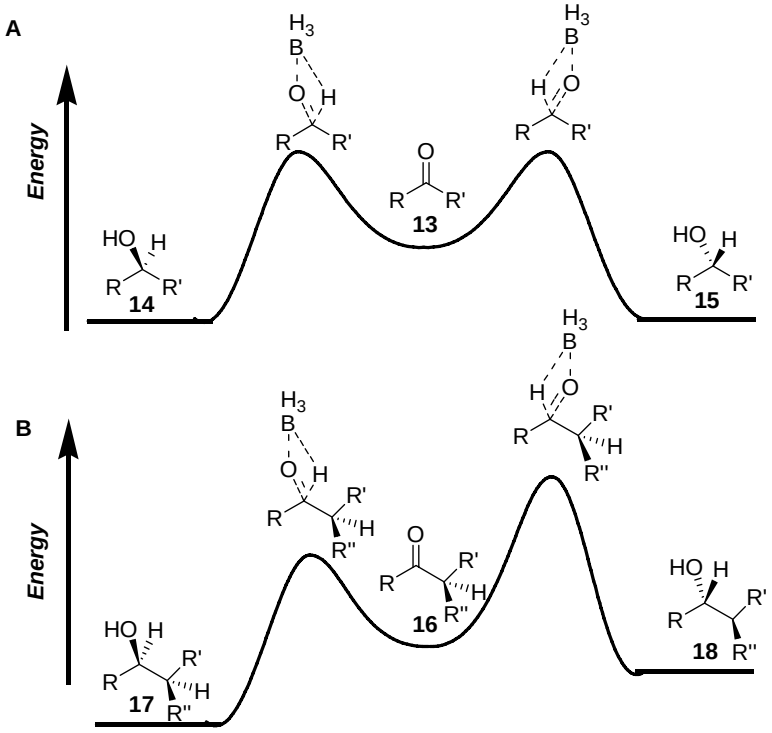

Figure 1.2.3.2: Reaction via enantiomeric and diastereomeric transition states.

When chiral ketone **16** is treated with the same achiral reducing agent, the resulting transition states are now diastereomers of one another (Figure 1.2.3.2, B). Given that the reduction is irreversible, the difference in energy between the two transition states will give alcohol **17** selectively via kinetic control.

In order to produce a single enantiomer selectively from a prochiral starting material, some external chiral element must be employed, such as a chiral catalyst or a chiral reagent. Enantioselective transformations using chiral catalysts are very important in the field of asymmetric synthesis. A vast number of asymmetric reactions using chiral catalysts have been illustrated, demonstrating the breadth and maturity of this field of research.[25-27] The far-reaching impact of catalytic asymmetric synthesis was acknowledged in 2001, when the Nobel Prize in Chemistry was awarded to three pioneers in this field; William S. Knowles, Ryoji Noyori and K. Barry Sharpless.[28]

In general, catalytic methods have gained a high profile due to their ability to synthesize large quantities of chiral products with the application of only small amounts of the expensive and potentially difficult to synthesize catalytic materials. However, stoichiometric asymmetric methods, in particular the application of chiral auxiliaries, have played an equally important role in the growth of stereoselective synthesis.[29-34]

One method for performing stoichiometric asymmetric synthesis involves the use of a chiral auxiliary. In this technique a chiral compound is attached to a prochiral substrate to convert enantiotopic atoms or faces of the substrate into diasterotopic atoms or faces. This method is illustrated with the asymmetric aldol reaction of aryl carboxylic acids **19** (Scheme 1.2.3.2). Amide **21** is formed by coupling the achiral carboxylic acid with pseudoephedrine. Protons Ha and Hb were enantiotopic in **19,** but now are diasterotopic, allowing the aldol reaction to proceed diastereoselectively to give isomer **22**. Hydrolysis of the amide bond liberates pseudoephedrine giving the *S* enantiomer of hydroxyl alcohol **23** preferentially. Performing this aldol reaction at –105 °C in the presence of zirconocene dichloride has been shown to give alcohol **22** with a diastereomeric excess of 98%.[35]

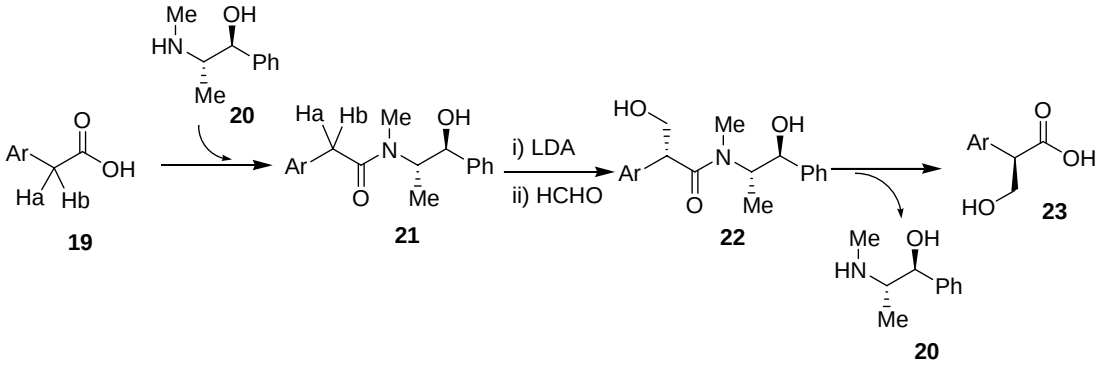

Scheme 1.2.3.2: Application of pseudoephedrine as a chiral auxiliary.

1.2.4 Oxazolidinone Chiral Auxiliaries

One of the most widely used and efficient chiral auxiliaries employed in asymmetric stoichiometric synthesis is the oxazolidinone (Figure 1.2.4.1).[36] These compounds were first introduced by Evans in 1981,[37] and since that time have been used extensively.[38]

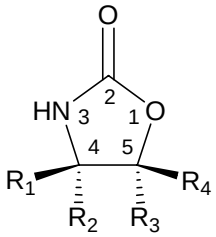

Figure 1.2.4.1: General structure of oxazolidinones.

For a molecule to function efficiently as a chiral auxiliary four basic criteria must be met. The auxiliary must be readily available as a single enantiomer, easily attached to a wide variety of achiral substrates, efficiently control the stereoselectivity of the necessary asymmetric transformation, and be efficiently and selectively removed following the introduction of the new stereogenic centre.

A wide variety of chiral oxazolidinones have been developed.[36,39] Chiral α-amino alcohols are the most obvious and practical feedstock to obtain functionalized oxazolidin-2-ones. These compounds are most commonly obtained from α-amino acids (Figure 1.2.4.2, **A**),[40] epoxides (Figure 1.2.4.2, **B**),[41] α-amino carbonyl compounds (Figure 1.2.4.2, **C**),[42] or hydroxy carbonyl compounds (Figure 1.2.4.2, **D**).[43]

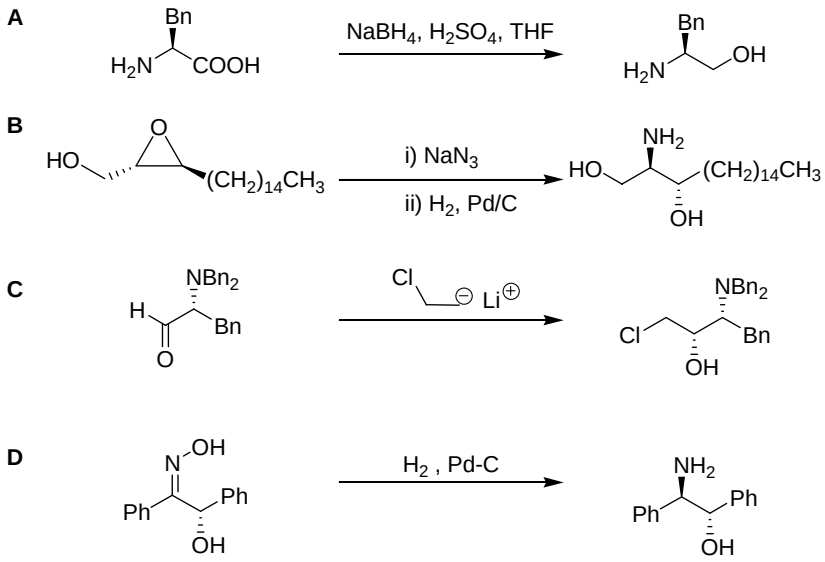

Figure 1.2.4.2: Methods for the synthesis of chiral α-amino alcohols. [40-43]

While numerous techniques exist to convert amino alcohols to the corresponding oxazolidinones,[38] several general strategies are most frequently employed. The necessary carbonyl functionality can be added to unprotected amino alcohol **24** by using phosgene or some appropriate reactive equivalent (Scheme 1.2.4.1, **A**).[44] Alternately, the corresponding *N*-carbamoyl derivatives **26** can be cyclized, either by using strong bases to promote addition to the carbamate carbonyl by the alkoxide (Scheme 1.2.4.1, **B**),[45] or by converting the alcohol to a leaving group, leading to S_N2 attack at the hydroxyl centre in **28** (Scheme 1.2.4.1, **C**).[46] These last two variations are particularly useful in generating different diastereomers of the target oxazolidinone, as the former proceeds with retention of stereochemistry at the 5 position, while the latter results in inversion.

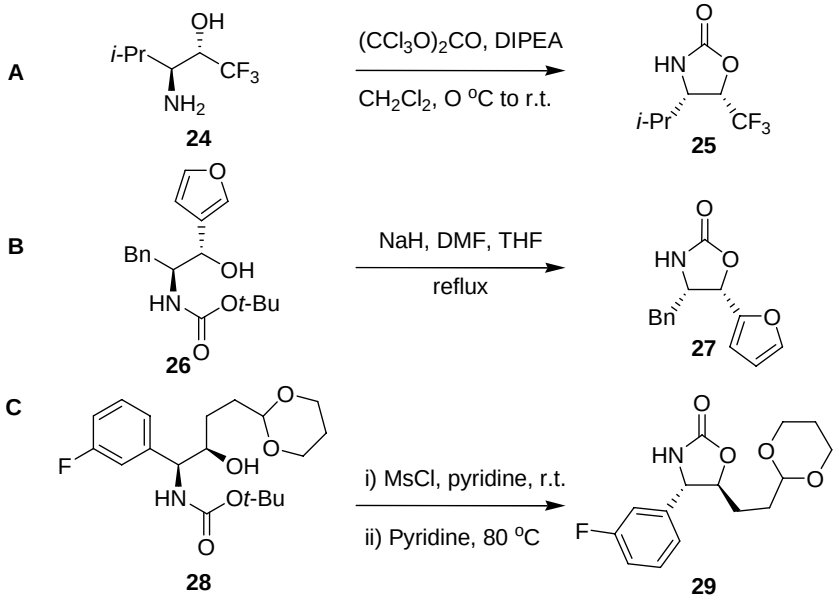

Scheme 1.2.4.1: Methods for the synthesis of oxazolidinones from amino alcohols.[44-46]

To apply these molecules to asymmetric synthesis, a prochiral substrate must be attached. Most commonly, this is accomplished by acylation of the oxazolidinone nitrogen with the appropriate carboxylic acid derivative. *N*-Acyloxazolidinones can be formed using standard amide formation or peptide-coupling techniques. In early applications, lithiated oxazolidinones such as **31** were generated using *n*-BuLi and reacted with the appropriate acid chloride, to yield the corresponding acyl derivative **32** (Scheme 1.2.4.2, **A**).[47] While this process can be very efficient certain sensitive carboxylic acids, such as α,β-unsaturated systems, do not tolerate strongly basic conditions. Acyl derivatives of these compounds can be prepared by using tertiary amine bases in combination with lithium chloride to give the corresponding *N*-enoyloxazolidinone **34** (Scheme 1.2.4.2, **B**).[48] Recently, more direct methods have been explored using peptide coupling agents such as HBTU to activate the carboxylic acid (Scheme 1.2.4.2, **C**).[49]

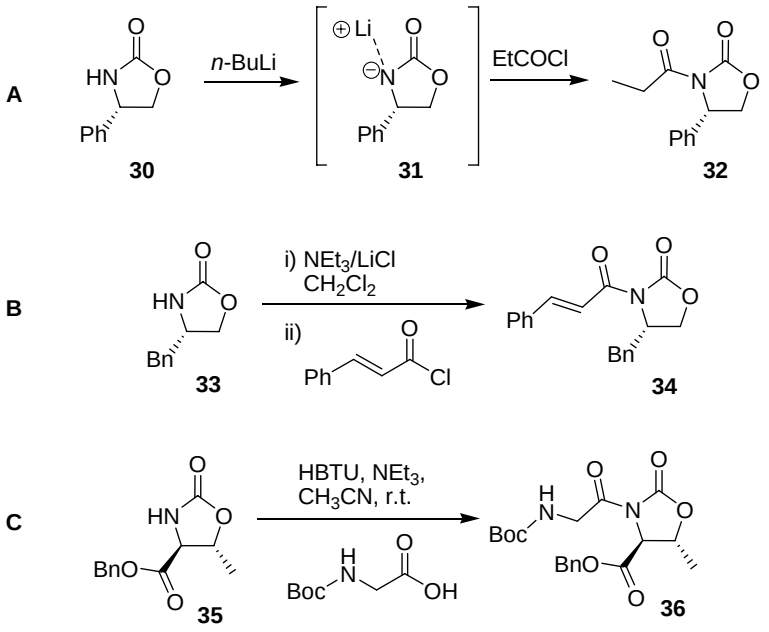

Scheme 1.2.4.2: Methods for the synthesis of *N*-acyloxazolidinones.[47-49]

Oxazolidinone chiral auxiliaries have been extensively employed in asymmetric chemistry.[29-31,38] Initially these auxiliaries were applied by Evans *et al.*[37] to asymmetric aldol reactions using boron enolates derived from oxazolidinone **37**. These reactions were tested with a variety of aldehydes and found to be highly selective for aldol product **38**.[37]

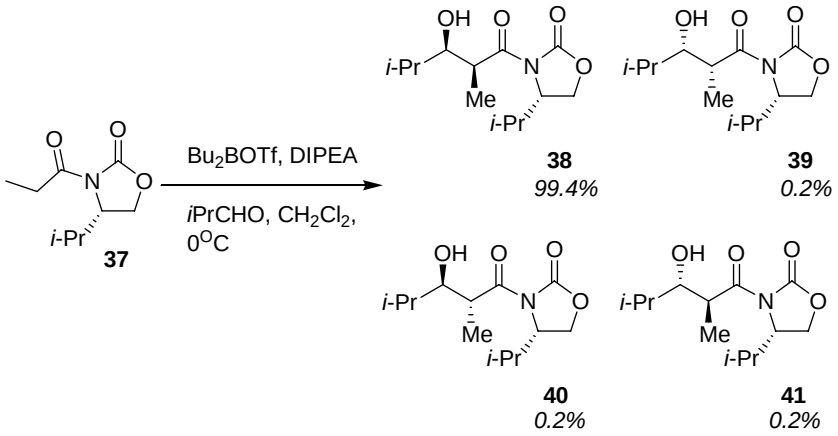

Scheme 1.2.4.3: Asymmetric aldol reactions using *N*-acyloxazolidinones.[37]

Oxazolidinones have since been employed in asymmetric alkylations,[50,51] α-substitutions,[52,53] nucleophilic conjugate additions,[54,55] and pericyclic reactions.[56,57] Representative examples of these reactions are shown in Scheme 1.2.4.4. Specific details regarding the mechanism of diastereoselectivity using *N*-acyloxazolidinones can be found in Section 1.5.

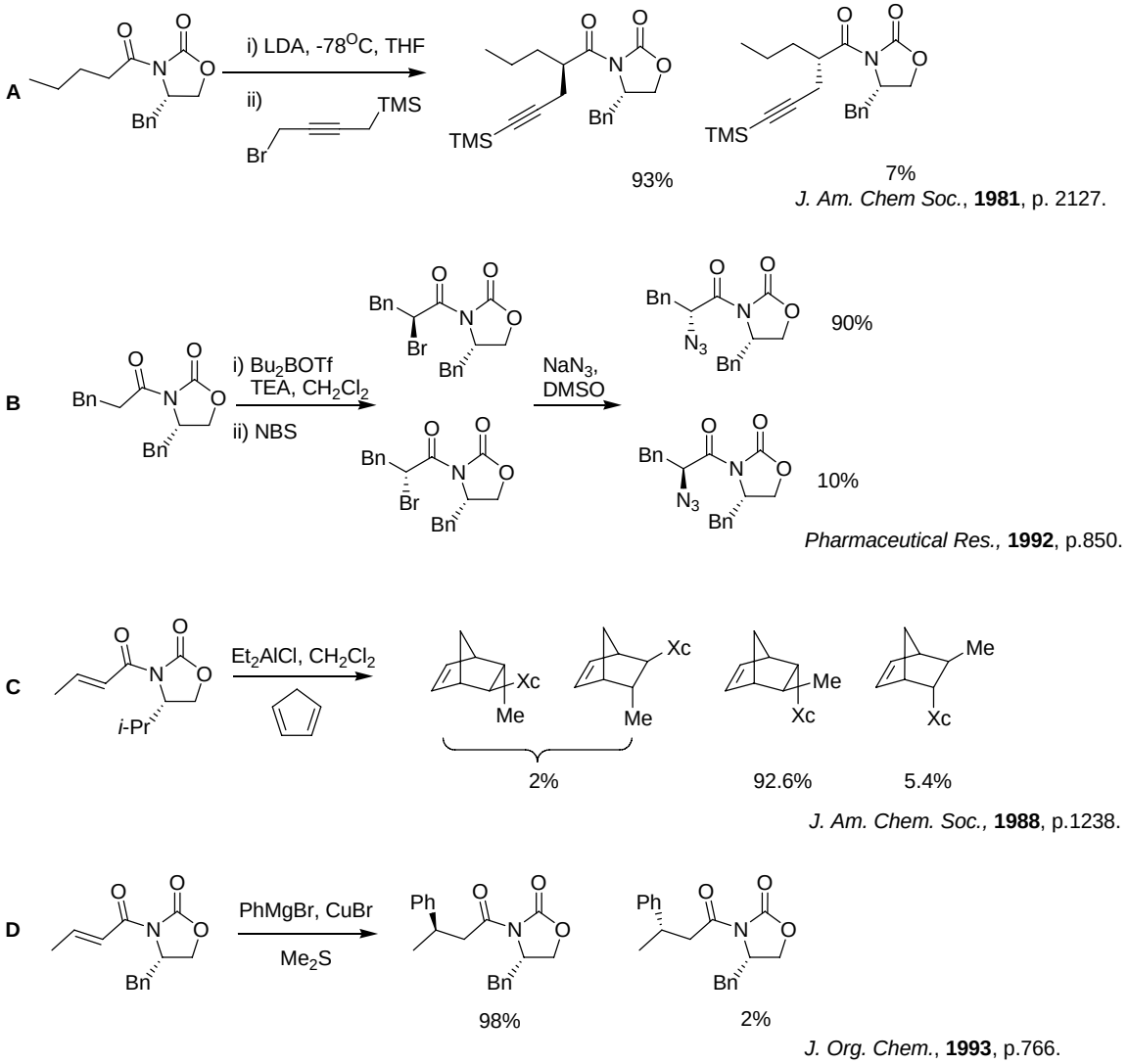

Scheme 1.2.4.4: Examples of asymmetric reactions using oxazolidinones.

Release of the acyl portion of the molecule following introduction of the new stereogenic centre can be accomplished using a number of techniques. The key challenge facing these protocols is the selective cleavage of the exocyclic amide bond without disrupting the endocyclic carbamate. The potential differences in selectivity have been demonstrated by Evans *et al*. (Scheme 1.2.4.5). [58] Hydroxide was shown to give poor selectivity, leading to cleavage via both the endo and exocyclic pathways. In contrast hydroperoxide ($^{-}$OOH) was found to be a superior reagent giving rise to the desired exocyclic mode of attack and minimizing endocyclic product **45**.

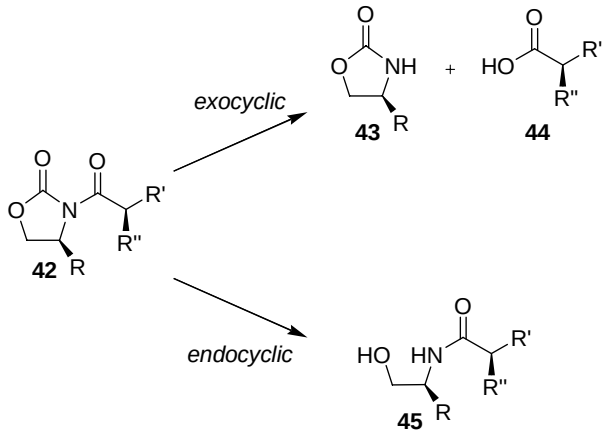

Scheme 1.2.4.5: Hydrolysis of *N*-acyloxazolidinones.

The *N*-acyl fragment of the oxazolidinone chiral auxiliary may also be cleaved by several other methods including transesterification,[59] transamination,[60] and direct reduction.[61] Examples of these procedures are listed in Scheme 1.2.4.6.

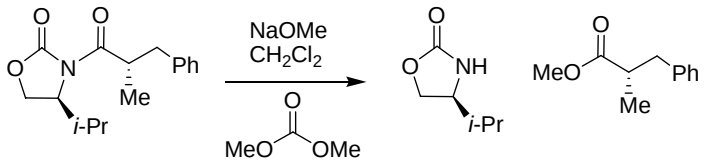

Tetrahedron Lett., **2003**, p.3599

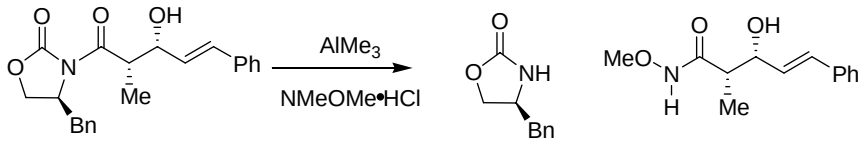

J. Am. Chem. Soc, **1988**, p.2506

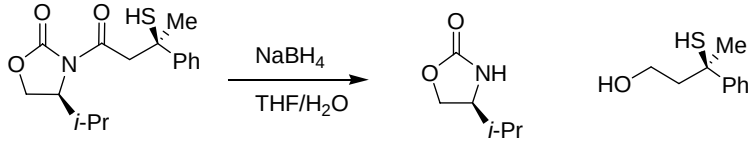

Angew. Chem. Int. Ed., **2004**, p.3307

Scheme 1.2.4.6: Examples for the deacylation of oxazolidinones.

Using this set of reactions it is possible to readily isolate the newly formed chiral material as a variety of carboxylic acid derivatives. This variability further adds to the versatility of employing oxazolidinone chiral auxiliaries.

1.3 Supported Synthesis

1.3.1 Background

Combinatorial chemistry now plays an important role in the lead discovery and hit optimization processes in the pharmaceutical world, and other areas of discovery chemistry.[62] Using a combinatorial approach, the synthesis of new compounds is designed such that a range of analogues can be produced under similar reaction conditions using semi-automated protocols.[63-65] In this technique, a small set of chemical building blocks are combined together in multiple ways, using standard chemistries, to create large libraries of compounds. This allows the preparation of many hundreds or thousands of compounds in the time usually taken to prepare only a few using standard methods. The process is schematically represented in Figure 1.3.1.1 where two starting materials and two pairs of reagents (A and B) can be combined using similar chemistry to give eight different products. Each of these products can then be tested in a biological system to identify structures or compounds for more detailed investigation.

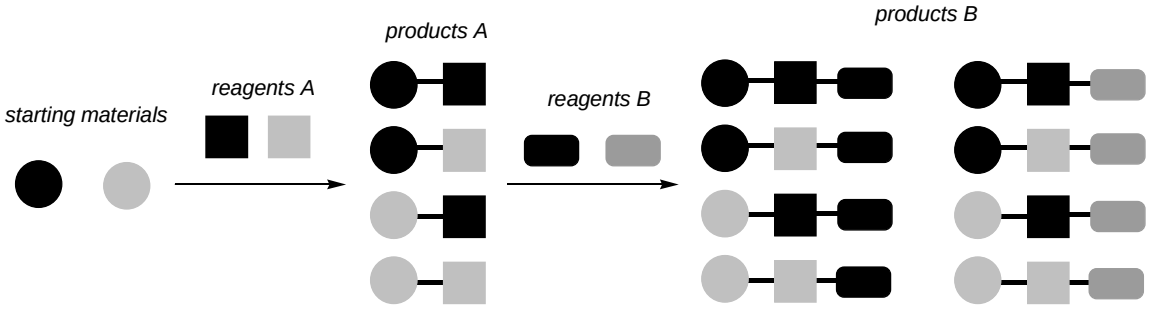

Figure 1.3.1.1: Schematic representation of a combinatorial synthesis.

Given the importance of chirality in biological systems it is imperative that asymmetric techniques be adapted to function in combinatorial applications. Many modern automated and parallel techniques, which are fundamental to combinatorial

chemistry, are predicated on the ability to rapidly and selectively isolate reaction materials.[66,67] Solid-phase or polymer-supported synthesis is the primary method of enabling reactions to be employed in these techniques. Therefore, established asymmetric reactions must be redeveloped on these media.

In polymer-supported organic synthesis, a target molecule is covalently attached to a polymer carrier. In most cases the polymer is not soluble in typical organic reactions, or can be precipitated from solution. This allows the "tagged" or polymer-bound molecules to be easily separated from other species simply using filtration. A schematic application of this protocol is shown in Figure 1.3.1.2. A small molecule is attached to the polymer-support during the loading stage, followed by a reaction to give a polymer-bound product. This product can be easily purified from the crude reaction simply by filtration due its difference in solubility. The product is then liberated from the support following transformation in the unloading step.

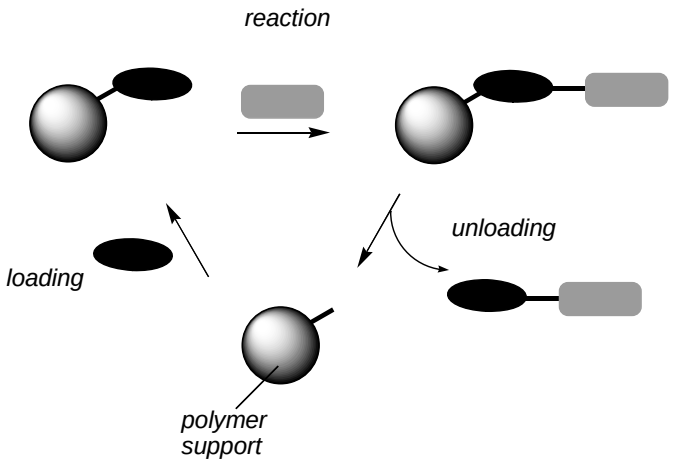

Figure 1.3.1.2: Supported organic synthesis.

In many cases chiral catalysts are supplanting stoichiometric auxiliaries in general synthetic methods. However, in supported synthesis there is no inherent disadvantage to

using a chiral auxiliary since it forms a part of the support itself. Moreover, chiral auxiliaries still offer the most dependable routes to high asymmetric induction in many cases. These properties make chiral auxiliaries applicable to combinatorial and parallel synthesis.

1.3.2 History of Supported Organic Synthesis

Before 1960, synthetic polymers were regarded as useful materials for a variety of macroscopic applications, but little attention was paid to their chemical reactivity.[68] During this early period, researchers began to recognize that these polymers were potentially susceptible to chemical transformations, and in many ways were analogous to their smaller organic counterparts. Merrifield was the first to demonstrate that large polymers could be functionalized and applied to standard organic synthetic protocols.[69] In his pioneering work on peptide synthesis, Merrifield demonstrated that an insoluble cross-linked polystyrene support could be used in place of a carboxylic acid protection group on the C-terminal amino acid residue. The remainder of the peptide could be synthesized on this insoluble support and the products rapidly purified by filtration.

Using this technique, it was possible to create tetrapeptides using a simple iterative protocol (Scheme 1.3.2.1). The first amino acid was loaded onto polymer **46** via an ester linkage to give **47**. Treating the now functionalized polymer with acetic acid and HBr removed the CBz protection group to give free base **48**, which was then coupled with the next amino acid residue in the presence of DCC to give the bound dipeptide **49**. The deprotection and coupling steps could then be repeated, sequentially lengthening the peptide one residue at a time. Once the desired sequence was constructed reaction with sodium hydroxide gave the hydroxylated polymer **50** and the free polypeptide **51**.

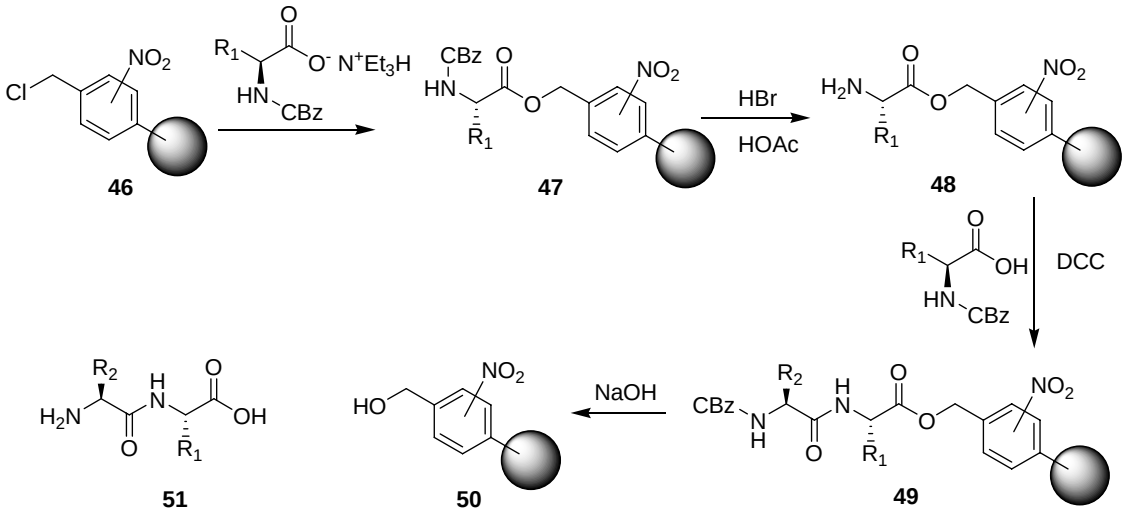

Scheme 1.3.2.1: Merrifield's protocol for solid-phase peptide synthesis.

The potential to replace the workup of a chemical reaction by a simple filtration step was a strong lure for many organic chemists. Aside from rapid and facile purification of reaction materials, reactions on polymeric supports offered other specific advantages including the ability to accelerate reactions and force them to completion by applying large excesses of reagents.[70] Soon after these initial studies, other researchers began to apply other methods to the solid phase, with the aim of synthesizing small molecules and natural products using this technique.

While many researchers contributed to the birth of solid phase organic synthesis, Leznoff's research group has accomplished outstanding pioneering work in this field.[66-68,70] In particular, the efficiency and adaptability of solid phase organic techniques were highlighted in their synthesis of a library of insect pheromones (Scheme 1.3.2.2).[70,71] Alcohol **53** could be loaded onto the resin and reacted using a variety of techniques. Oxidation produced terminal aldehyde **55**, which could be reacted with an appropriate ylide to give the corresponding *E* and *Z* alkenes **56** and **57** respectively. The compounds could then be liberated from the polymer by transesterification to produce pheromones **58**

and **59** in a ratio of approximately 3:7. Alternately, the loaded alcohol **54** could be converted to electrophile **60** and reacted with an alkynyl nucleophile to produce **61**. Reducing the alkyne with disiamylborane yielded the *Z* alkene selectively, which was liberated via transesterification to give pheromone **63**.

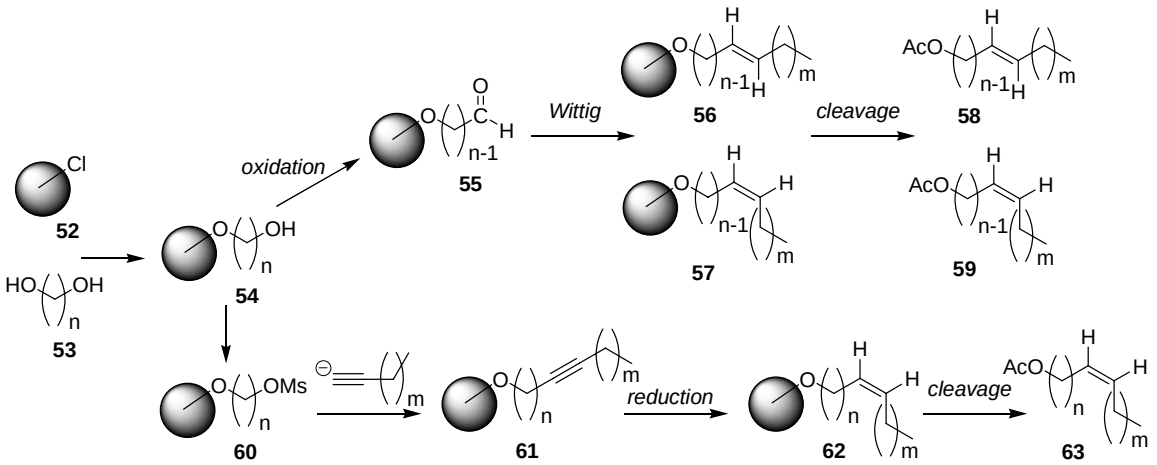

Scheme 1.3.2.2: Synthesis of *Z* and *E* insect pheromones using solid phase methods.[71]

Using this general solid phase technique, significant quantities of insect pheromones **58**, **59** and **63** were easily synthesized. In addition to the *Z/E* selectivity, the chain length in these compounds could be varied simply by altering the starting materials. Thus, it was possible to access a wide variety of structurally and conformationally unique pheromones with very little effort. This strategy could not be easily accomplished in the solution phase. Aside from the greater workload associated with workup and purification when the reactions are performed in the solution phase, it is difficult to use the symmetric diol **53** as a starting material. Using the polymer it is relatively easy to react a single alcohol group, in effect selectively protecting this centre and leaving the other free for further reaction.

1.3.3 Polymer-Supported Chiral Auxiliaries

The various benefits offered by solid phase chemistry led to a rapid expansion of synthetic methods, as many solution phase protocols were adapted to this new environment. Polymer-supported chiral catalysts[72] and chiral auxiliaries[73] have been developed and employed in various asymmetric transformations. While both these embodiments allow rapid purification of the chiral materials and potentially increase the efficiency of the asymmetric transformation, only the chiral auxiliary method simultaneously allows the introduction of asymmetry into the target molecule, and links the substrate to a carrier. This dual role, as stereochemical directing agent and synthetic support, makes the supported auxiliary very attractive to application in multi-step parallel or automated synthesis.

The first example of a polymer-supported chiral auxiliary was reported by Kawana *et al.* in 1972.[74] In this study, 1,2-*O*-cyclohexylidene-α-xylofuranose was attached to an insoluble polystyrene polymer (Scheme 1.3.3.1). The auxiliary was then esterified to form **65,** which was subsequently reacted in a Grignard reaction. Cleavage of the products gave the α-hydroxy acid **66** and the polymer-bound auxiliary **64**.

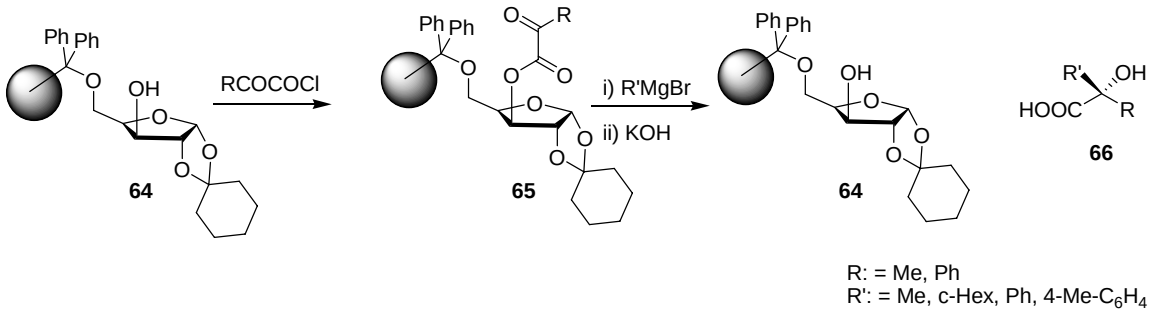

Scheme 1.3.3.1: Asymmetric synthesis using a polymer-bound carbohydrate auxiliary.

This reaction series was repeated with both benzoylformic and pyruvic acid, and a series of Grignard reagents. The yields for these reactions were between 18% and 84% and the enantiomeric excesses of the resulting α-hydroxy acids were consistently less than 65%.[74]

Since the initial report by Kawana *et al.*, many other polymer-supported chiral auxiliaries have been prepared. These can be divided into four categories: alcohol and carbohydrate auxiliaries,[75,76] amine and hydrazine auxiliaries,[77-79] sulfoxide, sulfinamide and sulfoximine auxiliaries,[80,81] and oxazolidinone auxiliaries.[82,83] Representative examples of these species and their application to asymmetric transformations can be found in Scheme 1.3.3.2.

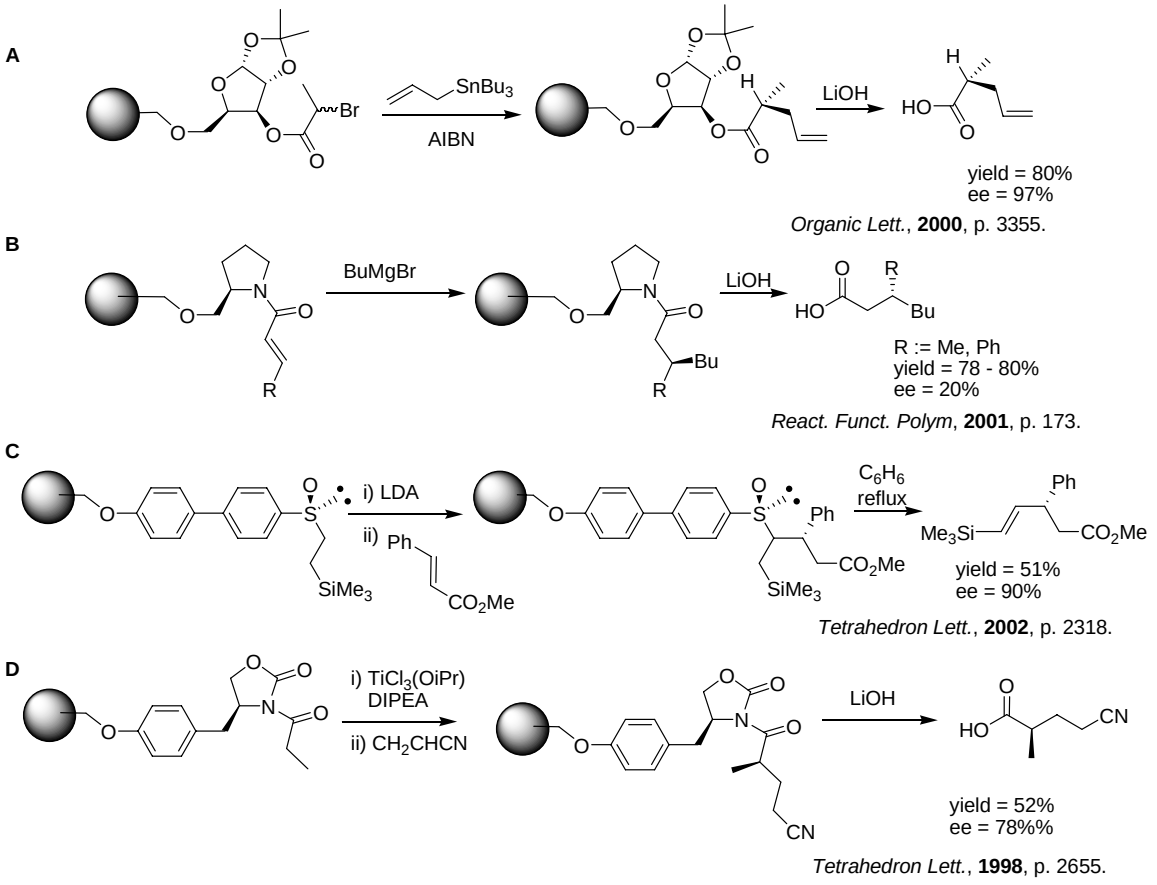

Scheme 1.3.3.2: Examples of polymer-supported chiral auxiliaries.[75,77,80,82]

The various developments in the application of polymer-supported chiral auxiliaries in asymmetric transformations over the last thirty years has recently been reviewed by Chung *et al*.[73] Although many examples are reported, this review highlights the fact that a relatively limited number of polymer-supported applications exist compared to the vast number of solution phase applications of chiral auxiliaries reported over the same period of time.[31,38,84,85]

In general, it was not always possible to obtain acceptable results using polymer-bound chiral auxiliaries.[73] There are a number of cases in which the polymer-bound auxiliary delivered very high yields and selectivities. The results reported by Itsuno *et al*.[86] are good examples of a successful application of a polymer-supported auxiliary (Scheme 1.3.3.3). In this work, imine **67** was treated with the allylzinc reagent prepared from allyl bromide to give the allylated product **68**. Reduction followed by treatment with hydroiodic acid and methyl amine gave the bound amine **69**, which could be released from the support to give **70** in 95% overall yield and greater than 99% ee.

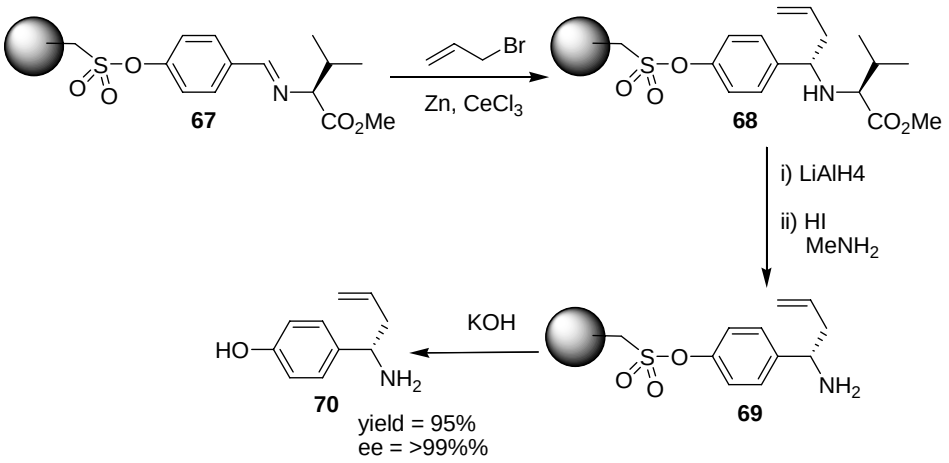

Scheme 1.3.3.3: Asymmetric allylation using a polymer bound chiral imine.[86]

However, in many cases the polymer-bound auxiliary does not replicate the performance of the analogous solution phase reactions. Proctor *et al.*[87] have reported the application of pseudoephedrine in both solution phase and solid phase reactions (Scheme 1.3.3.4). In both studies the propionyl derivatives **71** and **72** were treated with LDA to form the lithium enolate, which was then alkylated using benzyl bromide to give **73** and **74**. These compounds were then cleaved to give the primary alcohol **75**. Both methods yielded the *R* enantiomer selectively; however, the solution phase protocol gave **75** in a higher enantiomeric excess (91% cf. 87%).[87]

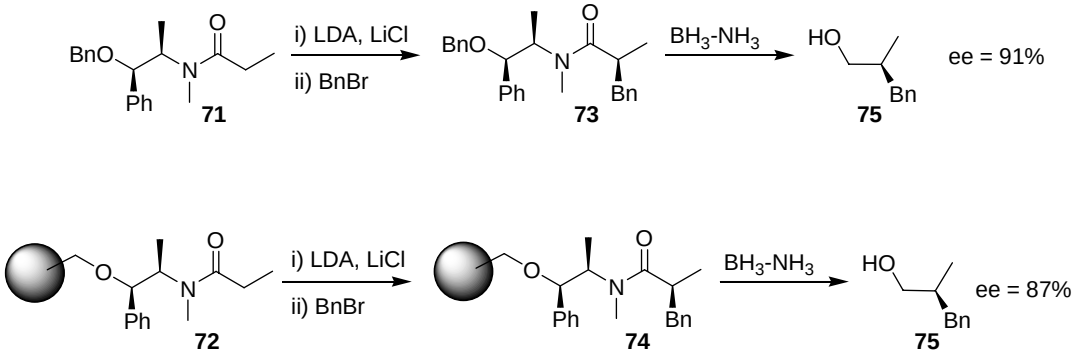

Scheme 1.3.3.4: Solid and solution phase alkylation using pseudoephedrine.[87]

The difference in performance observed between the solution phase and solid phase chiral auxiliaries can be attributed to the polymeric support itself. The literature reported for polymer-supported oxazolidinone chiral auxiliaries serves to highlight this fact. To date, three different varieties of polymer-supported oxazolidinones have been reported (Figure 1.3.3.1). Auxiliary **76** bound to Merrifield resin was the first supported oxazolidinone chiral auxiliary to be reported, and was synthesized from L-serine.[83] Auxiliary **77** is derived from L-tyrosine and has been supported on Merrifield resin,[82] Wang resin,[82,88] TentaGel®,[88] and non-crosslinked polystyrene.[89] More recently

auxiliary **78** has been synthesized from allophenylnorstatine and attached to Wang resin.[90]

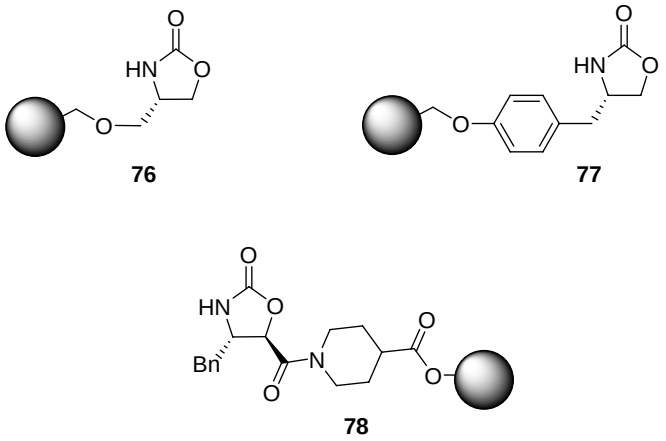

Figure 1.3.3.1: Polymer-supported oxazolidinone chiral auxiliaries.[83,88,91,92]

These supported oxazolidinones have been applied in stereoselective alkylations,[83,88,92] aldol condensations,[82,93] Diels-Alder reactions,[94] and 1,3 dipolar cycloadditions.[89,91,95] The results presented are promising but they have failed to reproduce the versatility, high stereoselectivity or general applicability of the analogous solution phase oxazolidinone chiral auxiliaries. The drawbacks associated with these supported auxiliaries stem from three specific issues intrinsic to the polymer support.

1) Interference or interaction with the polymer support

Several examples have been reported where the diastereoselectivity of the asymmetric transformation changes depending on the particular polymer employed. Burgess *et al.* have carried out a series of asymmetric alkylation reactions using an oxazolidinone bound to Merrifield resin, Wang resin and Tentagel (Scheme 1.3.3.5).[88] Treating *N*-propionyloxazolidinone **79** with LDA and benzyl bromide produced the alkylated product **80**, which could then be released from the polymer using reductive

cleavage to yield alcohol **81**. While the *R* geometry of alcohol **81** was the predominant product in all cases, the enantioselectivity varied from ~50% using Merrifield resin to 90% with Wang resin. In addition the reaction displayed a variation in selectivity when different electrophiles were applied. Wang resin provided acceptable results in reactions with benzyl bromide; however, using allyl bromide or benzyl chloromethyl ether produced the corresponding primary alcohols with lower enantiomeric excesses (81% and 71% respectively).[88]

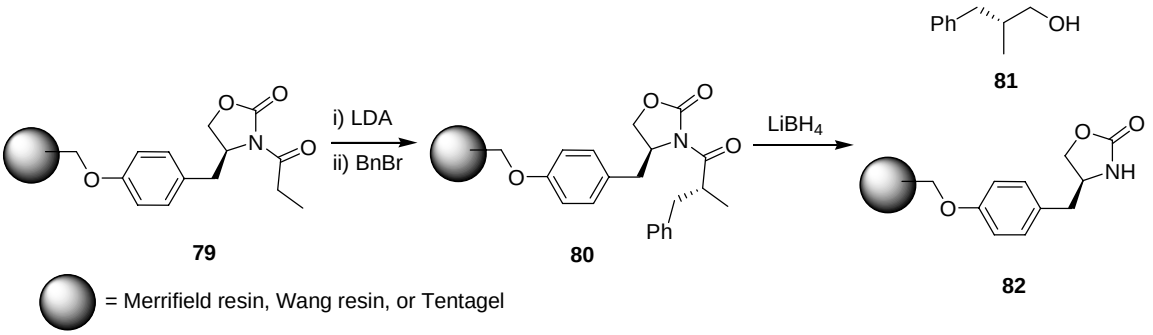

Scheme 1.3.3.5: Asymmetric alkylation using polymer supported oxazolidinones.

This wide variation in stereoselectivity clearly indicates that the polymer has an impact on these asymmetric transformations and possibly interferes with the formation of a well defined transition structure critical to obtaining a single isomer of the product. From these results, Burgess concluded that reaction at the oxazolidinone centre is very sensitive to the heterogeneous reaction environment. This is a fundamental disadvantage associated with the reactions on insoluble polymer supports.

In an attempt to address this issue, soluble polymer supports have been explored. These materials serve as an intermediate between solid-phase and solution-phase chemistry, allowing tagged materials to dissolve in organic solvents. Because these polymers can be precipitated and filtered, they are still able to assist purification.[96-98]

Soluble polymers afford more normal reaction kinetics and selectivities due to the homogeneous reaction conditions.[97,99] These characteristics have made soluble supports very attractive for applications with chiral auxiliaries.[73] Desimoni *et al.*[91] have explored this application by synthesizing *N*-crotonyloxazolidinone **83** bound to non-crosslinked polystyrene (Scheme 1.3.3.6). This material was soluble in dichloromethane and was subjected to a 1,3-dipolar cycloaddition reaction using diphenylnitrone to produce **84.** These cycloadducts were then treated with sodium borohydride to give isoxazolidines **85** and **86**. However, the dipolar cycloaddition still did not replicate the solution phase behavior of the analogous unsupported compounds. Isoxazolidines **85** and **86** were isolated with enantiomeric excesses of 90% and 27%, respectively, using a soluble polymer.[91] In contrast, performing the identical reaction with the unsupported oxazolidinone auxiliary gave **85** and **86** with 93% and >99% ee, respectively.[100] These results clearly demonstrate that reaction at the oxazolidinone centre is very sensitive to its environment. While the soluble polymer allowed the bound material to remain in solution the characteristics of the reaction are still altered when the material is supported on the polymer.

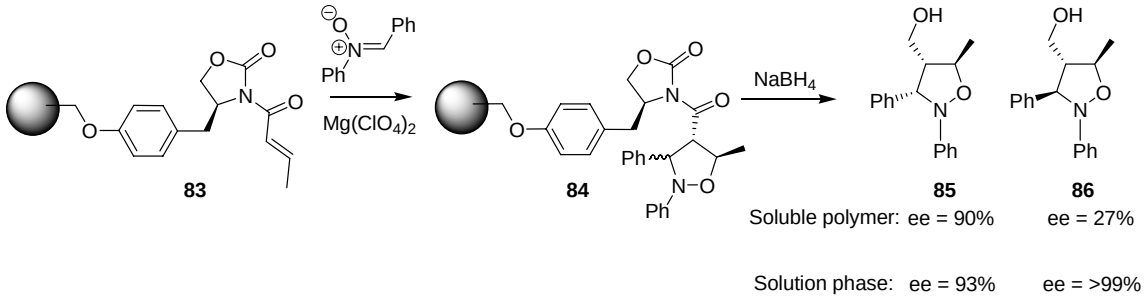

Scheme 1.3.3.6: Dipolar cycloaddition using a non-crosslinked polystyrene support.[91]

2) Difficulty characterizing polymer bound materials.

Identifying and characterizing compounds while they are bound to the polymer support is not always trivial. This difficulty has been illustrated by a series of studies examining the alkylation of a supported oxazolidinone derived from serine (Scheme 1.3.3.7). Allin and Shuttleworth prepared oxazolidinone **87** from L-serine and coupled it to Merrifield resin using potassium hydride. Under these conditions they proposed that the oxazolidinone formed the *O*-linked structure **88**, in which the oxazolidinone is bound to polystyrene via the 4 position. After removal of the Boc group propionyl derivative **89** could be formed and alkylated using LDA and benzyl bromide. Derivative **90** was then hydrolyzed using lithium hydroxide to give the free acid **91** and the bound auxiliary **92**. Using this protocol Allin and Shuttleworth reported obtaining **91** as the *S* enantiomer with a 96% ee.[83]

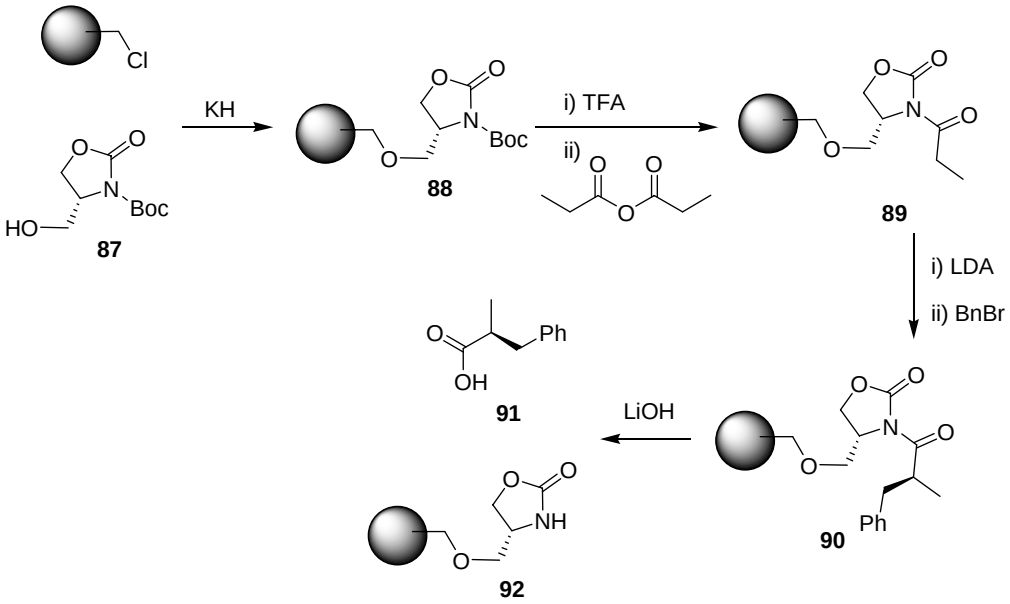

Scheme 1.3.3.7: Asymmetric alkylation using a supported oxazolidinone derived from L-serine.[83]

Davies and co-workers had been working with similar systems and felt these results were peculiar.[101] Using a model system, they had observed that the parent *N*-carbamoyl oxazolidinone **87** could undergo a rearrangement under basic conditions to give the *O*-Boc intermediate **94** via intramolecular attack by the alkoxide at the Boc carbonyl (Scheme 1.3.3.8). This gives rise to **93** and **94**, which can both act as a nucleophile with the Merrifield resin to produce the *O*- and *N*-linked species, **88** and **95** respectively.

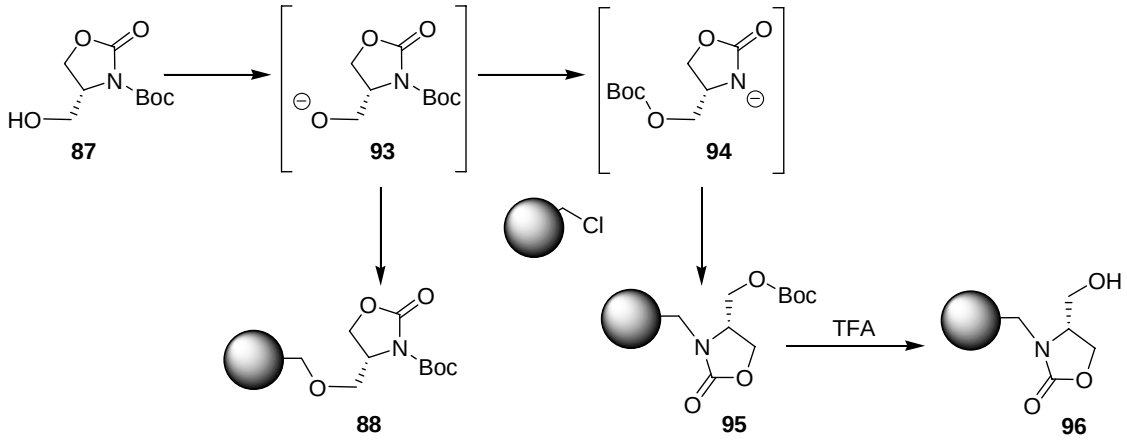

Scheme 1.3.3.8: Rearrangement to give *O*- and *N*-linked oxazolidinones.[102]

Recently, Allin and Shuttleworth have reexamined their results and confirmed that the *N*-linked derivative **95** and not the *O*-linked compound was formed preferentially, and thus auxiliary **96** was the reactive centre for the subsequent alkylation.[103] This presents a serious problem as illustrated in Scheme 1.3.3.9. Acylation produces ester **97**, which then undergoes enolization and addition to give **98**. This derivative is then hydrolyzed to give acid **92** and the bound auxiliary as alkoxide **99**, which can then undergo epimerization via intramolecular attack at the oxazolidinone carbonyl to form bicyclic intermediate **100** and giving rise to a mixture of **99** and **101**. Therefore, the high

selectivity observed from the initial application of bound auxiliary **96** would not be reproduced with subsequent reuse of the supported material.

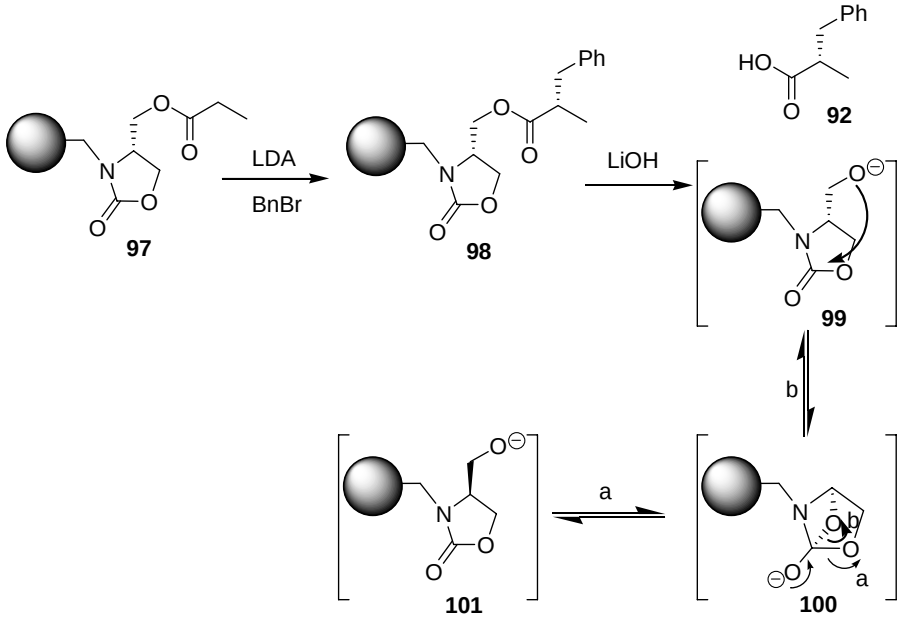

Scheme 1.3.3.9: Epimerization of the *N*-linked oxazolidinone.

This study has conclusively shown that the serine derived oxazolidinone is unsuitable as a supported auxiliary; however, its shortcomings were masked by the high selectively initially observed and the inability to characterize the material while it was bound to the polymer. In all it has taken the collective work of two research groups over the course of eight years to prove that the structure of the bound chiral compound is not as expected. [83,101-103] This failure could have easily been prevented if the material could be fully characterized, clearly demonstrating one of the major drawbacks of the polymer supported technique.

3) Poor recyclability of polymer-bound materials.

An additional difficulty encountered with polymer supported oxazolidinones is the inability to effectively recycle the supported materials. While this feature is often cited as a potential benefit to applying supported asymmetric systems, only two studies investigating the recovery and reuse of supported oxazolidinone chiral auxiliaries have been reported.[92,95] There are two major problems associated with recovering and efficiently reusing the polymer-supported oxazolidinones; difficulty removing trace impurities from the polymer and loss or modification of the supported auxiliary.

In some cases, polymer supports can be difficult to purify and often retain traces of Lewis acids, inorganic salts or solvents in the pores of the macromolecule. While this may not pose a problem for certain synthetic transformations, many asymmetric reactions can be very sensitive to even low levels of such impurities. This can lead to variations in the reaction conditions and consequently differing stereoselectivity as the supported material is reused. Faita *et al.* observed this trend when supported auxiliary **102** was used in stereoselective 1,3-dipolar cycloadditions (Scheme 1.3.3.10). The oxazolidinone could be easily acylated using crotonic anhydride and then reacted with diphenylnitrone to give **104**. The isoxazolidines **105** and **106** could be released from the support to regenerate the free auxiliary **102**. This process was repeated and the enantiomeric excesses of **105** and **106** were recorded. Over three cycles the stereoselectivity dropped sharply due to the presence of trace solvent and water, which participated in the cycloaddition and prevented the formation of a cyclic transition state necessary to obtain the product as a single enantiomer.[95]

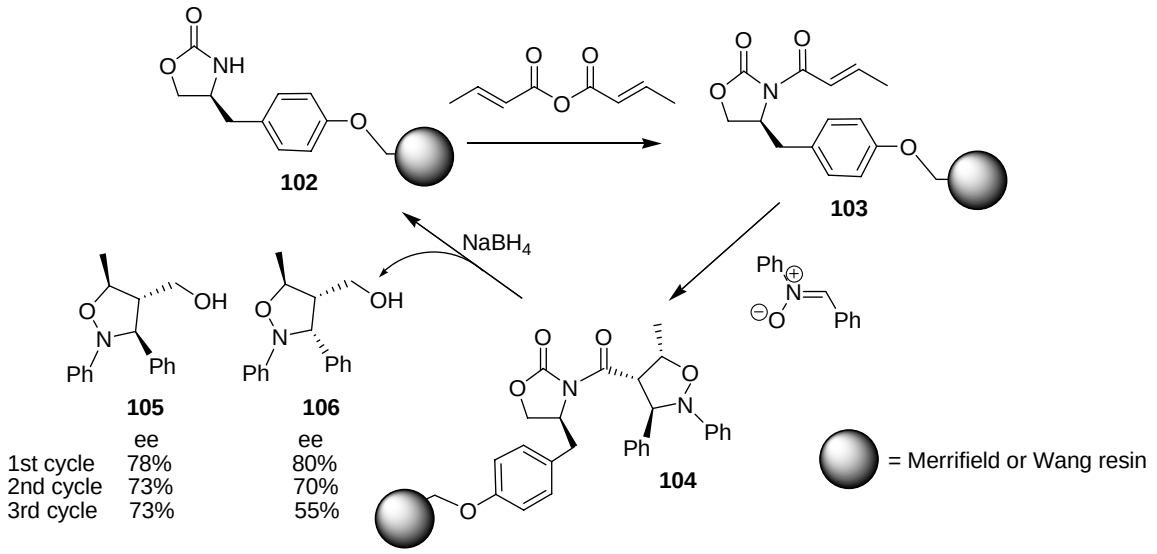

Scheme 1.3.3.10: Recycling study using supported oxazolidinones in 1,3 dipolar cycloadditions.[95]

An additional problem arises from modification or degradation of the chiral species bound to the polymeric support. This detrimental side-reaction can only be rectified by cleavage and refunctionalization. One example of this particular problem was observed by Kotake *et al.*, who demonstrated that supported oxazolidinone **106** could be acylated and then used in a stereoselective alkylation to produce **109** (Scheme 1.3.3.11).[92] Following alkylation, acid **110** could be released via hydrolysis to regenerate the supported auxiliary. This process could be repeated with no degradation in the stereoselectivity allowing acid **110** to be isolated with a 96% ee each time. However, the yield systematically decreased on each cycle due to the formation of the alkylated byproduct **111**. Although this material did not impact the stereoselectivity, the only way to recover the lost active sites was to cleave the auxiliary from the polymer and refunctionalize the support.

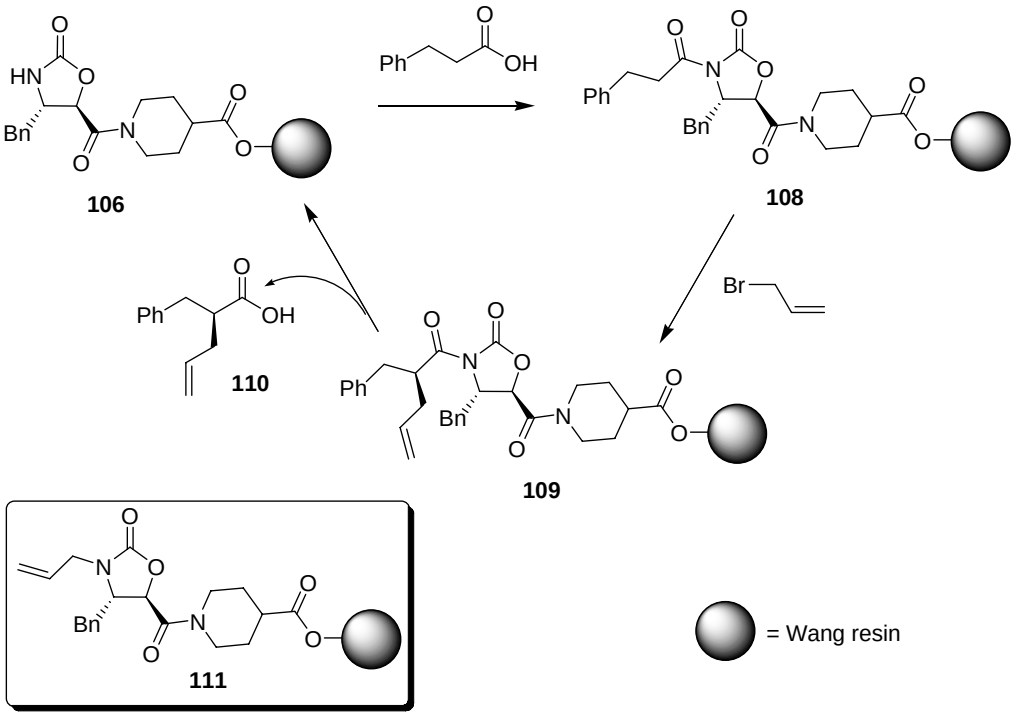

Scheme 1.3.3.11: Recycling study using asymmetric alkylation of a supported oxazolidinone chiral auxiliary.[92]

In summary, polymer-supported chiral auxiliaries can be successful in particular asymmetric transformations, yet in many cases the polymeric support interferes with the reaction resulting in poor stereoselectivity. At this time, no single polymer-supported chiral auxiliary has been able to match the broad applicability and versatility of the analogous unsupported compounds. Thus, there is a clear need for a more efficient and robust method of supporting these compounds to better mimic the solution phase performance of unsupported chiral auxiliaries.

1.4 Fluorous Organic Synthesis

1.4.1 Introduction

Fluorous synthetic methods have recently emerged as a powerful alternative to polymer supported techniques. The term *fluorous* was originally coined by Horváth and Rábai,[104] but has only recently begun to take on a solid definition. In 2002 Gladysz and Curran proposed that the adjective *fluorous* could be defined as "of, relating to, or having the characteristic of highly fluorinated saturated organic materials, molecules or molecular fragments."[105] This can be interpreted to mean sharing physical properties unique to poly-fluorinated sp^3-hybridized organic materials, including volatility, solubility, and an affinity to other fluorous molecules. It is this final property that allows fluorous compounds to be rapidly and efficiently separated from all other organic and inorganic materials, and allows these molecules to be used as supports for organic synthesis.

Fluorous and solid phase methods are similar in concept but different inpractice.[106] This is illustrated in the "tagging" technique similar to both fluorous and solid phase methods (Figure 1.4.1.1). In both techniques, a target compound is temporarily attached to a carrier molecule, allowing it to be rapidly isolated by exploiting the physical properties unique to the support or tag. When a polymer-support is employed (Figure 1.4.1.1,A), the insolubility or immiscibility allows the tagged compound to be isolated using filtration. Using fluorous methods (Figure 1.4.1.1,B), the reactant is typically attached to a molecule containing short perfluoroalkyl functional groups with the general formula $(CH_2)_m(CF_2)_nCF_3$. These perfluoroalkyl groups are termed fluorous tags or fluorous "ponytails"[107] and serve to label the target molecule

allowing it to be separated by taking advantage of the selective affinity fluorocarbon materials display for fluorocarbon phases.[104,108]

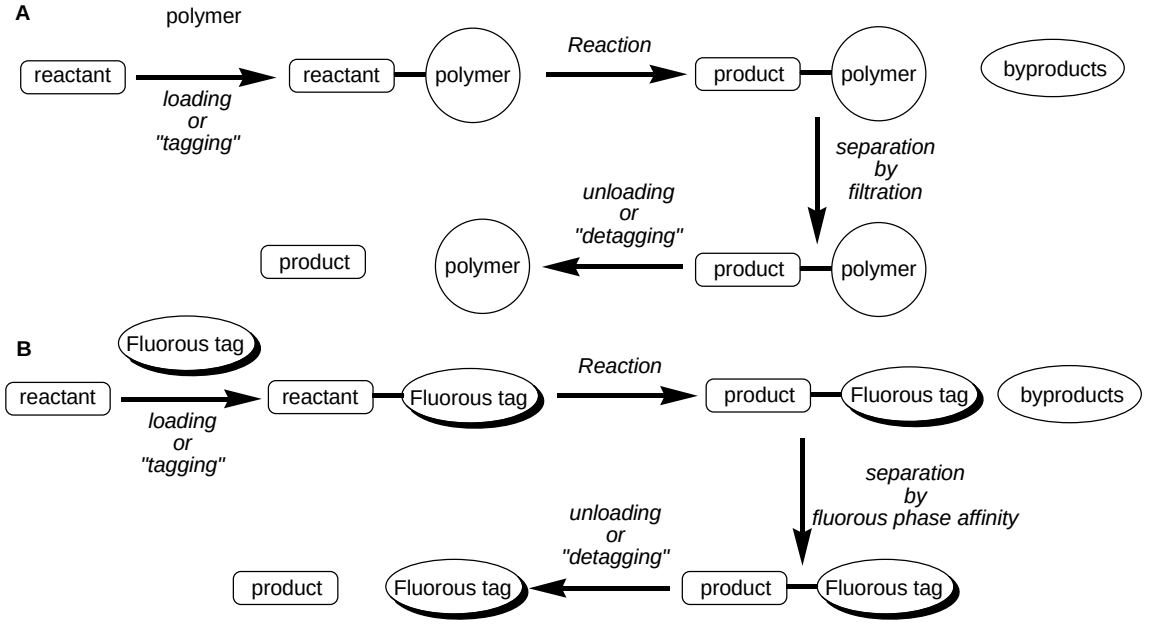

Figure 1.4.1.1: Schematic of polymer-supported and fluorous-supported methods.

While similar in concept to solid phase chemistry, fluorous techniques offer distinct advantages over both solid phase and traditional solution phase approaches. Typically fluorous tags are inert to many chemical reactions making them more robust than some polymeric materials. Also, many fluorous-tagged compounds are soluble in typical organic solvents, allowing the transformations to be carried out in a homogeneous environment. This often results in faster reactions than the corresponding polymer-bound heterogeneous protocols. Reactions using fluorous compounds are amenable to monitoring using conventional analytical methods such as TLC, HPLC, IR and NMR. Following completion of the reaction the products can be purified by fluorous separations as well as by regular and reverse-phase chromatography. In essence, fluorous supported synthesis combines the positive elements of small molecule organic synthesis with the

facile product isolation afforded by solid phase techniques. This duality has made fluorous techniques ideally suited for application in combinatorial and automated protocols.[109]

While fluorous supported chemistry is still relatively new, the potential of this field was recognized early on, leading to a rapid growth of fundamental knowledge and applications. The exuberance of these researchers combined with a multitude of uses for such a technology has allowed the field to expand quickly. The level of development is evident from the extent of literature available, including a number of review articles,[106,109-115] user guides,[116,117] and most recently a handbook published to summarize the most recent developments in the field.[108]

1.4.2 History and Development of Fluorous Supported Synthesis

The fluorous phase strategy makes use of the restricted solubility and miscibility of partially or fully fluorinated compounds with nonfluorinated compounds.[108] This limited miscibility is due to differences in the intermolecular forces between the fluorinated and nonfluorinated species.[104,118] As a result fluorocarbon compounds preferentially dissolve in perfluorocarbon solvents or associate with other fluorocarbon materials. This selective affinity displayed by fluorous compounds is illustrated by examining the equilibrium distribution of a fluorocarbon solute between immiscible fluorocarbon and organic liquid phases. This value is referred to as the fluorous/organic liquid/liquid partition coefficient[119] and is typically measured using commonly available fluorous solvents, such as FC-72 (perfluorohexanes) or perfluoromethylcyclohexane.[118]

Data from selected examples has been presented in Table 1.4.2.1 to illustrate the difference in phase affinity displayed for hydrocarbon and fluorocarbon materials.

Table 1.4.2.1: Selected examples of fluorous/hydrocarbon liquid/liquid partitioning.[119]

			partitioning ratio	
entry	**solute**	**solvent system**	**Fluorous**	**organic**
1	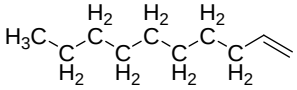	$CF_3C_6F_{11}$:$CH_3C_6H_5$	4.8	95.2
2	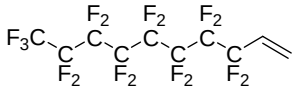	$CF_3C_6F_{11}$:$CH_3C_6H_5$	93.5	6.5
3	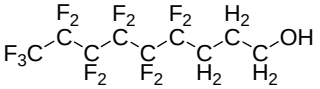	$CF_3C_6F_{11}$:$CH_3C_6H_5$	44.0	56.0
4	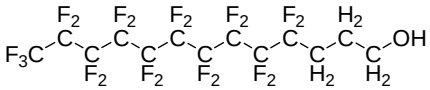	$CF_3C_6F_{11}$:$CH_3C_6H_5$	80.5	19.5
5	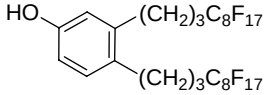	$CF_3C_6F_{11}$:$CH_3C_6H_5$	69.5	30.5
6	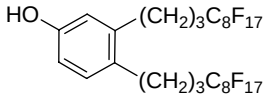	$CF_3C_6F_{11}$:CH_3OH	97.0	3.0

The solubility of a molecule in the fluorous phase is largely controlled by the solute's polarity and molecular size.[116] This is illustrated in the equal but opposite phase affinity seen between 1-decene and 1*H*,1*H*,2*H*-heptadecafluoro-1-decene (Table 1.4.2.1, entry 1 cf. 2). In general, perfluorinated species display very low intermolecular forces due to the high ionization energy of fluorine and its low polarizability, similar to the fluorocarbon solvent.[120] Thus dissolution in the fluorous solvent is rationalized by a "like dissolves like" phenomenon.[121] Due to these properties it follows that the affinity for the fluorocarbon phase is strongly affected by the fluorine content. 1*H*,1*H*,2*H*,2*H*,3*H*,3*H*-Tridecafluoro-1-nonanol is more polar than the perfluoroalkene, allowing it to show

equal hydrocarbon and fluorocarbon affinity (Table 1.4.2.1, entry 2 cf. 3). However, alcohols with longer fluorocarbon chains, such as 1*H*,1*H*,2*H*,2*H*,3*H*,3*H*-heneicosafluoro-1-tridecanol, have a strong preference for the fluorous phase (Table 1.4.2.1, entry 4). The phase affinity also depends strongly on the fluorous and organic solvents employed. Typically, fluorinated solutes show a higher preference for the fluorocarbon phase when the difference in polarity between the two liquids is greater. This is illustrated with 3,4-(perfluorooctyl)phenol, where the affinity for the fluorous phase increases when methanol is used in place of toluene (Table 1.4.2.1, entry 5 cf. 6).

Employing saturated fluorocarbon functional groups as supports for synthesis began in 1991 with Horváth and Rábai's study of fluorous biphasic catalysis (FBC), and was introduced to the general research community with their seminal paper in 1994.[104] This technique employs two immiscible liquid phases (organic and fluorous) that display a temperature-dependant miscibility, allowing the formation of a homogeneous reaction environment at high temperature (Scheme 1.4.2.1). In their initial report Horváth and Rábai carried out a series of hydroformylation reactions using several terminal alkenes **112** and a fluorous rhodium catalyst **113**. Partitioning studies revealed that **113** did not cross the fluorous-organic interface, and thus the fluorous ponytail sequesters the catalyst in the fluorous phase.[115]

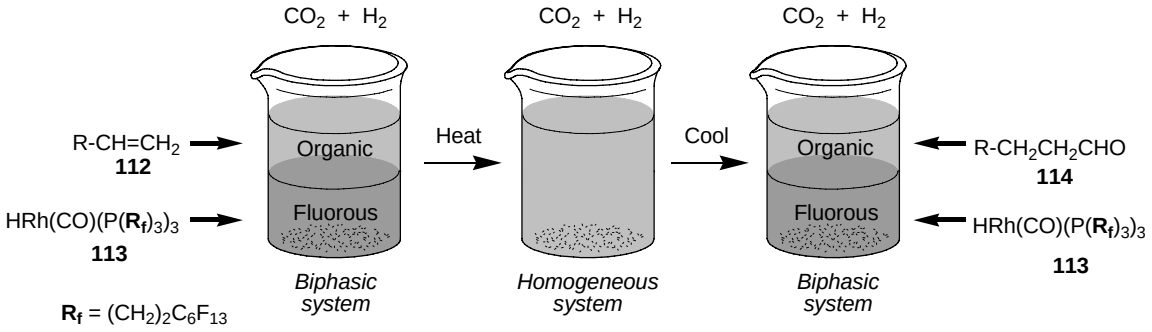

Scheme 1.4.2.1: Hydroformylation using fluorous biphasic catalysis.

Therefore, reaction was only observed when the two-phase system was heated to form a single phase. On cooling, the phases separate allowing the fluorous catalyst to be recovered from the fluorous solvent and the target aldehydes **114** are obtained from the organic phase. Simple liquid/liquid extraction allows the products and catalyst to be easily separated. In addition, the rhodium catalyst could be readily reused, making this process extremely efficient. The feature that sets this technique apart for other supported methods is that the system becomes homogenous on warming, as opposed to solid supported reagents, which can never achieve homogeneity.[114,115]

Following the success of fluorous biphasic catalysis, Curran *et al.*[122,123] introduced the concept of *fluorous synthesis* with perfluorinated compounds applied as supports for stoichiometric synthesis. In this technique the target molecule is temporarily rendered "fluorous" by attaching a protecting group containing several perfluoroalkyl ponytails. Tagging the molecule in this manner allows the compound to be selectively extracted due to its unique affinity for the fluorous phase. Following completion of the synthesis, the fluorous portion of the molecule can be removed. This process is represented schematically in Figure 1.4.1.1 B. One of the major differences between fluorous

synthesis and fluorous biphasic catalysis is in the role of fluorous solvents. Unlike biphasic catalysis, fluorous solvents are employed only at the separation stage in a fluorous synthetic protocol, not in the reaction.

Fluorous synthesis was first demonstrated in the preparation of small libraries of isoxazolines using a straightforward, three step protocol (Scheme 1.4.2.2).[122] Reacting fluorous silyl bromide **115** and allyl alcohol **116** produced the tagged alcohol **117**. After the reaction was completed, the products were purified using a three-phase extraction. Excess alcohol **116** remained in the organic phase, while any amine salts partitioned into the aqueous phase. Protected alcohol **117** was then recovered from the fluorous phase and applied in the dipolar cycloaddition using the Mukaiyama method. Again, three phase extraction was used to separate the excess reagent and byproducts from fluorous isoxazolines **119**. The fluorous tag could then be removed from **119** using a source of fluoride. Three phase extraction then gave the pure product isoxazolines **120** from the organic layer, while the recovered tag **121** was isolated from the fluorous phase with no chromatographic separation necessary.

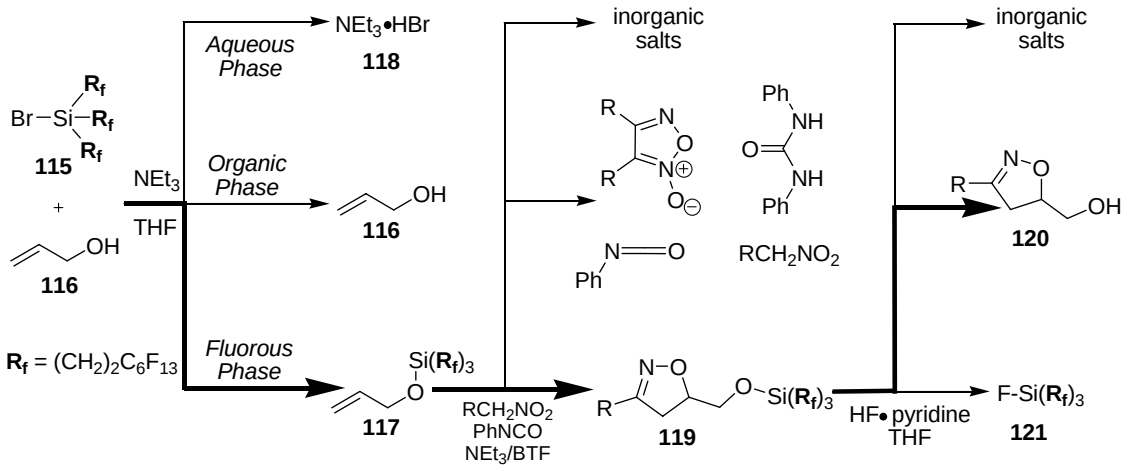

Scheme 1.4.2.2: Preparation of isoxazolidine libraries using fluorous synthesis.

This same selective protection, followed by triphasic or biphasic liquid/liquid extraction has been applied to Ugi condensations (Scheme 1.4.2.3,A),[123] Biginelli condensations (Scheme 1.4.2.3,B),[123] carbohydrate synthesis (Scheme 1.4.2.3,C),[124] and many other methods resulting in the synthesis of a number of small molecules and compound libraries.[106,109,114]

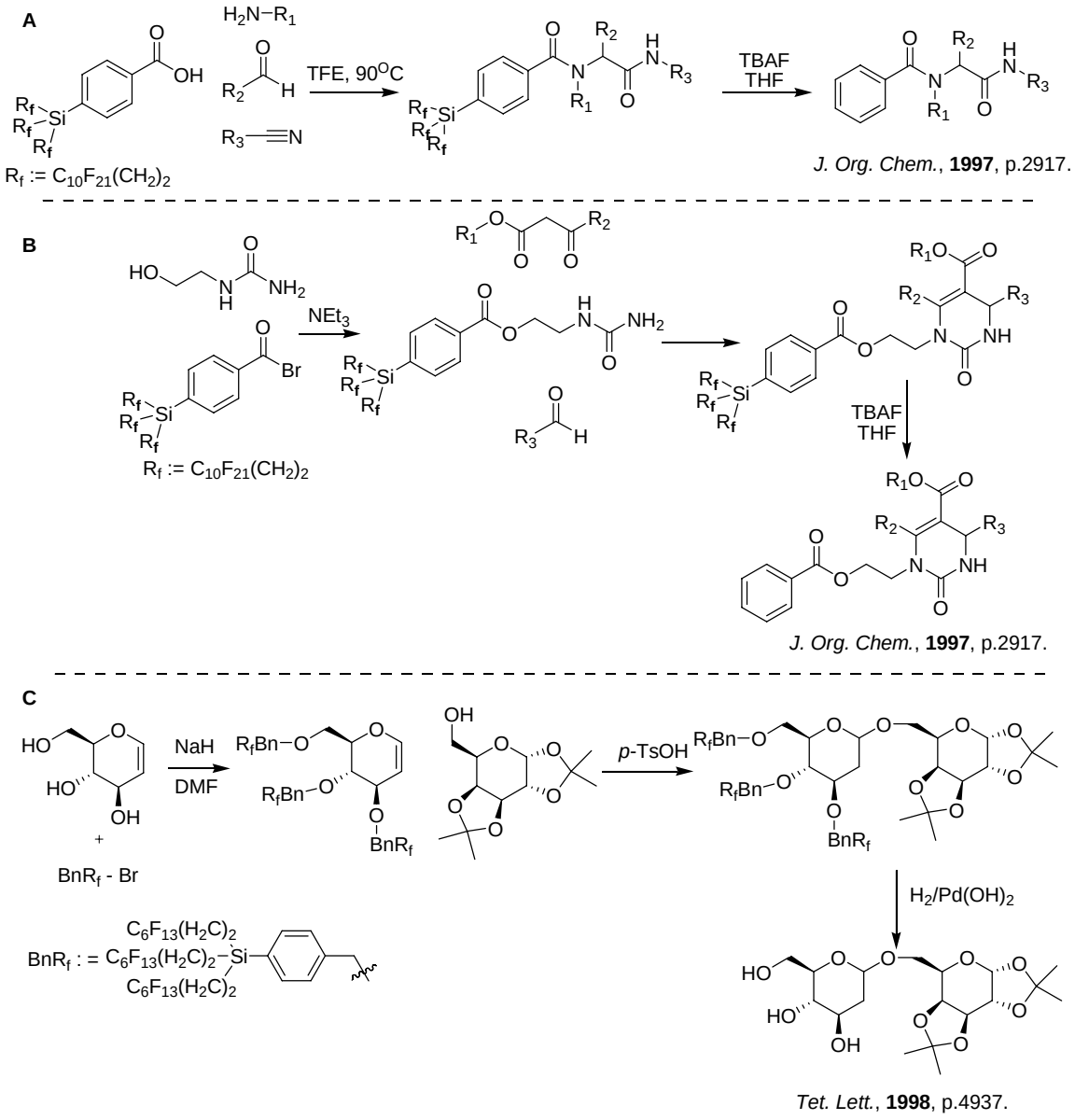

Scheme 1.4.2.3: Examples of fluorous synthetic protocols employing liquid/liquid separation.[122,124]

In each example the tagged fluorous materials were easily recovered using liquid/liquid extraction. However, the solubility of a compound in organic solvents is inversely related to its affinity for the fluorous liquid phase as represented in Figure 1.4.2.1. Thus a fine balance exists between optimal separation (purification) and solubility (reactivity) of the fluorous tagged materials.

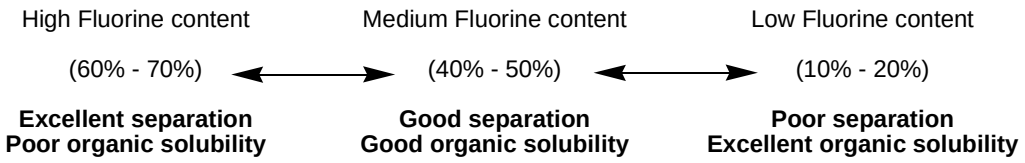

Figure 1.4.2.1: Balance between fluorous and organic solubility.

The dependence on selective partitioning into a fluorous liquid phase was the factor that demanded the creation of such highly fluorinated compounds.[125] In order for the tagged material to be selectively retained in the fluorous liquid phase, it had to display a very high partition coefficient, requiring approximately 60% fluorine by molecular weight. The dependence of the fluorous liquid/liquid partitioning coefficient on the fluorine content can be illustrated by examining a series of fluorous tin hydrides (Table 1.4.2.2).[126] The C_6F_{13} compound shows only a slight preference for the fluorous phase, despite having 50% fluorine by molecular weight (Table 1.4.2.2, entry 1). Increasing the fluorocarbon chain dramatically improved the affinity for the fluorocarbon phase, as illustrated with the C_8F_{17} and $C_{10}F_{21}$ compounds (Table 1.4.2.2, entry 2 and 3).

Table 1.4.2.2: Effect of fluorine content on liquid/liquid partitioning.[126]

entry	tin hydride	% fluorine	partition coefficient [a]
1	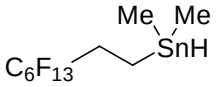	50%	2.4/1
2	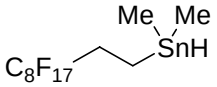	54%	14/1
3	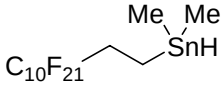	57%	48/1

[a] Ratio reflects distribution between FC-72 / CH_3CN.

This dependence on high fluorine content to obtain sufficient partitioning coefficients becomes particularly problematic with high molecular weight materials. Typically 60-120 fluorine atoms need to be incorporated into the molecule to permit adequate partition into the fluorous solvent, greatly reducing the tagged molecules' solubility in most organic solvents.[124] In other cases liquid/liquid extraction could be employed but repetitive extractions were necessary to adequately partition the fluorous materials.[123] As an alternative, Curran *et al.* introduced solid phase extraction (SPE) techniques using silica gel with a fluorocarbon bonded phase, termed fluorous silica gel, to replace liquid/liquid extraction.[112,127,128] The superiority of the solid/liquid extraction protocol was demonstrated in the radical allylation of several halides using fluorous allyl stannanes.[128,129] In one noteworthy example, bromide **122** was reacted with fluorous allyl stannane **123** to produce the ketone **124** (Scheme 1.4.2.4). Extracting the crude reaction mixture with FC-72 removed the fluorous tin byproduct **125** to yield the purified product **124**. This liquid/liquid extraction protocol was able to give ketone **124** free of tin

impurities in 67% yield but required a prolonged extraction procedure involving ten sequential washes with FC-72. In contrast, applying the reaction mixture to fluorous silica gel allowed the recovery of **124** free of tin byproducts in 92% yield.

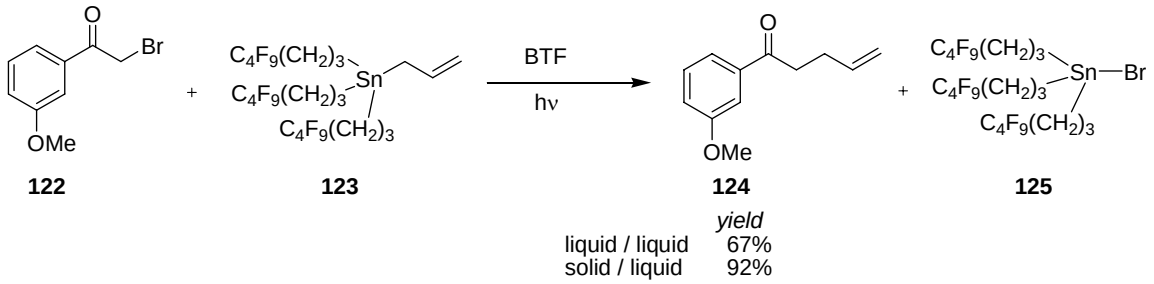

Scheme 1.4.2.4: Radical allylation using fluorous allyl stannane **123**.[129]

The greatly enhanced affinity that fluorous molecules exhibit for fluorous silica gel allows the facile separation of compounds bearing smaller perfluoroalkyl fragments. Reducing the number of fluorines in the fluorous tag greatly increases the organic solubility of tagged molecules, allowing reactions with these compounds to be carried out using standard solvents and conditions.[126,130] The reduction in fluorine content results in a simultaneous decrease in fluorous solvent solubility, while retaining the ability to be readily purified using solid/liquid extraction protocols.[127]

This switch in extraction protocols has given birth to the term "light" fluorous synthesis,[127,130] and thus the previous techniques depending on liquid/liquid extraction have been termed "heavy" fluorous synthesis.[117,127] While these two terms remain loosely defined, light fluorous compounds typically contain fewer than 21 fluorines, and can be easily purified using fluorous solid phase extraction (FSPE). In contrast, heavy fluorous species typically contain 39 fluorines or more, and show a high affinity for the fluorous liquid phase.[127]

1.4.3 Fluorous Solid Phase Extraction

Solid phase extraction (SPE) was originally designed as a means of cleaning or concentrating analytes prior to applying some other analytical technique.[131] However, it has found an increasing number of uses in synthetic protocols.[132,133] This is largely due to several advantages this technique has over classical liquid/liquid extraction or even preparative HPLC methods, including speed, low solvent usage, and high versatility. These features make solid phase extraction highly adaptable, and allow purifications using this technique to be readily automated. An in depth discussion on the fundamental principles and applications of solid phase extraction can be found in the recent monograph written by Thurman and Mills.[131]

In principle, solid phase extractions are similar to classical chromatographic methods, except that retention factors for the materials being separated by SPE are vastly different. In typical chromatographic separations, the two components display only moderately different affinities for the stationary phase, allowing each to be isolated by fractionation of the solvent as it is eluted (Figure 1.4.3.1, A). In solid phase extraction, the two components show sufficiently different affinities for the stationary phase that two different solvents are required to elute each material (Figure 1.4.3.1, B). Thus, solid phase extraction can be viewed as separation as a function of the solvent, while chromatography yields separation as a function of time. In a typical solid phase extraction protocol, the component mixture is added to the stationary phase and solvent A is applied to liberate the first component in a single fraction. The eluting solvent is then switched and a second fraction is collected, giving the second component.

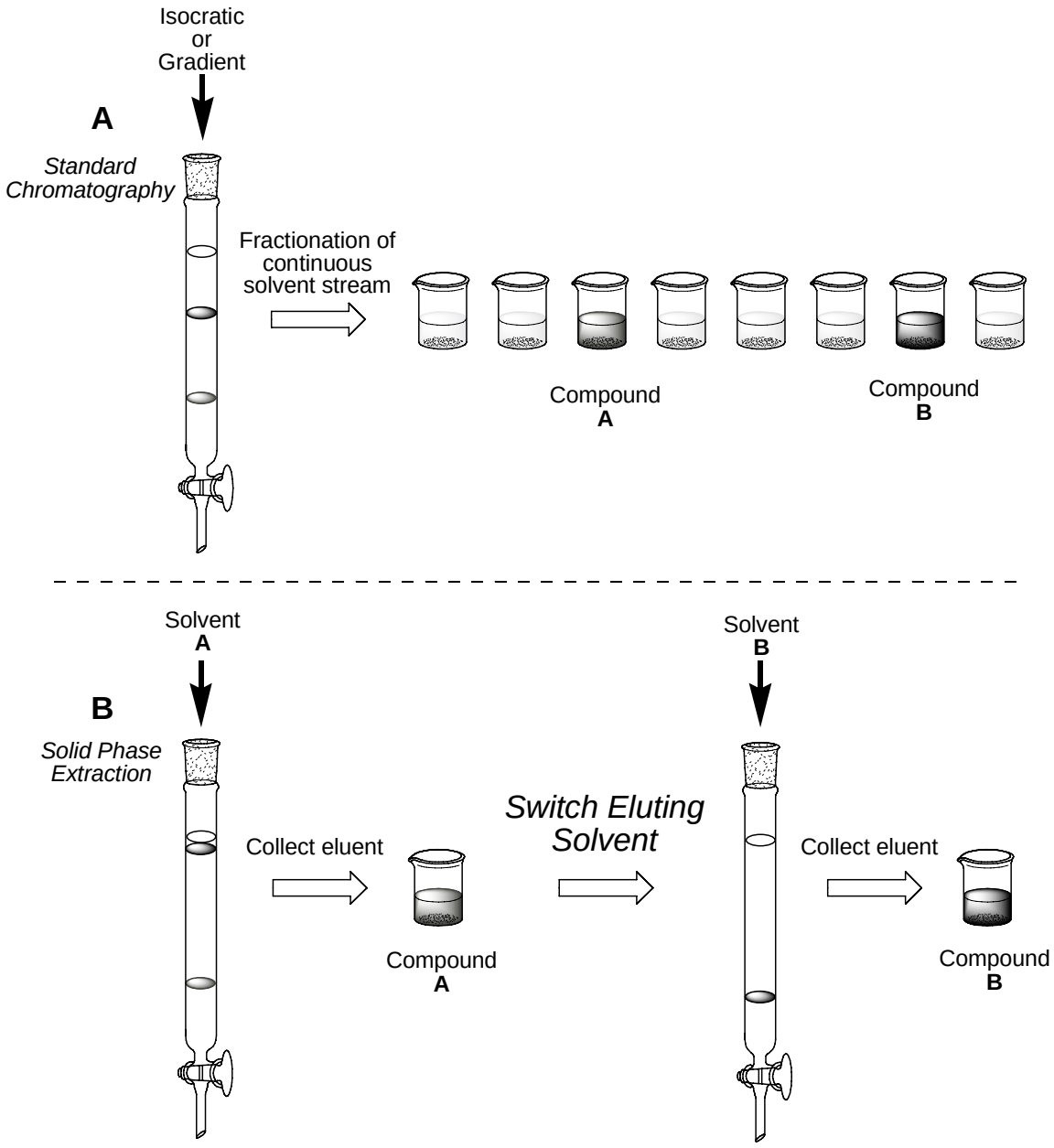

Figure 1.4.3.1: Comparison of chromatography and solid phase extraction.

Stationary phases for solid phase extraction are designed to have very high affinities for specific molecular properties.[131] Typical solid phase extraction stationary phases consist of silica gel covalently bonded to some functionalized organic moiety, such as hydrocarbon chains,[134] amines,[135] carboxylic or sulfonic acids,[131] or metal-chelating fragments.[136] In the case of fluorous solid phase extraction, the stationary

phase is modified by binding a C_nF_{2n+1} fragment (Scheme 1.4.3.1).[112] Typically, this bonded phase is generated by reacting the exposed hydroxyl groups with a perfluoroalkyl chlorosilane such as **126**.[137] Fluorous reverse phase silica gel was first developed as a non-polar sorbent for use in reverse phase liquid chromatography.[137-139] However, this material found only limited applications due to its extremely low retention of most organic molecules.[130]

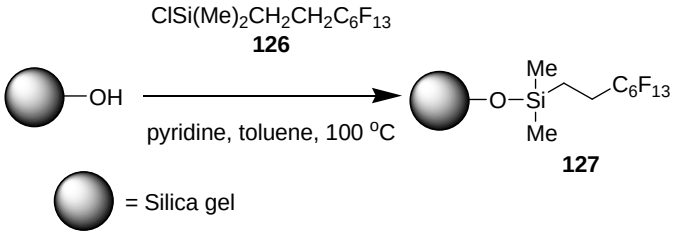

Scheme 1.4.3.1: Formation of fluorous reverse phase silica gel.

Fluorine-containing molecules exhibit selective retention on this bonded phase and this property has been illustrated in the separation of benzene and toluene from their fluorinated analogues, monofluorobenzene and α,α,α-trifluorotoluene. [140] On an *n*-decyl alkyl bonded phase (RP-10), the components display different retention times, allowing the materials to be separated by their polarity and geometry. In this environment toluene and α,α,α-trifluorotoluene can be separated, but monofluorobenzene and benzene are indistinguishable (Figure 1.4.3.2, A). When the same materials and conditions are applied to the fluorocarbon bonded phase (RPF-10) a sharp drop in the retention time was observed for both toluene and benzene (Figure 1.4.3.2, B). Monofluorobenzene and α,α,α-trifluorotoluene did not display the same reduction in retention times, allowing monofluorobenzene and benzene to be separated.

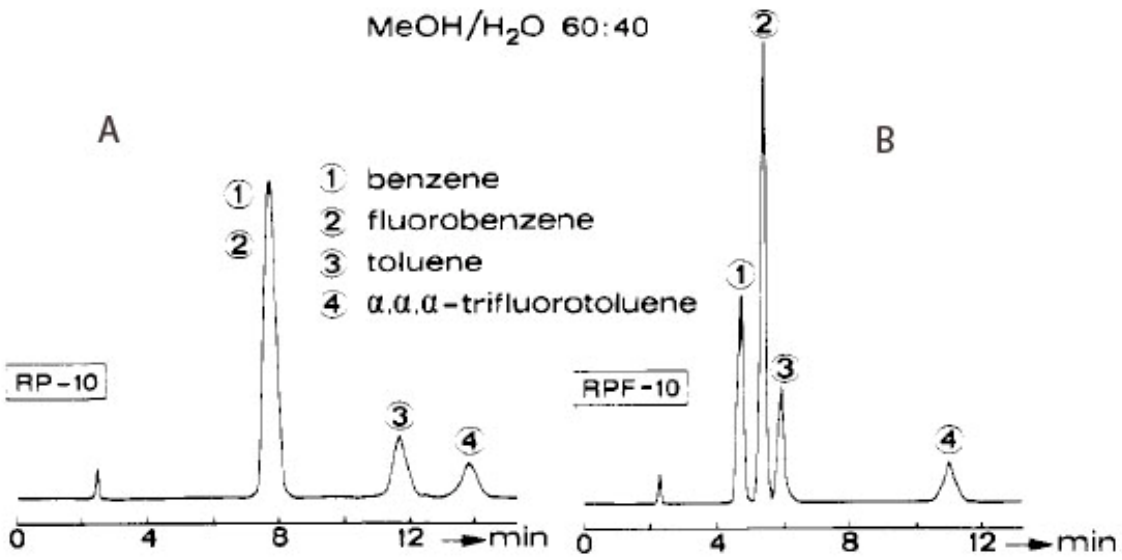

Figure 1.4.3.2: Comparison of retention times for fluorinated and non-fluorinated benzenes on alkyl (RP-10, A) and fluorocarbon (RPF-10, B) bonded phases.[137]

[Reprinted with permission *Anal. Chem.* **1980**, *52*, Copyright 1980 American Chemical Society]

Studies have indicated that while the fluorocarbon bonded phase can provide separation of components based on their polarity, its true potential lies in its ability to separate materials based on their fluorine content.[112] This property was illustrated in the separation of a series of amides with differing linear fluoroalkyl chains (Figure 1.4.3.3),[141] with retention times increasing as a function of the number of CF_2 groups in the perfluoroalkyl fragment. The separation is unique to fluorous bonded phase materials and cannot be reproduced on normal phase or standard reverse phase sorbents.[126] Due to this retention property, fluorous molecules can be viewed in terms of two separate domains; an organic domain which contains the reactive functionality, and a fluorous domain governing the selective isolation of the compound.[127]

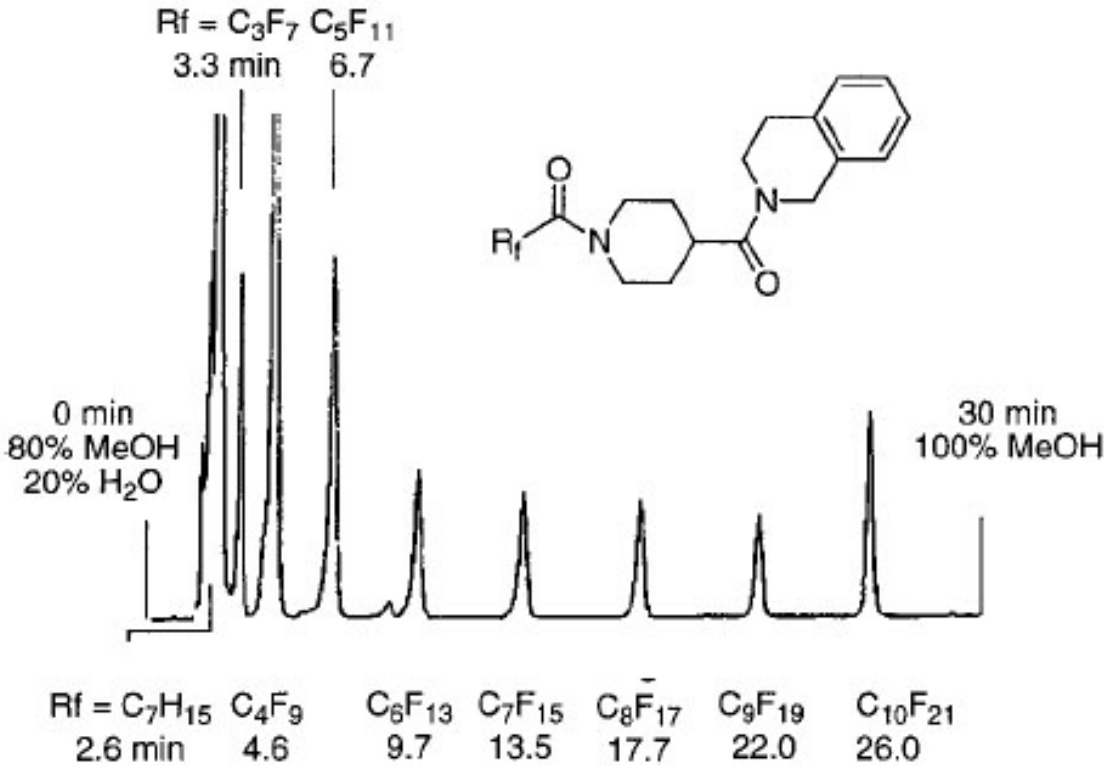

Figure 1.4.3.3: Separation of materials by fluorine content using fluorous silica gel[130]

[Reprinted with permission, *J. Org. Chem.* **2000**, *65*, 8866, Copyright 2000 American Chemical Society]

The selective retention of fluorine-containing compounds on perfluoroalkyl bonded phases is now well documented.[112,137,142-144] However, this phenomenon is not well explained by the models currently employed to rationalize the interactions seen with hydrocarbon bonded phases.[145] In general the mobility of a solute across a stationary phase bearing some covalently bound ligand can be pictured in terms of three key interactions: ligand-solvent, ligand-solute and solvent-solute.[146] The selective retention of fluorinated molecules on the fluoroalkyl bonded phase has been attributed to the presence of unique fluorine-fluorine interactions.[137,144] This suggests that a unique ligand-

solute interaction is present between fluorinated compounds and the fluorous solid phase, directly analogous to the affinity fluorous molecules display for perfluorinated liquids, with observations by Billiet *et al.*[142] supporting this hypothesis. In their work, the mobilities of fluorinated and non-fluorinated compounds on a fluoroalkyl stationary phase were monitored when methanol/water and 2,2,2-trifluoroethanol/water mixtures were employed as a mobile phase. Their results show that employing 2,2,2-trifluoroethanol in place of methanol led to a specific acceleration of fluorinated compounds relative to non-fluorinated ones.[142] This was interpreted as being due to specific fluorine-fluorine interactions between the highly fluorinated benzenes and the fluorinated mobile phase, leading to more rapid elution of pentafluoro- and hexafluorobenzene.

More recently Kamiusuki *et al.*[145] have proposed that the enhanced retention observed with fluorinated compounds on the perfluoroalkyl bonded phase is due to solvent-solute interactions. This conclusion is based on measurements of the contact angle made by a series of non-polar liquids applied to a silica surface modified with alkyl or fluoroalkyl silylating agents. In general the contact angle can be viewed as a measure of the ligand-solute interaction for a given bonded phase (Figure 1.4.3.4).[145]

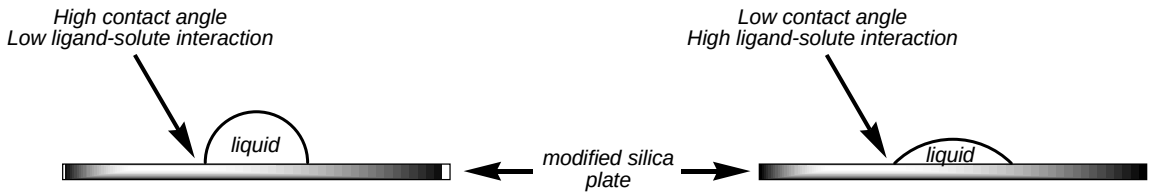

Figure 1.4.3.4: Schematic of liquid-surface contact angles.

The contact angles of benzene and fluorobenzene were shown to be inversely proportional to the retention factor for hydrocarbon bonded phases. This indicates that as contact angle decreases solute-ligand interactions increase leading to greater retention of the material on the hydrocarbon bonded phase. In contrast, the contact angles of both benzene and fluorobenzene were found to be independent of the retention factor with fluoroalkyl bonded phases, suggesting that the difference in retention cannot be due to ligand-solute interactions. Instead, the very high contact angles observed for all liquids applied to fluoroalkyl bonded phases suggest that ligand-solvent and ligand-solute interactions are minimal. Thus, separation of compounds on fluorous silica gel would be due to differences in solvent-solute interactions.

1.4.4 Light Fluorous Synthesis

Light fluorous synthesis has proved to be broadly applicable, and has greatly expanded the scope and versatility of fluorous techniques.[109,112,130] This development was largely made possible due to fluorous solid phase extraction, which allows facile purification of compounds bearing small perfluoroalkyl tags. One of the first applications of light fluorous synthesis was by Curran *et al.*[147] in the development and application of a fluorous amine protection group, now dubbed the fluorous Boc or ^{F}Boc group (Scheme 1.4.4.1). The fluorous Boc reagent **128** was mixed with amino acid **129** and triethylamine producing the *N*-carbamoyl derivative. The crude products from the *N* protection were purified by fluorous solid phase extraction to give the ^{F}Boc-protected amino acid **130.** Coupling of this species with amine **131** and purification of the crude products by FSPE gave amide **132.** Deprotection was accomplished by treating **132** with

HCl in MeOH and purifying the products using fluorous/organic biphasic extraction. Amide **133** was easily recovered from the organic phase, while alcohol **134** was isolated from the fluorous phase. The efficient recovery of alcohol **134** permitted the regeneration of the ^{F}Boc reagent **128**.[147]

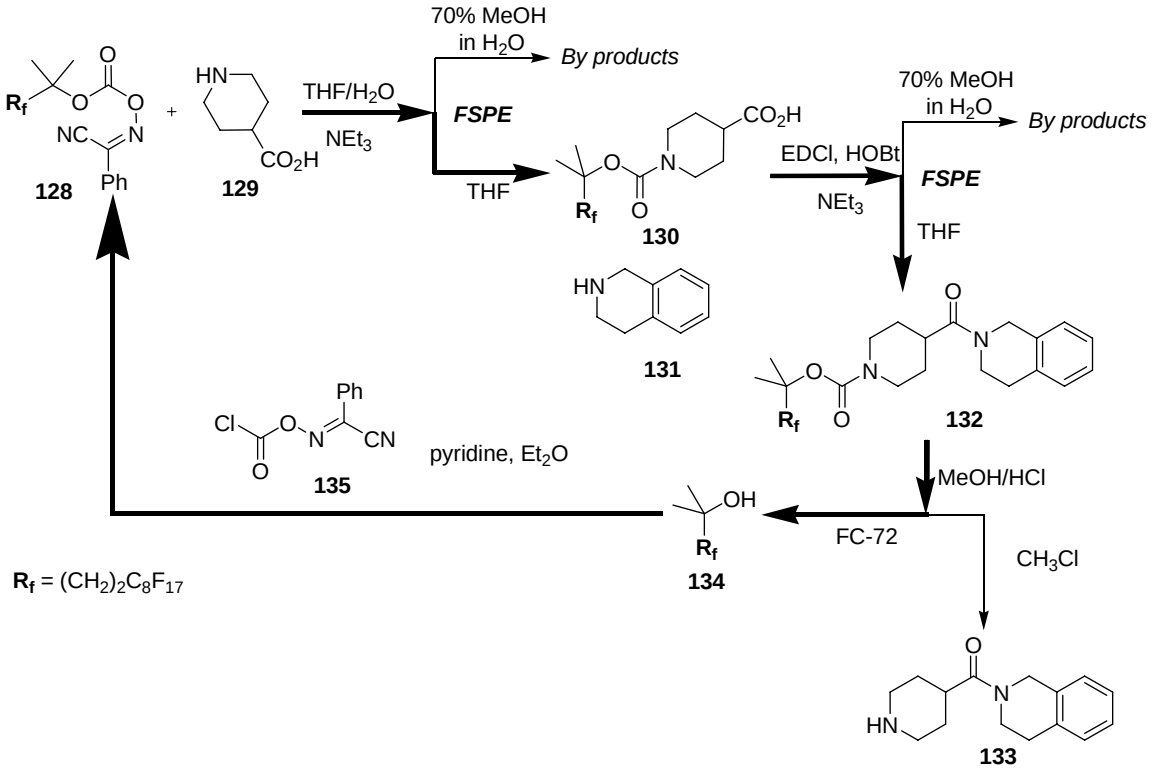

Scheme 1.4.4.1: Synthesis of amides using the ^{F}Boc protection group.

Rapid purification using FSPE made the amide formation very efficient and greatly reduced the workload required. To demonstrate the potential of this approach Curran *et al.*[147] have used the same general approach with a series of amino acids and amines to generate a library of amides (Scheme 1.4.4.2). Amino acids **129**, **136**, **137**, and **138** were sequentially protected with the fluorous Boc reagent **128** to give the four corresponding protected amino acids. These were coupled with amides **131**, **139**, **140**, and **141** to give sixteen unique amides. Removing the fluorous Boc group from these

compounds gave the free amides and fluorous alcohol **134**. Both the protection of the parent amino acids and the coupling to give the amides could be rapidly purified by FSPE. In all cases the fluorous materials were isolated from the fluorous solid phase, allowing immediate use in further chemistry.

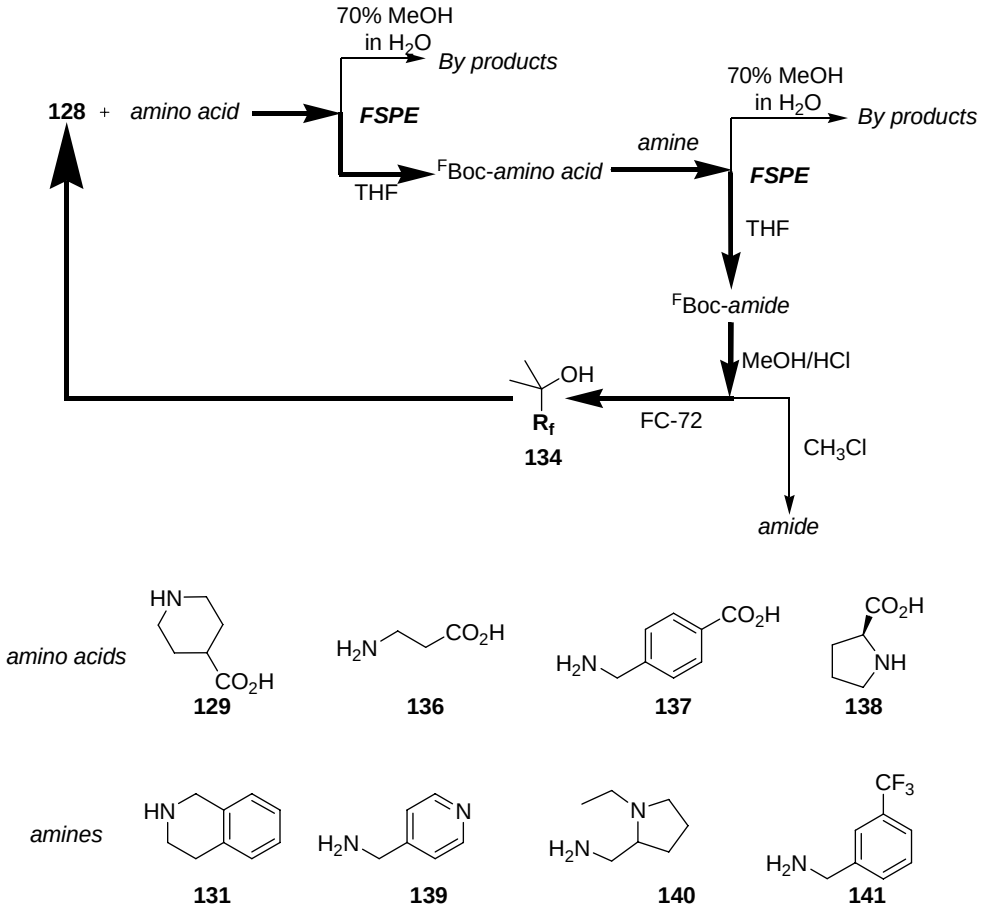

Scheme 1.4.4.2: Generation of a library of amides using the ^{F}Boc protection group.

This study served to demonstrate the utility of the light fluorous synthetic technique and its applicability to parallel and combinatorial synthesis. In addition, the application of this technique to peptide synthesis draws a parallel between these new developments and Merrifield's initial work, highlighting the similarity between fluorous synthetic methods and solid phase protocols.

1.5 Applications of Oxazolidinone Chiral Auxiliaries

1.5.1 Asymmetric Aldol Reactions

One of the first applications of oxazolidinones as chiral auxiliaries was in a series of asymmetric aldol reactions reported by Evans *et al.*[37,148-150] In general, the aldol addition between a ketone and some aldehyde gives rise to four possible isomers, usually classified by the relative configuration of the two new stereocentres and designated the *erythro* (E1and E2) and *threo* (T1 and T2) geometries (Scheme 1.5.1.1). Evans illustrated that several parameters are responsible for the control of stereoselectivity in this general reaction. In the end, these parameters may be manipulated to control both reaction diastereoselection (El and E2 *vs.* T1 and T2) and enantioselection (E1 *vs*. E2 or T1 *vs*.T2) for a range of substrates.

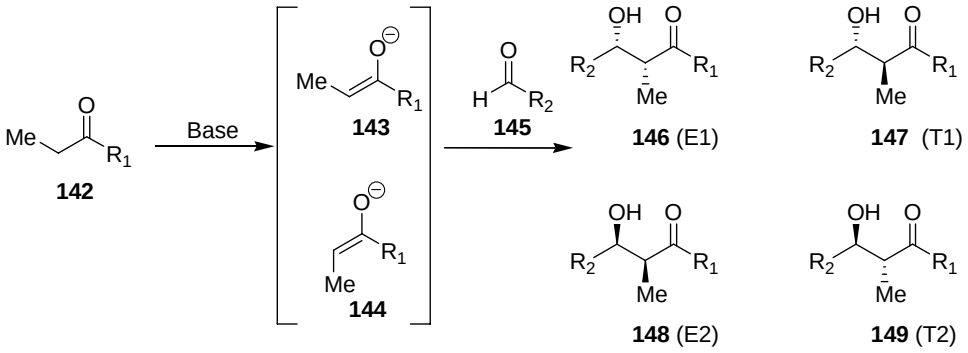

Scheme 1.5.1.1: Formation of *erythro* and *threo* isomers via the aldol reaction.

Fundamentally, there are two processes that must occur with high selectivity if a single isomer is to be formed via the aldol reaction. The first involves the selective formation of the *Z* or *E* enolate, **143** or **144** respectively, from ketone **142** using an appropriate base alone or in combination with some appropriate Lewis acid.[37,150] The

second step involves stereofacial control during the addition of aldehyde **145** to either enolate **143** or **144**.

The ratio of *Z* and *E* enolates can be controlled by varying the reaction conditions employed during their generation. These enolates are typically formed with either lithium amide bases (such as LDA or LiHMDS), or with tertiary amine bases in conjunction with some Lewis acid (such as dibutylboronyl triflate or titanium (IV) tetrachloride).[37,148] Regardless of the precise method employed, enolate generation occurs by first forming a Lewis acid-base complex which exists as two rotamers, **150** and **151** (Scheme 1.5.1.2, X = Li, Ti, or B).

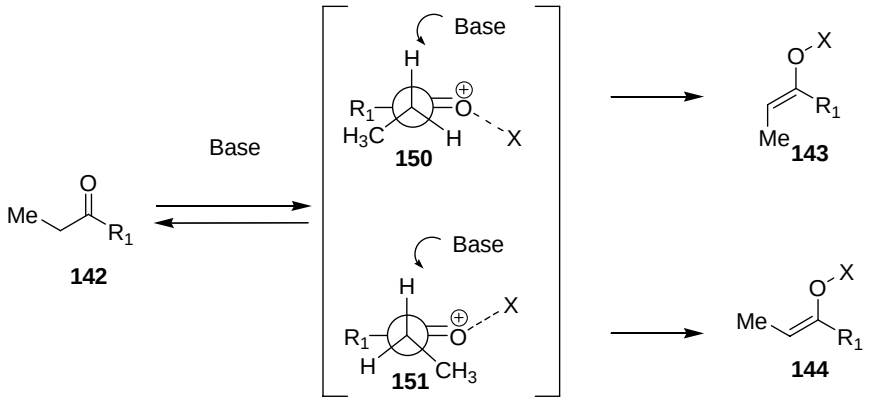

Scheme 1.5.1.2: Mechanism for the formation of the *Z* and *E* enolate of **142**.

Deprotonation of **150** or **151** gives the corresponding enolate **143** or **144** respectively. Thus the population of the two rotamers ultimately governs the ratio of enolates **143** and **144** provided that the deprotonation is irreversible. Studies have shown that performing this reaction using bulky and powerful amide bases, such as LDA, at low temperatures gives *Z* enolate **144** selectively, attributed to fast, irreversible deprotonation of rotamer **151**.[149,151] Performing the reaction at elevated temperatures, or using weaker

bases, such as 2,6-lutidine, allows the two enolates to equilibrate, resulting in the thermodynamically more favoured *E* enolate **143** as the major product.[152,153]

Following the formation of the enolate, nucleophilic addition to the aldehyde can occur. The observed diastereoselectivity for aldol reactions was explained by Zimmerman and Traxler who proposed that the reaction proceeds via a preferred chair-like transition state involving cooperative metal ion ligation by both the enolate and carbonyl substrates (Figure 1.5.1.1).[154] The chair-like geometry **152** should be energetically favoured compared to the corresponding boat structure **153**.

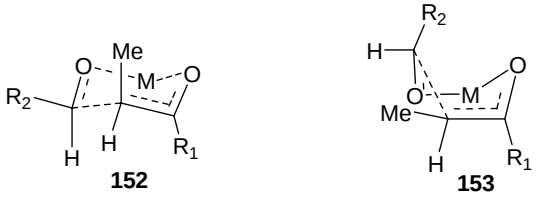

Figure 1.5.1.1: Chair and boat transition structures for aldol reactions.

The Zimmerman-Traxler model further predicts that chair-like transition structure **154** will be destabilized relative to **152**, due to the pseudo-axial orientation of R_2, in **154** leading to a steric interaction between the two alkyl groups R_1 and R_2. Therefore, addition to the aldehyde will proceed such that the alkyl group R_2 occupies the pseudo-equatorial geometry.[149,154]

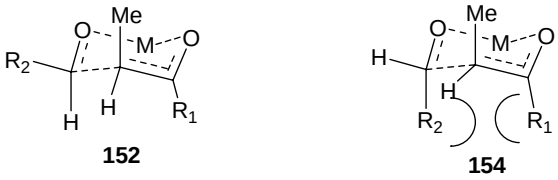

Figure 1.5.1.2: Orientation of the aldehyde and syn-axial interactions in aldol transition structures.

Given this model, the generation of the four possible diastereomers (E1, E2, T1, and T2) arising in the aldol addition can be explained. Ultimately, the two *erythro* geometries can be formed when *Z* enolate **144** is present, while the *threo* products are obtained from *E* enolate **143** (Figure 1.5.1.3). However, differentiation between *erythro* products E2 and E1, and likewise the selectivity between *threo* geometries T2 and T1, is a result of aldehyde addition to either the *si* or *re* face of the enolate via a chair transition state.

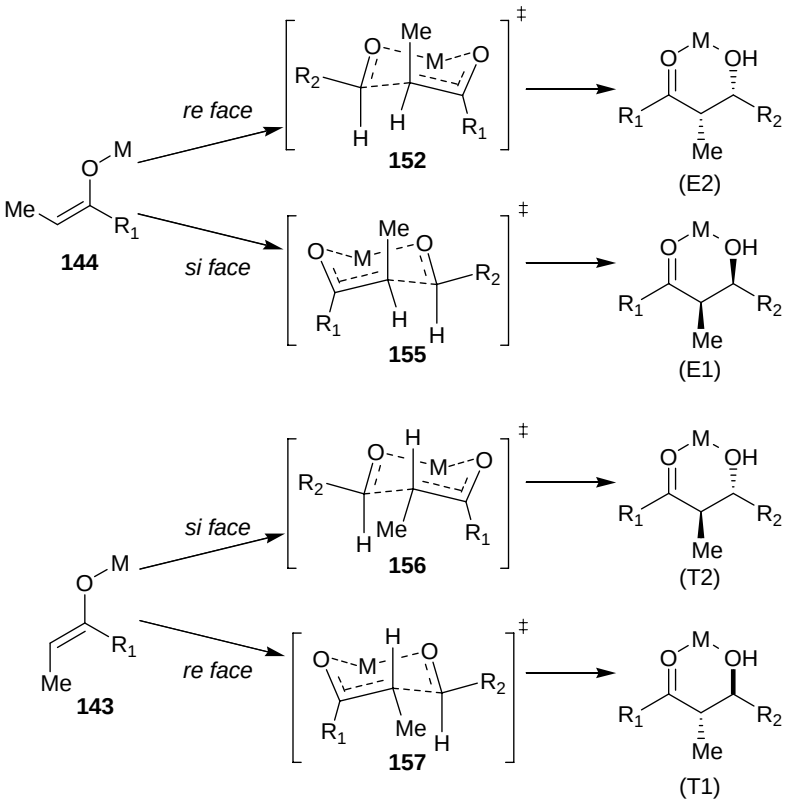

Figure 1.5.1.3: Generation of the four potential aldol addition diastereomers.

By using a chiral *N*-acyloxazolidinone such as **158** as the starting material a chiral enolate is generated, and thus the two faces of the enolate will be diasterotopic. Evans found that *N*-acyloxazolidinone derivatives undergo highly stereoselective enolization giving *Z* enolate **159** when treated with tertiary amine bases in conjunction with di-*n*-

butylboryl trifluoromethanesulfonate.[150] Assuming that the reaction follows the Zimmerman-Traxler model, chair-like transition structures **160** and **162** will be the lowest in energy, as the alkyl group from the incoming electrophile occupies the pseudo-equatorial position (Scheme 1.5.1.3). Using boronyl triflates it is expected that the oxazolidinone carbonyl and enolate oxygen will lie anti-periplanar to one another, leading to obstruction of the *re* face of the enolate. This leads to a destabilization of **162** due to the steric interaction between the aldehyde and the oxazolidinone benzyl group, allowing the selective formation of the E2 geometry.

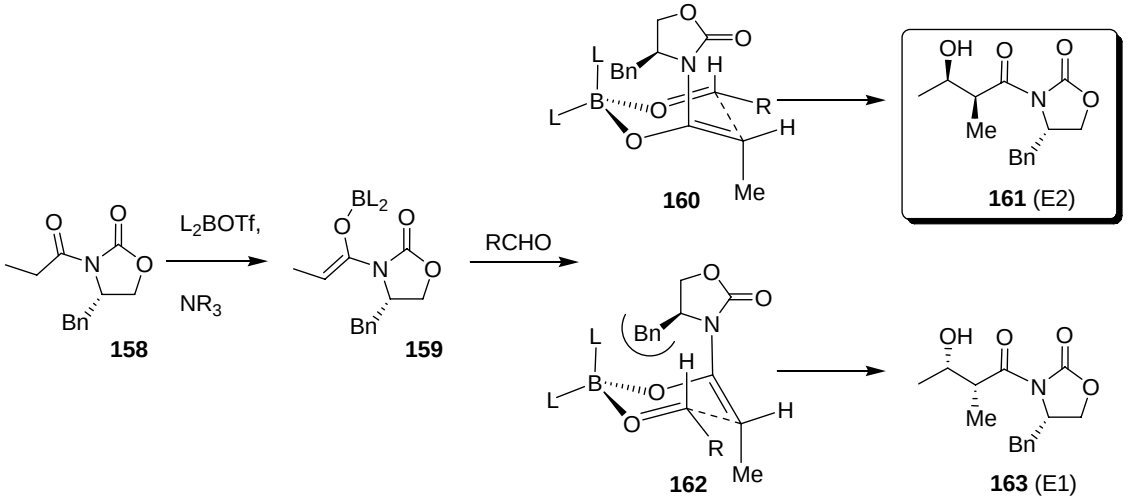

Scheme 1.5.1.3: Stereoselective aldol reactions using *N*-acyl oxazolidinones.

These methods have been extended through the study of other Lewis acids, including species derived from titanium.[155,156] Using these observations Crimmins *et al.* have been able to extend the model used to predict the stereoselectivity of aldol reactions involving oxazolidinone chiral auxilaries.[157] This new model centres around the equilibration of two coordinated intermediates, **164** and **165**, through the gain or loss of some ligand (Scheme 1.5.1.4).

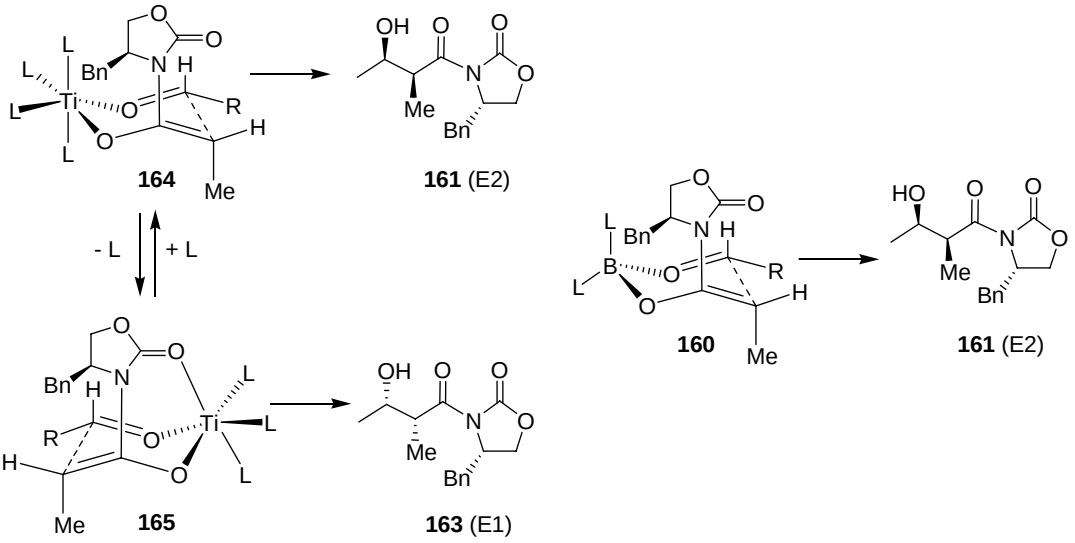

Scheme 1.5.1.4: Coordinated intermediates for aldol reactions with octahedral metals.

Boron can only form the tetravalent transition state **160**, involving the coordination to the aldehyde carbonyl and the enolate, and thus the E2 geometry will be generated selectively. Titanium and other species with higher coordination numbers can form the octahedral transition state **165**. This involves coordination to the oxazolidinone carbonyl as well as the aldehyde and enolate, selectively giving **163** with the E1 geometry. However, titanium is not restricted to this transition state, and may form **164**, which gives the E2 geometry selectively. The selectivity between **164** and **165** is a function of the stoichiometry of potential metal ligands, such as the aldehyde and amine base.[157] If these species are present in large excess they can bind to the titanium centre, displacing the oxazolidinone carbonyl and allowing the reaction to proceed via **164**. Conversely, if the aldehyde and amine are present in stoichiometric quantities **165** is favoured, and E1 is formed selectively.

Through the work of Evans and many others these methods have been developed into a highly reliable and general protocol for asymmetric aldol reaction using *N*-

acyloxazolidinones.[31,34,36,38,39] This technique has been widely adopted, allowing excellent stereoregulation of a very important carbon-carbon bond forming reaction, which gives rise to a great number of biologically significant natural products and intermediates.[158] These methods have been applied in a vast number of synthetic strategies, including Evans' work on the first stereoselective syntheses of Lonomycin A[159], Callipeltoside A[160] and Bryostatin 2.[161]

1.5.2 Stereoselective Radical Conjugate Additions

Asymmetric radical reactions have become important tools for synthetic chemists,[162,163] and in particular stereoselective radical additions to α,β-unsaturated carbonyl systems represent valuable transformations, furnishing synthetically useful carbon frameworks.[164-166] Methods for enantioselective bond construction using free radical addition to α,β-unsaturated systems have been developed.[167,168] However, examples of their use at the strategy level in the synthesis of natural products are only beginning to emerge.[169,170]

N-Acyloxazolidinones have played a central role in developing stereoselective conjugate additions of nucleophilic radicals.[171-173] Sibi *et al.* have proposed that addition to *N*-acyloxazolidinones proceeds via a chain mechanism, requiring activation of the α,β-unsaturated fragment by some Lewis acid (Scheme 1.5.2.1).[174] Initiation of the chain occurs by the reaction of triethylborane with molecular oxygen to produce an ethyl radical, which then generates alkyl radical R• from the corresponding alkyl halide RI. The initiator concentration must remain low to suppress addition of the ethyl radical to the *N*-acyloxazolidinone, forming intermediate **166** which gives ethyl byproduct **167** via hydrogen atom transfer. Following generation, alkyl radical R• then adds to the Lewis acid-activated alkene via reaction **R1**, to give radical **168**. Following addition via **R1** radical **168** reacts with tin hydride to produce the conjugate addition product **169** and the tributyl tin radical, which rapidly reacts with the alkyl halide to regenerate R• and complete the cycle.

Previous studies on these systems have not observed polymerization, or incorporation of tributyltin into the *N*-acyloxazolidinone when soluble Lewis acids are

used.[174] These results indicate that the kinetics of the reaction are balanced such that **R1**, **R2** and **R3** are significantly faster than the potential side reactions for the addition of a nucleophilic radical to the Lewis acid activated substrate. Furthermore, this activation by the Lewis acid has proven crucial to this reaction because addition to the unactivated *N*-acyloxazolidinone to produce **170** via **R7** is very slow. Thus, in the absence of the Lewis acid reduction via **R6** is preferred over addition via **R7** to give R-H preferentially.[175,176]

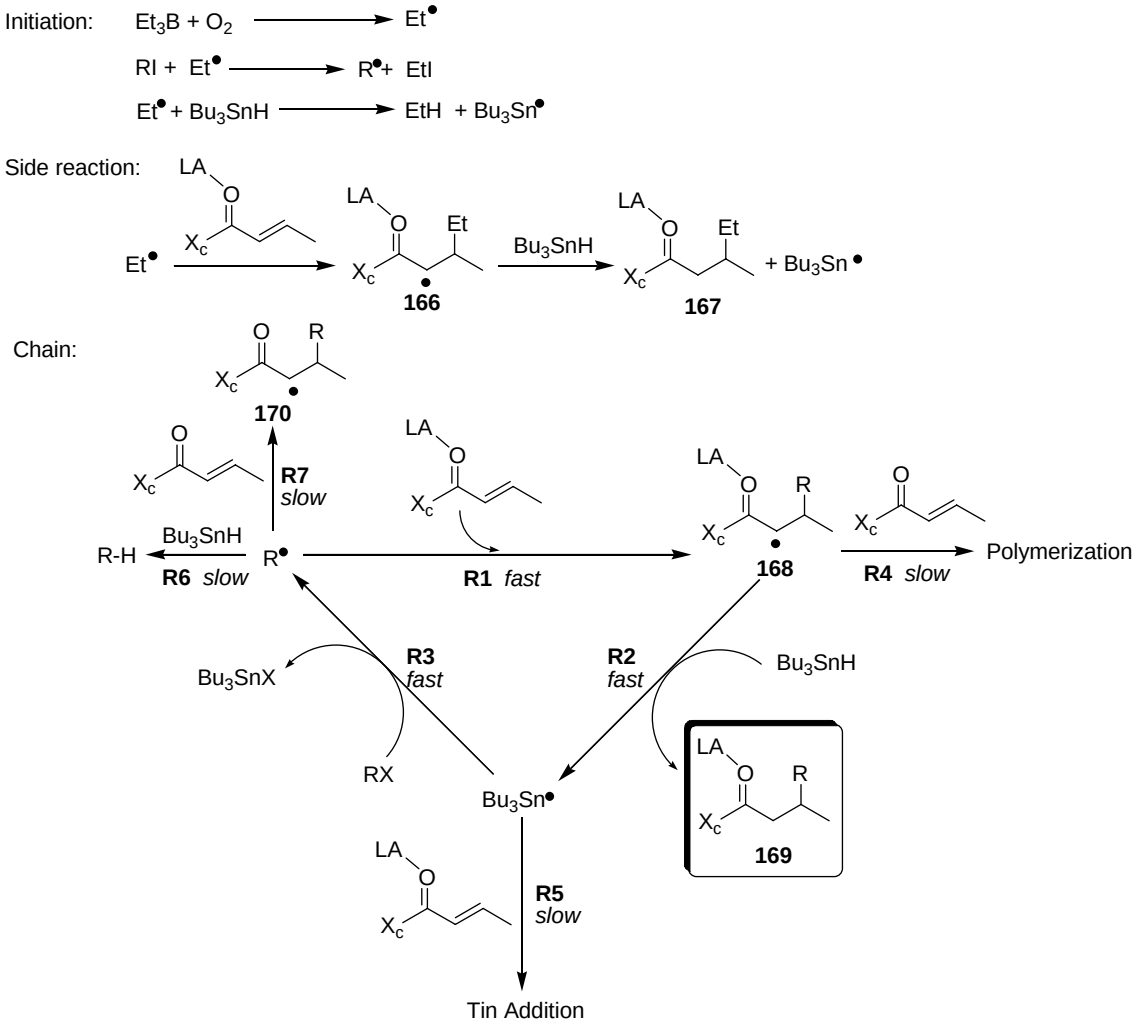

Scheme 1.5.2.1: Radical chain mechanism for conjugate addition to *N*-acyl oxazolidinones.[174]

Stereoselectivity of the radical conjugate addition to *N*-acyloxazolidinones arises by controlling the population of the rotamers present.[174,177] Four possible conformational isomers exist in solution due to rotation about the two bonds adjacent to the exocyclic carbonyl (Scheme 1.5.2.2). Conjugate radical additions to these molecules without Lewis acids lead to low selectivity due to a lack of rotamer control and subsequent reaction from all four possible conformations, **171 – 174**.[177] High stereoselectivity requires a dominant reactive rotamer in which one face of the enoyl substituent is effectively blocked. By applying a chelating Lewis acid rotamer **171** is expected be the primary reactive geometry present, as a result of the coordination of the endo and exocyclic carbonyls to form chelate **175**.

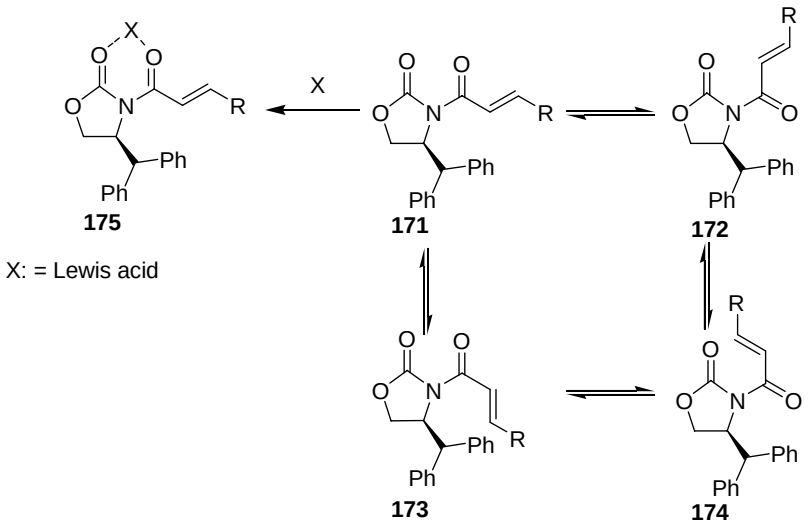

Scheme 1.5.2.2: Rotamers available for α,β-unsaturated *N*-acyloxazolidinones.

From this geometry the diphenyl substituent at the 4 position of the oxazolidinone effectively hinders the *re* face of the alkene (Scheme 1.5.2.3). Sibi *et al.* found that product **177**, resulting from conjugate addition from the *si* face of chelate **176**, could be

isolated as the major diastereomer for several *N*-enoyloxazolidinones (R = Me, Ph or COOEt).[169,174]

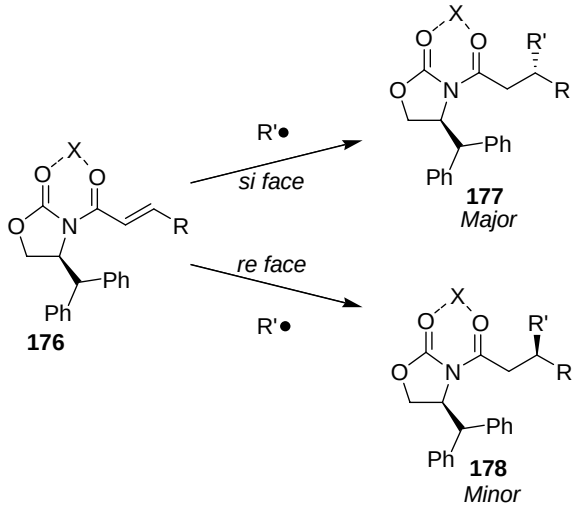

Scheme 1.5.2.3: Radical addition to α,β-unsaturated *N*-acyloxazolidinones.

While the presence of a Lewis acid is required to obtain high yield and stereoselectivity, the exact nature of the Lewis acid can have a dramatic effect on these parameters. Sibi *et al.* have shown that some Lewis acids increase the electrophilicity of the α,β-system to such a degree that direct reduction via hydrogen addition dominates (eg. $MeAlCl_2$, $TiCl_4$, Bu_2BOTf)).[174,178] These same studies have also shown that the diastereoselectivity of the conjugate radical additions using non-fluorous oxazolidinones depends primarily on the ionic radius of the metal rather than its Lewis acidity.[171,174] This conclusion was based on observations from a series of reactions performed with several lanthanide and prelanthanide triflates. Lewis acids with ionic radii near 0.9Å were found to provide sufficient activation and chelation, and gave efficient radical addition to the *N*-acyloxazolidinones.

In addition, these reactions pose an interesting problem with regard to the removal of pervasive and toxic alkyl tin species. Although practiced in the laboratory on a routine

basis, one of the major drawbacks to tin hydride-mediated radical chemistry is the difficulty in removal of the tin byproducts.[179,180] Several alternatives to tin hydride have been reported in the literature,[181-184] and in some cases specific methods have been developed to assist in tin removal.[185] While these methods have offered some promising alternatives, there is still a need for new methods or reagents that are able to provide metal free products via radical methodologies.

Fluorous synthetic methodologies are well suited to meet this challenge as the efficiency and selectivity with which fluorous materials can be separated from inorganic and organic reaction debris offers some unique advantages. Curran has demonstrated the utility of a fluorous tin hydride in radical chemistry and noted the ease with which pure reaction products could be isolated.[128,186-188] This technique allows the selective retention of the tin byproduct, yielding the organic reaction materials free of metal contamination.

While the initial goal of tin-free products has been met, further purification may still be necessary to obtain the target molecule free of other organic impurities. However, by applying the fluorous chiral auxiliary the target compound would be selectively purified from all unwanted reaction materials, including the alkyl tin species. This method provides a complementary technique to the work previously reported by Curran, allowing the selective extraction of reaction products, as opposed to capture of undesirable reagents. Combining these optimal purification characteristics with the fluorous auxiliary's ability to direct the stereochemistry of radical conjugate additions would provide a significant improvement over established methods.

1.5.3 Stereoselective 1,3 Dipolar Cycloadditions

The ability to construct multiple asymmetric centres in one synthetic transformation has made asymmetric cycloadditions a powerful method for the synthesis of complex chiral molecules. In particular 1,3-dipolar cycloadditions between nitrones and alkenes to form chiral isoxazolidines, with the general structures **179-182**, have received significant attention (Scheme 1.5.3.1).[189-191]

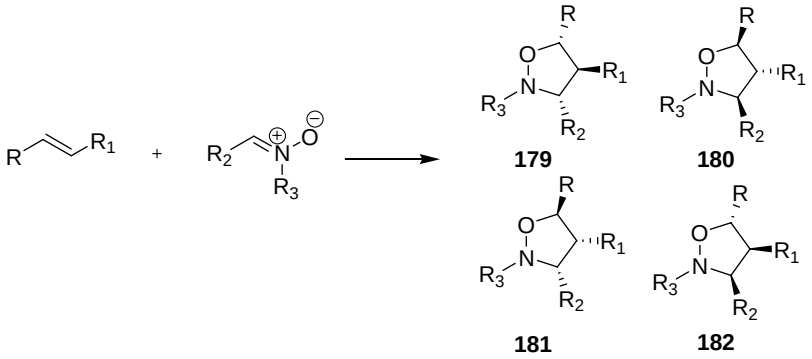

Scheme 1.5.3.1: 1,3-Dipolar cycloaddition forming chiral isoxazolidines.

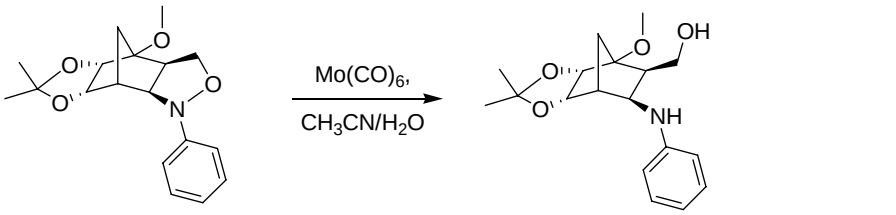

Tetrahedron Lett. **2005**, 3037.

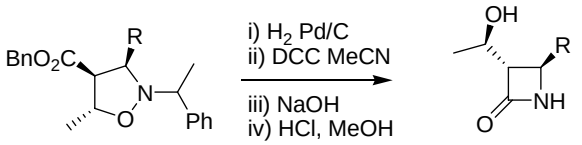

J Chem. Soc: Perk. Trans 1. **1989**, 2215.

Figure 1.5.3.1: Conversion of isoxazolidines to important precursors.[192,193]

Isoxazolidines themselves are not typically the primary synthetic target. However, many biologically important structures, such as 1,3-amino alcohols,[192,194,195] alkaloids,[190]

or β-lactams[196] can easily be formed through the reduction of the N-O bond. Examples of these transformations can be found in Figure 1.5.3.1.

While these cycloadditions do occur at room temperature and pressure they are often relatively slow.[190] In addition, many nitrones degrade rapidly in visible light and at elevated temperatures,[189,197] and thus do not tolerate extended reaction times. To solve these issues the rate of reaction can be dramatically increased through the application of a Lewis acid catalyst. Using a Frontier molecular orbital description, coordination of an α,β-unsaturated carbonyl to the Lewis acid lowers the energy of the LUMO of the alkene (Figure 1.5.3.2). This results in a decrease in the energy gap between the interacting Frontier molecular orbitals.[197]

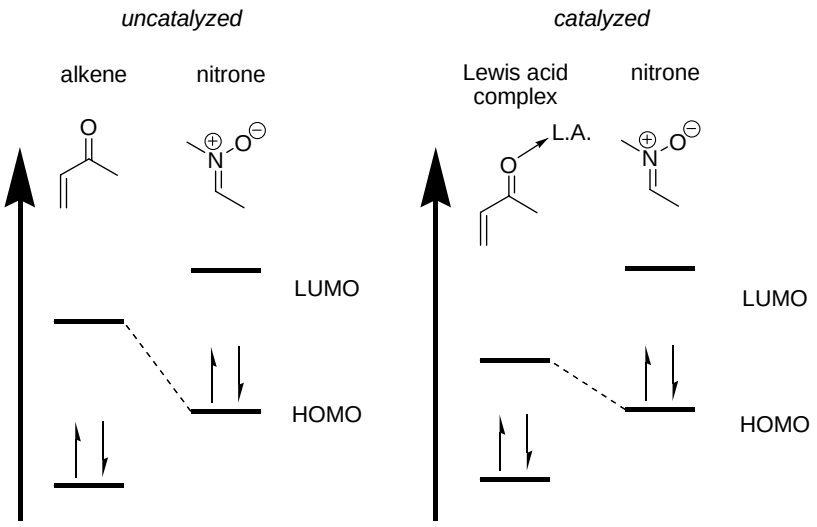

Figure 1.5.3.2: Molecular orbital interpretation of Lewis acid catalysis in 1,3 dipolar cycloadditions.

The 1,3 dipolar cycloaddition of nitrones to *N*-enoyloxazolidinones potentially can form three contiguous stereocentres at once. The ratio of regioisomers **183** and **184**

is controlled by a combination of steric and electronic factors which are largely influenced by the substitution of the nitrone and alkene.[189,198] Additions of diphenylnitrone to *N*-acyloxazolidinones containing non-terminal alkenes have been shown to give **183** exclusively (Scheme 1.5.3.2). This is attributed primarily to a more favourable orbital overlap, due to interaction of molecular orbitals of similar size.[189]

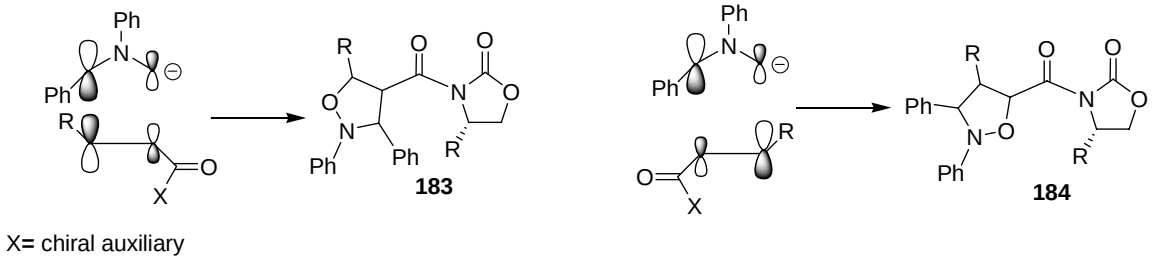

X= chiral auxiliary

Scheme 1.5.3.2: Regioisomers resulting from 1,3 dipolar cycloaddition to *N*-acyloxazolidinones.

Desimoni,[100] Faita,[89,95] and Jørgensen[195,199-201] have studied the factors affecting the stereoselectivity of the 1,3-dipolar cycloaddition between various nitrone dipoles and dipolarophiles linked to oxazolidinone chiral auxiliaries. Given that only regioisomer **183** is formed there are two issues of selectivity in these reactions: diastereofacial selectivity (which controls the 4',5' stereochemistry of the product) and *endo/exo* selectivity (which dictates the relative stereochemistry of the 3' and 4' centres).

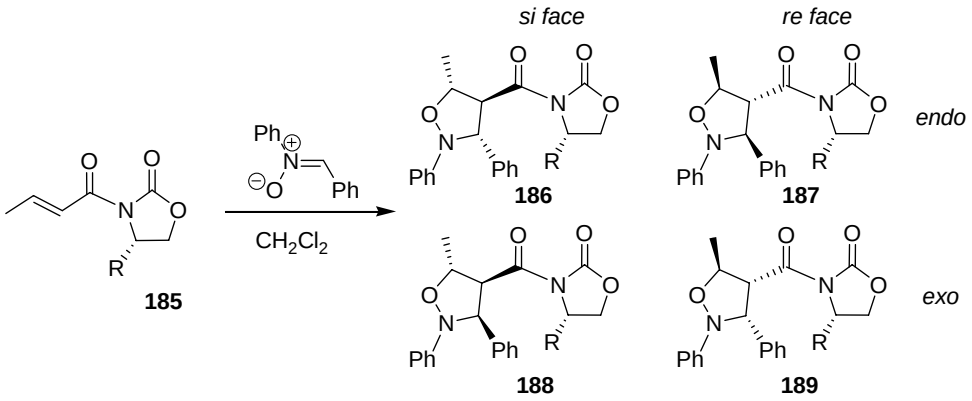

Scheme 1.5.3.3: 1,3-Dipolar cycloaddition between diphenylnitrone and *N*-acyloxazolidinones.

The facial selectivity of the cycloadditions is controlled by chelation of the carbonyls of the dipolarophile to the Lewis acid catalyst (Scheme 1.5.3.4).[89,95,100] The antiparallel arrangement of the two carbonyls seen in **190** is the predominant conformer in solution when no Lewis acid is present, giving rise to selective obstruction of the *si* face of the alkene. If a Lewis acid is added, coordination to the exocyclic carbonyl can occur to give the open coordinated structure **191**. Thus, both **190** and **191** are expected to direct dipolar addition at the *re* face of the alkene and give diastereomers **187** and **189**. The oxazolidinone can act as a bidentate ligand with many Lewis acids, such as $Mg(ClO_4)_2$, $TiCl_4$, and $Sc(OTf)_3$, allowing the formation of chelated structure **192**. In this orientation the *re* face is now obstructed, allowing addition to the *si* face of the alkene to give **186** and **188**. The balance between the open and chelated intermediate is crucial to obtain good facial selectivity, however this can be influenced by the reaction conditions. In most circumstances, the Lewis acid will prefer to form chelated geometry **192** over the open intermediate **191**.[197] However, species such as water and acetonitrile

can act as monodentate ligands, which displace the oxazolidinone carbonyl to give **191**, resulting in a switch in the facial selectivity of the dipole.[100,172]

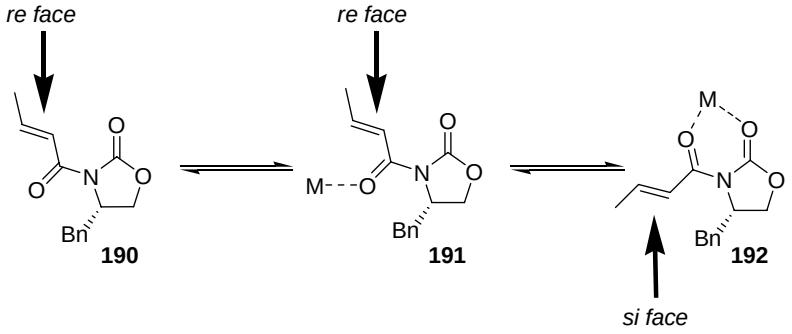

Scheme 1.5.3.4: Open and chelated intermediates for dipolar cycloaddition.

In Diels-Alder reactions the *endo/exo* selectivity is governed by secondary orbital overlap, leading to a net stabilization of the *endo* mode of approach (Figure 1.5.3.3). However, no analogous effect is possible in the 1,3 dipolar cycloaddition reactions due to the geometry of the system.[197]

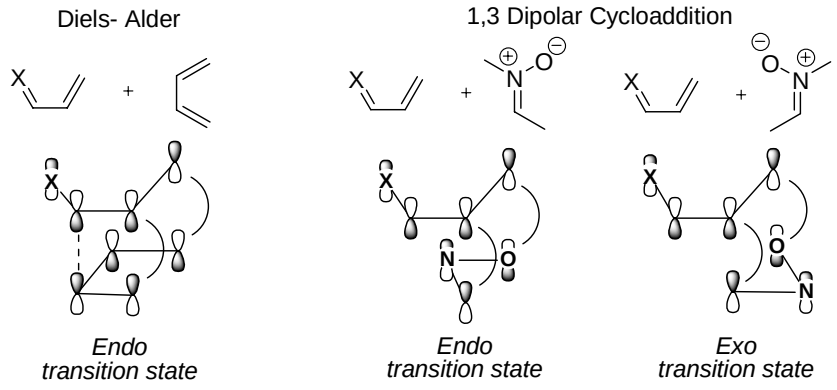

Figure 1.5.3.3: *Endo* and *exo* transition states in cycloaddition reactions.

Instead, the *endo/exo* selectivity is governed by the steric environment around the metal centre in the catalyzed cycloadditions (Scheme 1.5.3.5).[195,202] Assuming the nitrone exists in the *E* geometry, transition structure **194**, which gives the *exo* cycloadducts, will experience a steric interaction between the nitrone phenyl group and

the Lewis acid centre, thus making this approach higher in energy. Reaction via **193** to form the *endo* products is therefore favoured when bulkier ligands are used with the Lewis acids. Due to this effect the coordination geometry and ligands around the metal centre play a key role in determining its steric environment, and thus the *endo/exo* selectivity of the reaction.

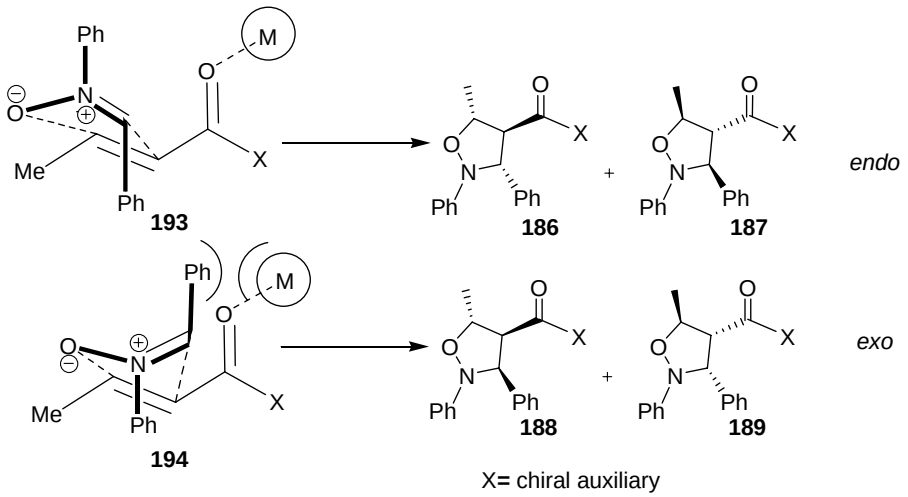

Scheme 1.5.3.5: Steric repulsion in *exo* dipolar cycloaddition transition state structure.

Chapter 2: THESIS OBJECTIVES

2.1.1 Design and Synthesis of a Fluorous Oxazolidinone

The initial goal of this work was to design an appropriate synthetic strategy to obtain chiral fluorous oxazolidinones. As discussed in Section 1.3 the most obvious starting material to accomplish this is an appropriately substituted chiral amino alcohol. Given this entry point, the main challenge became selecting the best method to attach a perfluoroalkyl fragment to some appropriate amino acid. Addition of perfluoroalkyl organometallic reagents derived from commercially available perfluoroalkyl halides have been studied in a number of systems.[203,204] By extending these studies, nucleophilic addition to an amino acid derived electrophile appeared to be a suitable choice.

Generation of substituted oxazolidinones using nucleophilic addition of some alkyl or aryl fragment to an amino acid electrophile can be classified into two basic categories as determined by the substitution pattern of the resulting oxazolidinone. Monosubstituted oxazolidinones functionalized at the 4 position are obtained when the amino acid side chain participates in the functional group transformations. One example of this approach is seen in the procedure developed by Sibi *et al.*[205] Serine is converted to amino ester **196**, and then treated with triphosgene to give oxazolidinone **197** (Scheme 2.1.1.1). The ester group at the 4 position is then reduced and the resulting alcohol is treated with tosyl chloride to produce electrophile **199**. This species can then be reacted with conventional Grignard or alkyl lithium reagents to give a wide variety of monosubstituted oxazolidinones.

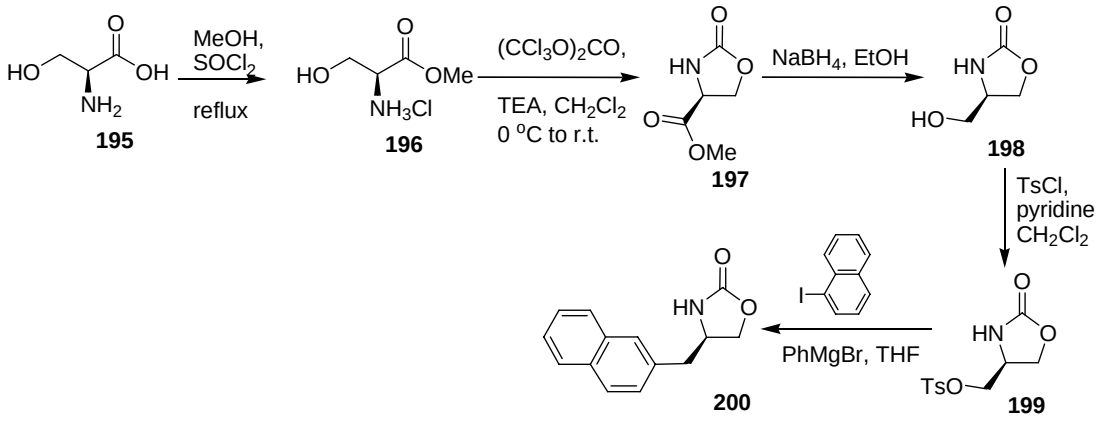

Scheme 2.1.1.1: Synthesis of a mono-functionalized oxazolidinone.[205]

Disubstituted oxazolidinones, or compounds bearing some substituent at both the 4 and 5 positions, are generated when nucleophilic addition occurs at the carboxylic acid centre of the amino acid starting material. This general strategy has been employed by Hoffman *et al.*[206] to generate 4,5 disubstituted oxazolidinone **207** (Scheme 2.1.1.2). In this instance, the amino acid is first converted to the corresponding *N*-carbamoyl derivative. After nucleophilic addition to the activated carboxylic acid centre several transformations are carried out, resulting in *N*-carbamoyl amino ketone **205**. This is reduced diastereoselectively to give a single isomer of the resulting hydroxycarbamate **206**, which is then cyclized to give oxazolidinone **207**.

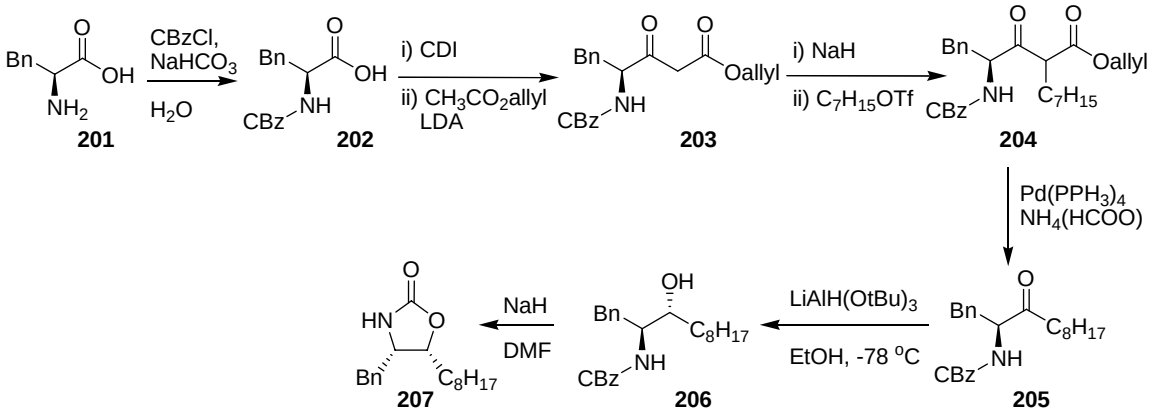

Scheme 2.1.1.2: Synthesis of a 4,5 disubstituted oxazolidinone.

Considering these two strategies, the protocol producing the 4,5 disubstituted material appeared to be the best option. Addition of the perfluoroalkyl group to the 4 position may alter the steric or electronic environment at this centre, resulting in an auxiliary that is unable to carry out asymmetric transformations with high diastereoselectivity. Instead, placing the perfluoroalkyl fragment at the more remote 5 centre should be less likely to interfere with reactions done on the *N*-alkyl or *N*-acyl portion of the chiral auxiliary.

In the synthesis of a 4,5 disubstituted oxazolidinone the control of the stereochemistry at the 5 position becomes an important consideration. The geometry at this position can be controlled by either diastereoselective reduction of an intermediate ketone,[206] or by controlling the stereoselectivity of the nucleophilic addition to some intermediate aldehyde.[207] The latter option was not seen as a favourable choice, as *N*-carbamoyl amino aldehydes have been shown to epimerize readily under mildly basic conditions.[208,209] In contrast, numerous examples exist where *N*-carbamoyl amino ketones have been reduced diastereoselectively using either chelation or steric control.[206,210] These two reduction methods would potentially allow both diastereomers to be easily accessed, giving rise to a more versatile synthetic method. For these reasons the route using the intermediate ketone was selected as the preferred pathway

The 4,5 disubstituted fluorous oxazolidinone can thus be obtained using a general procedure consisting of five steps (Scheme 2.1.1.3): synthesis of the *N*-carbamate and carbonyl activation of the parent α-amino acid producing **A**, perfluoroalkylation to give ketone **B**, diastereoselective reduction to selectively generate alcohol **C**, and finally cyclization to give oxazolidinone **D**.

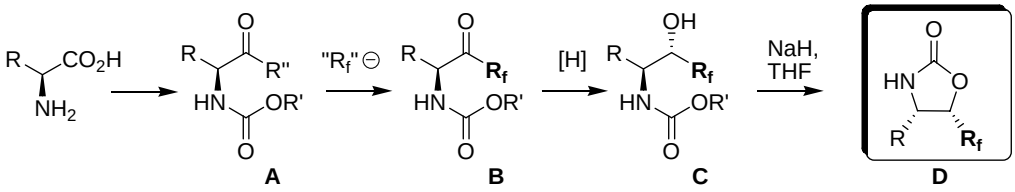

Scheme 2.1.1.3: General pathway for the synthesis of 4,5 disubstituted fluorous oxazolidinones.

This general route provided the framework for the investigation of these new chiral auxiliaries and their intermediate compounds. The objective now became identifying the most appropriate materials and conditions to generate an oxazolidinone with the general structure **D**. As the oxazolidinone derived from L-phenylalanine is by far the most commonly employed oxazolidinone-based auxiliary,[36] this amino acid was selected for the initial studies (Scheme 2.1.1.3, **R** = Bn).

2.1.2 Asymmetric Reactions using the Fluorous Auxiliary

Following the synthesis of the fluorous chiral auxiliary the focus of the research shifted to applying the new oxazolidinone to several model asymmetric transformations. These included aldol reactions, conjugate radical additions, and 1,3 dipolar cycloadditions. These model reactions were chosen specifically to evaluate three properties.

1) Stereoselectivity and versatility

All three asymmetric transformations represent important entry points to create diverse and useful carbon frameworks. In addition each reaction has been carried out using non-fluorous oxazolidinone chiral auxiliaries. Asymmetric aldol chemistry demonstrated by Evans *et al.* was one of the first applications of the oxazolidinones as

chiral auxiliaries.[37,149] Stereoselective radical conjugate additions and dipolar cycloadditions are newer applications for these auxiliaries first reported by Sibi *et al.*.[173] and Jørgensen *et al.*[199] respectively.

This set of three model systems offers a means of testing the new auxiliary in a variety of asymmetric transformations to produce relevant and synthetically important structures. In addition the reactivity and stereoselectivity can easily be compared with literature examples, permitting the direct comparison of the fluorous supported materials to non-fluorous analogs.

2) Demonstration of a superior support

One of the primary reasons for developing supported chiral auxiliaries is to effectively apply asymmetric transformations in automated and parallel synthetic techniques. As discussed in Section 1.3.3, polymer-supported oxazolidinones have been created, but lack the general applicability and versatility necessary to be efficiently employed in high-throughput chemistry.

In general the drawbacks reported in these studies stem from the nature of the polymer support itself. Reported transformations using polymer-supported materials have not been as reliable as the corresponding solution-phase methods. The variable yields and selectivities obtained suggest that the solid-phase environment may interfere with the formation of the well-defined complexes necessary for high stereoselectivity.[83,95,101,103]

This series of model reactions will test the perfluoroalkyl support to ensure it does not negatively impact the stereoselectivity, or reactivity of these systems. In particular the study of the 1,3-dipolar cycloaddition is ideal for this purpose, as these reactions have

been shown to exhibit dramatic changes in product distribution in the presence of different catalysts, solvents or additives.[100,172,195,198,211,212] This series of experiments combined with the literature data from the both solution phase and polymer-bound non-fluorous compounds will prove that fluorous synthesis is a superior method of supporting oxazolidinone auxiliaries.

3) Purification and isolation of supported materials

The auxiliary must be able to carry out reactions with high diastereoselectivity, but the fluorous support must also allow rapid and efficient purification of the products following completion of the transformation. As discussed in Section 1.4 light fluorous synthetic methods coupled with fluorous solid phase extraction (FSPE) can provide very efficient and selective recovery of supported materials.

The application of FSPE will be an asset for these model systems, allowing quick recovery on the chiral auxiliary and its derivates. While this is an important feature for all three model systems it will be particularly useful with the radical cycloadditions to efficiently remove alkyltin species.

In addition, the ability to rapidly purify the fluorous materials makes the auxiliary highly recyclable. Following unloading of the auxiliary to obtain the newly formed chiral fragment the fluorous oxazolidinone will be recovered and reused. This practice partially mitigates the extra synthetic effort required to create the auxiliary, but also demonstrates its superiority over non-fluorous oxazolidinones. The ability to reuse the auxiliary will be formally tested with the 1,3 dipolar cycloadditions, as this model system is most sensitive to external influences and may indicate if trace quantities of impurities are present in the recovered auxiliary.

Chapter 3: RESULTS AND DISCUSSION

3.1 Introduction

The research and findings from this project have been divided according to the two main objectives: design and synthesis of the fluorous oxazolidinone chiral auxiliary, and application of the new compounds to stoichiometric asymmetric synthesis. Each section will be discussed separately; however, the two topics are interrelated. For greater clarity areas of crossover have been highlighted and references have been made to the appropriate sections throughout this chapter.

3.2 Synthesis of the Fluorous Oxazolidinone Auxiliary

The development of a general and efficient synthesis of the fluorous chiral auxiliaries is the result of several specific investigations into the reactivity and properties of the required fluorous and non-fluorous intermediates. Early in our work, we identified several key challenges to the production of the chiral auxiliaries on multi-gram scales. Specifically, these included the selection of an appropriate chiral starting material, the efficient incorporation of a perfluoroalkyl functional group, and optimization of the reaction parameters to select for both high yield and rapid purification. Ultimately, these studies have led to first- and second-generation chiral auxiliaries based on α amino acids. This section discusses the initial goals and outlines the developments and improvements which led to the optimized synthetic protocol.

The nature of the perfluoroalkyl fragment is an important consideration. Typically, a linear perfluoroalkyl group is employed when creating a molecule to be used with fluorous synthetic methods (see Section 1.4). The chain length of the perfluoroalkyl

group determines the fluorine content of the resulting molecule, usually expressed as the percent by weight of fluorine. For molecules that are to be applied in fluorous synthetic methods the useful range is usually between 35% and 55% fluorine by weight.[117,127] This allows the compounds to be separable by FSPE, while remaining soluble in common organic solvents. Bearing in mind the potential applications of the chiral auxiliary, it was important to ensure that the oxazolidinone and any of its derivatives would have a sufficiently high fluorine content to guarantee easy separation. To meet this requirement a perfluorooctyl linear chain (C_8F_{17}) was employed.

3.2.1 First Generation Fluorous Oxazolidinone Chiral Auxiliaries

The primary undertaking was to select an appropriate nucleophilic fluorous organometallic reagent, and some suitable electrophile derived from L-phenylalanine. Initial studies centered on the reaction of perfluoroorganometallic reagents with the *N*-CBz methyl ester **208a**. The most commonly applied nucleophilic perfluoroorganometallic reagents are alkyl cuprates, alkyl lithiums, alkyl zinc species and Grignards.[203,204] However, only Grignard and lithium reagents were investigated because perfluoroalkyl cuprates and zinc reagents have afforded only modest yields in addition reactions with esters.[204,213]

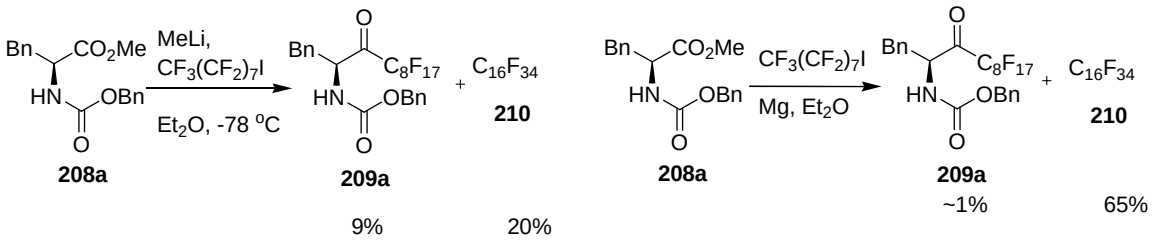

Scheme 3.2.1.1: Perfluoroalkyl Grignard and lithium additions to ester **208a**.

Nucleophilic additions using the perfluoroalkyllithium and Grignard reagent derived from $C_8F_{17}I$ were carried out (Scheme 3.2.1.1). While neither protocol gave efficient conversion to perfluoroketone **209a**, the Grignard reagent was extremely difficult to work with and typically gave the perfluoroalkyl dimer **210** rather than the desired addition. This result is similar to observations made by other groups,[204] who noted that Grignard reagents derived from perfluoroalkyl halides, such as $C_8F_{17}I$, are very sensitive to reaction conditions. Given these results the Grignard species was deemed unsuitable for our purposes.

While the lithium protocol did give the target perfluoroketone **209a,** the yield was only 9%. This was partly a result of the method necessary to form the required perfluoroalkyllithium compounds. Due to the instability of the lithiated species, even at low temperatures,[214,215] the trans-metalation must be carried out *in situ* through addition of MeLi to a solution containing $C_8F_{17}I$ and ester **208a**. As a result the ketone is but one of three products resulting from nucleophilic addition to the ester (Table 3.2.1.1). A series of different reaction conditions were evaluated in an attempt to selectively form ketone **209a** and minimize the generation of tertiary alcohols **211a** and **212**.

Table 3.2.1.1: Perfluoroalkyllithium addition to *N*-CBz phenylalanine methyl ester.

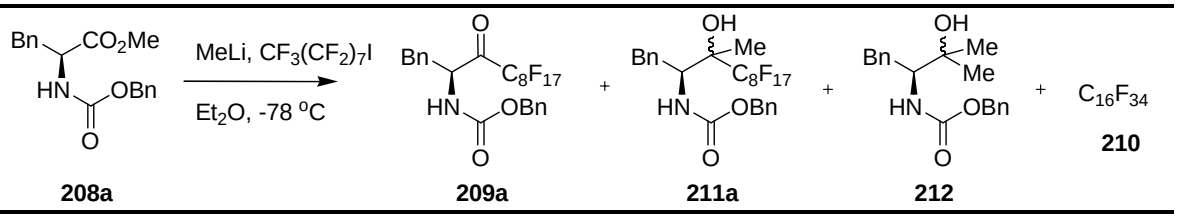

entry	eqv $C_8F_{17}I$	eqv MeLi	quench	209a [a]	211a [a]	212 [a]	210 [b]
1	1.5	1.6	–78 °C	9%	3%	35%	20%
2	2.5	2.6	–78 °C	12%	6%	38%	28%
3	3.5	3.6	–78 °C	15%	15%	44%	27%
4	2.5	3.6	–78 °C	18%	7%	52%	28%

[a] Yield based on percent conversion from ester **159a**; [b] Yields based on percent conversion from $C_8F_{17}I$ applied.

This study did not identify suitable reaction conditions to form the perfluoroketone exclusively, but several trends are evident. Increasing the quantity of the perfluoroalkyl iodide did improve the yield of ketone **209a**, but this was coupled with a simultaneous increase in the yields of the tertiary alcohols **211a** and **212** (Table 3.2.1.1, entries 1, 2 and 3). Also it is interesting to note that using a larger excess of MeLi increased the yield of the ketone (Table 3.2.1.1, entries 2 cf. 4). This observation is similar to results reported by Uno *et al.* In the lithiation of perfluorohexyl iodide **213**, Uno concluded that bis(perfluoroalkyl)iodinanide **214** was formed *in situ* and acted as a stable carrier of the reactive perfluoroalkyllithium (Scheme 3.2.1.2).[216] While the iodinanide was not nucleophilic, it served a crucial role by trapping the otherwise very unstable perfluoroalkyllithium in a reversible manner. Addition of an excess of the MeLi

helped to break up the unreactive iodinanide, increasing the concentration of the nucleophilic perfluoroalkyllithium species and resulting in a higher yield of the perfluoroalkylated product.[216]

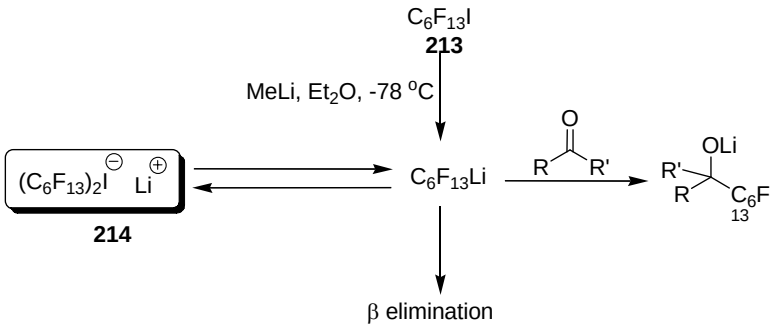

Scheme 3.2.1.2: Proposed mechanism for the stabilization of perfluoroalkyllithium reagents.[216]

The formation of the four isolated products **209a – 212** was a result of several competing reactions present during the *in situ* generation of the perfluoroalkyllithium reagent (Scheme 3.2.1.3).

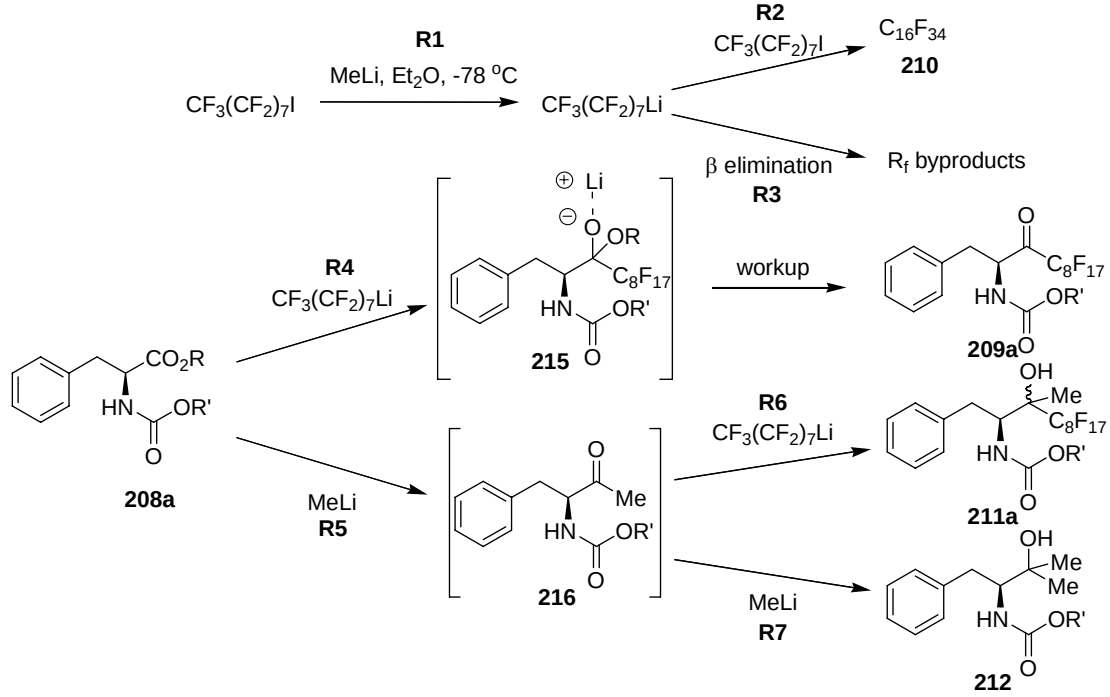

Scheme 3.2.1.3: Competitive reactions present during the perfluoroalkylation of **208a**.

The distribution of the four products is controlled by the relative rates of the individual reactions (Scheme 3.2.1.3, **R1** – **R7**). Ketone **209a** is formed though trans-metalation of the perfluorooctyl iodide, designated **R1**, followed by the addition to ester **208a** by pathway **R4.** This pathway generates tetrahedral intermediate **215**, which is stable at low temperatures and prevents further nucleophilic addition. As a result ketone **209a** is not present at low temperature and is only formed upon workup.[215,217,218] However, if the concentration of MeLi increases too quickly, then direct methylation of ester **208a** via **R5** can occur, forming intermediate ketone **216**. This ketone is more electrophilic than the parent ester, allowing rapid conversion to tertiary alcohols **211a** or **212** via **R6** or **R7** respectively. In order to isolate perfluoroketone **209a** as the major product the rate of **R1** must be faster than **R5**. This should occur if the perfluoroalkyl anion is more nucleophilic than the MeLi, or the concentration of the MeLi is kept much lower than the perfluoroalkyllithium reagent.

To complicate the situation further, the perfluorooctyl lithium reagent can react along two other pathways, **R2** and **R3** (Scheme 3.2.1.3). The more significant of these two reactions is **R3**, the degradation of the nucleophile via β-elimination. In the case of perfluorooctyl lithium the rate of **R3** is comparable to the rate of addition to the electrophile via **R4**,[216,218] thus making any conventional pregeneration protocol unsuitable. Reaction via **R2** occurs when low concentrations of the perfluorooctyl lithium are present with an excess of $C_8F_{17}I$, and gives rise to perfluoroalkane **210**. The propensity of perfluoroalkyl halides to produce symmetric dimers from the corresponding organometallic reagents has been noted in many cases.[203,204,219] Together, side reactions

R2 and **R3** are the primary cause for the low yield of the target ketone **209a**. In certain trials, cross coupling via **R3** has been responsible for an estimated loss of 30% of the perfluoroalkyl iodide originally applied, with the balance of the mass discrepancy for the fluorous materials being attributed to degradation via β-elimination. The multitude of competing reactions depicted in Scheme 3.2.1.3 begins to explain the low yields shown in Table 3.2.1.1.

Given these circumstances it is obvious that the production of perfluoroketone **209a** using this method is a delicate balancing act. In an attempt to obtain higher yields of the perfluoroketone, *N*-carbamoyl amino esters **208a-d** were tested under a variety of conditions (Table 3.2.1.2). The best overall yields were obtained when ester **208b** was treated with the perfluoroalkyllithium in the presence of $BF_3{\cdot}Et_2O$ (Table 3.2.1.2, entry 5). The results from the different starting materials indicate that **208b** and **208d** were superior to **208a** and **208c**, suggesting that the ethyl carbamate performed better than the larger benzyl carbamate (Table 3.2.1.2, entries 4, 5, 8, 9 cf. 2, 3, 6, 7). This observation may be attributed to the steric differences between the two carbamoyl groups, as the larger benzyl carbamate may hinder attack at the ester centre.

Table 3.2.1.2: Addition of perfluorooctyl lithium to *N*-carbamoyl amino esters.

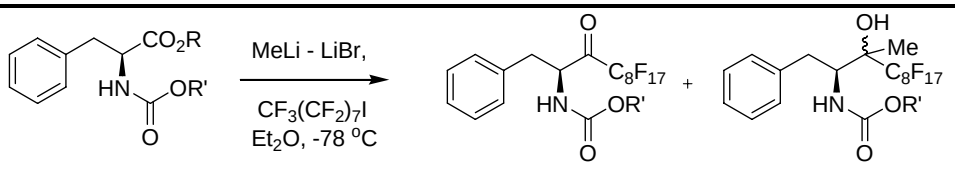

208a-d **209a,b** **211a,b**

208a: R = Me, R' = Bn
208b: R = Me, R' = Et
208c: R = Et, R' = Bn
208d: R = Et, R'= Et

209a, 211a: R' = Bn
209b, 211b: R' = Et

entry	**Ester**	**Lewis acid**	**time**	**ketone** [a]	**alcohol** [a]
1	**208a** [b]	—	2 h	**209a** (9%)	**211a** (1%)
2	**208a**	—	2 h	**209a** (13%)	**211a** (8%)
3	**208a**	$BF_3{\cdot}Et_2O$	1.5 h	**209a** (18%)	**211a** (5%)
4	**208b**	—	3 h	**209b** (29%)	**211b** (6%)
5	**208b**	$BF_3{\cdot}Et_2O$	2 h	**209b** (38%)	**211b** (1%)
6	**208c**	—	5 h	**209a** (9%)	**211a** (9%)
7	**208c**	$BF_3{\cdot}Et_2O$	2 h	**209a** (16%)	**211a** (4%)
8	**208d**	—	3 h	**209b** (20%)	**211b** (8%)
9	**208d**	$BF_3{\cdot}Et_2O$	2 h	**209b** (29%)	**211b** (2%)

[a] Yield represents percent conversion from corresponding ester; [b] R_fLi generated without LiBr

The presence of the lithium halide improved the incorporation of the perfluoroalkyl fragment, with the average yields increasing from <10% to 25% (Table

3.2.1.2, entries 1 vs. 2). This increase in yield may be due to the formation of a more nucleophilic perfluoroalkyllithium species. Alkyl lithium reagents typically exist in solution as dimeric or tetrameric homo-aggregates (Figure 3.2.1.1).[220] However, the addition of a lithium halide salt (LiX where X= Cl, Br, or I) can promote the formation of hetero-aggregates with the general structure $[(RLi)_x(LiX)_y]$.[221,222] The reactivity, stability and nucleophilicity of the carbanionic component of these hetero-aggregates can be markedly different from the parent $(RLi)_x$ species.[221,223]

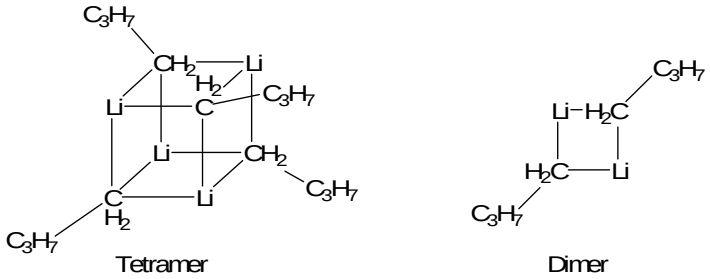

Figure 3.2.1.1: Homo-aggregates of *n*-butyllithium.[222]

This study indicates that the hetero-aggregate generated from the perfluoroalkyllithium reagent and lithium bromide is more reactive, leading to an increase in the yield of the perfluoroketones. While this enhancement is significant, there was also a simultaneous increase in the production of the corresponding tertiary alcohols **211a** and **b**. This indicates that the lithium salt leads to the formation of a more reactive hetero-aggregate of both the perfluoroalkyl and methyl lithium reagents. The result is an increase in the rates of both **R4** and **R5** (Scheme 3.2.1.3), and thus an increased yield of ketones **209a,b** and tertiary alcohols **211a,b**.

Addition of a Lewis acid improved the yield of the perfluoroketone without substantially increasing the production of the tertiary alcohol (Table 3.2.1.2, entries 3, 5,

7 and 9). In this method, the electrophilicity of **208a**–**d** is enhanced when the ester carbonyl interacts with $BF_3{\cdot}Et_2O$, resulting in a higher yield of ketone **209a** or **209b**. This result is similar to the observations reported by Uno *et al.*,[217,224] who noted that by performing the reaction in the presence of $BF_3{\cdot}Et_2O$ the yield of perfluoroketone **218** could be increased without simultaneously generating higher levels of ester **219** (Scheme 3.2.1.4).

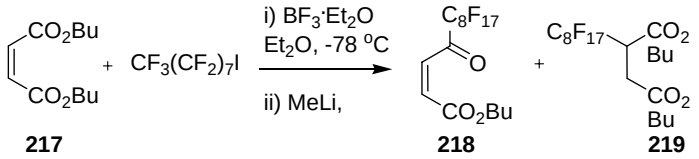

217 **218** **219**

Scheme 3.2.1.4: Improvement of the perfluoroalkylation of ester **217** using $BF_3{\cdot}EtO_2$.[217]

Using the conditions described in Table 3.2.1.2, entry 5 it was possible to synthesize multi-gram quantities of ketone **209b**. The efficiency of this synthesis was greatly enhanced through the application of fluorous solid phase extraction (FSPE). Following completion of the perfluoroalkylation, reactions were quenched, concentrated under reduced pressure and the residue was applied to fluorous-modified silica gel. Washing the solid phase with fluorophobic solvents, such as 70% MeOH in water or 30% *n*-PrOH in water, selectively removed organic and inorganic impurities. Fluorous products were then eluted by switching to a more fluorophilic solvent, such as MeOH, Et_2O, or *n*-PrOH. Despite extensive investigation, yields in excess of 50% could not be obtained. Additionally, the side reaction forming tertiary alcohol **211b** could not be fully suppressed. This was a particular nuisance as purification by FSPE could not be used to separate **209b** from **211b**, requiring the use of conventional chromatography on silica gel to separate the two fluorous products.

The next step in the synthesis of the fluorous oxazolidinone was to convert the perfluoroalkyl ketones to the corresponding alcohols. Because the stereochemical outcome of this reaction determines the final geometry at the 4 and 5 centres of the oxazolidinone, it was crucial that the reduction occurred with high diastereoselectivity. Studies by Hoffman *et al.*[206] have demonstrated that *N*-carbamoyl amino ketones can be selectively reduced to give either the *syn* or *anti N*-carbamoyl amino alcohol by varying the reaction conditions (Scheme 3.2.1.5). By choosing the correct solvent and reagents, it is possible to direct the reduction either through the Felkin-Anh transition structure **220**, leading to the *syn* alcohol **221**, or the chelated transition structure **222** to give the *anti* alcohol **223**.

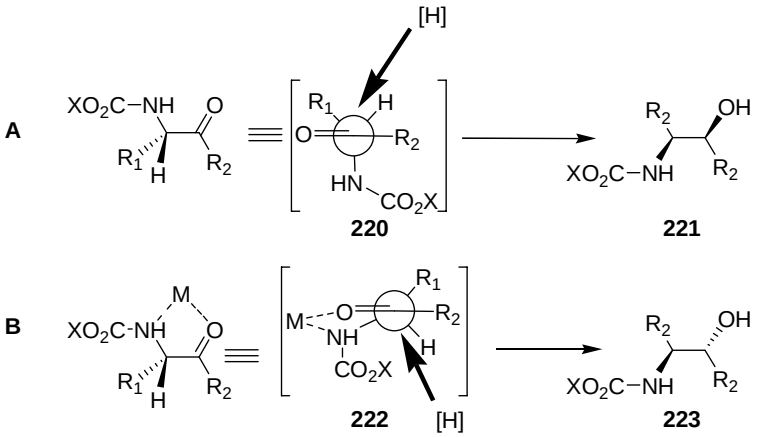

Scheme 3.2.1.5: Reduction of amino ketones via steric or chelation control.

Hoffman's results indicated that in most cases the reduction via a chelated intermediate gave significantly higher stereoselectivity than the corresponding sterically-controlled protocols, leading to the production of a single diastereomer in the best cases.[206] Therefore, reduction via chelation control became the primary focus for this research. Treating the perfluoroalkyl ketones with various reducing agents aimed to promote chelation proved to be somewhat problematic. Ketones **209a** and **209b** were

reacted under a variety of conditions to identify a highly diastereoselective reduction protocol (Table 3.2.1.3). In all cases the products were purified via FSPE and the diastereoselectivity of the reaction was assigned using ^{1}H NMR. While both ketones could be reduced to the corresponding alcohols cleanly and efficiently, we were unable to select for *anti* geometry **225** using chelation control.

Table 3.2.1.3: Attempted diastereoselective reduction of perfluoroketones.

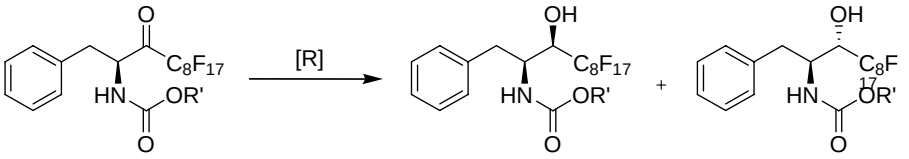

209a,b **224a,b** **225a,b**

a: R' = Bn
b: R' = Et

entry	ketone	solvent	[R]	yield	selectivity (*syn*:*anti*)
1	**209a**	THF	$NaBH_4$	96%	1 : 1
2	**209a**	EtOH	$NaBH_4$	98%	1 : 2.5
3	**209a**	EtOH	$LiAlH(OtBu)_3$	94%	1 : 4
4	**209b**	THF	$NaBH_4$	98%	1 : 1
5	**209b**	EtOH	$NaBH_4$	97%	1 : 3
6	**209b**	THF	$LiAlH(OtBu)_3$	98%	1 : 1
7	**209b**	EtOH	$LiAlH(OtBu)_3$	95%	1 : 5

The diastereoselectivity of these reductions showed a strong dependence on the solvent applied. Carrying out the reduction in THF produced a 1:1 mixture of both the *syn* and *anti* alcohols, **224** and **225** respectively, regardless of the reducing agent or

ketone applied (Table 3.2.1.3 entries 1, 4, and 6). Changing the solvent to EtOH allowed *anti* alcohol **225** to be formed as the major diastereomer (Table 3.2.1.3 entries 2, 3, 5, 7). With this solvent, both reducing agents favoured the formation of **225**, although the best stereoselectivity was obtained with $LiAlH(OtBu)_3$ (Table 3.2.1.3 entries 2, 5 cf. 3, 7).

These results agree with Hoffman *et al.*,[206] who reported that chelation-controlled reduction of *N*-carbamoyl amino ketones proceeds via intermediate **226**, involving the association of the aluminum or boron reagent to the carbamate nitrogen and ketone (Figure 3.2.1.2). This conclusion is based on the observation that the ratio of the *syn* and *anti* alcohols did not change when a series of borohydride regents was applied ($X^+(BH_4)^-$) where $X^+ = Li^+$, Na^+, K^+, Me_4N^+.[206] This indicates that intermediate **227** does not play a central role in the stereoselectivity.

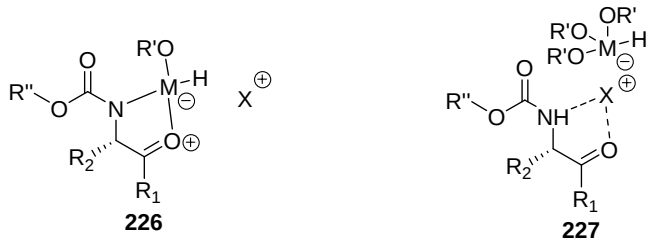

Figure 3.2.1.2: Possible chelated intermediates for the reduction of *N*-carbamoyl amino ketones.[206]

Intermediate **226** forms by dissociative ligand exchange involving disproportionation of alkoxy or hydride ligands by a dissociation/recombination mechanism (Scheme 3.2.1.6).[225] Chelate formation is likely initiated by the deprotonation of the carbamate group by an alkoxide species, forming **228**. This is necessary to form an appropriate anion, as boron and aluminum are known to form only weak complexes to neutral species.[226] Carbamate anion **228** then displaces a ligand from

the aluminum or boron centre to form the monodentate intermediate **229**. The chelated structure then forms through the displacement of a second ligand by the ketone carbonyl to give **226**.[227] This mechanism is directly analogous to the one proposed for the chelate formation of hydroxy ketones[227] and amino acids to aluminum.

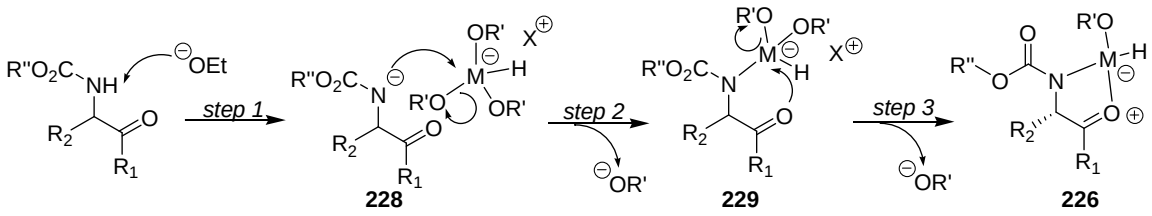

Scheme 3.2.1.6: Mechanism for chelate formation in alcoholic solvents.[206]

This mechanism demonstrates the role solvent plays in the diastereoselective reduction of these amino ketones. The solvent must promote ligand dissociation and exchange via participation of some alkoxide species. THF can not participate in this manner making it unsuitable for this application. Temperature control during the reduction is critical, as hydride reaction with EtOH becomes competitive with the reduction at temperatures above -50 ºC, requiring that the hydride reagent be introduced only after the reaction mixture has been cooled to -78 ºC.

Additionally, this mechanism explains the poor diastereoselectivity observed for the reduction of perfluoroalkyl ketones **209a** and **209b**. The coordination of the *N*-carbamoyl group of the fluorous ketone likely occurs in the same manner as proposed for non-fluorous ketones (Scheme 3.2.1.6, step 1 and 2). However, the strongly electron withdrawing perfluoroalkyl group reduces the basicity of the ketone carbonyl, preventing it from displacing a ligand from boron or aluminum to form the chelated intermediate **226**

(Scheme 3.2.1.6, step 3). As a result, the reduction takes place from intermediate **229**, giving the *syn* and *anti* alcohols, **224** and **225** respectively.

While it was not possible to select for a single diastereomer of the perfluoroalkyl alcohols, **224** and **225** could be separated with normal phase flash chromatography. These compounds were treated with KH in THF, forming an intermediate alkoxide which yields oxazolidinones **230** and **231** via intramolecular attack on the carbamate carbonyl (Scheme 3.2.1.7).

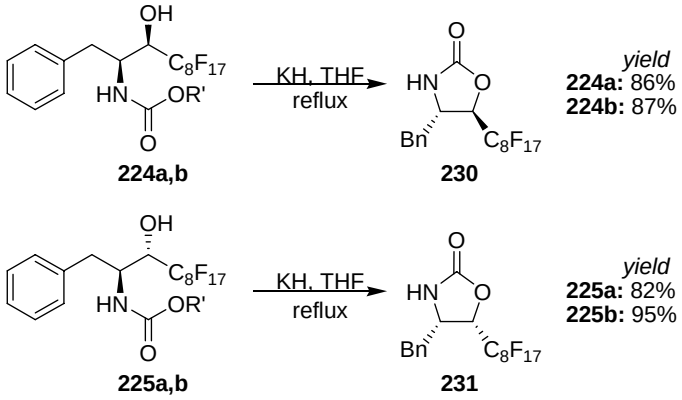

Scheme 3.2.1.7: Cyclization to form *syn* and *anti* oxazolidinones.

The relative geometry at the 4 and 5 centres of **230** and **231** was investigated using a combination of ^{1}H NMR and 1D selective NOE experiments. Examining the vicinal coupling constant between the two methine protons on the oxazolidinone ring it was possible to differentiate between the *syn* and *anti* geometries. In the case of the *syn* oxazolidinone **231** J_{H4H5} was 7.5 Hz, while **230** displayed a vicinal coupling constant of 5.5 Hz characteristic of an *anti* relationship between these centres. These values agree with the vicinal coupling constants reported for other *syn* and *anti* 4,5 disubstituted oxazolidinones.[92,206]

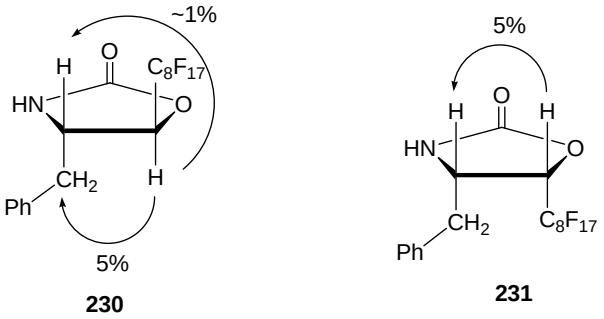

Figure 3.2.1.3: NOE results for *syn* and *anti* fluorous oxazolidinones.

Nuclear Overhauser effect experiments further confirmed the relative geometries of these two species (Figure 3.2.1.3). Oxazolidinone **230** showed < 1% NOE between H4 and H5, but displayed a strong signal between H5 and the benzyl methylene. This is consistent with the observed vicinal coupling constant confirming that **230** has the *anti* geometry at the 4 and 5 centres. In contrast, ~5% NOE was observed between the two methine protons in **231**, and no correlation to the benzyl methylene was present, confirming that the 4 and 5 centres in **231** have the *syn* relative geometry.

3.2.2 Second Generation Fluorous Oxazolidinone Chiral Auxiliaries

The synthesis of the first fluorous oxazolidinones, while successful, did not prove to be practical. The low efficiency of the perfluoroalkylation, coupled with the lack of diastereoselectivity in the subsequent reduction made this process a poor candidate for the production of large quantities of the target material. Examining the mechanisms of these processes and the observations in the literature it became clear that the difficulties encountered were a result of the chemical properties of the C_8F_{17} fragment itself. Further optimization using this perfluoroalkyl fragment did not appear to be possible. Instead, an alternate fluorous starting material was investigated.

A more robust fluorous nucleophile was required. Fluoroalkyl species containing an ethylene spacer, such as $C_6F_{13}(CH_2)_2Li$, behave much more like typical organometallic reagents.[127,130,228] The alkyl portion of these compounds helps to insulate the reactive site from the strongly electron withdrawing perfluorinated group, allowing the resulting carbanion to be more nucleophilic and less prone to β elimination. These properties provided several distinct advantages over the C_8F_{17} nucleophiles and their resulting products. First, the organometallic reagents derived from fluoroalkyl species with the general formula $CF_3(CF_2)_n(CH_2)_m$ can be pregenerated, eliminating side reactions associated with the *in situ* method of generation required for the C_8F_{17} nucleophiles. Secondly, the alkyl spacer in these fluoroalkyl fragments will insulate the carbonyl from the strongly electron withdrawing perfluoroalkyl group. This should increase the Lewis basicity of the carbonyl, allowing the compounds to form a chelated intermediate during reduction, and give a single diastereomer of the resulting alcohol.

Three *N*-protected amino esters **232a-c** were synthesized from L-phenylalanine via literature procedures,[229-232] and subjected to perfluoroalkylation with the Grignard derivatives of $C_6F_{13}(CH_2)_2I$ (Table 3.2.2.1).

Table 3.2.2.1: Perfluoroalkyl Grignard addition to *N*-carbamoyl amino esters.

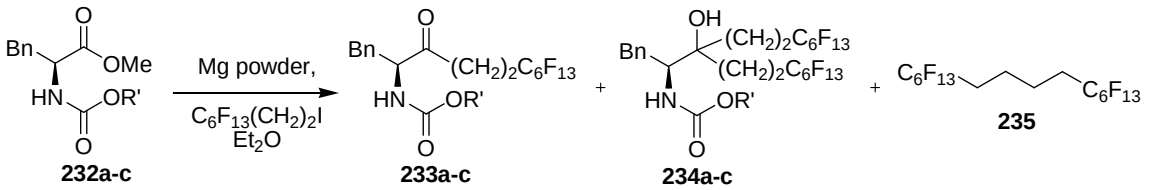

a: R' = Et
b: R' = *i*Pr
c: R' = Bn

entry	ester.	R'	$C_6F_{13}(CH_2)_2I$ eqv	ketone [a]	alcohol [a]
1	**232a**	Et	1.5	**233a** (25%)	**234a** (–)
2	**232a**	Et	3.0	**233a** (42%)	**234a** (36%)
3	**232b**	*i*Pr	2.0	**233b** (21%)	**234b** (6%)
4	**232b**	*i*Pr	3.0	**233b** (30%)	**234b** (17%)
5	**232c**	Bn	3.0	**233c** (15%)	**234c** (5%)

[a] Yield represents percent conversion from the corresponding electrophile.

Using the perfluoroalkyl iodide containing an alkyl spacer did produce a more stable fluorous nucleophile. Using the Grignard reagent derived from $C_6F_{13}(CH_2)_2I$ it was possible to obtain perfluoroketone **233** in yields of up to 42% (Table 3.2.2.1, entry 2), while the Grignard reagent generated from $C_8F_{17}I$ degraded too rapidly to be applied. However, using the $C_6F_{13}(CH_2)_2^-$ nucleophile also led to the formation of tertiary alcohols **234**. The increased stability and propensity to form dialkylated products both highlight the strong insulating effect methylene spacers can have when placed between perfluoroalkyl groups and reactive centres.[228] When nucleophiles derived from $C_8F_{17}I$

were reacted with ester **208**, only perfluoroalkyl ketones were generated, due to the stability of tetrahedral intermediate **215** (Scheme 3.2.2.1).[215,218] In the corresponding reaction with the nucleophile generated from $C_6F_{13}(CH_2)_2I$, the ethylene spacer insulates the reactive centre, removing any stabilizing effect the perfluoroalkyl group may impart on intermediate **236**. This allows the intermediate to decompose in solution, giving ketone **233** which then undergoes a second perfluoroalkylation to yield tertiary alcohol **234** (Scheme 3.2.2.1).

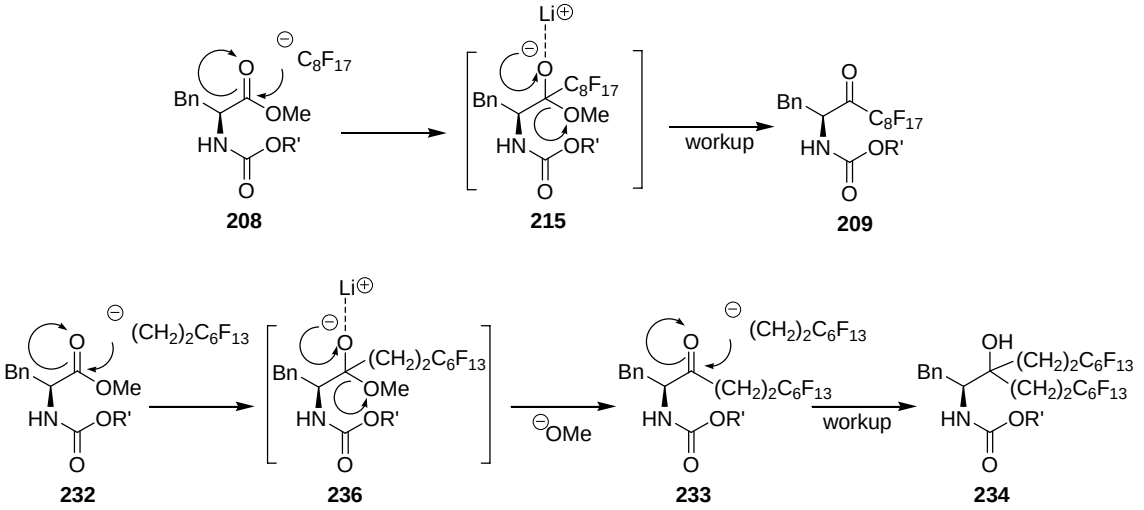

Scheme 3.2.2.1: Mechanism for mono- and bis-perfluoroalkylation of *N*-carbamoyl esters.

The Grignard reagent could be generated using finely powdered magnesium and $C_6F_{13}(CH_2)_2I$ in Et_2O; however, the results were highly dependant on the concentration of the perfluoroalkyl iodide and temperature during the formation of the Grignard reagent. Typically, if the reagent concentration exceeded 0.4M or the reaction temperature was greater than 25 ºC, then significant quantities of dimer **235** were generated via Wurtz coupling. The concentration of the free perfluoroalkyl iodide could be controlled by adjusting the addition rate of $C_6F_{13}(CH_2)_2I$ to the magnesium, provided the initiation of

the Grignard formation was sufficiently rapid. This swift initiation allowed the formation of the Grignard to proceed smoothly, but was very difficult to achieve, leading to poor reproducibility.

The presence of the fluorous tag permitted the use of FSPE to purify the products of these reactions. The quenched reactions were evaporated, and the crude residues were applied as concentrated solutions to short pads of FluoroFlash™ silica gel. Using this protocol, the fluorous compounds **233**, **234** and **235** could be easily separated from non-fluorous (organic and inorganic) materials. In addition it was possible to isolate products of differing fluorine content simply by adjusting the polarity of the eluting solvent, allowing the facile separation of perfluoroalkyl ketones **233a-c**, bis(perfluoroalkyl)alcohols **234a-c** and perfluoroalkyl dimer **235** in only three fractions from the FSPE pad. Washing the solid phase with 70% MeOH in water removed organic and inorganic byproducts. Ketones **233** could be selectively eluted using 85% MeOH in water, then washing with pure MeOH released tertiary alcohols **234**. Finally the perfluoroalkyl dimer could be eluted from the solid phase using diethyl ether.

Loss of perfluoroalkyl material via Wurtz coupling is a common problem with these Grignard reagents and has been noted previously.[203,219] In general, a three-fold excess of the fluorous iodide was required to give adequate conversion to the fluorous products (Table 3.2.2.1, entries 1 and 3). While many successful protocols for forming and applying this perfluoroalkyl Grignard regent have been reported,[117,188] we could not obtain consistent results in these studies.

Table 3.2.2.2: Effect of solvent composition on perfluoroalkyllithium addition.

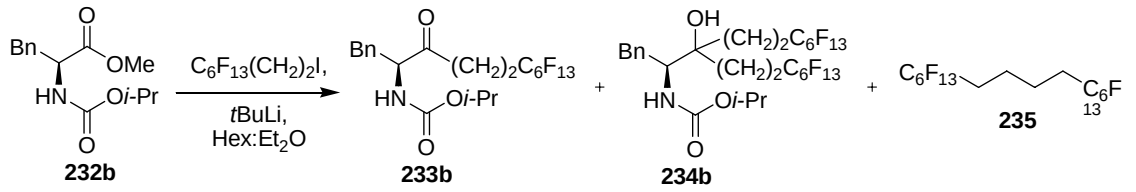

entry	solvent A	solvent B	ratio (A:B)	ketone [a]	alcohol [a]
1	Et_2O	–	–	10%	–
2	Et_2O	Hexanes	2:1	30%	15%
3	Hexanes	Et_2O	1:1	33%	21%
4	Hexanes	Et_2O	1.5:1	39%	19%
5	Hexanes	Et_2O	2:1	38%	18%
6	Hexanes	Et_2O	3:1	14%	–
7	Hexanes	Et_2O	5:1	–	–

[a] Yield represents percent conversion from the corresponding electrophile.

Perfluoroalkylation of esters using a lithium reagent was also investigated; however, initial studies revealed that this species displayed a strong dependence on the solvent composition (Table 3.2.2.2). In each case, the perfluoroalkyllithium regent was generated by dissolving $C_6F_{13}(CH_2)_2I$, cooling to –78 °C and adding one equivalent of *t*-BuLi. Ester **232b** was then dissolved separately and added to the perfluoroalkyllithium reagent dropwise. Performing the reaction in neat diethyl ether gave only poor conversion to perfluoroketone **233b** (Table 3.2.2.2, entry 1). Reports by Legros *et*

al.[233,234] suggested that better yields could be obtained by using a mixed ether-hydrocarbon solvent system. The yield of perfluoroalkylated product **233b** and **234b** increased when a mixed solvent system of up to 2:1 hexanes:ether was employed (Table 3.2.2.2, entries 2, 3, and 4), with 1.5:1 hexanes:ether being the optimal solvent mixture (Table 3.2.2.2, entry 4). At –78 °C, ester **232b** was not sufficiently soluble in solvent systems containing more than two parts hexanes, resulting in a drop in yield of **233b** and **234b** (Table 3.2.2.2, entry 6 and 7).

The change in yield observed in this study can be explained by examining the aggregation state of the perfluoroalkyllithium reagent. While the exact structures and geometries of these aggregates vary depending on the alkyl species, most organolithium reagents exist as the monomer, dimer or tetramer in solution (Figure 3.2.2.1). [221,222] The population of these three species is controlled to some extent by the Lewis basicity of the solvent, with the smaller dimeric and monomeric forms being favored in coordinating solvents, while the tetramer is more stable in hydrocarbon solvents.[235] With the perfluoroalkyllithium reagent lower yields were observed when a strongly coordinating solvent was used, but improved as the hydrocarbon content was increased. This indicates that the $C_6F_{13}(CH_2)_2Li$ tetramer is a better perfluoroalkylating agent than are the monomeric and dimeric aggregates. With most organolithium reagents, the monomer and dimer are typically more reactive than the tetramer.[236-238] However, it is possible that the smaller aggregates are more unstable, leading to decomposition instead of addition. Perfluoroalkyl species, such as $C_6F_{13}(CH_2)_2Li$, are known to decompose under strongly basic conditions, producing HF.[121,228] Therefore, the mixed solvent system gives rise to a

greater concentration of the stabilized tetramer, leading to better yields of the perfluoroalkylated products.

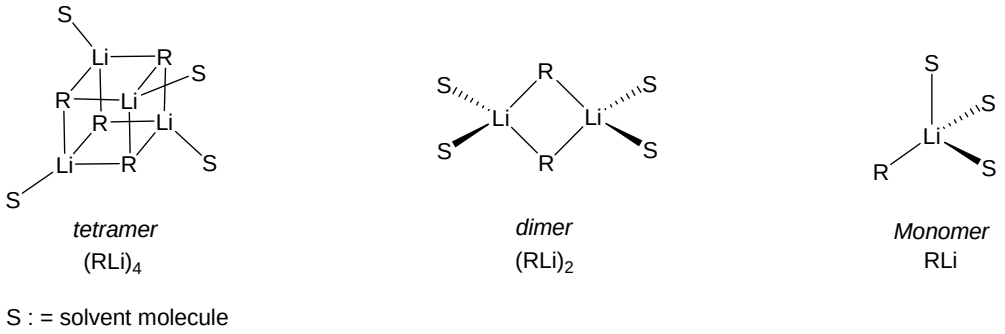

Figure 3.2.2.1: Solvated aggregates of organolithium reagents.[221]

The optimal solvent conditions for the generation and reaction of the perfluoroalkyllithium reagent were applied to amino esters **232a–c** (Table 3.2.2.3). In contrast to the results obtained with the perfluoroalkyl Grignard reagents, the lithium reagent gave moderate to good yields of fluorous materials using only 1.5 – 2.0 equivalents.

The best overall yields of perfluoroalkyl adducts were obtained using ester **232b** indicating the isopropyl carbamate was superior to the other protection groups. (Table 3.2.2.3). The previous Grignard studies indicated that *N*-ethyl carbamate **232a** was a superior electrophile (Table 3.2.2.1, entry 2); however, it was not sufficiently soluble in the mixed hexanes:ether solvent necessary for the generation and reaction of the perfluoroalkyl lithium reagents. Benzyl carbamate **232c** failed to perform well due to difficulties associated with its purification. The organometallic additions were quite sensitive to the presence of protonated impurities, including traces of water or alcohol contaminants left from the formation of the *N*-carbamoyl esters. Because these esters

were prepared in large batches (typically 5 – 15g), purification by chromatography was not a viable option. Instead, recrystallization, trituration, and solid phase extraction were relied upon to purify the necessary starting materials. It was quite simple to remove the more volatile ethanol byproduct from ester **232a** using reduced pressure and solid phase extraction from normal silica gel. Additionally, ester **232b** was a solid allowing it to be readily obtained on large scales by recrystallization. Benzyl carbamate **232c** was a viscous oil at room temperature, and presented some challenges due to traces of benzyl alcohol, which is significantly more non-polar and has a low volatility making it harder to remove with the methods available.

Table 3.2.2.3: Perfluoroalkyllithium addition to *N*-carbamoyl amino esters.

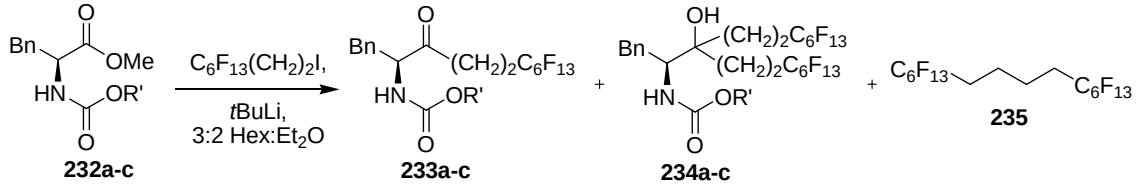

a: R' = Et
b: R' = *i*Pr
c: R' = Bn

entry	ester.	R'	$C_6F_{13}(CH_2)_2I$ eqv	ketone [a]	alcohol [a]
1	**232a**	Et	2.0	**233a** (18%)	**234a** (2%)
2	**232b**	*i*Pr	1.5	**233b** (39%)	**234b** (19%)
3	**232b**	*i*Pr	2.0	**233b** (47%)	**234b** (32%)
4	**232b**	*i*Pr	3.0	**233b** (12%)	**234b** (68%)
5	**232c**	Bn	2.0	**233c** (10%)	**234c** (0%)

[a] Yield represents percent conversion from the corresponding electrophile.

The ratio of **233** to **234** could be controlled to some extent by adjusting the amount of the perfluoroalkyllithium reagent applied. The tertiary alcohols **234** predominated when a three-fold excess of the perfluoroalkyllithium species was employed (Table 3.2.2.1, entry 6). The use of smaller amounts of the nucleophile to favour the formation of ketones **233a-c** could not be achieved without a significant sacrifice in the overall conversion of the reaction.

Although the perfluoroalkylation of the esters did not produce the required ketone selectively, the method for generating the perfluoroalkyllithium reagent proved to be very efficient and reliable. Given this achievement, the most obvious course of action was to modify the electrophile. Weinreb amides derived from amino acids readily undergo nucleophilic addition of a variety of organometallic reagents to give the corresponding amino ketones.[239] The formation of a stabilized tetrahedral intermediate *in situ* prevents further nucleophilic addition, similar to the behavior of intermediate **215**.[208,209] To investigate this pathway further, amides **240a-c** were prepared using a mixed anhydride protocol, according to reported procedures (Scheme 3.2.2.2).[240,241]

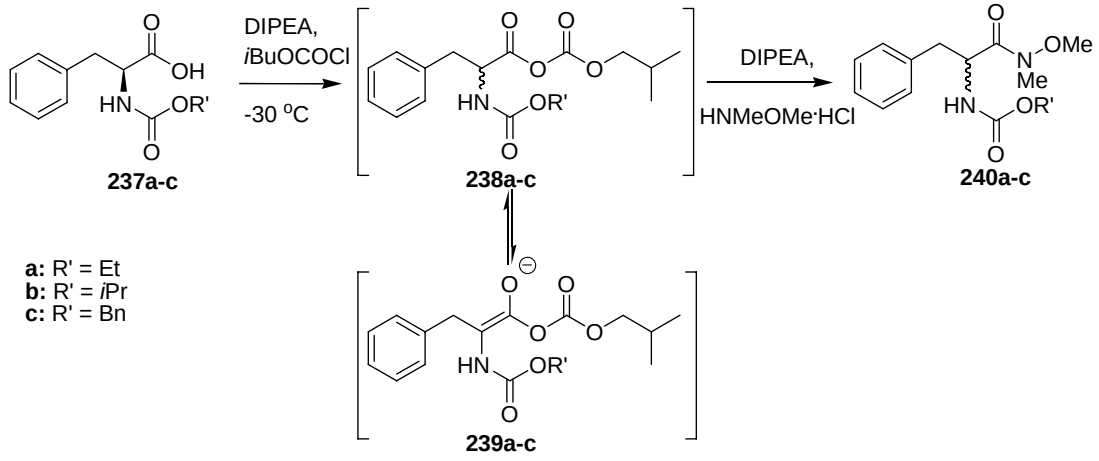

Scheme 3.2.2.2: Epimerization during the formation of Weinreb amides.

N-Carbamoyl amino acids **237a-c** were prepared using standard Schotten-Baumann conditions[242] and then treated with isobutyl chloroformate to form the mixed anhydride intermediates **238a-c**. Adding *N,O*-dimethoxyhydroxylamine hydrochloride to the reaction gave amides **240a-c**; however, the materials isolated in the preliminary studies displayed optical rotations significantly lower than the values reported in the literature,[240,243] indicating that epimerization had occurred at the α-centre. Under the basic conditions of the reaction, enolates **239a-c** can be generated, transforming the α position to an sp^2 centre and giving rise to both enantiomers of amides **240a-c**. However, the crude materials could be dissolved in dry diethyl ether, resulting in the selective crystallization of the racemic amides. Filtration of this solution yielded an enantiomerically enriched **240** from the mother liquor as a clear oil. To rectify this problem a series of reaction conditions were explored using *N*-carbamoyl amino acid **237c** (Table 3.2.2.4). In each case the acid was activated using some appropriate coupling agent, and then treated with *N,O*-dimethoxyhydroxylamine hydrochloride. The crude products were dissolved in Et_2O to remove the racemate allowing the degree of epimerization to be monitored.

Table 3.2.2.4: Formation of *N*-carbamoyl Weinreb amides.

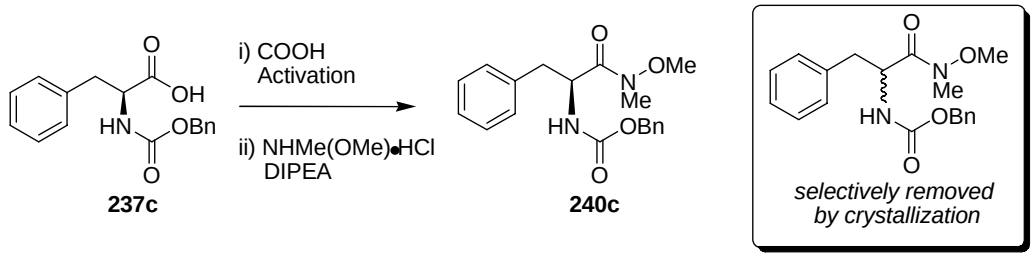

entry	Activating agent	temperature	amide [a]	racemate [a]
1	*i*BuOCOCl	–10 °C	56%	24%
2	*i*BuOCOCl	–20 °C	68%	17%
3 [b]	*i*BuOCOCl	–20 °C	34%	33%
4	*i*BuOCOCl	–30 °C	84%	6%
5	CMPI	reflux	65% [c]	–
6	CDMT	0 °C	78%	11%
7	TBTU	0 °C	85%	–

[a] Values represent mass recovered from solution after precipitation of racemic crystals from Et_2O; [b] Reaction performed in THF; [c] Recovered yield following flash chromatography.

Experimentation revealed that the extent of epimerization was increased when the reaction was performed in polar solvents such as THF (Table 3.2.2.4, entry 3), but could be minimized by carefully controlling the reaction temperature during the generation of the anhydride (Table 3.2.2.4, entries 1, 2 cf. 4). The coupling agent CDMT[244] was very convenient to use and gave products free of impurities, but significant epimerization was

still observed. Conversely, CMPI[245] did generate the target amides without detectable optical degradation, but flash chromatography on silica was required to sufficiently purify amide **240c** for use in further reactions. Ultimately TBTU was discovered as the superior coupling reagent, promoting Weinreb amide formation at 0 ºC without epimerization. Using this method, Weinreb amides could be readily prepared on gram scales with no need for further purification after simply extracting the products from the quenched reaction mixtures with ether (Table 3.2.2.4, entry 7).

Amides **240a-c** were submitted for perfluoroalkylation using the conditions developed for esters **232a-c** (Table 3.2.2.5). Despite the previous difficulty preparing and applying the perfluoroalkyl Grignard reagent, both the perfluoroalkyllithium and Grignard nucleophiles were evaluated. In all cases, only perfluoroketone **233** was isolated, with no evidence of the tertiary alcohol. This indicated that the Weinreb amides form a sufficiently stabilized intermediate *in situ*, preventing further addition of the perfluoroalkyl nucleophile. While it was possible to obtain ketones **233a-c** as the sole perfluoroalkylated product, an excess of the fluorous nucleophile was still required to obtain acceptable yields (Table 3.2.2.5, entry 2 vs. 7). This excess was necessary due to the carbamate NH, which can donate a proton to strongly basic species resulting in the loss of up to one equivalent of the Grignard or lithium reagent. While this point is common to all such organometallic additions to *N*-carbamoyl Weinreb amides, typically the nucleophile is simply applied in excess to ensure complete conversion.[208,209,239] In cases where the organometallic reagent is expensive or difficult to prepare the application of multiple equivalents is not acceptable.

Table 3.2.2.5: Perfluoroalkyl addition to *N*-carbamoyl Weinreb amides.

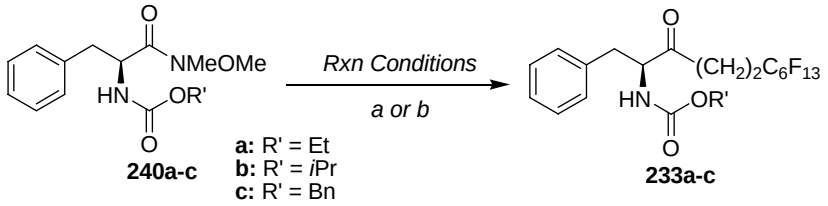

240a-c **a:** R' = Et **b:** R' = *i*Pr **c:** R' = Bn **233a-c**

entry	amide.	R'	rxn	$C_6F_{13}(CH_2)_2I$ eqv	ketone[c]
1	**240a**	Et	*a*	2.5	**233a** (19%)
2	**240a**	Et	*b*	1.5	**233a** (48%)
3	**240b**	*i*Pr	*a*	3.0	**233b** (18%)
4	**240b**	*i*Pr	*b*	2.3	**233b** (38%)
5	**240c**	Bn	*a*	2.5	**233c** (27%)
6	**240c**	Bn	*b*	1.5	**233c** (30%)
7	**240a**	Et	*b*	3.5	**233a** (61%)
8	**240a**	Et	*b*,[d]	1.5	**233a** (68%)
9	**240a**	Et	*b*,[e]	1.5	**233a** (75%)

[a] Mg powder, $C_6F_{13}(CH_2)_2I$, Et_2O; [b] *t*-BuLi, $C_6F_{13}(CH_2)_2I$, Ether:Hex, −78°C → r.t.; [c] Percent conversion from the corresponding electrophile; [d] *n*-BuLi used as sacrificial base; [e] *t*-BuLi used as sacrificial base.

To circumvent these problems, a sacrificial alkyllithium base can be employed to deprotonate the carbamate N-H prior to introducing the desired nucleophile (Scheme

3.2.2.3).[210,246] Thus Weinreb amide **240a** was dissolved in the required hexanes:ether mixed solvent and cooled to -78 ºC. Adding either *n*-BuLi or *t*-BuLi to the amide produced a faintly purple-colored solution, indicative of a lithium-stabilized anionic carbamate species, such as **241a**.[169] This deprotonated electrophile was added to a solution containing the perfluoroalkyllithium reagent to yield perfluoroketone **233a**. Using this protocol and only 1.5 equivalents of perfluoroalkyl iodide, the yield of ketone **233a** increased from 48% obtained without a sacrificial base, to 68% and 75% using *n*-BuLi and *t*-BuLi respectively (Table 3.2.2.5, entries 8 and 9).

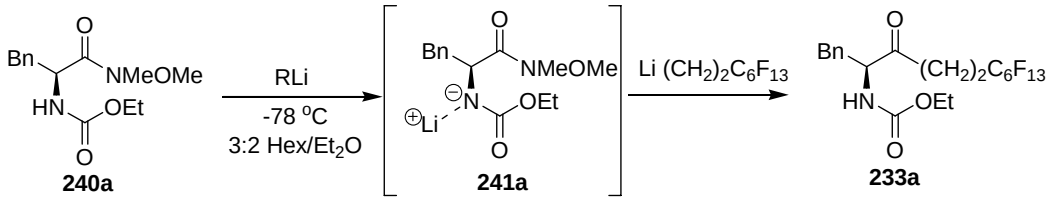

Scheme 3.2.2.3: Perfluoroalkyllithium addition using predeprotonation.

Perfluoroalkyl ketones **233a-c** could be reduced diastereoselectively using $LiAlH(OtBu)_3$ in EtOH at -78 ºC. The reduction proceeds via chelated intermediate **190** to give the *anti* diastereomer of the corresponding *N*-carbamoyl alcohol **191**. In all cases the alcohols were isolated in excellent yield and did not require further purification after simply extracting the products from the quenched reaction mixtures with ether (Table 3.2.2.6).

Table 3.2.2.6: Diastereoselective reduction of perfluoroalkyl ketones.

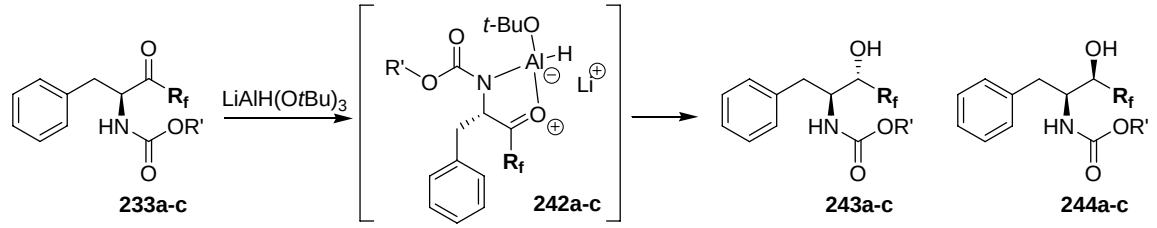

R_f: = $(CH_2)_2C_6F_{13}$ **a**: R' = Et
b: R' = *i*Pr
c: R' = Bn

entry	ketone	R'	solvent	yield	selectivity (*syn*:*anti*)
1	**233a**	Et	EtOH	95%	1 : >99
2	**233a**	Et	THF	95%	1 : 2.4
3	**233b**	*i*Pr	EtOH	99%	1 : >99
4	**233c**	Bn	EtOH	97%	1 : >99

Unlike ketones **209a** and **209b**, which contain a C_8F_{17} perfluoroalkyl fragment, ketones **233a-c** were reduced with excellent diastereoselectivity to give only *anti* alcohol **243a-c** with no evidence of *syn N*-carbamoyl alcohol **244a-c**. Clearly, by adding the ethylene spacer the strong electron withdrawing effects of the perfluoroalkyl group have been sufficiently masked. The carbonyl of ketones **233a-c** is now a strong enough Lewis base to effectively displace one of the O*t*Bu ligands from the aluminum centre, permitting the formation of chelated transition structure **242**. From this intermediate, the hydride reduction proceeds with excellent diastereoselectivity giving only the *anti* geometry of the corresponding alcohol. The nature of the solvent proved critical to achieving high diastereoselectivity, as reactions in THF showed only a slight preference for the

chelation-controlled pathway (Table 3.2.2.6, entries 1 vs. 2). This agrees with our previous results (Section 3.2.1, Table 3.2.1.3), and with the observation made by Hoffman *et al.*[206] indicating that the solvent participates in the formation of chelated intermediate **242** by promoting ligand exchange (Section 3.2.1, Scheme 3.2.1.6).

Alcohols **243a-c** were treated with NaH in THF to give the corresponding mono(perfluoroalkyl) oxazolidinone **245**. Bis(perfluoroalkyl) alcohols **234a-c** could also be converted to 5,5 disubstituted oxazolidinone **246** using similar conditions (Scheme 3.2.2.4). In both cases the cyclization proceeded smoothly at room temperature, but required long reaction times to ensure complete conversion. It was possible to accelerate the cyclization by performing the reaction at elevated temperatures, but this was accompanied the production of an uncharacterized polar byproduct and a corresponding drop in the yield of **245**. The added time needed to remove this byproduct following cyclization at elevated temperatures offset any benefit offered by this route, making the room temperature protocol more favourable.

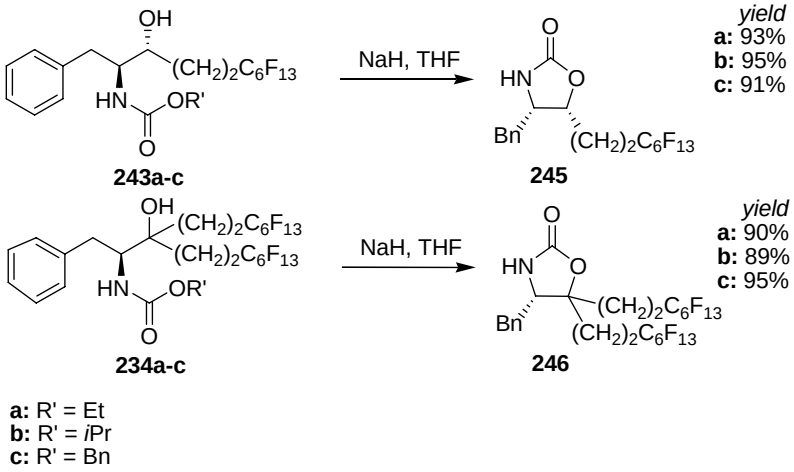

Scheme 3.2.2.4: Cyclization of perfluoroalkyl alcohols to oxazolidinones

The relative geometry at the 4 and 5 centres of **245** was investigated using a combination of ^{1}H NMR and 1D selective NOE experiments. The vicinal coupling constant between the two methine protons was 7.2 Hz, which is indicative of a *syn* geometry at *C*4 and *C*5 in **245**. Nuclear Overhauser effect experiments further confirmed the *syn* geometry at the 4 and 5 centres, as 5% NOE was observed between the two oxazolidinone methine protons (Figure 3.2.2.2). This result is consistent with literature results,[206] and with our previous observations from the first generation oxazolidinones, **230** and **231**.

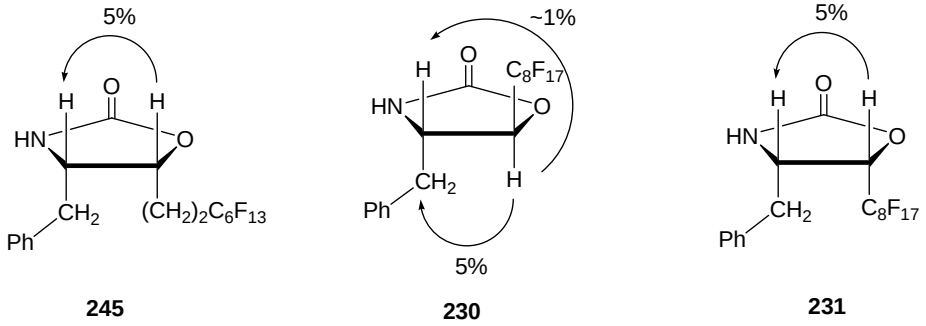

Figure 3.2.2.2: NOE results for *syn* and *anti* 4,5 disubstituted oxazolidinones.

To further study the structure of oxazolidinone **245** crystals were grown using slow evaporation from diethyl ether and submitted for characterization by X-ray diffraction. Analysis revealed that the correct diastereomer had been synthesized as the substituents at C4 and C5 (labeled C2 and C3 in Figure 3.2.2.3) were arranged with a *syn* geometry. However, the crystal was found to be triclinic with a $P\bar{1}$ space group, indicating that both enantiomers of the oxazolidinone were present in the unit cell. This result alerted us to the degree of epimerization which was occurring during the generation of Weinreb amide **240**a (see Scheme 3.2.2.2)**.** The epimerization of amide **240a** can be rectified by using TBTU (Table 3.2.2.4).

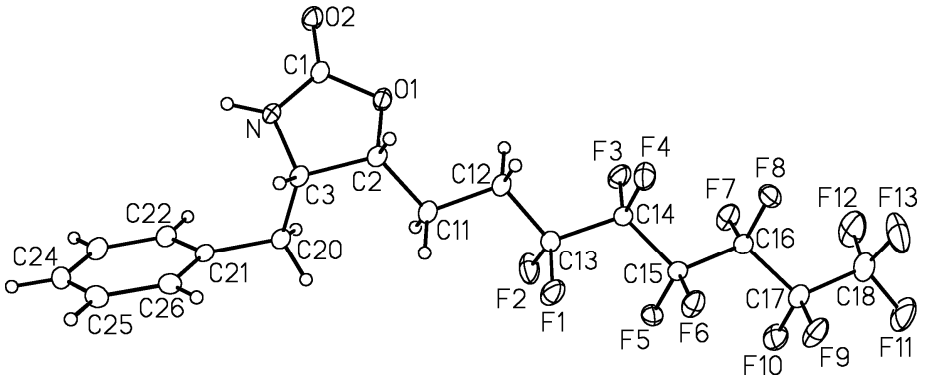

Figure 3.2.2.3: X-ray structure of oxazolidinone **245**.

To ensure that a single enantiomer was being produced from the enantiomerically pure amide **240a** the enantiomeric excess of amino alcohol **243a**, generated using the TBTU protocol, was measured by conversion to the corresponding (*S*) and (*R*)-MTPA esters (Scheme 3.2.2.5). The ^{1}H and ^{19}F NMR spectra of esters **247** and **248** clearly indicated that only one diastereomer was present, confirming that alcohol **243a** was generated as a single enantiomer. This result indicates that oxazolidinone **245** must also be of sufficiently high enantiomeric excess.

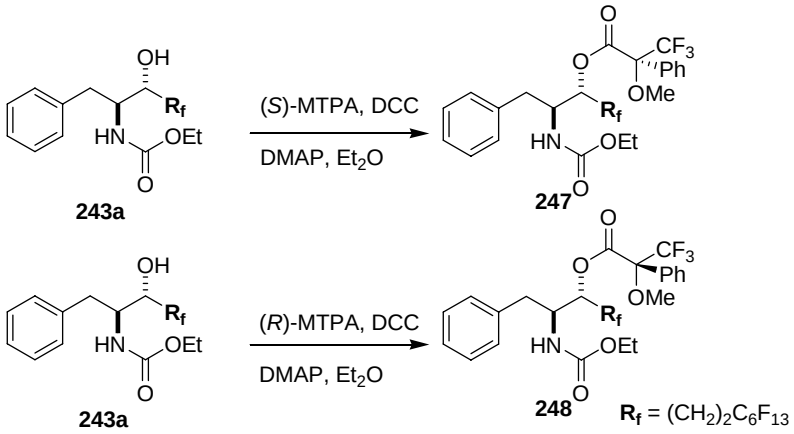

Scheme 3.2.2.5: Esterification of alcohol **243a** with (*R*) and (*S*) MTPA.

3.2.3 Extension of the General Synthetic Route

After extensive investigation, the most favourable route had been identified, allowing the synthesis of oxazolidinone **245** from L-phenylalanine in five steps (Scheme 3.2.3.1). While many of the parent *N*-carbamoyl electrophiles (esters **232a-c** and amides **240 a-c**) could be prepared with approximately the same ease, the efficiency with which ketone **233a** could be produced was the ultimate deciding factor in selecting the best candidate for production of the target oxazolidinone.

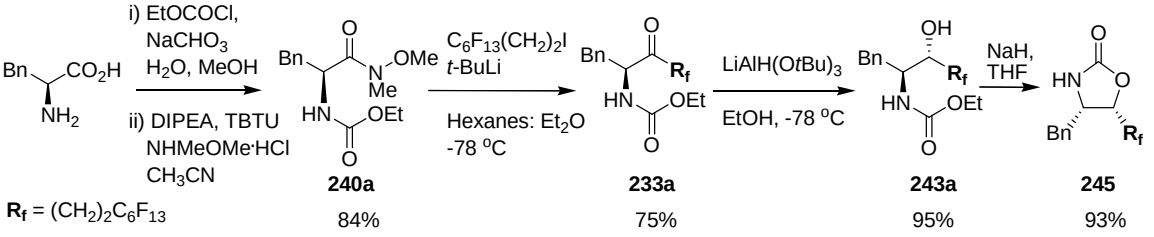

Scheme 3.2.3.1: Optimized synthesis of oxazolidinone **245**

While the initial studies were focused on L-phenylalanine as the primary starting point, it is evident that the same protocol could be applied to almost any chiral α amino acid with only minor modifications. Some compounds containing protonated or acidic functional groups, such as serine, tyrosine or aspartic acid, would require some appropriate protection prior to perfluoroalkylation; however, amino acids with unfunctionalized side chains (Scheme 3.2.3.2, R = alkyl or aryl) should react under analogous conditions to give the corresponding oxazolidinones.

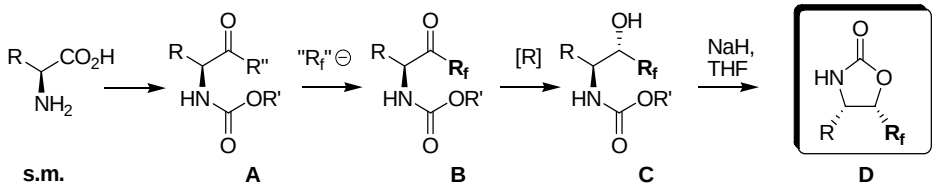

Scheme 3.2.3.2: General synthetic pathway for the synthesis of fluorous oxazolidinones

To investigate the breadth of the synthetic pathway, esters **249** and **252** were synthesized from L-valine and D-phenylglycine respectively and submitted for perfluoroalkylation using the optimized conditions employed for amide **240a** (Scheme 3.2.3.3). The corresponding perfluoroketones **250** and **253** were obtained in moderate yields along with tertiary alcohols **251** and **254**.

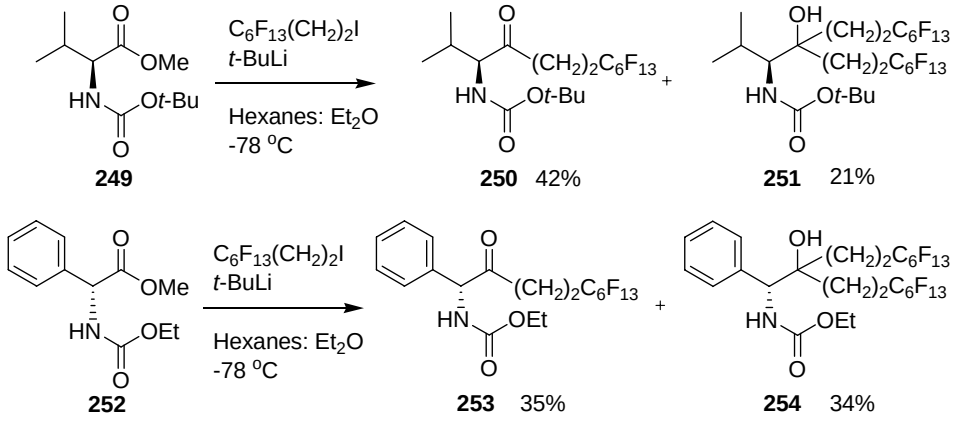

Scheme 3.2.3.3: Perfluoroalkylation of *N*-carbamoyl amino esters **249** and **252**.

These results correlated with observations from the L-phenylalanine systems, and as before the ketones **250** and **253** could be separated from tertiary alcohols **251** and **254** simply by using FSPE. The two bis(perfluoroalkyl) species were then easily cyclized to give the corresponding 5,5 disubstituted oxazolidinones **203** and **204** (Scheme 3.2.3.4).

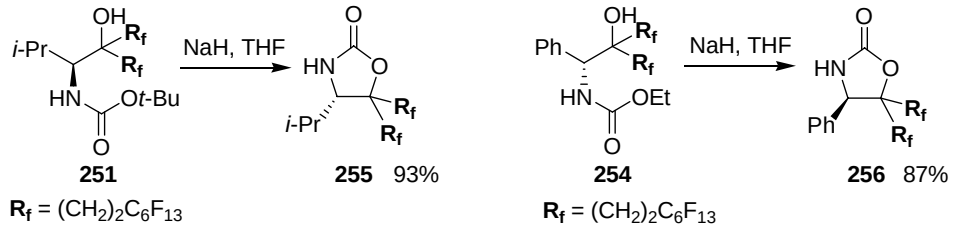

Scheme 3.2.3.4: Cyclization of bis(perfluoroalkyl) alcohols.

As in the case of the L-phenylalanine system, using the corresponding *N*-carbamoyl Weinreb amides led to the selective formation of the perfluoroketones. In the

case of the L-valine system the identical reaction conditions originally developed for L-phenylalanine could be directly applied to give similar yields and selectivities (Scheme 3.2.3.5). Amide **257** was submitted for perfluoroalkylation using $(CH_2)_2C_6F_{13}Li$ and *t*-BuLi as a sacrificial base to give ketone **250**. This was reduced diastereoselectively, yielding alcohol **258** as the sole product, indicating that the reaction was proceeding through a chelated transition structure. The perfluoroalkyl alcohol was then cyclized to give oxazolidinone **259**. The *syn* geometry of the 4 and 5 substituents was confirmed in the same fashion as the previous oxazolidinones using ^{1}H NMR and nuclear Overhauser effect experiments.

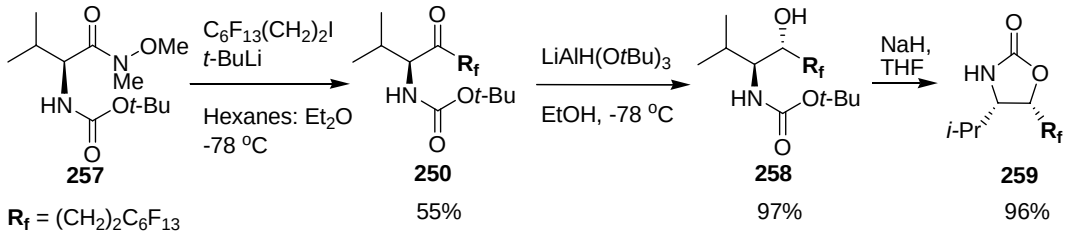

Scheme 3.2.3.5: Synthesis of fluorous oxazolidinone from L-valine.

As with the L-phenylalanine system, the enantiomeric excess of the oxazolidinone **259** was estimated by conversion of the intermediate alcohol **258** to the corresponding (*S*) and (*R*)-MTPA esters (Scheme 3.2.3.6). The ^{1}H and ^{19}F NMR spectra of esters **260a** and **260b** clearly indicated that only diastereomer was present in each case.

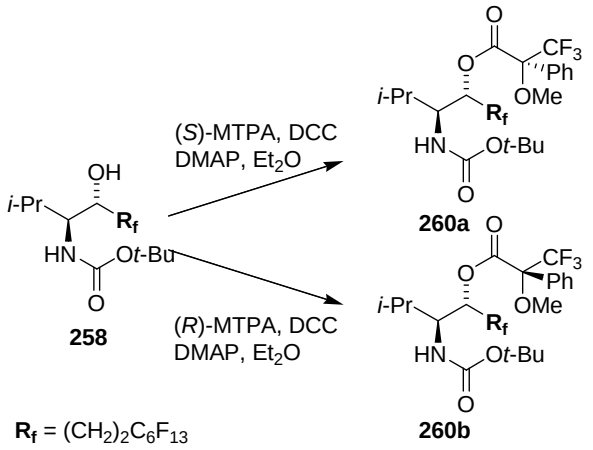

Scheme 3.2.3.6: Esterification of alcohol **258** with (*R*) and (*S*) MTPA.

Conducting the perfluoroalkylation with D-phenylglycine did not prove to be as successful (Scheme 3.2.3.7). Amide **261** could be converted to ketone **262** using the same method of perfluoroalkylation applied to amides **257** and **240a** derived from L-valine and L-phenylalanine respectively. This ketone could be reduced diastereoselectively using chelation control to give *anti* alcohol **263** as the sole product. However, the optical rotations of ketone **262** and alcohol **263** were both near zero.

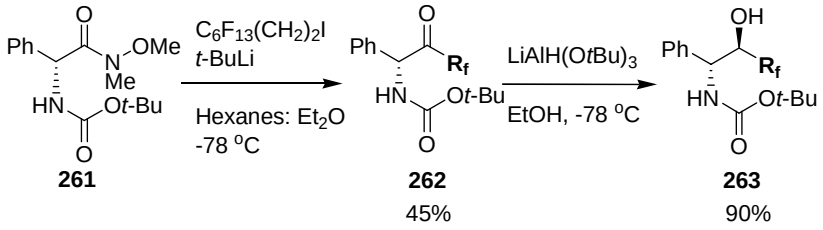

Scheme 3.2.3.7: Perfluoroalkylation of amide **261** derived from D-phenylglycine.

This observation raised concerns about loss of enantiomeric purity during this synthesis. To examine the situation further, the enantiomeric excess of alcohol **263** was measured by conversion to the corresponding (*S*) and (*R*)-MTPA esters (Scheme 3.2.3.8). Esters **264a** and **264b** were both isolated as a 1:1 mixture of diastereomers, indicating

that alcohol **263** must be racemic. The loss of enantiomeric purity in the D-phenylglycine system likely occurs at the perfluoroalkylation stage, indicating that the strongly basic perfluoroorganometallic reagent is acting to deprotonate the α centre in the amide **261**. This is not surprising, as the relatively milder cyclization conditions also resulted in epimerization at this centre.

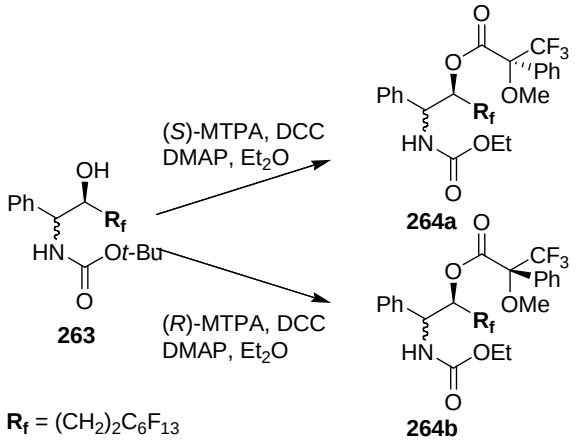

Scheme 3.2.3.8: Esterification of alcohol **263** with (*R*) and (*S*) MTPA.

Alcohol **263** was submitted for cyclization using the same procedure applied to the L-valine and L-phenylalanine systems, despite the presence of both enantiomers. Unlike the previous system, cyclization using NaH in THF resulted in the generation of two diastereomeric oxazolidinones (Scheme 3.2.3.9). ^{1}H NMR and 1D selective NOE experiments confirmed that both the *syn* and *anti* oxazolidinones, **265** and **266** respectively, had been generated.

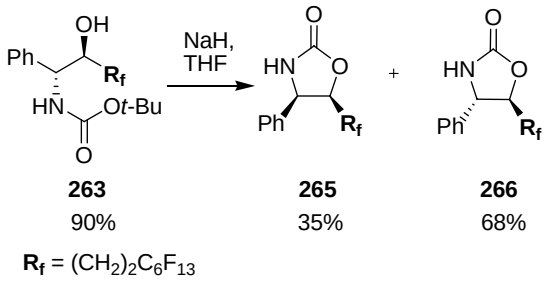

263 90%

265 35%

266 68%

$R_f = (CH_2)_2C_6F_{13}$

Scheme 3.2.3.9: Cyclization of alcohol **263** derived from L-phenylglycine.

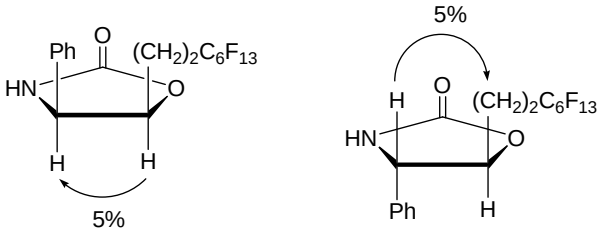

J_{H4H5} = 7.3 Hz

265

J_{H4H5} = 3.2 Hz

266

Figure 3.2.3.1: Coupling constants and NOE results from oxazolidinones **265** and **266**.

Alcohol **263** was studied using HPLC and NMR allowing us to confirm that it had been isolated as a single diastereomer. Thus, the generation of both diastereomers was not due to poor diastereoselectivity in the reduction of ketone **262**. Instead, the two geometries likely arise via deprotonation at the α position resulting in anion **267** (Scheme 3.2.3.10). Due to resonance stabilization of this resulting carbanion, epimerization can readily occur.[247] Protonation of this species then gives rise to either the original alcohol **263** or the *syn* alcohol **268**, which both can undergo cyclization resulting in the *syn* and *anti* oxazolidinones **265** and **266**.

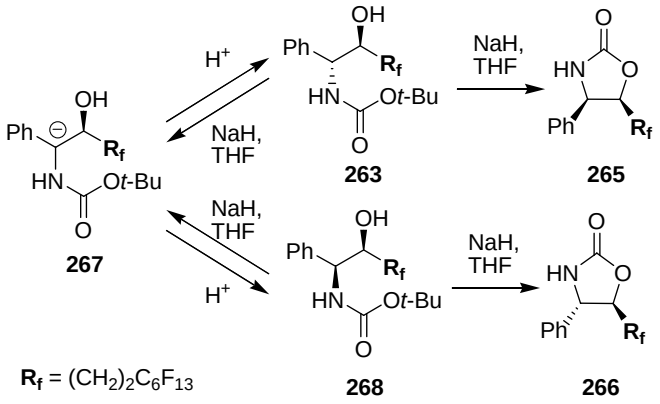

Scheme 3.2.3.10: Epimerization of perfluoroalcohol **263**.

While these results conclusively show L-valine and similarly unfunctionalized amino acids can be successfully employed in the general five step synthesis, compounds possessing a particularly acidic α proton are not suitable. At the present time, the loss of enantiomeric purity in the phenylglycine case does not appear reconcilable, as the major problem lies in the nucleophilic perfluoroalkylation central to this method. Extension of this synthesis to a wide variety of other unfunctionalized or suitably protected α-amino acids should be straight forward.

3.3 Application of the New Auxiliaries to Asymmetric Synthesis

Following the production of the two generations of oxazolidinone chiral auxiliaries, the focus of this research turned to evaluating these new compounds in stoichiometric asymmetric synthesis. As the goal of this project was to create a new auxiliary to rival the currently employed supported oxazolidinone auxiliaries, it was crucial that these new auxiliaries could meet three major criteria. First, the auxiliaries must be able to participate in a variety of asymmetric reactions, giving high stereoselectivity and good conversion for some particular isomer of the target molecule. Second, the fluorous support must assist in the purification of the desired products, allowing the supported materials to be selectively and rapidly recovered using FSPE. Finally, the auxiliary must be robust to allow recycling following completion of the asymmetric transformation, further improving the efficiency of this method and mitigating the large synthetic investment needed to produce the fluorous compound. To demonstrate the superiority of the fluorous chiral auxiliaries three model systems have been selected for study. Each investigation has been tailored to illustrate the fluorous auxiliaries' ability to meet the stated criteria, and allow direct comparison to results from other supported and non-supported oxazolidinone auxiliaries.

3.3.1 Asymmetric Aldol Reactions using Titanium Enolates

The first generation auxiliaries **230** and **231** were acylated with propionyl chloride, to give derivatives **269** and **270**. Both compounds were converted to the corresponding titanium enolates using $Ti(Cl)_4$ and a variety of tertiary amine bases. This enolate was reacted with a series of aldehydes to give the corresponding aldol products.

By purifying the products using FSPE, the selectivity resulting from each variation could be quickly determined. Following quenching of the aldol reactions the solvents were removed under vacuum to yield crude residues. The residue was dissolved in a small volume of *n*-propanol and applied to column charged with perfluoroalkyl-modified silica gel (Tridecafluoro- 2™, Silicycle Inc.). Fluorophobic solvents, such as 30% *n*-PrOH in water, allowed impurities to be selectively washed from the column. The fluorous aldol products could then be eluted by using more fluorophilic solvents, such as THF or acetone. Following this purification the reaction products could be easily analyzed by HPLC and NMR to determine the diastereoselectivity of the reactions.

Table 3.3.1.1: Titanium mediated aldol reactions using the *anti* oxazolidinone **269**.

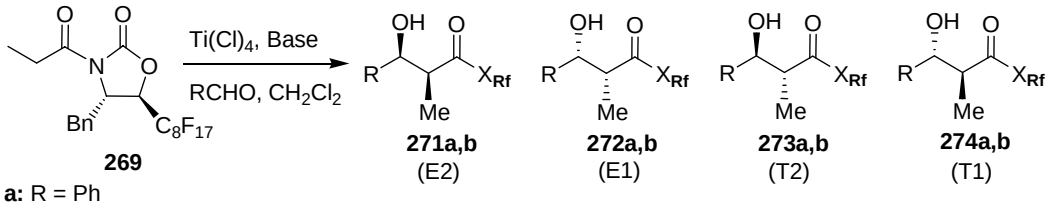

entry	aldehyde	temperature	base	yield [a]	selectivity [b] (271: 272 : 273 : 274)
1	PhCHO	–25 °C	TMEDA	78%	1 : 0.2: 0.4 : 0.3
2	PhCHO	0 °C	DIPEA	95%	1 : 1 : 1 : 1
3	PhCHO	–25 °C	DIPEA	91%	1 : 0.5 : 1 : 1
4	Me_2CHCHO	–25 °C	TMEDA	79%	1 : 1 : 1 : 1
5	Me_2CHCHO	–25 °C	DIPEA	84%	1 : 1 : 1 : 1

[a] Yields refer to recovery of aldol products; [b] Selectivity was measured using HPLC

Aldol reactions with propionyl derivative **269** derived from *anti* oxazolidinone **230** were not selective and gave mixtures of **271 – 274** (Table 3.3.1.1). This is not surprising when the transition structures predicted by the Zimmerman-Traxler model are considered (Scheme 3.3.1.1). Crimmins *et al.*[157] have shown that using these reaction conditions *N*-propionyl oxazolidinones are converted to the *Z* enolate selectively. Using the non-fluorous oxazolidinone derived from L-phenylalanine, addition of the aldehyde

proceeds selectively via a cyclic transition structure similar to **276**, to give the E2 geometry selectively.

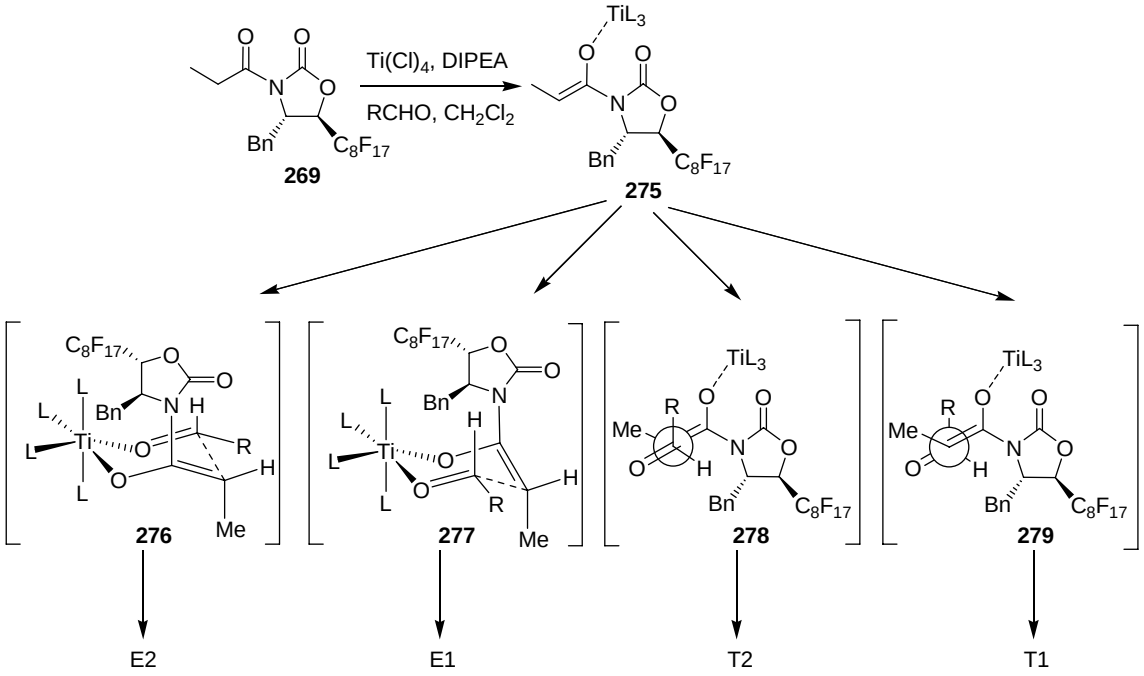

Scheme 3.3.1.1: Aldol transition structures for reaction supported on *anti* 4,5 disubstituted oxazolidinone **269**.

Using these conditions, *Z* enolate **275** should be formed, however the *anti* 4,5 substitution of the oxazolidinone ring complicates the aldol addition. Although the linear perfluoroalkyl chain will not have the same degree of steric influence as the benzyl group, it is clear from transition structures **276** and **277** that these two functional groups act to obstruct both the *re* and *si* faces of the enolate. As a result neither cyclic transition structure is energetically favoured, allowing both *erythro* products to be generated. The lack of facial selectivity in the cyclic transition structures explains the generation of both E1 and E2 but does not account for the *threo* products. It is possible that this competitive interaction between the benzyl and perfluoroalkyl groups destabilizes the cyclic transition states sufficiently to permit reaction via acyclic structures **278** and **279**,[39,248] giving the

T2 and T1 *threo* geometries respectively. From these results it is clear that 4,5 *anti* oxazolidinone **230** is a poor chiral auxiliary for this reaction.

Table 3.3.1.2: Titanium mediated aldol reactions using the *syn* oxazolidinone **270**.

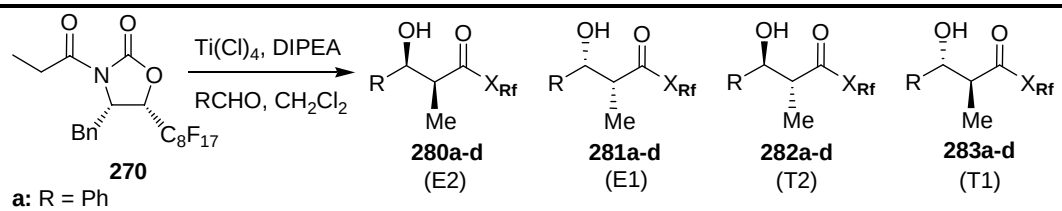

270

a: R = Ph
b: R = *i*Pr
c: R = $CH_3(CH_2)_5$
d: R = MeCH=CH
X_{Rf} : Fluorous auxiliary

280a-d (E2) | **281a-d** (E1) | **282a-d** (T2) | **283a-d** (T1)

entry	**aldehyde**	**major product**	**yield** [a]	**selectivity** [b] **(280: 281 : 282 : 283)**
1	PhCHO	**280a**	94%	>99 : <1 : 0 : 0 :
2	Me_2CHCHO	**280b**	74%	>99 : <1 : 0 : 0
3	$CH_3(CH_2)_5CHO$	**280c**	81%	93 : 0 : 7 : 0
4	MeCH=CHCHO	**280d**	80%	86 : 14 : 0: 0

[a] Yields refer to the purified major diastereomer; [b] Selectivity was measured using HPLC

Reactions with **270** derived from *syn* oxazolidinone **231** produced much better results, giving diastereomer **280** as the major product in each case (Table 3.3.1.2). These results agree with the observations reported by Crimmins *et al.*[157] indicating that kinetic enolate **284** is forming selectively, and that the reaction proceeds through bidentate transition structure **285** (Scheme 3.3.1.2). The *syn* auxiliary selectively blocks the *si* face of the enolate leading to the formation of the aldol product with the E2 geometry.

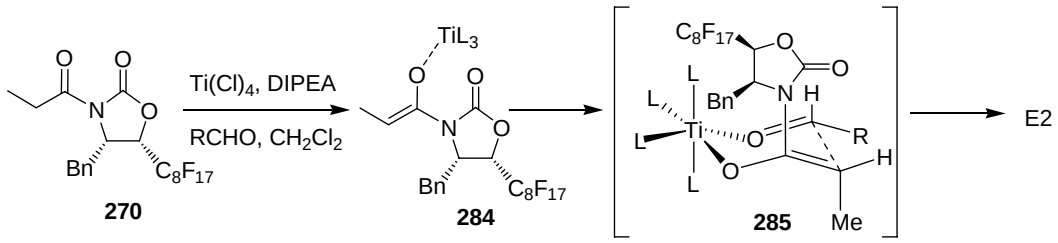

Scheme 3.3.1.2: Aldol transition structure for *syn* 4,5 disubstituted oxazolidinone.

The identities of the diastereomeric aldol products were assigned from their NMR spectra, after FSPE purification and, where necessary, separation of the diastereomers by preparative HPLC. The *erythro* and *threo* adducts were easily differentiated by the vicinal coupling constant between their α and β protons located at the two newly formed chiral centres.[155] Following characterization by NMR, the absolute geometries of the major adducts **280a-c** were assigned by conversion to the corresponding hydroxyacids **288a-c** and by comparison with literature optical rotations.[152,249,250] The acids were obtained by LiOOH hydrolysis of the aldol products,[58] which proceeds via nucleophilic attack at the exocyclic carbonyl to form tetrahedral intermediate **286** (Scheme 3.3.1.3). Addition of sodium sulfite leads to deacylation of the auxiliary by nucleophilic attack by the sulfur as shown in **287**,[251] to give oxazolidinone **231** and carboxylic acids **288a-c**.

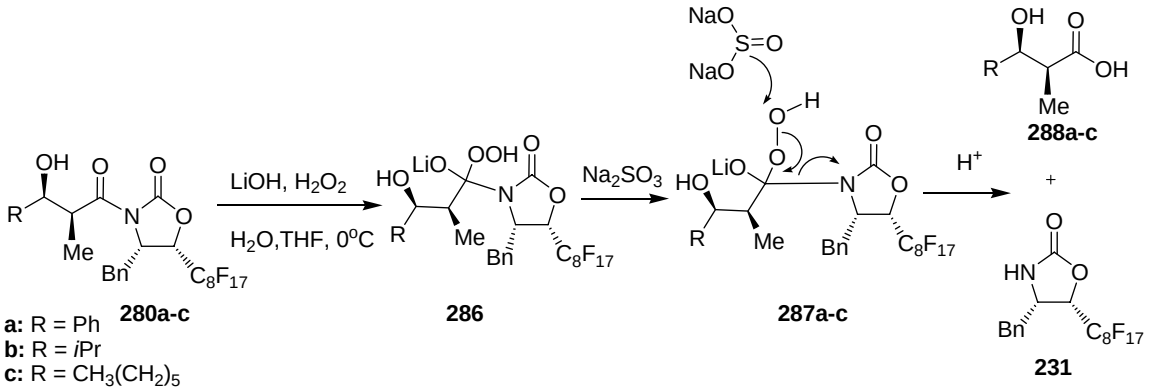

Scheme 3.3.1.3: Mechanism for LiOOH hydrolysis of *N*-acyl oxazolidinones.

No literature data was available for the carboxylic acid derived from crotyl aldol product **280d**. Instead, reductive cleavage to give diol **289** was necessary,[252] in order to correlate with literature values and confirm the absolute stereochemistry (Scheme 3.3.1.4).[250]

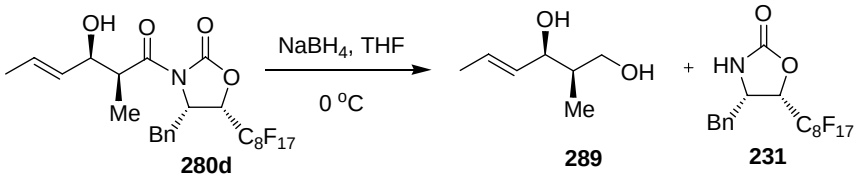

Scheme 3.3.1.4: Reductive cleavage of crotyl aldol product.

These results show that the *syn* fluorous auxiliary **231** is fully compatible with classical enolate reaction conditions, and behaves analogously to the well-known Evans auxiliaries for the set of aldehydes employed. This success should allow the application of the fluorous auxiliary in any synthetic strategy where an asymmetric aldol reaction using a non-fluorous oxazolidinones has been employed. In addition, the fluorous portion of the new auxiliary endows this compound with the benefits associated with standard supported protocols, allowing rapid screening of reaction conditions and facile purification.

A second key observation obtained from this study relates to the optimal relative geometry of the chiral auxiliary. Oxazolidinone **230** with the 4,5 *anti* geometry was found to be unsuitable for this reaction due to steric repulsion at both faces of the enolate. While the Zimmerman-Traxler model is unique to enolate reactions, a similar competing facial selectivity is predicted for other asymmetric transformations. Thus, only the *syn* geometry of the fluorous auxiliary was explored in further investigations.

3.3.2 Lewis Acid Mediated Radical Conjugate Additions

The second system investigated involved addition of nucleophilic radicals to α,β-unsaturated carboxylic acid derivatives. To begin the study of the fluorous oxazolidinone system, the required crotyl starting material **290a** was synthesized using a standard acylation protocol.[48] This material was reacted using a standard protocol developed by Sibi *et al.* [171,253] in conjunction with a series of Lewis acids.

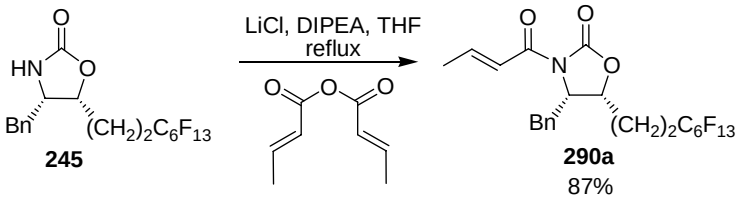

Scheme 3.3.2.1: Synthesis of *N*-crotyl fluorous oxazolidinone **290a**.

The purpose of the initial study was to identify reaction conditions capable of promoting conjugate addition to give **291a** and **292a** in preference to direct reduction yielding **293a** (Table 3.3.2.1). In general, the rare earth Lewis acids (in particular $Yb(OTf)_3$) gave the best results. Good stereoselectivity was observed with a number of Lewis acids but reduction product **293a** was a significant byproduct in some cases (Table 3.3.2.1, entries 2, 5, 11). This side reaction could be effectively suppressed at -78 ºC (Table 3.3.2.1, entry 5 *vs.* 6, 11 *vs.* 12).

Table 3.3.2.1: Effect of Lewis acids on radical conjugate additions.

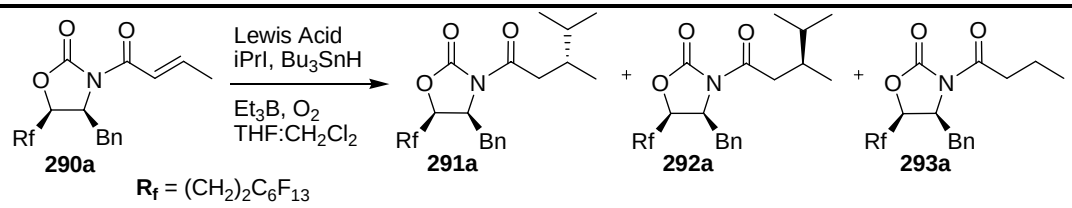

entry	Lewis acid	yield (%) [a,b]	temperature	selectivity (291a : 292a) [c]
1	—	58	0°C	1.1:1
2	$ZrCl_4$	44 (45)	0°C	6:1
3	$Fe(ClO_4)_3$	34 (22)	0°C	1.2:1
4	$Cu(OTf)_2$	31 (12)	0°C	2:1
5	$Sc(OTf)_3$	62 (16)	0°C	2:1
6	$Sc(OTf)_3$	82	–78 °C	5:1
7	$La(OTf)_3$	65	0°C	1.7:1
8	$Yb(OTf)_3$	88	0°C	4:1
9	$Yb(OTf)_3$	91	–78 °C	7.2:1
10	$Pr(OTf)_3$	89	0°C	3:1
11	$Dy(OTf)_3$	60 (25)	0°C	3:1
12	$Dy(OTf)_3$	79	–78 °C	6:1

[a] Yield based on conversion to **291a** determined by ^{1}H NMR; [b] Values in parentheses represent yield of **293a** determined by HPLC. [c] Diastereomer ratios were determined by ^{1}H NMR.

The formation of alkylation products **291a** and **292a** follows a radical chain mechanism as outlined in Section 1.5.2 (see Scheme 1.5.2.1). The radical addition relies on sufficient activation of the α,β-unsaturated system. Direct addition to the unactivated **290a** to give the radical adduct **294** is expected to be much slower than the radical addition to the Lewis acid complex **295**.[174] However, the presence of a strongly activating species, such as $Fe(ClO_4)_3$ or $Sc(OTf)_3$, will promote reduction of the crotyl group via **297** resulting in byproduct **293a** (Table 3.3.2.1, entries 3 and 5).[173,174]

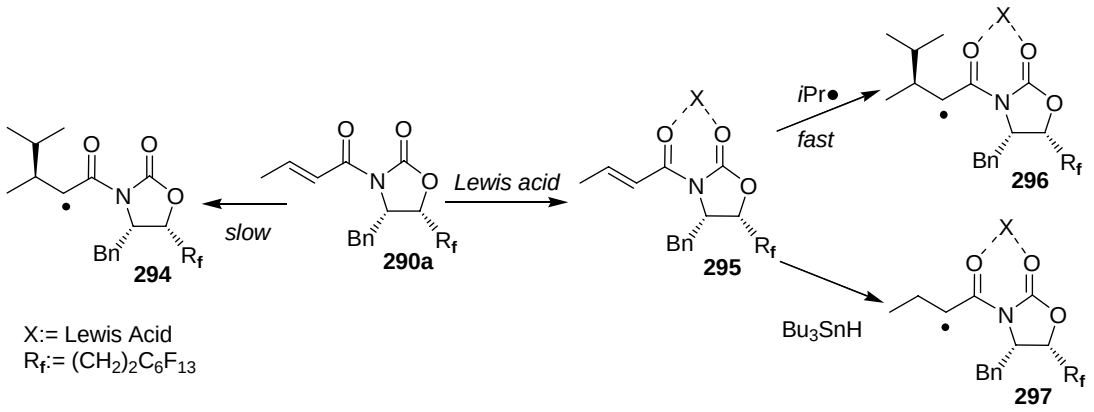

Scheme 3.3.2.2: Radical addition to *N*-crotyl fluorous oxazolidinone.

The diastereoselectivity of the conjugate radical addition varied depending on the nature of the Lewis acid applied. As good to excellent yields were obtained regardless of the Lewis acid present the α,β-system must be sufficiently activated, leading to rapid addition of the isopropyl radical. The difference in diastereoselectivity must then be due to reaction from both chelated and open intermediates, **295** and **298** respectively (Scheme 3.3.2.3). The observed stereoselectivity thus reflects the preference of the Lewis acid to bind the oxazolidinone as a bidentate ligand.

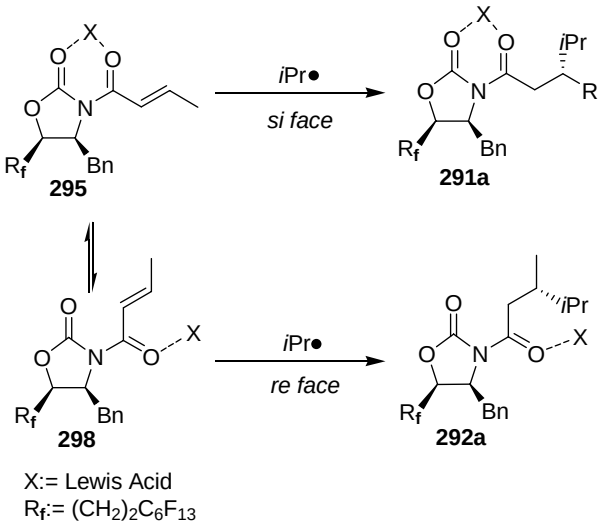

Scheme 3.3.2.3: Chelated and open intermediates in radical conjugate addition.

Sibi *et al.* reported similar results,[171,174] demonstrating that Yb(III) and other late lanthanide triflates favour a bidentate geometry similar to **295**. This conclusion is based on results from a systematic study of the dependence of diastereoselectivity of the radical conjugate addition on lanthanide and prelanthanide triflates as Lewis acids. While the yields obtained were consistently high, the late lanthanide triflates (eg. $Yb(OTf)_3$ and $Tm(OTf)_3$) gave higher diastereoselectivity than the earlier lanthanides (eg. $La(OTf)_3$ and $Ce(OTf)_3$).[174]

To examine the variability and generality of this reaction the chemistry was extended to other *N*-acyl fluorous oxazolidinones. Cinnamoyl derivative **290b** was synthesized from fluorous auxiliary **245** using similar conditions to those employed for crotyl derivative **290a**. Monoethyl fumaroyl derivative **290c** was obtained by coupling oxazolidinone **245** with monoethyl fumarate using TBTU (Scheme 3.3.2.4).

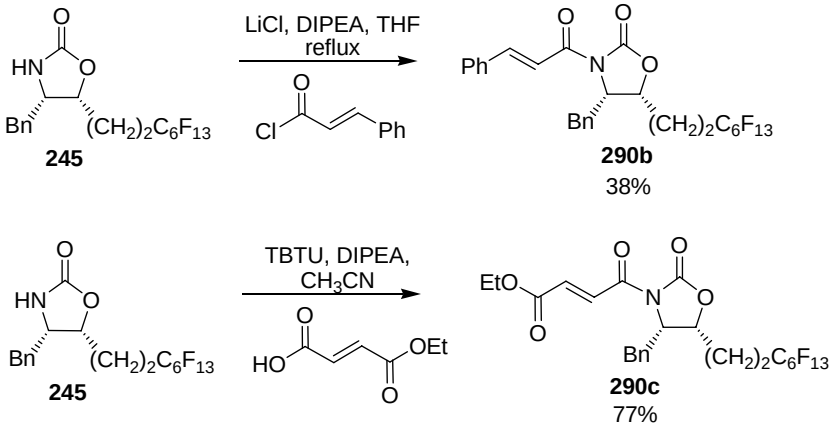

Scheme 3.3.2.4: Synthesis of cinnamoyl and monoethyl fumaroyl derivatives.

Table 3.3.2.2: Examination of substrate variability

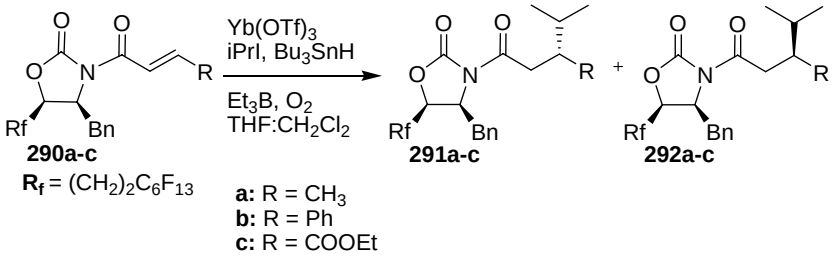

entry	starting material	temperature	yield (%) [a]	selectivity (291 : 292) [b]
1	**290a**	0 °C	86	4:1
2	**290a**	–78 °C	89	7.2:1
3	**290b**	0 °C	87	2.2:1
4	**290b**	–78 °C	89	4.7:1
5	**290c**	0 °C	93	3:1
6	**290c**	–78 °C	85	6.6:1

[a] Isolated yield of major diastereomer **291**; [b] Diastereomer ratios were determined by ^{1}H NMR

Cinnamoyl and monoethyl fumarate derivatives **290b** and **290c** were alkylated using $Yb(OTf)_3$, which proved to be the best Lewis acid from the initial study (Table 3.3.2.2). Following radical addition, purification by FSPE and measurement of the diastereoselectivity, the diastereomers **291a-c** were separated from the minor products **292a-c** using HPLC. In each case, the new stereocentre in the major diastereomer had the *R* configuration, as determined by hydrolysis of the addition products **291a-c** to the known carboxylic acids **299a-c**[175,254,255] (Scheme 3.3.2.5). This observed stereochemistry represents radical addition to chelated intermediate **295** from the less hindered face of the alkene, which is consistent with the behavior of other oxazolidinone chiral auxiliaries under similar conditions.[169,173,174]

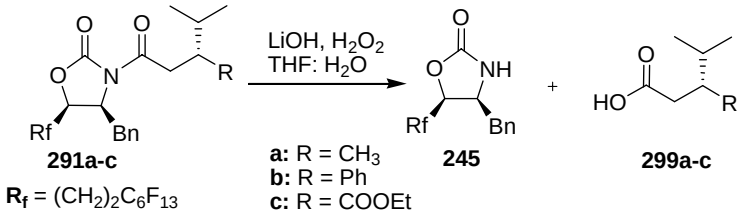

Scheme 3.3.2.5: Hydrolysis of radical addition products using LiOOH.

Performing the radical additions at –78 ºC significantly improved the diastereoselectivity of the reaction, reflecting better differentiation between the two faces of the alkene due to the lower kinetic energy of the system (Scheme 3.3.2.6). While acceptable levels of stereoselectivity were obtainable even at 0 °C using the fluorous oxazolidinone, it was not possible to select for a single diastereomer of the product. This is a problem shared by the non-fluorous oxazolidinone auxiliaries, which were only able to give moderate diastereoselectivity in many cases.[174] While the reaction is thought to proceed through chelated intermediate **295**, the distance between the reactive β-centre

and the chiral carbon is still significant, limiting the degree to which the benzyl group at the 4 position can shield the *si* face of the alkene.

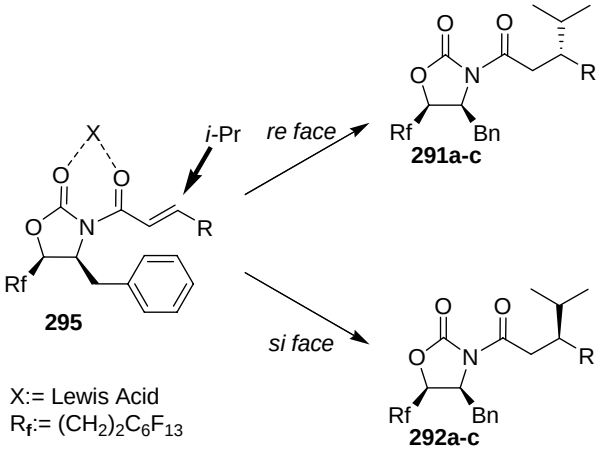

Scheme 3.3.2.6: Facial selectivity for the Lewis acid-mediated radical conjugate addition.

It is significant that the 4,5 disubstituted oxazolidinone was able to give good diastereoselectivity at 0 ºC, while the mono-functionalized auxiliary derived from L-phenylalanine required the reactions to be conducted at -78 ºC to produce comparable results. While the steric effect of the perfluoroalkyl group cannot be directly responsible for this result, it is possible that its presence hinders the rotation of the benzyl group, forcing it to occupy the environment near the alkene, ultimately increasing the stereoselectivity (Scheme 3.3.2.7).

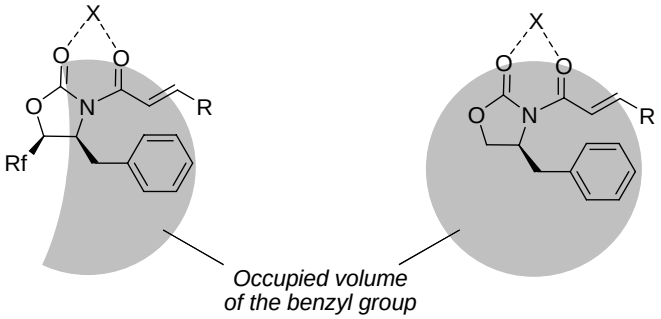

Scheme 3.3.2.7: Steric volume of benzyl group in mono and disubstituted oxazolidinones.

Following FSPE cleanup of the products no further purification was necessary, even when a large excess (5 eq.) of tributyltin hydride was present. Based on the preliminary ^{1}H NMR results it appeared as if the fluorous cleanup protocol had effectively removed the bulk of the alkyltin species. However, to get a sense of how efficient this protocol was at dealing with persistent heavy metal impurities a more sensitive analytical technique, such as atomic absorption spectroscopy was required. Furthermore, to prove the purification was being accomplished selectively due to the fluorous portion of the chiral auxiliary the results had to be compared to some analogous non-fluorous system. Oxazolidinone **301** derived from norephedrine was chosen to act as the non-fluorous comparison model, and was synthesized, acylated, and applied to the same radical addition conditions used for the fluorous compounds (Scheme 3.3.2.8). The effectiveness of the FSPE technique was evaluated quantitatively by measuring the residual tin content of the crude reaction products obtained from both fluorous and non-fluorous chiral auxiliaries.

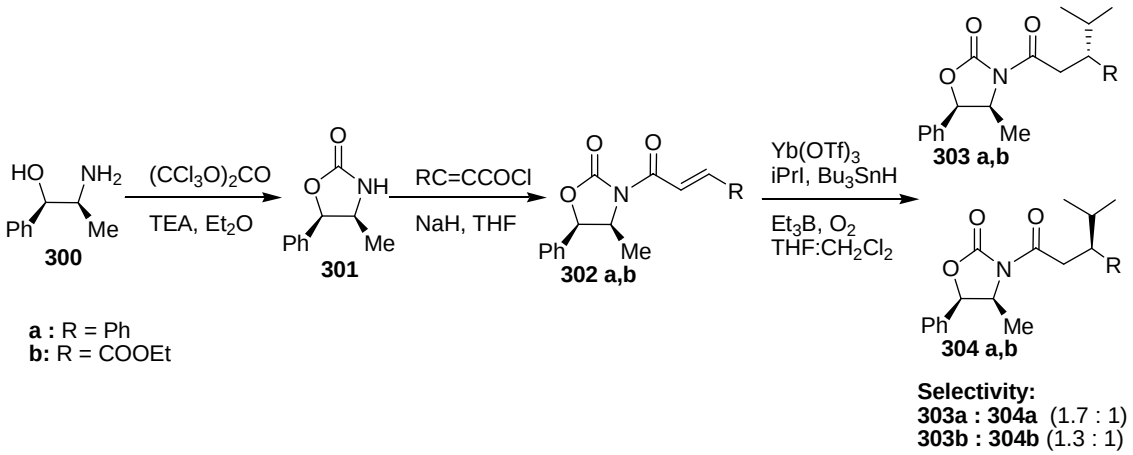

Scheme 3.3.2.8: Synthesis and radical conjugate addition using norephedrine derivatives.

Fluorous products **291** and **292** and norephedrine compounds **303** and **304** were purified using a combination of silica and fluorous solid phase extractions as described previously. The total tin content was measured after each step using atomic absorption spectroscopy, allowing the changes in tin levels to be monitored after each stage in the purification (Table 3.3.2.3). To ensure that the total tin level was being assayed in these trials the samples were digested using hot nitric acid prior to analysis,[256,257] resulting in the conversion of all alkyltin species to inorganic tin nitrate. While this removes the possibility of measuring the tin speciation in the samples, it prevents any anomalies due to the different emission responses of dissimilar alkyltin compounds.[257]

Table 3.3.2.3: Residual tin in samples following purification by various methods.

entry	compound	silica pad (%w/w)	FSPE (%w/w)	flash column (%w/w)
1	**291a**	3.7%	0.054%	–
2	**291b**	6.4%	0.070%	–
3	**303a**	6.6%	6.6% [a]	0.013%
4	**303b**	4.5%	4.5% [a]	0.023%

[a] Material was not retained on FSPE cartridge and isolated in 7:3 MeOH:H_2O wash.

The first step for the purification using standard silica gel gave similar results for all compounds, leaving behind between 3.7% and 6.6% tin by weight. Following this purification the material was then subjected to FSPE. Table 3.3.2.3 shows that FSPE is very effective at removing alkyltin species from fluorous materials **291a** and **291b**, while the non-fluorous substances **303a** and **303b** co-eluted with the alkyltin compounds. It is

also evident that the fluorous solid phase is not sequestering alkyltin species (Table 3.3.2.3, entries 1,2 vs 3,4). In order to remove the excess tin from the norephedrine derivatives, a third flash chromatography step was required. The tin levels in the norephedrine samples following this final purification using flash chromatography were lower than those in the fluorous materials; however, significantly more time and effort was required. The FSPE purification was faster than standard chromatographic methods, did not require tedious fraction collection, and used far less solvent to obtain a comparable removal of tin.

In conclusion, this study demonstrated that the fluorous chiral auxiliary is an effective tool for stereoselective radical chemistry, offering good stereocontrol and superior purification properties. These results represent the first example of a supported stereoselective radical conjugate addition and the efficient removal of tin byproducts from the desired product.

3.3.3 Stereoselective 1,3 Dipolar Cycloadditions with Diphenylnitrone

The investigations related to the asymmetric aldol and conjugate radical additions had proven that the fluorous oxazolidinone was an effective supported chiral auxiliary. The results from the aldol and conjugate addition reactions also suggested that the perfluoroalkyl chain does not negatively impact the stereoselectivity or reactivity of these systems. In both cases, the observations were similar to those reported for the analogous non-fluorous oxazolidinones, indicating that the standard solution phase models were applicable to the new auxiliary.

To fully test the extent to which the perfluoroalkyl tag may participate in asymmetric transformations auxiliary **245** was applied to a series of 1,3 dipolar cycloadditions. Crotyl derivative **290a** was generated using the acylation protocol developed for the radical conjugate addition study (Scheme 3.3.3.1). The vicinal coupling constant between H2' and H3' was 15.8 Hz, confirming the alkene had been formed with the *E* geometry.

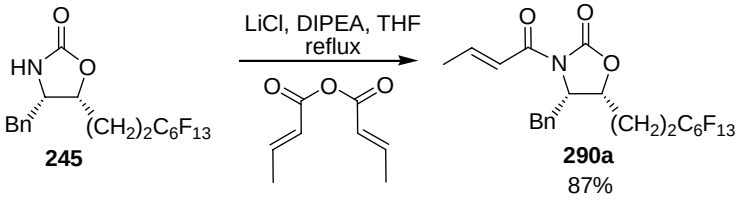

Scheme 3.3.3.1: Synthesis of *N*-crotyl fluorous oxazolidinone **290a**.

Diphenylnitrone was synthesized according to literature proceduresREF by reducing nitrobenzene to give *N*-phenylhydroxylamine **306**, which was then reacted with benzaldehyde (Scheme 3.3.3.2). This protocol generates diphenylnitrone in the *Z* geometry selectively,REF as seen in **307**.

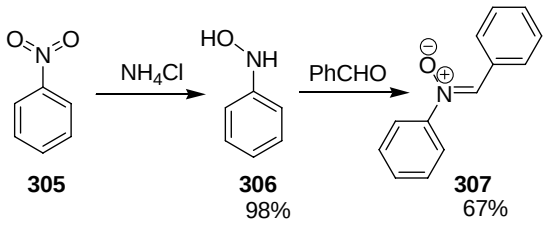

Scheme 3.3.3.2: Synthesis of diphenylnitrone.

N-Crotyl derivative **290a** was then allowed to react with diphenylnitrone, and monitored by conventional TLC. On completion, the volatile components were removed under vacuum and the residue was adsorbed onto FluoroFlash™ before being applied to an FSPE cartridge. The cartridge was rinsed with 70% MeOH in water to remove organic and inorganic impurities. Subsequent elution with MeOH liberated a mixture of cycloaddition products **308 – 311**.

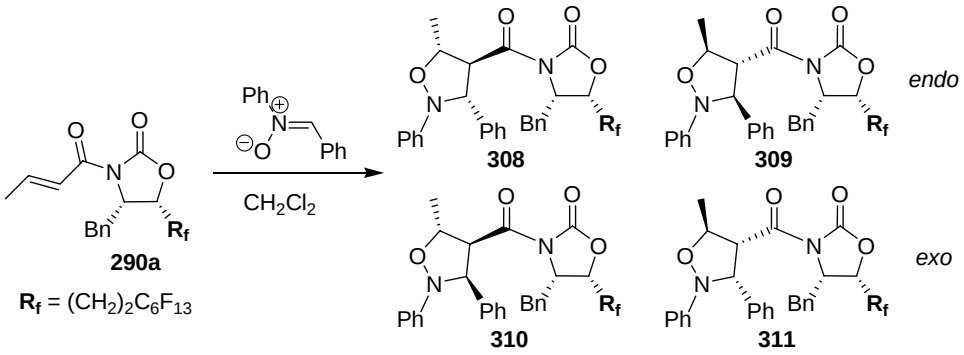

Scheme 3.3.3.3: 1,3 Dipolar cycloaddition of diphenylnitrone and **290a**.

Performing the reaction without a Lewis acid present led to an extremely long reaction time. After seven days the cycloaddition only showed approximately 50% conversion to the isoxazolidine product, with a corresponding quantity of the dipolarophile **290a** still present. Monitoring the reaction over the next several days showed no further conversion; however, the reaction continued after a second equivalent of diphenylnitrone was added giving the isoxazolidines **308 – 311** in an overall yield of

92% after two weeks. The need for a second equivalent of the nitrone dipole after an extended time is not entirely surprising, as this species is photosensitive and readily undergoes photolysis in the presence of visible light. The drop in rate indicates that the nitrone had been completely exhausted after one week, preventing further reaction.

Following completion of the reaction the individual cycloaddition products **308 – 311** were obtained in pure form by preparative HPLC. The absolute stereochemistry of each isoxazolidine was then assigned. Given that the crotyl dipolarophile had the *E* geometry and the nitrone was synthesized in the *Z* geometry two general approach geometries are possible (Scheme 3.3.3.4). Regardless of which approach pathway is followed, the 4' and 5' positions of the resulting isoxazolidines will have the *anti* relative configuration due to the initial configuration of crotyl dipolarophile **290a**. Reaction via the *endo* transition state **312** gives rise to an *anti* relative geometry between the 3' and 4' substituents in products **308** and **309**. Conversely, reaction via *exo* transition structure **313** results in a *syn* relationship between the 3' and 4' centres, as seen in **310** and **311**. These differences make it possible to readily distinguish between the diastereomers resulting from the *exo* or *endo* mode of attack simply by examining the H3' – H4' coupling constants. Compounds **308** and **309** both showed a $J_{H3'H4'}$ of 7.5 Hz, characteristic of the expected *anti* relationship at these centres, while compounds **310** and **311** were observed to have a $J_{H3'H4'}$ of 10.6 Hz, indicating a *syn* relationship. [199]

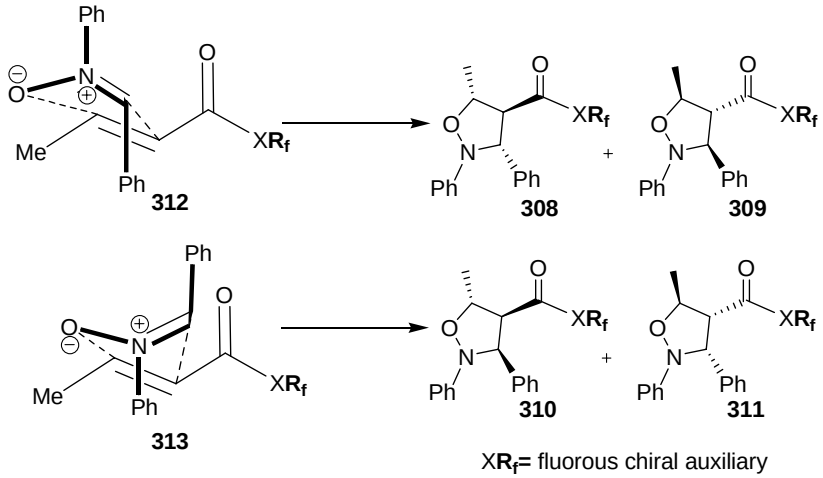

Scheme 3.3.3.4: *Endo* and *exo* cycloaddition pathways.

To establish the absolute stereochemistry of the isoxazolidine ring it was necessary to convert **308** to the known isopropyl ester **314** (Scheme 3.3.3.5). Comparing the $[\alpha]_D$ value reported in the literature[201] to that obtained for **314** confirmed that the configuration in the parent isoxazolidine **308** was (3'*R*,4'*S*,5'*R*). The absolute stereochemistry of the other *endo* product **309** was then inferred as (3'*S*,4'*R*,5'*S*).

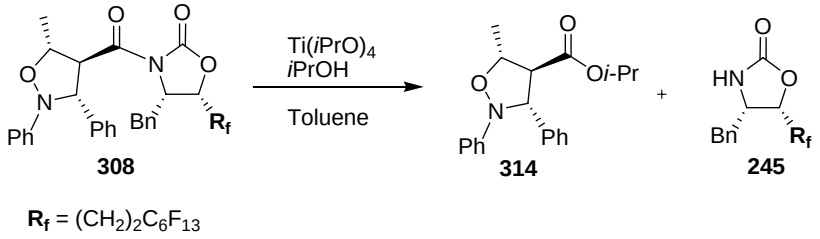

Scheme 3.3.3.5: Lewis acid mediated transesterification.

Chemical conversion to assign the geometry of the two *exo* products via this route was not possible. Treating either *exo* product **310** or **311** with titanium(IV) isopropoxide led to degradation and complex mixtures of materials. This same behavior has been noted by Jørgensen *et al.*,[195,212] although it is unclear why the *endo* and *exo* products display such a striking difference in their reactivity. To obtain a comparison standard, the

1,3 dipolar cycloaddition was carried out using the dipolarophile **315** and diphenylnitrone (Scheme 3.3.3.6). This reaction has been studied by Desimoni *et al.*[100] and the absolute geometries of all cycloaddition products have been assigned.

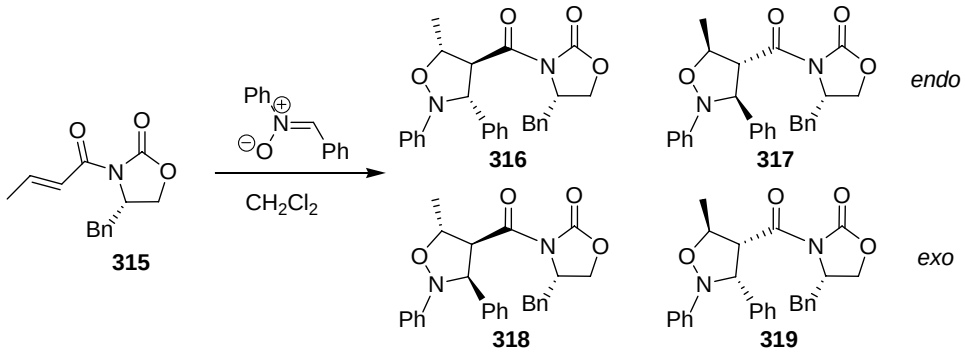

Scheme 3.3.3.6: Dipolar cycloaddition using non-fluorous dipolarophile **315**.

Following completion of the reaction the individual diastereomers **316 – 319** were isolated using flash chromatography. *Exo* isoxazolidines **316**, **310**, and **311** were then converted to the oxazolidinones **245** and **322** and corresponding isoxazolidine alcohols **320** and **321** via reductive cleavage (Scheme 3.3.3.7). *Exo* cycloadduct **318** has been fully characterized, and the absolute stereochemistry of the isoxazolidine ring assigned as (3'*S*,4'*S*,5'*R*) by analysis of the crystal structure obtained from X-ray diffraction.[100] Comparison of the isoxazolidine alcohols revealed that both cycloaddition products **310** and **318** gave rise to the alcohol **320**, while enantiomer **321** was generated from cycloadduct **311**. This information allowed us to suggest that compounds **310** and **318** share similar stereochemistry in their isoxazolidine fragments, indicating that **310** could be assigned as (3'*S*,4'*S*,5'*R*), while **311** would then be (3'*R*,4'*R*,5'*S*).

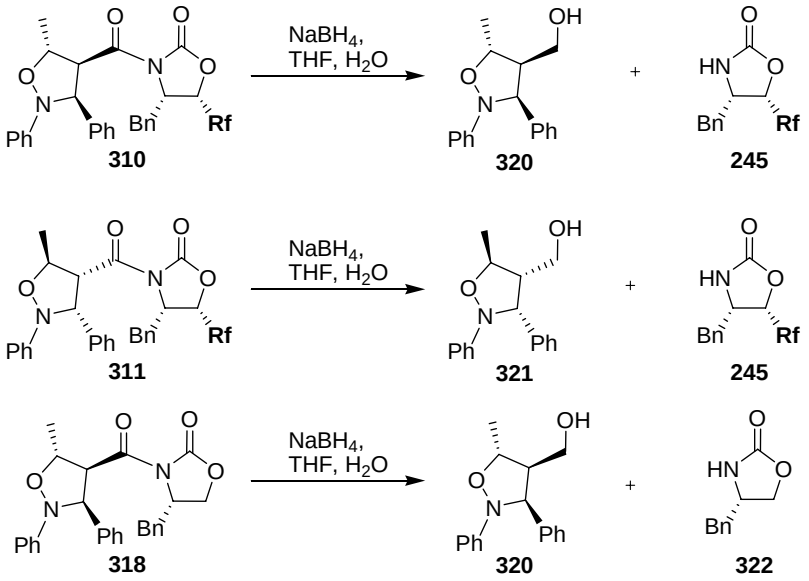

Scheme 3.3.3.7: Reductive cleavage of *exo* isoxazolidine products.

While these results allowed us to propose the absolute stereochemistry of the two *exo* cycloadducts, a more definitive analysis was required to confirm these observations. Both **310** and **311** were recrystallized to obtain material suitable for X-ray analysis. After considerable experimentation clear needles of **310** were obtained by slow evaporation from ethanol/water. The crystal structure of this material is shown in Figure 3.3.3.1. These crystals were orthorhombic with a Pcnb space group, indicating that the unit cell contained both enantiomers of the isoxazolidine and that the crystal was racemic. Further analysis revealed that the pure enantiomer of **310** remained in the filtrate of the ethanol/water solution. On evaporation it was obtained as a clear yellow oil.

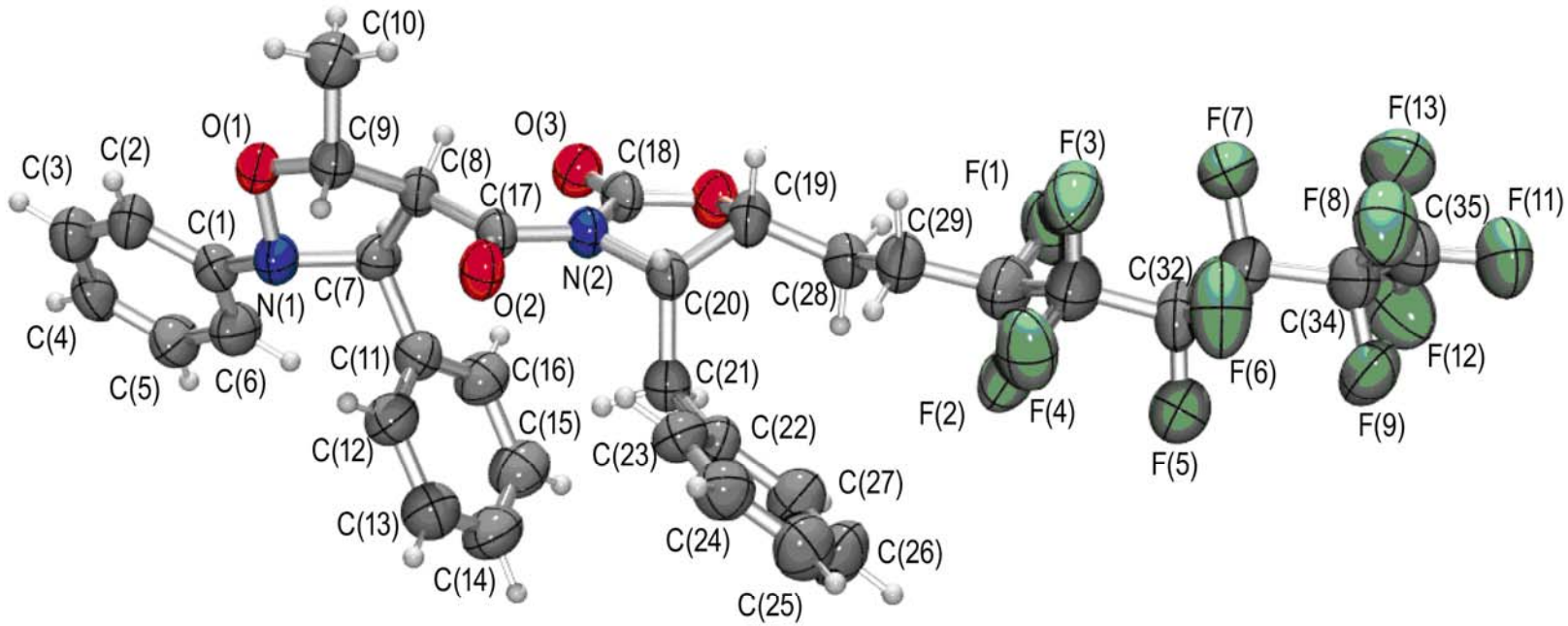

Figure 3.3.3.1: X-ray structure of dipolar cycloaddition product **310.**

The presence of both enantiomers in the crude **310** was a result of the enantiomeric purity of the particular batch of oxazolidinone **245** used in these investigations. At this point in our experiments the production of the fluorous oxazolidinone was not yet optimized, and the enantiomeric excess of **245** used to prepare cycloadduct **310** was only 98%. The propensity for isoxazolidine cycloadducts such as **310** to crystallize as racemates has been observed in other cases.[258] Thus, it was not surprising that racemic **310** selectively crystallized from the mixture given that a small quantity of the minor enantiomer was present in solution.

Using the X-ray structure, the absolute and relative stereochemistry of the isoxazolidine ring could now be confirmed. Given that **245** predominantly had the 4*S*,5*R* (Figure 3.3.3.1, C(20) and C(19) respectively) configuration, the C3' and C4' centres (Figure 3.3.3.1, C(7) and C(8) respectively) can be assigned. The major enantiomer of cycloadduct **310** was confirmed to be (3'*S*,4'*S*,5'*R*). This result agrees with the observations from the chemical conversion to alcohol **320**. The geometry of the other *exo* product **311** was then inferred to be (3'*R*,4'*R*,5'*S*).

Following characterization of cycloadducts **308 – 311** the effects of various reaction conditions were explored. By applying the convenient FSPE cleanup protocol it was possible to rapidly investigate the effect of different Lewis acid catalysts, solvents and additives on the diastereoselectivity of the cycloaddition. Each of these parameters has been shown to affect the diastereoselectivity of the cycloaddition reaction.[91,100,172,201] As such these conditions were specifically chosen to compare the behavior of the fluorous auxiliary to other systems reported in the literature. In each case the reaction

was initially purified using FSPE, and the product ratios were measured by HPLC on silica gel or C18 columns.

The first parameter under scrutiny was the effect catalytic amounts of different Lewis acids had on the rate and selectivity of the cycloaddition (Table 3.3.3.1). Regardless of the nature of the Lewis acid the rate of reaction was significantly increased in each case. This acceleration in rate has been attributed to coordination of the Lewis acid to the dipolarophile, resulting in a net activation of the α,β-unsaturated system.[199]

Table 3.3.3.1: 1,3-Dipolar cycloaddition using Lewis acid catalysts.

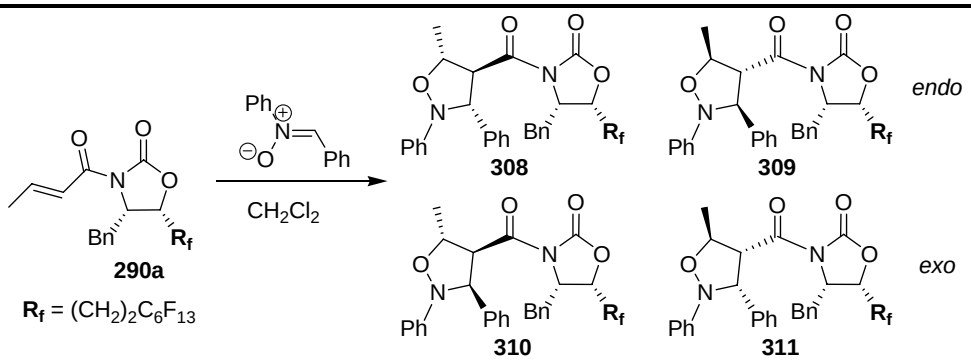

entry	catalyst	time/yield	*exo:endo*	% de exo [a]	% de endo [a]
1	—	14 d/92%	68:32	76 (**311**)	50 (**308**)
2	$Mg(ClO_4)_2$	24 h/98%	69:31	88 (**310**)	81 (**308**)
3	$Sc(OTf)_3$	16 h/98%	30:70	60 (**310**)	86 (**308**)
4	$Cu(OTf)_2$	18 h/87%	60:40	64 (**310**)	84 (**308**)
5	$Yb(OTf)_3$	16 h/91%	17:83	65 (**310**)	89 (**308**)

[a] Compound number in parentheses refers to major diastereomer

While the yields and rates of the cycloaddition were similar with all Lewis acids, the diastereoselectivity varied considerably. Most notably, the configuration of the major *exo* diastereomer changed from **311** in the uncatalyzed case to **310** in the presence of the Lewis acids (Table 3.3.3.1, entry 1 cf. entries 2,3,4,5). There were also significant differences in the *endo/exo* selectivity, with Mg^{2+} and Cu^{2+} species giving good selectivity from the *exo* diastereomers, while Sc^{3+} and Yb^{3+} both favoured the *endo* products (Table 3.3.3.1, entry 2,4 cf. entries 3,5).

As discussed in Section 1.5.3 the factors affecting the stereoselectivity of the 1,3-dipolar cycloaddition between various nitrone dipoles and dipolarophiles linked to oxazolidinone chiral auxiliaries have been studied by Desimoni,[100] Faita,[89,95] and Jørgensen.[195,201] Ultimately, there are two issues of selectivity in these reactions: diastereofacial selectivity (which controls the 4',5' stereochemistry of the product) and *endo/exo* selectivity (which dictates the relative stereochemistry of the 3' and 4' centres). The facial selectivity of the cycloadditions (with *si* face attack on **290a** giving rise to **308** and **310** but *re* face addition giving **309** and **311**) is controlled by chelation of the carbonyls of the dipolarophile to the metal catalyst (Scheme 3.3.3.8).[89,95,100]

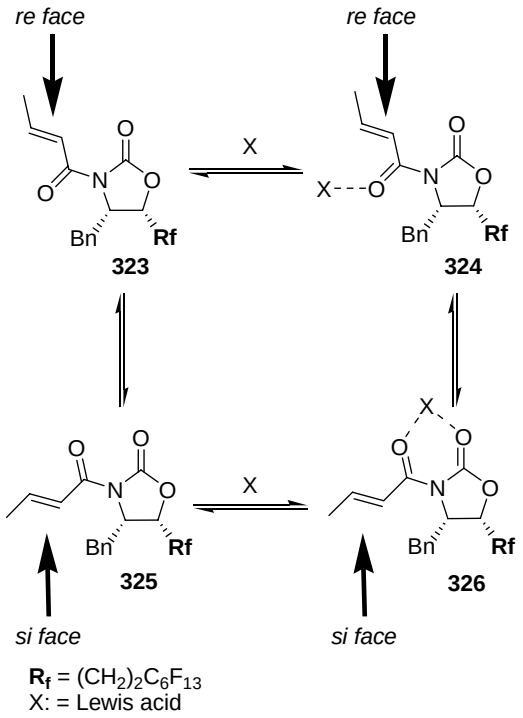

Scheme 3.3.3.8: Open and chelated intermediates for dipolar cycloaddition.

Assuming the exocyclic enoyl fragment adopts the *s-cis* geometry preferentially[100,195] the dipolarophile can exist as two rotamers, **323** and **325**. Rotamer **323**, where the two carbonyls adopt an antiparallel arrangement, is the predominant conformer in solution when no Lewis acid is present,[57,100] giving rise to selective obstruction of the *si* face of the alkene. If a Lewis acid is added the two coordinated structures **324** and **326** can be formed. Coordination to the exocyclic carbonyl to form **326** activates the α,β-unsaturated system, but still directs dipolar addition from the *re* face. The Lewis acids used in this study readily form the chelated structure **326**, causing the *re* face to be selectively hindered. The observed switch in the stereoselectivity of the major *exo* product between uncatalyzed and catalyzed reaction may be explained by a shift in the reactive geometry from **323** when no catalyst is present to **326** upon addition of a Lewis acid.

As discussed in Section 1.5.3 the *endo/exo* selectivity is governed by a steric interaction between the nitrone phenyl group and the Lewis acid centre (Scheme 3.3.3.9).[195,202] Therefore, the coordination geometry and ligands around the metal centre play a key role in determining the degree of this steric effect. Species such as Cu^{2+} and Mg^{2+} prefer to adopt square planar[211] and tetrahedral[100] geometries respectively. Therefore cycloaddition proceeds via **328** to give *exo* diastereomers **310** and **311** (Table 3.3.3.1, entries 2 and 4). Conversely, both Sc^{3+} and Yb^{3+} prefer to form more bulky octahedral complexes,[100,172,259] giving rise to reaction via **327** and producing the *endo* diastereomers **308** and **309** preferentially (Table 3.3.3.1, entries 3 and 5).

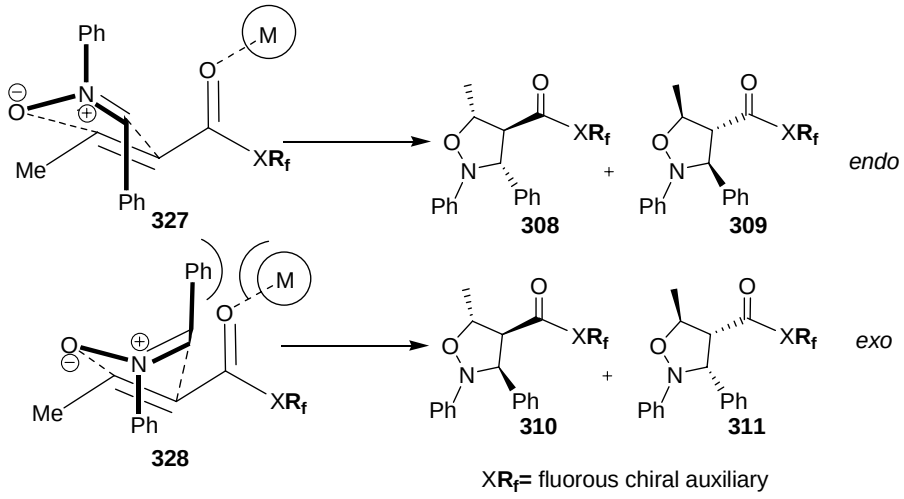

Scheme 3.3.3.9: Steric repulsion in *exo* dipolar cycloaddition transition structure.

Based on these two models, the *exo/endo* and diastereofacial selectivity can be tuned by adjusting the reaction conditions (Table 3.3.3.2). By adding a ligand capable of coordination to the metal, such as *o*-phenanthroline, the steric bulk of the Lewis acid is increased. This increases the steric repulsion seen in transition state **328**, resulting in an increase in the *endo* selectivity (Table 3.3.3.2, entry 1 cf. 2,3). Changing the Lewis acid from $Mg(ClO_4)_2$ to MgI_2 also had little effect on the diastereoselectivity observed (Table

3.3.3.2, entry 2 cf. 3), indicating that *o*-phenanthroline likely displaces the counter-ion in solution, and thus is responsible for the stereochemical outcome. Using this ligand in the presence of $Sc(OTf)_3$ did not have a significant effect on the *endo/exo* selectivity, but the diastereoselectivity of the *exo* compounds did decrease (Table 3.3.3.2, entry 4 vs. 5). This result indicates the steric bulk of the octahedral complex is not significantly increased; however, the reduction in stereoselectivity between *exo* compounds **310** and **311** may indicate that this ligand is interfering with the formation of the chelated intermediate **326**, leading to poor facial differentiation.

Table 3.3.3.2: 1,3-Dipolar cycloadditions using **290a** and *o*-phenanthroline.

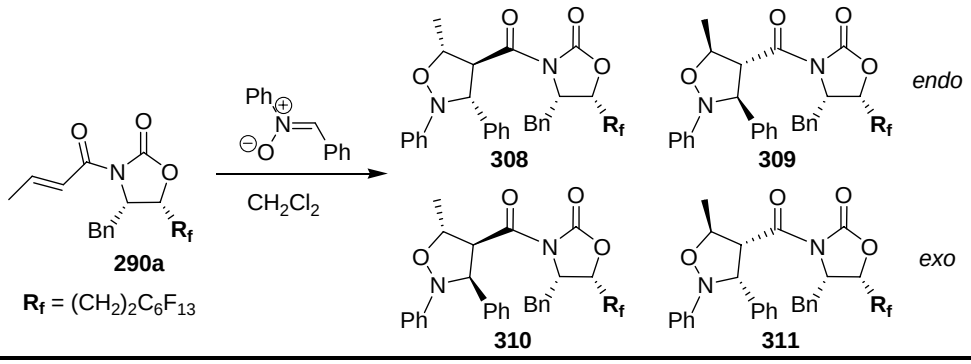

entry	catalyst	time/yield	*exo:endo*	% de exo [a]	% de endo [a]
1	$Mg(ClO_4)_2$	24 h/98%	69:31	88 (**310**)	81 (**308**)
2 [b]	$Mg(ClO_4)_2$	2 d/87%	35:65	54 (**310**)	94 (**308**)
3 [b]	MgI_2	36 h/67%	49:51	64 (**310**)	91 (**308**)
4	$Sc(OTf)_3$	16 h/98%	30:70	60 (**310**)	86 (**308**)
5 [b]	$Sc(OTf)_3$	24 h/75%	29:71	42 (**310**)	88 (**308**)

[a] Compound number in parentheses refers to major diastereomer; [b] Reaction run in the presence of *o*-phenanthroline

Table 3.3.3.3: 1,3-Dipolar cycloadditions using **290a** and 4Å molecular sieves.

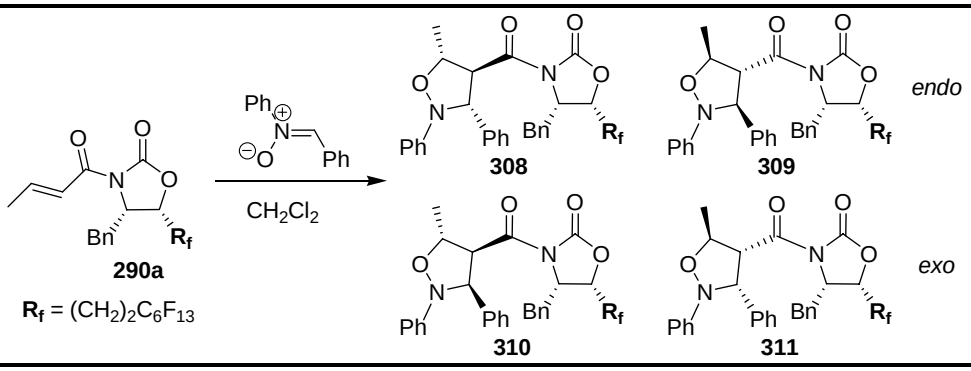

entry	catalyst	time/yield	*exo:endo*	% de exo [a]	% de endo [a]
1	$Mg(ClO_4)_2$	24 h/98%	69:31	88 (**310**)	81 (**308**)
2 [b]	$Mg(ClO_4)_2$	2 d/92%	30:70	64 (**310**)	92 (**308**)
3	$Sc(OTf)_3$	16 h/98%	30:70	60 (**310**)	86 (**308**)
4 [b]	$Sc(OTf)_3$	24 h/92%	22:78	71 (**310**)	98 (**308**)
5	$Yb(OTf)_3$	16 h/91%	17:83	65 (**310**)	89 (**308**)
6 [b]	$Yb(OTf)_3$	24 h/98%	20:80	56 (**310**)	95 (**308**)
7 [b,c]	$Yb(OTf)_3$	24 h/58%	62:38	53 (**311**)	30 (**308**)
8 [b,d]	$Yb(OTf)_3$	24 h/62%	24:76	74 (**310**)	76 (**308**)

[a] Compound number in parentheses refers to major diastereomer; [b] Reaction performed in the presence of 4Å molecular sieves; [c] Reaction performed in CH_3CN; [b] reaction performed in toluene.

Molecular sieves have also been shown to influence the diastereoselectivity of nitrone cycloadditions.[100,195,211] In general, performing the reaction in the presence of 4Å molecular sieves results in an increase in the *endo* selectivity of the cycloaddition (Table

3.3.3.3,entries 1,3,5 cf. 2,4,6). Studies by Jørgensen *et al.* have shown that molecular sieves participate in these processes by binding the Lewis acid.[195] This dramatically changes the steric environment at the metal centre, and directs the cycloaddition via the *endo* transition structure **327**.

In addition, the molecular sieves will remove trace amounts of water from solution, thus depleting a monodentate ligand which may coordinate to the metal centre interfering with the formation of chelated transition structure **326** (Scheme 3.3.3.10). Adding coordinating solvents, such as acetonitrile, has the opposite effect, promoting the formation of open structure **324.** This results in a switch in the facial selectivity allowing the reaction to occur at the *re* face to give higher quantities of **309** and **311** (Table 3.3.3.3, entry 6 vs. 7).

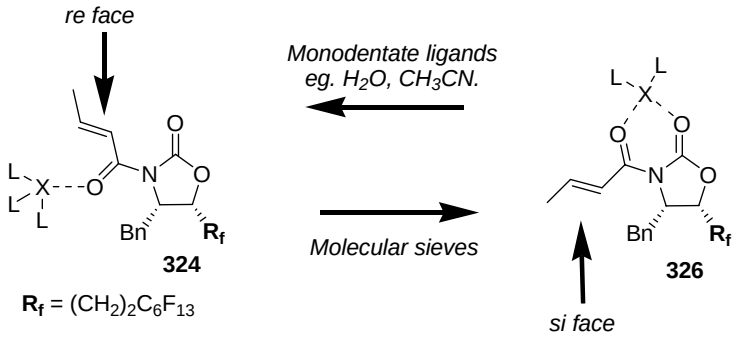

Scheme 3.3.3.10: Switching facial selectivity of catalyzed dipolar cycloaddition.

In general, using molecular sieves results in a strong preference for the attack at the *si* face of the alkene giving the *endo* geometry. This shift in diastereoselectivity is accompanied by an increase in the reaction times, which would be expected if the Lewis acid were bound to the surface of the molecular sieves. In this instance the Lewis acid is effectively acting as heterogeneous catalyst.

The ability to reuse the chiral auxiliary is a key advantage of supported oxazolidinones, adding to the efficiency and value of these materials. While the auxiliary had been easily recovered and reused following the aldol reactions and radical conjugate additions, no formal measurement of the yield on a cycle to cycle basis had been completed. To investigate this aspect further the auxiliary was tested by repeating the cycloaddition reactions and monitoring the yields and selectivity over several cycles (Scheme 3.3.3.11). Diphenylnitrone and dipolarophile **290a** were reacted in the presence of $Mg(ClO_4)_2$ or $Sc(OTf)_3$ catalysts. Following measurement of product ratios, the cycloadducts **308 – 311** were reductively cleaved. The free auxiliary **245** was then acylated to reform dipolarophile **290a**, which was immediately subjected to a further cycloaddition. Following each reaction the fluorous and organic materials were separated using FSPE, making the process extremely fast and efficient.

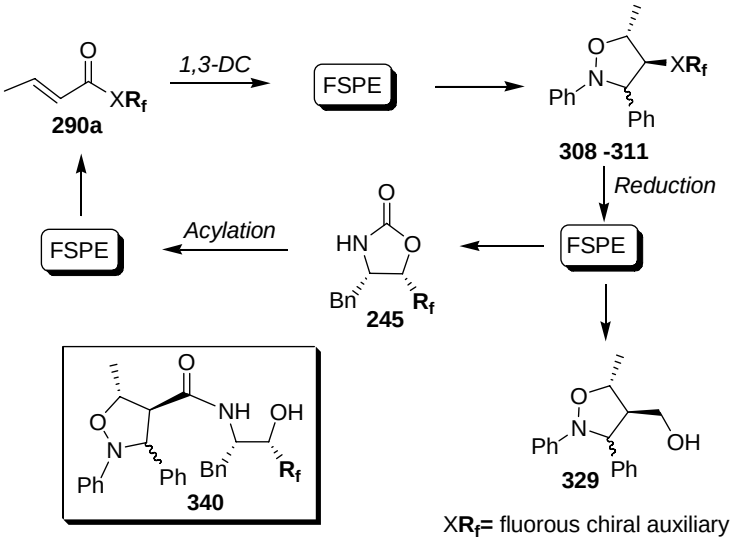

Scheme 3.3.3.11: Recycling of **290a** in 1,3-dipolar cycloadditions with diphenylnitrone.

This cycle was repeated a total of five times using $Mg(ClO_4)_2$ as catalyst, and three cycles using $Sc(OTf)_3$ (Table 3.3.3.4). Over this series no change in

stereoselectivity or yield was observed, but a small amount of alcohol **340** was isolated. This degraded material accounted for <2% of the fluorous material recovered after five reaction cycles. The presence of this material did not affect the stereoselectivity of the cycloadditions. Furthermore, alcohol **340** was easily separated from auxiliary **245** using chromatography. This demonstrates a distinct advantage of the fluorous support over polymeric materials. Modification or degradation of the chiral species on a polymer can only be rectified by cleavage and refunctionalization. The fluorous material, on the other hand, can be readily purified using conventional methods, such as flash chromatography or crystallization, allowing it to be rapidly returned to service.

Table 3.3.3.4: Recovery and recycling of **290a** in 1,3-dipolar cycloadditions.

entry	catalyst [a]	cycle	*exo:endo*	%de endo	%de exo	yield/time
1	$Mg(ClO_4)_2$	1st	69:31	81	88	24 h/92%
2	$Mg(ClO_4)_2$	2nd	68:32	82	88	24 h/90%
3	$Mg(ClO_4)_2$	3rd	68:32	80	89	24 h/91%
4	$Mg(ClO_4)_2$	4th	69:31	81	88	24 h/91%
5	$Mg(ClO_4)_2$	5th	67:33	80	88	24 h/91%
6	$Sc(OTf)_3$	1st	30:70	86	60	16 h/95%
7	$Sc(OTf)_3$	2nd	32:68	87	58	16 h/93%
8	$Sc(OTf)_3$	3rd	31:69	86	59	16 h/95%

[a] Reaction conditions: CH_2Cl_2, r.t, , 10 mol% catalyst

Despite the formation of small amounts of **340**, auxiliary **245** was highly reusable. In contrast, Faita *et al.*[95] found that these reactions performed on Wang or Merrifield resins provided significantly lower selectivity after repetitive use. They attributed this deterioration to the presence of trace water retained in the polymer matrix, which may modify the reactive geometry at the metal centre.[95] The fluorous-supported auxiliary circumvents this problem, as trace metals, water and other impurities are removed during FSPE workup.

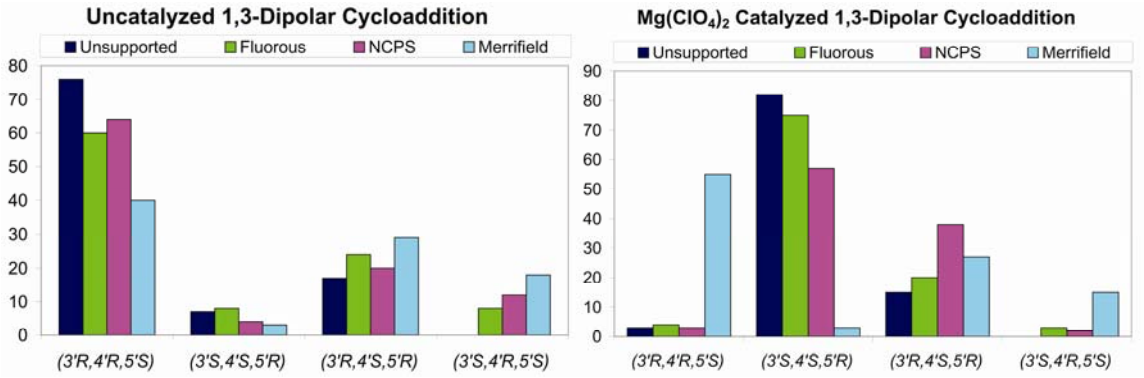

Figure 3.3.3.2: Comparison of polymer-supported, fluorous-supported, and unsupported oxazolidinones in 1,3-dipolar cycloadditions.

The observations from these reaction conditions were compared to results of cycloadditions using unsupported dipolarophiles.[100,202] The fluorous chiral auxiliary **245** followed the same trends in selectivity, indicating that the fluorous tag had a negligible electronic and steric effect on the behavior of the auxiliary. Faita *et al.*[95] have observed that this was not the case when the polymer supported auxiliaries were applied. The differing behavior of the cycloaddition performed on an insoluble polymer versus the reactions in solution is displayed in Figure 3.3.3.2. Regardless of the reaction conditions, the oxazolidinones bound to insoluble supports favoured the production of the

isoxazolidine with the (3'*R*,4'*R*,5'*S*) geometry. Furthermore the reaction times were much longer when the cycloaddition was performed with the insoluble polymer support.

This increase in reaction time was also accompanied by a drop in the yield of the cycloaddition products.[89,95] In contrast, the solution-phase reactions afforded the (3'*S*,4'*S*,5'*R*) product in the presence of Mg^{2+}, but gave the (3'*R*,4'*R*,5'*S*) product in the absence of the metal ion. Desimoni found that the auxiliary supported with non-crosslinked polystyrene gave diastereoselectivities more similar to the unsupported oxazolidinone,[91] due to the solubility of this material in certain organic solvents. The fluorous auxiliary still afforded a significantly higher ratio of major product to minor products than did either the soluble or insoluble polymeric supports (2.8:1 versus 1.3:1 or 1.2:1 respectively) in the presence of metal catalysts. It is clear that both the soluble and insoluble polymeric supports alter the behavior of the chiral auxiliary and have a more significant impact on the diastereoselectivity of the dipolar cycloaddition than the fluorous support.

Chapter 4: CONCLUSIONS AND FUTURE WORK

4.1 Conclusions

This work has demonstrated the successful completion of the two main goals presented at the beginning of this thesis.

Through a series of studies an efficient five-step synthetic protocol has been developed and optimized to produce a series of fluorous chiral oxazolidinones. Auxiliaries **230** and **231**, employing a C_8F_{17} perfluoroalkyl fragment, could be synthesized from the *N*-carbamoyl esters derived from L-phenylalanine using an *in situ* generating method to obtain the required perfluoroalkyl nucleophile. Perfluoroalkylation by this technique did not result in suitable yields due to poor control over competing side reactions. Furthermore, the intermediate ketones **209a** and **209b** could not be reduced diasteroselectively, giving rise to both the *syn* and *anti* auxiliaries. Ultimately, the combination of these shortcomings made this pathway unsuitable for the generation of the fluorous chiral auxiliary.

By employing a fluorous iodide containing an ethylene spacer the efficiency of the perfluoroalkylation was dramatically improved. Optimal results were obtained when Weinreb amide **240a** was first deprotonated using *t*-BuLi and then reacted with $C_6F_{13}(CH_2)_2Li$ in a mixed solvent made up of 3:2 hexane:ether. The resulting ketone **233a** was reduced to alcohol **243a** with excellent diastereoselectivity, and subsequently cyclized yielding auxiliary **245**. These methods have been adapted to enable the practical syntheses of the new fluorous oxazolidinone chiral auxiliary on a large scale. Coupling the optimized synthesis with FSPE allowed the material to be rapidly processed, making

it possible to generate multigram quantities of the oxazolidinone rapidly and efficiently.[260]

These methods have been extended successfully to L-valine to give the corresponding oxazolidinone **259**, indicating that the synthetic protocols are relatively general and can be extended to other α amino acids. L-Phenylglycine was found to be incompatible with these reactions, leading only to racemic oxazolidinones **265** and **266**, due to epimerization at the α-centre. In general, these synthetic protocols should be applicable to any chiral α-amino acid, requiring only minor modifications or initial protection of acidic functional groups.[260]

Oxazolidinones **230** and **231** have been applied in a series of asymmetric aldol reactions.[261] This study revealed that only auxiliary **231,** which had the *syn* geometry at the C4 and C5 centres, gave high diastereoselectivity in these reactions and behaves analogously to the well-known Evans auxiliaries for the set of aldehydes employed. In addition, the fluorous portion of the new auxiliary allows rapid screening of reaction conditions and facile purification of this compound and its derivatives.

Purification of the new oxazolidinone **245** was found to be extremely efficient, as demonstrated from the study of radical conjugate additions.[262] High diastereoselectivity was possible when the *N*-enoyl derivatives **290a-c** were treated with $Yb(OTf)_3$ at -78 ºC and reacted with the nucleophilic isopropyl radical. Products could then be rendered free of organic and inorganic impurities using a combination of silica and fluorous solid phase extraction. In particular the compounds were found to contain very low levels of tin after applying this cleanup protocol. In reactions using the non-fluorous oxazolidinone **301** it

was necessary to employ flash chromatography to remove the alkyltin species following radical conjugate additions.

Auxiliary **245** has been further employed to study the 1,3 dipolar cycloaddition of *N*-crotyl oxazolidinones with diphenylnitrone.[263] Using a series of reactions that, while not necessarily highly stereoselective, were extremely sensitive to changes in reaction conditions the impact of the fluorous support was investigated. In all cases the new auxiliary gave results that were qualitatively identical and quantitatively very similar to those obtained using unsupported oxazolidinone auxiliaries. This was not always the case when the analogous polymer-supported systems were applied. Furthermore, auxiliary **245** was demonstrated to be highly reusable, and was successfully recycled in 1,3 dipolar cycloaddition catalyzed by both $Mg(ClO_4)_2$ and $Sc(OTf)_3$. The alcohol side product **340** was detected after several cycles, but it could be easily removed using standard flash chromatography, allowing auxiliary **245** to be easily purified and immediately reused.

These studies have successfully shown that the fluorous chain is a superior means of supporting the oxazolidinone auxiliary. Fluorous solid phase extraction allows auxiliary **245** and its derivatives to be selectively and rapidly isolated, with the same efficiency reported for the analogous polymer-supported materials, without interfering with the asymmetric reactions. Unlike many of the polymer supported compounds, the fluorous supported chiral auxiliary could be used under standard solution phase conditions, affording yields and stereoselectivities comparable to those reported for corresponding non-fluorous oxazolidinones. This combination of high stereoselectivity

and rapid purification confirms that fluorous oxazolidinones can be used to carry out stoichiometric asymmetric synthesis efficiently.

4.2 Future Studies

4.2.1 Large-Scale Production of Fluorous Oxazolidinone

The production of oxazolidinone **245** on large scales has always been a priority, and as such the special requirements synthesis on this scale demands were considered in the development of the optimized pathway. Aside from good conversion and high yield issues surrounding product isolation were of paramount importance. When batch sizes became larger than 10 grams some conventional workup methods, such as flash chromatography and to some extent liquid/liquid extraction, became impractical. To address these issues purifications were limited to silica and fluorous solid-phase extractions, and recrystallization.

Synthesis of the oxazolidinone on scales up 25 g does not require specialized equipment other than typical glassware, a supply of inert gas, and standard syringe techniques. In principle, much larger batches could be produced; however, two key factors limit the scale of reaction in a typical organic laboratory. The first is related to the application of *t*-BuLi, which is a pyrophoric lithium reagent requiring caution and care when handling. While transferring large quantities of this type of reagent is not uncommon in industrial settings, typical research laboratories are ill-equipped to deal with this operation, potentially leading to reduced efficiency, loss of products and numerous safety concerns. The second limitation is the result of the cryogenic conditions necessary for two of the five steps. The temperatures necessary for the perfluoroalkylation and diastereoselective reduction can easily be achieved using a bath

of dry ice and acetone; however, it is impractical to use this method of cooling if the reaction volume is much larger than one liter. Furthermore, heat dissipation becomes less efficient as the reaction vessel increases in size, leading to complications with these temperature sensitive processes. These issues can likely be overcome with the use of appropriate reaction vessels and equipment.

4.2.2 Application of the Auxiliary to Multi-Step Synthesis

This work has shown that auxiliary **245** can be synthesized on large scales, and applied to a variety of asymmetric reactions. The success of these investigations indicates that the fluorous oxazolidinone can likely be employed in any asymmetric transformation that currently uses non-fluorous oxazolidinones. While the application of the fluorous auxiliaries to such methods would be valuable, their potential use in multi-step supported syntheses makes them truly powerful tools for drug discovery and high-throughput chemistry.

The synthesis of methylphenidate analogues represents an interesting model system under consideration. These analogues represent pharmaceutically and biologically important structures, and thus are an excellent testing ground for the fluorous auxiliaries. Methylphenidate, also known by the brand name Ritalin®, is the most common treatment for attention deficit hyperactivity disorder (ADHD) and is typically given as a racemic mixture of (±)-*threo* compounds (Figure 4.2.2.1).[264]

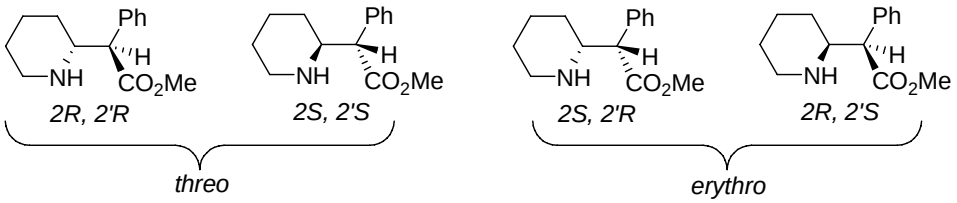

Figure 4.2.2.1: Stereoisomers of methylphenidate.

Aside from its role in the treatment of ADHD in children, methylphenidate is active generally as a dopamine reuptake inhibitor by binding to the dopamine transport protein (DAT) found in the synaptic cleft. Thus methylphenidate, or its structural analogues, may have broader application in the treatment of a variety of neurological conditions where the density or activity of DAT is altered, such as Parkinson's disease.

Methylphenidate also offers a lead structure for a specific cocaine agonist. Although cocaine has a number of target receptors in the body, its abuse potential is generally attributed to the inhibition of dopamine reuptake in the mesolimbic system.[265] Therefore, a methylphenidate analogue could compete with cocaine for the DAT binding sites, reducing cravings and blocking its pleasurable effects.[266]

Recent studies examining the possibility of using methylphenidate in replacement therapy for cocaine addicts indicate that a more potent and specific inhibitor is needed to offer effective treatment. [266] The array of analogues synthesised to date is large,[267-269] but little diversity has been achieved. This lack of diversity is inherent in the exsisting synthetic pathways, which in most cases cannot be adapted to generate alternate functionalization while maintaining good stereoselectivity and practical yields.

We have devised a combinatorial pathway that exploits our fluorous chiral auxiliary, allowing us to generate a library of methylphenidate analogues using a modular assembly approach (Scheme 4.2.2.1). This versatile pathway will allow us to vary the

aromatic substituent, the stereochemistry of the compound, the size of the heteroatom ring and substituents on that ring, as well as the heteroatom itself.

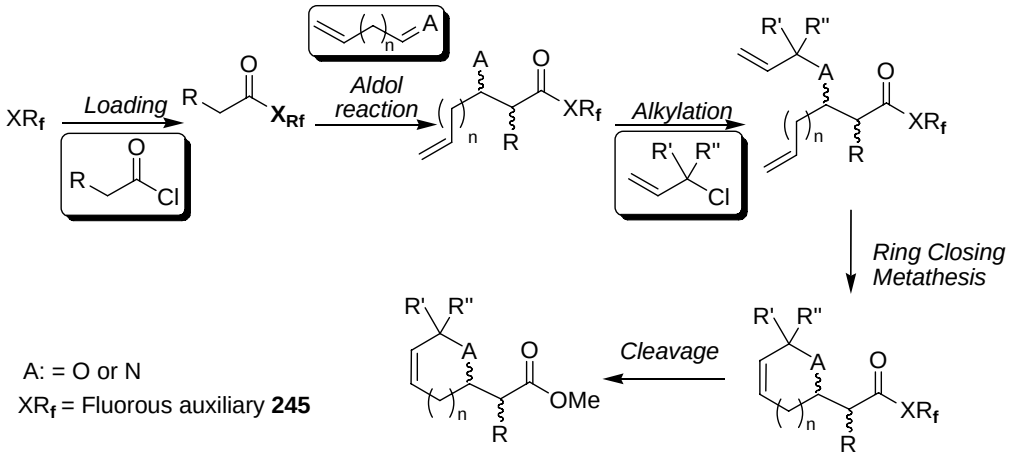

Scheme 4.2.2.1: General synthesis of methylphenidate analogues using a fluorous chiral auxiliary.

The initial aldol reaction is the key to the diversity of the library. By changing the acid chloride used to load the auxiliary we can vary the aromatic substituent. Changing the electrophile will vary a number of properties of the final heteroatom ring. The chain length and functional group present between the electrophilic centre and the alkene will determine the ring size and substitution respectively. Also, using the aldehyde or imine to give the corresponding oxygen and nitrogen compounds allows us to vary the nature of heteroatom itself.

Alkylation of the heteroatom with an appropriately substituted allyl chloride will prepare the molecule for ring closing metathesis, giving rise to the heterocyclic ring. The remaining alkene can then be reduced to give the unsubstituted ring, or used as a functional group to further diversify the library.

Throughout the synthesis of these analogues the molecule will remain loaded on the auxiliary. Thus, after the initial introduction of stereochemistry the auxiliary will function as a soluble support facilitating the rapid generation of this chiral library. Following each synthetic step the crude product will be rapidly purified using the fluorous solid phase extraction techniques, allowing a number of reactions to be carried out quickly and efficiently.

Chapter 5: EXPERIMENTAL PROCEDURES

General Procedures

All melting points were measured on an Electrothermal® melting point apparatus and are uncorrected. ^{1}H NMR (300 MHz, 400 MHz, or 500 MHz), ^{13}C NMR (75 MHz, 100MHz, or 125MHz) and ^{19}F NMR (282 MHz) spectra were recorded with a Bruker Avance 300 spectrometer, Varian Unity/Inova-400 NB or Bruker AMX 500 spectrometer. Chemical shifts are reported in parts per million (ppm) down field from TMS, using residual $CDCl_3$ (7.27 ppm) or $CDCl_3$ (77.00 ppm) as internal standards. Chemical shifts for ^{19}F are reported with respect to external $CFCl_3$ (0.00 ppm). Atom connectivity and assignment for ^{1}H and ^{13}C were determined using combinations of standard gradient ^{1}H-COSY, {^{1}H,^{13}C}-HSQC and {^{1}H,^{13}C}-HMBC techniques. Specific rotation was measured on an Autopol® III automatic polarimeter. Atomic absorbance spectroscopy was performed on a Varian SpectrAA-20. Preparative HPLC was performed using a Waters high throughput LC-MS-UV auto-purification system. Flash chromatography was performed using Silicycle Silica-P flash silica gel (230-400 mesh). Thin-layer chromatography was carried out on precoated (0.2 mm) Alugram® Sil G/UV silica gel plates. Fluorous solid phase extraction was performed using bulk FluoroFlash™ silica gel obtained from Fluorous Technologies Incorporated and packed into blank SPE cartridges.

Dichloromethane, triethylamine and diisopropylethylamine were distilled from calcium hydride under nitrogen prior to use. Tetrahydrofuran was distilled from sodium benzophenone under nitrogen. Tributyltin hydride was freshly distilled under vacuum from the reaction of tributyltin oxide with poly(methylhydrosiloxane). Lewis acids were

purchased from various suppliers (Aldrich, Lancaster, Acros), and stored in a desiccator. In most cases the Lewis acids were simply handled under normal atmosphere and used without further drying or purification. If required (as indicated in specific procedures) the Lewis acids were dried at 50 °C and 0.1 Torr for 24 h prior to use. All glassware was oven dried, assembled hot and cooled under a stream of nitrogen before use. Reactions with air sensitive materials were carried out by standard syringe techniques.

General procedures for purification using FSPE

Method A: Purification of fluorous material using a liquid loading protocol; Isolation of (*E*)-(4*S*,5*R*)-4-benzyl-3-(2'-butenoyl)-5-(1'*H*,-1'*H*,2'*H*,2'*H*-perfluorooctyl)-2-oxazolidinone (290a):

The crude material obtained after concentrating the reaction under vacuum (~1.5 g) was then dissolved in a minimum of Et_2O and applied to a pad of dry FluoroFlash™ (7-10 × crude weight) and driven onto the column using compressed air. The column was blown dry until no evidence of the loading solvent remained. The solid phase was then washed with 70% methanol in water (100 - 300 mL) to remove organic and inorganic impurities. (*E*)-(4*S*,5*R*)-4-benzyl-3-(2'-butenoyl)-5-(1'*H*,1'*H*,2'*H*,2'*H*-perfluoro-octyl)-2-oxazolidinone, **290a** (0.98 g, 1.7 mmol, 87 % yield) was then selectively eluted by washing the column with 85% methanol in water (200 - 400 mL).

Method B: Purification of fluorous material using adsorption protocol; Isolation of (*E*)-(4*S*,5*R*)-4-benzyl-3-(3'-phenyl-2'-propenoyl)-5-(1'*H*,-1'*H*,2'*H*,-2'*H*-perfluorooctyl)-2-oxazolidinone (290b):

The crude material obtained after quenching the reaction and concentrating under vacuum was adsorbed onto silica gel (2 × crude weight). The loaded silica gel was applied to a pad of silica (50 g), and washed with 4:1-Hex/EtOAc (100-250 mL) to give the desired product as a lightly colored oil. This material was then further purified by adsorbing onto fluorous-modified silica gel (2 × crude weight) and applied to an FPSE cartridge charged with 5.5 g of dry FluoroFlash™. The solid phase was washed with 70% methanol in water (100-250 mL) to remove organic and inorganic impurities. Washing the column with 85% methanol in water (100-250 mL) gave (*E*)-(4*S*,5*R*)-4-benzyl-3-(3'-phenyl-2'-propenoyl)-5-(1'*H*,1'*H*,2'*H*,2'*H*-perfluorooctyl)-2-oxazolidinone, **290b** (0.457 g, 0.699 mmol, 36.6 % yield) as a white crystalline solid.

Method C: Removal of alkyltin from fluorous material; Isolation of (3'*R*,4*S*,5*R*)-4-benzyl-3-(3',4'-dimethyl-pentanoyl)-5-(1'*H*,1'*H*,-2'*H*,2'*H*-perfluorooctyl)-2-oxazolidinone (291a):

The reaction was quenched with silica gel (1g) and the volatile material was removed under vacuum. The loaded silica was transferred to a fritted filter and washed with hexanes (~20 mL) to remove the bulk of the alkyltin compounds. The silica was then eluted with Et_2O to give the desired product as a crude oil, which was then adsorbed onto fluorous-modified silica gel (2 × crude weight) and applied to an FPSE cartridge charged with 5.5 g of dry FluoroFlash™. The solid phase was washed with 70%

methanol in water (500 mL) to remove organic and inorganic impurities. Washing the column with methanol (250 mL) gave (3'*R*,4*S*,5*R*)-4-benzyl-3-(3',4'-dimethyl-pentanoyl)-5-(1'*H*,1'*H*,-2'*H*,2'*H*-perfluorooctyl)-2-oxazolidinone, **291a** as a mixture of diastereomers (0.051 g, 95 % yield).

Synthesis of Amino Acid Electrophiles

General Procedure for the Synthesis of Amino Ester Hydrochlorides; Preparation of Methyl phenylalaninate hydrochloride:

MeOH (250 mL) was added to L-phenylalanine (15.0 g, 90.8 mmol) and the mixture was cooled to 0°C. $SOCl_2$ (13.2 mL, 182 mmol) was added dropwise over a period of 45 min, during which time the solution cleared and began to boil gently. The reaction mixture was then refluxed for 4 h before cooling and removing the solvent using a rotary evaporator. This produced a crude white solid, which was resuspended in MeOH and evaporated under reduced pressure to remove excess HCl. The product was then triturated with hexane and filtered, yielding 19.2g (~99%) of methyl phenylalaninate hydrochloride. After drying the material under high vacuum it was carried through without further purification.

Methyl phenylalaninate hydrochloride:

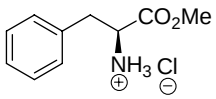

Synthesized from L-phenylalanine. Isolated as a white powder whose ^{1}H and ^{13}C NMR spectra matched literature values.[231]

Ethyl phenylalaninate hydrochloride:

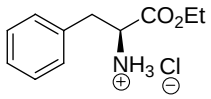

Synthesized from L-phenylalanine. Isolated as a white powder whose ^{1}H and ^{13}C NMR spectra matched literature values.[270]

Methyl phenylglycinate hydrochloride:

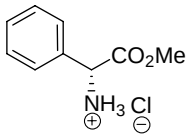

Synthesized from D-phenylglycine. Isolated as a white powder whose ^{1}H and ^{13}C NMR spectra matched literature values.[232]

Methyl (*S*)-*N*-(benzyloxycarbonyl)-phenylalaninate (208a):

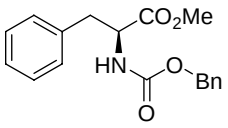

N-(Benzyloxycarbonyl)-phenylalaninate (5.00 g, 16.7 mmol) was dissolved in methanol (100 mL) and cooled to 0°C. $BF_3 \cdot Et_2O$ (4.5 mL, 35 mmol) was added dropwise over a period of 15 min. The reaction mixture was then removed from the ice bath and heated to reflux for 1 h before cooling and removing the solvent using a rotary evaporator. The crude residue was suspended with ice water and extracted with EtOAc. The combined organic extracts were washed successively with 1 M $NaHCO_3$, and brine, then the organic layer was dried with $MgSO_4$ and evaporated to dryness to give (4.5 g, 86%) of **208a** as a clear oil whose ^1H and ^{13}C NMR spectra matched literature values.[230] After drying the material thoroughly under high vacuum it was carried through without further purification.

Methyl (*S*)-*N*-(ethoxycarbonyl)-phenylalaninate (208b):

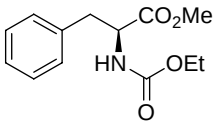

Methyl phenylalaninate hydrochloride (10.0 g, 46.4 mmol) was suspended in THF (100 mL) and cooled to 0°C. TEA (27.8 mL, 200 mmol) was added dropwise, during which time the solution cleared. Ethyl chloroformate (4.85 mL, 51.0 mmol) was then added dropwise and the solution was allowed warm to room temperature and then was

stirred for 2 hrs. After this time the reaction mixture was concentrated using a rotary evaporator, and the resulting residue was dissolved in EtOAc and water. The organic fraction was separated and washed successively with 1M HCl, 1M $NaHCO_3$, and brine. The organic fraction was then dried with $MgSO_4$ and evaporated to give a crude oil. The material was eluted through a 10 cm pad of silica gel with 4:1 Hex:EtOAc to produce (10.14 g, 87%) of **208b** as a clear oil whose ^1H and ^{13}C NMR spectra matched literature values.[232]

Ethyl (*S*)-*N*-(benzyloxycarbonyl)-phenylalaninate (208c):

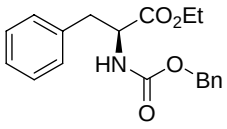

N-(Benzyloxycarbonyl)-phenylalaninate (5.00 g, 16.7 mmol) was dissolved in ethanol (100 mL) and cooled to 0°C. $BF_3{\cdot}Et_2O$ (4.45 mL, 35.1 mmol) was added dropwise over a period of 15 min. The reaction mixture was then removed from the ice bath and heated to reflux for 1 h before cooling and removing the solvent using a rotary evaporator. The crude residue was suspended with ice water and extracted with EtOAc. The combined organic extracts were washed successively with 1 M $NaHCO_3$, and brine, and then dried with $MgSO_4$ and evaporated to dryness to give (4.5 g, 86%) of **208c** as a clear oil whose ^1H and ^{13}C NMR spectra matched literature values.[271] After drying the material thoroughly under high vacuum it was carried through without further purification.

Ethyl (*S*)-*N*-(ethoxycarbonyl)-phenylalaninate (208d):

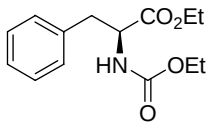

N-(Ethoxycarbonyl)-phenylalaninate (10.0 g, 46.4 mmol) was dissolved in ethanol (100 mL) and cooled to 0°C. $BF_3 \cdot Et_2O$ (12.65 mL, 92.00 mmol) was added dropwise over a period of 15 min. The reaction mixture was then removed from the ice bath and heated to reflux for 1 h before cooling and removing the solvent using a rotary evaporator. The crude residue was suspended with ice water and extracted with EtOAc. The combined organic extracts were washed successively with 1 M $NaHCO_3$, and brine, then were dried with $MgSO_4$ and evaporated to dryness to give (11.7 g, 83%) of **208d** as a clear oil whose ^1H and ^{13}C NMR spectra matched literature values.[272] After drying the material thoroughly under high vacuum it was carried through without further purification.

Methyl (*S*)-*N*-(*iso*-propoxycarbonyl)-phenylalaninate (232b):

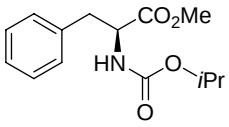

Methyl phenylalaninate hydrochloride (20.0 g, 92.8 mmol) was suspended in THF (100 mL) and cooled to 0°C. TEA (27.85 mL, 199.5 mmol) was added dropwise, during which time the solution cleared. Isopropyl chloroformate (102 mL of a 1M solution in hexane, 102 mmol) was then added dropwise and the solution was allowed to stir at 0°C

for 2 hrs. After this time the reaction mixture was concentrated using a rotary evaporator, and the resulting residue was dissolved in EtOAc and water. The organic fraction was separated and washed successively with 1M HCl, 1M $NaHCO_3$, and brine. The organic fraction was then dried with $MgSO_4$ and evaporated to give a crude white solid. The material was recrystallized from petroleum ether to produce **232b** (14.43 g, 70%) as a cottony white material whose ^1H and ^{13}C NMR spectra matched literature values.[273]

Methyl (*S*)-*N*-(ethoxycarbonyl)-phenylglycinate (252):

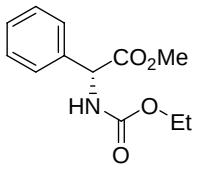

Methyl phenylglycinate hydrochloride (5.00 g, 24.8 mmol) was dissolved in water. $NaHCO_3$ (13.14 g, 124.0 mmol) was added slowly and the reaction was stirred vigorously to effectively dissipate any gas generated. Ethyl chloroformate (3.35 mL, 34.7 mmol) was then added dropwise over 5 min, producing a clear solution. The reaction was then stirred for 5 h at r.t.. After this time a white precipitate had formed and was easily isolated by filtration. The crystals were washed with cold water, giving **252** (5.70 g, 24.0 mmol, 97 % yield) as a white powder whose ^1H and ^{13}C NMR spectra matched literature values.[232]

General Procedure for the Synthesis of *N*-Carbamoyl Amino Acids via Modified Schotten-Baumann Conditions; Preparation of 2(*S*)-*N*-(ethoxycarbonyl) phenylalanine (237a):

L-Phenylalanine (20.00 g, 121.1 mmol) was suspended in 200 mL of 50% methanol in water. Sodium carbonate (25.7 g, 242 mmol) was added slowly and the reaction was stirred vigorously to effectively dissipate gas generation. Ethyl chloroformate (17.45 mL, 182.0 mmol) was added dropwise over 25 min, producing a clear solution. The reaction was then stirred at r.t. overnight. After this time the reaction was poured into a separatory funnel and the alkaline solution was extracted with Et_2O. The organic layer was discarded and the aqueous portion was acidified with sufficient 2M HCl to produce an acidic solution (pH ~ 5). The aqueous solution was then extracted with Et_2O and the combined organic layers were washed with brine, dried over magnesium sulfate, and evaporated to dryness. This gave a clear oil that could be triturated with petroleum ether to give 2(*S*)-*N*-(ethoxylcarbonyl) phenylalanine (24.0 g, 101 mmol, 84 % yield) as a white powder, whose ^{1}H NMR and ^{13}C spectra matched those reported in the literature.[208] The material was carried forward without further purification.

2(*S*)-*N*-(Ethoxycarbonyl)-phenylalaninate (237a):

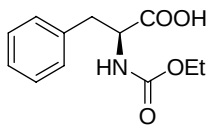

Material prepared using general Schotten-Baumann procedure described in this document. The compound is also commercially available. CAS = [19887-32-2]

2(*S*)-*N*-(iso-Propoxycarbonyl)-phenylalaninate (237b):

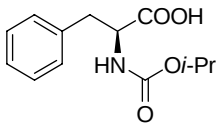

Material prepared using general Schotten-Baumann procedure described in this document. The compound is also commercially available. CAS = [19887-32-2]

N-(Benzyloxycarbonyl)-phenylalaninate (237c):

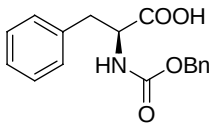

L-Phenylalanine (5.00 g, 30.3 mmol) was suspended in THF (500 mL) and refluxed for 1 h to produce a concentrated solution. While the solution was still at reflux benzyl chloroformate (4.35 mL, 30.3 mmol) was added producing a milky solution. The mixture was refluxed for an additional 2 hrs, after which the reaction was cooled to room temperature and filtered to remove unreacted L-phenylalanine present as a fine white precipitate. The filtrate was concentrated under vacuum to produce a clear oil, which solidified when triturated with petroleum ether. The solid was filtered to give *N*-CBz phenylalanine (7.0 g 77%) as a white solid. The ^{1}H and ^{13}C NMR matched literature values[229] allowing the material to be carried forward without further purification.

(*S*)-*N*-(*tert*-Butoxycarbonyl)-valaninate:

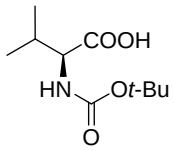

Material prepared using general Schotten-Baumann procedure described in this document. The compound is also commercially available. CAS = [13734-41-3]

(*R*)-*N*-(*tert*-Butoxycarbonyl)-phenylglycinate:

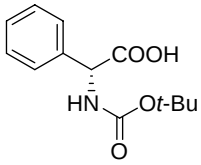

Material prepared using general Schotten-Baumann procedure described in this document. The compound is also commercially available. CAS = [33125-05-2]

General Procedure for the Synthesis of *N*-Carbamoyl Weinreb Amides Using Isobutyl Chloroformate; 2(S)-*N*-(Ethoxycarbonyl)-*N*'-methoxy-*N*'-methyl-phenylalaninamide (240a):

2(*S*)-*N*-(Ethoxycarbonyl) phenylalanine (21.00 g, 89.00 mmol) was dissolved in CH_2Cl_2 (250 mL) and cooled to -30 °C. DIPEA (17.0 mL, 97.1 mmol) was added dropwise, and the solution was allowed to stir at -30 °C for 15 min. Isobutyl chloroformate (12.75 mL, 97.04 mmol) was added dropwise while monitoring the reaction temperature with a digital thermometer. The addition rate was carefully

controlled to keep the internal temperature between −30 °C and –25 °C. Following completion of the addition stirring was continued at −30 °C for an additional 15 min, at which time DIPEA (20.8 mL, 119 mmol) was added dropwise. Solid *N*,*O*-dimethylhydroxylamine hydrochloride (11.66 g, 119.0 mmol) was added in one portion, followed by DMF (10 mL). The reaction was allowed to warm to r.t. over 3 h, and was then quenched with 1M HCl and diluted with CH_2Cl_2. The layers were separated, and the organic layer was washed successively with 1M HCl, $NaHCO_3$ and brine. The organic layer was dried ($MgSO_4$) and concentrated. The residual oil was eluted through a pad of silica gel (4:1−hexanes/ethyl acetate) to produce **240a** (22.12 g, 79.04 mmol, 89 % yield) as a clear oil.

General Procedure for the Synthesis of *N*-Carbamoyl Weinreb Amides Using 3-Chloro-methylpyridinium iodide; 2(*S*)-*N*-(Benzyloxycarbon-yl)-*N*'-methoxy-*N*'-methyl-phenylalaninamide (240c):

2(*S*)-*N*-(Benzyloxycarbonyl) phenylalanine (12.00 g, 41.11 mmol) was dissolved in CH_2Cl_2 (250 mL). DIPEA (17.45 mL, 100.0 mmol) was added dropwise, followed by CMPI (20.49 g, 80.12 mmol) and *N*,*O*-dimethylhydroxylamine hydrochloride (6.26 g, 64.1 mmol). The solution was then refluxed for 24 h, and then cooled to r.t.. The reaction was then quenched with 1M HCl and diluted with CH_2Cl_2. The layers were separated, and the organic layer was washed successively with 1M HCl, $NaHCO_3$ and brine. The organic layer was dried ($MgSO_4$) and concentrated. The residual oil was purified using flash column chromatography on silica (9:1 hexane: EtOAc) to yield the desired product **240c** (9.25 g, 27.0 mmol, 67.4 % yield) as a clear oil.

General Procedure for the Synthesis of *N*-Carbamoyl Weinreb Amides Using 2-chloro-4,6-dimethoxy-[1,3,5]triazine; 2(*S*)-*N*-(Benzyloxy-carbonyl)-*N*'-methoxy-*N*'-methyl-phenylalaninamide (240c):

2(*S*)-*N*-(Benzyloxycarbonyl) phenylalanine (5.00 g, 16.7 mmol) was dissolved in THF (100 mL). *N*-Methylmorpholine (4.59 mL, 41.8 mmol) was added dropwise, followed by CDMT (3.67 g, 20.9 mmol). The solution was allowed to stir at r.t. for 1 h, then *N,O*-dimethylhydroxylamine hydrochloride was added. The solution was allowed to stir at r.t and monitored by TLC. Upon completion the reaction quenched with H_2O and extracted with twice with Et_2O. The organic extracts were washed successively with 1M HCl, $NaHCO_3$ and brine. The organic layer was dried ($MgSO_4$) and concentrated. The residual oil was then triturated with Et_2O and then eluted through a pad of silica gel (4:1−hexanes/ethyl acetate) to produce **240c** (4.46 g, 13.0 mmol, 78 % yield) as a clear oil.

General Procedure for the Synthesis of *N*-Carbamoyl Weinreb Amides Using TBTU; 2(*S*)-*N*-(*tert*-Butoxycarbonyl)-*N*'-methoxy-*N*'-methyl-valinamide (251):

Solid (*S*)-*N*-(*tert*-Butoxycarbonyl)-valinate (1.50 g, 6.90 mmol), *N,O*-dimethoxyhydroxylamine hydrochloride (1.01 g, 10.4 mmol) and TBTU (3.33 g, 10.4 mmol) were combined. The powders were dissolved in freshly distilled acetonitrile (25 mL) and then the reaction was cooling to 0 °C. The solution was stirred at 0 °C for 10 min, and then DIPEA (3.61 ml, 20.7 mmol) was added dropwise. The solution turned

yellow, and quickly became opaque. The reaction was allowed to warm to r.t. over 3 h. After this time the reaction was concentrated under vacuum, and the residue was taken up in Et_2O. The mixture was washed sequentially with 1M HCl, 1M $NaHCO_3$ and brine. The organic fraction was dried with $MgSO_4$ and evaporated to dryness. The resulting crude yellow oil was applied to a 10 cm pad of silica gel and eluted with 4:1−hexanes/ethyl acetate, providing **251** (0.102 g, 0.346 mmol, 87 % yield) as clear oil.

2(*S*)-*N*-(Ethoxycarbonyl)-*N*'-methoxy-*N*'-methyl-phenylalaninamide (240a):

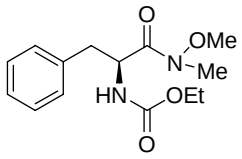

^{1}H NMR (300 MHz, $CDCl_3$) δ 7.29 – 7.14 (m, 5H, −C_6H_5), 5.45 (d, 1H, ^3J = 8.3 Hz, N*H*), 4.96 (ddd, 1H, $^3J_1$ = 8.3 Hz, $^3J_2$ = 7.2 Hz, $^3J_3$ = 6.4 Hz, −C*H*Bn), 4.03 (q, 2H, ^3J = 7.2 Hz, −OCH_2CH$_3$), 3.64 (s, 3H, −OCH_3), 3.14 (s, 3H, −NCH_3OMe), 3.04 (dd, 1H, $^3J_1$ = 13.6 Hz, $^3J_2$ = 6.2 Hz, −C*H*HC_6H_5), 2.88 (dd, 1H, $^3J_1$ = 13.6 Hz, $^3J_2$ = 7.2 Hz, −CH*H*C_6H_5), 1.17 (t, 3H, ^3J = 7.2 Hz, −OCH$_2$CH_3); ^{13}C (75 MHz, $CDCl_3$) δ 14.5 (−OCH$_2$*C*H$_3$), 32.0 (−N*C*H$_3$OMe), 38.6 (−*C*H$_2$C$_6$H$_5$), 52.0 (Bn*C*H−), 61.2 (−O*C*H$_2$CH$_3$), 62.0 (−OCH$_3$), 126.8, 128.4, 129.4, 136.5 (*C*$_6$H$_5$−), 156.1 (−*C*OOEt), 172.1 (−*C*OONMeOMe); $[\alpha]_D$ = +15.2° (c = 1.0, $CHCl_3$); Anal. Calc'd for formula $C_{14}H_{20}N_2O_4$: C, 59.99; H, 7.19; N, 9.99. Found: C, 59.94; H, 7.40; N, 10.20.

2(*S*)-*N*-(iso-Propoxycarbonyl)-*N*'-methoxy-*N*'-methyl-phenylalanin-amide (240b):

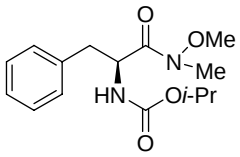

^{1}H NMR (300 MHz, $CDCl_3$) δ 7.31 – 7.17 (m, 5H, −C_6H_5), 5.54 (d, 1H, ^{3}J = 8.3 Hz, N*H*), 4.89 (ddd, 1H, $^{3}J_1$ = 8.3 Hz, $^{3}J_2$ = 7.3 Hz, $^{3}J_3$ = 6.4 Hz, −C*H*Bn), 4.03 (m, 1H, −OC*H*$(CH_3)_2$), 3.70 (s, 3H, −OCH_3), 3.21 (s, 3H, −NCH_3OMe), 3.06 (dd, 1H, $^{3}J_1$ = 13.4 Hz, $^{3}J_2$ = 6.4 Hz, −C*H*HC_6H_5), 2.88 (dd, 1H, $^{3}J_1$ = 13.6 Hz, $^{3}J_2$ = 7.3 Hz, −CH*H*C_6H_5), 1.17 (d, 3H, ^{3}J = 7.2 Hz, −OCHCH_3CH_3), 1.10 (d, 3H, ^{3}J = 7.5 Hz, −OCHCH_3CH_3); ^{13}C (75 MHz, $CDCl_3$) δ 12.9 (−OCH(*C*$H_3)_2$), 14.4 (−OCH(*C*$H_3)_2$), 33.2 (−N*C*H_3OMe), 38.9 (−*C*$H_2C_6H_5$), 52.9 (Bn*C*H−), 61.7 (−O*C*H$(CH_3)_2$), 62.1 (−O*C*H_3), 126.7, 128.6, 128.2, 136.7 (*C*$_6H_5$−), 155.9 (−*C*OO*i*Pr), 173.0 (−*C*OONMeOMe); $[\alpha]_D$ = +14.1˚ (c = 0.8, $CHCl_3$); Anal. Calc'd for formula $C_{15}H_{22}N_2O_4$: C, 61.21; H, 7.53; N, 9.52. Found: C, 61.34; H, 7.45; N, 9.78.

2(*S*)-*N*-(Benzyloxycarbonyl)-*N*'-methoxy-*N*'-methyl-phenylalaninamide (240c):

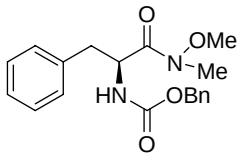

Chemical and spectroscopic properties matched those reported in the literature.[240]

2(*S*)-*N*-(*tert*-Butoxycarbonyl)-*N*'-methoxy-*N*'-methyl-valaninamide (257):

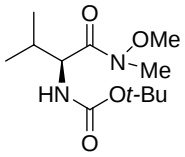

^{1}H NMR (300MHz, $CDCl_3$) δ 5.09 (br d, 1H, ^3J = 9.4 Hz, N*H*), 4.47 – 4.41 (m, 1H, *i*PrC*H*−), 3.64 (s, 3H, −OCH_3), 3.08 (s, 3H, −NCH_3OMe), 1.86 (dqq, 1H, $^3J_1$ = 6.8 Hz, $^3J_2$ = 6.7 Hz, $^3J_3$ = 6.7 Hz, $(CH_3)_2CH$−), 1.30 (s, 9H, $(CH_3)_3C$−), 0.82 (d, 3H, ^3J = 6.7 Hz, CH_3CHCH_3), 0.78 (d, 3H, $^3J_1$ = 6.7 Hz, CH_3CHCH_3); ^{13}C (75MHz, $CDCl_3$) δ 17.4 (CH_3CHCH_3), 19.4 (CH_3CHCH_3), 28.3 ($(CH_3)_3C$−), 31.3 (CH_3CHCH_3), 31.8 (−NMe), 54.9 (*i*PrCHN−), 61.5 (−OMe), 61.8 ($(CH_3)_3C$−), 155.8 (−COOtBu), 172.9 (−CONMeOMe); $[\alpha]_D$ = +6.88˚ (c = 1.2, $CHCl_3$); Anal. Calc'd for formula $C_{12}H_{24}N_2O_4$: C, 55.36; H, 9.29; N, 10.76. Found: C, 55.12; H, 8.99; N, 10.66.

2(*R*)-*N*-(*tert*-Butoxycarbonyl)-*N*'-methoxy-*N*'-methyl-phenylglycin-amide (261):

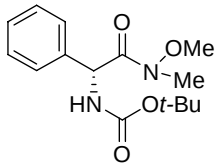

^{1}H NMR (300MHz, $CDCl_3$) δ 7.33 – 7.22 (m, 5H, −C_6H_5), 5.79 (d, 1H, ^{3}J = 8.0 Hz, N*H*), 5.65 (d, 1H, ^{3}J = 8.0 Hz, N*H*), 3.38 (s, 3H, −OC*H*$_3$), 3.10 (s, 3H, −NC*H*$_3$OMe), 1.35 (s, 9H, (C*H*$_3$)$_3$C−); ^{13}C (75MHz, $CDCl_3$) δ 28.3 ((*C*H$_3$)$_3$C−), 32.2 (−N*C*H$_3$OMe), 54.9 (Ph*C*H−), 61.0 (−NMeO*C*H$_3$), 79.6 ((CH$_3$)$_3$*C*−), 127.7, 128.0, 128.7, 138.0 (−*C*$_6$H$_5$), 154.9 (−*C*OOtBu), 171.2 (−*C*ONMeOMe); $[\alpha]_D$ = −133.0° (c = 1.6, $CHCl_3$); Anal. Calc'd for formula $C_{15}H_{22}N_2O_4$: C, 61.21; H, 7.53; N, 9.52. Found: C, 61.37; H, 7.55; N, 9.31.

Nucleophilic Perfluoroalkyl Additions Using Perfluoroalkyl Grignard and Perfluoroalkyllithium Reagents

General Procedure for Perfluoroalkylation of *N*-Carbamoyl Amino Esters using Perfluoroalkyllithium Reagents Derived from $C_8F_{17}I$: 2(*S*)-(Ethoxycarbonylamino)-4,4,5,5,6,6,7,7,8,8,9,9,10,10,11,-11,11-heptadecafluoro-1-phenyl-undecan-3-one (209b):

Amino ester **208b** (0.750 g, 2.98 mmol) was dissolved in dry ethyl ether (250 mL). $BF_3{\cdot}OEt_2$ (0.404 mL, 3.28 mmol) was added to the solution, followed by $C_8F_{17}I$ (0.90 mL, 3.28 mmol). The reaction mixture was cooled to –78ºC and MeLi − LiBr (3.55 mL, 1.5M solution in ether) was added dropwise over 15 min. The reaction proceeded at

–78ºC for 2 h, and was then quenched with dilute NH_4Cl before allowing the solution to warm to room temperature. The aqueous layer was then extracted with Et_2O and the combined extracts were washed with brine, dried with $MgSO_4$, and evaporated to dryness. The crude material (2.0 g) was dissolved in a minimum of *n*−PrOH and purified by FSPE using general method **A**. Fluorous products were further purified using flash chromatography on silica gel, eluting with a solvent gradient (hexane to 9:1 hexane: EtOAc) to give ketone **209b** (0.725 g, 1.14 mmol, 38% yield) and tertiary alcohol **211b** (0.020 g, 0.030 mmol, 1% yield).

2(*S*)-(Benzyloxycarbonylamino)-4,4,5,5,6,6,7,7,8,8,9,9,10,10,11,11,11-heptadecafluoro-1-phenyl-undecan-3-one (209a):

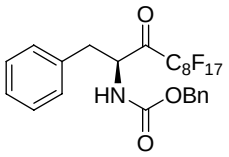

Mp = 62 – 66˚C, ^{1}H NMR (300 MHz, acetone-d_6) δ 7.74 – 7.12 (m, 10H, 2 × C_6H_5), 5.46 (d, 1H, ^3J = 8.1 Hz, N*H*), 5.11 – 5.01 (m, 1H, BnC*H*N−), 5.11 (s, 2H, PhCH_2O−), 3.27 (dd, 1H, $^3J_1$ = 13.2 Hz, $^3J_2$ = 4.5 Hz, PhC*H*H−), 2.78 (dd, 1H, $^3J_1$ = 13.4 Hz, $^3J_2$ = 7.9 Hz, PhCH*H*−); ^{13}C (75 MHz, $CDCl_3$) δ 36.9 (Ph*C*H$_2$−), 59.1 (Bn*C*HN−), 68.1 (Bn*C*H$_2$O−), 126.5 − 148.1 (2 × *C*$_6$H$_5$−), 155.9 (−NH*C*OO−), 199.2 (−CO*C*$_8$F$_{17}$); ^{19}F (282 MHz, $CDCl_3$) δ −81.32, −114.98, −122.16, −123.31, −123.99, −124.28, −124.83, −126.43; Anal. Calc'd for formula $C_{25}H_{16}F_{17}NO_3$: C, 42.81; H, 2.30; N, 2.00. Found: C, 42.99; H, 2.00; N, 1.84.

2(*S*)-(Ethoxycarbonylamino)-4,4,5,5,6,6,7,7,8,8,9,9,10,10,11,11,11-heptadecafluoro-1-phenyl-undecan-3-one (209b):

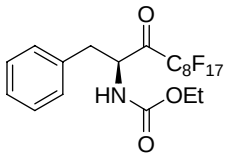

mp = 55 – 57˚C, ^{1}H NMR (300 MHz, acetone-d_6) δ 7.33 – 7.22 (m, 5H, C_6H_5), 5.34 (d, 1H, ^{3}J = 8.3 Hz, N*H*), 5.23 – 5.04 (m, 1H, BnC*H*N−), 4.06 (q, 2H, ^{3}J = 7.2 Hz, −OC*H*$_2$CH$_3$), 3.25 (dd, 1H, $^{3}J_1$ = 14.1 Hz, $^{3}J_2$ = 4.3 Hz, PhC*H*H−), 2.90 (dd, 1H, $^{3}J_1$ = 13.8 Hz, $^{3}J_2$ = 7.9 Hz, PhCH*H*−), 1.17 (t, 3H, ^{3}J = 7.2 Hz, −OCH$_2$C*H*$_3$); ^{13}C (75 MHz, $CDCl_3$) δ 14.2 (−OCH$_2$*C*H$_3$), 36.7 (Ph*C*H$_2$−), 57.1 (Bn*C*HN−), 61.6 (−O*C*H$_2$CH$_3$), 127.5 − 134.2 (*C*$_6$H$_5$−), 155.5 (−NH*C*OO−), 193.13 (−CO*C*$_8$F$_{17}$); ^{19}F (282 MHz, $CDCl_3$) δ −81.25, −114.93, −122.36, −123.32, −123.93, −124.88, −124.99, −126.58; Anal. Calc'd for formula $C_{20}H_{14}F_{17}NO_3$: C, 37.58; H, 2.21; N, 2.19. Found: C, 37.42; H, 2.01; N, 2.04.

2(*S*)-(Benzyloxycarbonylamino)-4,4,5,5,6,6,7,7,8,8,9,9,10,10,11,11,11-heptadecafluoro-3-methly-1-phenyl-undecan-3-ol (211a):

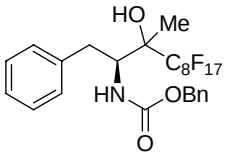

Mp = 83 – 85˚C, ^{1}H NMR (300 MHz, acetone-d_6) δ 7.67 – 7.09 (m, 10H, 2 × C_6H_5), 5.57 (d, 1H, ^{3}J = 7.1 Hz, N*H*), 5.45 – 5.42 (m, 1H, BnC*H*N−), 5.35 (s, 2H, PhC*H*$_2$O−), 3.44 – 3.14 (m, 2H, PhC*H*$_2$−), 1.88 (s, 3H, −CH$_3$); ^{13}C (75 MHz, $CDCl_3$) δ 21.0 (−*C*H$_3$), 38.1 (Ph*C*H$_2$−), 57.1 (Bn*C*HN−), 68.1 (Bn*C*H$_2$O−), 71.2 (CH$_3$*C*(OH)−),

127.1 − 139.0 (2 × C_6H_5−), 151.6 (−NH*C*OO−); ^{19}F (282 MHz, $CDCl_3$) δ −82.12, −115.12, −122.34, −123.31, −123.29, −123.78, −125.13, −125.93; Anal. Calc'd for formula $C_{26}H_{20}F_{17}NO_3$: C, 43.53; H, 2.81; N, 1.95. Found: C, 43.21; H, 2.75; N, 1.86.

2(*S*)-(Ethoxycarbonylamino)-4,4,5,5,6,6,7,7,8,8,9,9,10,10,11,11,11-heptadecafluoro-3-methyl-1-phenyl-undecan-3-ol (211b):

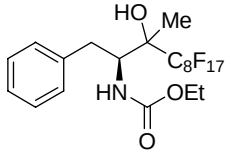

mp = 55 – 57°C, ^{1}H NMR (300 MHz, acetone-d_6) δ 7.32 – 7.29 (m, 5H, C_6H_5), 5.45 (d, 1H, ^{3}J = 7.9 Hz, N*H*), 5.26 – 5.07 (m, 1H, BnC*H*N −), 4.12 (q, 2H, ^{3}J = 7.5 Hz, −OC*H*$_2$CH$_3$), 3.67 (dd, 1H, $^3J_1$ = 13.7 Hz, $^3J_2$ = 4.1 Hz, PhC*H*H−), 2.87 (dd, 1H, $^3J_1$ = 13.9 Hz, $^3J_2$ = 8.3 Hz, PhCH*H*−), 1.39 (s, 3H, −CH$_3$), 1.23 (t, 3H, ^{3}J = 7.5 Hz, −OCH$_2$C*H*$_3$); ^{13}C (75 MHz, $CDCl_3$) δ 15.7 (−OCH$_2$*C*H$_3$), 38.1 (Ph*C*H$_2$−), 55.5 (Bn*C*HN−), 63.1 (−O*C*H$_2$CH$_3$), 71.8 (CH$_3$*C*(OH)−), 128.2 − 145.1 (*C*$_6$H$_5$−), 157.1 (−NH*C*OO−); ^{19}F (282 MHz, $CDCl_3$) δ −84.15, −113.34, −123.16, −123.72, −124.23, −124.88, −125.23, −126.12; Anal. Calc'd for formula $C_{21}H_{18}F_{17}NO_3$: C, 38.49; H, 2.77; N, 2.14. Found: C, 37.41; H, 2.34; N, 2.03.

General Procedure for Perfluoroalkylation of *N*-Carbamoyl Amino Esters using Perfluoroalkyl Grignard Reagents Derived from $C_6F_{13}(CH_2)_2I$; 2(*S*)-(Benzyloxycarbonylamino)-6,6,7,7,8,8,9,9,10,10,-11,11,11-tridecafluoro-1-phenyl-undecan-3-one (233c):

Magnesium powder (0.15 g, 6.5 mmol) was placed into a flask and flame-dried under vacuum. The magnesium powder was covered with a minimum of dry Et_2O and then 1*H*,1*H*,2*H*,2*H*-perfluorooctyl iodide (0.150 g, 0.633 mmol) was added. The suspension was stirred vigorously for 1 h. After this time a solution of 1*H*,1*H*,2*H*,2*H*-perfluorooctyl iodide (1.35 mL, 5.70 mmol) in Et_2O (25 mL) was added dropwise over 45 min. After the addition was completed the solution was dark grey in color characteristic of a Grignard reagent. In a separate flask amino ester **232c** (0.661 g, 2.11 mmol) was dissolved in dry Et_2O and added dropwise to the Grignard solution. The reaction was allowed to stir for 4 h, and then quenched with dil. NH_4Cl. The solution was then extracted with Et_2O and the combined ether extracts were washed with brine, dried with $MgSO_4$, and evaporated to dryness. The crude material was then purified by FSPE using the general method **A** to give ketone **233c** (0.200 g, 0.317 mmol, 15% yield) (from 85% MeOH in water) and tertiary alcohol **234c** (0.103 g, 0.105 mmol, 5% yield) (from MeOH eluent).

General Procedure for Perfluoroalkylation of *N*-Carbamoyl Amino Esters or *N*-Carbamoyl Weinreb Amides using Perfluoroalkyllithium Reagents Derived from $C_6F_{13}(CH_2)_2I$; 3(*S*)-(*tert*-Butoxycarbonylamino)-7,7,8,8,9,9,10,10,11,11,12,12,12-tridecafluoro-2-methyl-dodecan-4-one (250):

1*H*,1*H*,2*H*,2*H*-Perfluorooctyl iodide (4.60 ml, 19.5 mmol) was dissolved in ether:hexane (3:2) and cooled to −78 ºC. *t*-BuLi (12.20 ml, 20.75 mmol) was added dropwise via cannula, taking care to keep the reaction temperature below −60 ºC. In a separate flask amino ester **249** (3.00 g, 13.0 mmol) was dissolved in dry Et_2O and added via cannula to the perfluoroalkyl lithium reagent. Again the addition rate was adjusted to maintain an internal temperature below −60 ºC. The reaction was then stirred at −78 ºC for 15 min and then allowed to warm to r.t over 4 h. The reaction was quenched with dilute aqueous NH_4Cl, and then extracted with Et_2O. The combined ether extracts were washed with brine, dried ($MgSO_4$), and evaporated to dryness. The crude material was then purified by FSPE using general method A to give ketone **250** (3.00 g, 5.46 mmol, 42.1 % yield) (from 85% MeOH in water wash) and tertiary acohol **251** (2.49 g, 2.78 mmol, 21.1 % yield) (from MeOH wash).

General Procedure for the Application of a Sacrificial Base in the Perfluoroalkylation of *N*-Carbamoyl Weinreb Amides; 2(*S*)-(Ethoxycarbonylamino)-6,6,7,7,8,8,9,9,10,10,11,11,11-tridecafluoro-1-phenyl-undecan-3-one (233a):

1*H*,1*H*,2*H*,2*H*-Perfluorooctyl iodide (26.6 ml, 112 mmol) was dissolved in ether:hexane (3:2, 500 mL) and cooled to −78 ºC. *t*-BuLi (70.5 ml, 120 mmol) was added dropwise via cannula, taking care to keep the reaction temperature below −60 ºC. In a separate flask **240a** (21.0 g, 74.9 mmol) was dissolved in dry Et_2O, cooled to −78 ºC and deprotonated by adding *t*-BuLi (48.5 ml, 82.0 mmol). The solution of deprotonated amide was then transferred via cannula into the perfluoroalkyllithium reagent. The reaction was then stirred at −78ºC for ~15 min and then allowed to warm to r.t over 4 h. The reaction was quenched with dilute aqueous NH_4Cl, and extracted with Et_2O. The combined ether extracts were washed with brine, dried ($MgSO_4$), and evaporated to dryness. The crude material was then purified by FSPE according to general **A** to give ketone **233a** (28.88 g, 51.1 mmol, 68.2% yield).

2(*S*)-(Ethoxycarbonylamino)-6,6,7,7,8,8,9,9,10,10,11,11,11-tridecafluoro-1-phenyl-undecan-3-one (233a):

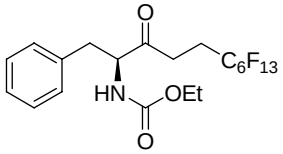

R_f = 0.3 (9:1−hexanes/ethyl acetate); mp = 57−60 °C; ^{1}H NMR (300 MHz, $CDCl_3$) δ 7.31 – 7.14 (m, 5H, −C_6H_5), 5.4 (br d, 1H, ^{3}J = 7.0 Hz, −N*H*−), 4.58 (ddd, 1H, $^3J_1$ = 7.5 Hz, $^3J_2$ = 7.0 Hz, $^3J_3$ = 7.0 Hz, BnC*H*(NH)−), 4.09 (q, 2H, ^{3}J = 7.0 Hz, −OCH_2CH$_3$), 3.04 (dd, 1H, $^3J_1$ = 13.8 Hz, $^3J_2$ = 7.0 Hz, PhCH*H*−), 3.04 (dd, 1H, $^3J_1$ = 13.8 Hz, $^3J_2$ = 7.5 Hz, PhC*H*H−), 2.75 – 2.69 (m, 1H, −C*H*HCH$_2$C$_6$F$_{13}$), 2.60 – 2.53 (m, 1H,

−CH*H*CH$_2$C$_6$F$_{13}$), 2.43 – 2.23 (m, 2H, −CH$_2$C*H*$_2$C$_6$F$_{13}$), 1.20 (t, 3H, ^{3}J = 7.0 Hz, −OCH$_2$C*H*$_3$); ^{13}C NMR (75 MHz, CDCl$_3$) δ 14.4 (−OCH$_2$*C*H$_3$), 24.9 (−CH$_2$*C*H$_2$C$_6$F$_{13}$), 31.8 (−*C*H$_2$CH$_2$C$_6$F$_{13}$), 37.8 (Ph*C*H$_2$−), 60.5 (Bn*C*HN−), 61.4 (−O*C*H$_2$CH$_3$), 127.4, 128.9, 129.0, 135.6 (−C$_6$H$_5$), 156.1 (−NH*C*OOEt), 206.4 (−*C*OCH$_2$CH$_2$C$_6$F$_{13}$); ^{19}F NMR (282 MHz,CDCl$_3$) δ −81.25, −114.93, −122.36, −123.32, −123.93, −126.58; $[\alpha]^{25}_D$ +15.0 (*c* 1.00, CHCl$_3$); Anal. Calc'd for formula C$_{20}$H$_{18}$F$_{13}$NO$_3$: C, 42.34; H, 3.20; N, 2.47. Found: C, 42.44; H, 3.43; N, 2.34.

2(*S*)-(iso-Propoxycarbonylamino)-6,6,7,7,8,8,9,9,10,10,11,11,11-trideca-fluoro-1-phenyl-undecan-3-one (233b):

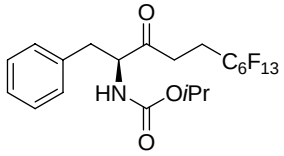

R_f = 0.35 (9:1−hexanes/ethyl acetate); mp = 71−75 °C; ^{1}H NMR (300 MHz, CDCl$_3$) δ 7.35 – 7.15 (m, 5H, −C$_6$*H*$_5$), 5.12 (br d, 1H, ^{3}J = 7.1 Hz, −N*H*−), 4.87 (qq, 1H, ^{3}J$_1$ = 6.3 Hz, ^{3}J$_2$ = 6.2 Hz, (CH$_3$)$_2$C*H*O−), 4.56 (ddd, 1H, ^{3}J$_1$ = 7.1 Hz, ^{3}J$_2$ = 7.0 Hz, ^{3}J$_3$ = 6.8 Hz, BnC*H*−), 3.04 (dd, 1H, ^{3}J$_1$ = 14.5 Hz, ^{3}J$_2$ = 6.8 Hz, PhCH*H*−), 3.00 (dd, 1H, ^{3}J$_1$ = 14.5 Hz, ^{3}J$_2$ = 7.8 Hz, PhC*H*H−), 2.77 – 2.66 (m, 1H, −CH*H*CH$_2$C$_6$F$_{13}$), 2.61 – 2.50 (m, 1H, −C*H*HCH$_2$C$_6$F$_{13}$), 2.45 – 2.23 (m, 2H, −CH$_2$C*H*$_2$C$_6$F$_{13}$), 1.21 (d, 6H, ^{3}J = 6.3 Hz, (C*H*$_3$)$_2$CH−); ^{13}C NMR (75 MHz, CDCl$_3$) δ 21.9 ((*C*H$_3$)$_2$CH−), 24.9 (−CH$_2$*C*H$_2$C$_6$F$_{13}$), 31.7 (−*C*H$_2$CH$_2$C$_6$F$_{13}$), 37.7 (Ph*C*H$_2$−), 60.5 (Bn*C*HN−), 61.4 ((CH$_3$)$_2$*C*HO−), 127.3, 128.8, 129.0, 135.7 (−*C*$_6$H$_5$), 155.7 (−NH*C*OO*i*Pr), 206.4 (−*C*OCH$_2$CH$_2$C$_6$F$_{13}$); ^{19}F NMR (282 MHz,CDCl$_3$) δ −81.22, −115.02, −122.12, −123.45, −124.23, −126.78; $[\alpha]^{25}_D$ +11.8

(*c* 0.78, $CHCl_3$); Anal. Calc'd for formula $C_{21}H_{20}F_{13}NO_3$: C, 43.38; H, 3.47; N, 2.41. Found: C, 43.64; H, 3.87; N, 2.79.

2(*S*)-(Benzyloxycarbonylamino)-6,6,7,7,8,8,9,9,10,10,11,11,11-trideca-fluoro-1-phenyl-undecan-3-one (233c):

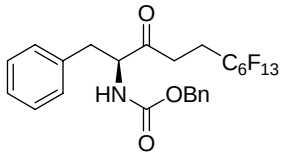

R_f = 0.39 (9:1−hexanes/ethyl acetate); mp = 68−70 °C; ^{1}H NMR (300 MHz, $CDCl_3$) δ 7.37 – 7.11 (m, 10H, 2×−C_6H_5), 5.31 (br d, 1H, ^{3}J = 7.4 Hz, −N*H*−), 5.09 (s, 2H, PhCH_2O−), 4.60 (ddd, 1H, $^3J_1$ = 7.4 Hz, $^3J_2$ = 7.1 Hz, $^3J_3$ = 6.3 Hz, BnC*H*−), 3.06 (dd, 1H, $^3J_1$ = 14.5 Hz, $^3J_2$ = 6.3 Hz, PhCH*H*−), 3.02 (dd, 1H, $^3J_1$ = 14.5 Hz, $^3J_2$ = 7.1 Hz, PhC*H*H−), 2.77 – 2.51 (m, 2H, −CH_2CH$_2$C$_6$F$_{13}$), 2.44 – 2.22 (m, 2H, −CH$_2$CH_2C$_6$F$_{13}$); ^{13}C NMR (75 MHz, $CDCl_3$) δ 24.9 (−CH$_2$*C*H$_2$C$_6$F$_{13}$), 31.8 (−*C*H$_2$CH$_2$C$_6$F$_{13}$), 37.8 (Ph*C*H$_2$−), 60.7 (Bn*C*HN−), 67.2 (Bn*C*H$_2$O−), 127.4, 128.1, ,128.3, 128.9, 129.0, 135.4, 136.0 (2×−*C*$_6$H$_5$), 155.8 (−NH*C*OOBn), 206.0 (−*C*OCH$_2$CH$_2$C$_6$F$_{13}$); ^{19}F NMR (282 MHz,$CDCl_3$) δ −81.42, −114.85, −122.64, −123.12, −123.83, −126.10; $[\alpha]^{25}_D$ +13.6 (*c* 0.69, $CHCl_3$); Anal. Calc'd for formula $C_{25}H_{20}F_{13}NO_3$: C, 47.71; H, 3.20; N, 2.23. Found: C, 47.67; H, 2.85; N, 2.34.

3(*S*)-(*tert*-Butoxycarbonylamino)-7,7,8,8,9,9,10,10,11,11,12,12,12-tridecafluoro-2-methyl-dodecan-4-one (250):

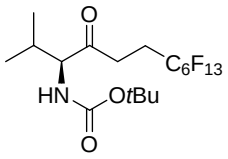

R_f = 0.4 (9:1−hexanes/ethyl acetate); mp = 36−37 °C; ^{1}H NMR (300 MHz, $CDCl_3$) δ 5.05 (d, 1H, ^{3}J = 8.2 Hz, −N*H*−), 4.25 (dd, 1H, $^3J_1$ = 8.2 Hz, $^3J_2$ = 4.6 Hz, *i*PrC*H*−), 2.90 – 2.72 (m, 2H, −C*H*$_2$CH$_2$C$_6$F$_{13}$), 2.51 – 2.33 (m, 2H, −CH$_2$C*H*$_2$C$_6$F$_{13}$), 2.24 – 2.29 (m, 1H, (CH$_3$)$_2$C*H*−), 1.43 (s, 9H, (C*H*$_3$)$_3$C−), 1.01 (d, 3H, ^{3}J = 7.1 Hz, C*H*$_3$CHCH$_3$), 0.82 (d, 3H, ^{3}J = 7.0 Hz, CH$_3$CHC*H*$_3$); ^{13}C NMR (75 MHz, $CDCl_3$) δ 16.9 (*C*H$_3$CHCH$_3$), 19.7 (CH$_3$CHC*H*$_3$), 25.0 (−CH$_2$*C*H$_2$C$_6$F$_{13}$), 28.3 ((*C*H$_3$)$_3$C−), 30.0 ((CH$_3$)$_2$*C*H−), 31.5 (−*C*H$_2$CH$_2$C$_6$F$_{13}$), 64.3 (*i*Pr*C*HN−), 80.03 ((CH$_3$)$_3$*C*−), 156.4 (−NH*C*OOEt), 206.6 (−*C*OCH$_2$CH$_2$C$_6$F$_{13}$); ^{19}F NMR (282 MHz,$CDCl_3$) δ −81.29, −114.69, −122.36, −123.34, −123.94, −126.61; $[\alpha]^{25}_D$ +17.0 (*c* 1.06, $CHCl_3$); Anal. Calc'd for formula $C_{18}H_{22}F_{13}NO_3$: C, 39.50; H, 4.05; N, 2.56. Found: C, 39.64; H, 3.89; N, 2.55.

1(*R*)-(Ethoxycarbonylamino)-5,5,6,6,7,7,8,8,9,9,10,10,10-tridecafluoro-1-phenyl-decan-2-one (253):

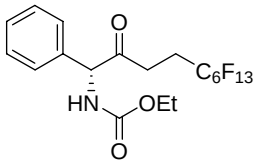

R_f = 0.1 (9:1−hexanes/ethyl acetate); mp = 71 − 76 °C; ^{1}H NMR (300 MHz, $CDCl_3$) δ 7.42 – 7.29 (m, 5H, −C_6H_5), 5.94 (d, 1H, ^{3}J = 6.1 Hz, −N*H*−), 5.37 (d, 1H, ^{3}J = 6.1 Hz, PhC*H*−), 4.11 – 4.03 (m, 2H, CH_3CH_2O−), 2.79– 2.59 (m, 2H, −$CH_2CH_2C_6F_{13}$), 2.52 – 2.20 (m, 2H, −$CH_2CH_2C_6F_{13}$), 1.22 (t, 3H, 3J = 7.0 Hz, CH_3CH_2O−); ^{13}C NMR (75 MHz, $CDCl_3$) δ 14.4 (CH_3CH_2O−), 25.0 (−$CH_2CH_2C_6F_{13}$), 30.5 (−$CH_2CH_2C_6F_{13}$), 61.3 (CH_3CH_2O−), 64.5 (PhCH(NH)−), 127.8, 129.0, 129.5, 135.8 (−C_6H_5), 155.6 (−NHCOOEt), 202.7 (−$COCH_2CH_2C_6F_{13}$); ^{19}F NMR (282 MHz,$CDCl_3$) δ −81.32, −114.90, −122.41, −123.37, −124.03, −126.63; $[\alpha]^{25}_D$ −21.8 (*c* 1.21, $CHCl_3$); Anal. Calc'd for formula $C_{19}H_{16}F_{13}NO_3$: C, 41.24; H, 2.91; N, 2.53. Found: C, 41.13; H, 2.81; N, 2.64

.

1(*R*)-(*tert*-Butoxycarbonylamino)-5,5,6,6,7,7,8,8,9,9,10,10,10-trideca-fluoro-1-phenyl-decan-2-one (262):

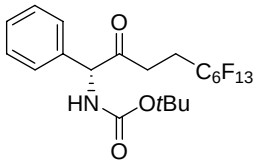

R_f = 0.3 (9:1−hexanes/ethyl acetate); mp = 80 − 82 °C; ^{1}H NMR (300 MHz, $CDCl_3$) δ 7.42 – 7.29 (m, 5H, −C_6H_5), 5.72 (d, 1H, ^{3}J = 5.5 Hz, −N*H*−), 5.32 (d, 1H, ^{3}J = 5.5 Hz, PhC*H*−), 2.77– 2.60 (m, 2H, −CH_2CH_2C$_6$F$_{13}$), 2.52 – 2.20 (m, 2H, −CH$_2$CH_2C$_6$F$_{13}$), 1.42 (s, 9H, (CH_3)$_3$C−); ^{13}C NMR (75 MHz, $CDCl_3$) δ 25.1 (−CH$_2$*C*H$_2$C$_6$F$_{13}$), 28.3 ((*C*H$_3$)$_3$C−), 30.4 (−*C*H$_2$CH$_2$C$_6$F$_{13}$), 64.4 (Ph*C*H(NH)−), 80.2 ((CH$_3$)$_3$*C*O−), 127.8, 128.9, 129.4, 135.9 (−*C*$_6$H$_5$), 154.9 (−NH*C*O*O*tBu), 203.1 (−*C*OCH$_2$CH$_2$C$_6$F$_{13}$); ^{19}F NMR (282 MHz,$CDCl_3$) δ −81.20, −114.86, −122.37, −123.32, −123.99, −126.58; $[\alpha]^{25}_D$ +0.48 (*c* 1.3, $CHCl_3$); Anal. Calc'd for formula $C_{21}H_{20}F_{13}NO_3$: C, 43.38; H, 3.47; N, 2.41. Found: C, 43.06; H, 2.99; N, 2.37.

2(*S*)-(Ethoxycarbonylamino)-3,3-bis(1'*H*,1'*H*,2'*H*,2'*H*-perfluorooctyl)-1-phenyl-propan-3-ol (234a):

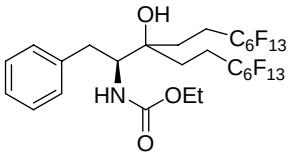

R_f = 0.35 (9:1−hexanes/ethyl acetate); mp = 67 − 69 °C; ^{1}H NMR (500 MHz, $CDCl_3$) δ 7.44 – 7.26 (m, 5H, −C_6H_5), 4.84 (d, 1H, ^{3}J = 7.5 Hz, −N*H*−), 4.11 (q, 2H, ^{3}J = 6.9 Hz, CH$_3$CH_2O−), 3.90 (ddd, 1H, ^{3}J$_1$ = 11.1 Hz, ^{3}J$_2$ = 7.5 Hz, ^{3}J$_3$ = 3.3 Hz, BnC*H*−),

3.70 (s, 1H, −OH), 3.12 (dd, 1H, $^3J_1$ = 14.5 Hz, $^3J_2$ = 3.3 Hz, PhCH*H*−), 2.75 (dd, 1H, $^3J_1$ = 14.5 Hz, $^3J_2$ = 11.1 Hz, PhC*H*H−), 2.51– 2.37 (m, 2H, 2×−CH_2CH*H*C_6F_{13}), 2.34– 2.19 (m, 2H, 2×−CH_2C*H*HC_6F_{13}), 2.11 – 1.80 (m, 4H, 2×−C*H*$_2CH_2C_6F_{13}$), 1.24 (t, 3H, ^3J = 6.9 Hz, C*H*$_3CH_2O$−); ^{13}C NMR (75 MHz, $CDCl_3$) δ 14.2 (*C*H_3CH_2O−), 25.3 (2×−CH_2*C*$H_2C_6F_{13}$), 25.7 (−*C*$H_2CH_2C_6F_{13}$), 26.7 (−*C*$H_2CH_2C_6F_{13}$), 35.4 (Ph*C*H−), 58.9 (Bn*C*H(NH)−), 61.7 (CH_3*C*H_2O−), 74.5 (*C*(OH)($CH_2CH_2C_6F_{13}$)$_2$), 126.9, 128.9, 129.4, 137.2 (−*C*$_6H_5$), 158.1 (−NH*C*OOEt); ^{19}F NMR (282 MHz,$CDCl_3$) δ −81.19, −114.81, −122.20, −122.98, −124.06, −126.29; $[\alpha]^{25}_D$ +10.96 (*c* 0.37, $CHCl_3$); Anal. Calc'd for formula $C_{28}H_{23}F_{26}NO_3$: C, 36.74; H, 2.53; N, 1.53. Found: C, 36.86; H, 2.07; N, 1.61.

2(*S*)-(iso-Propoxycarbonylamino)-3,3-bis(1'*H*,1'*H*,2'*H*,2'*H*-perfluoro-octyl)-1-phenyl-propan-3-ol (234b):

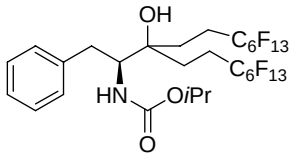

Mp = 78 − 81 °C; ^{1}H NMR (300 MHz, $CDCl_3$) δ 7.38 – 7.14 (m, 5H, −C_6H_5), 4.76 (qq, 1H, $^3J_1$ = 6.3 Hz, $^3J_1$ = 5.9 Hz, $(CH_3)_2$C*H*O−), 4.62 (d, 1H, ^3J = 7.9 Hz, −N*H*−), 3.78 (ddd, 1H, $^3J_1$ = 11.3 Hz, $^3J_2$ = 8.3 Hz, $^3J_3$ = 3.1 Hz, BnC*H*−), 3.55 (s, 1H, −OH), 3.01(dd, 1H, $^3J_1$ = 14.2 Hz, $^3J_2$ = 3.1 Hz, PhCH*H*−), 2.65 (dd, 1H, $^3J_1$ = 14.2 Hz, $^3J_2$ = 11.3 Hz, PhC*H*H−), 2.43– 2.08 (m, 4H, 2×−CH_2C*H*$_2C_6F_{13}$), 2.02– 1.67 (m, 4H, 2×−C*H*$_2CH_2C_6F_{13}$), 1.18 (d, 3H, ^3J = 5.9 Hz, C*H*$_3CHCH_3$), 1.06 (d, 3H, ^3J = 6.3 Hz, CH_3CHCH_3); ^{13}C NMR (75 MHz, $CDCl_3$) δ 18.4 (*C*H_3CHCH_3), 19.9 (CH_3CHCH_3), 25.6 (2×−CH_2*C*$H_2C_6F_{13}$), 26.7 (2×−*C*$H_2CH_2C_6F_{13}$), 35.4 (Ph*C*H−), 59.1 (Bn*C*H(NH)−), 61.0

((CH$_3$)$_2$*C*HO−), 75.5 (*C*(OH)(CH$_2$CH$_2$C$_6$F$_{13}$)$_2$), 126.9, 128.8, 129.2, 137.6 (−*C*$_6$H$_5$), 159.0 (−NH*C*OO*i*Pr); ^{19}F NMR (282 MHz,CDCl$_3$) δ −81.23, −114.62, −122.34, −123.04, −124.23, −126.14; [α]$^{25}_D$ −1.67 (*c* 1.01, CHCl$_3$); Anal. Calc'd for formula $C_{29}H_{25}F_{26}NO_3$: C, 37.47; H, 2.71; N, 1.51. Found: C, 37.63; H, 2.81; N, 1.26.

2(*S*)-(Benzyloxycarbonylamino)-3,3-bis(1'*H*,1'*H*,2'*H*,2'*H*-perfluoro-octyl)-1-phenyl-propan-3-ol (234c):

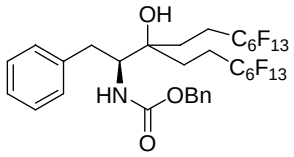

^{1}H NMR (300 MHz, CDCl$_3$) δ 7.39 – 7.13 (m, 5H, −C$_6$H$_5$), 5.01 (s, 2H, PhC*H*$_2$O−), 4.62 (d, 1H, ^{3}J = 7.6 Hz, −N*H*−), 3.77 (ddd, 1H, ^{3}J$_1$ = 11.0 Hz, ^{3}J$_2$ = 8.2 Hz, ^{3}J$_3$ = 3.7 Hz, BnC*H*−), 3.51 (s, 1H, −OH), 3.00 (dd, 1H, ^{3}J$_1$ = 14.6 Hz, ^{3}J$_2$ = 3.7 Hz, PhCH*H*−), 2.63 (dd, 1H, ^{3}J$_1$ = 14.6 Hz, ^{3}J$_2$ = 11.0 Hz, PhC*H*H−), 2.38– 2.07 (m, 4H, 2×−CH$_2$C*H*$_2$C$_6$F$_{13}$), 2.02– 1.69 (m, 4H, 2×−C*H*$_2$CH$_2$C$_6$F$_{13}$); ^{13}C NMR (75 MHz, CDCl$_3$) δ 25.3 (2×−CH$_2$*C*H$_2$C$_6$F$_{13}$), 26.2 (2×−*C*H$_2$CH$_2$C$_6$F$_{13}$), 35.7 (Ph*C*H−), 58.9 (Bn*C*H(NH)−), 66.7 (Bn*C*H$_2$O−), 75.2 (*C*(OH)(CH$_2$CH$_2$C$_6$F$_{13}$)$_2$), 126.8, 127.6, 128.2, 128.7, 128.8, 128.9, 136.2, 136.9 (2×−*C*$_6$H$_5$), 158.1 (−NH*C*OO*t*Bu); ^{19}F NMR (282 MHz,CDCl$_3$) δ −81.23, −114.67, −122.43, −123.04, −124.24, −126.23; [α]$^{25}_D$ +14.90 (*c* 0.39, CHCl$_3$); Anal. Calc'd for formula $C_{33}H_{25}F_{26}NO_3$: C, 40.55; H, 2.58; N, 1.43. Found: C, 40.59; H, 2.37; N, 1.14.

3(*S*)-(*tert*-Butoxycarbonylamino)-4,4-bis(1'*H*,1'*H*,2'*H*,2'*H*-perfluoro-octyl)-2-methyl-butan-4-ol (251):

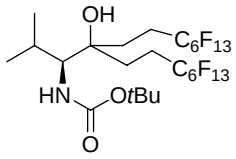

R_f = 0.47 (9:1−hexanes/ethyl acetate); mp = 42 − 49 °C; ^{1}H NMR (300 MHz, $CDCl_3$) δ 4.86 (d, 1H, ^{3}J = 9.8 Hz, −N*H*−), 3.50 (d, 1H, ^{3}J = 9.8 Hz, *i*PrC*H*−), 2.84 (s, 1H, −OH), 2.36– 2.16 (m, 2H, 2×−CH_2CH*H*C_6F_{13}), 2.11– 1.99 (m, 3H, 2×−CH*H*$CH_2C_6F_{13}$, $(CH_3)_2$C*H*−), 1.97 – 1.77 (m, 2H, 2 × −CH_2C*H*HC_6F_{13}), 1.78 – 1.65 (m, 2H, 2×−CH*H*$CH_2C_6F_{13}$), 1.44 (s, 9H, $(CH_3)_3$C−), 0.98 (d, 3H, ^{3}J = 7.0 Hz, C*H*$_3$CHCH_3), 0.94 (d, 3H, ^{3}J = 7.2 Hz, CH_3CHC*H*$_3$); ^{13}C NMR (75 MHz, $CDCl_3$) δ 16.7 (*C*H_3CHCH_3), 22.1 (CH_3CHCH_3), 25.5 (2×−CH_2*C*$H_2C_6F_{13}$), 25.9 (−*C*$H_2CH_2C_6F_{13}$), 26.9 (−*C*$H_2CH_2C_6F_{13}$), 27.6 ((CH_3)$_2$*C*H−), 28.0 ((*C*H_3)$_3$C−), 59.2 (*i*Pr*C*H(NH)−), 75.6 (*C*(OH)($CH_2CH_2C_6F_{13}$)$_2$), 80.3 ((CH_3)$_3$C−), 157.3 (−NH*C*OO*t*Bu); ^{19}F NMR (282 MHz,$CDCl_3$) δ −81.71, −115.17, −122.68, −123.64, −123.97, −126.99; $[\alpha]^{25}_D$ +11.67 (*c* 0.42, $CHCl_3$); Anal. Calc'd for formula $C_{26}H_{27}F_{26}NO_3$: C, 34.87; H, 3.04; N, 1.56. Found: C, 34.59; H, 2.92; N, 1.34.

1(*R*)-(Ethoxycarbonylamino)-2,2-bis(1'*H*,1'*H*,2'*H*,2'*H*-perfluorooctyl)-1-phenyl-ethan-2-ol (254):

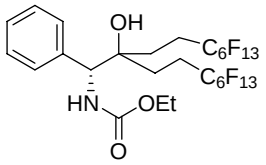

R_f = 0.27 (9:1−hexanes/ethyl acetate); mp = 87 − 91 °C; ^{1}H NMR (500 MHz, $CDCl_3$) δ 7.38 – 7.25 (m, 5H, −C_6H_5), 5.62 (d, 1H, ^{3}J = 7.9 Hz, −N*H*−), 4.70 (d, 1H, ^{3}J = 7.9 Hz, PhC*H*−), 4.13 – 4.04 (m, 2H, CH_3CH_2O−), 2.57 (s, 1H, −OH), 2.31– 2.17 (m, 2H, 2× −CH_2CH*H*C_6F_{13}), 2.16– 2.04 (m, 2H, 2×−CH*H*$CH_2C_6F_{13}$), 1.92 – 1.72 (m, 2H, 2× −CH_2C*H*HC_6F_{13}), 1.66 – 1.56 (m, 2H, 2×−CH*H*$CH_2C_6F_{13}$), 1.22 (t, 3H, ^{3}J = 6.5 Hz, (C*H*$_3CH_2O$−); ^{13}C NMR (75 MHz, $CDCl_3$) δ 14.1 (*C*H_3CH_2O−), 25.1 (−CH_2*C*$H_2C_6F_{13}$), 25.5 (−CH_2*C*$H_2C_6F_{13}$), 26.0 (*C*$H_2CH_2C_6F_{13}$), 26.2 (−*C*$H_2CH_2C_6F_{13}$), 60.5 (PhCH(NH)−), 61.5 (CH_3*C*H_2O−), 74.7 (*C*(OH)($CH_2CH_2C_6F_{13}$)$_2$), 128.1, 128.2, 128.6, 137.8 (−*C*$_6H_5$), 156.9 (−NH*C*OO*t*Bu); ^{19}F NMR (282 MHz,$CDCl_3$) δ −81.79, −115.05, −115.38, −122.66, −123.66, −123.93, −124.22, −127.00; $[\alpha]^{25}_D$ −0.34 (*c* 0.67, $CHCl_3$); Anal. Calc'd for formula $C_{27}H_{21}F_{26}NO_3$: C, 35.98; H, 2.35; N, 1.55. Found: C, 36.16; H, 2.32; N, 1.43.

Reduction of the Perfluoroalkyl Ketones

General Procedure for Reductions of Perfluoroalkylketone; *syn* and *anti* 2-(Ethoxycarbonylamino)-4,4,5,5,6,6,7,7,8,8,9,9,10,10,11,11,11-heptadec-afluoro-1-phenyl-undecan-3-ol (224b, 225b):

Ketone **209b** (3.00 g, 5.12 mmol) and $NaBH_4$ (0.27 g, 7.00 mmol) was dissolved in THF (200 mL), and stirred for 1 h. The reaction was then quenched with 1M HCl and allowed to stir for 20 min. The reaction was then concentrated under vacuum, and the aqueous residue was extracted with Et_2O. The combined ether extracts were then dried ($MgSO_4$) and evaporated to dryness, giving alcohols **224b** and **225b** (2.65 g, ~98% yield) as a mixture of diastereomers. The alcohols were then separated using flash chromatography on silica (9:1 hexane: EtOAc) to give the individual alcohols **224b** (1.21 g, 1.89 mmol, 40.2% yield) and **225b** (1.02 g, 1.59 mmol, 33.9% yield).

General Procedure for Diastereoselective Reductions of Perfluoro-alkylketones Using Chelation Control; (2S,3R)-2-(Ethoxy-carbonylamino)-6,6,7,7,8,8,9,9,10,10,11,11,11-tridecafluoro-1-phenyl-undecan-3-ol (243a):

A solution of ketone **233a** (21.0 g, 35.3 mmol) in anhydrous ethanol (2.0 L) at −78 °C was treated with powdered $LiAlH(OtBu)_3$ (26.9 g, 106 mmol). The reaction was allowed to warm to r.t. over 16 h., and was then quenched by gradual addition of 1M HCl while stirring vigorously. Following addition of HCl the solution became translucent, and was then concentrated under vacuum. The crude residue was taken up in distilled

water and extracted with Et_2O. The combined ether extracts were dried ($MgSO_4$) and evaporated to dryness to give **243a** (20.0 g, 33.5 mmol, 95 % yield) as a white powder. This material was used without further purification.

(2*S*,3*R*)-2-(Benzyloxycarbonylamino)-4,4,5,5,6,6,7,7,8,8,9,9,10,10,11,11,-11-heptadecafluoro-1-phenyl-undecan-3-ol (224a):

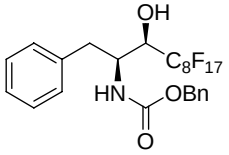

Mp = 92˚C, ^{1}H NMR (300 MHz, acetone−d_6), δ 7.43 – 7.09 (m, 10H, 2 × C_6H_5−), 5.87 (d, 1H, ^{3}J = 8.2 Hz, NH), 5.79 (d, 1H, ^{3}J = 7.2 Hz, OH), 5.36 (br s, 2H, PhC*H*$_2$O−), 4.45 (m, 1H, −C*H*(OH)C_8F_{17}), 4.53 (d, 1H, ^{3}J = 6.9 Hz, BnC*H*N −), 3.27 (d, 2H, ^{3}J = 8.5 Hz, PhC*H*$_2$−); ^{13}C NMR (75 MHz, acetone−d_6) δ 37.5 (Ph*C*H$_2$), 55.2 (Bn*C*HNH−), 66.7 (Bn*C*H$_2$O−), 69.0 (−*C*H(OH)C_8F_{17}), 129.2 − 141.5 (C_6H_5−), 155.7 (−NH*C*OO−), Anal. Calc'd for formula $C_{25}H_{18}F_{17}NO_3$: C, 42.69; H, 2.58; N, 1.99. Found: C, 42.96; H, 2.45; N, 2.05.

(2*S*,3*R*)-2-(Ethoxycarbonylamino)-4,4,5,5,6,6,7,7,8,8,9,9,10,10,11,11,11-heptadecafluoro-1-phenyl-undecan-3-ol (224b):

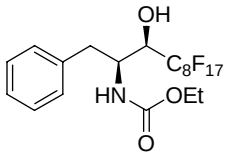

Mp = 78˚C, ^{1}H NMR (300 MHz, acetone−d_6), δ 7.28 (m, 5H, C_6H_5−), 6.22 (d, 1H, ^{3}J = 8.7 Hz, N*H*), 5.99 (d,1H, ^{3}J = 8.7 Hz, OH), 4.36 (m, 1H, −C*H*(OH)C_8F_{17}), 4.31 (d, 1H, ^{3}J = 7.8 Hz, BnC*H*NH−), 4.03 (q, 2H, ^{3}J = 6.9 Hz, OC$H_2$$CH_3$), 3.06 (d, 2H, ^{3}J = 7.1Hz, PhCH_2−), 1.16 (t, 3H, ^{3}J = 7.4 Hz, −OCH_2CH_3), ^{13}C NMR (75 MHz, acetone−d_6) δ 14.4 (−OCH_2CH_3), 39.4 (Ph*C*H2), 53.4 (Bn*C*HNH−), 61.6 (−O*C*H_2CH_3), 68.0 (−*C*H(OH)C_8F_{17}), 127.3 − 138.5 (C_6H_5−), 157.7 (−NH*C*OO−), Anal. Calc'd for formula $C_{20}H_{16}F_{17}NO_3$: C, 37.46; H, 2.51; N, 2.18. Found: C, 37.92; H, 2.36; N, 2.18.

(2*S*,3*S*)-2-(Benzyloxycarbonylamino)-4,4,5,5,6,6,7,7,8,8,9,9,10,10,11,11,-11-heptadecafluoro-1-phenyl-undecan-3-ol (225a):

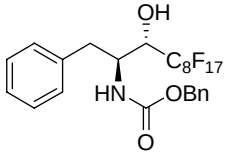

Mp = 112 – 117 ˚C, ^{1}H NMR (300 MHz, acetone−d_6), δ 7.47 – 7.13 (m, 10H, 2 × C_6H_5−), 5.98 (d, 1H, ^{3}J = 7.6 Hz, NH), 5.73 (d, 1H, ^{3}J = 7.2 Hz, OH), 5.53 (br s, 2H, PhCH_2O−), 4.76 (m, 1H, −C*H*(OH)C_8F_{17}), 4.24 (m, 1H, BnC*H*N −), 3.27 (dd, 1H, $^3J_1$ = 14.3 Hz, 4.2 Hz, PhCH*H*−), 2.71 (dd, 1H, $^3J_1$ = 13.9 Hz, 8.1 Hz, PhC*H*H−); ^{13}C NMR (75

MHz, acetone−d_6) δ 38.3 (Ph*C*H_2), 59.2 (Bn*C*HNH−), 67.2 (Bn*C*H_2O−), 68.1 (−*C*H(OH)C_8F_{17}), 127.1 − 139.2 (C_6H_5−), 156.2 (−NH*C*OOCH_2−), Anal. Calc'd for formula $C_{25}H_{18}F_{17}NO_3$: C, 42.69; H, 2.58; N, 1.99. Found: C, 42.58; H, 2.55; N, 2.01.

(2S,3S)-2-(Ethoxycarbonylamino)-4,4,5,5,6,6,7,7,8,8,9,9,10,10,11,11,11-heptadecafluoro-1-phenyl-undecan-3-ol (225b):

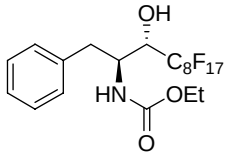

Mp = 108 – 111˚C, ^{1}H (300 MHz, acetone−d_6) δ 7.25 (m, 5H, C_6H_5), 6.40 (d, 1H, ^{3}J = 8.3 Hz, N*H*), 5.74 (d, 1H, ^{3}J = 7.9 Hz, OH), 4.53 (m,−C*H*(OH)C_8F_{17}), 4.26 (m, 1H, −C*H*(NHR)CH−), 3.93 (q, 2H, ^{3}J = 7.4 Hz, −OC*H*$_2$$CH_3$), 3.16 (dd, 1H, $^3J_1$= 14.1 Hz, $^3J_2$= 3.3 Hz, PhC*H*H−), 2.99 (dd, 1H, $^3J_1$ = 14.1 Hz, $^3J_2$ = 11.5 Hz, PhCH*H*−), 1.08 (t, 3H, ^{3}J = 7.4 Hz) ^{13}C NMR (75 MHz, acetone−d_6) δ 14.4 (*C*$H_3$$CH_2$O−), 36.1 (Ph*C*$H_2$−), 54.2 (−Bn*C*HNH−), 61.7 (−O*C*$H_2$$CH_3$), 71.9 (−*C*H(OH) C_8F_{17}), 127.3 – 140.1 (C_6H_5), 157.3, (−NH*C*OO−) ppm, Anal. Calc'd for formula $C_{20}H_{16}F_{17}NO_3$: C, 37.46; H, 2.51; N, 2.18. Found: C, 38.0; H, 2.43; N, 2.08.

(2S,3R)-2-(Ethoxycarbonylamino)-6,6,7,7,8,8,9,9,10,10,11,11,11-tridecafluoro-1-phenyl-undecan-3-ol (243a):

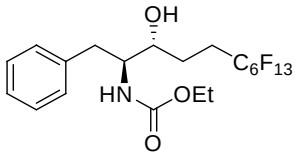

R_f = 0.37 (9:1−hexanes/ethyl acetate); mp =116−120 °C; ^{1}H NMR (300 MHz, $CDCl_3$) δ 7.34 – 7.17 (m, 5H, −C_6H_5), 4.67 (br d, 1H, ^{3}J = 7.4 Hz, −N*H*−), 4.10 – 4.01 (m, 2H, −OCH_2CH_3), 3.96 – 3.88 (m, 1H, BnC*H*(NH)−), 3.75 – 3.70 (m, 1H, −C*H*(OH)CH_2−), 3.24 (br s, 1H, −O*H*−), 2.91 (dd, 1H, $^3J_1$ = 14.3 Hz, $^3J_2$ = 5.2 Hz, PhC*H*H−), 2.77 (dd, 1H, $^3J_1$ = 14.3 Hz, $^3J_2$ = 9.5 Hz, PhCH*H*−), 2.55 – 2.36 (m, 1H, −CH_2C*H*HC_6F_{13}), 2.22 – 2.00 (m, 1H, − CH_2CH*H*C_6F_{13}), 1.86 – 1.67 (m, 2H, −C$H_2CH_2C_6F_{13}$), 1.19 (t, 3H, ^{3}J = 7.0 Hz, −OCH_2CH_3); ^{13}C NMR (75 MHz, $CDCl_3$) δ 14.4 (−OCH_2CH_3), 23.5 (−$CH_2CH_2C_6F_{13}$), 27.8 (−$CH_2CH_2C_6F_{13}$), 36.0 (PhCH_2−), 57.4 (Bn*C*H(NH)−), 61.4 (−OCH_2CH_3), 73.0 (−*C*H(OH)CH_2−), 126.8, 128.7, 129.0, 137.3 (−C_6H_5), 157.4 (−NH*C*OOEt); ^{19}F (282 MHz, $CDCl_3$) δ −81.27, −114.95, −122.38, −123.38, −124.01, −126.60; $[\alpha]^{25}_D$ –6.5 (*c* 1.00, $CHCl_3$); Anal. Calc'd for formula $C_{20}H_{20}F_{13}NO_3$: C, 42.19; H, 3.54; N, 2.46. Found: C, 42.59; H, 3.14; N, 2.65.

(2S,3R)-2-(iso-Propoxycarbonylamino)-6,6,7,7,8,8,9,9,10,10,11,11,11-tridecafluoro-1-phenyl-undecan-3-ol (243b):

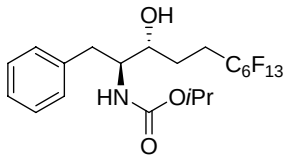

R_f = 0.40 (9:1−hexanes/ethyl acetate); mp =123−126 °C; ^{1}H NMR (300 MHz, $CDCl_3$) δ 7.34 – 7.17 (m, 5H, −C_6H_5), 4.82 (qq, 1H, $^3J_1$ = 11.1 Hz, $^3J_2$ = 6.3 Hz, $(CH_3)_2CHO$−), 4.63 (br s, 1H, −N*H*−), 3.95 – 3.88 (m, 1H, BnC*H*(NH)−), 3.75 – 3.69 (m, 1H, −C*H*(OH)CH_2−), 3.37 (br s, 1H, −O*H*−), 2.91 (dd, 1H, $^3J_1$ = 14.1 Hz, $^3J_2$ = 4.7 Hz, PhC*H*H−), 2.77 (dd, 1H, $^3J_1$ = 14.1 Hz, $^3J_2$ = 9.2 Hz, PhCH*H*−), 2.53 – 2.38 (m, 1H, −$CH_2CHHC_6F_{13}$), 2.21 – 2.01 (m, 1H, − $CH_2CHHC_6F_{13}$), 1.86 – 1.67 (m, 2H, −$CH_2CH_2C_6F_{13}$), 1.24 (d, 3H, ^3J = 11.1 Hz, CH_3CHCH_3), 1.15 (d, 3H, ^3J = 6.3 Hz, CH_3CHCH_3); ^{13}C NMR (75 MHz, $CDCl_3$) δ 21.5 ($CH_3)_2CH$−), 23.6 (−$CH_2CH_2C_6F_{13}$), 27.9 (−$CH_2CH_2C_6F_{13}$), 36.2 (PhCH_2−), 57.7 (BnCH(NH)−), 68.4 (($CH_3)_2CH$)−), 73.7 (−CH(OH)CH_2−), 126.8, 129.0, 129.2, 137.1 (−C_6H_5), 157.6 (−NHCOO*i*Pr); ^{19}F (282 MHz, $CDCl_3$) δ −81.34, −115.02, −122.26, −123.36, −124.12, −126.34; $[\alpha]^{25}_D$ +13.0 (*c* 1.00, $CHCl_3$); Anal. Calc'd for formula $C_{21}H_{22}F_{13}NO_3$: C, 43.23; H, 3.80; N, 2.40. Found: C, 42.78; H, 3.98; N, 2.43.

(2S,3R)-2-(Benzyloxycarbonylamino)-6,6,7,7,8,8,9,9,10,10,11,11,11-tridecafluoro-1-phenyl-undecan-3-ol (243c):

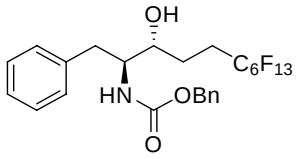

R_f = 0.52 (9:1−hexanes/ethyl acetate); mp =131−135 °C; ^{1}H NMR (300 MHz, $CDCl_3$) δ 7.35 – 7.16 (m, 10H, 2×−C_6H_5), 5.03 (s, 2H, BnCH_2O−), 4.86 (br d, 1H, ^3J = 7.0 Hz, −N*H*−), 3.98 – 3.90 (m, 1H, BnC*H*(NH)−), 3.76 – 3.69 (m, 1H, −C*H*(OH)CH_2−), 3.16 (br s, 1H, −O*H*−), 2.92 (dd, 1H, $^3J_1$ = 14.1 Hz, $^3J_2$ = 4.8 Hz, PhC*H*H−), 2.76 (dd, 1H, $^3J_1$ = 14.1 Hz, $^3J_2$ = 9.3 Hz, PhCH*H*−), 2.54 – 2.38 (m, 1H, − CH_2C*H*HC_6F_{13}), 2.19 – 2.02 (m, 1H, − CH_2CH*H*C_6F_{13}), 1.85 – 1.68 (m, 2H, −C$H_2CH_2C_6F_{13}$); ^{13}C NMR (75 MHz, $CDCl_3$) δ 23.6 (−*C*$H_2CH_2C_6F_{13}$), 27.8 (−CH_2*C*$H_2C_6F_{13}$), 35.9 (Ph*C*H_2−), 57.5 (Bn*C*H(NH)−), 67.1 (Bn*C*H_2O−), 72.9 (−*C*H(OH)CH_2−), 126.9, 128.0, 128.3, 128.6, 128.8, 129.0, 136.1, 137.2 (2×−*C*$_6H_5$), 157.1 (−NH*C*OOBn); ^{19}F (282 MHz, $CDCl_3$) δ −81.34, −115.02, −122.26, −123.36, −124.12, −126.34; $[\alpha]^{25}_D$ +11.54 (*c* 1.00, $CHCl_3$); Anal. Calc'd for formula $C_{25}H_{22}F_{13}NO_3$: C, 47.55; H, 3.51; N, 2.22. Found: C, 47.18; H, 3.01; N, 2.07.

(3S,4R)-3-(*tert*-Butoxycarbonylamino)-7,7,8,8,9,9,10,10,11,11,12,12,12-tridecafluoro-2-methyl-dodecan-4-ol (258):

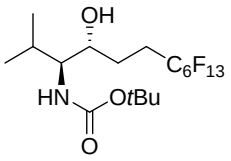

R_f = 0.32 (9:1−hexanes/ethyl acetate); mp =101−107 °C; ^{1}H NMR (300 MHz, $CDCl_3$) δ 4.54 (d, 1H, ^{3}J = 9.0 Hz, −N*H*−), 3.64 – 3.57 (m, 1H, −C*H*(OH)CH_2−), 3.53 – 3.46 (m, 1H, *i*PrC*H*(NH)−), 2.57 – 2.36 (m, 1H, −CH_2C*H*HC_6F_{13}), 2.20 – 1.98 (m, 1H, −CH_2CH*H*C_6F_{13}), 1.90 (dqq, 1H, $^3J_1$ = 7.1 Hz, $^3J_2$ = 7.1 Hz, $^3J_3$ = 7.0 Hz, $(CH_3)_2$C*H*−), 1.79 – 1.55 (m, 2H, −C*H*$_2$$CH_2C_6F_{13}$), 1.42 (s, 9H, $(CH_3)_3$C−), 0.93 (d, 3H, ^{3}J = 7.1 Hz, C*H*$_3$CHCH_3), 0.89 (d, 3H, ^{3}J = 7.1 Hz, CH_3CHC*H*$_3$); ^{13}C NMR (75 MHz, $CDCl_3$) δ 17.6 (*C*H_3CHCH_3), 18.2 (CH_3CH*C*H_3), 23.2 (−*C*$H_2$$CH_2C_6F_{13}$), 27.6 (−$CH_2$*C*$H_2$$C_6F_{13}$), 28.1 ((*C*$H_3$)$_3$C−), 28.4 ($(CH_3)_2$CH−), 60.5 (*i*Pr*C*H(NH)−), 71.4 (−*C*H(OH)CH_2−), 80.0 ($(CH_3)_3$*C*−), 157.2 (−NH*C*OO*t*Bu); ^{19}F (282 MHz, $CDCl_3$) δ −81.49, −114.98, −122.54, −123.50, −124.08, −126.80; $[\alpha]^{25}_D$ –3.2 (*c* 0.760 $CHCl_3$); Anal. Calc'd for formula $C_{18}H_{24}F_{13}NO_3$: C, 39.35; H, 4.40; N, 2.55. Found: C, 38.94; H, 3.99; N, 2.38.

(1R,2S)-1-(*tert*-Butoxycarbonylamino)-5,5,6,6,7,7,8,8,9,9,10,10,10-tri-decafluoro-1-phenyl-decan-2-ol (263):

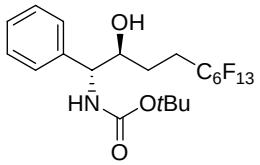

R_f = 0.5 (9:1−hexanes/ethyl acetate); mp =130−132 °C; ^{1}H NMR (300 MHz, $CDCl_3$) δ 7.42 – 7.25 (m, 5H, −C_6H_5), 5.23 (br s, 1H, −N*H*−), 4.69 (br s, 1H, PhC*H*(NH)−), 3.92 – 3.88 (m, 1H, C*H*(OH)CH_2−), 2.44 – 2.27 (m, 1H, −CH_2C*H*HC_6F_{13}), 2.20 – 2.02 (m, 1H, −CH_2CH*H*C_6F_{13}), 1.86 – 1.76 (m, 2H, CH*H*$CH_2C_6F_{13}$, −OH), 1.58 – 1.48 (m, 1H, −C*H*H$CH_2C_6F_{13}$), 1.43 (s, 9H, (C*H*$_3$)C−); ^{13}C NMR (75 MHz, $CDCl_3$) δ 23.9 (−*C*$H_2CH_2C_6F_{13}$), 27.5 (−CH_2*C*$H_2C_6F_{13}$), 28.3 ((*C*H_3)$_3$C−), 59.7 (Ph*C*H(NH)−), 73.4 (−*C*H(OH)CH_2−), 80.3 ((CH$_3$)$_3$*C*−), 127.4, 127.5, 128.2, 129.0, 137.9 (−*C*$_6$H$_5$), 155.7 (−NH*C*OO*t*Bu); ^{19}F (282 MHz, $CDCl_3$) δ −81.22, −114.83, −122.36, −123.36, −123.99, −126.57; $[\alpha]^{25}_D$ –0.31 (*c* 0.97 $CHCl_3$); Anal. Calc'd for formula $C_{21}H_{22}F_{13}NO_3$: C, 43.23; H, 3.80; N, 2.40. Found: C, 42.82; H, 4.28; N, 2.13.

Synthesis of MTPA Derivatives for Determination of Enantiomeric Excess

General procedure for synthesis of MTPA esters from (perfluoroalkyl)alcohols; (2S,2'R,3R)-2-(Ethoxycarbonylamino)-3-(2'-methoxy-2'-trifluoromethyl-phenylacetyl)-6,6,7,7,8,8,9,9,10,10,11,11,-11-tridecafluoro-1-phenyl-undecan-3-ol (248):

Alcohol **13a** (0.100 g, 0.176 mmol), **(*R*)**-(+)-MTPA (0.090 g, 0.386 mmol), DCC (0.091 g, 0.439 mmol), and DMAP (3.22 mg, 0.026 mmol) were dissolved in dry ethyl ether. The solution was stirred at r.t. for 10 min, then DIPEA (0.092 ml, 0.527 mmol) was added dropwise. The solution was allowed to stir overnight at r.t. The reaction was quenched with 1M HCl and diluted with Et_2O. The mixture was washed sequentially with 1M HCl, 1M $NaHCO_3$, and brine. The combined organic fraction was dried with $MgSO_4$ and evaporated to dryness. Flash column chromatography (9:1−hexanes/ethyl acetate as eluent) provided **15a** (.078 g, 0.099 mmol, 56.5 % yield) as crystalline solid.

(2S,2'S,3R)-2-(Ethoxycarbonylamino)-3-(2'-methoxy-2'-trifluoromethyl-phenylacetyl)-6,6,7,7,8,8,9,9,10,10,11,11,11-tridecafluoro-1-phenyl-undecan-3-ol (247):

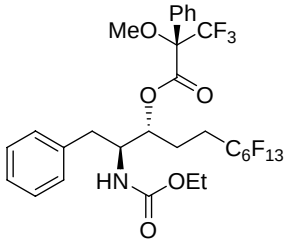

^{1}H NMR (300 MHz, $CDCl_3$) δ 7.65 – 7.06 (m, 10H, 2×−C_6H_5), 5.24 – 5.20 (m, 1H, −C*H*(O)CH_2CH_2−), 4.36 (d, 1H, ^{3}J = 8.7 Hz, −N*H*−), 4.16 – 4.07 (m, 1H, BnC*H*(NH)−), 3.99 (q, 2H, ^{3}J = 7.3 Hz, CH_3CH_2O−), 3.52 (s, 3H, CH_3O−), 2.87 (dd, 1H, $^{3}J_1$ = 14.4 Hz, $^{3}J_2$ = 4.4 Hz, PhC*H*H−), 2.52 (dd, 1H, $^{3}J_1$ = 14.4 Hz, $^{3}J_2$ = 9.7 Hz, PhCH*H*−), 2.18 – 1.87 (m, 4H, − $CH_2CH_2C_6F_{13}$, −$CH_2CH_2C_6F_{13}$), 1.14 (t, 3H, ^{3}J = 7.3 Hz, CH_3CH_2O−); ^{13}C NMR (75 MHz, $CDCl_3$) δ 14.4 (CH_3CH_2O−), 21.4 (−$CH_2CH_2C_6F_{13}$), 26.8 (−$CH_2CH_2C_6F_{13}$), 36.0 (PhCH_2−), 53.7 (BnCH(NH)−), 55.4 (−OCH_3), 61.2 (CH_3CH_2O−), 76.5 (−CH(O)CH_2 CH_2−), 84.5 ((CF_3)(Ph)(OMe)C−) 127.0, 127.3, 127.3, 128.7, 128.7, 129.0, 129.1, 131.7, 136.2 (2×−C_6H_5), 155.8 (−NHCOOEt), 166.3 (−CCOO−); ^{19}F (282 MHz, $CDCl_3$) δ −70.95, −81.19, −115.01, −122.35, −123.27, −123.94, −126.56; $[\alpha]^{25}_{D}$ +17.5 (*c* 0.26, $CHCl_3$); Anal. Calc'd for formula $C_{30}H_{27}F_{16}NO_5$: C, 45.87; H, 3.46; N, 1.78. Found: C, 45.91; H, 3.08; N, 1.74.

(2S,2'R,3R)-2-(Ethoxycarbonylamino)-3-(2'-methoxy-2'-trifluoromethyl-phenylacetyl)-6,6,7,7,8,8,9,9,10,10,11,11,11-tridecafluoro-1-phenyl-undecan-3-ol (248):

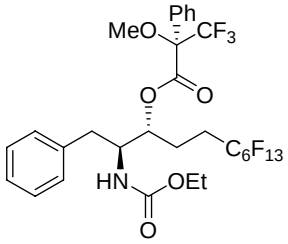

^{1}H NMR (300 MHz, $CDCl_3$) δ 7.59 – 7.02 (m, 10H, 2×−C_6H_5), 5.32 – 5.27 (m, 1H, −C*H*(O)CH_2CH_2−), 4.34 (d, 1H, ^{3}J = 8.4 Hz, −N*H*−), 4.10 – 3.94 (m, 2H, BnC*H*(NH)−, CH_3CH_2O−) 3.56 (s, 3H, CH_3O−), 2.84 (dd, 1H, $^{3}J_1$ = 14.2 Hz, $^{3}J_2$ = 4.4 Hz, PhC*H*H−), 2.45 (dd, 1H, $^{3}J_1$ = 14.2 Hz, $^{3}J_2$ = 9.8 Hz, PhCH*H*−), 2.23 – 1.92 (m, 4H, −$CH_2CH_2C_6F_{13}$, −$CH_2CH_2C_6F_{13}$), 1.15 (t, 3H, ^{3}J = 7.3 Hz, CH_3CH_2O−); ^{13}C NMR (75 MHz, $CDCl_3$) δ 14.4 (CH_3CH_2O−), 22.0 (−$CH_2CH_2C_6F_{13}$), 27.1 (−$CH_2CH_2C_6F_{13}$), 35.2 (PhCH_2−), 53.7 (BnCH(NH)−), 55.4 (−OCH_3), 61.2 (CH_3CH_2O−), 76.4 (−CH(O)CH_2 CH_2−), 84.3 ((CF_3)(Ph)(OMe)C−) 126.8, 127.1, 127.2, 128.6, 128.7, 129.0, 129.9, 131.9, 136.4 (2×−C_6H_5), 155.9 (−NHCOOEt), 166.3 (−CCOO−); ^{19}F (282 MHz, $CDCl_3$) δ −70.97, −81.18, −115.11, −122.35, −123.31, −123.88, −126.55; $[\alpha]^{25}_{D}$ –48.5 (*c* 0.78, $CHCl_3$); Anal. Calc'd for formula $C_{30}H_{27}F_{16}NO_5$: C, 45.87; H, 3.46; N, 1.78. Found: C, 46.12; H, 3.64; N, 1.81

(2'S,3S,4R)-3-(*tert*-Butoxycarbonylamino)-4-(2'-methoxy-2'-trifluoro-methyl-phenylacetyl)-7,7,8,8,9,9,10,10,11,11,12,12,12-tridecafluoro-2-methyl-dodecan-4-ol (260a):

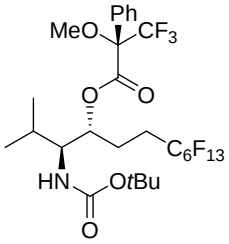

^{1}H NMR (300 MHz, $CDCl_3$) δ 7.58 – 7.38 (m, 5H, −C_6H_5), 5.16 – 5.11 (m, 1H, −C*H*(O)CH_2CH_2−), 4.30 (d, 1H, ^{3}J = 10.5 Hz, −N*H*−), 3.79 – 3.70 (m, 1H, *i*PrC*H*(NH)−), 3.52 (s, 3H, CH_3O−), 2.37 – 1.92 (m, 3H, − $CH_2CH_2C_6F_{13}$, −CH*H*$CH_2C_6F_{13}$), 1.75 – 1.54 (m, 2H, $(CH_3)_2$CH−, CH*H*$CH_2C_6F_{13}$), 1.42 (s, 9H, ^{t}C$H_3)_3$CO−), 0.85 (d, 3H, ^{3}J = 6.7 Hz, CH_3CHCH_3), 0.71 (d, 3H, ^{3}J = 6.7 Hz, CH_3CHCH_3); ^{13}C NMR (75 MHz, $CDCl_3$) δ 15.6 (*C*H_3CHCH_3), 19.9 (CH_3CH*C*H_3), 25.2 (−*C*$H_2CH_2C_6F_{13}$), 26.0 (−CH_2*C*$H_2C_6F_{13}$), 27.2 (($CH_3)_2$CH−), 28.1 ((*C*$H_3)_3$C−), 55.3 (*i*Pr*C*H(NH)−), 55.4 (−O*C*H_3), 74.7 (−*C*H(OH)CH_2CH_2−), 80.0 (($CH_3)_3$*C*−), 85.1 ((CF_3)(Ph)(OMe)C−), 127.0 , 128.6, 128.7, 129.8, 131.8 (−*C*$_6$H$_5$), 155.7 (−NH*C*OO*t*Bu), 166.1 (−C*C*OO−); ^{19}F (282 MHz, $CDCl_3$) δ −71.27, −81.22, −115.25, −122.38, −123.31, −123.98, −126.56; $[\alpha]^{25}_{D}$ −15.5 (*c* 1.01, $CHCl_3$); Anal. Calc'd for formula $C_{28}H_{31}F_{16}NO_5$: C, 43.93; H, 4.08; N, 1.83. Found: C, 43.94; H, 4.29; N, 2.32

(2'R,3S,4R)-3-(*tert*-Butoxycarbonylamino)-4-(2'-methoxy-2'-trifluoro-methyl-phenylacetyl)-7,7,8,8,9,9,10,10,11,11,12,12,12-tridecafluoro-2-methyl-dodecan-4-ol (260b):

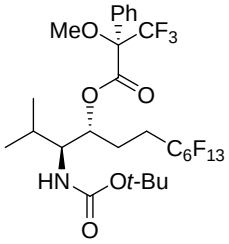

^{1}H NMR (300 MHz, $CDCl_3$) δ 7.58 – 7.39 (m, 5H, −C_6H_5), 5.15 – 5.09 (m, 1H, −C*H*(O)CH_2CH_2−), 4.32 (d, 1H, ^{3}J = 10.5 Hz, −N*H*−), 3.82 – 3.75 (m, 1H, *i*PrC*H*(NH)−), 3.54 (s, 3H, CH_3O−), 2.20 – 1.67 (m, 5H, − $CH_2CH_2C_6F_{13}$, −$CH_2CH_2C_6F_{13}$, $(CH_3)_2CH$−), 1.42 (s, 9H, $(CH_3)_3$CO−), 0.92 (d, 3H, ^{3}J = 6.7 Hz, CH_3CHCH_3), 0.80 (d, 3H, ^{3}J = 6.7 Hz, CH_3CHCH_3); ^{13}C NMR (75 MHz, $CDCl_3$) δ 16.2 (CH_3CHCH_3), 19.9 (CH_3CHCH_3), 24.5 (−$CH_2CH_2C_6F_{13}$), 25.4 (−$CH_2CH_2C_6F_{13}$), 28.1 ($(CH_3)_2CH$−), 28.2 ($(CH_3)_3C$−), 55.5 (*i*PrCH(NH)−), 55.7 (−OCH_3), 74.8 (−CH(OH)CH_2CH_2−), 80.0 ($(CH_3)_3C$−), 84.9 ((CF_3)(Ph)(OMe)C−), 127.0, 127.1, 128.6, 128.7, 129.7, 131.8 (−C_6H_5), 155.7 (−NHCOO*t*Bu), 166.3 (−CCOO−); ^{19}F (282 MHz, $CDCl_3$) δ −71.18, −81.22, −115.21, −122.40, −123.32, −123.99, −126.53; $[\alpha]^{25}_{D}$ +19.4 (*c* 0.18, $CHCl_3$); Anal. Calc'd for formula $C_{28}H_{31}F_{16}NO_5$: C, 43.93; H, 4.08; N, 1.83. Found: C, 43.54; H, 3.94, N, 1.78

(1R,2S,2'S)-1-(*tert*-Butoxycarbonylamino)-2-(2'-methoxy-2'-trifluoro-methyl-phenylacetyl)-5,5,6,6,7,7,8,8,9,9,10,10,10-tridecafluoro-1-phenyl-decan-2-ol (264a):

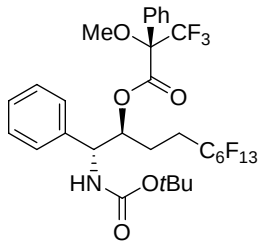

^{1}H NMR (300 MHz, $CDCl_3$) δ 7.54 – 7.01 (m, 10H, 2×−C_6H_5), 5.60 – 5.52 (m, 1H, C*H*(O)CH_2−), 4.96 (br s, 1H, −N*H*−), 4.80 (d, 1H, ^{3}J = 8.3 Hz, PhC*H*(NH)−), 3.40 (s, 3H, CH_3O−), 2.21 – 1.75 (m, 4H, −$CH_2CH_2C_6F_{13}$, −$CH_2CH_2C_6F_{13}$), 1.43 (s, 9H, (CH_3)C−); ^{13}C NMR (75 MHz, $CDCl_3$) δ 22.0 (−$CH_2CH_2C_6F_{13}$), 26.3 (−$CH_2CH_2C_6F_{13}$), 28.2 ((*C*H_3)$_3$C−), 55.1 (Ph*C*H(NH)−), 55.4 (−O*C*H_3), 76.0 (−*C*H(OH)CH_2−), 80.4 ($(CH_3)_3C$−), 84.5 ((CF_3)(Ph)(OMe)C−), 127.0, 127.3, 127.3, 128.7, 128.7, 129.0, 129.1, 131.7, 136.2 (2×−C_6H_5), 154.7 (−NH*C*OO*t*Bu), 166.1 (−C*C*OO−); ^{19}F (282 MHz, $CDCl_3$) δ −71.31, −81.25, −115.23, −122.40, −123.31, −124.01, −126.59; Anal. Calc'd for formula $C_{31}H_{29}F_{16}NO_5$: C, 46.57; H, 3.66; N, 1.75. Found: C, 46.90; H, 3.65; N; 1.97; Isolated as a mixture of diastereomers (1.2:1)

(1R,2S,2'R)-1-(*tert*-Butoxycarbonylamino)-2-(2'-methoxy-2'-trifluoro-methyl-phenylacetyl)-5,5,6,6,7,7,8,8,9,9,10,10,10-tridecafluoro-1-phenyl-decan-2-ol (264b):

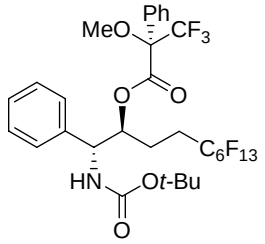

^{1}H NMR (300 MHz, $CDCl_3$) δ 7.54 – 7.01 (m, 10H, 2×−C_6H_5), 5.60 – 5.52 (m, 1H, C*H*(O)CH_2−), 4.90 (br s, 1H, −N*H*−), 4.68 (d, 1H, ^{3}J = 8.3 Hz, PhC*H*(NH)−), 3.27 (s, 3H, CH_3O−), 2.21 – 1.75 (m, 4H, −$CH_2CH_2C_6F_{13}$, −$CH_2CH_2C_6F_{13}$), 1.42 (s, 9H, (CH_3)C−); ^{13}C NMR (75 MHz, $CDCl_3$) δ 22.0 (−$CH_2CH_2C_6F_{13}$), 26.3 (−$CH_2CH_2C_6F_{13}$), 28.2 ((*C*H_3)$_3$C−), 55.1 (Ph*C*H(NH)−), 55.4 (−O*C*H_3), 76.0 (−*C*H(OH)CH_2−), 80.4 ((CH_3)$_3$*C*−), 84.5 ((CF_3)(Ph)(OMe)C−), 127.0, 127.3, 127.3, 128.7, 128.7, 129.0, 129.1, 131.7, 136.2 (2×−*C*$_6$H$_5$), 154.7 (−NH*C*OO*t*Bu), 166.1 (−C*C*OO−); ^{19}F (282 MHz, $CDCl_3$) δ −71.15, −81.25, −115.23, −122.40, −123.31, −124.01, −126.59; Anal. Calc'd for formula $C_{31}H_{29}F_{16}NO_5$: C, 46.57; H, 3.66; N, 1.75. Found:C, 46.09; H, 3.68; N, 2.15; Isolated as a mixture of diastereomers (1.1:1)

Cyclization of Perfluoroalkyl Alcohols to Oxazolidinones

General Procedure for Cyclization of Mono and Bis(perfluoroalkyl)-alcohols; (4*S*,5*R*)-4-Benzyl-5-(1'*H*,1'*H*,2'*H*,2'*H*-perfluorooctyl)-2-oxazolidinone (245):

NaH (4.210 g, 50% suspension in oil, 105.3 mmol) was added to a stirred solution of alcohol **243a** (20.0 g, 35.1 mmol) in THF (250 mL). The reaction was stirred at r.t. for 12 h, and then quenched (1M HCl) with vigorous stirring. The solution was then evaporated to yield a crude colored product (~21g). This material was dissolved in a minimum of Et_2O and purified by FSPE using general method **A** to give oxazolidinone **245** (17.1 g, 32.7 mmol, 93 % yield) as a white crystalline solid.

Alternate Cyclization Protocol Employing Refluxing THF; (4S,5S)-4-Benzyl-5-heptadecafluorooctyl-oxazolidin-2-one (231):

NaH (0.2 g, 50% suspension in oil, 2.5 mmol) was placed under nitrogen, washed with hexane, and suspended in THF (50 mL). Alcohol **225b** (0.2 g, 0.31 mmol) was dissolved in THF (20 mL), added to the slurry, and heated to reflux for 2 h. The reaction was then cooled to r.t, and quenched with sat. NH_4Cl (10 mL), stirred until no further gas was evolved, and extracted with Et_2O. The combined ether extracts were then dried with $MgSO_4$ and evaporated to dryness to yield a crude residue. The crude material was purified by FSPE using general method **B** to give oxazolidinone 231 (0.18 g, 0.30 mmol, 95% yield) as a white crystalline solid.

(4*S*,5*R*)-4-Benzyl-5-heptadecafluorooctyl-oxazolidin-2-one (230):

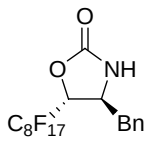

Mp = 108−111˚C, ^{1}H NMR (300MHz, acetone−d_6) δ 7.37 – 7.23 (m, 5H, C_6H_5−), 5.04 (m, 1H, −C*H*C_8F_{17}), 4.43 (ddd, 1H, $^{3}J_1$ = 3.6 Hz, $^{3}J_2$ = 7.0Hz, $^{3}J_3$ = 6.1 Hz, BnC*H*−), 3.13 (dd, 1H, $^{3}J_1$ = 13.7 Hz, $^{3}J_2$ = 6.1 Hz, PhC*H*H−), 3.10 (dd, 1H, $^{3}J_1$ = 13.7 Hz, $^{3}J_2$ = 7.0 Hz, PhCH*H*−); ^{13}C NMR (75MHz, acetone−d_6) δ 42.4 (Ph*C*H_2−), 54.1 (Bn*C*HNH−), 75.8 (−*C*H(O)C_8F_{17}), 128.4 − 136.7 (−C_6H_5), 156.8 (−NH*C*OO−); $[\alpha]_D$ = −11.1˚ (c = 1.0, Acetone); Anal. Calc'd for formula $C_{18}H_{10}F_{17}NO_2$: C, 36.32; H, 1.69; N, 2.35. Found: C, 36.77; H, 1.73; N, 2.37.

(4S,5S)-4-Benzyl-5-heptadecafluorooctyl-oxazolidin-2-one (231):

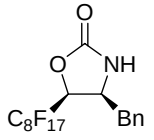

Mp = 148−151˚C, ^{1}H NMR (300MHz, acetone−d_6) δ 7.42 – 7.24 (m, 5H, C_6H_5−), 7.02 (br s, 1H, NH), 5.48 (dd, 1H, $^{3}J_1$ = 8.0 Hz, $^{3}J_2$ = 26.8 Hz, −C*H*C_8F_{17}), 4.74 (ddd, 1H, $^{3}J_1$= 3.2 Hz, $^{3}J_2$= 8.2 Hz, $^{3}J_3$ = 11.4 Hz, BnC*H*−), 3.30 (ddd, 1H, $^{3}J_1$ = 3.1Hz, $^{3}J_2$ = 7.3 Hz, $^{3}J_3$ = 13.5 Hz, PhC*H*H−), 2.97 (ddd, 1H, $^{3}J_1$ = 11.3 Hz, $^{3}J_2$ = 2.2 Hz, $^{3}J_3$ = 13.6 Hz, PhCH*H*−) ppm, ^{13}C NMR (75MHz, acetone−d_6) δ 37.1 (Ph*C*H_2−), 57.1 (Bn*C*HNH−), 73.7 (−*C*H(O)C_8F_{17}), 128.2 − 138.5 (−C_6H_5), 156.7 (−NH*C*OO−); $[\alpha]_D$ = −18.1˚ (c = 1.0,

Acetone); Anal. Calc'd for formula $C_{18}H_{10}F_{17}NO_2$: C, 36.32; H, 1.69; N, 2.35. Found: C, 36.82; H, 1.48; N, 2.46.

(4*S*,5*R*)-4-Benzyl-5-(1'*H*,1'*H*,2'*H*,2'*H*-perfluorooctyl)-2-oxazolidinone (245):

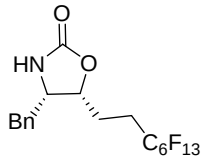

Mp = 100−101˚C, ^{1}H NMR (300MHz, $CDCl_3$) δ 7.39 – 7.17 (m, 5H, −C_6H_5), 4.93 (br s, 1H, N*H*), 4.69 (ddd, 1H, $^3J_1$ = 7.2 Hz, $^3J_2$ = 7.2 Hz, $^3J_3$ = 7.2 Hz, −C*H*$CH_2CH_2C_6F_{13}$), 4.05 (ddd, 1H, $^3J_1$ = 7.2 Hz, $^3J_2$ = 7.2 Hz, $^3J_3$ = 7.2 Hz, BnC*H*−), 2.89 (dd, 1H, $^3J_1$ = 14.1 Hz, $^3J_2$ = 4.3 Hz, PhC*H*H−), 2.71 (dd, 1H, $^3J_1$ = 14.1 Hz, $^3J_2$ = 7.9 Hz, PhCH*H*−), 2.62 − 2.43 (m, 1H, −CH_2C*H*HC_6F_{13}), 2.30 – 2.08 (m, 2H, −CH_2CH*H*C_6F_{13}, −C*H*H$CH_2C_6F_{13}$), 2.06 – 1.94 (m, 1H, −CH*H*$CH_2C_6F_{13}$); ^{13}C (75MHz, $CDCl_3$) δ 21.1 (−*C*$H_2CH_2C_6F_{13}$), 28.0 (−CH_2*C*$H_2C_6F_{13}$), 36.3 (Ph*C*H_2−), 56.6 (Bn*C*H−), 78.3 (−*C*H$CH_2CH_2C_6F_{13}$), 127.3, 128.9, 129.1, 136.1 (*C*$_6H_5$−), 158.0 (−NH*C*OO−); ^{19}F (282 MHz, $CDCl_3$) δ −81.32, −115.18, −122.34, −123.23, −124.18, −126.91; $[\alpha]_D$ = −30.0˚ (c = 1.0, $CHCl_3$); Anal. Calc'd for formula $C_{18}H_{14}F_{13}NO_2$: C, 41.31; H, 2.70; N, 2.68. Found: C, 41.34; H, 2.64; N, 2.69.

4(*S*)-Benzyl-5,5-bis(1'*H*,1'*H*,2'*H*,2'*H*-perfluorooctyl)-2-oxazolidinone (246):

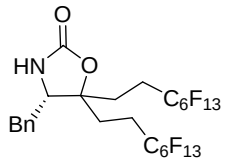

Mp = 112−115˚C, ^{1}H NMR (300MHz, $CDCl_3$) δ 7.41 – 7.17 (m, 5H, −C_6H_5), 4.88 (s, 1H, N*H*), 3.86 (dd, 1H, $^3J_1$ = 10.0 Hz, $^3J_2$ = 4.4 Hz, BnC*H*−), 2.88 (dd, 1H, $^3J_1$ = 13.2 Hz, $^3J_2$ = 4.4 Hz, PhCH*H*−), 2.80 (dd, 1H, $^3J_1$ = 13.2 Hz, $^3J_2$ = 10.0 Hz, PhC*H*H−), 2.45 – 1.87 (m, 8H, 2×−$CH_2CH_2C_6F_{13}$, 2× −$CH_2CH_2C_6F_{13}$); ^{13}C (75MHz, $CDCl_3$) δ 23.7 (−$CH_2CH_2C_6F_{13}$), 24.3 (−$CH_2CH_2C_6F_{13}$), 25.2 (−$CH_2CH_2C_6F_{13}$), 26.2 (−$CH_2CH_2C_6F_{13}$), 36.5 (PhCH_2−), 61.0 (Bn*C*H−), 83.3 (−$C(CH_2CH_2C_6F_{13})_2$), 127.8, 128.7, 129.5, 135.6 (−C_6H_5), 156.1 (−NH*C*OO−); ^{19}F (282 MHz, $CDCl_3$) δ −81.34, −115.32, −122.15, −122.98, −124.16, −126.86; Anal. Calc'd for formula $C_{26}H_{17}F_{26}NO_2$: C, 35.92; H, 1.97; N, 1.61. Found: C, 35.68; H, 2.07; N, 1.61.

4(*S*)-*iso*-Propyl-5,5-bis(1'*H*,1'*H*,2'*H*,2'*H*-perfluorooctyl)-2-oxazolidinone (255):

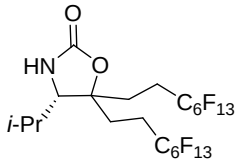

Mp = 109 − 114˚C, ^{1}H NMR (300MHz, $CDCl_3$) δ 5.68 (s, 1H, N*H*), 3.36 (d, 1H, ^3J = 8.9 Hz *i*PrC*H*−), 2.41 – 2.12 (m, 4H, 2×−$CH_2CHHC_6F_{13}$, 2× −$CHHCH_2C_6F_{13}$), 1.98

– 1.68 (m, 5H, 2×−$CH_2CHHC_6F_{13}$, 2× −$CHHCH_2C_6F_{13}$, $(CH_3)_2CH$−), 1.05 (d, 3H, ^3J = 6.8 Hz, CH_3CHCH_3), 0.99 (d, 3H, ^3J = 6.6 Hz, CH_3CHCH_3); ^{13}C (75MHz, $CDCl_3$) δ 20.3 (CH_3CHCH_3), 20.7 (CH_3CHCH_3), 25.8 (2×−$CH_2CH_2C_6F_{13}$), 28.2 ($(CH_3)CH$−), 28.3 (2×−$CH_2CH_2C_6F_{13}$), 65.7 (*i*Pr*C*H−), 84.2 (−$C(CH_2CH_2C_6F_{13})_2$), 157.4 (−NH*C*OO−); ^{19}F (282 MHz, $CDCl_3$) δ −81.25, −115.80, −115.08, −122.32, −123.30, −123.75, −126.54; Anal. Calc'd for formula $C_{22}H_{17}F_{26}NO_2$: C, 32.17; H, 2.09; N, 1.71. Found: C, 32.60; H, 1.83; N, 1.34.

4(*R*)-Phenyl-5,5-bis(1'*H*,1'*H*,2'*H*,2'*H*-perfluorooctyl)-2-oxazolidinone (256):

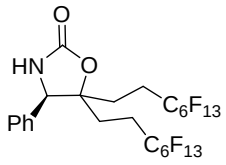

Mp = 115 – 120 ˚C, ^1H NMR (300MHz, $CDCl_3$) δ 7.45 – 7.25 (m, 5H, −C_6H_5), 6.45 (s, 1H, N*H*), 4.79 (s, 1H, PhC*H*−), 2.42 – 2.04 (m, 4H, 2×−$CH_2CHHC_6F_{13}$, 2× −$CHHCH_2C_6F_{13}$), 1.89 – 1.41 (m, 4H, 2×−$CH_2CHHC_6F_{13}$, 2× −$CHHCH_2C_6F_{13}$); ^{13}C (75MHz, $CDCl_3$) δ 25.2 (−$CH_2CH_2C_6F_{13}$), 25.4 (−$CH_2CH_2C_6F_{13}$), 28.2 (2×−$CH_2CH_2C_6F_{13}$), 63.6 (Ph*C*H−), 84.7 (−$C(CH_2CH_2C_6F_{13})_2$), 126.6, 127.7, 129.4, 129.7, 134.7 (−C_6H_5), 156.9 (−NH*C*OO−); ^{19}F (282 MHz, $CDCl_3$) δ −81.24, −114.62, −115.63, −122.34, −123.30, −124.03, −126.59; Anal. Calc'd for formula $C_{25}H_{15}F_{26}NO_2$: C, 35.10; H, 1.77; N, 1.64. Found: C, 35.32; H, 1.67; N, 1.91

(4*S*,5*R*)-4-*iso*-Propyl-5-(1'*H*,1'*H*,2'*H*,2'*H*-perfluorooctyl)-2-oxazolidinone (259):

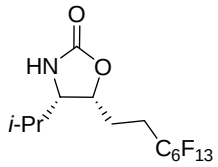

Mp = 96−99˚C, ^{1}H NMR (300MHz, $CDCl_3$) δ 6.90 (br s, 1H, N*H*), 4.58 (ddd, 1H, $^3J_1$ = 10.6 Hz, $^3J_2$ = 7.5 Hz, $^3J_3$ = 2.6 Hz, −C*H*(O)CH_2−), 3.6 (dd, 1H, $^3J_1$ = 7.5 Hz, $^3J_2$ = 7.5 Hz, *i*PrC*H*−), 2.58 – 2.37 (m, 1H, −CH_2C*H*HC_6F_{13}), 2.28 – 1.97 (m, 2H, −CH_2CH*H*C_6F_{13}, $(CH_3)_2$C*H*−), 1.94 – 1.80 (m, 2H, −C*H*$_2CH_2C_6F_{13}$), 1.01 (d, 3H, ^3J = 6.4 Hz, C*H*$_3$CHCH_3), 0.93 (d, 3H, ^3J = 6.4 Hz, CH_3CHC*H*$_3$); ^{13}C (75MHz, $CDCl_3$) δ 19.0 (*C*H_3CHCH_3), 19.7 (CH_3CH*C*H_3), 20.2 (−*C*$H_2CH_2C_6F_{13}$), 27.7 ((*C*$H_3)_3$C−), 27.7 (−CH_2*C*$H_2C_6F_{13}$), 28.2 ($(CH_3)_2$*C*H−), 62.0 (*i*Pr*C*H−), 78.7 (−*C*H$CH_2CH_2C_6F_{13}$), 159.8 (−NH*C*OO−); ^{19}F (282 MHz, $CDCl_3$) δ −81.12, −115.56, −122.12, −123.34, −124.23, −126.83; $[\alpha]_D$ = −46.0˚ (c = 0.43, $CHCl_3$); Anal. Calc'd for formula $C_{14}H_{14}F_{13}NO_2$: C, 35.38; H, 2.97; N, 2.95. Found: C, 35.12; H, 2.73; N, 2.68.

Titanium-Mediated Aldol Reactions

General Acylation Protocol for Fluorous Oxazolidinones; (4*S*,5*R*)-4-Benzyl-5-heptadecafluorooctyl-3-propionyl-oxazolidin-2-one (269):

KH (0.2 g, 30% suspension in oil, 1.5 mmol) was placed under nitrogen, washed with hexane, and suspended in THF (50 mL). Oxazolidinone **230** (0.5 g, 0.85 mmol) was then dissolved in THF (25 mL), added dropwise to the slurry and allowed to stir for 15 min. Propionyl chloride (0.22 mL, 2.55 mmol) was added dropwise, and the solution was brought to reflux for 2 h. The reaction was then cooled to r.t, quenched with 1M HCl, and extracted with Et_2O. The combined ether extracts were then dried with $MgSO_4$ and evaporated to dryness to yield the crude product. The crude material (0.62 g) was dissolved in a minimum of *n*-PrOH and purified by FSPE using general method **A**. This protocol yielded *N*-propionyloxazolidinone **269** (0.51g 0.783 mmol, 93% yield) of as a white solid.

(4*S*,5*R*)-4-Benzyl-5-heptadecafluorooctyl-3-propionyl-oxazolidin-2-one (269):

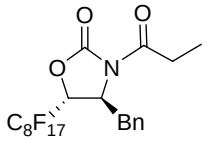

Mp = 85−87˚C, ^{1}H NMR (300 MHz, $CDCl_3$) δ 7.26 (m, 5H, C_6H_5−), 4.93 (m, 1H, BnC*H*(NH)−), 4.73 (m, 1H, −C*H*C_8F_{17}), 3.33 (dd, 1H, $^3J_1$ = 13.7 Hz, $^3J_2$ = 3.2 Hz, PhC*H*H−), 2.97 (dd, 1H, $^3J_1$ = 13.2 Hz, $^3J_2$ = 10.7 Hz, PhCH*H*−), 2.94 (q, 2H, ^3J = 7.2 Hz,

CH_3CH_2CON-), 1.21 (t, 3H, ^3J = 7.4 Hz, CH_3CH_2CON-); ^{13}C NMR (75MHz, $CDCl_3$) δ 7.9 (CH_3CH_2CON-), 29.1 (CH_3CH_2CON-), 37.7 ($PhCH_2-$), 54.6 ($BnCH(NH)-$), 72.4 ($-CH(O)C_8F_{17}$), 127.8 − 133.5 (C_6H_5-), 151.1 ($-NCOO-$), 173.2 (CH_3CH_2CON-); Anal. Calc'd for formula $C_{21}H_{14}F_{17}NO_3$: C, 38.73; H, 2.17; N, 2.15. Found: C, 37.43; H, 2.37; N, 2.14.

(4S,5S)-4-Benzyl-5-heptadecafluorooctyl-3-propionyl-oxazolidin-2-one (270):

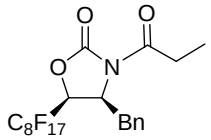

Mp = 99−103˚C, ^1H NMR (300MHz,$CDCl_3$) δ 7.26 (m, 5H, C_6H_5-), 5.15 (dd, 1H, $^3J_1$ = 13.7 Hz, $^3J_2$ = 6.9 Hz, $BnCH(NH)-$), 4.96 (ddd, 1H, $^3J_1$ = 18.8 Hz, $^3J_2$ = 6.3 Hz, $^3J_3$ = 5.1 Hz, $-CHC_8F_{17}$), 3.24 (dd, 1H, $^3J_1$ = 14.1 Hz, $^3J_2$ = 6.0 Hz, $PhCHH-$), 3.07 (dd, 1H, $^3J_1$ = 14.1 Hz, $^3J_2$ = 5.1 Hz, $PhCHH-$), 2.76 (q, 2H, ^3J = 7.4 , CH_3CH_2CONH-), 1.01 (t, 3H, ^3J = 7.4 Hz, CH_3CH_2CONH-); ^{13}C NMR (75MHz, $CDCl_3$) 8.1 (CH_3CH_2CONH-), 29.1 (CH_3CH_2CONH-), 35.0 ($PhCH_2-$), 57.0 ($BnCH(NH)-$), 71.4 ($-CH(O)C_8F_{17}$), 127.3 135.20 (C_6H_5-), 150.9 ($-NCOO-$), 172.3 (CH_3CH_2CON-); Anal. Calc'd for formula $C_{21}H_{14}F_{17}NO_3$: C, 38.73; H, 2.17; N, 2.15. Found: C, 39.03; H, 2.71; N, 2.0.

General Procedure for Titanium-Mediated Aldol Reactions: (4S,5S,2'S,3'S)-4-Benzyl-5-heptadecafluorooctyl-3-(3'-hydroxy-2'-methyl-3'-phenyl-propionyl)-oxazolidin-2-one (280a):

Propionyl derivative **270** (0.1 g, 0.15 mmol) was dissolved in CH_2Cl_2 (5 mL), and cooled to –20ºC. $TiCl_4$ (0.169 mL, 1M solution in CH_2Cl_2) was added dropwise over ~5 min. DIEA (0.742 mL, 0.38 mmol) was then added and the reaction was stirred for 20 min, resulting in the development of a deep red color characteristic of a titanium enolate. Benzaldehyde (0.0386mL, 0.38mmol) was added dropwise, and the solution was stirred at –20ºC for 3 h. The reaction was quenched with saturated NH_4Cl (5 mL), and extracted with Et_2O. The combined extracts were dried with $MgSO_4$ and evaporated to yield a crude residue (0.25g) which was purified using general method **A**. This gave aldol product **280a** (0.11 g, 0.145mmol, 95% yield), which was then analyzed by HPLC.

(4S,5S,2'S,3'S)-4-Benzyl-5-heptadecafluorooctyl-3-(3'-hydroxy-2'-methyl-3'-phenyl-propionyl)-oxazolidin-2-one (280a):

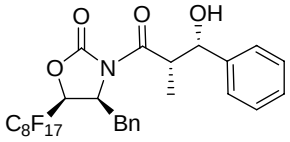

^{1}H NMR (300 MHz, $CDCl_3$) δ 7.26 (m, 10H, C_6H_5 × 2), 5.58 (m, 1H, BnC*H*(NH)−), 4.61 (m, 1H, −C*H*C_8F_{17}), 4.50 (s, 1H, ^3J = 2.5 Hz, PhC*H*(OH)CH(CH_3)−), 4.42 (s, 1H, −OH), 3.34 (dd, 1H, $^3J_1$ = 13.3 Hz, $^3J_2$ = 13.0 Hz, PhC*H*H−), 3.24 (dd, 1H, $^3J_1$ = 13.3 Hz, $^3J_2$ = 4.2 Hz, PhCH*H*−), 2.60 (dq, 1H, $^3J_1$ = 7.6 Hz, $^3J_2$ = 2.5 Hz, −CH(OH)C*H*(CH_3)CO−), 0.94 (d, 3H, $^3J_1$ = 7.6 Hz, CH_3−); ^{13}C NMR (75 MHz, $CDCl_3$)

δ 9.7 (CH_3−), 32.5 (Ph*C*H_2−), 41.8 (PhCH(OH)*C*H(CH_3)CO−), 51.6 (Bn*C*H(NH)−), 72.2 (−*C*HC_8F_{17}), 77.8 (Ph*C*H(OH)CH(CH_3)−), 125.2 – 136.6 (C_6H_5 × 2), 152.2 (−N*C*OO−), 171.3 (−CH(CH_3)*C*ON−).

(4*S*,5*S*,2'S,3'*R*)-Benzyl-5-heptadecafluorooctyl-3-(3'-hydroxy-2',4'-dimethyl-pentanoyl)-oxazolidin-2-one (280b):

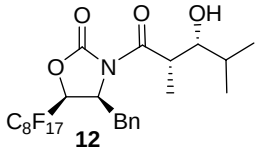

12

^{1}H NMR (300 MHz, $CDCl_3$) δ 7.21 (m, 5H, C_6H_5), 5.51 (m, 1H, BnC*H*(NH)−), 4.70 (br s, 1H, −OH), 4.58 (m, 1H, −C*H*C_8F_{17}), 3.31 (dd, 1H, $^3J_1$ = 13.2 Hz, $^3J_2$ = 13.1 Hz, PhC*H*H−), 3.20 (dd, 1H, $^3J_1$ = 13.2 Hz, $^3J_2$ = 5.3 Hz, PhCH*H*−), 2.70 (dd, 1H, $^3J_1$ = 9.92 Hz, $^3J_2$ = 2.0 Hz, $(CH_3)_2$CHC*H*(OH)−), 2.46 (dq, 1H, $^3J_1$ = 7.3 Hz, $^3J_2$ = 2.0 Hz, CH(OH)C*H*(CH_3)CO−), 1.78 (m, 1H, $(CH_3)_2$C*H*−), 1.08 (d, 1H, ^3J = 7.3 Hz, −CH(OH)CH(C*H*$_3$)CO−), 0.98 (d, 3H, ^3J = 6.7 Hz, (C*H*$_3$)(CH_3)CH−), 0.69 (d, 3H, ^3J = 6.3 Hz, (CH_3)(C*H*$_3$)CH−); ^{13}C NMR (75MHz, $CDCl_3$) δ 8.5 (CH(OH)CH(*C*H_3)CO−), 17.1 ((*C*H_3)(CH_3)CH−), 19.0 ((CH_3)(*C*H_3)CH−), 27.7 ((CH_3)$_2$*C*H−), 32.0 (Ph*C*H_2), 37.7 (CH(OH)*C*H(CH_3)CO−), 51.3 (Bn*C*H(NH)−), 71.5 (−*C*HC_8F_{17}), 82.7 ((CH_3)$_2$CH*C*H(OH)−), 127.0 – 136.61 (C_6H_5), 152.9 (−N*C*OO−), 171.8 (−CH(CH_3)*C*ON−).

(4*S*,5*S*,2'*S*,3'*R*)-4-Benzyl-5-heptadecafluorooctyl-3-(3'-hydroxy-2'-methyl-nonanoyl)-oxazolidin-2-one (280c):

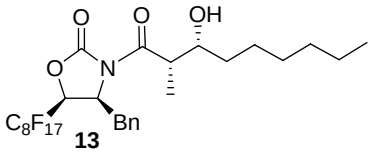

13

^{1}H NMR (300 MHz, acetone−d_6) δ 7.19 (m, 5H, C_6H_5), 5.75 (s, 1H, −OH), 5.35 (m, 1H, BnC*H*(NH)−), 5.09 (m, 1H, −C*H*C_8F_{17}), 3.56 (m, 1H, −$(CH_2)_4$C*H*(OH)−), 3.36 (dd, 1H, $^3J_1$ = 12.5 Hz, $^3J_2$ = 3.9 Hz, PhC*H*H−), 3.18 (dd, , $^3J_1$ = 12.5 Hz, $^3J_2$ = 12.4 Hz, PhCH*H*−), 2.33 (dq, 1H, $^3J_1$ = 7.2 Hz, $^3J_2$ = 2.5 Hz, CH(OH)C*H*(CH_3)CO−), 1.50 (m, 2H, CH_2CH(OH)−), 1.25 (br m, 8H, −$(CH_2)_4$−), 0.96 (d, 3H, ^{3}J = 7.2 Hz, CH(OH)CH(C*H*$_3$)CO−), 0.86 (t, 3H, ^{3}J = 6.2 Hz, C*H*$_3(CH_2)_4$−); ^{13}C NMR (75 MHz, acetone−d_6) δ 8.9 (CH(OH)CH(*C*H_3)CO−), 14.1 (*C*$H_3(CH_2)_4$−), 22.9 (−(*C*$H_2)_4$−), 25.3 (−(*C*$H_2)_4$−), 29.3 (−(*C*$H_2)_4$−), 29.8 (−$(CH_2)_4$*C*H(OH)−), 32.0 (−(*C*$H_2)_4$−), 34..3 ($PhCH_2$), 39.4 (CH(OH)*C*H(CH_3)CO−), 51.6 (BnC*H*(NH)−), 69.0 (−*C*HC_8F_{17}), 77.9 (CH_2*C*H(OH)−), 127.3 – 137.6 (C_6H_5), 151.4 (−N*C*OO−), 171.9 (−CH(CH_3)*C*ON−).

(*E*)-(4*S*,5*S*,2'*S*,3'*R*)-4-Benzyl-5-heptadecafluorooctyl-3-(3'-hydroxy-2'-methyl-hex-4'-enoyl)-oxazolidin-2-one (280d):

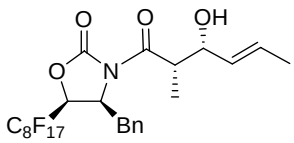

^{1}H NMR (300 MHz, $CDCl_3$) δ 7.23 (m, 5H, C_6H_5), 5.78 (m, 1H, CH_3C*H*=CH−), 5.53 (m, 1H, BnC*H*(NH)−), 5.30 (m, 1H, CH_3CH=C*H*−), 4.54 (m, 1H, −C*H*C_8F_{17}), 4.01

(br s, 1H, −OH), 3.33 (dd, 1H, $^3J_1$ = 13.2 Hz, $^3J_2$ = 13.1 Hz, PhC*H*H−), 3.17 (dd, 1H, $^3J_1$ = 13.2 Hz, $^3J_2$ = 4.6 Hz, PhCH*H*−), 2.32 (dq, 1H, $^3J_1$ = 7.1 Hz, $^3J_2$ = 3.0 Hz, CH(OH)C*H*(CH_3)CO−), 1.73 (d, 3H, ^3J = 6.2 Hz, C*H*$_3$CH=CH−), 1.06 (d, 3H, ^3J = 7.1 Hz, , CH(OH)CH(C*H*$_3$)CO−); ^{13}C NMR (75 MHz ,$CDCl_3$) δ 9.5 (CH(OH)CH(*C*H_3)CO−), 17.7 (*C*H_3CH=CH−), 32.5 (CH(OH)*C*H(CH_3)CO−), 51.6 (BnC*H*(NH)−), 72.1 (−*C*HC_8F_{17}), 78.3 (CH=CH*C*H(OH)−), 122.3 (CH_3CH=*C*H−), 127.1 – 136.6 (C_6H_5), 134.1 (CH_3*C*H=CH−), 152.3 (−N*C*OO−), 171.1 (−CH(CH_3)*C*ON−).

General Procedure for LiOOH Hydrolysis of Aldol Products; (2S,3S)-3-Hydroxy-2-methyl-3-phenylpropanoic acid (288a):

Aldol product **280a** obtained by HPLC (0.090 g, 0.119 mmol) was dissolved in THF : H_2O (3 : 1 v/v, 2.5mL) and cooled to 0ºC. H_2O_2 (30% solution, 0.115 mL) was then added, followed by LiOH (5.7 mg, 0.238 mmol). The reaction was stirred at 0ºC for 3h, and then quenched with Na_2SO_3 (7 mL, 1M solution) and extracted with Et_2O to give Fraction #1. The aqueous layer was then acidified and extracted with Et_2O to give Fraction #2. Both organic extracts were separately dried and concentrated under vacuum. The residue from Fraction #1 was dissolved in *n*-PrOH and purified by FSPE using general method **A**, to give oxazolidinone **231** (.069 g, 0.116 mmol, 98% yield). Fraction #2 yielded the desired (2*S*,3*S*)-3-hydroxy-2-methyl-3-phenylpropanoic acid **288a** (0.018 g, 0.108 mmol, 91% yield).

(2S,3S)-3-Hydroxy-2-methyl-3-phenylpropanoic acid (288a):

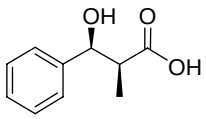

^{1}H NMR, and ^{13}C NMR identical to literature[152]; Measured $[\alpha]_D = -10^\circ$ (c = 0.3, $CHCl_3$); Lit.[152] $[\alpha]_D = -29.3^\circ$ (c = 0.8, $CHCl_3$).

(2S,3R)-3-Hydroxy-2,4-dimethylpentanoic acid (288b):

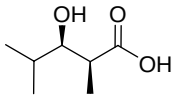

^{1}H NMR, and ^{13}C NMR identical to literature[152]; Measured $[\alpha]_D = -6.8^\circ$ (c = 0.2, $CHCl_3$); Lit.[152] $[\alpha]_D = -9.5^\circ$ (c = 0.4, CH_2Cl_2)

(2S,3R)-3-Hydroxy-2-methylnonanoic acid (288c):

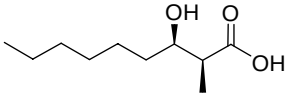

^{1}H NMR, and ^{13}C NMR identical to literature[249]; Measured $[\alpha]_D = +3.3^\circ$ (c = 0.32, $CHCl_3$); Lit.[249] for (2*R*,3*S*) enantiomer $[\alpha]_D = -11.3^\circ$ (c = 0.98, $CHCl_3$).

(*E*)-(2S,3R)-2-Methyl-4-hexene-1,3-diol (289):

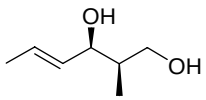

Aldol product **280d** (17 mg, 0.024 mmol) was dissolved in THF (2.5 mL) and cooled to 0ºC. A solution of $NaBH_4$ (4 mg, 0.1 mmol) in H_2O (1 mL) was added to the reaction dropwise. The solution was stirred at 0ºC for 3 h, after which the reaction was quenched with 1N HCl. The reaction mixture was then concentrated under vacuum and extracted with Et_2O. The combined extracts were washed with brine, dried with $MgSO_4$ and evaporated to dryness under vacuum. The products were purified using flash column chromatography on silica (9:1 hexane: EtOAc) to yield the desired diol, **289** (0.9 mg, 6.91 μmol, 30% yield). The ^1H and ^{13}C NMR spectra matched literature values.[250] Measured $[\alpha]_D = -1.11^\circ$ (c = 0.90, $CHCl_3$); Lit.[250] $[\alpha]_D = -0.35^\circ$ (c = 0.865, $CHCl_3$).

Radical Conjugate Additions

(*E*)-(4*S*,5*R*)-4-Benzyl-3-(2'-butenoyl)-5-(1'*H*,1'*H*,2'*H*,2'*H*-perfluorooct-yl)-2-oxazolidinone (290a):

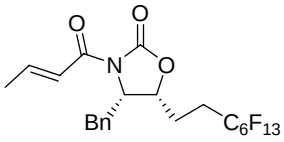

Powdered and dried LiCl (0.406 g, 9.55 mmol) was added to a solution of oxazolidinone **245** (1.00 g, 1.91 mmol) in THF (200 mL) and allowed to stir until the solution was homogeneous. *E*-Crotonic anhydride (1.40 mL, 9.55 mmol) was then added

dropwise, followed by DIPEA (1.66 mL, 9.55 mmol). The solution was then heated to reflux for 24 h. After this time, the reaction was cooled, and the solvent was removed under vacuum to give a crude oil. This material was purified by FSPE using method **A** to give *N*-enoyloxazolidinone **290a** (0.98 g, 1.66 mmol, 87 % yield) as a white crystalline solid; R_f 0.49 (4:1-hexanes/ethyl acetate); ^{1}H NMR (300 MHz, $CDCl_3$) δ 7.35 – 7.16 (m, 7H, −C_6H_5, CH_3CH=C*H*−), 4.91 (ddd, 1H, $^3J_1$ = 9.8 Hz, $^3J_2$ = 6.9 Hz, $^3J_3$ = 3.4 Hz, BnC*H*N−), 4.53 (ddd, 1H, $^3J_1$ = 10.1 Hz, $^3J_2$ = 6.9 Hz, $^3J_3$ = 3.3 Hz, −C*H*$CH_2CH_2C_6F_{13}$), 3.13 (dd, 1H, $^3J_1$ = 14.5 Hz, $^3J_2$ = 3.2 Hz, PhC*H*H−); 2.96 (dd, 1H, $^3J_1$ = 14.5 Hz, $^3J_2$ = 9.7 Hz, PhCH*H*−), 2.41 – 2.26 (m, 1H, −CH_2C*H*HC_6F_{13}), 2.22 – 2.10 (m, 1H, −C*H*$HCH_2C_6F_{13}$), 1.97 (apt d, 4H, ^3J = 5.4 Hz, C*H*$_3$CH=CH−, −CH_2C*H*HC_6F_{13}), 1.81 – 1.70 (m, 1H, −CH*H*$CH_2C_6F_{13}$); ^{13}C NMR (75 MHz, $CDCl_3$) δ 18.5 (*C*H_3CH=CH−), 21.1 (−*C*$H_2CH_2C_6F_{13}$), 27.9 (−CH_2*C*$H_2C_6F_{13}$), 34.0 (Ph*C*H_2−), 58.42 (Bn*C*H−), 77.7 (−*C*$HCH_2CH_2C_6F_{13}$), 121.7 (−*C*H=CH−), 127.1, 128.9, 129.0, 136.2 (−*C*$_6H_5$), 152.5 (−N*C*OO−), 164.5 (−CH=CH*C*ON−); ^{19}F (282 MHz, $CDCl_3$) δ −81.25, −114.93, −122.36, −123.32, −123.93, −126.58; $[\alpha]^{25}_D$ +13.4 (*c* 1.00, $CHCl_3$); Anal. Calc for formula $C_{22}H_{18}F_{13}NO_3$: C, 44.68; H, 3.07; N, 2.37. Found: C, 44.68; H, 3.30; H, 2.35.

(*E*)-(4*S*,5*R*)-4-Benzyl-3-(3'-phenyl-2'-propenoyl)-5-(1'*H*,1'*H*,2'*H*,2'*H*-perfluorooctyl)-2-oxazolidinone (290b):

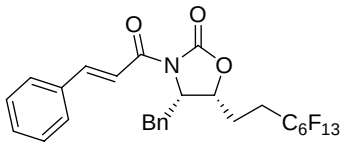

Powdered and dried LiCl (0.406 g, 9.55 mmol) was added to a solution of oxazolidinone **245** (1.00 g, 1.91 mmol) and cinnamoyl chloride (0.573 g, 3.44 mmol) in CH_2Cl_2 (200 mL) and stirred as a suspension. DIPEA (1.66 mL, 9.55 mmol) was then added dropwise and the solution was left overnight at r.t.. After this time the solvent was removed under vacuum to give a crude colored oil. The products were purified by FSPE using method **B** to give *N*-enoyloxazolidinone **290b** (.457 g, 0.699 mmol, 36.6 % yield) as a white crystalline solid; R_f 0.56 (4:1-hexanes/ethyl acetate); ^{1}H NMR (400 MHz, $CDCl_3$) δ 7.88 (d, 1H, ^{3}J = 15.8 Hz, −C*H*=CH−), 7.83 (d, 1H, ^{3}J = 15.8 Hz, −CH=C*H*−) 7.62 – 7.59 (m, 2H, 2 × −C_6H_5), 7.39 – 7.37 (m, 3H, 2 × −C_6H_5), 7.31 – 7.30 (m, 4H, 2 × −C_6H_5), 7.27 – 7.21 (m, 1H, 2 × −C_6H_5), 4.97 (ddd, 1H, $^3J_1$ = 9.8 Hz, $^3J_2$ = 6.7 Hz, $^3J_3$ = 3.6 Hz, BnC*H*N−), 4.54 (ddd, 1H, $^3J_1$ = 10.3 Hz, $^3J_2$ = 6.9 Hz, $^3J_3$ = 3.4 Hz, −C*H*$CH_2CH_2C_6F_{13}$), 3.22 (dd, 1H, $^3J_1$ = 14.5 Hz, $^3J_2$ = 3.4 Hz, PhC*H*H−), 2.98 (dd, 1H, $^3J_1$ = 14.5 Hz, $^3J_2$ = 9.6 Hz, PhC*H*H−), 2.39 – 2.27 (m, 1H, − CH_2C*H*HC_6F_{13}), 2.23 – 2.12 (m, 1H, −C*H*H$CH_2C_6F_{13}$), 2.04 – 1.87 (m, 1H, −CH_2CH*H*C_6F_{13}), 1.81 – 1.73 (m, 1H, −CH*H*$CH_2C_6F_{13}$); ^{13}C NMR (100 MHz, $CDCl_3$) δ 21.3 (−*C*$H_2CH_2C_6F_{13}$), 28.1 (−CH_2*C*$H_2C_6F_{13}$), 34.3 (Ph*C*H_2−), 58.8 (Bn*C*H−), 78.8 (−*C*H$CH_2CH_2C_6F_{13}$), 117.0 (−*C*H=CH−), 127.4, 128.9, 129.1, 129.1, 129.3, 131.0, 134.7, 136.4 (2 × −C_6H_5), 147.0 (−CH=*C*H−), 152.8 (−N*C*OO−), 165.0 (−CH=CH*C*ON); ^{19}F (282 MHz, $CDCl_3$) δ −81.22,

−114.90, −122.34, −123.29, −123.89, −126.55; $[\alpha]^{25}_{D}$ –3.21 (*c* 1.06, $CHCl_3$); Anal. Calc for formula: $C_{27}H_{20}F_{13}NO_3$; C, 49.63; H, 3.09; N, 2.14. Found: C, 50.00; H, 3.27; H, 2.11.

(*E*)-(4*S*,5*R*)-4-Benzyl-3-(3'-ethoxycarbonyl-2'-propenoyl)-5-(1'H,1'H,-2'H,2'H-perfluorooctyl)-2-oxazolidinone (290c):

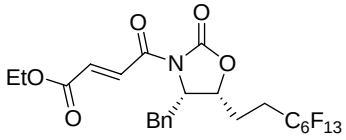

2-Chloro-1-methyl-pyridinium iodide (0.244 g, 0.955 mmol) was added to a solution of oxazolidinone **245** (0.200 g, 0.382 mmol) and monoethyl fumarate (0.138 g, 0.955 mmol) in THF (10 mL) and stirred at r.t. for 25 min. DIPEA (0.166 mL, 0.955 mmol) was then added dropwise and the solution was left to stir at r.t. for 48 h. After this time the solvent was removed under vacuum to give a crude colored solid. The products were purified by FSPE using method **B** to give *N*-enoyloxazolidinone **290c** (0.191 g, 0.294 mmol, 77 % yield) as a white crystalline solid: R_f 0.36 (4:1−hexanes/ethyl acetate); ^{1}H NMR (300 MHz, $CDCl_3$) δ 8.09 (d, 1H, ^{3}J = 15.5 Hz, −C*H*=CH−) 7.35 – 7.26 (m, 5H, −C_6H_5), 6.91 (d, 1H, ^{3}J = 15.5 Hz, −CH=C*H*−), 4.93 (ddd, 1H, $^3J_1$ = 9.3 Hz, $^3J_2$ = 6.6 Hz, $^3J_3$ = 3.88 Hz, BnC*H*N−), 4.59 (ddd, 1H, $^3J_1$ = 10.2 Hz, $^3J_2$ = 6.7 Hz, $^3J_3$ = 3.2 Hz, −C*H*$CH_2CH_2C_6F_{13}$), 4.27 (q, 2H, ^{3}J = 7.1 Hz, −OC$H_2$$CH_3$), 3.17 (dd, 1H, $^3J_1$ = 14.4 Hz, $^3J_2$ = 3.9 Hz, PhC*H*H−), 2.98 (dd, 1H, $^3J_1$ = 14.4 Hz, $^3J_2$ = 9.4 Hz, PhC*H*H−), 2.44 – 2.28 (m, 1H, − CH_2C*H*HC_6F_{13}), 2.20 – 2.11 (m, 1H, −C*H*$HCH_2C_6F_{13}$), 2.09 – 1.93 (m, 1H, −CH_2CH*H*C_6F_{13}), 1.85 – 1.74 (m, 1H, −CH*H*$CH_2C_6F_{13}$) 1.33 (t, 3H, ^{3}J = 7.1 Hz, −OCH_2C*H*$_3$); ^{13}C NMR (75 MHz, $CDCl_3$) δ 14.1 (−OCH_2*C*H_3), 21.1 (−*C*$H_2CH_2C_6F_{13}$),

27.8 (−CH_2*C*$H_2C_6F_{13}$), 33.9 (Ph*C*H_2−), 58.5 (Bn*C*H−), 61.5 (−O*C*H_2CH_3), 78.2 (−*C*$HCH_2CH_2C_6F_{13}$), 127.3, 128.9, 129.0, 134.7 (−*C*$_6H_5$), 132.0 (−*C*H=CH−), 135.7 (−CH=*C*H−), 152.1 (−N*C*OO−), 163.2 (EtO*C*O−), 164.8 (−CH=CH*C*ON); ^{19}F (282 MHz, $CDCl_3$) δ −81.27, −114.92, −122.37, −123.33, −123.93, −126.60; $[\alpha]^{25}_D$ +20.22 (*c* 0.44, $CHCl_3$); Anal. Calc for formula: $C_{24}H_{20}F_{13}NO_5$; C, 44.39; H, 3.10; N, 2.16. Found: C, 44.05; H, 2.89; H, 1.96.

Synthesis of the Norephedrine Oxazolidinone Auxiliary; (4*S*,5*R*)-4-methyl-5-phenyl-2-oxazolidinone (301):

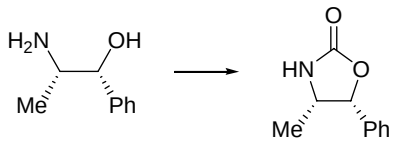

(−)-(1*R*,2*S*)-Norephedrine (3.00 g, 19.84 mmol) and triphosgene (7.07 g, 23.81 mmol) were dissolved in CH_2Cl_2 and cooled to −78 °C. TEA (5.58 mL, 39.7 mmol) was then added dropwise and the mixture was left to stir vigorously for 2 h. After this time the reaction was warmed slowly to 0 °C and left to stir for an additional 2 h. Et_2O (~100 mL) was added and the solution was again cooled to −78 °C, forcing TEA·HCl to precipitate out of solution. While the solution was cold, the precipitate was filtered, and the filtrate was concentrated under vacuum. The crude products (3.8 g) were adsorbed onto silica gel (10 g), applied to a pad of silica (40 mL), and eluted with EtOAc (200 mL). Removal of the volatile material produced oxazolidinone **301** (2.700 g, 15.24 mmol, 77 % yield) as a white solid. R_f = 0.125 (2:1−hexanes/ethyl acetate); 118−120 °C, lit.[274] 121−122 °C; ^{1}H NMR (300 MHz, $CDCl_3$) δ 7.35 – 7.23 (m, 5H, −C_6H_5), 6.90 (br s, 1H, −N*H*), 5.65 (d,

1H, ^{3}J = 8.8 Hz, PhC*H*−), 4.17 (dq, 1H, $^{3}J_1$ = 8.0 Hz, $^{3}J_2$ = 6.8 Hz, CH_3CH(N)−), 0.76 (d, 3H, ^{3}J = 6.8 Hz,CH_3CH(N)−); ^{13}C NMR (75 MHz, $CDCl_3$) δ 17.7 (CH_3CH(N)−), 52.7 (CH_3CH(N)−), 81.2 (−*C*HPh), 126.2, 128.6, 128.7, 135.3 (−C_6H_5), 160.2 (−N*C*OO−);

(*E*)-(4*S*,5*R*)-4-Methyl-3-(3'-phenyl-2'-propenoyl)-5-phenyl-2-oxazolidinone (302a):

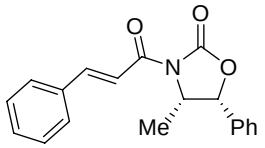

To oxazolidinone **301** (0.600 g, 3.39 mmol) in THF (10 mL) was added *n*-butyllithium (2.5M hexanes, 1.35 mL, 3.39 mmol) dropwise at −78 °C. At the endpoint of the addition the solution was deep purple in color. After complete addition the solution was stirred at −78 °C for ~5 min. A solution of cinnamoyl chloride (0.677 g, 4.06 mmol) in THF (5 mL) was added dropwise at −78 °C over 10 min, and the mixture was stirred at −78 °C for 3 h. The reaction was quenched with NH_4Cl at −78 °C and extracted with Et_2O (3 × 35 mL). The extracts were combined and washed with brine, dried over $MgSO_4$, and evaporated to dryness. Flash chromatography (9:1−hexanes/ethyl acetate as eluent) gave *N*-enoyloxazolidinone **302a** (0.91 g, 2.96 mmol, 87 % yield) as crystalline solid whose ^{1}H and ^{13}C NMR matched those reported in the literature.[275]

(*E*)-(4*S*,5*R*)-3-(3'-Ethoxycarbonyl-2'-propenoyl)-4-methyl-5-phenyl-2-oxazolidinone (302b):

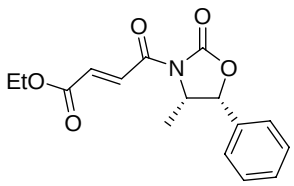

Oxazolidinone **301** (0.800 g, 4.51 mmol), mono-ethyl fumaric acid (0.781 g, 5.42 mmol), and TBTU (1.740 g, 5.42 mmol) were combined as powders and dissolved in dry CH_3CN. The solution was stirred at r.t. for 10 min, then TEA (1.27 mL, 9.03 mmol) was added dropwise. The solution turned yellow in color, and quickly became opaque, and was allowed to stir overnight at r.t. After this time the reaction was concentrated under vacuum, and the residue taken up in Et_2O (50 mL). The mixture was extracted sequentially with brine, 1M HCl, and 1M $NaHCO_3$. The organic fraction was dried with $MgSO_4$ and evaporated to dryness. Flash column chromatography (4:1−hexanes/ethyl acetate as eluent) provided *N*-enoyloxazolidinone **302b** (0.91 g, 3.00 mmol, 66.5 % yield) as crystalline solid. . R_f 0.29 (9:1−hexanes/ethyl acetate); ^{1}H NMR (300 MHz, $CDCl_3$) δ 8.17 (d, 1H, ^{3}J = 15.6 Hz, −C*H*=CH−) 7.46 – 7.30 (m, 5H, −C_6H_5), 6.96 (d, 1H, ^{3}J = 15.6 Hz, −CH=C*H*−), 5.73 (d, 1H, ^{3}J = 7.5 Hz, PhC*H*−), 4.83 (dq, 1H, $^3J_1$ = 6.8 Hz, $^3J_2$ = 6.7 Hz, CH_3C*H*−), 4.29 (q, 2H, ^{3}J = 7.1 Hz, −OC*H*$_2$CH$_3$), 1.34 (t, 3H, $^3J_1$ = 7.2 Hz, −OCH$_2$C*H*$_3$), 0.96 (d, 3H, ^{3}J = 6.5, C*H*$_3$CH(N)−); ^{13}C NMR (75 MHz, $CDCl_3$) δ 14.5 (*C*H$_3$CH(N)−), 14.9 (−OCH$_2$*C*H$_3$), 55.5 (CH$_3$*C*H(N)−), 61.8 (−O*C*H$_2$CH$_3$), 79.8 (Ph*C*H−), 126.1, 129.2, 129.4, 133.3 (−*C*$_6$H$_5$), 132.7 (−*C*H=CH−), 134.8 (−CH=*C*H−), 153.0 (−N*C*OO−), 163.9 (EtO*C*O−), 165.3 (−CH=CH*C*ON); Anal. Calc for formula: $C_{16}H_{17}NO_5$; C, 63.36; H, 5.65; N, 4.62. Found: C, 62.98; H, 5.42; H, 4.53.

General Experimental Procedure for Lewis Acid-Mediated Conjugate Radical Addition to Enoates; (3'*R*,4*S*,5*R*)-4-benzyl-3-(3',4'-dimethyl-pentanoyl)-5-(1'*H*,1'*H*,2'*H*,2'*H*-perfluorooctyl)-2-oxazolidinone (291a):

N-enoyloxazolidinone **290a** (0.050 g, 0.085 mmol) and $Yb(OTf)_3$ (0.105 g, 0.169 mmol) were dissolved in 1.0 mL of CH_2Cl_2/THF (4:1) and cooled to 0 °C. After stirring for 15 min 2-iodopropane (0.042 mL, 0.423 mmol), tributyltin hydride (0.056 mL, 0.211 mmol), and triethylborane (0.423 mL, 0.423 mmol) were added. The reaction was immediately initiated by adding O_2 (10 mL) via syringe and then monitored by TLC. After 1 h, a second equivalent of 2-iodopropane (0.042 mL, 0.423 mmol), tributyltin hydride (0.056 mL, 0.211 mmol), and triethylborane (0.423 mL, 0.423 mmol) was added, followed again by immediate initiation by O_2 (10 mL). After an additional 1 h the reaction was quenched with silica gel (1g) and the crude material purified by FSPE using method **C** to give radical addition product **291a** as a mixture of diastereomers (0.051 g, 95 % yield).

(3'*R*,4*S*,5*R*)-4-Benzyl-3-(3',4'-dimethyl-pentanoyl)-5-(1'*H*,1'*H*,2'*H*,2'*H*-perfluorooctyl)-2-oxazolidinone (291a):

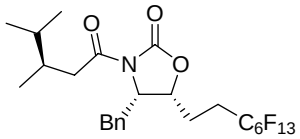

R_f = 0.45 (9:1−hexanes/ethyl acetate); ^{1}H NMR (300 MHz, $CDCl_3$) δ 7.34 – 7.22 (m, 5H, −C_6H_5), 4.89 (ddd, 1H, $^3J_1$ = 9.7 Hz, $^3J_2$ = 6.4 Hz, $^3J_3$ = 3.5 Hz, BnC*H*N−), 4.52

(ddd, 1H, $^3J_1$ = 10.2 Hz, $^3J_2$ = 6.5 Hz, $^3J_3$ = 3.2 Hz, −C*H*$CH_2CH_2C_6F_{13}$), 3.12 (dd, 1H, $^3J_1$ = 14.0 Hz, $^3J_2$ = 3.2 Hz, PhC*H*H−), 2.92 (m, 2H, PhC*H*H−, −C*H*HCON−), 2.67 (dd, 1H, $^3J_1$ = 16.4 Hz, $^3J_2$ = 9.1 Hz, −CH*H*CON−), 2.41 – 2.21 (m, 1H, − $CH_2CHHC_6F_{13}$), 2.18 – 2.08 (m, 1H, −C*H*H$CH_2C_6F_{13}$), 2.01 – 1.89 (m, 2H, −$CH_2CHHC_6F_{13}$, *i*PrC*H*−), 1.81 – 1.70 (m, 1H, −CH*H*$CH_2C_6F_{13}$) 1.67 – 1.57 (m, 1H, $(CH_3)_2CH$−), 0.90 (d, 3H, ^3J = 6.7 Hz, $(CH_3)_2$CH−), 0.86 (d, 3H, ^3J = 6.4 Hz, $(CH_3)_2$CH−); ^{13}C NMR (75 MHz, $CDCl_3$) δ 15.7 (*C*H_3CH(*i*Pr)−), 18.2 ((*C*H_3)$_2$CH−), 20.0 ((*C*H_3)$_2$CH−), 21.1 (−*C*$H_2CH_2C_6F_{13}$), 27.9 (−CH_2*C*$H_2C_6F_{13}$), 32.1 ($(CH_3)_2$*C*H−), 34.1 (Ph*C*H_2−), 35.0 (CH_3(*i*Pr)*C*H−), 40.0 (−CH*C*H_2CON−), 58.2 (Bn*C*H−), 77.7 (−*C*H$CH_2CH_2C_6F_{13}$), 127.2, 128.9, 129.0, 136.1 (−*C*$_6H_5$), 152.5 (−N*C*OO−), 172.7 (−CHCH_2*C*ON); ^{19}F (282 MHz, $CDCl_3$) δ −81.22, −114.92, −122.34, −123.30, −123.92, −126.56; Anal. Calc for formula: $C_{25}H_{26}F_{13}NO_3$; C, 47.25; H, 4.12; N, 2.20. Found: C, 46.95; H, 3.90; H, 2.16.

(3'*R*,4*S*,5*R*)-4-Benzyl-3-(4'-methyl-3'-phenyl-pentanoyl)-5-(1'H,1'H,-2'H,2'H-perfluorooctyl)-2-oxazolidinone (291b):

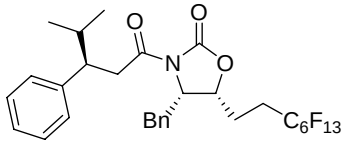

R_f = 0.52 (9:1−hexanes/ethyl acetate); ^{1}H NMR (300 MHz, $CDCl_3$) δ 7.31 – 7.09 (m, 10H, 2 × −C$_6H_5$), 4.57 (ddd, 1H, $^3J_1$ = 9.9 Hz, $^3J_2$ = 6.5 Hz, $^3J_3$ = 3.6 Hz, BnC*H*N−), 4.11 (ddd, 1H, $^3J_1$ = 10.1 Hz, $^3J_2$ = 6.6 Hz, $^3J_3$ = 3.3 Hz, −C*H*$CH_2CH_2C_6F_{13}$), 3.52 (dd, 1H, $^3J_1$ = 15.8 Hz, $^3J_2$ = 10.6 Hz, −C*H*HCON−), 3.12 (dd, 1H, $^3J_1$ = 15.9 Hz, $^3J_2$ = 4.6 Hz, −CH*H*CON−), 3.01 – 2.90 (m, 2H, PhC*H*H−, −iPrC*H*CH_2−), 2.77 (dd, 1H, $^3J_1$ = 14.5 Hz,

$^3J_2$ = 9.6 Hz, PhCH*H*−), 2.32 – 2.16 (br m, 1H, −$CH_2CHHC_6F_{13}$), 2.07 – 1.97 (m, 1H, −$CHHCH_2C_6F_{13}$), 1.96 – 1.84 (m, 2H, −$CH_2CHHC_6F_{13}$, $(CH_3)_2CH$−), 1.67 – 1.57 (m, 1H, −$CHHCH_2C_6F_{13}$) 1.00 (d, 3H, ^3J = 6.6 Hz, $(CH_3)_2CH$−), 0.76 (d, 3H, ^3J = 6.6 Hz, $(CH_3)_2CH$−); ^{13}C NMR (75 MHz, $CDCl_3$) δ 20.6 ($(CH_3)_2CH$−), 20.9 (−$CH_2CH_2C_6F_{13}$), 27.7 (−$CH_2CH_2C_6F_{13}$), 33.3 ($(CH_3)_2CH$−), 33.9 (PhCH_2−), 39.0 (CHCH_2CON−), 49.2 (Ph(*i*Pr)CH−), 58.3 (BnCH−), 77.4 (−$CHCH_2CH_2C_6F_{13}$), 126.4, 127.1, 128.1, 128.4, 128.7, 129.0, 136.1, 142.9 (2 × −C_6H_5), 152.5 (−NCOO−), 172.1 (−$CHCH_2CON$); ^{19}F (282 MHz, $CDCl_3$) δ −81.27, −114.92, −122.37, −123.33, −123.93, −126.60; Anal. Calc for formula: $C_{30}H_{28}F_{13}NO_3$; C, 51.66; H, 4.05; N, 2.01. Found: C, 51.90; H, 3.85; H, 1.94.

(3'*R*,4*S*,5*R*)-4-Benzyl-3-(3'-ethoxycarbonyl-4'-methyl-pentanoyl)-5-(1'*H*,1'*H*,2'*H*,2'*H*-perfluorooctyl)-2-oxazolidinone (291c):

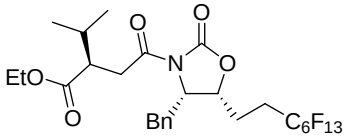

R_f = 0.32 (9:1−hexanes/ethyl acetate); ^1H NMR (300 MHz, $CDCl_3$) δ 7.33 – 7.25 (m, 5H, −C_6H_5), 4.84 (ddd, 1H, $^3J_1$ = 9.8 Hz, $^3J_2$ = 6.7 Hz, $^3J_3$ = 3.7 Hz, BnC*H*N−), 4.54 (ddd, 1H, $^3J_1$ = 10.1 Hz, $^3J_2$ = 6.9 Hz, $^3J_3$ = 3.2 Hz, −C*H*$CH_2CH_2C_6F_{13}$), 4.21 (dq, 1H, $^3J_1$ = 10.8 Hz, $^3J_2$ = 7.1 Hz, −OCH*H*CH_3), 4.15 (dq, 1H, $^3J_1$ = 10.8 Hz, $^3J_2$ = 7.1 Hz, −OC*H*HCH_3), 3.35 (dd, 1H, $^3J_1$ = 18.3 Hz, $^3J_2$ = 11.4 Hz, −C*H*HCON−), 3.13 (dd, 1H, $^3J_1$ = 14.5 Hz, $^3J_2$ = 3.7 Hz, PhC*H*H−), 2.96 – 2.88 (m, 2H, PhC*H*H−, −CH*H*CON−), 2.78 (ddd, 1H, $^3J_1$ = 11.4 Hz, $^3J_2$ = 5.3 Hz, $^3J_3$ = 3.0 Hz, PhC*H*H−), 2.36 – 2.24 (m, 1H, −$CH_2CHHC_6F_{13}$), 2.19 – 1.89 (m, 3H, −C*H*H$CH_2C_6F_{13}$, −$CH_2CHHC_6F_{13}$, $(CH_3)_2CH$−),

1.77 – 1.66 (m, 1H, −CH*H*$CH_2C_6F_{13}$), 1.28 (t, 3H, ^3J = 7.1 Hz, −OCH_2CH_3), 0.99 (d, 3H, ^3J = 4.4 Hz), 0.96 (d, 3H, ^3J = 4.4 Hz); ^{13}C NMR (75 MHz, $CDCl_3$) δ 14.3 (*C*H_3CH_2O−), 19.6 ((*C*H_3)$_2$CH−), 20.2 ((*C*H_3)$_2$CH−), 21.1 (−*C*$H_2CH_2C_6F_{13}$), 27.9 (−CH_2*C*$H_2C_6F_{13}$), 30.0 ((CH$_3$)$_2$*C*H−), 34.0 (Ph*C*H_2−), 34.6 (CH*C*H_2CON−), 46.7 ((*i*Pr)*C*H−), 58.3 (Bn*C*H−), 60.5 (−O*C*H_2CH_3), 78.0 (−*C*H$CH_2CH_2C_6F_{13}$), 127.2, 128.8, 129.0, 136.0 (−*C*$_6$H$_5$), 152.6 (−N*C*OO−), 171.7 (−CHCH_2*C*ON), 174.6 (EtO*C*O−); ^{19}F (282 MHz, $CDCl_3$) δ −81.27, −114.92, −122.37, −123.33, −123.93, −126.60; Anal. Calc for formula: $C_{27}H_{28}F_{13}NO_5$; C, 46.76; H, 4.07; N, 2.02. Found: C, 47.14; H, 3.80; H, 1.74.

(4*S*,5*R*)-4-Benzyl-3-(butanoyl)-5-(1'*H*,1'*H*,2'*H*,2'*H*-perfluorooctyl)-2-oxazolidinone (293a):

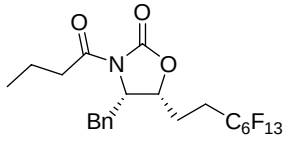

R_f = 0.49 (4:1−hexanes/ethyl acetate); ^1H NMR (300 MHz, $CDCl_3$) δ 7.35 – 7.24 (m, 5H, −C_6*H*$_5$), 4.87 (ddd, 1H, $^3J_1$ = 9.3 Hz, $^3J_2$ = 6.7 Hz, $^3J_3$ = 3.8 Hz, BnC*H*N−), 4.52 (ddd, 1H, $^3J_1$ = 10.2 Hz, $^3J_2$ = 6.9 Hz, $^3J_3$ = 3.3 Hz, −C*H*$CH_2CH_2C_6F_{13}$), 3.12 (dd, 1H, $^3J_1$ = 14.3 Hz, $^3J_2$ = 3.5 Hz, PhC*H*H−), 2.98 – 2.78 (m, 3H, PhC*H*H−, −CH_2CO−), 2.42 – 2.22 (m, 1H, −CH_2C*H*HC_6F_{13}), 2.20 – 2.09 (m, 1H, −C*H*H$CH_2C_6F_{13}$), 2.07 – 1.92 (m, 1H, −CH_2CH*H*C_6F_{13}), 1.82 – 1.72 (m, 1H, −CH*H*$CH_2C_6F_{13}$) 1.67 (tq, 2H, $^3J_1$ = 7.5 Hz, $^3J_2$ = 7.0 Hz, CH_3C*H*$_2CH_2$CO−), 0.97 (t, 3H, ^3J = 7.4 Hz, C*H*$_3CH_2CH_2$CO−); ^{13}C NMR (75 MHz, $CDCl_3$) δ 13.6 (*C*$H_3CH_2CH_2$CO−), 17.2 (CH_3*C*H_2CH_2CO−), 21.1 (−*C*$H_2CH_2C_6F_{13}$), 27.9 (−CH_2*C*$H_2C_6F_{13}$), 34.1 (Ph*C*H_2−), 34.4 (−*C*H_2CON−), 58.2

(Bn*C*H−), 77.7 (−*C*HCH$_2$CH$_2$C$_6$F$_{13}$), 127.3, 128.9, 129.0, 136.1 (−*C*$_6$H$_5$), 152.4 (−N*C*OO−), 164.8 (−CH$_2$CH$_2$*C*ON); ^{19}F (282 MHz, CDCl$_3$) δ −81.19, −114.91, −122.34, −123.31, −123.92, −126.58; Anal. Calc for formula: $C_{22}H_{20}F_{13}NO_3$; C, 44.53; H, 3.40; N, 2.36. Found: C, 44.86; H, 3.10; H, 2.08.

(3'*R*,4*S*,5*R*)-4-Methyl-3-(4'-methyl-3'-phenyl-pentanoyl)-5-phenyl-2-oxazolidinone (303a):

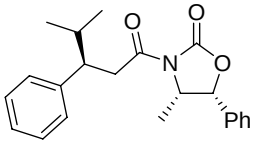

R_f = 0.41 (9:1−hexanes/ethyl acetate); ^{1}H NMR (300 MHz, CDCl$_3$) δ 7.41 – 7.15 (m, 10H, 2 × −C$_6$*H*$_5$), 5.54 (d, 1H, ^{3}J = 7.4 Hz, PhC*H*CH−), 4.59 (dq, 1H, ^{3}J$_1$ = 7.2 Hz, ^{3}J$_2$ = 6.3 Hz, CH$_3$C*H*(N)CH−), 3.68 (dd, 1H, ^{3}J$_1$ = 15.6 Hz, ^{3}J$_2$ = 10.2 Hz, −C*H*HCON−), 3.25 (dd, 1H, ^{3}J$_1$ = 15.8 Hz, ^{3}J$_2$ = 4.7 Hz, −CH*H*CON−), 2.98 (ddd, 1H, ^{3}J$_1$ = 10.2 Hz, ^{3}J$_2$ = 6.6 Hz, ^{3}J$_3$ = 4.7 Hz, PhC*H*(*i*Pr)−), 1.93 (qqd, 1H, ^{3}J$_1$ = 6.8 Hz, ^{3}J$_2$ = 6.8 Hz, ^{3}J$_3$ = 6.6 Hz, (CH$_3$)$_2$C*H*−), 1.03 (d, 3H, ^{3}J = 6.1 Hz, (C*H*$_3$)$_2$CH−), 1.00 (d, 3H, ^{3}J = 6.1 Hz, (C*H*$_3$)$_2$CH−), 0.77 (d, 3H, ^{3}J = 6.5 Hz, C*H*$_3$CH(N)−); ^{13}C NMR (75 MHz, CDCl$_3$) δ 14.4 (*C*H$_3$CH(N)−), 20.7 ((*C*H$_3$)$_2$CH−), 20.8 ((*C*H$_3$)$_2$CH−), 33.4 ((CH$_3$)$_2$*C*H−), 39.3 (−CH*C*H$_2$CO−), 49.2 (PhCH(*i*Pr)−), 54.8 (CH$_3$*C*H(N)−), 78.9 (Ph*C*H−), 125.7, 126.4, 128.1, 128.5, 128.7, 128.7, 133.3, 143.0 (2 × −*C*$_6$H$_5$), 153.1 (−N*C*OO−), 172.5 (−CH$_2$*C*ON); Anal. Calc for formula: $C_{22}H_{25}NO_3$; C, 75.19; H, 7.17; N, 3.99. Found: C, 75.40; H, 7.02; H, 4.22.

(3'*R*,4*S*,5*R*)-4-Methyl-3-(3'-ethoxycarbonyl-4'-methyl-pentanoyl)-5-phenyl-2-oxazolidinone (303b):

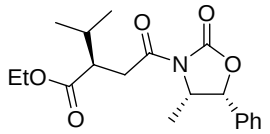

R_f = 0.41 (9:1−hexanes/ethyl acetate); ^{1}H NMR (300 MHz, $CDCl_3$) δ 7.45 – 7.26 (m, 5H, −C$_6$*H*$_5$), 5.69 (d, 1H, ^{3}J = 6.9 Hz, PhC*H*CH−), 4.74 (dq, 1H, $^3J_1$ = 7.2 Hz, $^3J_2$ = 6.8 Hz, CH_3C*H*(N)CH−), 4.21 (dq, 1H, $^3J_1$ = 10.8 Hz, $^3J_2$ = 7.3 Hz, −OC*H*$_2$CH$_3$), 4.13 (dq, 1H, $^3J_1$ = 10.8 Hz, $^3J_2$ = 7.3 Hz, −OC*H*$_2$CH$_3$), 3.47 (dd, 1H, $^3J_1$ = 19.2 Hz, $^3J_2$ = 11.9 Hz, −C*H*HCON−), 3.04 (dd, 1H, $^3J_1$ = 19.2 Hz, $^3J_2$ = 3.4 Hz, −CH*H*CON−), 2.80 (ddd, 1H, $^3J_1$ = 11.9 Hz, $^3J_2$ = 6.6 Hz, $^3J_3$ = 3.3 Hz, EtOCOC*H*(*i*Pr)−), 2.05 (qqd, 1H, $^3J_1$ = 6.7 Hz, $^3J_2$ = 6.7 Hz, $^3J_3$ = 6.6 Hz, $(CH_3)_2$C*H*−), 1.28 (t, 3H, ^{3}J = 7.4 Hz, −OCH$_2$C*H*$_3$), 0.99 (d, 6H, ^{3}J = 7.0 Hz, (C*H*$_3$)$_2$CH−), 0.88 (d, 3H, ^{3}J = 6.5 Hz, C*H*$_3$CH(N)−); ^{13}C NMR (75 MHz, $CDCl_3$) δ 14.3 (*C*H$_3$CH(N)−), 14.5 (−O*C*H$_2$CH$_3$), 19.8 ((*C*H$_3$)$_2$CH−), 20.3 ((*C*H$_3$)$_2$CH−), 30.1 ((CH$_3$)$_2$*C*H−), 35.0 (−CH*C*H$_2$CO−), 47.0 (EtOCO*C*H(*i*Pr)−), 54.9 (CH$_3$*C*H(N)−), 60.4 (CH$_3$*C*H$_2$O−), 79.1 (Ph*C*H−), 125.6, 128.7, 128.8, 133.3 (−*C*$_6$H$_5$), 153.1 (−N*C*OO−), 172.0 (−CH$_2$*C*ON), 174.7 (EtO*C*O−); Anal. Calc for formula: $C_{22}H_{25}NO_3$; C, 75.19; H, 7.17; N, 3.99. Found: C, 65.95; H, 7.02; H, 3.71.

General Procedure for LiOOH Hydrolysis of Radical Products; (*R*)-3,4-dimethylpentanoic acid (229a):

To a flask containing (3'*R*,4*S*,5*R*)-4-benzyl-3-(3',4'-dimethyl-pentanoyl)-5-(1'*H*,1'*H*,2'*H*,2'*H*-perfluorooctyl)-2-oxazolidinone (0.162 g, 0.255 mmol), THF (1 mL)

and H_2O (1 mL) was added H_2O_2 (30%) (0.104 mL, 1.022 mmol) at 0 °C. $LiOH{\cdot}H_2O$ (0.021 g, 0.511 mmol) was then added as a solid and the mixture was stirred at 0 °C for 3 h. After completion, the reaction was acidified to ~pH 1 and all volatile material was removed under vacuum. The crude products were adsorbed onto fluorous-modified silica gel (2 × crude weight) and applied to an FPSE cartridge charged with 5.5 g of dry Fluroflash™. The solid phase was washed with 70% methanol in water (200 mL) yielding (*R*)-3,4-dimethylpentanoic acid **299a** (.028 g, 0.215 mmol, 84 % yield) as a white solid. Washing the column with methanol (250 mL) allowed oxazolidinone **245** to be recovered (0.118 g, 0.225 mmol, 88 % yield).

(*R*)-3,4-Dimethylpentanoic acid (299a):

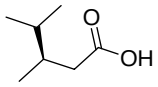

$[\alpha]^{25}_D$ +17.6 (*c* 1.4, benzene), lit $[\alpha]^{25}_D$ –10.7 (*c* 0.55, benzene) (for *(S)*-3,4-dimethylpentanoic acid).[174]

(3R)-3-Methyl-4-phenylpentanoic acid (299b):

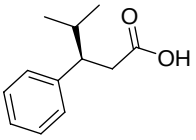

$[\alpha]^{25}_D$ +18.2 (*c* 1.2, $CHCl_3$), lit. $[\alpha]^{25}_D$ +16.1 (*c* 1.17, $CHCl_3$).[276]

(*R*)-2-*iso*-Propylfumaric acid (299c):

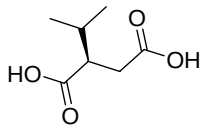

$[\alpha]^{25}_{D}$ +17.1 (*c* 1.0, $CHCl_3$), lit. $[\alpha]^{25}_{D}$ +18.0 (*c* 1.2, $CHCl_3$).[255]

Procedure for the Measurement of Tin Following Various Purification Protocols:

Each sample was weighed into a 10 dram vial and dissolved in MeOH (1 mL) and conc HNO_3 (3 mL). The vials were then capped and heated to 40°C for 24 h. The samples were then evaporated to dryness under reduced pressure and reconstituted with conc HNO_3 (3.5 mL) and divided into equal portions (7 × 0.5 mL samples). Each vial was then diluted with 1.5 mL of distilled water, or one of six standard tin solutions. (standard tin solutions = 200 ppm, 100 ppm, 50 ppm, 25 ppm, 12.5 ppm, 6.25 ppm). Each vial was then measured using an acetylene flame with a standard Sn atomic absorbance lamp at 283.3 nm (slit width = 1mm). The absorbance recorded was plotted against the known concentrations of tin, taking into account the 1 in 4 dilution of each tube. Plotting the best fit line gave the tin content in the unknown sample by extrapolation to the negative *x*-intercept. This allowed the total tin content (mass) to be calculated in the parent sample. The amount of tin was then expressed as a percent by weight given the total mass of the sample prior to digestion in HNO_3.

1,3-Dipolar Cycloadditions Using Diphenylnitrone

General Procedure for 1,3-Dipolar Cycloaddition; (3'*R*,4*S*,4'*S*,5*R*,5'*R*)-4-benzyl-3-((5'-methyl-2',3'-diphenylisoxazolidin-4'-yl)carbonyl)-5-(1'*H*,1'*H*,2'*H*,-2'*H*-perfluorooctyl)-2-oxazolidinone (308):

Magnesium perchlorate (0.219 g, 0.981 mmol) and **2** (0.58 g, 0.981 mmol) were dissolved in CH_2Cl_2 (0.5 mL). The solution was then stirred for 15 min at r.t., after which diphenylnitrone (0.193 g, 0.981 mmol) was added. The reaction was monitored by TLC and was allowed to stir in the dark for 24 h. After this time, the crude products were adsorbed onto FluoroFlash^{TM} fluorous-modified silica gel (~0.5 g) and applied to an FPSE cartridge charged with 5.5 g of dry Fluroflash^{TM}. The solid phase was washed with 70% methanol in water (100 mL), removing organic and inorganic by-products. Washing the solid phase with methanol liberated cycloaddition products **308**, **309**, **310**, and **311**. The diastereoselectivity was assigned by HPLC, and the individual diastereomers were separated by preparative HPLC.

(3'*R*,4*S*,4'*S*,5*R*,5'*R*)-4-Benzyl-3-((5'-methyl-2',3'-diphenylisoxazolidin-4'-yl)carbonyl)-5-(1'*H*,1'*H*,2'*H*,-2'*H*-perfluorooctyl)-2-oxazolidinone (308):

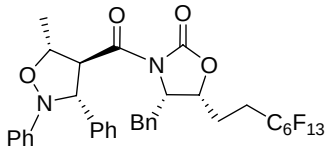

Isolated as a yellow oil; ^{1}H NMR (300MHz, $CDCl_3$) δ 7.48 – 6.91 (m, 15H), 5.12 (d, ^{3}J = 6.7 Hz, 1H), 4.90 – 4.84 (m, 1H), 4.79 (dd, $^{3}J_1$ = 7.3 Hz, $^{3}J_2$ = 7.3 Hz, 1H), 4.52 – 4.43 (m, 2H), 3.07 (dd, $^{3}J_1$ = 14.5 Hz, $^{3}J_1$ = 3.5 Hz, 1H), 2.89 (dd, $^{3}J_1$ = 14.5 Hz, $^{3}J_2$ = 9.5 Hz, 1H), 2.36 – 2.16 (m, 1H), 2.13 – 2.04 (m, 1H), 1.99 – 1.86 (m, 1H), 1.79 – 1.69 (m, 1H), 1.52 (d, ^{3}J = 6.7 Hz, 3H); ^{13}C (75MHz, $CDCl_3$) δ 18.0, 20.9, 27.8, 33.8, 58.7, 62.9, 71.8, 74.6, 79.4, 114.7, 121.8, 126.6, 127.4, 127.9, 128.6, 128.8, 128.9, 129.0, 135.5, 140.6, 151.4, 151.8, 170.3; ^{19}F (282 MHz, $CDCl_3$) δ −81.18, −114.86, −122.35, −123.30, −123.92, −126.55; $[\alpha]_D$ = +99.1 (*c* 0.8, Et_2O); Anal. Calc. for formula $C_{35}H_{29}F_{13}N_2O_4$; C, 53.31; H, 3.71; N, 3.55; Found, C: 52.93; H, 3.44; N, 3.74.

(3'*S*,4*S*,4'*R*,5*R*,5'*S*)-4-Benzyl-3-((5'-methyl-2',3'-diphenylisoxazolidin-4'-yl)carbonyl)-5-(1'*H*,1'*H*,2'*H*,-2'*H*-perfluorooctyl)-2-oxazolidinone (309):

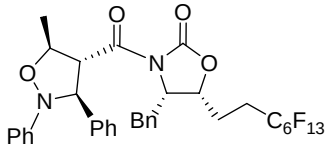

Isolated as a yellow oil; ^{1}H NMR (300MHz, $CDCl_3$) δ 7.46 – 6.91 (m, 15H), 5.09 (d, ^{3}J = 7.2 Hz, 1H), 4.93 – 4.85 (m, 1H), 4.68 (dd, $^{3}J_1$ = 7.5 Hz, $^{3}J_2$ = 7.4 Hz, 1H), 4.49 – 4.41 (m, 1H), 4.31 (dq, $^{3}J_1$ = 7.4 Hz, $^{3}J_2$ = 6.3 Hz, 1H), 3.02 (dd, $^{3}J_1$ = 14.4 Hz, $^{3}J_1$ = 4.6 Hz, 1H), 2.94 (dd, $^{3}J_1$ = 14.4 Hz, $^{3}J_2$ = 8.6 Hz, 1H), 2.37 – 2.23 (m, 1H), 2.22 – 2.05 (m, 2H), 2.00 – 1.88 (m, 1H), 1.53 (d, ^{3}J = 6.3 Hz, 3H); ^{13}C (75MHz, $CDCl_3$) δ 18.2, 21.3, 27.7, 33.0, 58.9, 63.1, 72.1, 74.3, 79.1, 114.7, 121.7, 126.5, 127.3, 128.0, 128.6, 128.8, 128.9, 129.0, 135.5, 140.6, 151.4, 152.1, 170.1; ^{19}F (282 MHz, $CDCl_3$) δ −81.20, −114.89, −122.34, −123.29, −123.90, −126.55; $[\alpha]_D$ = +32.8 (*c* 0.5, Et_2O); Anal. Calc. for formula $C_{35}H_{29}F_{13}N_2O_4$; C, 53.31; H, 3.71; N, 3.55; Found: C, 53.68; H, 3.98; N, 3.12.

(3'*S*,4*S*,4'*S*,5*R*,5'*R*)-4-Benzyl-3-((5'-methyl-2',3'-diphenylisoxazolidin-4'-yl)carbonyl)-5-(1'*H*,1'*H*,2'*H*,-2'*H*-perfluorooctyl)-2-oxazolidinone (310):

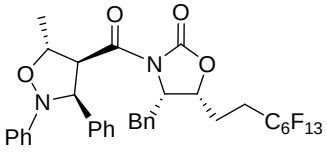

Isolated as a yellow oil; ^{1}H NMR (300MHz, $CDCl_3$) δ 7.58 – 6.90 (m, 15H), 5.12 (dq, $^{3}J_1$ = 9.7 Hz, $^{3}J_2$ = 6.0 Hz, 1H), 5.10 (d, ^{3}J = 10.9 Hz, 1H), 4.60 – 4.53 (m, 1H), 4.43 – 4.37 (m, 1H), 4.25 (dd, $^{3}J_1$ = 10.7 Hz, $^{3}J_2$ = 9.7 Hz, 1H), 2.88 (dd, $^{3}J_1$ = 13.9 Hz, $^{3}J_1$ = 5.2 Hz, 1H), 2.78 (dd, $^{3}J_1$ = 13.9 Hz, $^{3}J_2$ = 8.4 Hz), 2.29 – 2.09 (m, 1H), 1.94 – 1.71 (m, 4H), 1.61 – 1.52 (m, 1H), 1.48 (d, ^{3}J = 6.0 Hz, 3H); ^{13}C (75MHz, $CDCl_3$) δ 17.1, 20.7, 27.7, 32.0, 58.2, 60.3, 71.9, 74.8, 77.7, 115.9, 122.3, 127.0, 128.4, 128.5, 128.6, 128.8, 128.9, 136.3, 138.6, 149.8, 151.9, 168.7; ^{19}F (282 MHz, $CDCl_3$) δ −81.19, −114.97,

−122.36, −123.30, −123.94, −126.54; $[\alpha]_D$ = +88.5 (*c* 0.5, Et_2O); Anal. Calc. for formula $C_{35}H_{29}F_{13}N_2O_4$; C, 53.31; H, 3.71; N, 3.55; Found: C, 53.64; H, 3.60; N, 3.38.

(3'*R*,4*S*,4'*R*,5*R*,5'*S*)-4-Benzyl-3-((5'-methyl-2',3'-diphenylisoxazolidin-4'-yl)carbonyl)-5-(1'*H*,1'*H*,2'*H*,-2'*H*-perfluorooctyl)-2-oxazolidinone (311):

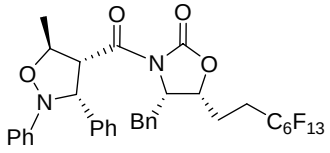

Isolated as a yellow oil; ^{1}H NMR (300MHz, $CDCl_3$) δ 7.39 – 7.17 (m, 15H), 5.01 (dq, $^3J_1$ = 9.3 Hz, $^3J_2$ = 6.1 Hz, 1H), 4.81 (d, ^3J = 10.7 Hz, 1H), 4.35 (dd, $^3J_1$ = 10.7 Hz, $^3J_2$ = 9.3 Hz, 1H), 4.08 – 4.02 (m, 1H), 3.51 – 3.43 (m, 1H), 2.88 (dd, $^3J_1$ = 13.9 Hz, $^3J_1$ = 5.2 Hz, 1H), 2.78 (dd, $^3J_1$ = 13.9 Hz, $^3J_2$ = 8.4 Hz, 1H), 2.29 – 2.09 (m, 1H), 2.04 – 1.81 (m, 2H), 1.64 – 1.55 (m, 1H), 1.39 (d, ^3J = 6.1 Hz, 3H); ^{13}C (75MHz, $CDCl_3$) δ 17.8, 21.2, 26.8, 34.8, 58.3, 60.3, 71.8, 74.6, 78.6, 116.6, 122.8, 127.2, 128.4, 128.5, 128.6, 128.8, 129.1, 135.7, 138.5, 149.6, 152.1, 168.5; ^{19}F (282 MHz, $CDCl_3$) δ −81.17, −114.79, −122.32, −123.27, −123.86, −126.53; $[\alpha]_D$ = +27.4 (*c* 0.32, Et_2O); Anal. Calc. for formula $C_{35}H_{29}F_{13}N_2O_4$; C, 53.31; H, 3.71; N, 3.55; Found: C, 53.54; H, 3.56; N, 3.41.

(3*R*,4*S*,5*R*)-4-Isoxazolidinecarboxylic acid, 5-methyl-2,3-diphenyl-, isopropyl ester (314)

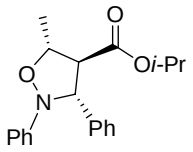

Following the procedure described in the literature,[201] Ti(*i*PrO)$_4$ (0.074 ml, 0.254 mmol) and *i*PrOH (0.039 ml, 0.507 mmol) were added to a solution of **308** (0.02 g, 0.025 mmol) in toluene (2 mL). The reaction then heated to reflux and left to stir for 5 h, after which the reaction was cooled and the reaction was evaporated to dryness. The crude mixture was adsorbed onto Fluoroflash^{TM} fluorous-modified silica gel (~0.1 g) and applied to an FPSE cartridge charged with 5.5 g of dry Fluroflash^{TM}. The solid phase was washed with 70% methanol in water (150 mL), allowing **314** (0.0076 g, 0.023 mmol, 92 % yield) to be isolated as a colorless oil. Washing the solid phase with methanol gave oxazolidinone **245** (0.011 g, 0.021 mmol, 83 % yield) as a crystalline solid. ^{1}H NMR values for **314** matched those reported in the literature. Absolute configuration was determined by chemical correlation to literature results; $[\alpha]_D$ = +43.7 (*c* 0.65, $CHCl_3$); lit.[201] $[\alpha]_D$ = +35.

Reductive Cleavage Applied in Recyclability Study

Sodium borohydride (0.179 ml, 5.07 mmol) was dissolved in water (2 mL) and added to a solution of cycloadditions products **308**, **309**, **310**, and **311** (1 g, 1.268 mmol) in THF (20 mL). The reaction was left to stir at r.t. for 5 h, after which the reaction was quenched with 1M HCl (5 mL) and evaporated to dryness. The crude mixture was

adsorbed onto Fluoroflash™ fluorous-modified silica gel (~0.5 g) and applied to an FPSE cartridge charged with 5.5 g of dry Fluroflash™. The solid phase was washed with 70% methanol in water (250 mL), to give alcohols **320** and **321** (0.2 g, 0.743 mmol, 58.6 % yield). Washing the solid phase with methanol gave oxazolidinone **245** (0.59 g, 1.127 mmol, 89 % yield) as a crystalline solid.

(3*S*,4*S*,5*R*)-5-Methyl-2,3-diphenyl-isoxazolidine-4-methanol (320):

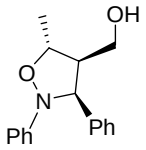

Obtained as a mixture of stereoisomers, ^{1}H and ^{13}C NMR values matched those reported in the literature;[95] $[\alpha]_D = +17.1$ (*c* 0.79, $CHCl_3$).

(3*R*,4*R*,5*S*)-5-Methyl-2,3-diphenyl-isoxazolidine-4-methanol (321):

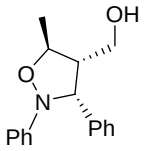

Obtained as a mixture of stereoisomers, ^{1}H and ^{13}C NMR values matched those reported in the literature;[95] $[\alpha]_D = -9.6$ (*c* 0.56, $CHCl_3$).

2-((5'-Methyl-2',3'-diphenylisoxazolidin-4'-yl)carbonylamino)-6,6,7,7,8,8,9,9,10,10,11,11,11-trideafluoro-1-phenyl-undecan-3-ol (340):

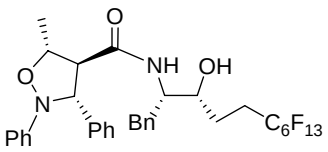

^{1}H NMR (300MHz, $CDCl_3$) 7.54 – 6.89 (m, 15H), 5.90 (d, ^3J = 7.3 Hz, 1H), 4.90 (d, ^3J = 8.7 Hz), 4.15 (dq, $^3J_1$ = 8.7 Hz, $^3J_2$ = 6.7 Hz, 1H), 3.93 – 3.87 (m, 1H), 3.34 (dd, $^3J_1$ = 8.7 Hz, $^3J_2$ = 4.1 Hz, 1H), 3.15 – 3.09 (m, 1H), 2.81 (dd, $^3J_1$ = 14.1 Hz, $^3J_2$ = 4.8 Hz, 1H), 2.53 (dd, $^3J_1$ = 14.1 Hz, $^3J_2$ = 11.1 Hz, 1H), 2.34 (d, ^3J = 6.5 Hz, 1H), 3.32 – 2.14 (m, 1H), 2.01 – 1.79 (m, 1H), 1.41 – 1.23 (m, 2H), 1.11 (d, ^3J = 6.5 Hz, 3H).

APPENDICES

X-Ray Structure Report for Oxazolidinone 245

University of Alberta Department of Chemistry

X-Ray Crystallography Laboratory

STRUCTURE REPORT

XCL Code: MAN0301

Date: 6 May 2003

Compound: 4-Benzyl-5-(3,3,4,4,5,5,6,6,7,7,8,8,8-tridecafluorooctyl)-1,3-oxazolidin-2-one

Formula: $C_{18}H_{14}F_{13}NO_2$

Supervisor: P. Hultin, University of Manitoba

Crystallographer: R. McDonald

Figure Legends

Figure 1. Perspective view of the 4-benzyl-5-(3,3,4,4,5,5,6,6,7,7,8,8,8-tridecafluorooctyl)-1,3-oxazolidin-2-one molecule showing the atom labelling scheme. Non-hydrogen atoms are represented by Gaussian ellipsoids at the 20% probability level. Hydrogen atoms are shown with arbitrarily small thermal parameters.

Figure 2. Illustration of hydrogen-bonded interactions between adjacent molecules. Primed atoms are related to unprimed ones via the crystallographic inversion centre (0, 0, 0).

Figure 3. Illustration of crystal packing. View direction is parallel to the *a* axis of the crystal unit cell.

Figure 4. Illustration of crystal packing. View direction is parallel to the *b* axis of the crystal unit cell.

Figure 5. Illustration of crystal packing. View direction is parallel to the *c* axis of the crystal unit cell.

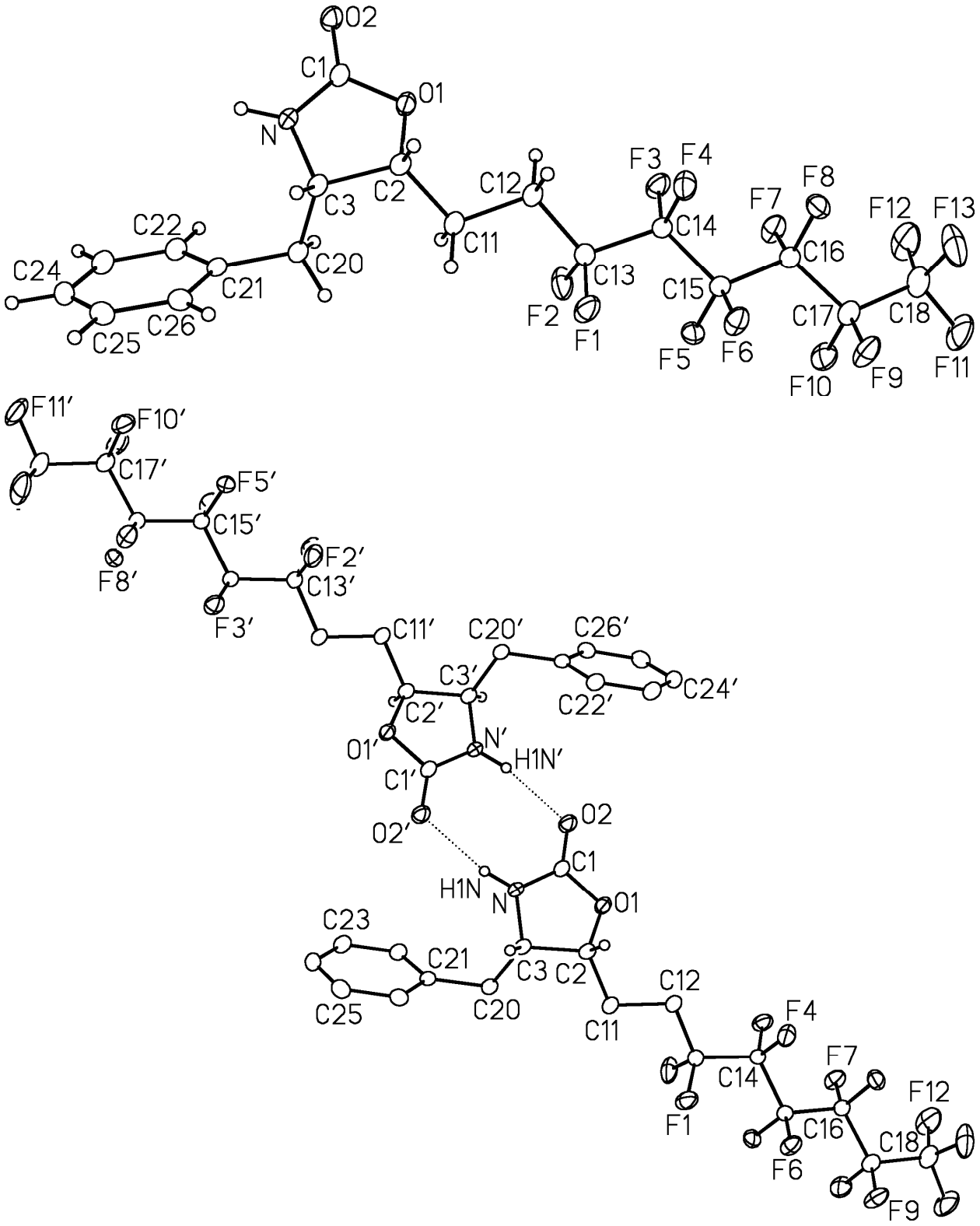
O2
C1
O1
N
C3
C2
C12
F3
F4
F8
F7
F12
F13
C22
C24
C21
C20
C11
C14
C16
C13
C15
C17
C18
C25
C26
F2
F1
F5
F6
F10
F9
F11
F11′
F10′
C17′
F5′
C15′
F8′
F2′
C13′
F3′
C11′
C20′
C26′
C3′
C24′
C2′
C22′
O1′
N′
H1N′
C1′
O2
O2′
C1
H1N
N
O1
C23
C21
C3
C2
C12
C25
C20
C11
F4
F7
C14
F12
F1
C16
C18
F6
F9

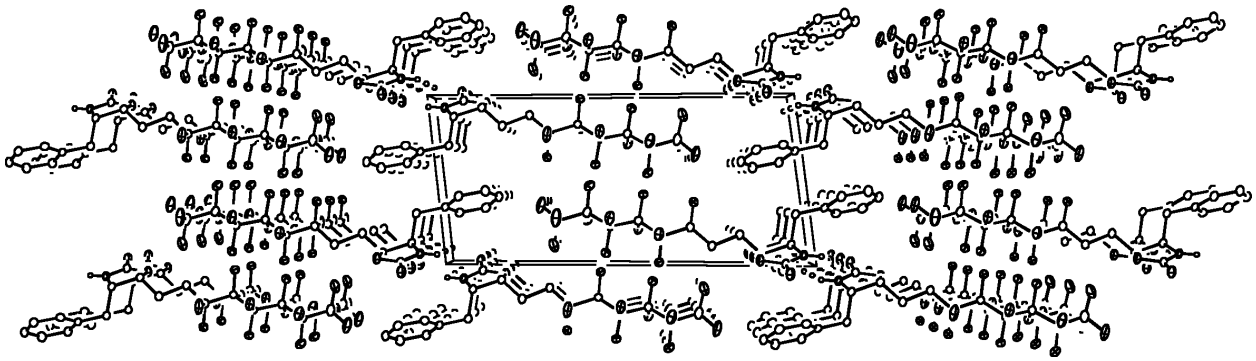

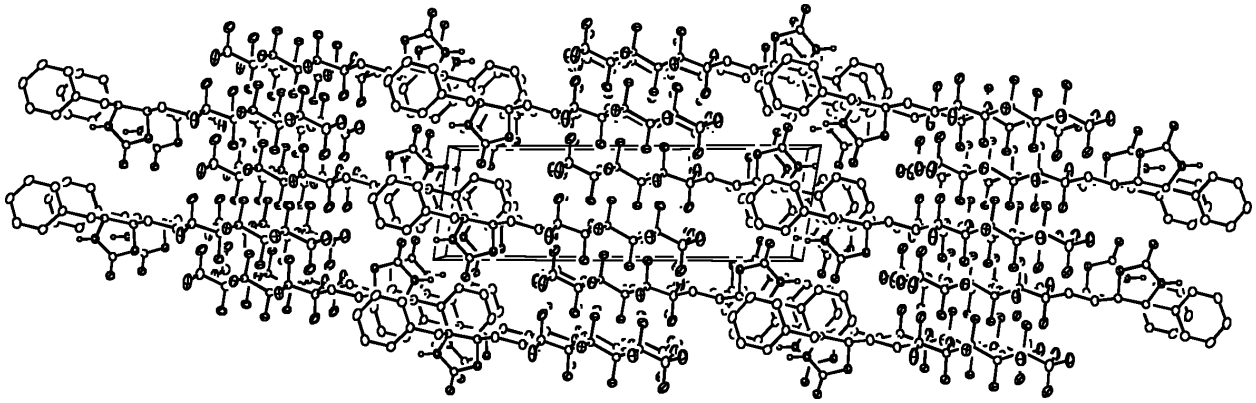

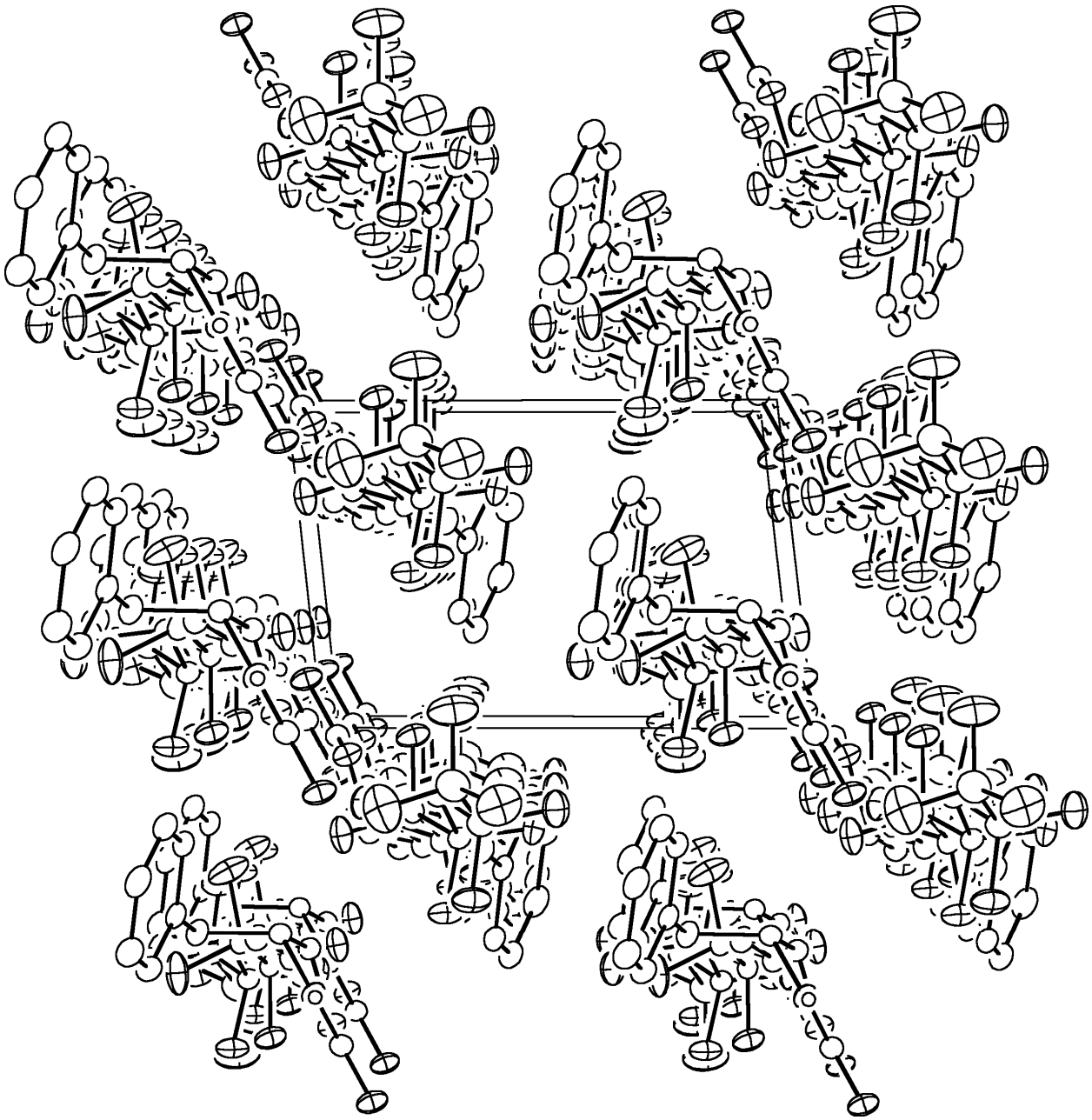

List of Tables

Table 1. Crystallographic Experimental Details

Table 2. Atomic Coordinates and Equivalent Isotropic Displacement Parameters

Table 3. Selected Interatomic Distances

Table 4. Selected Interatomic Angles

Table 5. Torsional Angles

Table 6. Anisotropic Displacement Parameters

Table 7. Derived Atomic Coordinates and Displacement Parameters for Hydrogen Atoms

Table 1. Crystallographic Experimental Details

A. Crystal Data	
formula	$C_{18}H_{14}F_{13}NO_2$
formula weight	523.30
crystal dimensions (mm)	0.88 × 0.43 × 0.09
crystal system	triclinic
space group	$P\bar{1}$ (No. 2)
unit cell parameters[a]	
a (Å)	6.0687 (4)
b (Å)	9.0312 (6)
c (Å)	19.3560 (12)
α (deg)	82.0899 (10)
β (deg)	80.8538 (10)
γ (deg)	82.6018 (10)
V (Å^3)	1031.19 (12)
Z	2
ρ_{calcd} (g cm^{-3})	1.685
μ (mm^{-1})	0.188
B. Data Collection and Refinement Conditions	
diffractometer	Bruker PLATFORM/SMART 1000 CCD[b]
radiation (λ [Å])	graphite-monochromated Mo Kα (0.71073)
temperature (°C)	–80
scan type	ω scans (0.3°) (20 s exposures)
data collection 2θ limit (deg)	52.80
total data collected	8248 ($-7 \le h \le 7$, $-11 \le k \le 11$, $-24 \le l \le 24$)
independent reflections	4220 (R_{int} = 0.0148)
number of observed reflections (*NO*)	3439 [$F_o^2 \ge 2\sigma(F_o^2)$]
structure solution method	direct methods (*SHELXS–86*[c])
refinement method	full-matrix least-squares on F^2 (*SHELXL–93*[d])
absorption correction method	multi-scan (*SADABS*)
range of transmission factors	0.9833–0.8520
data/restraints/parameters	4220 [$F_o^2 \ge -3\sigma(F_o^2)$] / 0 / 307
goodness-of-fit (S)[e]	1.043 [$F_o^2 \ge -3\sigma(F_o^2)$]
final R indices[f]	
$R1$ [$F_o^2 \ge 2\sigma(F_o^2)$]	0.0453
$wR2$ [$F_o^2 \ge -3\sigma(F_o^2)$]	0.1293
largest difference peak and hole	0.390 and –0.288 e Å^{-3}

[a]Obtained from least-squares refinement of 6335 reflections with $4.82° < 2\theta < 52.77°$.

(continued)

Table 1. Crystallographic Experimental Details (continued)

[b]Programs for diffractometer operation, data collection, data reduction and absorption correction were those supplied by Bruker.

[c]Sheldrick, G. M. *Acta Crystallogr.* **1990**, *A46*, 467–473.

[d]Sheldrick, G. M. *SHELXL-93*. Program for crystal structure determination. University of Göttingen, Germany, 1993. Refinement on F_o^2 for all reflections (all of these having $F_o^2 \geq -3\sigma(F_o^2)$). Weighted *R*-factors *wR*2 and all goodnesses of fit *S* are based on F_o^2; conventional *R*-factors *R*1 are based on F_o, with F_o set to zero for negative F_o^2. The observed criterion of $F_o^2 > 2\sigma(F_o^2)$ is used only for calculating *R*1, and is not relevant to the choice of reflections for refinement. *R*-factors based on F_o^2 are statistically about twice as large as those based on F_o, and *R*-factors based on ALL data will be even larger.

[e]$S = [\Sigma w(F_o^2 - F_c^2)^2/(n-p)]^{1/2}$ (n = number of data; p = number of parameters varied; $w = [\sigma^2(F_o^2) + (0.0589P)^2 + 0.4509P]^{-1}$ where $P = [\mathrm{Max}(F_o^2, 0) + 2F_c^2]/3$).

[f]$R1 = \Sigma||F_o| - |F_c||/\Sigma|F_o|$; $wR2 = [\Sigma w(F_o^2 - F_c^2)^2/\Sigma w(F_o^4)]^{1/2}$.

Table 2. Atomic Coordinates and Equivalent Isotropic Displacement Parameters

Atom	*x*	*y*	*z*	U_{eq}, Å^2
F1	0.5390(2)	0.2401(2)	0.32258(7)	0.0820(5)*
F2	0.2176(3)	0.36938(14)	0.31271(7)	0.0798(5)*
F3	0.00731(19)	0.19417(16)	0.41387(6)	0.0573(3)*
F4	0.3002(3)	0.03254(12)	0.42136(6)	0.0604(4)*
F5	0.2791(2)	0.41246(12)	0.44142(6)	0.0531(3)*
F6	0.52567(18)	0.22208(16)	0.46434(6)	0.0558(3)*
F7	-0.03916(18)	0.28358(16)	0.53631(6)	0.0582(3)*
F8	0.1982(2)	0.08604(13)	0.55715(6)	0.0561(3)*
F9	0.4770(2)	0.27750(18)	0.59471(7)	0.0693(4)*
F10	0.2136(3)	0.46059(15)	0.57975(7)	0.0695(4)*
F11	0.1960(3)	0.3524(2)	0.71305(8)	0.1017(6)*
F12	-0.0757(3)	0.2828(3)	0.67483(8)	0.1048(7)*
F13	0.2080(4)	0.1264(2)	0.69180(8)	0.1090(7)*
O1	0.0757(2)	0.05164(16)	0.16246(6)	0.0460(3)*
O2	-0.1506(2)	-0.01712(18)	0.09427(7)	0.0525(4)*
N	0.1814(3)	0.07747(17)	0.04788(8)	0.0399(4)*
C1	0.0209(3)	0.0337(2)	0.09943(9)	0.0382(4)*
C2	0.3107(3)	0.0804(2)	0.15251(9)	0.0381(4)*
C3	0.3643(3)	0.1334(2)	0.07304(9)	0.0367(4)*
C11	0.3403(4)	0.1879(2)	0.20245(10)	0.0462(5)*
C12	0.2725(3)	0.1255(2)	0.27917(9)	0.0437(4)*
C13	0.3179(3)	0.2287(2)	0.32891(10)	0.0444(4)*

C14	0.2327(3)	0.17892(19)	0.40674(9)	0.0362(4)*
C15	0.3065(3)	0.2646(2)	0.46209(9)	0.0369(4)*
C16	0.1786(3)	0.2343(2)	0.53737(9)	0.0382(4)*
C17	0.2562(3)	0.3119(2)	0.59449(10)	0.0468(5)*
C18	0.1426(5)	0.2673(3)	0.66992(12)	0.0652(6)*
C20	0.3692(4)	0.3019(2)	0.05143(9)	0.0439(4)*
C21	0.4283(3)	0.3375(2)	-0.02731(9)	0.0392(4)*
C22	0.2679(3)	0.4006(2)	-0.06950(10)	0.0469(5)*
C23	0.3245(4)	0.4308(3)	-0.14174(11)	0.0554(5)*
C24	0.5418(4)	0.3966(2)	-0.17322(11)	0.0559(6)*
C25	0.7034(4)	0.3331(2)	-0.13221(11)	0.0524(5)*
C26	0.6472(3)	0.3044(2)	-0.05992(10)	0.0455(4)*

Anisotropically-refined atoms are marked with an asterisk (*). The form of the anisotropic displacement parameter is: $\exp[-2\pi^2(h^2a^{*2}U_{11} + k^2b^{*2}U_{22} + l^2c^{*2}U_{33} + 2klb^*c^*U_{23} + 2hla^*c^*U_{13} + 2hka^*b^*U_{12})]$.

Table 3. Selected Interatomic Distances (Å)

Atom1	Atom2	Distance	Atom1	Atom2	Distance
F1	C13	1.344(2)	C2	C3	1.542(2)
F2	C13	1.355(2)	C2	C11	1.506(2)
F3	C14	1.344(2)	C3	C20	1.525(3)
F4	C14	1.338(2)	C11	C12	1.526(3)
F5	C15	1.337(2)	C12	C13	1.506(2)
F6	C15	1.342(2)	C13	C14	1.538(3)
F7	C16	1.342(2)	C14	C15	1.555(2)
F8	C16	1.336(2)	C15	C16	1.545(3)
F9	C17	1.336(2)	C16	C17	1.549(3)
F10	C17	1.334(2)	C17	C18	1.536(3)
F11	C18	1.311(3)	C20	C21	1.509(2)
F12	C18	1.304(3)	C21	C22	1.386(3)
F13	C18	1.316(3)	C21	C26	1.391(3)
O1	C1	1.350(2)	C22	C23	1.384(3)
O1	C2	1.460(2)	C23	C24	1.377(3)
O2	C1	1.213(2)	C24	C25	1.378(3)
N	C1	1.335(2)	C25	C26	1.383(3)
N	C3	1.452(2)			

Table 4. Selected Interatomic Angles (deg)

Atom1	Atom2	Atom3	Angle	Atom1	Atom2	Atom3	Angle
C1	O1	C2	108.57(13)	F6	C15	C16	108.22(14)
C1	N	C3	113.44(14)	C14	C15	C16	114.47(15)
O1	C1	O2	122.08(16)	F7	C16	F8	108.88(15)
O1	C1	N	109.85(15)	F7	C16	C15	108.65(15)
O2	C1	N	128.07(16)	F7	C16	C17	106.59(15)
O1	C2	C3	104.30(13)	F8	C16	C15	108.62(14)
O1	C2	C11	109.35(15)	F8	C16	C17	108.20(15)
C3	C2	C11	116.83(15)	C15	C16	C17	115.72(16)
N	C3	C2	99.74(14)	F9	C17	F10	108.66(17)
N	C3	C20	111.70(15)	F9	C17	C16	110.02(15)
C2	C3	C20	117.02(14)	F9	C17	C18	106.60(17)
C2	C11	C12	111.80(16)	F10	C17	C16	108.98(16)
C11	C12	C13	111.44(16)	F10	C17	C18	107.85(17)
F1	C13	F2	106.47(17)	C16	C17	C18	114.55(18)
F1	C13	C12	110.54(17)	F11	C18	F12	107.4(2)
F1	C13	C14	108.29(15)	F11	C18	F13	108.1(2)
F2	C13	C12	110.31(16)	F11	C18	C17	110.1(2)
F2	C13	C14	107.19(15)	F12	C18	F13	108.0(2)
C12	C13	C14	113.73(15)	F12	C18	C17	112.2(2)
F3	C14	F4	107.32(15)	F13	C18	C17	110.76(19)
F3	C14	C13	106.99(14)	C3	C20	C21	111.43(14)
F3	C14	C15	108.83(14)	C20	C21	C22	121.67(18)
F4	C14	C13	108.61(15)	C20	C21	C26	120.37(18)
F4	C14	C15	108.11(14)	C22	C21	C26	117.95(17)
C13	C14	C15	116.62(15)	C21	C22	C23	120.9(2)
F5	C15	F6	108.57(14)	C22	C23	C24	120.4(2)
F5	C15	C14	109.32(14)	C23	C24	C25	119.55(19)
F5	C15	C16	108.44(14)	C24	C25	C26	120.0(2)
F6	C15	C14	107.66(14)	C21	C26	C25	121.2(2)

Table 5. Torsional Angles (deg)

Atom1	Atom2	Atom3	Atom4	Angle	Atom1	Atom2	Atom3	Atom4	Angle
C2	O1	C1	O2	166.79(18)	F5	C15	C16	F7	59.28(18)
C2	O1	C1	N	-12.4(2)	F5	C15	C16	F8	177.58(13)
C1	O1	C2	C3	19.78(18)	F5	C15	C16	C17	-60.5(2)
C1	O1	C2	C11	145.46(16)	F6	C15	C16	F7	176.88(13)
C3	N	C1	O1	-1.0(2)	F6	C15	C16	F8	-64.82(18)
C3	N	C1	O2	179.88(19)	F6	C15	C16	C17	57.1(2)
C1	N	C3	C2	12.73(19)	C14	C15	C16	F7	-63.1(2)
C1	N	C3	C20	-111.63(17)	C14	C15	C16	F8	55.2(2)
O1	C2	C3	N	-18.63(16)	C14	C15	C16	C17	177.12(15)
O1	C2	C3	C20	101.94(17)	F7	C16	C17	F9	-175.03(16)
C11	C2	C3	N	-139.44(16)	F7	C16	C17	F10	-56.0(2)
C11	C2	C3	C20	-18.9(2)	F7	C16	C17	C18	64.9(2)
O1	C2	C11	C12	59.4(2)	F8	C16	C17	F9	68.0(2)
C3	C2	C11	C12	177.50(16)	F8	C16	C17	F10	-172.94(15)
N	C3	C20	C21	-67.2(2)	F8	C16	C17	C18	-52.0(2)
C2	C3	C20	C21	178.75(16)	C15	C16	C17	F9	-54.1(2)
C2	C11	C12	C13	175.99(17)	C15	C16	C17	F10	64.9(2)
C11	C12	C13	F1	-63.3(2)	C15	C16	C17	C18	-174.16(17)
C11	C12	C13	F2	54.2(2)	F9	C17	C18	F11	66.3(3)
C11	C12	C13	C14	174.65(16)	F9	C17	C18	F12	-174.1(2)
F1	C13	C14	F3	169.28(15)	F9	C17	C18	F13	-53.2(3)
F1	C13	C14	F4	-75.17(19)	F10	C17	C18	F11	-50.2(3)
F1	C13	C14	C15	47.2(2)	F10	C17	C18	F12	69.4(3)
F2	C13	C14	F3	54.77(19)	F10	C17	C18	F13	-169.8(2)
F2	C13	C14	F4	170.33(15)	C16	C17	C18	F11	-171.74(19)
F2	C13	C14	C15	-67.3(2)	C16	C17	C18	F12	-52.1(3)
C12	C13	C14	F3	-67.4(2)	C16	C17	C18	F13	68.7(3)
C12	C13	C14	F4	48.1(2)	C3	C20	C21	C22	105.4(2)
C12	C13	C14	C15	170.52(16)	C3	C20	C21	C26	-73.3(2)
F3	C14	C15	F5	-75.15(18)	C20	C21	C22	C23	-179.19(17)
F3	C14	C15	F6	167.08(14)	C26	C21	C22	C23	-0.6(3)
F3	C14	C15	C16	46.7(2)	C20	C21	C26	C25	178.55(17)
F4	C14	C15	F5	168.58(14)	C22	C21	C26	C25	-0.1(3)
F4	C14	C15	F6	50.81(19)	C21	C22	C23	C24	0.9(3)
F4	C14	C15	C16	-69.5(2)	C22	C23	C24	C25	-0.6(3)
C13	C14	C15	F5	45.9(2)	C23	C24	C25	C26	-0.1(3)
C13	C14	C15	F6	-71.8(2)	C24	C25	C26	C21	0.4(3)
C13	C14	C15	C16	167.80(15)					

Table 6. Anisotropic Displacement Parameters (*U*ij, Å2)

Atom	*U*11	*U*22	*U*33	*U*23	*U*13	*U*12
F1	0.0662(9)	0.1469(15)	0.0456(7)	-0.0358(8)	0.0105(6)	-0.0567(9)
F2	0.1564(16)	0.0412(7)	0.0399(7)	-0.0012(5)	-0.0149(8)	-0.0071(8)
F3	0.0417(6)	0.0868(9)	0.0501(7)	-0.0192(6)	-0.0077(5)	-0.0190(6)
F4	0.1024(10)	0.0371(6)	0.0433(7)	-0.0067(5)	-0.0200(6)	-0.0001(6)
F5	0.0794(9)	0.0373(6)	0.0450(6)	-0.0055(5)	-0.0064(6)	-0.0177(5)
F6	0.0330(6)	0.0922(9)	0.0455(7)	-0.0212(6)	-0.0046(5)	-0.0066(6)
F7	0.0325(6)	0.0941(10)	0.0503(7)	-0.0229(6)	-0.0030(5)	-0.0044(6)
F8	0.0795(9)	0.0445(6)	0.0442(6)	-0.0021(5)	-0.0022(6)	-0.0178(6)
F9	0.0456(7)	0.1124(12)	0.0590(8)	-0.0334(8)	-0.0159(6)	-0.0073(7)
F10	0.1013(11)	0.0521(8)	0.0615(8)	-0.0209(6)	-0.0171(7)	-0.0099(7)
F11	0.1204(14)	0.1475(17)	0.0498(9)	-0.0459(10)	0.0121(9)	-0.0256(12)
F12	0.0666(10)	0.191(2)	0.0568(9)	-0.0388(11)	0.0156(7)	-0.0200(11)
F13	0.1673(19)	0.1008(14)	0.0450(8)	0.0080(8)	-0.0009(10)	0.0017(13)
O1	0.0442(7)	0.0660(9)	0.0316(6)	-0.0101(6)	-0.0053(5)	-0.0155(6)
O2	0.0405(7)	0.0810(10)	0.0411(7)	-0.0122(7)	-0.0074(6)	-0.0191(7)
N	0.0465(9)	0.0470(9)	0.0309(7)	-0.0088(6)	-0.0084(6)	-0.0146(7)
C1	0.0391(9)	0.0448(10)	0.0325(9)	-0.0084(7)	-0.0082(7)	-0.0037(7)
C2	0.0391(9)	0.0415(9)	0.0359(9)	-0.0080(7)	-0.0083(7)	-0.0062(7)
C3	0.0369(9)	0.0421(9)	0.0334(9)	-0.0117(7)	-0.0062(7)	-0.0039(7)
C11	0.0587(12)	0.0501(11)	0.0334(9)	-0.0079(8)	-0.0094(8)	-0.0133(9)
C12	0.0546(11)	0.0464(10)	0.0336(9)	-0.0070(8)	-0.0100(8)	-0.0109(8)
C13	0.0548(12)	0.0457(10)	0.0348(9)	-0.0059(8)	-0.0047(8)	-0.0144(8)
C14	0.0401(9)	0.0348(9)	0.0350(9)	-0.0042(7)	-0.0074(7)	-0.0068(7)
C15	0.0349(9)	0.0409(9)	0.0366(9)	-0.0076(7)	-0.0043(7)	-0.0079(7)
C16	0.0363(9)	0.0433(10)	0.0360(9)	-0.0073(7)	-0.0040(7)	-0.0064(7)
C17	0.0466(11)	0.0551(12)	0.0413(10)	-0.0145(9)	-0.0084(8)	-0.0040(9)
C18	0.0736(16)	0.0833(18)	0.0392(12)	-0.0168(11)	-0.0056(11)	-0.0037(13)
C20	0.0594(12)	0.0422(10)	0.0341(9)	-0.0107(7)	-0.0048(8)	-0.0161(8)
C21	0.0522(11)	0.0356(9)	0.0336(9)	-0.0100(7)	-0.0036(8)	-0.0161(8)
C22	0.0486(11)	0.0548(12)	0.0405(10)	-0.0126(8)	-0.0036(8)	-0.0140(9)
C23	0.0676(14)	0.0631(13)	0.0414(11)	-0.0069(9)	-0.0154(10)	-0.0189(11)
C24	0.0794(16)	0.0575(12)	0.0338(10)	-0.0105(9)	0.0037(10)	-0.0287(11)
C25	0.0576(12)	0.0492(11)	0.0503(12)	-0.0145(9)	0.0099(10)	-0.0175(9)

C26	0.0518(11)	0.0393(10)	0.0471(11)	-0.0072(8)	-0.0042(9)	-0.0130(8)

The form of the anisotropic displacement parameter is:
$\exp[-2\pi^2(h^2a^{*2}U_{11} + k^2b^{*2}U_{22} + l^2c^{*2}U_{33} + 2klb^*c^*U_{23} + 2hla^*c^*U_{13} + 2hka^*b^*U_{12})]$

Table 7. Derived Atomic Coordinates and Displacement Parameters for Hydrogen Atoms

Atom	*x*	*y*	*z*	*U*eq, Å^2
H1N	0.1768	0.0729	0.0030	0.048
H2	0.4051	-0.0166	.1636	0.046
H3	0.5101	0.0789	0.0536	0.044
H11A	0.2478	0.2845	0.1917	0.055
H11B	0.4994	0.2079	0.1954	0.055
H12A	0.1106	0.1124	0.2872	0.052
H12B	0.3573	0.0256	0.2890	0.052
H20A	0.2202	0.3551	0.0670	0.053
H20B	0.4809	0.3385	0.0752	0.053
H22	0.1170	0.4234	-0.0485	0.056
H23	0.2129	0.4754	-0.1698	0.067
H24	0.5799	0.4167	-0.2229	0.067
H25	0.8535	0.3091	-0.1536	0.063
H26	0.7600	0.2612	-0.0321	0.055

X-ray Crystal Structure Report for Dipolar Cycloaddition Product 310

Prepared for Jason Hein, University of Manitoba
Prepared by Laura Harrington and Jim Britten
McMaster Analytical X-ray (MAX) Diffraction Facility
11 May 2005

The crystal (0.5 x 0.025 x 0.01 mm) was mounted by gluing it to a thin glass fiber attached to a brass pin. The data were collected on a Bruker Smart 6000 CCD 3-circle D8 diffractometer with a Cu RA (Rigaku) X-ray source. Cross-coupled parallel focusing mirrors were used to monochromate the X-ray radiation. The data were collected using 60 s frames for the detector at -40° 2θ and using 120 s frames for the detector at -100° 2θ, and a total of 3000 frames were collected. There was very little diffraction observed at high angle.

The structure was solved by routine direct methods using SHELXTL. The hydrogens were placed in calculated positions based on the framework of the molecule. All relevant crystallographic data and derived bond lengths and angles are included in Tables 1-6.

All pictures are made with 30% thermal ellipsoids.

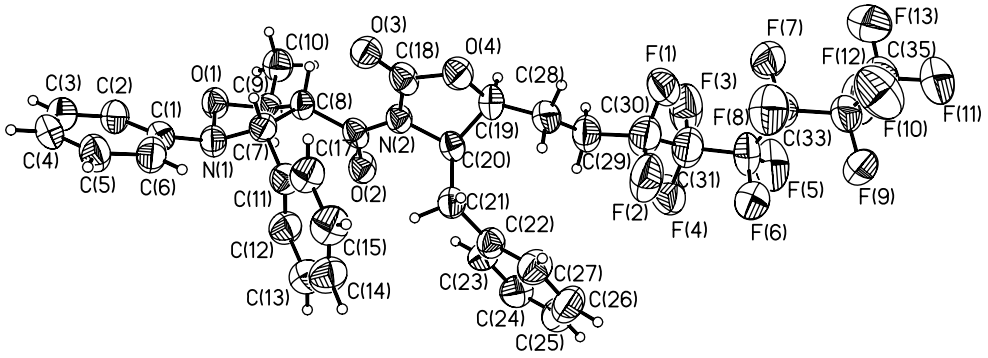

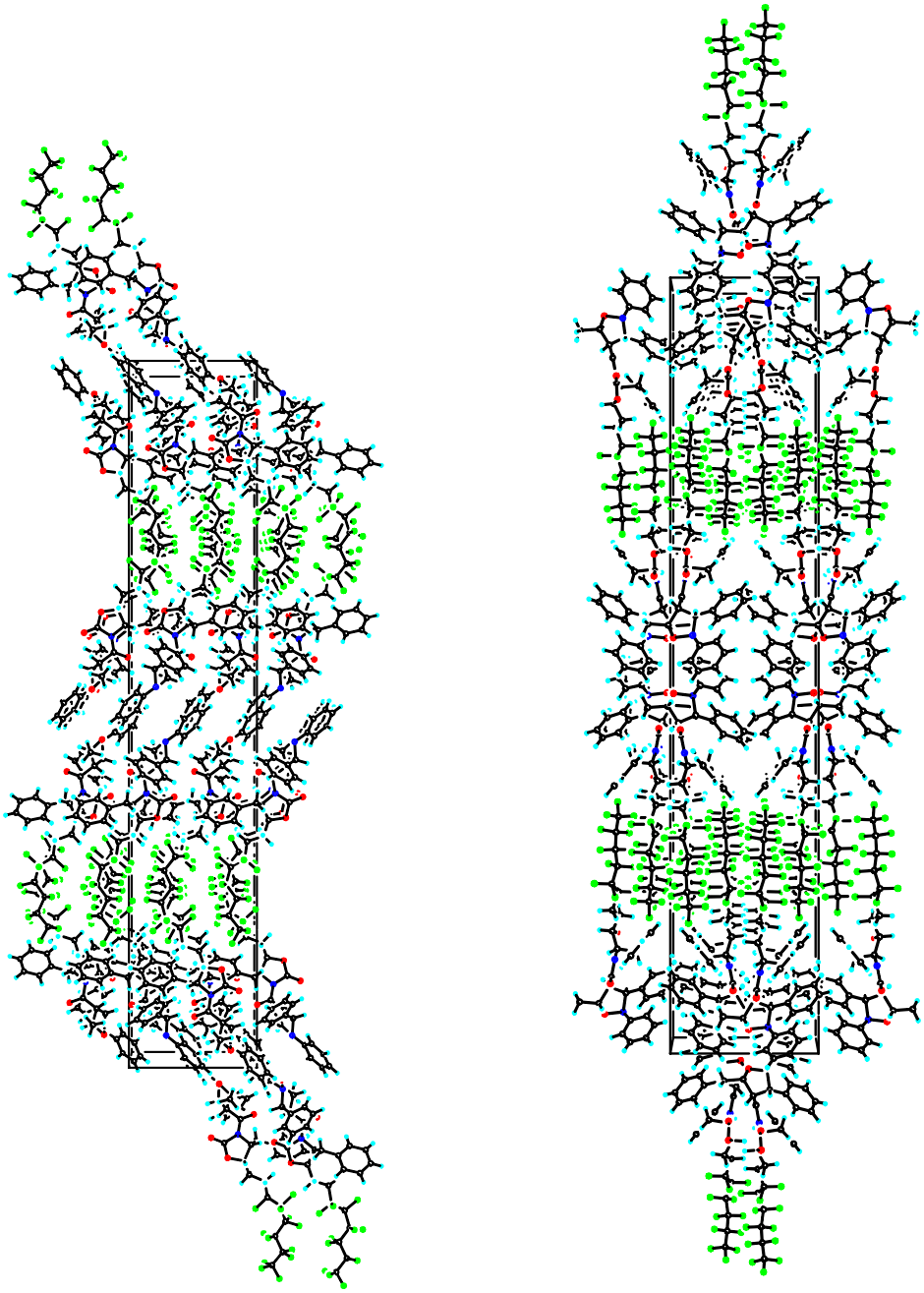

Table 1. Crystal data and structure refinement for jh01.

Identification code	jh01	
Empirical formula	$C_{35}H_{29}F_{13}N_2O_4$	
Formula weight	788.60	
Temperature	295(2) K	
Wavelength	1.54178 Å	
Crystal system	Orthorhombic	
Space group	Pbcn	
Unit cell dimensions	a = 58.6236(13) Å	α= 90°
	b = 11.2628(3) Å	β= 90°
	c = 10.6713(2) Å	γ = 90°
Volume	7045.9(3) $Å^3$	
Z	8	
Density (calculated)	1.487 Mg/m^3	
Absorption coefficient	1.272 mm^{-1}	
F(000)	3216	
Crystal size	0.50 x 0.025 x 0.01 mm^3	
θ range for data collection	3.02 to 44.52°	
Index ranges	$-53 \le h \le 53$, $-9 \le k \le 10$, $-8 \le l \le 9$	
Reflections collected	21337	
Independent reflections	2767 [R(int) = 0.0911]	
Completeness to θ = 44.52°	99.9 %	
Absorption correction	Sadabs	
Refinement method	Full-matrix least-squares on F^2	
Data / restraints / parameters	2767 / 210 / 488	
Goodness-of-fit on F^2	1.044	
Final R indices [I>2σ(I)]	R1 = 0.0756, wR2 = 0.1962	
R indices (all data)	R1 = 0.1361, wR2 = 0.2499	
Extinction coefficient	0.00069(11)	
Largest diff. peak and hole	0.361 and -0.247 $e.Å^{-3}$	
Ratio of min. to max. apparent transmission	0.778	

Table 2. Atomic coordinates (x 10^4) and equivalent isotropic displacement parameters ($Å^2$ x 10^3) for jh01. U(eq) is defined as one third of the trace of the orthogonalized U^{ij} tensor.

	x	y	z	U(eq)
F(1)	7189(1)	1075(7)	5027(7)	159(3)
N(1)	5385(2)	1558(8)	2126(8)	93(2)
O(1)	5356(1)	275(7)	2103(6)	93(2)
C(1)	5254(2)	2031(11)	1147(10)	85(3)
O(2)	5811(1)	770(6)	4882(7)	98(2)
N(2)	6110(2)	1026(6)	3610(8)	80(2)
C(2)	5062(2)	1454(10)	669(11)	103(3)
F(2)	7035(1)	2582(7)	6067(9)	181(3)
O(3)	6161(1)	1130(6)	1461(8)	102(2)
C(3)	4933(2)	1957(12)	-242(12)	113(4)
F(3)	7155(1)	-233(8)	7004(10)	194(4)
F(4)	6990(1)	1227(8)	8062(7)	166(3)
O(4)	6456(1)	1156(6)	2793(7)	106(2)
C(4)	4980(2)	3064(12)	-719(11)	113(4)
F(5)	7432(1)	793(9)	8518(9)	189(4)
C(5)	5164(2)	3659(10)	-242(12)	119(4)
F(6)	7377(1)	2493(9)	7733(7)	160(3)
C(6)	5302(2)	3158(12)	679(12)	117(4)
F(7)	7583(1)	122(7)	6025(8)	167(3)
C(7)	5636(2)	1744(9)	2052(9)	83(3)
F(8)	7584(1)	2021(8)	5718(7)	171(3)
C(8)	5729(2)	599(8)	2702(9)	80(3)
F(9)	7828(1)	2184(8)	7983(7)	168(3)
C(9)	5515(2)	-87(9)	3024(10)	89(3)
F(10)	7869(1)	248(8)	7833(8)	183(3)
C(10)	5534(2)	-1430(9)	2934(10)	111(3)
C(11)	5704(2)	2889(10)	2697(12)	93(3)
F(11)	8220(1)	1349(8)	6956(9)	198(4)
C(12)	5602(2)	3207(11)	3784(13)	111(4)
F(12)	8027(2)	2427(9)	5785(10)	215(4)
C(13)	5669(2)	4268(14)	4392(13)	134(4)

F(13)	8039(2)	556(10)	5516(10)	218(5)
C(14)	5833(3)	4956(12)	3868(16)	137(5)
C(15)	5939(2)	4649(12)	2799(15)	130(4)
C(16)	5874(2)	3584(11)	2187(11)	110(3)
C(17)	5881(2)	797(8)	3815(13)	85(3)
C(18)	6236(2)	1101(9)	2508(16)	94(3)
C(19)	6492(2)	869(9)	4112(11)	98(3)
C(20)	6265(2)	1246(8)	4673(9)	80(3)
C(21)	6239(2)	2551(9)	5123(9)	90(3)
C(22)	6305(2)	2746(10)	6467(12)	90(3)
C(23)	6185(2)	2151(10)	7380(14)	103(3)
C(24)	6239(2)	2308(11)	8634(14)	123(4)
C(25)	6410(3)	3032(14)	8989(13)	134(5)
C(26)	6530(2)	3647(13)	8114(16)	144(5)
C(27)	6480(2)	3496(11)	6831(13)	126(4)
C(28)	6710(2)	1426(9)	4532(11)	105(3)
C(29)	6791(2)	943(10)	5781(12)	121(4)
C(30)	7036(3)	1364(14)	5991(18)	150(5)
C(31)	7151(3)	967(15)	7064(19)	157(5)
C(32)	7387(2)	1349(15)	7426(16)	128(5)
C(33)	7595(2)	1178(13)	6606(14)	119(4)
C(34)	7829(2)	1254(14)	7208(16)	127(4)
C(35)	8023(3)	1389(17)	6360(20)	153(5)

Table 3. Bond lengths [Å] and angles [°] for jh01.

F(1)-C(30)	1.405(17)	C(8)-C(9)	1.513(11)
N(1)-C(1)	1.400(12)	C(8)-H(8A)	0.9800
N(1)-O(1)	1.455(9)	F(9)-C(34)	1.335(13)
N(1)-C(7)	1.491(11)	C(9)-C(10)	1.520(12)
O(1)-C(9)	1.416(10)	C(9)-H(9A)	0.9800
C(1)-C(6)	1.392(13)	F(10)-C(34)	1.335(14)
C(1)-C(2)	1.396(13)	C(10)-H(10C)	0.9600
O(2)-C(17)	1.211(11)	C(10)-H(10B)	0.9600
N(2)-C(17)	1.383(12)	C(10)-H(10A)	0.9600
N(2)-C(18)	1.392(13)	C(11)-C(12)	1.352(13)
N(2)-C(20)	1.478(10)	C(11)-C(16)	1.381(13)
C(2)-C(3)	1.356(13)	F(11)-C(35)	1.321(17)
C(2)-H(2A)	0.9300	C(12)-C(13)	1.415(15)
F(2)-C(30)	1.374(14)	C(12)-H(12A)	0.9300
O(3)-C(18)	1.199(13)	F(12)-C(35)	1.319(17)
C(3)-C(4)	1.375(14)	C(13)-C(14)	1.356(16)
C(3)-H(3A)	0.9300	C(13)-H(13A)	0.9300
F(3)-C(31)	1.354(14)	F(13)-C(35)	1.302(17)
F(4)-C(31)	1.454(17)	C(14)-C(15)	1.343(16)
O(4)-C(18)	1.327(12)	C(14)-H(14A)	0.9300
O(4)-C(19)	1.459(11)	C(15)-C(16)	1.417(15)
C(4)-C(5)	1.369(14)	C(15)-H(15A)	0.9300
C(4)-H(4A)	0.9300	C(16)-H(16A)	0.9300
F(5)-C(32)	1.348(14)	C(19)-C(28)	1.494(12)
C(5)-C(6)	1.392(13)	C(19)-C(20)	1.516(12)
C(5)-H(5A)	0.9300	C(19)-H(19A)	0.9800
F(6)-C(32)	1.331(14)	C(20)-C(21)	1.554(12)
C(6)-H(6A)	0.9300	C(20)-H(20A)	0.9800
F(7)-C(33)	1.344(13)	C(21)-C(22)	1.502(12)
C(7)-C(11)	1.515(13)	C(21)-H(21B)	0.9700
C(7)-C(8)	1.563(12)	C(21)-H(21A)	0.9700
C(7)-H(7A)	0.9800	C(22)-C(23)	1.377(13)
F(8)-C(33)	1.343(13)	C(22)-C(27)	1.385(13)
C(8)-C(17)	1.501(13)	C(23)-C(24)	1.386(14)

C(23)-H(23A)	0.9300	C(18)-O(4)-C(19)	110.6(9)
C(24)-C(25)	1.350(15)	C(5)-C(4)-C(3)	117.6(12)
C(24)-H(24A)	0.9300	C(5)-C(4)-H(4A)	121.2
C(25)-C(26)	1.357(16)	C(3)-C(4)-H(4A)	121.2
C(25)-H(25A)	0.9300	C(4)-C(5)-C(6)	121.4(11)
C(26)-C(27)	1.409(15)	C(4)-C(5)-H(5A)	119.3
C(26)-H(26A)	0.9300	C(6)-C(5)-H(5A)	119.3
C(27)-H(27A)	0.9300	C(5)-C(6)-C(1)	120.5(11)
C(28)-C(29)	1.515(13)	C(5)-C(6)-H(6A)	119.8
C(28)-H(28B)	0.9700	C(1)-C(6)-H(6A)	119.8
C(28)-H(28A)	0.9700	N(1)-C(7)-C(11)	110.8(8)
C(29)-C(30)	1.530(17)	N(1)-C(7)-C(8)	101.9(8)
C(29)-H(29B)	0.9700	C(11)-C(7)-C(8)	114.2(8)
C(29)-H(29A)	0.9700	N(1)-C(7)-H(7A)	109.9
C(30)-C(31)	1.402(18)	C(11)-C(7)-H(7A)	109.9
C(31)-C(32)	1.499(18)	C(8)-C(7)-H(7A)	109.9
C(32)-C(33)	1.515(17)	C(17)-C(8)-C(9)	112.8(9)
C(33)-C(34)	1.517(16)	C(17)-C(8)-C(7)	115.8(8)
C(34)-C(35)	1.463(19)	C(9)-C(8)-C(7)	103.4(7)
		C(17)-C(8)-H(8A)	108.1
C(1)-N(1)-O(1)	107.6(8)	C(9)-C(8)-H(8A)	108.1
C(1)-N(1)-C(7)	116.5(8)	C(7)-C(8)-H(8A)	108.1
O(1)-N(1)-C(7)	104.7(7)	O(1)-C(9)-C(8)	104.0(8)
C(9)-O(1)-N(1)	101.4(7)	O(1)-C(9)-C(10)	106.9(8)
C(6)-C(1)-C(2)	117.1(11)	C(8)-C(9)-C(10)	115.6(8)
C(6)-C(1)-N(1)	120.4(11)	O(1)-C(9)-H(9A)	110.0
C(2)-C(1)-N(1)	122.3(11)	C(8)-C(9)-H(9A)	110.0
C(17)-N(2)-C(18)	131.3(10)	C(10)-C(9)-H(9A)	110.0
C(17)-N(2)-C(20)	120.6(9)	C(9)-C(10)-H(10C)	109.5
C(18)-N(2)-C(20)	108.1(9)	C(9)-C(10)-H(10B)	109.5
C(3)-C(2)-C(1)	121.1(11)	H(10C)-C(10)-H(10B)	109.5
C(3)-C(2)-H(2A)	119.4	C(9)-C(10)-H(10A)	109.5
C(1)-C(2)-H(2A)	119.4	H(10C)-C(10)-H(10A)	109.5
C(2)-C(3)-C(4)	122.2(12)	H(10B)-C(10)-H(10A)	109.5
C(2)-C(3)-H(3A)	118.9	C(12)-C(11)-C(16)	120.5(11)
C(4)-C(3)-H(3A)	118.9	C(12)-C(11)-C(7)	119.9(11)

C(16)-C(11)-C(7)	119.5(12)	C(20)-C(21)-H(21B)	108.7
C(11)-C(12)-C(13)	119.7(12)	C(22)-C(21)-H(21A)	108.7
C(11)-C(12)-H(12A)	120.1	C(20)-C(21)-H(21A)	108.7
C(13)-C(12)-H(12A)	120.1	H(21B)-C(21)-H(21A)	107.6
C(14)-C(13)-C(12)	119.3(13)	C(23)-C(22)-C(27)	118.6(11)
C(14)-C(13)-H(13A)	120.4	C(23)-C(22)-C(21)	118.2(11)
C(12)-C(13)-H(13A)	120.4	C(27)-C(22)-C(21)	123.3(12)
C(15)-C(14)-C(13)	122.0(14)	C(22)-C(23)-C(24)	120.3(11)
C(15)-C(14)-H(14A)	119.0	C(22)-C(23)-H(23A)	119.8
C(13)-C(14)-H(14A)	119.0	C(24)-C(23)-H(23A)	119.8
C(14)-C(15)-C(16)	119.2(13)	C(25)-C(24)-C(23)	121.2(13)
C(14)-C(15)-H(15A)	120.4	C(25)-C(24)-H(24A)	119.4
C(16)-C(15)-H(15A)	120.4	C(23)-C(24)-H(24A)	119.4
C(11)-C(16)-C(15)	119.3(12)	C(24)-C(25)-C(26)	120.0(13)
C(11)-C(16)-H(16A)	120.3	C(24)-C(25)-H(25A)	120.0
C(15)-C(16)-H(16A)	120.3	C(26)-C(25)-H(25A)	120.0
O(2)-C(17)-N(2)	118.8(10)	C(25)-C(26)-C(27)	120.1(13)
O(2)-C(17)-C(8)	122.6(10)	C(25)-C(26)-H(26A)	120.0
N(2)-C(17)-C(8)	118.5(11)	C(27)-C(26)-H(26A)	120.0
O(3)-C(18)-O(4)	124.5(13)	C(22)-C(27)-C(26)	119.9(12)
O(3)-C(18)-N(2)	126.6(12)	C(22)-C(27)-H(27A)	120.1
O(4)-C(18)-N(2)	109.0(12)	C(26)-C(27)-H(27A)	120.1
O(4)-C(19)-C(28)	108.7(9)	C(19)-C(28)-C(29)	112.4(9)
O(4)-C(19)-C(20)	101.1(7)	C(19)-C(28)-H(28B)	109.1
C(28)-C(19)-C(20)	120.9(9)	C(29)-C(28)-H(28B)	109.1
O(4)-C(19)-H(19A)	108.5	C(19)-C(28)-H(28A)	109.1
C(28)-C(19)-H(19A)	108.5	C(29)-C(28)-H(28A)	109.1
C(20)-C(19)-H(19A)	108.5	H(28B)-C(28)-H(28A)	107.9
N(2)-C(20)-C(19)	101.0(8)	C(28)-C(29)-C(30)	108.2(11)
N(2)-C(20)-C(21)	109.5(8)	C(28)-C(29)-H(29B)	110.1
C(19)-C(20)-C(21)	118.3(8)	C(30)-C(29)-H(29B)	110.1
N(2)-C(20)-H(20A)	109.2	C(28)-C(29)-H(29A)	110.1
C(19)-C(20)-H(20A)	109.2	C(30)-C(29)-H(29A)	110.1
C(21)-C(20)-H(20A)	109.2	H(29B)-C(29)-H(29A)	108.4
C(22)-C(21)-C(20)	114.0(8)	F(2)-C(30)-C(31)	105.8(14)
C(22)-C(21)-H(21B)	108.7	F(2)-C(30)-F(1)	106.1(14)

C(31)-C(30)-F(1)	102.5(14)
F(2)-C(30)-C(29)	108.3(12)
C(31)-C(30)-C(29)	118.2(15)
F(1)-C(30)-C(29)	115.0(12)
F(3)-C(31)-C(30)	106.7(14)
F(3)-C(31)-F(4)	104.3(14)
C(30)-C(31)-F(4)	102.7(14)
F(3)-C(31)-C(32)	106.5(13)
C(30)-C(31)-C(32)	124.2(16)
F(4)-C(31)-C(32)	110.7(14)
F(6)-C(32)-F(5)	104.2(14)
F(6)-C(32)-C(31)	107.5(13)
F(5)-C(32)-C(31)	105.5(13)
F(6)-C(32)-C(33)	107.6(12)
F(5)-C(32)-C(33)	106.5(12)
C(31)-C(32)-C(33)	124.0(15)
F(8)-C(33)-F(7)	107.3(12)
F(8)-C(33)-C(32)	106.2(12)
F(7)-C(33)-C(32)	109.7(12)
F(8)-C(33)-C(34)	107.6(12)
F(7)-C(33)-C(34)	107.1(12)
C(32)-C(33)-C(34)	118.5(12)
F(10)-C(34)-F(9)	110.9(14)
F(10)-C(34)-C(35)	105.3(13)
F(9)-C(34)-C(35)	107.8(13)
F(10)-C(34)-C(33)	108.7(12)
F(9)-C(34)-C(33)	107.7(12)
C(35)-C(34)-C(33)	116.5(15)
F(13)-C(35)-F(12)	108.5(17)
F(13)-C(35)-F(11)	104.4(15)
F(12)-C(35)-F(11)	103.9(15)
F(13)-C(35)-C(34)	114.0(16)
F(12)-C(35)-C(34)	113.2(16)
F(11)-C(35)-C(34)	112.1(17)

Symmetry transformations used to generate equivalent atoms:

Table 4. Anisotropic displacement parameters ($Å^2$ x 10^3) for jh01. The anisotropic displacement factor exponent takes the form: $-2\pi^2[h^2 a^{*2}U^{11} + ... + 2 h k a^* b^* U^{12}]$

	U^{11}	U^{22}	U^{33}	U^{23}	U^{13}	U^{12}
F(1)	96(5)	248(9)	132(6)	-27(6)	8(4)	29(5)
N(1)	79(7)	96(8)	104(7)	1(5)	-15(5)	2(5)
O(1)	74(5)	90(6)	115(5)	-2(4)	-14(4)	-6(4)
C(1)	74(7)	89(8)	93(8)	-1(7)	-1(7)	9(7)
O(2)	71(5)	129(6)	95(5)	1(5)	6(4)	-13(4)
N(2)	62(6)	96(6)	84(6)	0(5)	3(6)	-5(4)
C(2)	78(8)	116(8)	115(8)	-4(7)	-10(7)	-7(7)
F(2)	162(7)	113(6)	268(9)	10(6)	-97(6)	-14(5)
O(3)	95(6)	117(6)	93(5)	-5(5)	2(5)	-8(4)
C(3)	93(8)	128(10)	119(9)	-14(8)	-12(8)	5(8)
F(3)	145(6)	118(6)	320(11)	25(7)	-73(7)	-19(5)
F(4)	119(5)	248(9)	131(6)	1(6)	16(5)	11(5)
O(4)	75(6)	140(6)	102(6)	-7(5)	15(4)	-13(4)
C(4)	86(8)	125(10)	127(9)	-7(9)	-17(7)	30(7)
F(5)	124(6)	263(10)	180(7)	69(7)	-17(5)	-21(6)
C(5)	109(9)	101(8)	147(10)	5(8)	-28(8)	13(8)
F(6)	136(6)	162(7)	183(7)	-33(6)	-27(5)	1(5)
C(6)	114(9)	108(9)	130(9)	-5(8)	-37(8)	9(8)
F(7)	140(6)	136(6)	226(8)	-54(6)	-45(5)	16(5)
C(7)	87(8)	80(7)	81(7)	-2(6)	-9(6)	2(6)
F(8)	166(7)	201(8)	146(6)	63(6)	-24(5)	-14(6)
C(8)	61(6)	89(7)	90(7)	0(6)	-8(6)	-4(6)
F(9)	127(6)	210(8)	167(7)	-75(6)	-6(5)	-25(5)
C(9)	70(7)	94(8)	102(8)	0(6)	-2(6)	-5(6)
F(10)	161(7)	182(8)	207(8)	71(7)	-41(6)	-8(6)
C(10)	110(8)	107(9)	116(8)	9(7)	-7(6)	-3(6)
C(11)	87(8)	90(8)	101(9)	0(7)	2(7)	-5(7)
F(11)	103(6)	238(10)	253(10)	-22(8)	-3(6)	-2(6)

C(12)	111(9)	100(9)	122(9)	-8(8)	-9(8)	-9(7)
F(12)	173(8)	198(9)	273(11)	58(8)	66(8)	-2(7)
C(13)	124(10)	136(11)	140(10)	-24(9)	-4(8)	0(8)
F(13)	170(8)	252(11)	231(9)	-94(9)	36(7)	-2(7)
C(14)	147(11)	101(9)	162(12)	-17(9)	-22(10)	-14(9)
C(15)	147(10)	105(10)	140(11)	14(9)	-9(9)	-16(8)
C(16)	121(9)	96(8)	112(8)	8(8)	-11(7)	-11(7)
C(17)	58(8)	80(7)	117(9)	4(7)	4(8)	-3(5)
C(18)	63(9)	88(7)	132(11)	1(8)	9(10)	-10(6)
C(19)	70(8)	113(8)	111(9)	8(7)	-18(7)	-6(6)
C(20)	62(7)	83(7)	96(7)	8(6)	0(6)	-1(5)
C(21)	78(7)	103(8)	89(8)	3(6)	-3(6)	-2(6)
C(22)	80(7)	88(7)	101(9)	1(7)	-5(7)	-7(6)
C(23)	108(8)	96(8)	105(9)	-17(7)	-8(8)	-3(6)
C(24)	127(10)	122(9)	119(11)	-7(8)	0(8)	2(8)
C(25)	135(11)	157(11)	109(10)	-9(9)	-15(9)	7(9)
C(26)	128(10)	172(12)	132(11)	-31(10)	-22(9)	-26(9)
C(27)	124(9)	131(9)	121(10)	-8(8)	-2(8)	-16(8)
C(28)	76(7)	117(8)	123(9)	-11(7)	0(6)	-3(6)
C(29)	89(8)	122(9)	151(10)	-1(8)	-22(7)	-7(7)
C(30)	137(12)	131(11)	181(13)	-7(10)	-54(11)	3(10)
C(31)	128(12)	142(12)	199(14)	-13(11)	-51(12)	0(10)
C(32)	86(10)	138(11)	161(12)	33(10)	-36(9)	-10(9)
C(33)	99(10)	118(10)	139(11)	-3(9)	-11(9)	-7(8)
C(34)	87(10)	136(11)	157(11)	-9(10)	9(9)	-12(9)
C(35)	107(12)	157(13)	196(14)	-1(12)	9(12)	-5(11)

Table 5. Hydrogen coordinates (x 10^4) and isotropic displacement parameters ($Å^2$ x 10^3) for jh01.

	x	y	z	U(eq)
H(2A)	5022	712	982	124
H(3A)	4809	1538	-556	136
H(4A)	4890	3398	-1343	135
H(5A)	5198	4415	-540	143
H(6A)	5427	3578	984	141
H(7A)	5685	1762	1174	99
H(8A)	5815	142	2078	96
H(9A)	5461	141	3859	107
H(10C)	5392	-1785	3173	166
H(10B)	5653	-1703	3484	166
H(10A)	5570	-1650	2087	166
H(12A)	5489	2730	4130	133
H(13A)	5601	4491	5144	160
H(14A)	5873	5663	4259	164
H(15A)	6053	5129	2466	157
H(16A)	5946	3355	1448	132
H(19A)	6506	5	4193	118
H(20A)	6226	708	5363	96
H(21B)	6332	3057	4596	108
H(21A)	6081	2790	5013	108
H(23A)	6067	1643	7155	123
H(24A)	6155	1906	9242	147
H(25A)	6447	3110	9833	161
H(26A)	6644	4168	8360	173
H(27A)	6565	3900	6230	151
H(28B)	6689	2277	4602	126
H(28A)	6827	1284	3905	126
H(29B)	6785	83	5777	145
H(29A)	6693	1230	6450	145

Table 6. Torsion angles [°] for jh01.

C(1)-N(1)-O(1)-C(9)	173.3(7)
C(7)-N(1)-O(1)-C(9)	48.8(8)
O(1)-N(1)-C(1)-C(6)	-159.4(9)
C(7)-N(1)-C(1)-C(6)	-42.3(13)
O(1)-N(1)-C(1)-C(2)	26.0(12)
C(7)-N(1)-C(1)-C(2)	143.1(9)
C(6)-C(1)-C(2)-C(3)	2.3(15)
N(1)-C(1)-C(2)-C(3)	177.1(9)
C(1)-C(2)-C(3)-C(4)	-1.8(17)
C(2)-C(3)-C(4)-C(5)	0.1(17)
C(3)-C(4)-C(5)-C(6)	0.9(17)
C(4)-C(5)-C(6)-C(1)	-0.4(17)
C(2)-C(1)-C(6)-C(5)	-1.2(15)
N(1)-C(1)-C(6)-C(5)	-176.1(9)
C(1)-N(1)-C(7)-C(11)	90.0(11)
O(1)-N(1)-C(7)-C(11)	-151.3(8)
C(1)-N(1)-C(7)-C(8)	-148.2(8)
O(1)-N(1)-C(7)-C(8)	-29.5(9)
N(1)-C(7)-C(8)-C(17)	-122.7(9)
C(11)-C(7)-C(8)-C(17)	-3.2(13)
N(1)-C(7)-C(8)-C(9)	1.3(9)
C(11)-C(7)-C(8)-C(9)	120.8(10)
N(1)-O(1)-C(9)-C(8)	-47.1(8)
N(1)-O(1)-C(9)-C(10)	-169.9(7)
C(17)-C(8)-C(9)-O(1)	154.0(8)
C(7)-C(8)-C(9)-O(1)	28.1(9)
C(17)-C(8)-C(9)-C(10)	-89.1(11)
C(7)-C(8)-C(9)-C(10)	145.0(9)
N(1)-C(7)-C(11)-C(12)	39.9(13)
C(8)-C(7)-C(11)-C(12)	-74.4(13)
N(1)-C(7)-C(11)-C(16)	-142.0(9)
C(8)-C(7)-C(11)-C(16)	103.7(11)
C(16)-C(11)-C(12)-C(13)	1.0(16)
C(7)-C(11)-C(12)-C(13)	179.1(10)

C(11)-C(12)-C(13)-C(14)	0.5(18)
C(12)-C(13)-C(14)-C(15)	-2(2)
C(13)-C(14)-C(15)-C(16)	1(2)
C(12)-C(11)-C(16)-C(15)	-1.4(16)
C(7)-C(11)-C(16)-C(15)	-179.5(9)
C(14)-C(15)-C(16)-C(11)	0.3(17)
C(18)-N(2)-C(17)-O(2)	179.5(10)
C(20)-N(2)-C(17)-O(2)	-0.5(13)
C(18)-N(2)-C(17)-C(8)	-1.0(15)
C(20)-N(2)-C(17)-C(8)	179.0(8)
C(9)-C(8)-C(17)-O(2)	-22.6(13)
C(7)-C(8)-C(17)-O(2)	96.4(11)
C(9)-C(8)-C(17)-N(2)	157.9(8)
C(7)-C(8)-C(17)-N(2)	-83.1(11)
C(19)-O(4)-C(18)-O(3)	-169.0(11)
C(19)-O(4)-C(18)-N(2)	12.0(11)
C(17)-N(2)-C(18)-O(3)	10.7(19)
C(20)-N(2)-C(18)-O(3)	-169.3(11)
C(17)-N(2)-C(18)-O(4)	-170.3(9)
C(20)-N(2)-C(18)-O(4)	9.6(11)
C(18)-O(4)-C(19)-C(28)	-155.8(9)
C(18)-O(4)-C(19)-C(20)	-27.6(10)
C(17)-N(2)-C(20)-C(19)	154.3(8)
C(18)-N(2)-C(20)-C(19)	-25.7(10)
C(17)-N(2)-C(20)-C(21)	-80.2(10)
C(18)-N(2)-C(20)-C(21)	99.9(9)
O(4)-C(19)-C(20)-N(2)	30.5(9)
C(28)-C(19)-C(20)-N(2)	150.4(10)
O(4)-C(19)-C(20)-C(21)	-88.8(10)
C(28)-C(19)-C(20)-C(21)	31.0(14)
N(2)-C(20)-C(21)-C(22)	155.2(9)
C(19)-C(20)-C(21)-C(22)	-89.9(11)
C(20)-C(21)-C(22)-C(23)	-61.6(12)
C(20)-C(21)-C(22)-C(27)	118.7(11)
C(27)-C(22)-C(23)-C(24)	0.1(16)
C(21)-C(22)-C(23)-C(24)	-179.6(10)

C(22)-C(23)-C(24)-C(25)	-0.6(18)
C(23)-C(24)-C(25)-C(26)	2(2)
C(24)-C(25)-C(26)-C(27)	-2(2)
C(23)-C(22)-C(27)-C(26)	-0.7(17)
C(21)-C(22)-C(27)-C(26)	179.0(11)
C(25)-C(26)-C(27)-C(22)	1.9(19)
O(4)-C(19)-C(28)-C(29)	-166.3(9)
C(20)-C(19)-C(28)-C(29)	77.7(13)
C(19)-C(28)-C(29)-C(30)	168.2(10)
C(28)-C(29)-C(30)-F(2)	63.3(16)
C(28)-C(29)-C(30)-C(31)	-176.5(14)
C(28)-C(29)-C(30)-F(1)	-55.1(15)
F(2)-C(30)-C(31)-F(3)	-179.8(13)
F(1)-C(30)-C(31)-F(3)	-68.8(16)
C(29)-C(30)-C(31)-F(3)	59(2)
F(2)-C(30)-C(31)-F(4)	70.9(15)
F(1)-C(30)-C(31)-F(4)	-178.1(11)
C(29)-C(30)-C(31)-F(4)	-50.6(18)
F(2)-C(30)-C(31)-C(32)	-55(2)
F(1)-C(30)-C(31)-C(32)	56(2)
C(29)-C(30)-C(31)-C(32)	-176.9(15)
F(3)-C(31)-C(32)-F(6)	-167.8(14)
C(30)-C(31)-C(32)-F(6)	68(2)
F(4)-C(31)-C(32)-F(6)	-55.1(18)
F(3)-C(31)-C(32)-F(5)	-57.0(19)
C(30)-C(31)-C(32)-F(5)	178.6(17)
F(4)-C(31)-C(32)-F(5)	55.7(18)
F(3)-C(31)-C(32)-C(33)	66(2)
C(30)-C(31)-C(32)-C(33)	-59(3)
F(4)-C(31)-C(32)-C(33)	178.5(13)
F(6)-C(32)-C(33)-F(8)	-49.3(14)
F(5)-C(32)-C(33)-F(8)	-160.6(11)
C(31)-C(32)-C(33)-F(8)	77.0(18)
F(6)-C(32)-C(33)-F(7)	-164.9(11)
F(5)-C(32)-C(33)-F(7)	83.8(14)
C(31)-C(32)-C(33)-F(7)	-39(2)

F(6)-C(32)-C(33)-C(34)	71.8(16)
F(5)-C(32)-C(33)-C(34)	-39.5(19)
C(31)-C(32)-C(33)-C(34)	-161.9(15)
F(8)-C(33)-C(34)-F(10)	-163.1(12)
F(7)-C(33)-C(34)-F(10)	-48.0(16)
C(32)-C(33)-C(34)-F(10)	76.6(18)
F(8)-C(33)-C(34)-F(9)	76.7(15)
F(7)-C(33)-C(34)-F(9)	-168.3(12)
C(32)-C(33)-C(34)-F(9)	-43.7(18)
F(8)-C(33)-C(34)-C(35)	-44.4(19)
F(7)-C(33)-C(34)-C(35)	70.7(18)
C(32)-C(33)-C(34)-C(35)	-164.8(15)
F(10)-C(34)-C(35)-F(13)	64(2)
F(9)-C(34)-C(35)-F(13)	-177.5(15)
C(33)-C(34)-C(35)-F(13)	-56(2)
F(10)-C(34)-C(35)-F(12)	-171.3(15)
F(9)-C(34)-C(35)-F(12)	-53(2)
C(33)-C(34)-C(35)-F(12)	68(2)
F(10)-C(34)-C(35)-F(11)	-54.2(19)
F(9)-C(34)-C(35)-F(11)	64.2(19)
C(33)-C(34)-C(35)-F(11)	-174.8(14)

Symmetry transformations used to generate equivalent atoms:

REFERENCES

1. Smith, M. B.; March, J. *March's Advanced Organic Chemistry: Reactions, Mechanisms, and Structure, 5th Edition*, 2000.

2. Eliel, E. L.; Wilen, S. H.; Mander, L. N. *Stereochemistry of Organic Compounds*, 1994.

3. Caldwell, J. *Modern Drug Discovery* **1999,** *2*, 51, 54-55, 57, 59-60.

4. Nicolaou, K. C.; Sorensen, E. J.; Editors *Classics in Total Synthesis*, 1996.

5. Baker, G. B.; Prior, T. I. *Annal. Med.* **2002,** *34*, 537-543.

6. Agranat, I.; Caner, H.; Caldwell, J. *Nature Reviews Drug Discovery* **2002,** *1*, 753-768.

7. Lehninger, A. L.; Nelson, D. L.; Cox, M. M. *Principles of Biochemistry, Pt. 1. 2nd Ed*, 1993.

8. Burke, D.; Henderson, D. J. *Brit. J. Anaesthesia* **2002,** *88*, 563-576.

9. Mehvar, R.; Brocks, D. R.; Vakily, M. *Clin. Pharmacokinet.* **2002,** *41*, 533-558.

10. Stoschitzky, K.; Zernig, G.; Lindner, W. *J Clin Basic Cardiol* **1998,** *1*, 14-18.

11. Horwitt, M. K. *J. Nutr.* **1986,** *116*, 1371-7.

12. Laufer, M. C.; Bonrath, W.; Hoelderich, W. F. *Catalysis Lett.* **2005,** *100*, 101-103.

13. Weiser, H.; Vecchi, M. *Internat. J. Vit. Nut. Res.* **1982,** *52*, 351-70.

14. Andersson, T.; Rohss, K.; Bredberg, E.; Hassan-Alin, M. *Ailment. Pharmacol. Theraputics* **2001,** *15*, 1563-1569.

15. Mansfield, P.; Henry, D.; Tonkin, A. *Clin. Pharmacokinet.* **2004,** *43*, 287-290.

16. Thayer, A. *Chem. Eng. News.* **2005,** *83*, 49.

17. Matsuura, T.; Koshima, H. *J. Photochem. Photobio. C* **2005,** *6*, 7-24.

18. Lough, W. J. *Chirality in Nat. App. Sci.* **2002**, 179-202.

19. Thompson, R. *J. Liquid Chromatogr.* **2005,** *28*, 1215-1231.

20. Ema, T. *Tetrahedron: Asymmetry* **2004,** *15*, 2765-2770.

21. Pellissier, H. *Tetrahedron* **2003,** *59*, 8291-8327.

22. Calmes, M.; Glot, C.; Michel, T.; Rolland, M.; Martinez, J. *Tetrahedron: Asymmetry* **2000,** *11*, 737-741.

23. Liebscher, J.; Jin, S.; Otto, A.; Woydowski, K. *J. Heterocyclic Chem.* **2000,** *37*, 509-518.

24. Juaristi, E.; Lopez-Ruiz, H. *Curr. Med. Chem.* **1999,** *6*, 983-1004.

25. Ager, D. J.; Allen, D. R.; Laneman, S. A.; Schaad, D. R. *Speciality Chemicals* **1997,** *17*, 356-358, 360.

26. Tye, H. *J. Chem. Soc., Perkin Trans. 1* **2000**, 275-298.

27. Ma, J.-A. *Angew. Chem., Int. Ed. Engl.* **2003,** *42*, 4290-4299.

28. Stibbs, B. *Can. Chem. News.* **2002,** *54*, 26-27.

29. O'Brien, P. *J. Chem. Soc., Perkin Trans. 1* **2001**, 95-113.

30. Regan, A. C. *J. Chem. Soc., Perkin Trans. 1* **1999**, 357-374.

31. Jones, S. *J. Chem. Soc., Perkin Trans. 1* **2002**, 1-21.

32. Hultin, P. G.; Earle, M. A.; Sudharshan, M. *Tetrahedron* **1997,** *53*, 14823-14870.

33. Groaning, M. D.; Meyers, A. I. *Tetrahedron* **2000,** *56*, 9843-9873.

34. Seyden-Penne, J. *Chiral Auxiliaries and Ligands in Symmetric Synthesis*; Wiley-Interscience, 1995.

35. Vicario, J. L.; Badia, D.; Dominguez, E.; Rodriguez, M.; Carrillo, L. *J. Org. Chem.* **2000,** *65*, 3754-3760.

36. Ager, D. J.; Prakash, I.; Schaad, D. R. *Aldrichimica Acta* **1997,** *30*, 3-12.

37. Evans, D. A.; Bartroli, J.; Shih, T. L. *J. Am. Chem. Soc.* **1981,** *103*, 2127-2129.

38. Ager, D. J.; Prakash, I.; Schaad, D. R. *Chem. Rev.* **1996,** *96*, 835-875.

39. Vicario, J. L.; Badia, D.; Carrillo, L.; Reyes, E.; Etxebarria, J. *Curr. Org. Chem.* **2005,** *9*, 219-235.

40. Abiko, A.; Masamune, S. *Tetrahedron Lett.* **1992,** *33*, 5517-18.

41. Takanami, T.; Tokoro, H.; Kato, D.-I.; Nishiyama, S.; Sugai, T. *Tetrahedron Lett.* **2005,** *46*, 3291-3295.

42. Beaulieu, P. L.; Wernic, D.; Duceppe, J.-S.; Guindon, Y. *Tetrahedron Lett.* **1995,** *36*, 3317-20.

43. Davis, F. A.; Haque, M. S.; Przeslawski, R. M. *J. Org. Chem.* **1989,** *54*, 2021-2024.

44. Andres, J. M.; Pedrosa, R.; Perez-Encabo, A. *Eur. J. Org. Chem.* **2004**, 1558-1566.

45. Tromp, R. A.; Van Der Hoeven, M.; Amore, A.; Brussee, J.; Overhand, M.; Van Der Marel, G. A.; Van Der Gen, A. *Tetrahedron: Asymmetry* **2003,** *14*, 1645-1652.

46. Urban, F. J.; Jasys, V. J. *Org. Proc. Res. Dev.* **2004,** *8*, 169-175.

47. Koch, S. S. C.; Chamberlin, A. R. *J. Org. Chem.* **1993,** *58*, 2725-2737.

48. Soloshonok, V. A.; Uekia, H.; Jianga, C.; Caib, C.; Hruby, V. J. *Helv. Chim. Acta* **2002,** *85*, 3616-3623.

49. Luppi, G.; Soffre, C.; Tomasini, C. *Tetrahedron: Asymmetry* **2004,** *15*, 1645-1650.

50. Evans, D. A.; Ennis, M. D.; Mathre, D. J. *J. Am. Chem. Soc.* **1982,** *104*, 1737-1739.

51. Hauck, R. S.; Nau, H. *Pharm. Res.* **1992,** *9*, 850-855.

52. Evans, D. A.; Britton, T. C.; Ellman, J. A.; Dorow, R. L. *J. Am. Chem. Soc.* **1990,** *112*, 4011-4030.

53. Dharanipragada, R.; Nicolas, E.; Toth, G.; Hruby, V. J. *Tetrahedron Lett.* **1989,** *30*, 6841-6844.

54. Nicolas, E.; Russell, K. C.; Hruby, V. J. *J. Org. Chem.* **1993,** *58*, 766-70.

55. Williams, D. R.; Kissel, W. S.; Li, J. J. *Tetrahedron Lett.* **1998,** *39*, 8593-8596.

56. Evans, D. A.; Chapman, K. T.; Bisaha, J. *Tetrahedron Lett.* **1984,** *25*, 4071-4.

57. Evans, D. A.; Chapman, K. T.; Bisaha, J. *J. Am. Chem. Soc.* **1988,** *110*, 1238-1256.

58. Evans, D. A.; Britton, T. C.; Ellman, J. A. *Tetrahedron Lett.* **1987,** *28*, 6141-6144.

59. Kanomata, N.; Maruyama, S.; Tomono, K.; Anada, S. *Tetrahedron Lett.* **2003,** *44*, 3599-3603.

60. Evans, D. A.; Bender, S. L.; Morris, J. *J. Am. Chem. Soc.* **1988,** *110*, 2506-2526.

61. Palomo, C.; Oiarbide, M.; Dias, F.; Lopez, R.; Linden, A. *Angew. Chem., Int. Ed. Engl.* **2004,** *43*, 3307-3310.

62. Boyle, N. A.; Janda, K. D. *Curr. Op. Chem. Biol.* **2002,** *6*, 339-346.

63. Gordon, E. M.; Barrett, R. W.; Dower, W. J.; Fodor, S. P. A.; Gallop, M. A. *J. Med. Chem.* **1994,** *37*, 1385-1401.

64. Balkenhohl, F.; von dem Bussche-Huennefeld, C.; Lansky, A.; Zechel, C. *Angew. Chem., Int. Ed. Engl.* **1996,** *35*, 2288-2337.

65. Terrett, N. K.; Gardner, M.; Gordon, D. W.; Kobylecki, R. J.; Steele, J. *Tetrahedron* **1995,** *51*, 8135-8173.

66. Lorsbach, B. A.; Kurth, M. J. *Chem. Rev.* **1999,** *99*, 1549-1581.

67. Brown, R. D. *J. Chem. Soc., Perkin Trans. 1* **1998**, 3293-3320.

68. Akelah, A.; Sherrington, D. C. *Chem. Rev.* **1981,** *81*, 557-587.

69. Merrifield, R. B. *J. Am. Chem. Soc.* **1963,** *85*, 2149-54.

70. Leznoff, C. C. *Acc. Chem. Res.* **1978,** *11*, 327-333.

71. Fyles, T. M.; Leznoff, C. C.; Weatherston, J. *Can. J. Chem.* **1977,** *55*, 4135-4143.

72. Benaglia, M.; Puglisi, A.; Cozzi, F. *Chem. Rev.* **2003,** *103*, 3401-3429.

73. Chung, C. W. Y.; Toy, P. H. *Tetrahedron: Asymmetry* **2004,** *15*, 387-399.

74. Kawana, M.; Emoto, S. *Tetrahedron Lett.* **1972**, 4855-8.

75. Enholm, E. J.; Gallagher, M. E.; Jiang, S.; Batson, W. A. *Org. Lett.* **2000,** *2*, 3355-3357.

76. Enholm, E. J.; Gallagher, M. E. *Org. Lett.* **2001,** *3*, 3397-3399.

77. Huang, J.; Li, Y.; Ren, J.; Zhou, Y.; Hou, J. *React. Funct. Polym.* **2001,** *49*, 173-178.

78. McArthur, C. R.; Worster, P. M.; Jiang, J. L.; Leznoff, C. C. *Can. J. Chem.* **1982,** *60*, 1836-41.

79. Frechet, J. M. J.; Halgas, J.; Sherrington, D. C. *React. Polym.* **1983,** *1*, 227-36.

80. Nakamura, S.; Uchiyama, Y.; Ishikawa, S.; Fukinbara, R.; Watanabe, Y.; Toru, T. *Tetrahedron Lett.* **2002,** *43*, 2381-2383.

81. Hachtel, J.; Gais, H.-J. *Eur. J. Org. Chem.* **2000**, 1457-1465.

82. Phoon, C. W.; Abell, C. *Tetrahedron Lett.* **1998,** *39*, 2655-2658.

83. Allin, S. M.; Shuttleworth, S. J. *Tetrahedron Lett.* **1996,** *37*, 8023-8026.

84. Roos, G. H.; Editor *Compendium of Chiral Auxiliary Applications*, 2001.

85. Nogradi, M. *Stereoselective Synthesis: A Practical Approach.*, 2nd ed., 1994.

86. Itsuno, S.; El-Shehawy, A. A.; Abdelaal, M. Y.; Ito, K. *New. J. Chem.* **1998,** *22*, 775-777.

87. Hutchison, P. C.; Heightman, T. D.; Procter, D. J. *Org. Lett.* **2002,** *4*, 4583-4585.

88. Burgess, K.; Lim, D. *Chem. Commum.* **1997**, 785-786.

89. Faita, G.; Paio, A.; Quadrelli, P.; Rancati, F.; Seneci, P. *Tetrahedron Lett.* **2000,** *41*, 1265-1269.

90. Kotake, T.; Rajesh, S.; Hayashi, Y.; Mukai, Y.; Ueda, M.; Kimura, T.; Kiso, Y. *Tetrahedron Lett.* **2004,** *45*, 3651-3654.

91. Desimoni, G.; Faita, G.; Galbiati, A.; Pasini, D.; Quadrelli, P.; Rancati, F. *Tetrahedron: Asymmetry* **2002,** *13*, 333-337.

92. Kotake, T.; Hayashi, Y.; Rajesh, S.; Mukai, Y.; Takiguchi, Y.; Kimura, T.; Kiso, Y. *Tetrahedron* **2005,** *61*, 3819-3833.

93. Purandare, A.; Natarajan, S. *Tetrahedron Lett.* **1997,** *38*, 8777-8780.

94. Winkler, J. D.; McCoull, W. *Tetrahedron Lett.* **1998,** *39*, 4935-4936.

95. Faita, G.; Paio, A.; Quadrelli, P.; Rancati, F.; Seneci, P. *Tetrahedron* **2001,** *57*, 8313-8322.

96. Delgado, M.; Janda, K. D. *Curr. Org. Chem.* **2002,** *6*, 1031-1043.

97. Toy, P. H.; Janda, K. D. *Acc. Chem. Res.* **2000,** *33*, 546-554.

98. Dickerson, T. J.; Reed, N. N.; Janda, K. D. *Chem. Rev.* **2002,** *102*, 3325-3343.

99. Harwig, C. W.; Gravert, D. J.; Janda, K. D. *Chemtracts* **1999,** *12*, 1-26.

100. Desimoni, G.; Faita, G.; Mella, M.; Righetti, P.; Zemat, M. *Tetrahedron* **1999,** *55*, 8509-8524.

101. Bew, S. P.; Bull, S. D.; Davies, S. G. *Tetrahedron Lett.* **2000,** *41*, 7577-7581.

102. Bew, S. P.; Bull, S. D.; Davies, S. G.; Savory, E. D.; Watkin, D. J. *Tetrahedron* **2002,** *58*, 9387-9401.

103. Allin, S. M.; Johnson, C. A.; Timm, A. *Tetrahedron Lett.* **2005,** *46*, 2495-2497.

104. Horvath, I. T.; Rabai, J. *Science* **1994,** *266*, 72-75.

105. Gladysz, J. A.; Curran, D. P. *Tetrahedron* **2002,** *58*, 3823-3825.

106. Curran, D. P. *Angew. Chem., Int. Ed. Engl.* **1998,** *37*, 1175-1196.

107. Horvath, I. T.; Curran, D. P.; Gladysz, J. A. "Fluorous chemistry: scope and definition"; In *Handbook of Fluorous Chemistry;* Gladysz, J. A.; Curran, D. P.; Horvath, I. T. Eds.; Wiley: New York, 2004; pp. 1-4.

108. Gladysz, J. A.; Curran, D. P.; Horvath, I. T.; Editors *Handbook of Flurorous Chemistry*, 2004.

109. Zhang, W. *Tetrahedron* **2003,** *59*, 4475-4489.

110. Luo, Z.; Zhang, Q.; Oderaotoshi, Y.; Curran, D. P. *Science* **2001,** *291*, 1766-1769.

111. Zhang, W. *Chem. Rev.* **2004,** *104*, 2531-2556.

112. Curran, D. P. *Synlett* **2001**, 1488-1496.

113. Curran, D. P. *Actual. Chim.* **2003**, 67-71.

114. Dobbs, A. P.; Kimberley, M. R. *J. Fluorine Chem.* **2002,** *118*, 3-17.

115. Horvath, I. T. *Acc. Chem. Res.* **1998,** *31*, 641-650.

116. Barthel-Rosa, L. P.; Gladysz, J. A. *Coord. Chem. Rev.* **1999,** *190-192*, 587-605.

117. Curran, D. P.; Hadida, S.; Studer, A.; He, M.; Kim, S.-Y.; Luo, Z.; Larhed, M.; Hallberg, A.; Linclau, B. *Comb. Chem.* **2000**, 327-352.

118. Gladysz, J. A.; Emnet, C. “Fluorous solvents and related media”; In *Handbook of Fluorous Chemistry;* Gladysz, J. A.; Curran, D. P.; Horvath, I. T. Eds.; Wiley: New York, 2004; pp. 11-23.

119. Gladysz, J. A.; Emnet, C.; Rabai, J. “Partition coefficients involving fluorous solvents”; In *Handbook of Fluorous Chemistry;* Gladysz, J. A.; Curran, D. P.; Horvath, I. T. Eds.; Wiley: New York, 2004; pp. 56-100.

120. Metrangolo, P.; Pilati, T.; Resnati, G.; Stevenazzi, A. *Curr. Op. Colloid Interface Sci.* **2003,** *8*, 215-222.

121. Rocaboy, C.; Rutherford, D.; Bennett, B. L.; Gladysz, J. A. *J. Phys. Org. Chem.* **2000,** *13*, 596-603.

122. Studer, A.; Hadida, S.; Ferritto, R.; Kim, S.-Y.; Jeger, P.; Wipf, P.; Curran, D. P. *Science* **1997,** *275*, 823-826.

123. Studer, A.; Jeger, P.; Wipf, P.; Curran, D. P. *J. Org. Chem.* **1997,** *62*, 2917-2924.

124. Curran, D. P.; Ferritto, R.; Hua, Y. *Tetrahedron Lett.* **1998,** *39*, 4937-4940.

125. Zhang, Q.; Luo, Z.; Curran, D. P. *J. Org. Chem.* **2000,** *65*, 8866-8873.

126. Curran, D. P. *Pure and Applied Chemistry* **2000,** *72*, 1649-1653.

127. Curran, D. P. “Light fluorous chemistry-a user's guide”; In *Handbook of Fluorous Chemistry;* Gladysz, J. A.; Curran, D. P.; Horvath, I. T. Eds.; Wiley, 2004; pp. 128-155.

128. Curran, D. P.; Hadida, S.; He, M. *J. Org. Chem.* **1997,** *62*, 6714-6715.

129. Curran, D. P.; Luo, Z.; Degenkolb, P. *Bioorg. Med. Chem. Let.* **1998,** *8*, 2403-2408.

130. Curran, D. P.; Luo, Z. *J. Am. Chem. Soc.* **1999,** *121*, 9069-9072.

131. Thurman, E. M.; Mills, M. S. *Solid-Phase Extraction: Principles and Practice.*; Wiley: New York, 1998.

132. Neue, U. D.; Mallet, C. R.; Lu, Z.; Cheng, Y.-F.; Mazzeo, J. R. *Handbook of Analytical Separations* **2003,** *4*, 73-90.

133. Ye, L. *Molec. Imp. Mater.* **2005**, 603-618.

134. Guenu, S.; Hennion, M.-C. *J. Chromatogr.* **1996,** *737*, 15-24.

135. Stella, C.; Rudaz, S.; Veuthey, J. L.; Tchapla, A. *Chromatographia* **2001,** *53*, S113-S131.

136. Stella, C.; Rudaz, S.; Veuthey, J. L.; Tchapla, A. *Chromatographia* **2001,** *53*, S132-S140.

137. Berendsen, G. E.; Pikaart, K. A.; De Galan, L.; Olieman, C. *Anal. Chem.* **1980,** *52*, 1990-3.

138. Berendsen, G. E.; De Galan, L. *J. Liquid Chromatogr.* **1978,** *1*, 403-426.

139. De Miguel, I.; Exbrayat, S.; Samain, D. *Chromatographia* **1987,** *24*, 849-53.

140. Berendsen, G. E.; De Galan, L. *J. Chromatogr.* **1980,** *196*, 21-37.

141. ftp://ftp.fluorous.com/FTIprimer.pdf. Fluorous Technologies Inc., 2005.

142. Billiet, H. A. H.; Schoenmakers, P. J.; De Galan, L. *J. Chromatogr.* **1981,** *218*, 443-54.

143. Varughese, P.; Gangoda, M. E.; Gilpin, R. K. *J. Chromatograpic Sci.* **1988,** *26*, 401-5.

144. Danielson, N. D.; Beaver, L. G.; Wangsa, J. *J. Chromatogr.* **1991,** *544*, 187-99.

145. Kamiusuki, T.; Monde, T.; Nakayama, N.; Yano, K.; Yoko, T.; Konakahara, T. *J. Colloid Interface Sci.* **1999,** *220*, 123-127.

146. McGuffin, V. L. *J. Chromatography. Lib.* **2004,** *69A*, 1-93.

147. Luo, Z.; Williams, J.; Read, R. W.; Curran, D. P. *J. Org. Chem.* **2001,** *66*, 4261-4266.

148. Evans, D. A.; Vogel, E.; Nelson, J. V. *J. Am. Chem. Soc.* **1979,** *101*, 6120-6123.

149. Evans, D. A.; Nelson, J. V.; Vogel, E.; Taber, T. R. *J. Am. Chem. Soc.* **1981,** *103*, 3099-3111.

150. Evans, D. A.; Takacs, J. M.; McGee, L. R.; Ennis, M. D.; Mathre, D. J.; Bartroli, J. *Pure and Applied Chemistry* **1981,** *53*, 1109-27.

151. Inoue, T.; Mukaiyama, T. *Bull. Chem. Soc. Jpn.* **1980,** *53*, 174-8.

152. Van Draanen, N. A.; Arseniyadis, S.; Crimmins, M. T.; Heathcock, C. H. *J. Org. Chem.* **1991,** *56*, 2499-2506.

153. Vaino, A. R.; Janda, K. D. *J. Comb. Chem.* **2000,** *2*, 579-596.

154. Zimmerman, H. E.; Traxler, M. D. *J. Am. Chem. Soc.* **1957,** *79*, 1920-1923.

155. Nerz-Stormes, M.; Thornton, E. R. *J. Org. Chem.* **1991,** *56*, 2489-2498.

156. Crimmins, M. T.; She, J. *Synlett* **2004**, 1371-1374.

157. Crimmins, M. T.; King, B. W.; Tabet, E. A.; Chaudhary, K. *J. Org. Chem.* **2001,** *66*, 894-902.

158. Nicolaou, K. C.; Vourloumis, D.; Winssinger, N.; Baran, P. S. *Angew. Chem., Int. Ed. Engl.* **2000,** *39*, 44-122.

159. Evans, D. A.; Ratz, A. M.; Huff, B. E.; Sheppard, G. S. *J. Am. Chem. Soc.* **1995,** *117*, 3448-3467.

160. Evans, D. A.; Hu, E.; Burch Jason, D.; Jaeschke, G. *J. Am. Chem. Soc.* **2002,** *124*, 5654-5655.

161. Evans, D. A.; Carter, P. H.; Carreira, E. M.; Charette, A. B.; Prunet, J. A.; Lautens, M. *J. Am. Chem. Soc.* **1999,** *121*, 7540-7552.

162. Sibi, M. P.; Manyem, S.; Zimmerman, J. *Chem. Rev.* **2003,** *103*, 3263-3295.

163. Curran, D. P.; Porter, N. A.; Giese, B. *Heterocycles* **1996,** *43*, 936.

164. Zhang, W. *Tetrahedron* **2001,** *57*, 7237-7262.

165. Leonard, J.; Dıez-Barra, E.; Merino, S. *Eur. J. Org. Chem.* **1998**, 2051-2061.

166. Christoffers, J.; Baro, A. *Angew. Chem., Int. Ed. Engl.* **2003,** *42*, 1688-1690.

167. Bar, G.; Parsons, A. F. *Chem. Soc. Rev.* **2003,** *32*, 251-263.

168. Sibi, M. P.; Manyem, S. *Tetrahedron* **2000,** *56*, 8033-8061.

169. Sibi, M. P.; Liu, P.; Ji, J.; Hajra, S.; Chen, J.-X. *J. Org. Chem.* **2002,** *67*, 1738-1745.

170. Sibi, M. P.; He, L. *Org. Lett.* **2004,** *6*, 1749-1752.

171. Sibi, M. P.; Manyem, S. *Org. Lett.* **2002,** *4*, 2929-2932.

172. Minakata, S.; Ezoe, T.; Nakamura, K.; Ryu, I.; Komatsu, M. *Tetrahedron Lett.* **1998,** *39*, 5205-5208.

173. Sibi, M. P.; Jasperse, C. P.; Ji, J. *J. Am. Chem. Soc.* **1995,** *117*, 10779-10780.

174. Sibi, M. P.; Ji, J.; Sausker, J. B.; Jasperse, C. P. *J. Am. Chem. Soc.* **1999,** *121*, 7517-7526.

175. Sibi, M. P.; Ji, J.; Wu, J. H.; Guertler, S.; Porter, N. A. *J. Am. Chem. Soc.* **1996,** *118*, 9200-9201.

176. Giese, B.; Harnisch, H.; Lachhein, S. *Synthesis* **1983**, 733.

177. Crich, D.; Davies, J. W. *Tetrahedron Lett.* **1987,** *28*, 4205-8.

178. Sibi, M. P.; Ji, J. *J. Am. Chem. Soc.* **1996,** *118*, 9200-9201.

179. Baguley, P. A.; Walton, J. C. *Angew. Chem., Int. Ed. Engl.* **1998,** *37*, 3072-3082.

180. Parsons, A. *Chem. Brit.* **2002,** *38*, 42-44.

181. Chatgilialoglu, C. *Acc. Chem. Res.* **1992,** *25*, 188-194.

182. Graham, S. R.; Murphy, J. A.; Kennedy, A. R. *J. Chem. Soc., Perkin Trans. 1* **1999**, 3071-3073.

183. Khan, T. A.; Tripoli, R.; Crawford, J. J.; Martin, C. G.; Murphy, J. A. *Org. Lett.* **2003,** *5*, 2971-2974.

184. Studer, A.; Amrein, S.; Schleth, F.; Schulte, T.; Walton, J. C. *J. Am. Chem. Soc.* **2003,** *125*, 5726-5733.

185. Harrowven, D. C.; Guy, I. L. *Chem. Commun.* **2004**, 1968-1969.

186. Curran, D. P.; Hadida, S.; Kim, S.-Y.; Luo, Z. *J. Am. Chem. Soc.* **1999,** *121*, 6607-6615.

187. Curran, D. P.; Hadida, S. *J. Am. Chem. Soc.* **1996,** *118*, 2531-2532.

188. Crombie, A.; Kim, S.-Y.; Hadida, S.; Curran, D. P. *Organic Syntheses* **2003,** *79*, 1-10.

189. Torssell, K. B. G. *Nitrile Oxides, Nitrones, and Nitronates in Organic Synthesis. Novel Strategies in Synthesis*; VHC, 1988.

190. Frederickson, M. *Tetrahedron* **1997,** *53*, 403-425.

191. Gothelf, K. V.; Jørgensen, K. A. *Chem. Commum.* **2000**, 1449-1458.

192. Kaliappan, K. P.; Das, P.; Kumar, N. *Tetrahedron Lett.* **2005,** *46*, 3037-3040.

193. Ihara, M.; Takahashi, M.; Fukumoto, K.; Kametani, T. *J. Chem. Soc., Perkin Trans. 1* **1989**, 2215-2221.

194. Murahashi, S.; Imada, Y.; Kohno, M.; Kawakami, T. *Synlett* **1993**, 395-396.

195. Gothelf, K. V.; Hazell, R. G.; Jørgensen, K. A. *J. Org. Chem.* **1998,** *63*, 5483-5488.

196. Kobayashi, S.; Kawamura, M. *J. Am. Chem. Soc.* **1998,** *120*, 5840-5841.

197. Gothelf, K. V.; Jørgensen, K. A. *Chem. Rev.* **1998,** *98*, 863-909.

198. Dugovic, B.; Fisera, L.; Cyranski, M. K.; Hametner, C.; Pronayova, N.; Obranec, M. *Helv. Chim. Acta* **2005,** *88*, 1432-1443.

199. Gothelf, K. V.; Joergensen, K. A. *J. Org. Chem.* **1994,** *59*, 5687-5691.

200. Gothelf, K. V.; Joergensen, K. A. *J. Chem. Soc., Perkin Trans. 2* **1997**, 111-115.

201. Gothelf, K. V.; Hazell, R. G.; Jørgensen, K. A. *J. Org. Chem.* **1996,** *61*, 346-355.

202. Gothelf, K. V.; Thomsen, I.; Jørgensen, K. A. *J. Am. Chem. Soc.* **1996,** *118*, 59-64.

203. Burton, D. J.; Lu, L. *Top. Current Chem.* **1997,** *193*, 45-89.

204. Burton, D. J.; Yang, Z. Y. *Tetrahedron* **1992,** *48*, 189-275.

205. Sibi, M. P.; Rutherford, D.; Sharma, R. *J. Chem. Soc., Perkin Trans. 1* **1994**, 1675-1678.

206. Hoffman, R. V.; Maslouh, N.; Cervantes-Lee, F. *J. Org. Chem.* **2002,** *67*, 1045-1056.

207. Zlatoidsky, P. *Tetrahedron Lett.* **1995,** *36*, 7281-4.

208. Cupps, T. L.; Boutin, R. H.; Rapoport, H. *J. Org. Chem.* **1985,** *50*, 3972-3979.

209. Boutin, R. H.; Rapoport, H. *J. Org. Chem.* **1986,** *51*, 5320-5327.

210. So, R. C.; Ndonye, R.; Izmirian, D. P.; Richardson, S. K.; Guerrera, R. L.; Howell, A. R. *J. Org. Chem.* **2004,** *69*, 3233-3235.

211. Sibi, M. P.; Ma, Z.; Jasperse, C. P. *J. Am. Chem. Soc.* **2004,** *126*, 718-719.

212. Jensen, K.; Gothelf, K. V.; Hazell, R. G.; Jørgensen, K. A. *J. Org. Chem.* **1997,** *62*, 2471-2477.

213. Gopal, H.; Tamborski, C. *J. Fluorine Chem.* **1979,** *13*, 337-351.

214. Gassman, P. G.; O'Reilly, N. J. *Tetrahedron Lett.* **1985,** *26*, 5243-5246.

215. Uno, H.; Shiraishi, Y.; Simokawa, K.; Suzuki, H. *Chem. Let.* **1987**, 1153-1156.

216. Uno, H.; Suzukib, H. *Synlett* **1993**, 91-6.

217. Uno, H.; Shiraishi, Y.; Suzuki, H. *Bull. Chem. Soc. Jpn.* **1989,** *62*, 2636-2642.

218. Chen, L. S.; Chen, G. J.; Tamborski, C. *J. Fluorine Chem.* **1984,** *26*, 341-58.

219. Richter, B.; de Wolf, E.; van Koten, G.; Deelman, B.-J. *J. Org. Chem.* **2000,** *65*, 3885-3893.

220. Kottke, T.; Stalke, D. *Angew. Chem., Int. Ed. Engl.* **1993,** *32*, 580-582.

221. Gossage, R. A.; Jastrzebski, J. T. B. H.; van Koten, G. *Angew. Chem., Int. Ed. Engl.* **2005,** *44*, 1448-1454.

222. Pratt, L. M. *Mini-Rev. Org. Chem.* **2004,** *1*, 209-217.

223. Ewin, R. A.; MacLeod, A. M.; Price, D. A.; Simpkins, N. S.; Watt, A. P. *J. Chem. Soc., Perkin Trans. 1* **1997**, 401-415.

224. Uno, H.; Shiraishi, Y.; Shimokawa, K.; Suzuki, H. *Chem. Let.* **1988**, 729-732.

225. Johnson, M. R.; Rickborn, B. *J. Org. Chem.* **1970,** *35*, 1041-1045.

226. Mathur, V.; Kanoongo, N.; Mathur, R.; Narang, C. K.; Mathur, N. K. *J. Chromatogr.* **1994,** *685*, 360-4.

227. Ishihara, K.; Funahashi, S.; Tanaka, M. *Inorg. Chem.* **1986,** *25*, 2898-2901.

228. Gladysz, J. A. “Ponytails: structural and electronic considerations”; In *Handbook of Fluorous Chemistry;* Gladysz, J. A.; Curran, D. P.; Horvath, I. T. Eds.; Wiley: New York, 2004; pp. 41-55.

229. Kruse, C. H.; Holden, K. G. *J. Org. Chem.* **1985,** *60*, 2792-2794.

230. Edmonds, M. K.; Abell, A. D. *J. Org. Chem.* **2001,** *66*, 3747-3752.

231. You, J.; Wróblewski, A. E.; Verkade, J. G. *Tetrahedron* **2004,** *60*, 7877-7883.

232. Lewis, N.; McKillop, A.; Taylor, R. J. K.; Watson, R. J. *Synth. Commun.* **1995,** *25*, 561-568.

233. Legros, J.; Crousse, B.; Bourdon, J.; Bonnet-Delpon, D.; Begue, J.-P. *Tetrahedron Lett.* **2001,** *42*, 4463-4466.

234. Legros, J.; Crousse, B.; Bonnet-Delpon, D.; Begue, J.-P. *Tetrahedron* **2002,** *58*, 3993-3998.

235. Bauer, W.; Winchester, W. R.; Schleyer, P. v. R. *Organometallics* **1987,** *6*, 2371-2379.

236. McGarrity, J. F.; Ogle, C. A. *J. Am. Chem. Soc.* **1985,** *107*, 1805-1810.

237. Brown, T. L. *Pure and Applied Chemistry* **1970,** *23*, 447-62.

238. Peascoe, W.; Applequist, D. E. *J. Org. Chem.* **1973,** *38*, 1510-1512.

239. Singh, J.; Satyamurthi, N.; Aidhen, I. S. *J. Praktische Chem.* **2000,** *342*, 340-347.

240. Angelastro, M. R.; Peet, N. P.; Bey, P. *J. Org. Chem.* **1989,** *54*, 3913-3916.

241. Benetti, S.; De Risi, C.; Marchetti, P.; Pollini, G. P.; Zanirato, V. *Synthesis* **2002**, 331-338.

242. Morita, J.-I.; Nakatsuji, H.; Misaki, T.; Tanabe, Y. *Green Chemistry* **2005,** *7*, 711-715.

243. Acton, J. J., III; Adams, A. D.; Hermes, J. D.; Jones, A. B.; Parsons, W. H.; Sinclair, P. J.*;* US Ed.; Merck and Co., Inc.: US, 1998; p. 38.

244. De Luca, L.; Giacomelli, G.; Taddei, M. *J. Org. Chem.* **2001,** *66*, 2534-2537.

245. Sibi, M. P.; Stessman, C. C.; Schultz, J. A.; Christensen, J. W.; Lu, J.; Marvin, M. *Synth. Commun.* **1995,** *25*, 1255-64.

246. Liu, J.; Ikemoto, N.; Petrillo, D.; Armstrong, J. D., III. *Tetrahedron Lett.* **2002,** *43*, 8223-8226.

247. Walborsky, H. M.; Hornyak, F. M. *J. Am. Chem. Soc.* **1955,** *77*, 6026-6029.

248. Walker, M. A.; Heathcock, C. H. *J. Org. Chem.* **1991,** *56*, 5747-5750.

249. Rychnovsky, S. D.; Buckmelter, A. J.; Dahanukar, V. H.; Skalitzky, D. J. *J. Org. Chem.* **1999,** *64*, 6849-6860.

250. Evans, D. A.; Rieger, D. L.; Jones, T. K.; Kaldor, S. W. *J. Org. Chem.* **1990,** *55*, 6260-6268.

251. Pettit, G. R.; Burkett, D. D.; Barkoczy, J.; Breneman, G. L.; Pettit, W. E. *Synthesis* **1996**, 719-725.

252. Wu, Y.; Shen, X.; Tang, C.-J.; Chen, Z.-L. *Helv. Chim. Acta* **2001,** *84*, 3428-3432.

253. Sibi, M. P.; Porter, N. A. *Acc. Chem. Res.* **1999,** *32*, 163-171.

254. Enders, D.; Rendenbach, B. E. M. *Tetrahedron* **1986,** *42*, 2235-42.

255. Lawston, I. W.; Inch, T. D. *J. Chem. Soc., Perkin Trans. 1* **1983**, 2629-35.

256. Rose, M.; Knaggs, M.; Owen, L.; Baxter, M. *J. Anaytical Atom. Spec.* **2001,** *16*, 1101-1106.

257. Skoog, D. A.; Holler, F. J.; Nieman, T. A. *Principles of Instrumental Analysis*, 5th ed.; Harcourt Brace & Company: Toronto, 1998.

258. Simonsen, K. B.; Bayon, P.; Hazell, R. G.; Gothelf, K. V.; Jørgensen, K. A. *J. Am. Chem. Soc.* **1999,** *121*, 3845-3853.

259. Kawamura, M.; Kobayashi, S. *Tetrahedron Lett.* **1999,** *40*, 3213-3216.

260. Hein, J. E.; Geary, L. M.; Jaworski, A. A.; Hultin, P. G. *J. Org. Chem.* **2005,** *70*, 9940-9946.

261. Hein, J. E.; Hultin, P. G. *Synlett* **2003**, 635-638.

262. Hein, J. E.; Zimmerman, J.; Sibi, M. P.; Hultin, P. G. *Org. Lett.* **2005,** *7*, 2755-2758.

263. Hein, J. E.; Hultin, P. G. *Tetrahedron: Asymmetry* **2005,** *16*, 2341-2347.

264. Glase, S. A.; Robertson, D. W.; Wise, L. D. *Annual Reports in Medicinal Chemistry* **2002,** *37*, 11-20.

265. Schweri, M. M.; Deutsch, H. M.; Massey, A. T.; Holtzman, S. G. *Journal of Pharmacology and Experimental Therapeutics* **2002,** *301*, 527-535.

266. Kim, D.-I.; Ye, X.; Deutsch, H.; Schweri, M. M.; Holtzman, S. G.; Spealman, R. D. *Abstracts of Papers, 223rd ACS National Meeting, Orlando, FL, United States, April 7-11, 2002* **2002**, MEDI-051.

267. Axten, J. M.; Krim, L.; Kung, H. F.; Winkler, J. D. *J. Org. Chem.* **1998,** *63*, 9628-9629.

268. Matsumura, Y.; Kanda, Y.; Shirai, K.; Onomura, O.; Maki, T. *Org. Lett.* **1999,** *1*, 175-178.

269. Deutsch, H. M.; Ye, X.; Shi, Q.; Liu, Z.; Schweri, M. M. *European Journal of Medicinal Chemistry* **2001,** *36*, 303-311.

270. Welch, J. T.; Seper, K. W. *J. Org. Chem.* **1988,** *53*, 2991-9.

271. Saha, A. K.; Rapoport, H.; Schultz, P. *J. Am. Chem. Soc.* **1989,** *111*, 4856-9.

272. Huang, Z.-H.; Wang, J.; Gage, D. A.; Watson, J. T.; Sweeley, C. C.; Husek, P. *J. Chromatogr.* **1993,** *635*, 271-81.

273. Matsuda, F.; Matsumoto, T.; Ohsaki, M.; Ito, Y.; Terashima, S. *Bull. Chem. Soc. Jpn.* **1992,** *65*, 360-365.

274. Evans, D. A.; Mathre, D. J.; Scott, W. L. *J. Org. Chem.* **1985,** *50*, 1830-1835.

275. Kise, N.; Mashiba, S.-I.; Ueda, N. *J. Org. Chem.* **1998,** *63*, 7931-7938.

276. Murakata, M.; Tsutsui, H.; Hoshino, O. *Org. Lett.* **2001,** *3*, 299-302.

NMR SECTION

SpinWorks 2.4: 2(S)-N-(Ethoxycarbonyl)-N'-methoxy-N'-methyl-phenylalaninamide

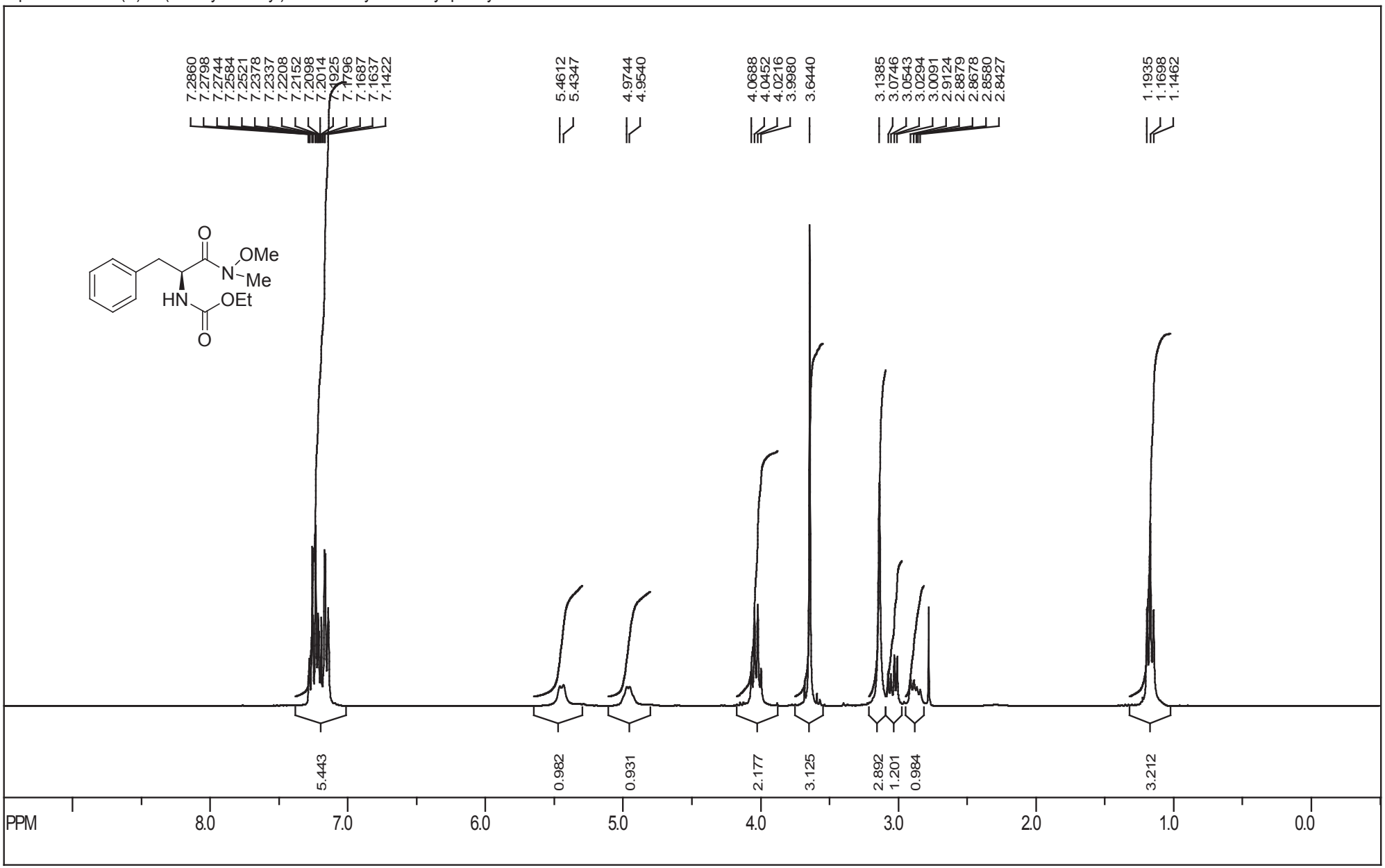

file: C:\NMR\Laina\40-50\lmg43_55\1\fid expt: <zg30>

freq. of 0 ppm: 300.130006 MHz

SpinWorks 2.4: 2(S)-N-(Ethoxycarbonyl)-N'-methoxy-N'-methyl-phenylalaninamide

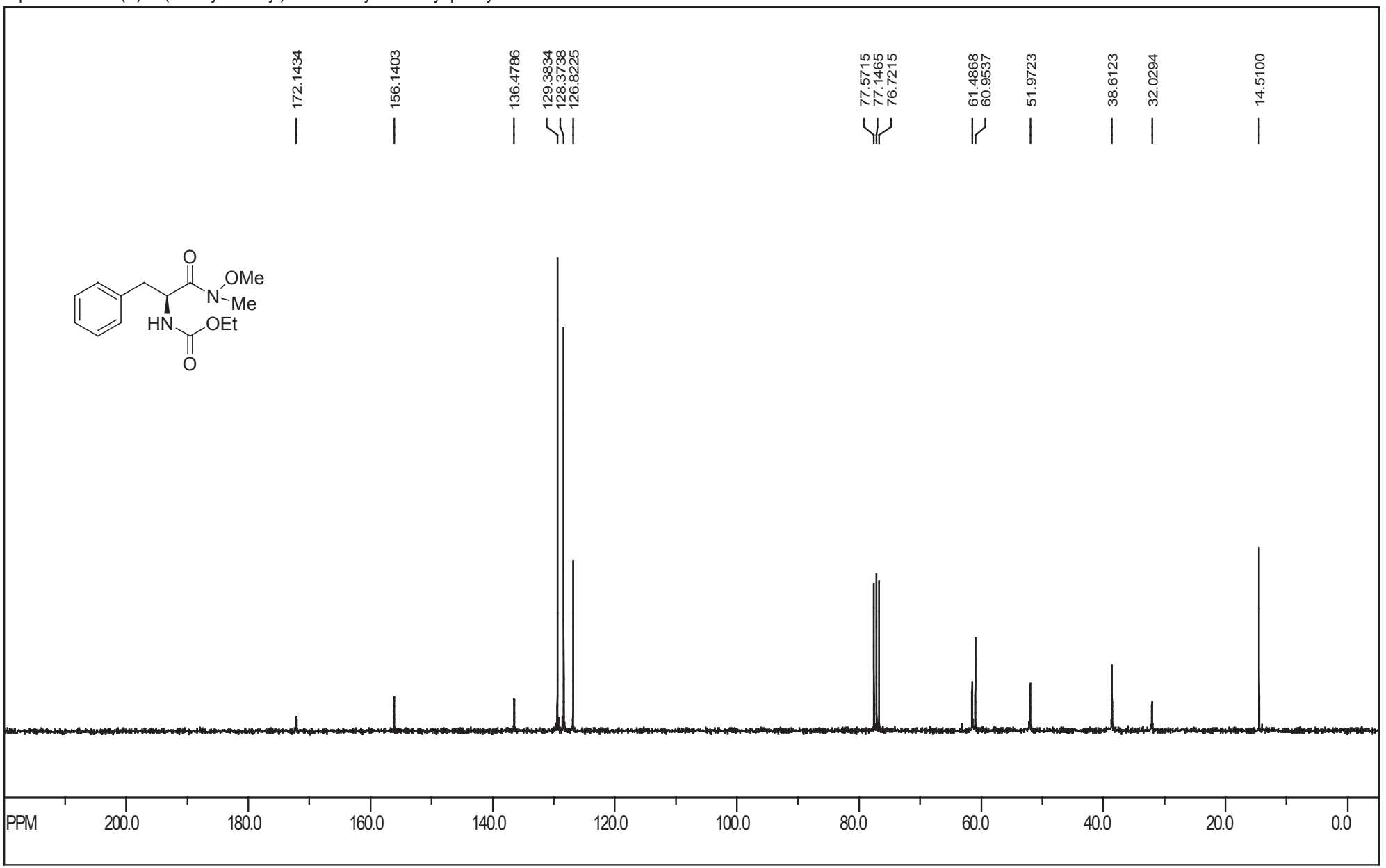

file: C:\NMR\Lainal\40-50\lmg43_55\2\fid expt: <zgpg30>
transmitter freq.: 75.476020 MHz
time domain size: 65536 points
width: 18832.39 Hz = 249.514902 ppm = 0.287359 Hz/pt
number of scans: 512

freq. of 0 ppm: 75.467749 MHz
processed size: 32768 complex points
LB: 0.000 GB: 0.0000

SpinWorks 2.4: 2(S)-N-(tert-Butoxyoxycarbonyl)-N'-methoxy-N'-methyl-valinamide

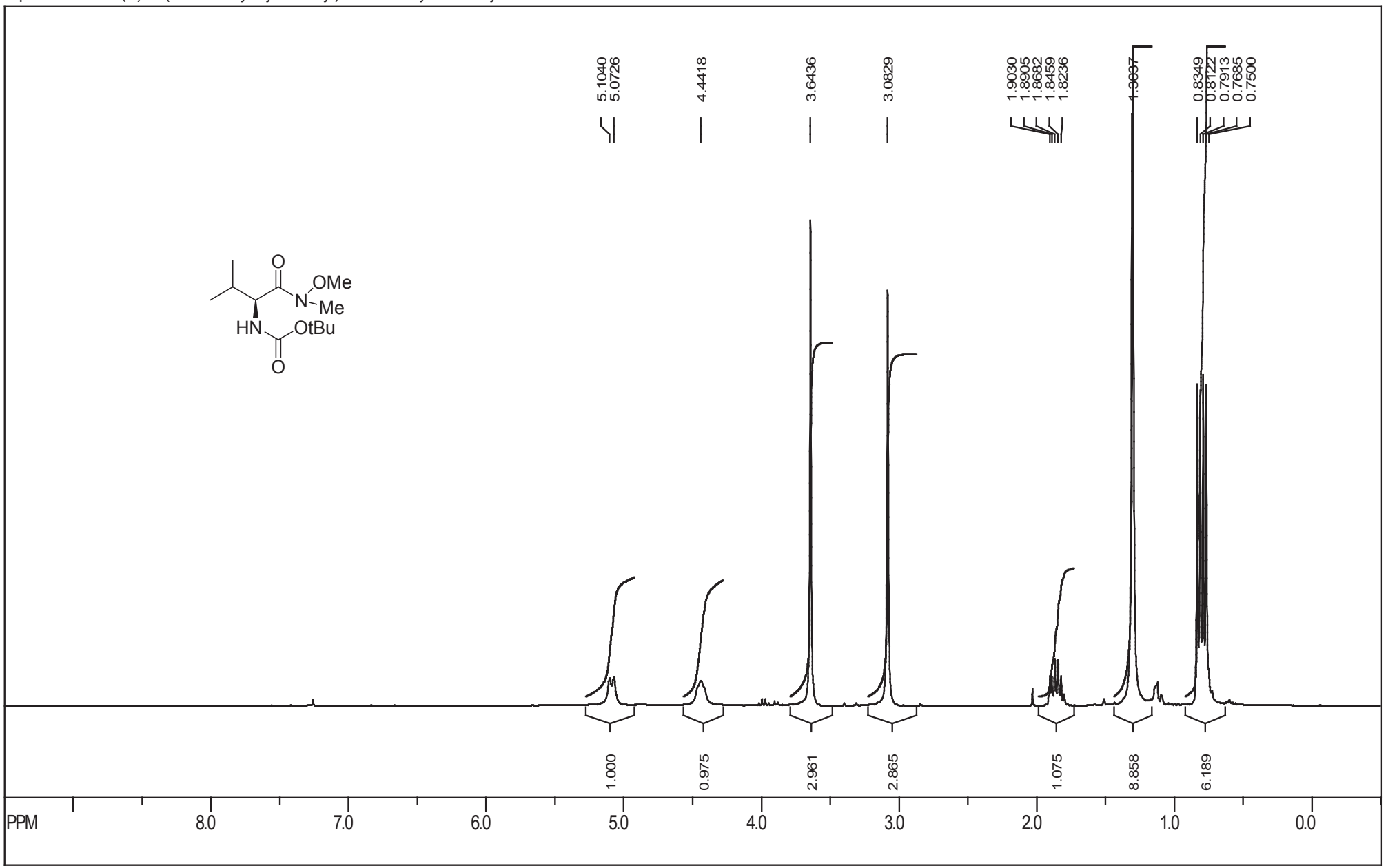

file: C:\NMR\Laina\lmg76\1\fid expt: <zg30>

freq. of 0 ppm: 300.130006 MHz

SpinWorks 2.4: 2(S)-N-(tert-Butoxycarbonyl)-N'-methoxy-N'-methyl-valaninamide

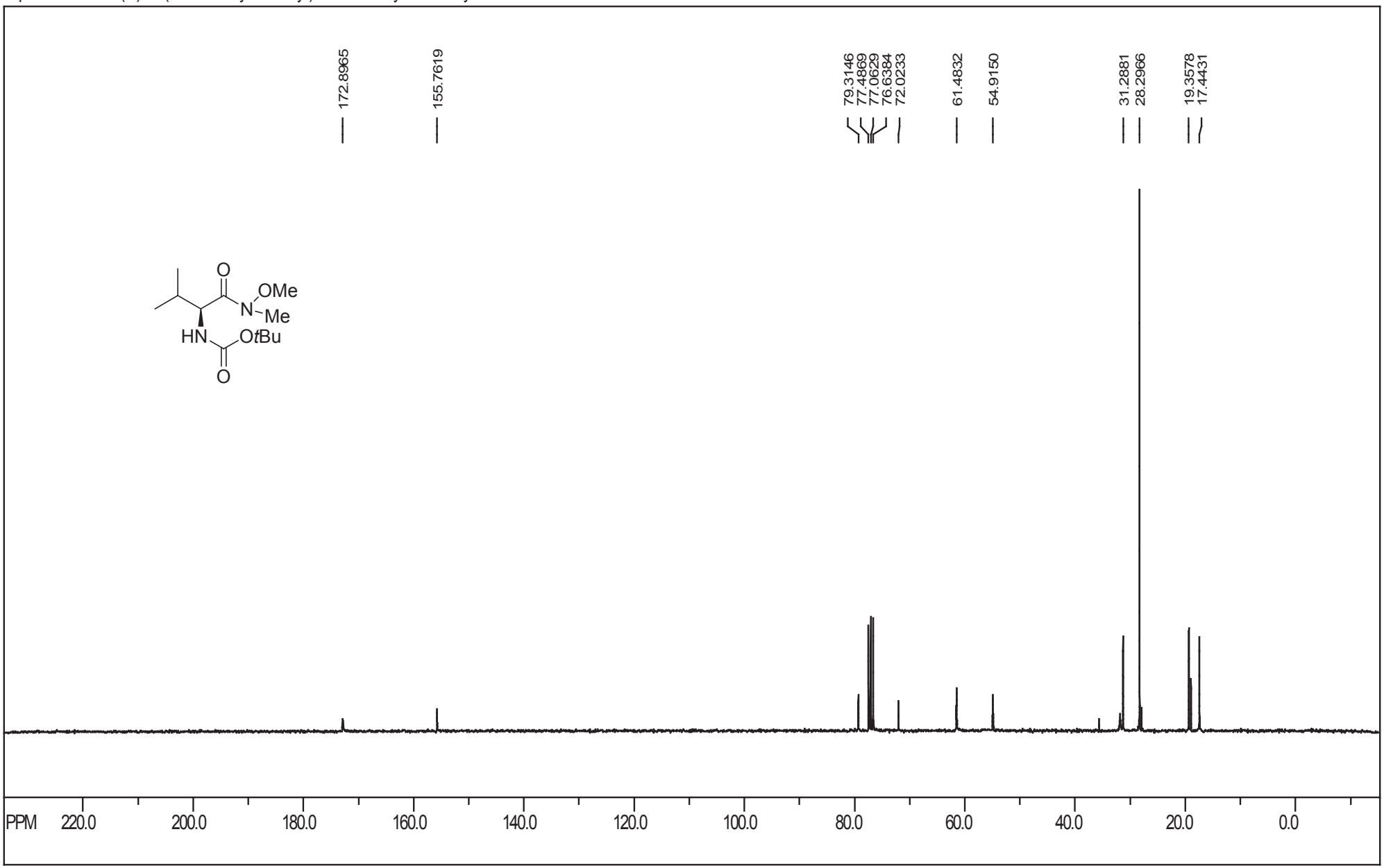

file: C:\NMR\Laina\lmg64\2\fid expt: <zgpg30>

freq. of 0 ppm: 75.467749 MHz

SpinWorks 2.4: 2(R)-N-(tert-Butoxycarbonyl)-N'-methoxy-N'-methyl-phenylglycinamide

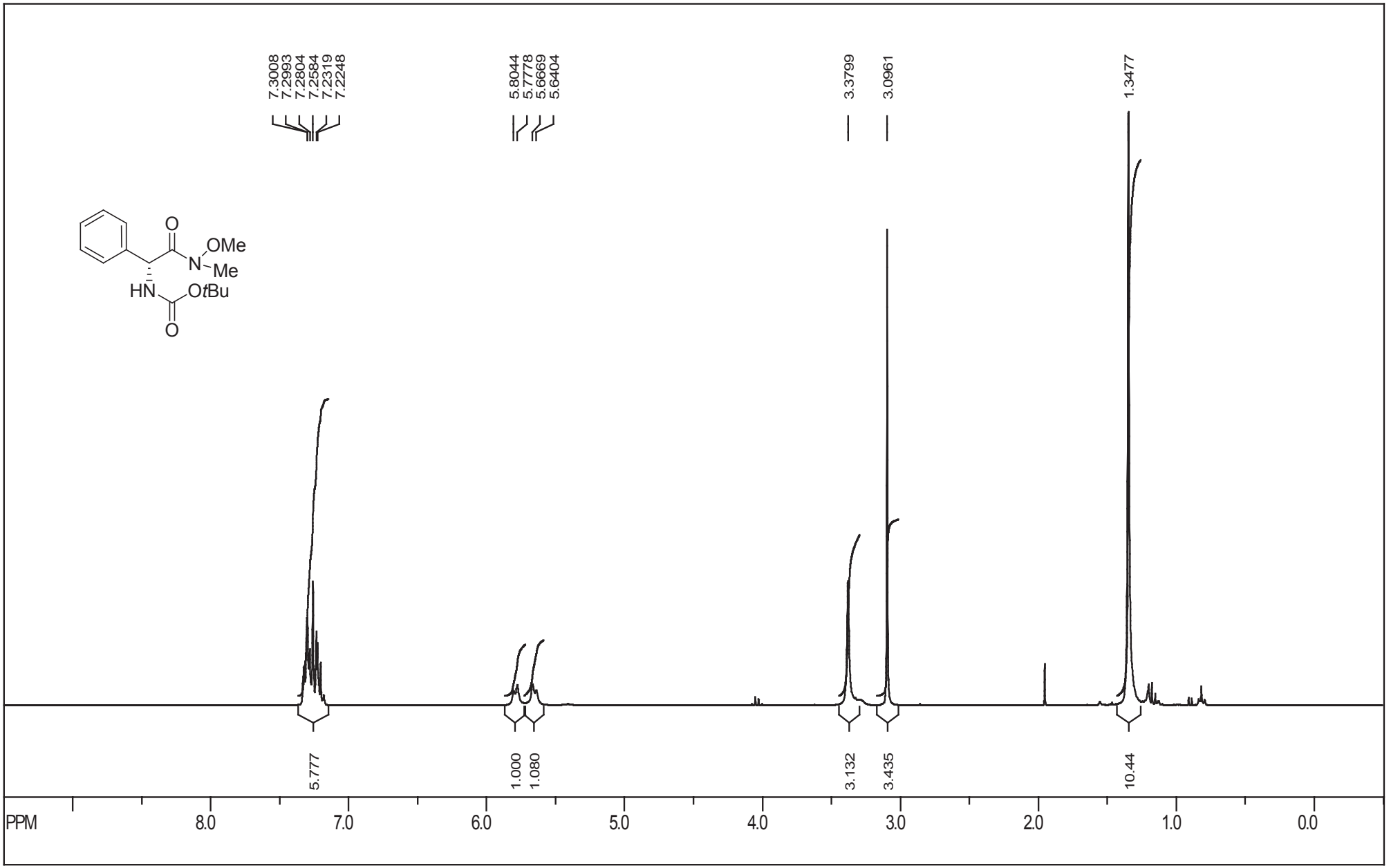

file: C:\NMR\Laina\70-80\lmg75\1\fid expt: <zg30>

freq. of 0 ppm: 300.130006 MHz

SpinWorks 2.4: 2(R)-N-(tert-Butoxycarbonyl)-N'-methoxy-N'-methyl-phenylglycinamide

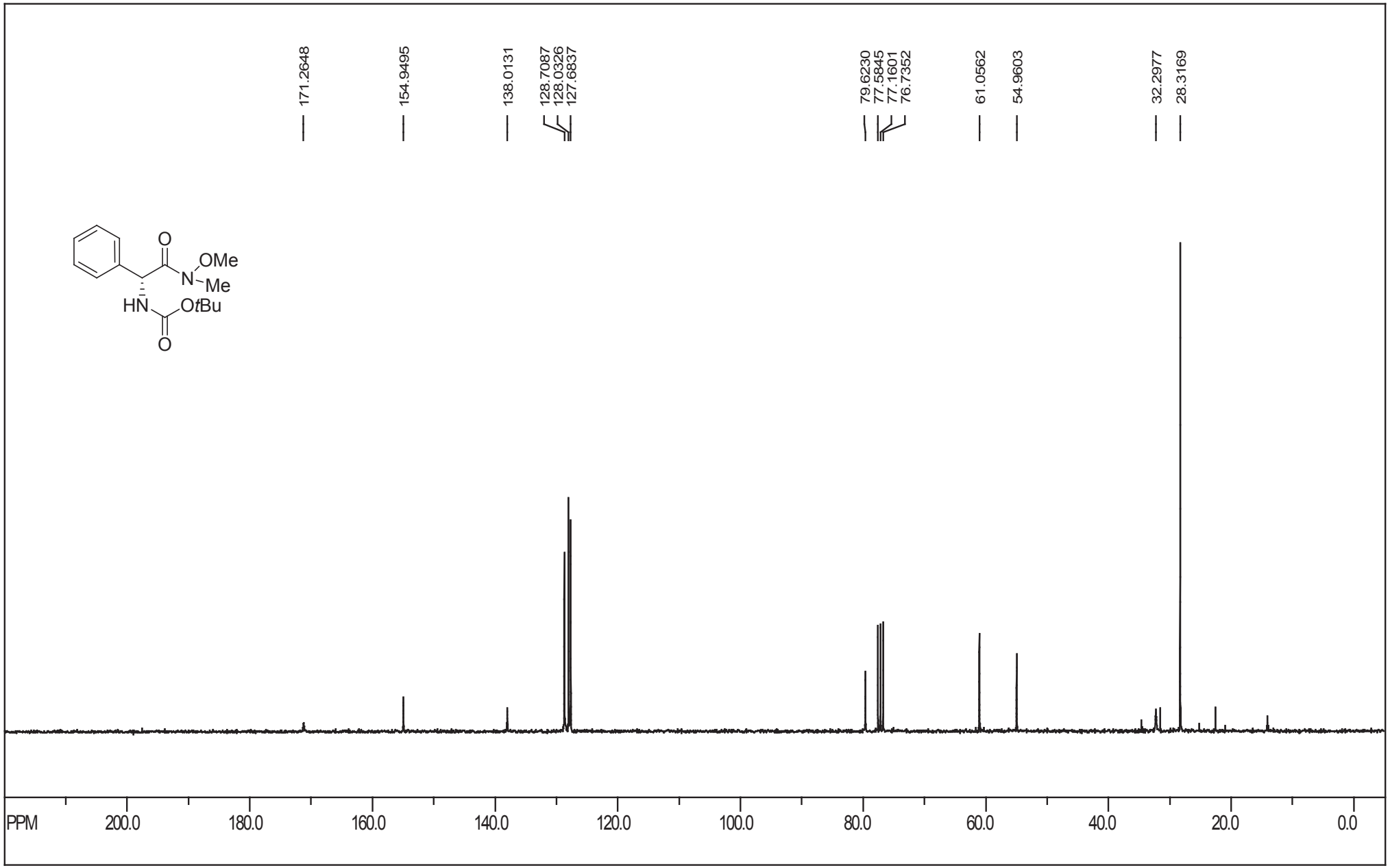

file: C:\NMR\Laina\70-80\lmg74\3\fid expt: <zgpg30>

freq. of 0 ppm: 75.467749 MHz

SpinWorks 2.4: 2(S)-(Ethoxycarbonylamino)-6,6,7,7,8,8,9,9,10,10,11,11,11-tridecafluoro-1-phenyl-undecan-3-one

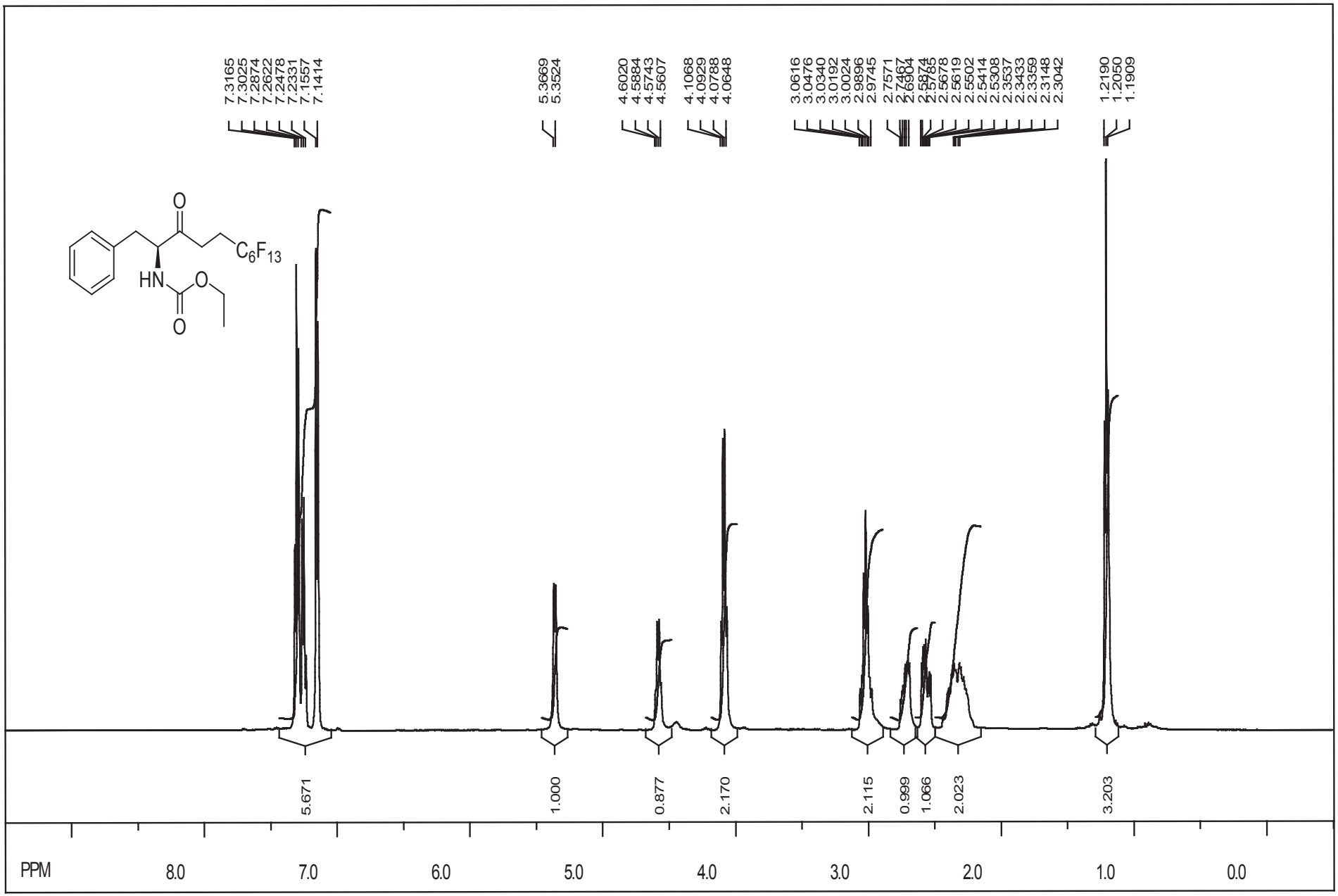

file: C:\NMR\Jehvi_10_1\1\fid expt: <zg30>

SpinWorks 2.4: 2(S)-(Ethoxycarbonylamino)-6,6,7,7,8,8,9,9,10,10,11,11,11-tridecafluoro-1-phenyl-undecan-3-one

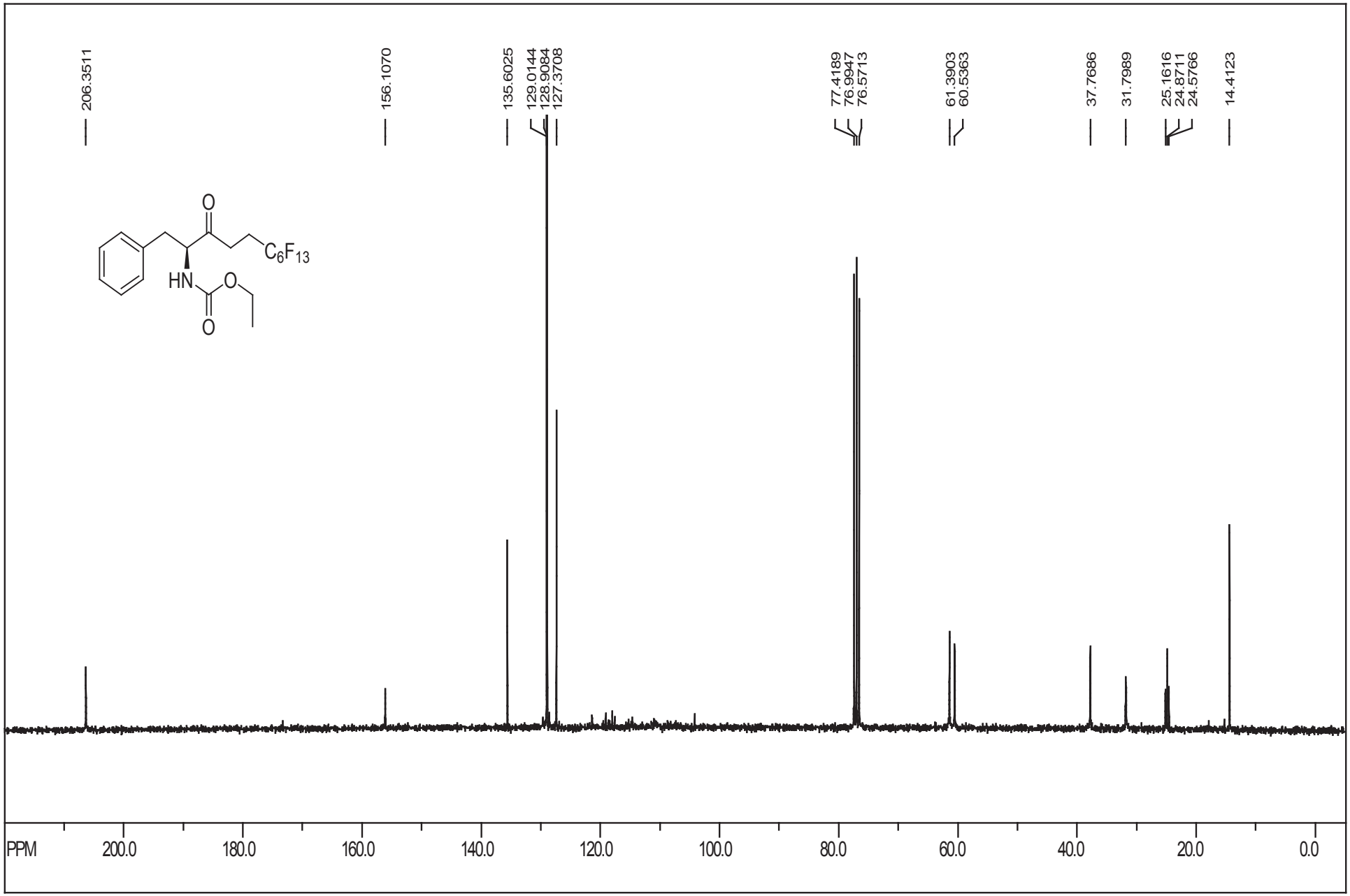

file: C:\NMRJehv_84\7\fid expt: <zgpg30>

SpinWorks 2.4: 3(S)-(tert-Butoxyoxycarbonylamino)-7,7,8,8,9,9,10,10,11,11,12,12,12-tridecafluoro-2-methyl-dodecan-4-one

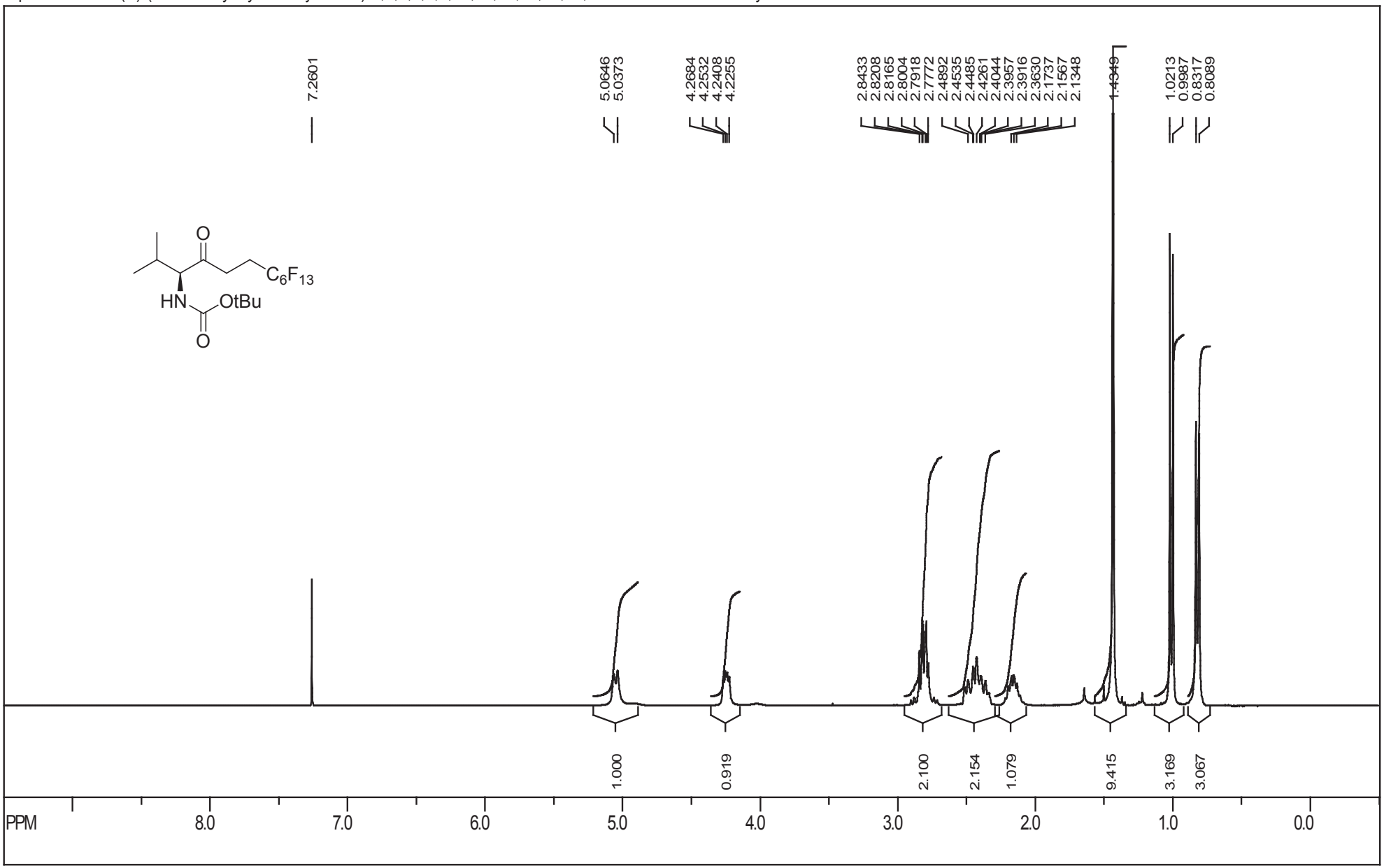

file: C:\NMR\70-80\Jehvi_72a_1b\1\fid expt: <zg30>

freq. of 0 ppm: 300.130006 MHz

SpinWorks 2.4: 3(S)-(tert-Butoxycarbonylamino)- 7,7,8,8,9,9,10,10,11,11,12,12,12-tridecafluoro-2-methyl-dodecan-4-one

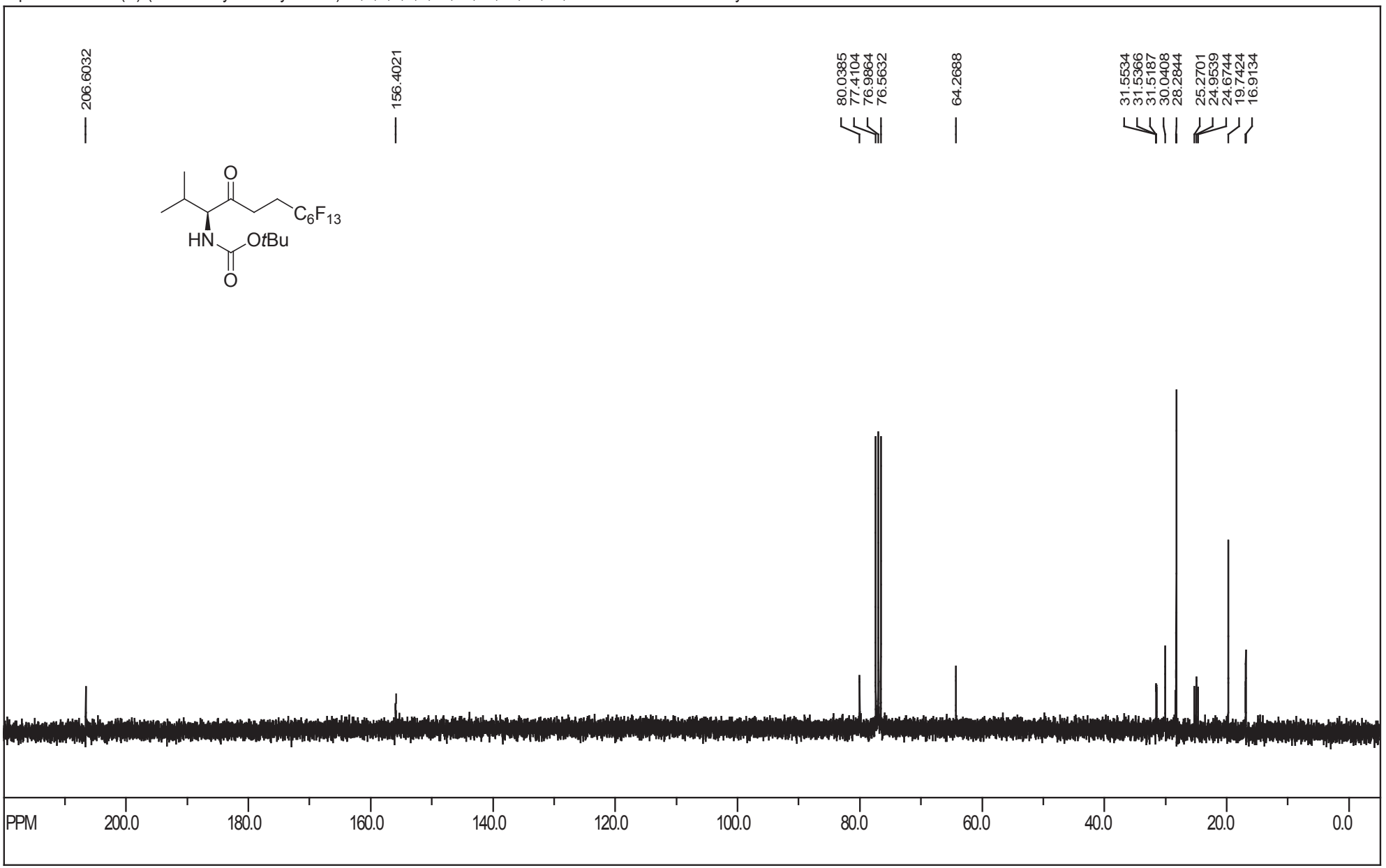

file: C:\NMR\70-80\jehvi_72a_1\6\fid expt: <zgpg30>

freq. of 0 ppm: 75.467749 MHz

SpinWorks 2.4: 1(R)-(tert-Butoxycarbonylamino)-5,5,6,6,7,7,8,8,9,9,10,10,10-tridecafluoro-1-phenyl-decan-2-one

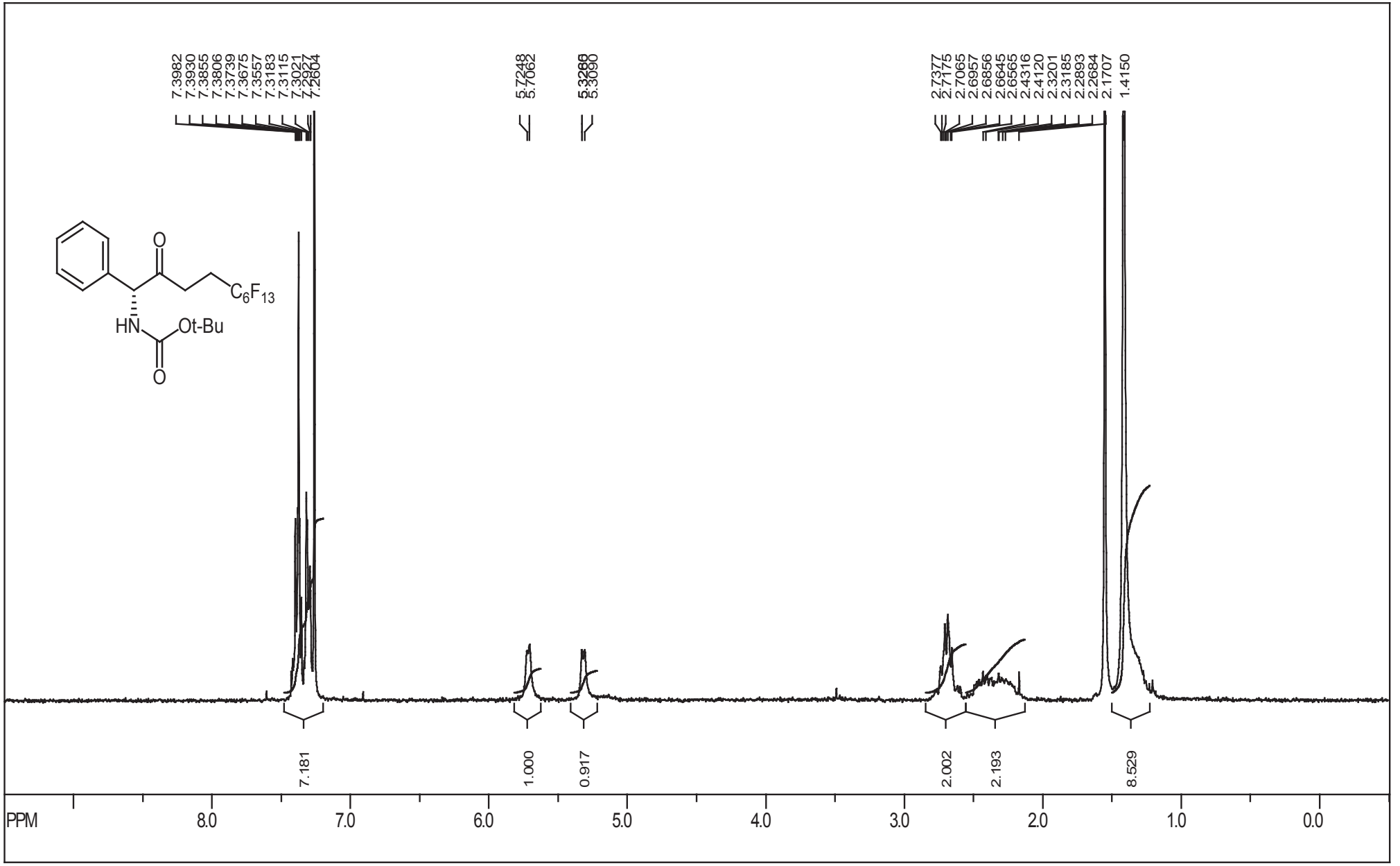

file: C:\NMR\Laina\60-70\lmg66\2\fid expt: <zg30>

freq. of 0 ppm: 300.130006 MHz

SpinWorks 2.4: 1(R)-(tert-Butoxycarbonylamino)-5,5,6,6,7,7,8,8,9,9,10,10,10-tridecafluoro-1-phenyl-decan-2-one

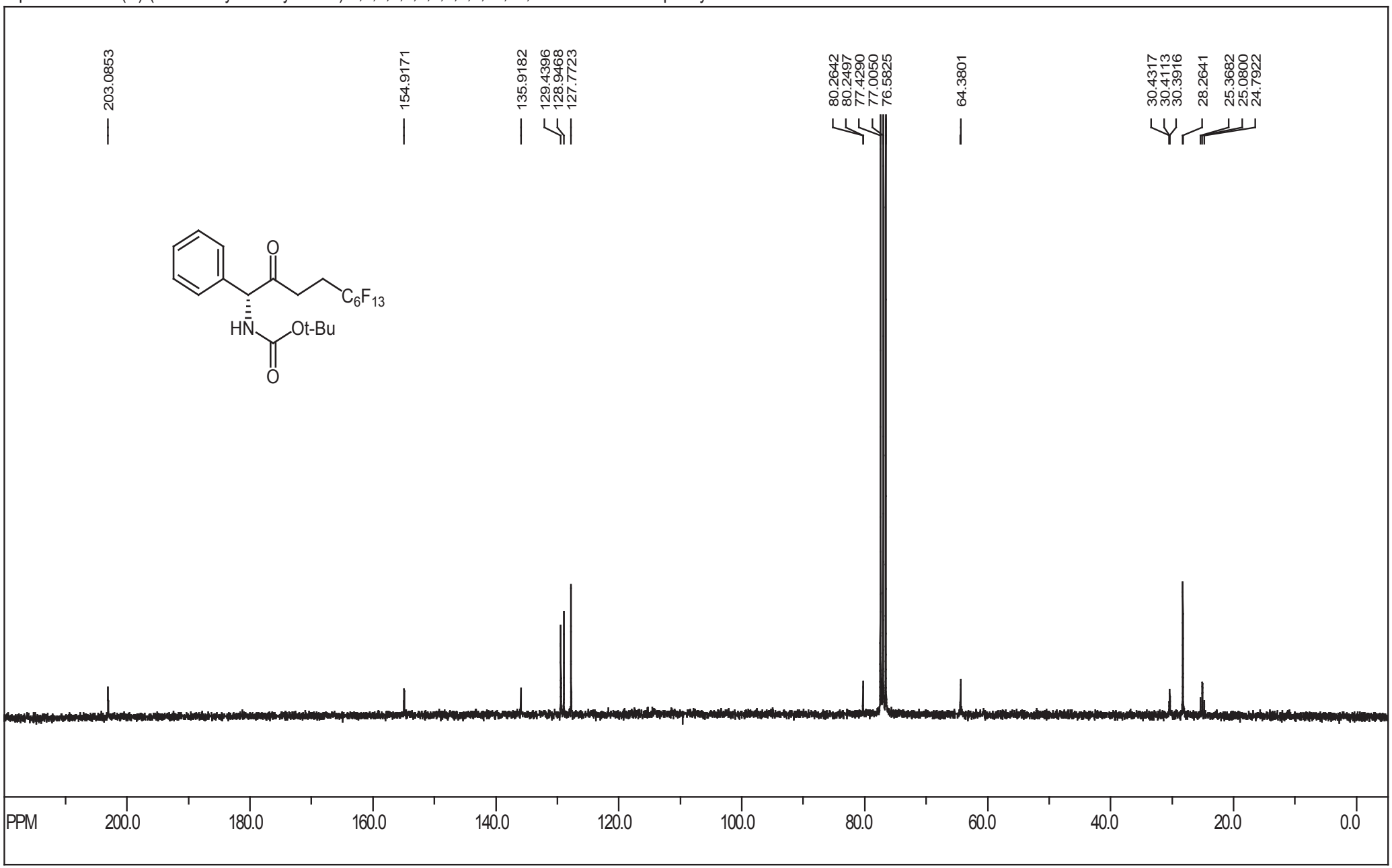

file: C:\NMR\Laina\60-70\lmg66\9\fid expt: <zgpg30>

freq. of 0 ppm: 75.467749 MHz

SpinWorks 2.4: 2(S)-(Ethoxycarbonylamino)-3,3-bis(1H,1H,2H,2H-perfluorooctyl)-1-phenyl-propan-3-ol

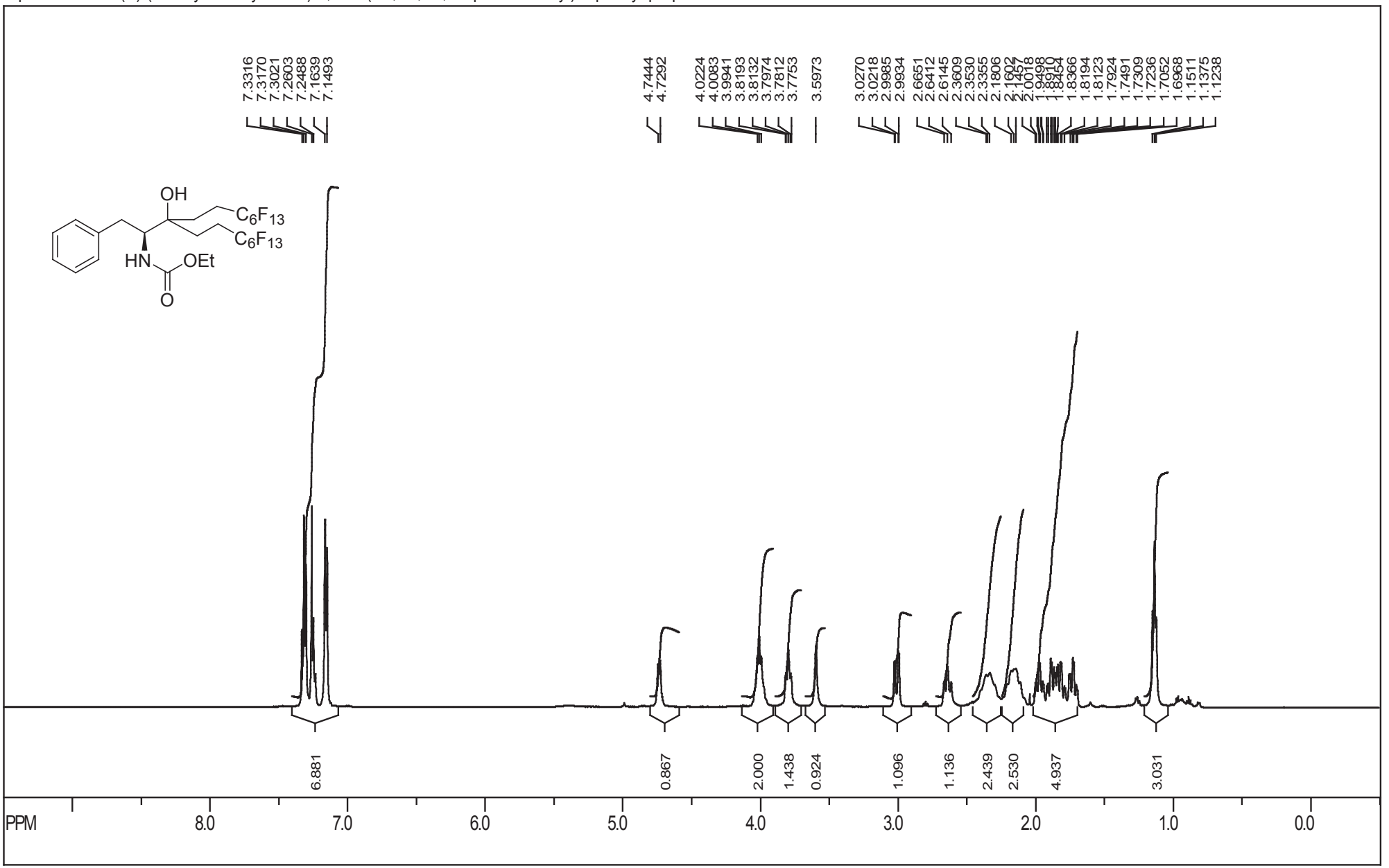

file: C:\NMR\V\80-90\Jehv_84d\1\fid expt: <zg30>

freq. of 0 ppm: 500.135421 MHz

SpinWorks 2.4: 2(S)-(Ethoxycarbonylamino)-3,3-bis(1H,1H,2H,2H-perfluorooctyl)-1-phenyl-propan-3-ol

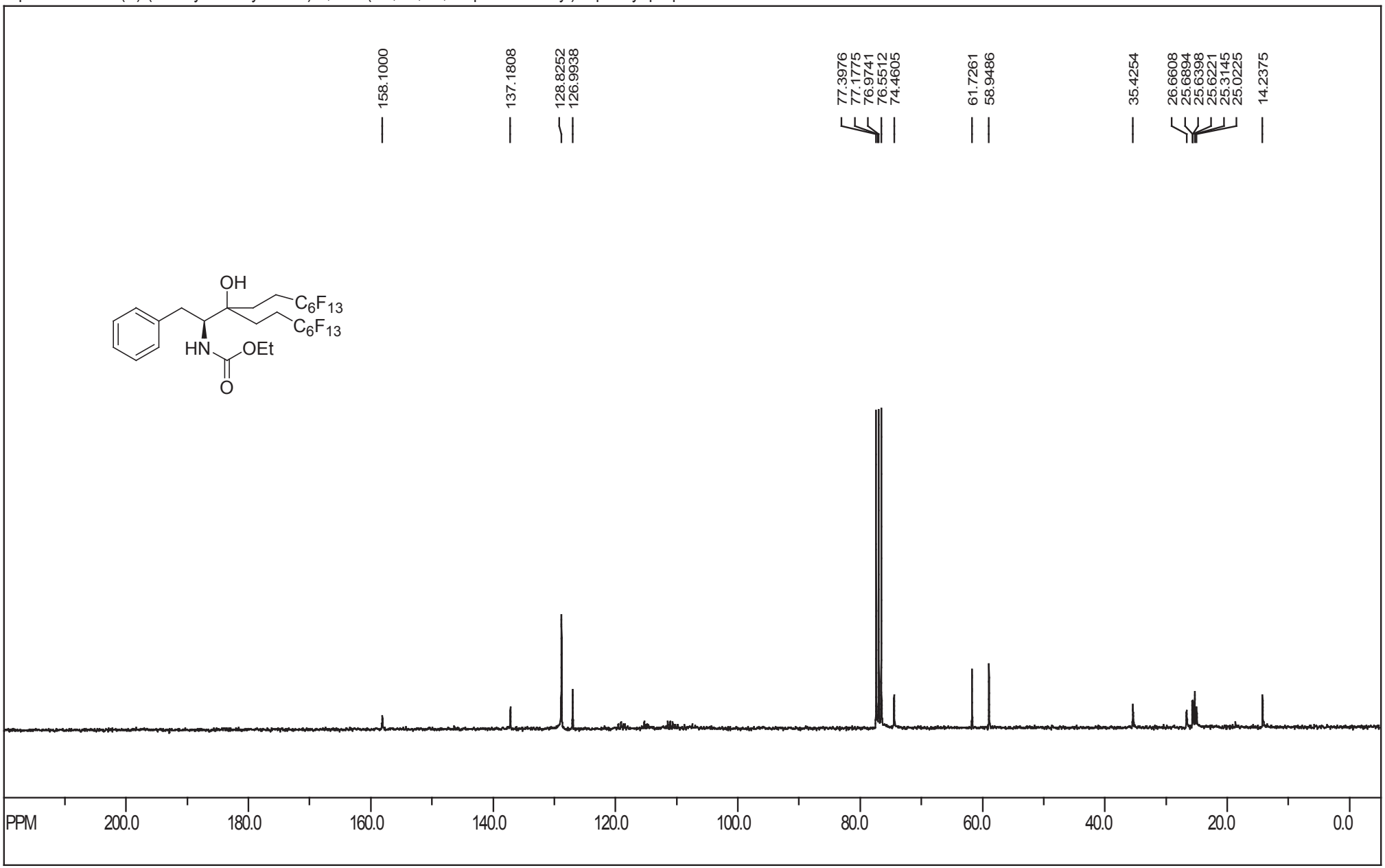

file: C:\NMR\V\80-90\Jehv_84cl4\fid expt: <zgpg30>

freq. of 0 ppm: 75.467749 MHz

SpinWorks 2.4: 3(S)-(tert-Butoxycarbonylamino)-4,4-bis(1'H,1'H,2'H,2'H-perfluorooctyl)-2-methyl-butan-4-ol

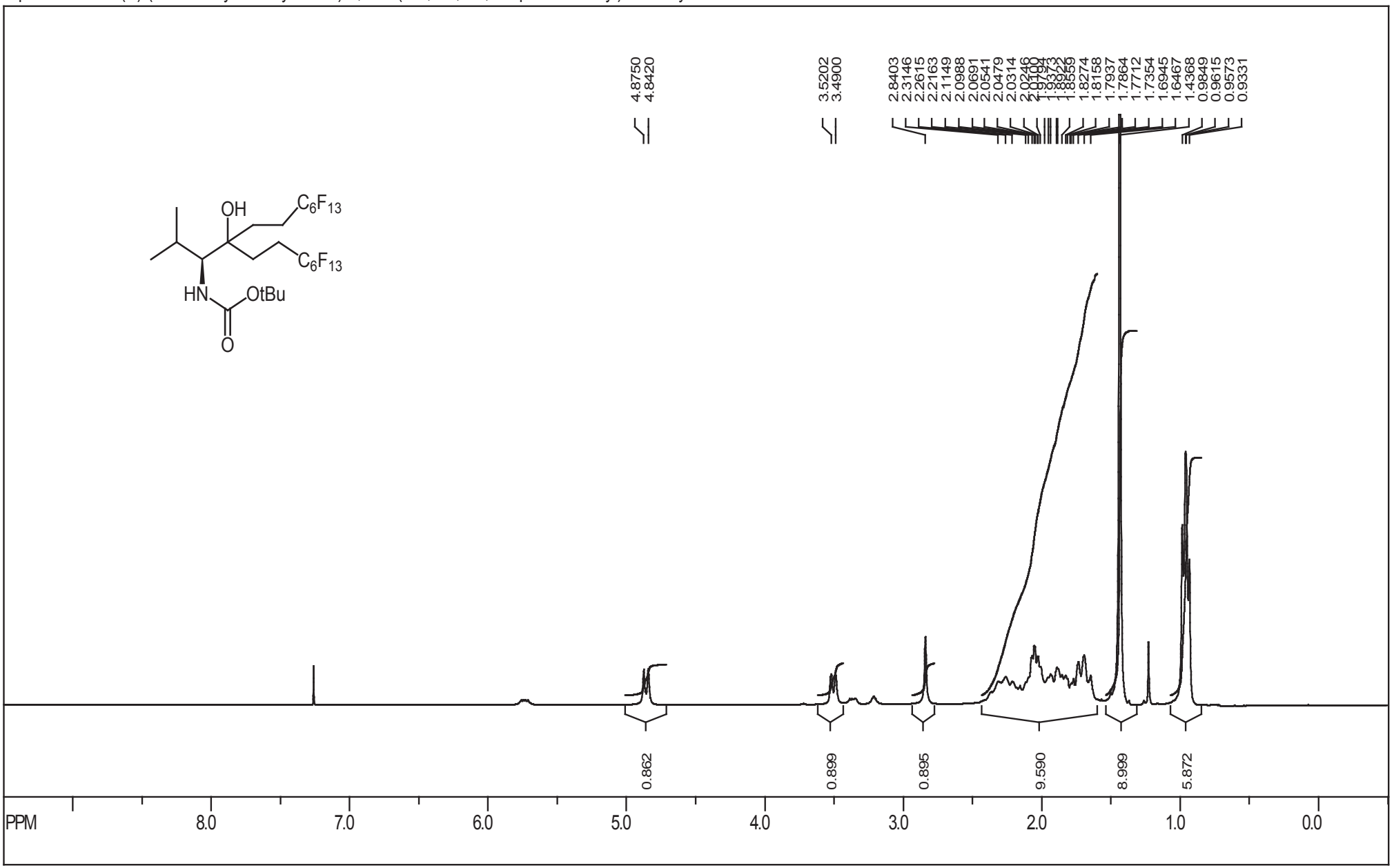

file: C:\NMRJason\vi\70-80\Jehvi_72a_2b\1\fid expt: <zg30>

freq. of 0 ppm: 300.130006 MHz

SpinWorks 2.4: 3(S)-(tert-Butoxycarbonylamino)-4,4-bis(1'H,1'H,2'H,2'H-perfluorooctyl)-2-methyl-butan-4-ol

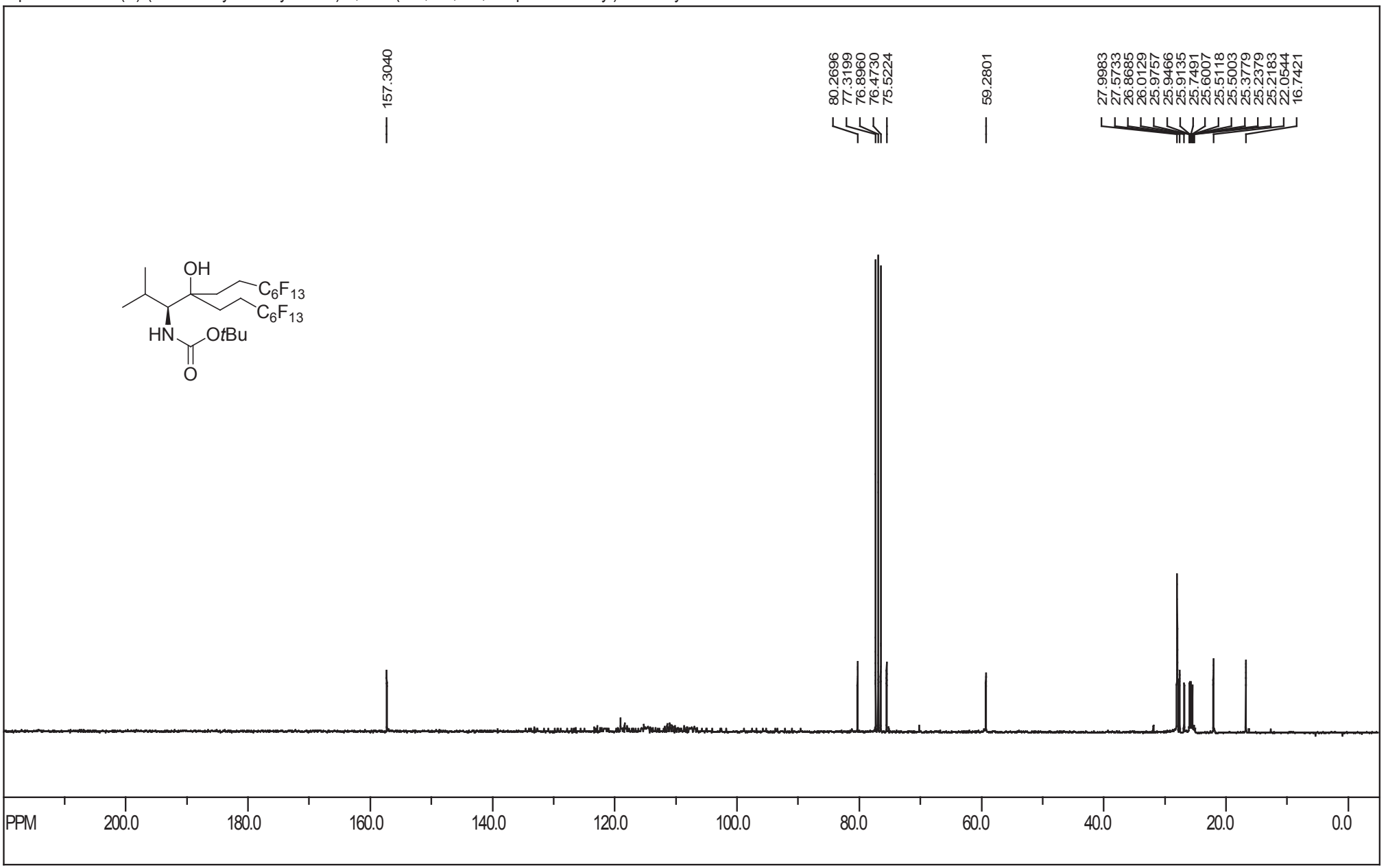

file: C:\NMR\70-80\Jehvi_72a_2b\5\fid expt: <zgpg30>

freq. of 0 ppm: 75.467749 MHz

SpinWorks 2.4: 1(R)-(Ethoxycarbonylamino)-2,2-bis(1'H,1'H,2'H,2'H-perfluorooctyl)-1-phenyl-ethan-2-ol

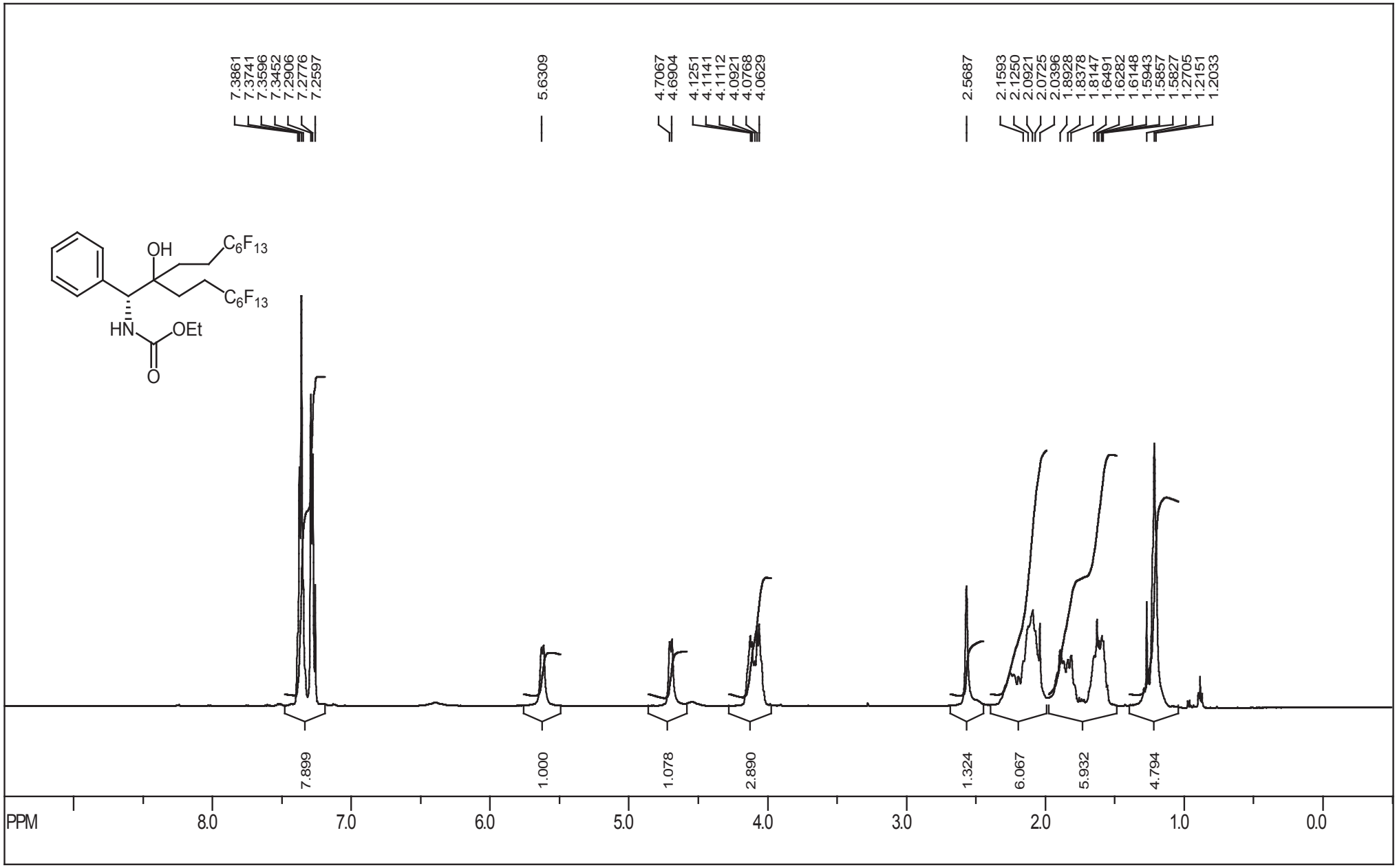

file: C:\NMR\Jason\vi\70-80\Jehvi_72b_15\1\fid expt: <zg30>

freq. of 0 ppm: 500.135421 MHz

SpinWorks 2.4: 1(R)-(Ethoxycarbonylamino)-2,2-bis(1'H,1'H,2'H,2'H-perfluorooctyl)-1-phenyl-ethan-2-ol

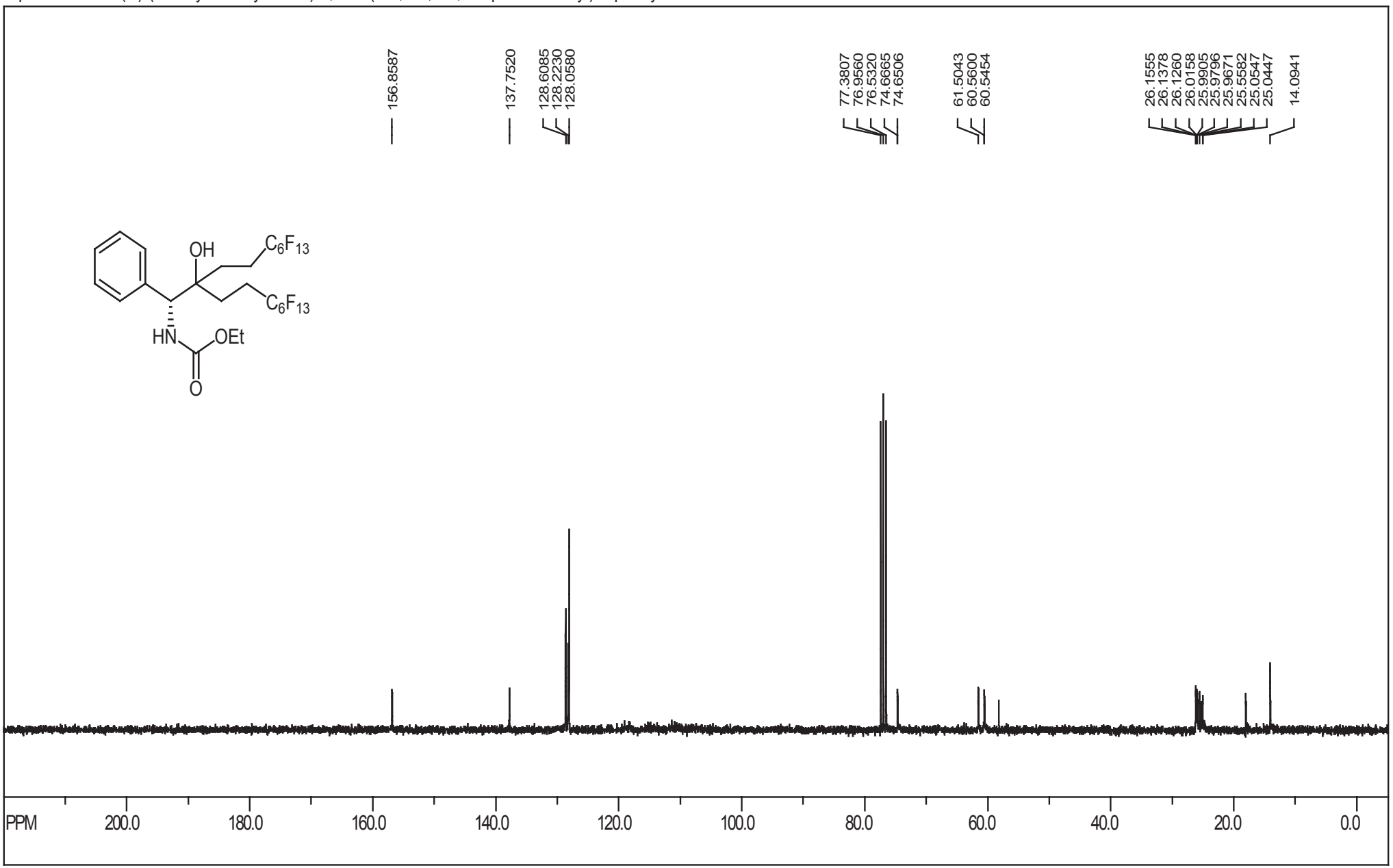

file: C:\NMR\Jason\vi\70-80\Jehvi_72b_15ch\5\fid expt: <zgpg30>

freq. of 0 ppm: 75.467749 MHz

SpinWorks 2.4: (2S,3R)-(Ethoxycarbonylamino)-6,6,7,7,8,8,9,9,10,10,11,11,11-tridecafluoro-1-phenyl-undecan-3-ol

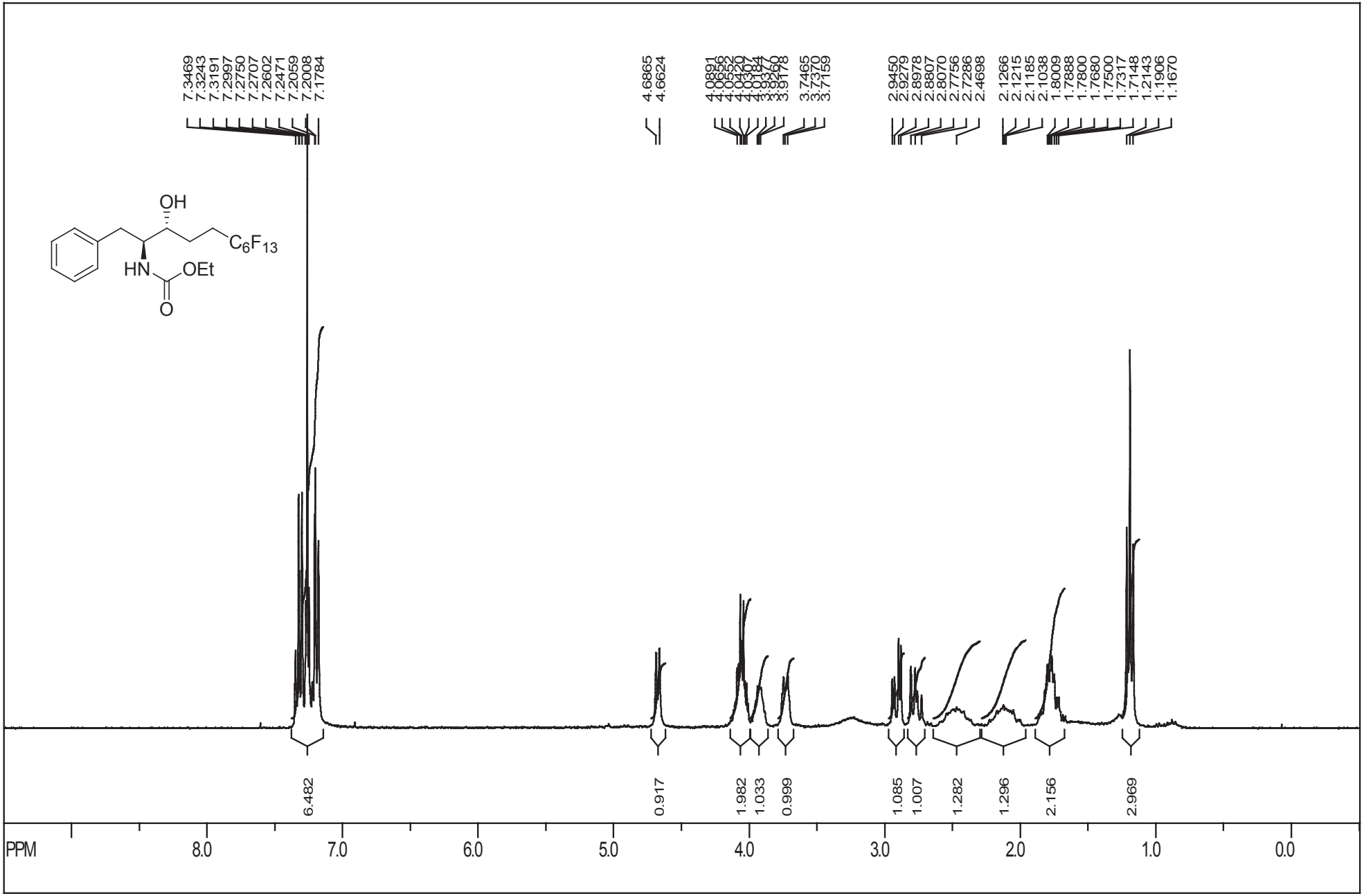

file: C:\NMR\Jehv_91b\1\fid expt: <zg30>

SpinWorks 2.4: (2S,3R)-(Ethoxycarbonylamino)-6,6,7,7,8,8,9,9,10,10,11,11,11-tridecafluoro-1-phenyl-undecan-3-ol

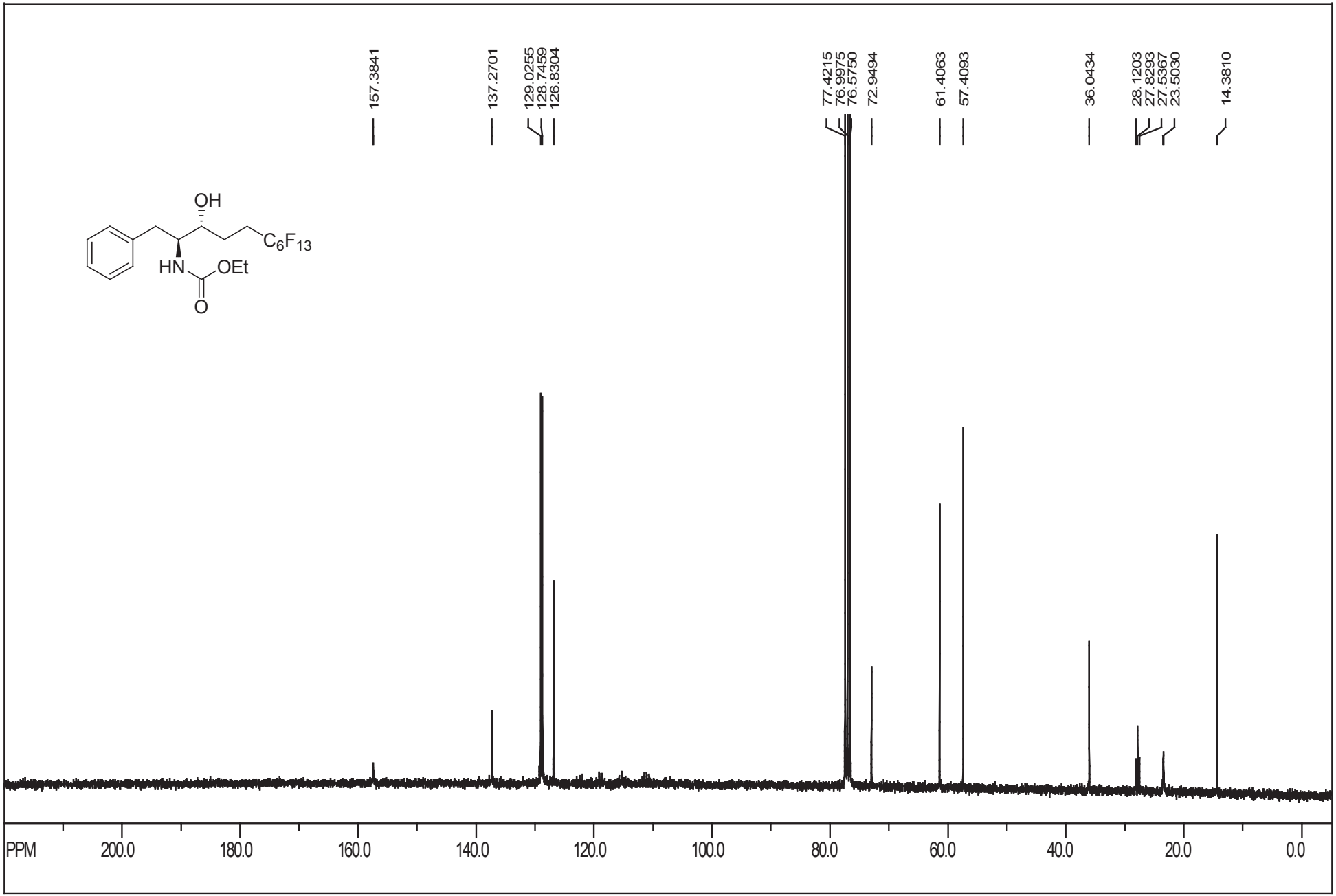

file: C:\NMRJehv_91b\23\fid expt: <zgpg30>

SpinWorks 2.4: (3S,4R)-(tert-Butoxyoxycarbonylamino)-7,7,8,8,9,9,10,10,11,11,12,12,12-tridecafluoro-2-methyl-dodecan-4-ol

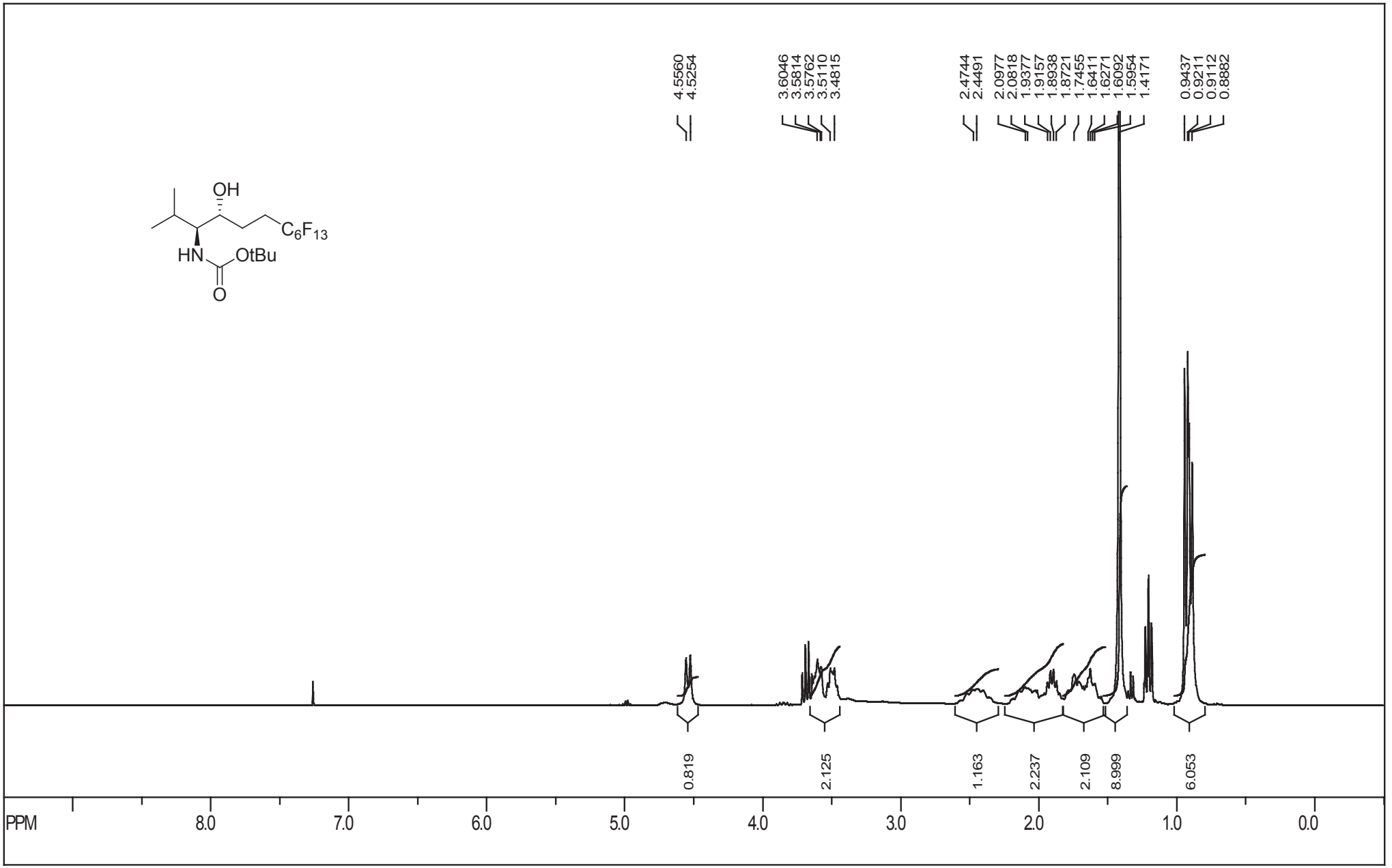

file: C:\NMR\70-80\Jehvi_75b\1\fid expt: <zg30>

freq. of 0 ppm: 300.130006 MHz

SpinWorks 2.4: (3S,4R)-(tert-Butoxyoxycarbonylamino)-7,7,8,8,9,9,10,10,11,11,12,12,12-tridecafluoro-2-methyl-dodecan-4-ol

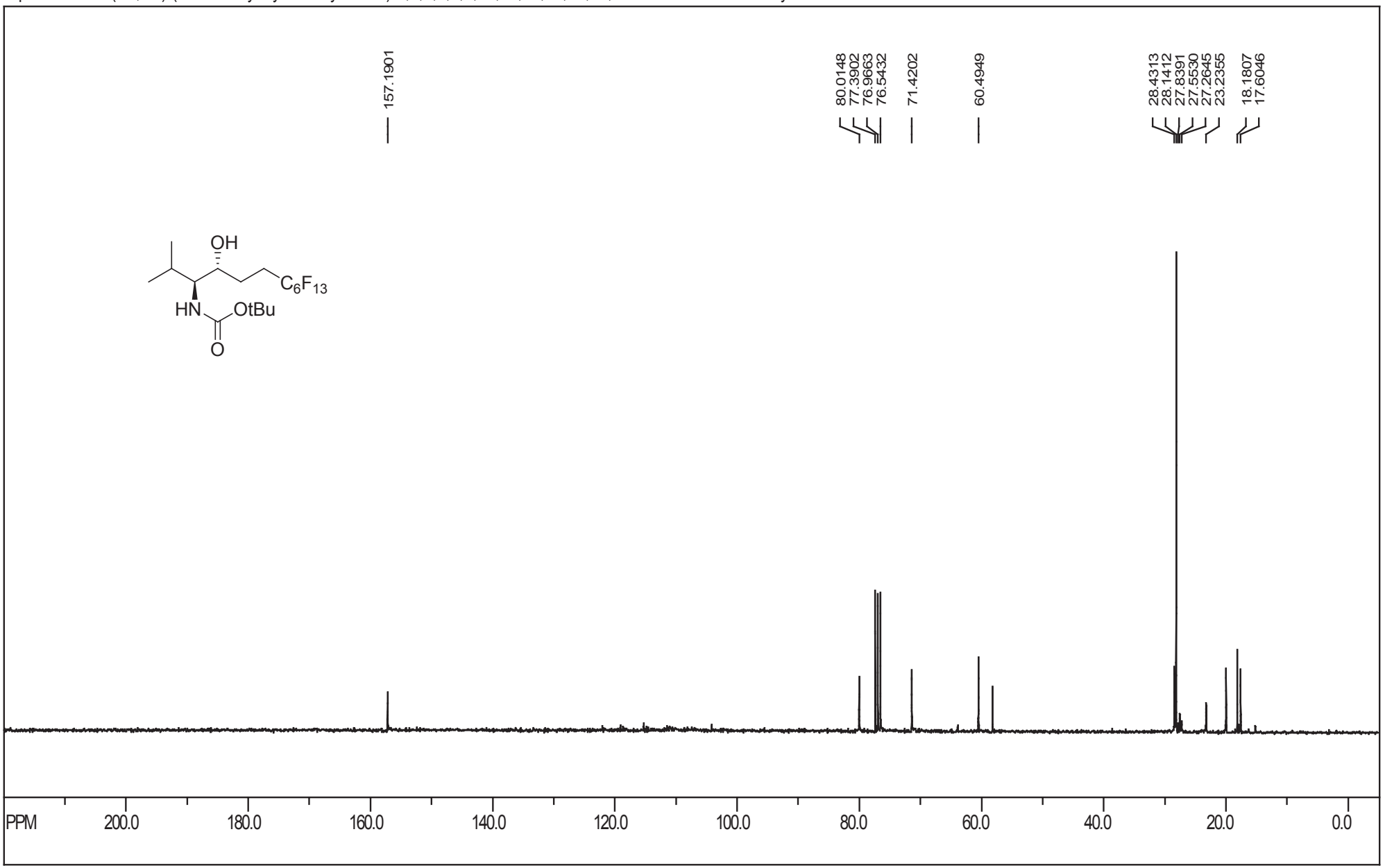

file: C:\NMR\70-80\Jehvi_75b\4\fid expt: <zgpg30>

freq. of 0 ppm: 75.467749 MHz

SpinWorks 2.4: (1R,2S)-1-(tert-Butoxycarbonylamino)-5,5,6,6,7,7,8,8,9,9,10,10,10-tridecafluoro-1-phenyl-decan-2-ol

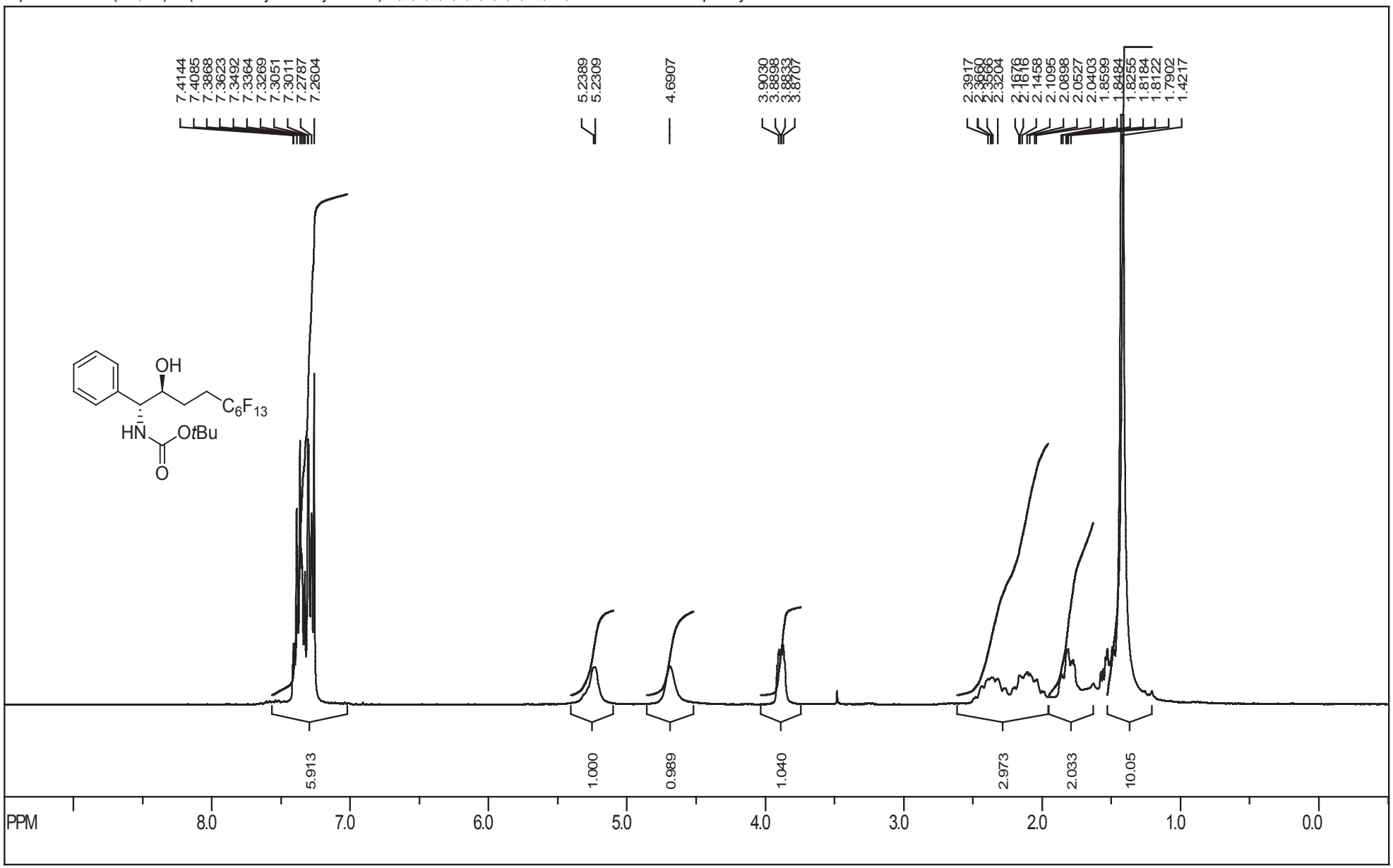

file: C:\NMR\Laina\70-80\lmg70\2\fid expt: <zg30>

freq. of 0 ppm: 300.130006 MHz

SpinWorks 2.4: (1R,2S)-1-(tert-Butoxycarbonylamino)-5,5,6,6,7,7,8,8,9,9,10,10,10-tridecafluoro-1-phenyl-decan-2-ol

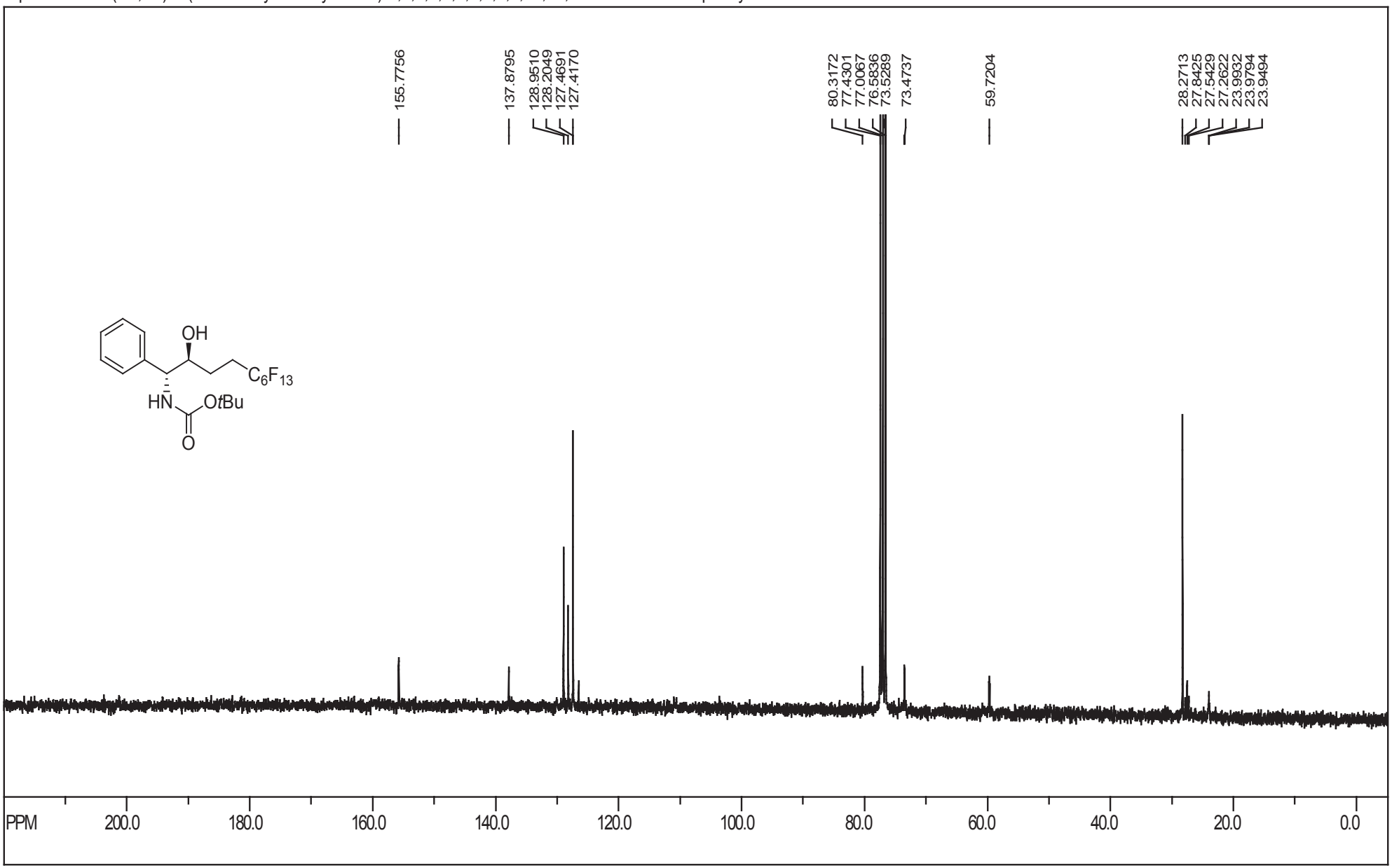

file: C:\NMR\Laina\70-80\lmg70\6\fid expt: <zgpg30>

freq. of 0 ppm: 75.467749 MHz

SpinWorks 2.4: (4S,5R)-4-Benzyl-5-(1'H,1'H,2'H,2'R-perfluorooctyl)-2-oxazolidinone

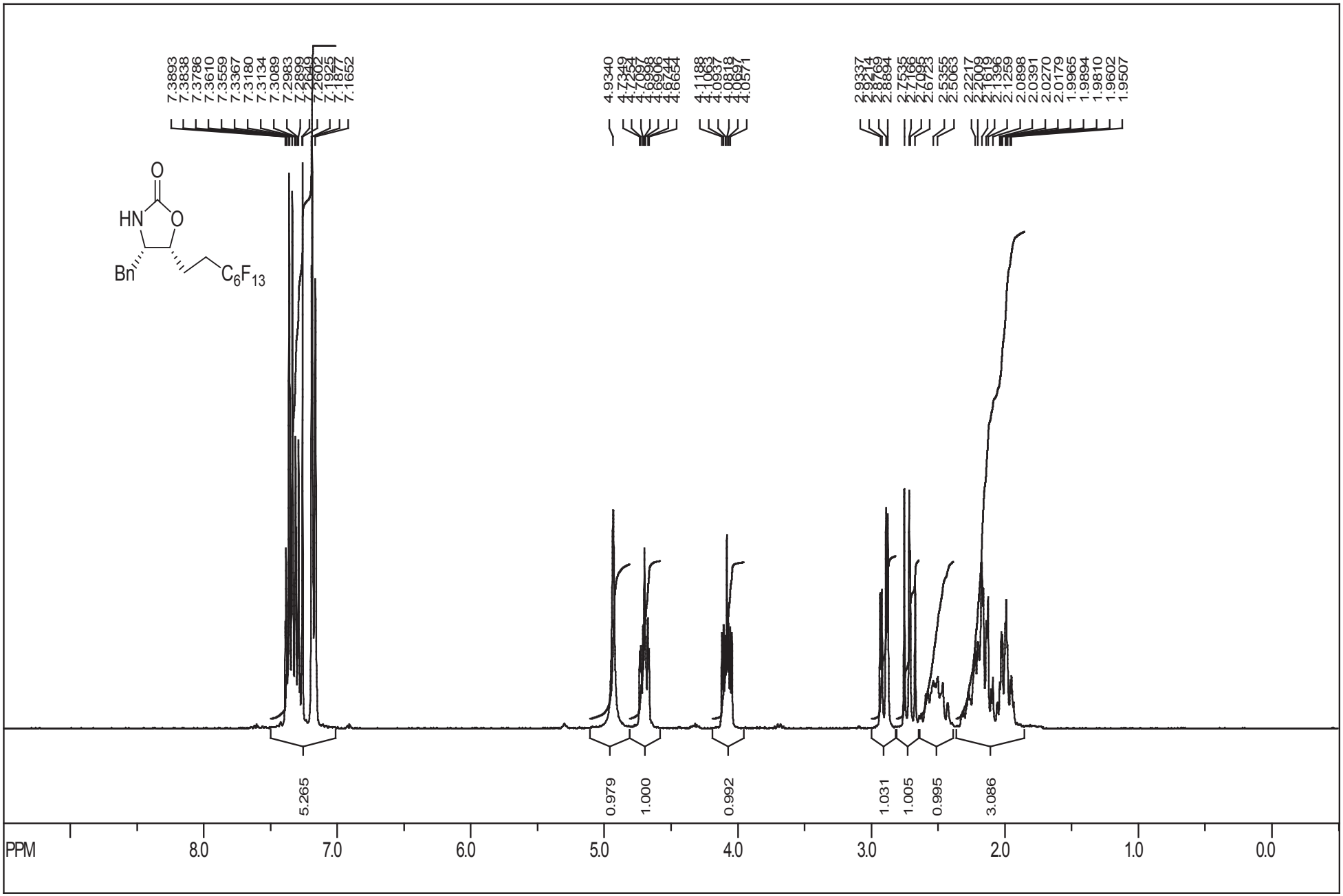

file: C:\NMR\jehv_88c\2\fid expt: <zg30>

SpinWorks 2.4: (4S,5R)-4-Benzyl-5-(1'H,1'H,2'H,2'H-perfluorooctyl)-2-oxazolidinone

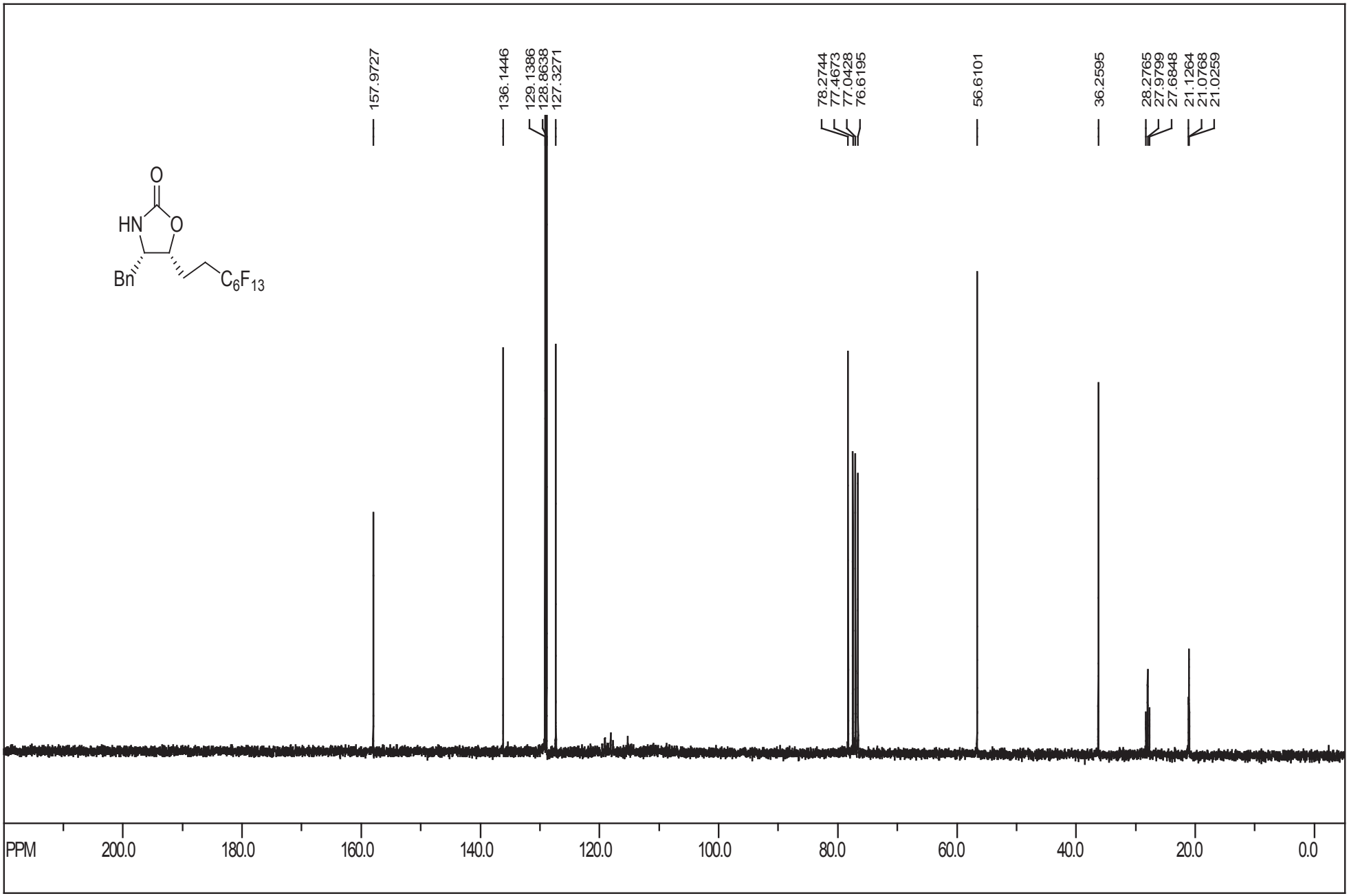

file: C:\NMR\Jehvi_29\5\fid expt: <zgpg30>

SpinWorks 2.4: (4S,5R)-4-iso-Propyl-5-(1'H,1'H,2'H,2'H-perfluorooctyl)-oxazolidin-2-one

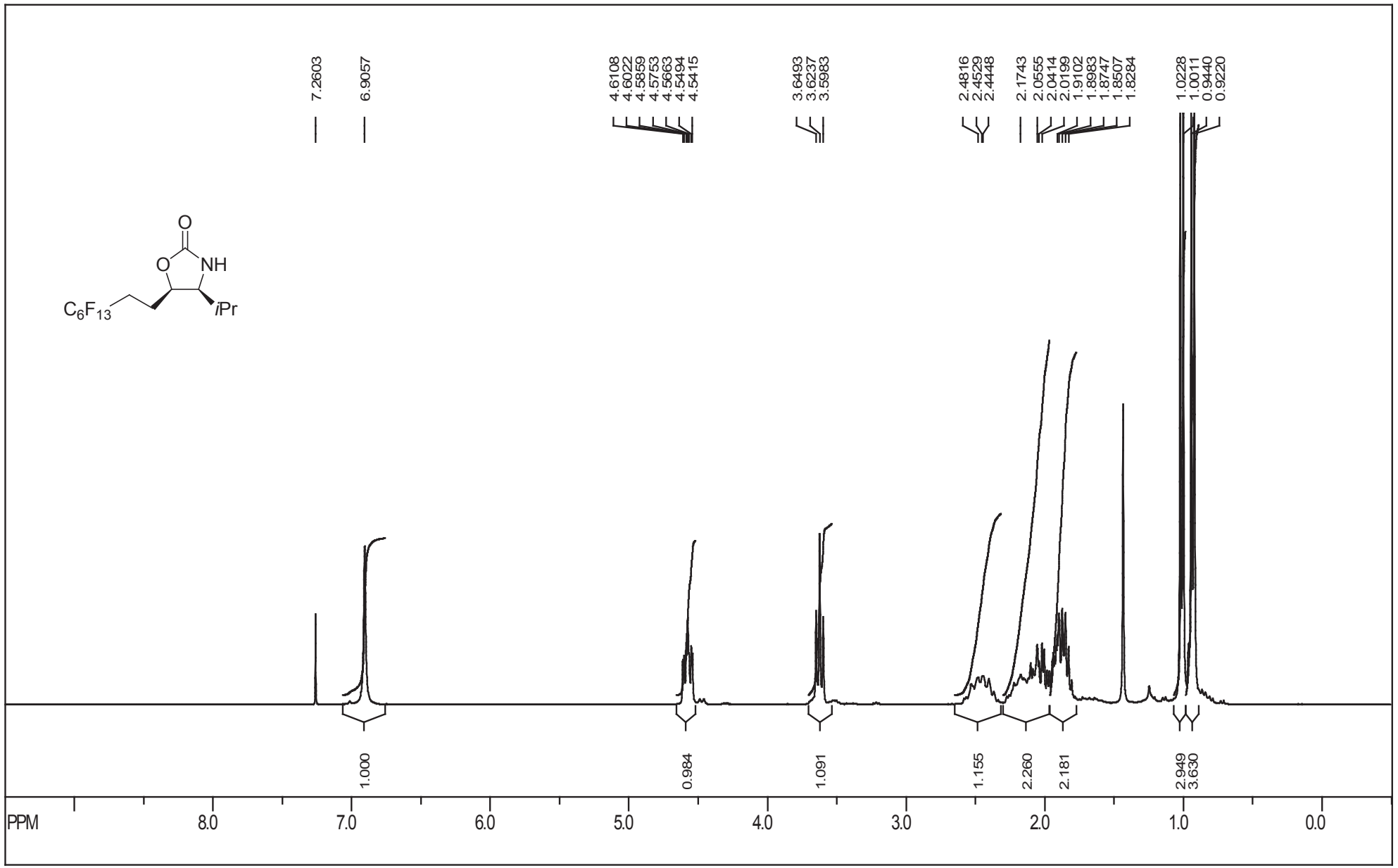

file: C:\NMR\Jason\vi\70-80\Jehvi_77c\1\fid expt: <zg30>

freq. of 0 ppm: 300.130006 MHz

SpinWorks 2.4: (4S,5R)-4-iso-Propyl-5-(1'H,1'H,2'H,2'H-perfluorooctyl)-oxazolidin-2-one

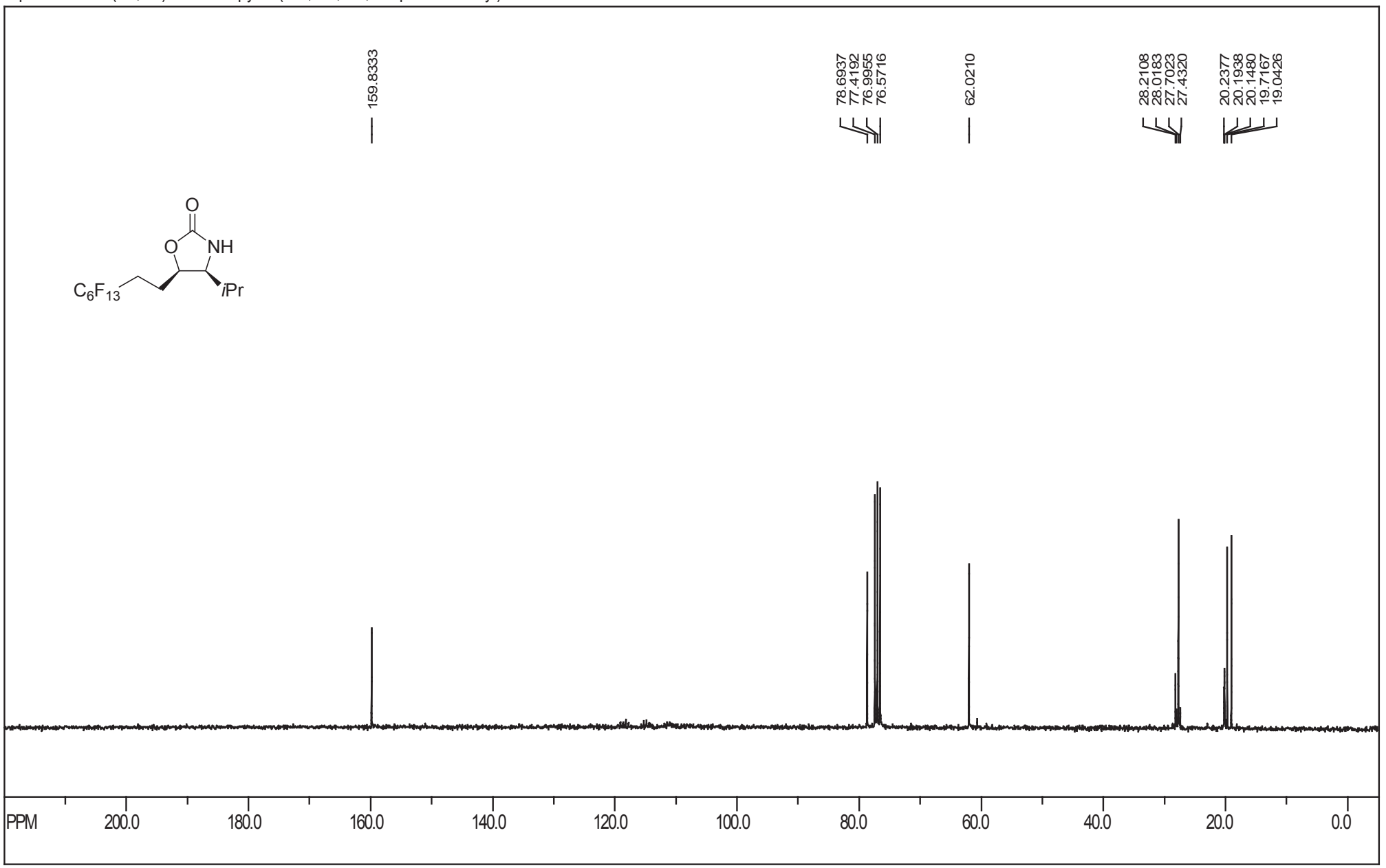

file: C:\NMR\70-80\Jehvi_77c\5\fid expt: <zgpg30>

freq. of 0 ppm: 75.467749 MHz

SpinWorks 2.4: 4(S)-Benzyl-5,5-bis(1H,1H,2H,2H-perfluorooctyl)-oxazolidin-2-one

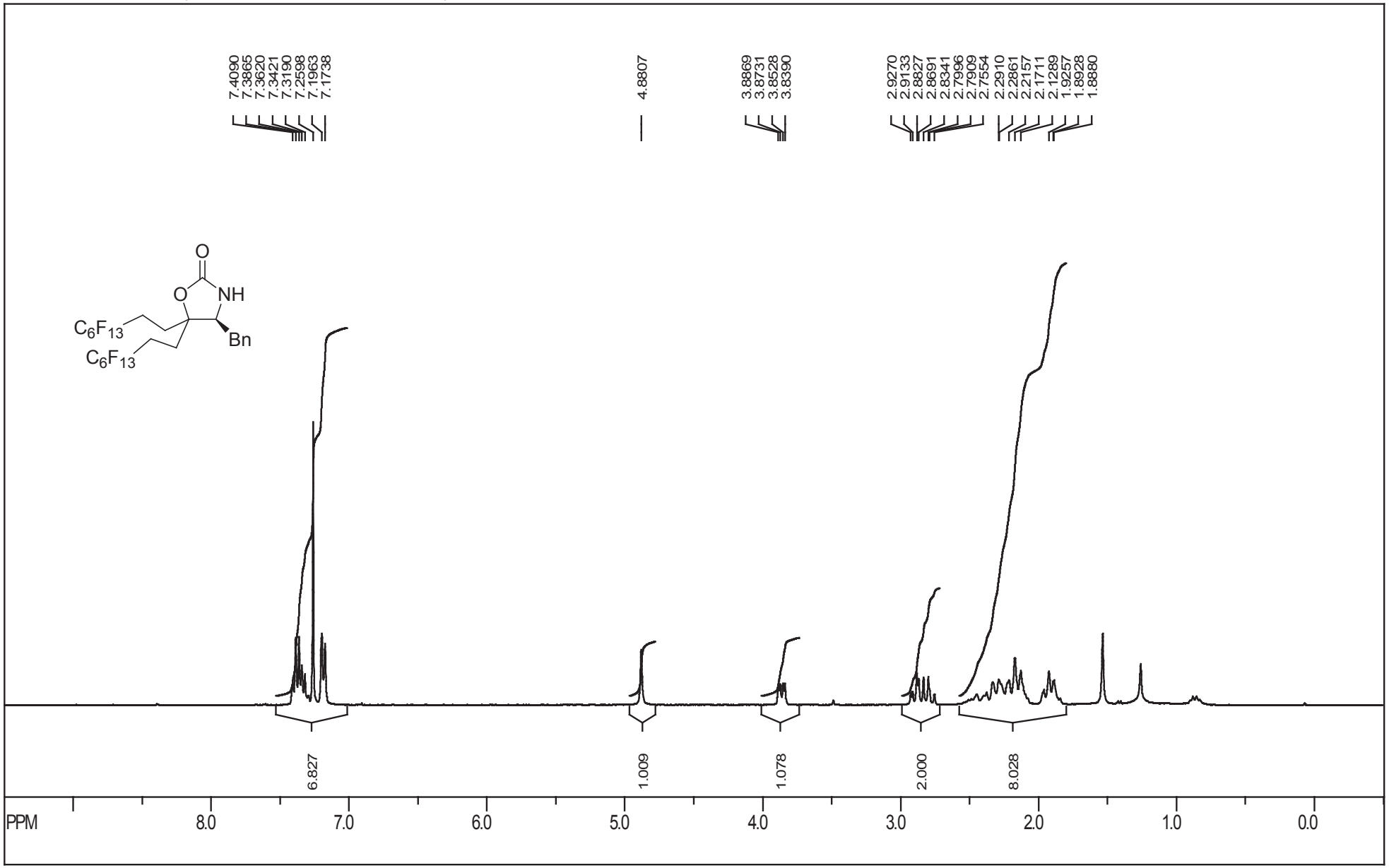

file: C:\NMR\V\80-90\Jehv_86\6\fid expt: <zg30>

freq. of 0 ppm: 300.130006 MHz

SpinWorks 2.4: 4(S)-Benzyl-5,5-bis(1'H,1'H,2'H,2'H-perfluorooctyl)-oxazolidin-2-one

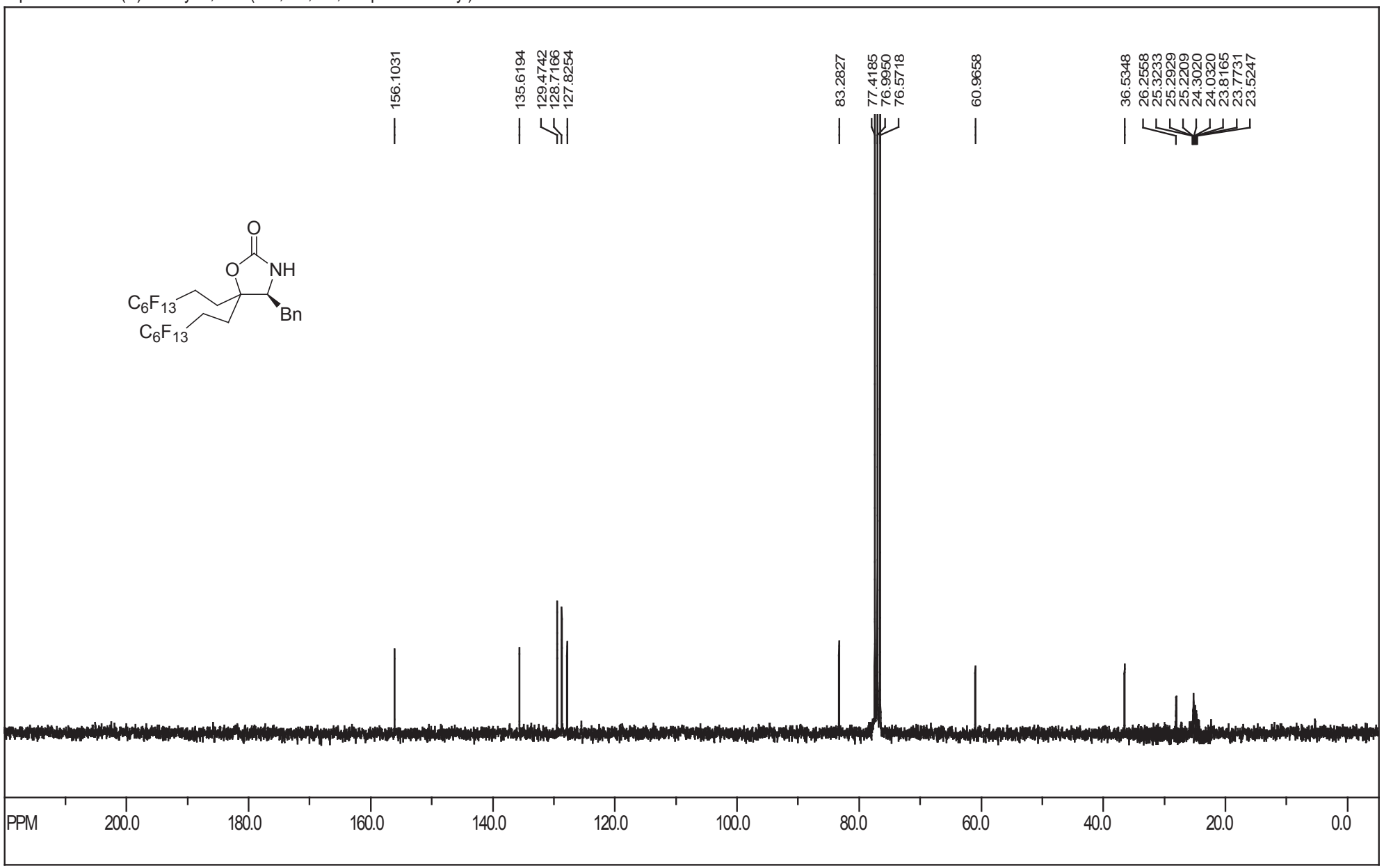

file: C:\NMR\V\80-90\Jehv_86\8\fid expt: <zgpg30>

freq. of 0 ppm: 75.467749 MHz

SpinWorks 2.4: 4(S)-iso-Propyl-5,5-bis(1'H,1'H,2'H,2'H-perfluorooctyl)-2-oxazolidinone

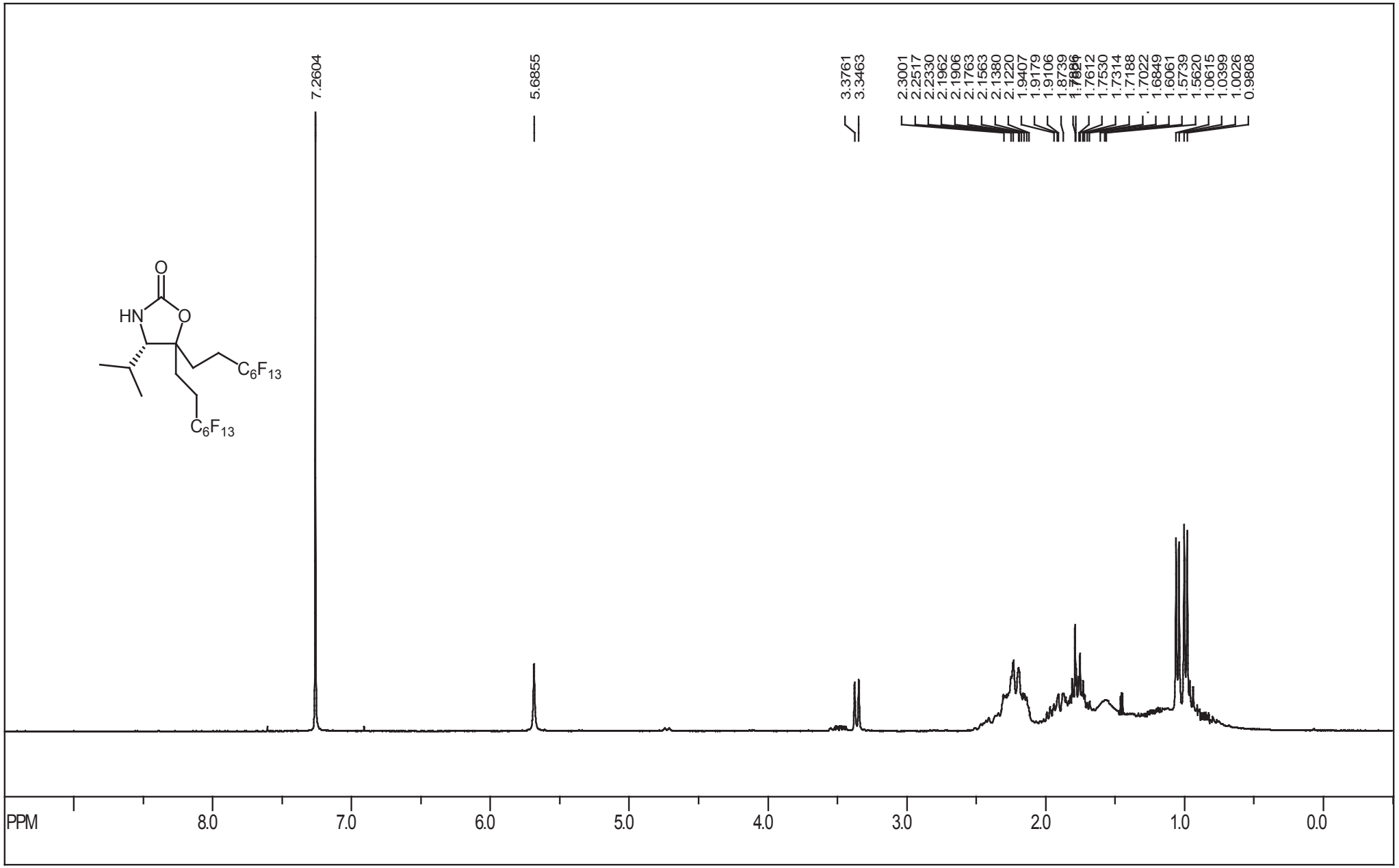

file: C:\NMR\Jason\vi\70-80\Jehvi_77d\8\fid expt: <zg30>

freq. of 0 ppm: 300.130006 MHz

SpinWorks 2.4: 4(S)-iso-Propyl-5,5-bis(1'H,1'H,2'H,2'H-perfluorooctyl)-2-oxazolidinone

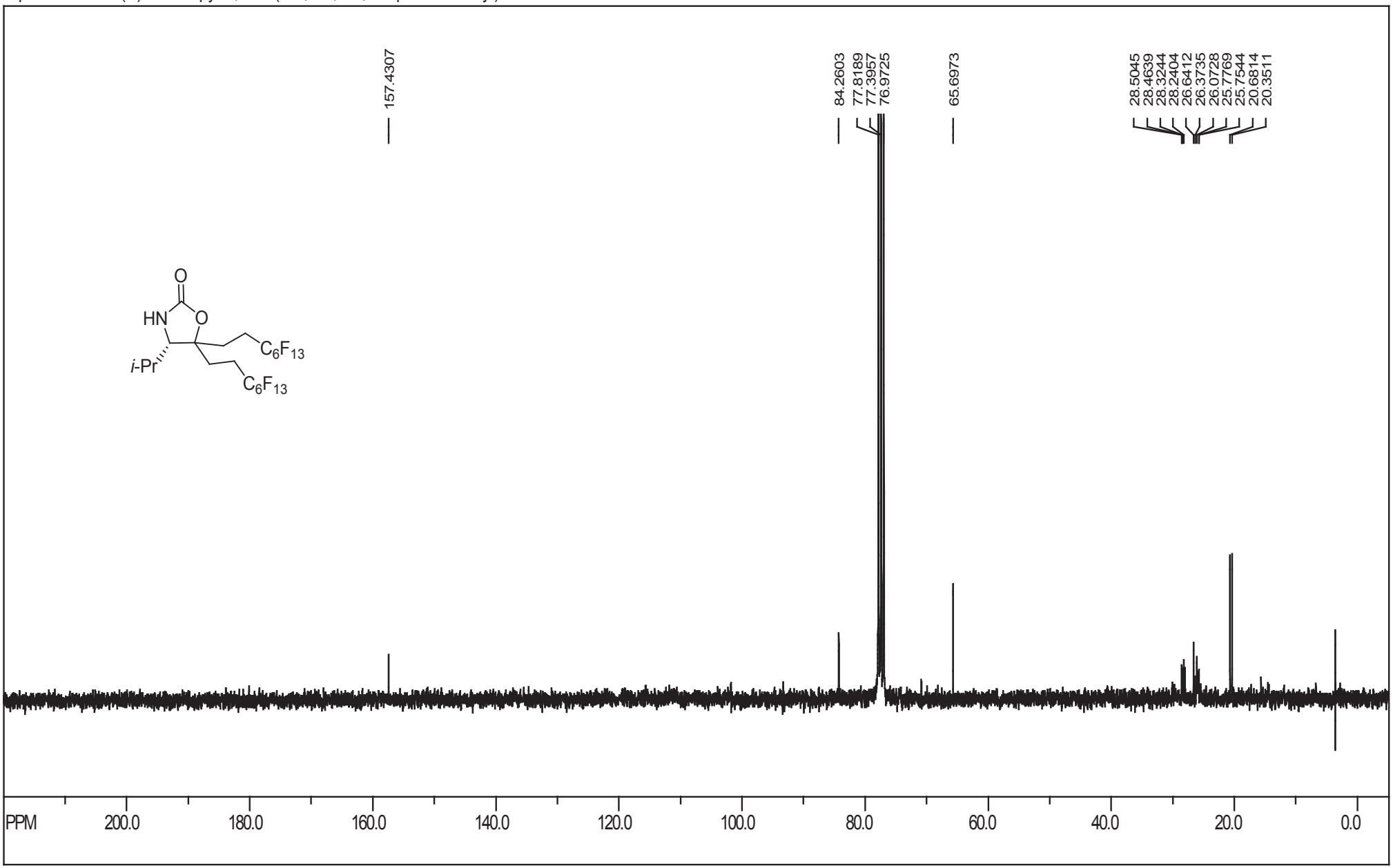

file: C:\NMR\Jason\vi\70-80\Jehvi_77d\5\fid expt: <zgpg30>

freq. of 0 ppm: 75.467719 MHz

SpinWorks 2.4: 4(R)-Phenyl-5,5-bis(1'H,1'H,2'H,2'H-perfluorooctyl)-2-oxazolidinone

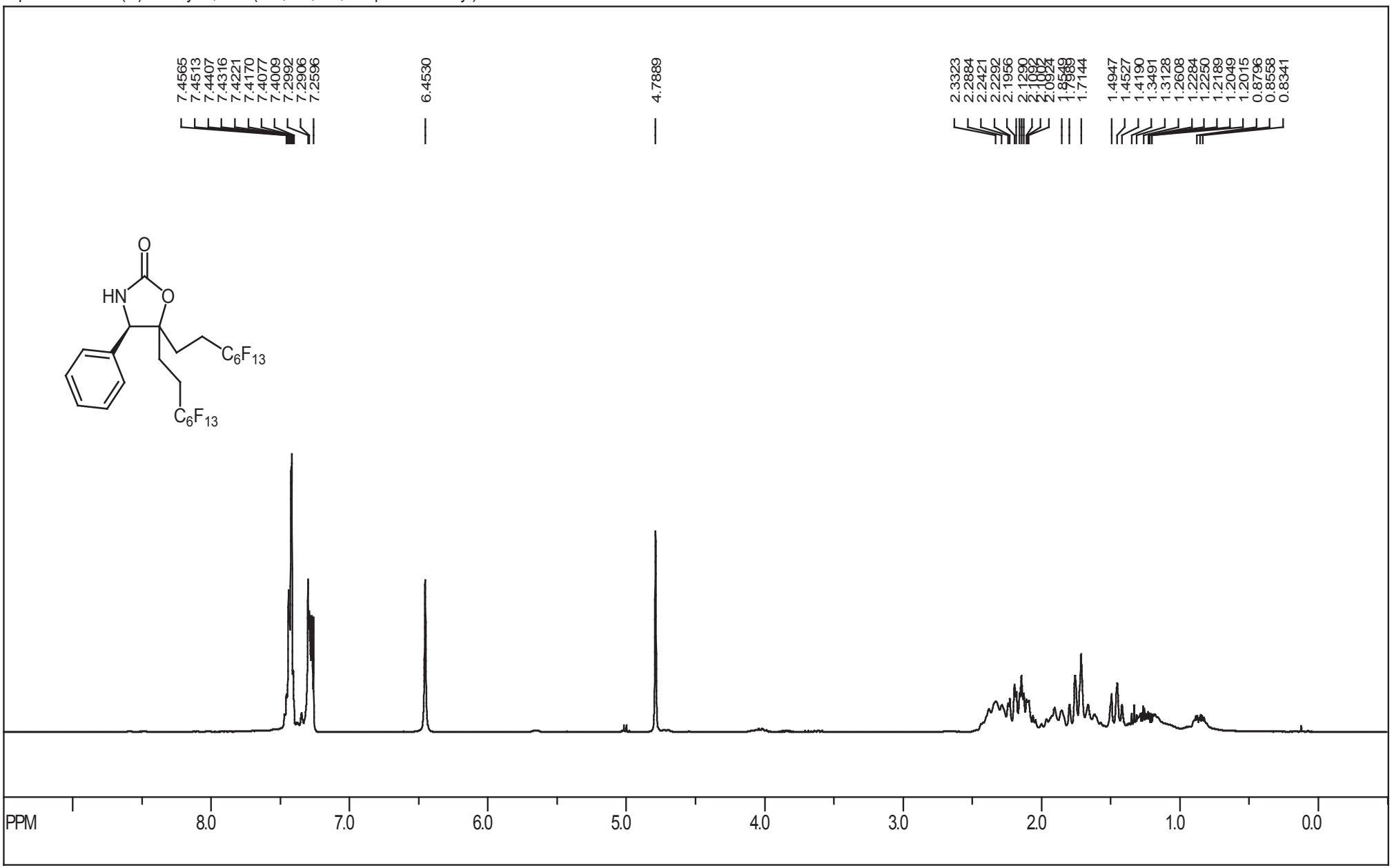

file: C:\NMR\Jason\vi\70-80\Jehvi_77b_2\1\fid expt: <zg30>

freq. of 0 ppm: 300.130006 MHz

SpinWorks 2.4: 4(R)-Phenyl-5,5-bis(1'H,1'H,2'H,2'H-perfluorooctyl)-2-oxazolidinone

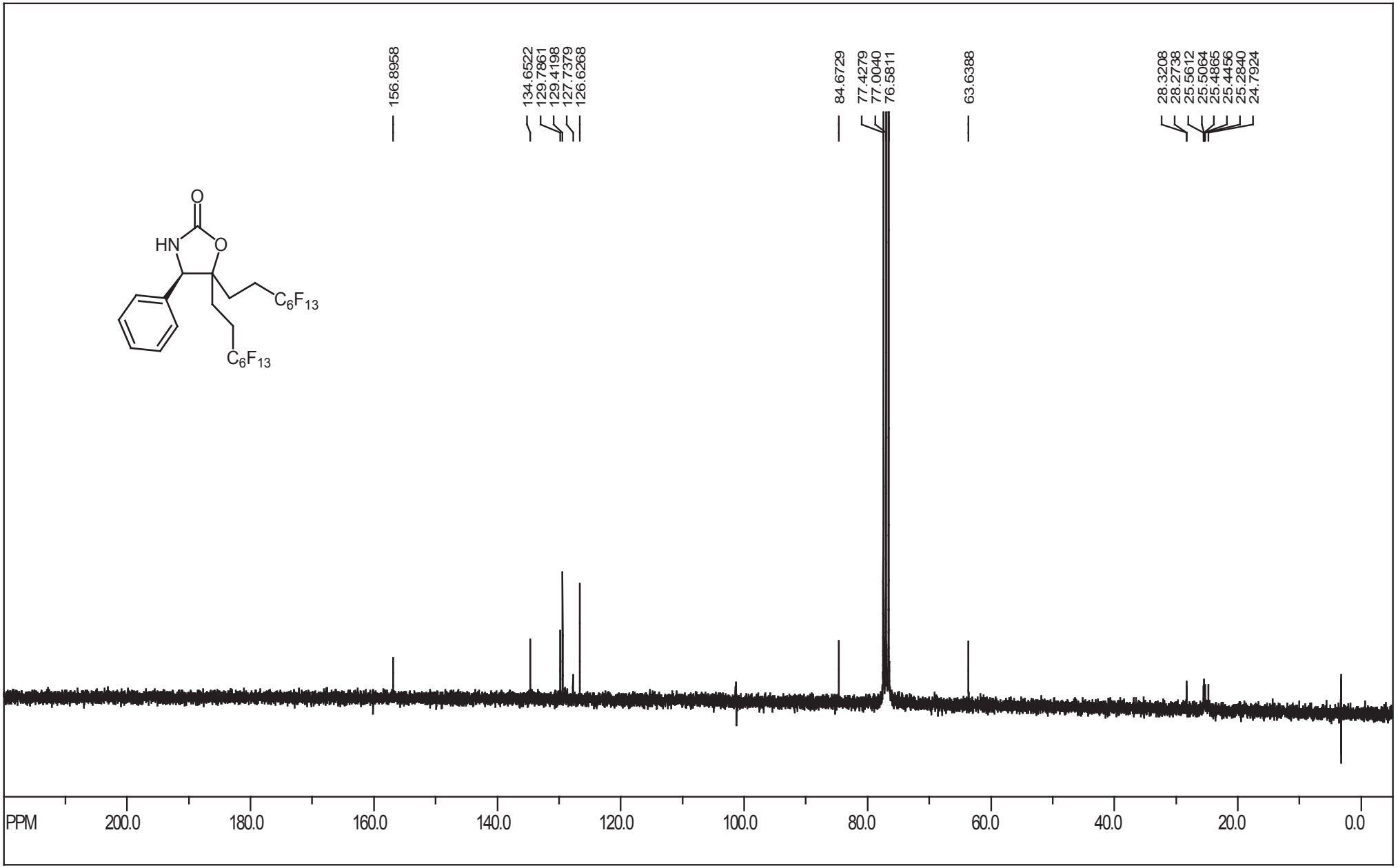

file: C:\NMR\Jason\vi\70-80\Jehvi_77b\3\fid expt: <zgpg30>

freq. of 0 ppm: 75.467749 MHz

SpinWorks 2.4: (2S,2'R,3R)-2-(Ethoxycarbonylamino)-3-(2'-methoxy-2'-trifluoromethyl-phenylacetyl)-6,6,7,7,8,8,9,9,10,10,11,11,11-tridecafluoro-1-phenyl-undecan-3-ol

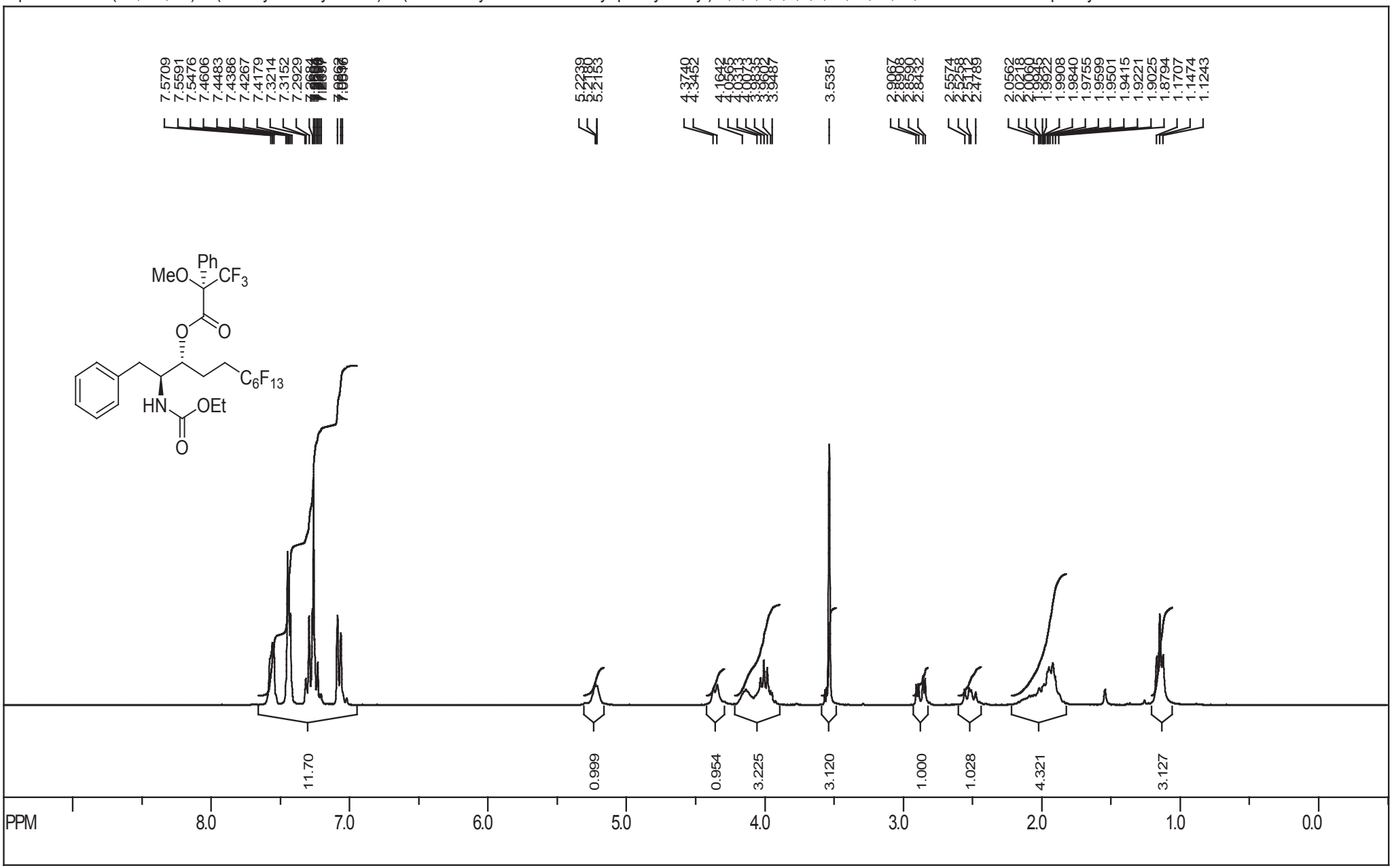

file: C:\NMR\Jason\V\90-100\Jehv_96a\6\fid expt: <zg30>

freq. of 0 ppm: 300.130006 MHz

SpinWorks 2.4: (2S,2'R,3R)-2-(Ethoxycarbonylamino)-3-(2'-methoxy-2'-trifluoromethyl-phenylacetyl)-6,6,7,7,8,8,9,9,10,10,11,11,11-tridecafluoro-1-phenyl-undecan-3-ol

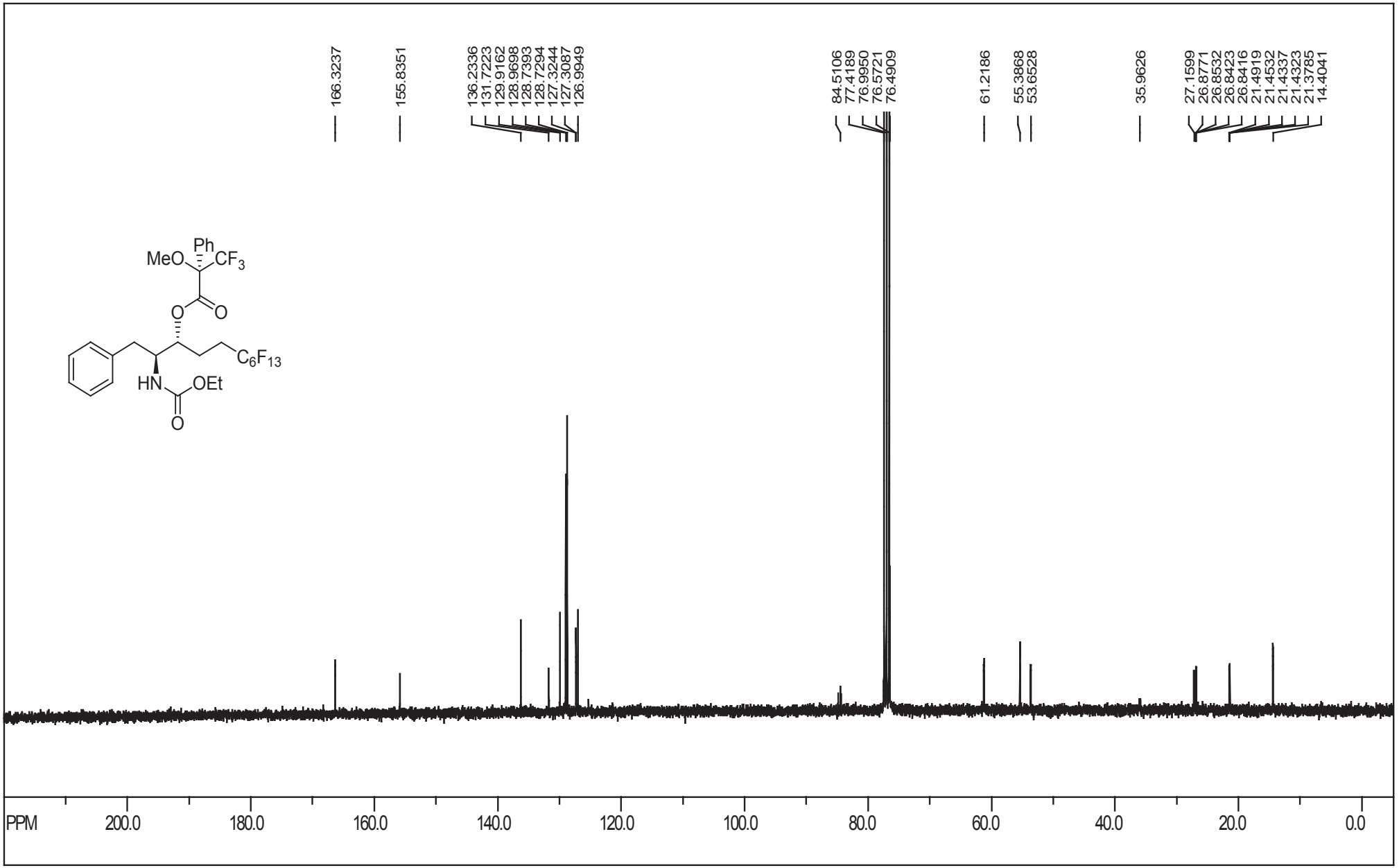

file: C:\NMR\Jason\V\90-100\Jehv_96a\11\fid expt: <zgpg30>

freq. of 0 ppm: 75.467749 MHz

SpinWorks 2.4: (2S,2'R,3R)-2-(Ethoxycarbonylamino)-3-(2'-methoxy-2'-trifluoromethyl-phenylacetyl)-6,6,7,7,8,8,9,9,10,10,11,11,11-tridecafluoro-1-phenyl-undecan-3-ol

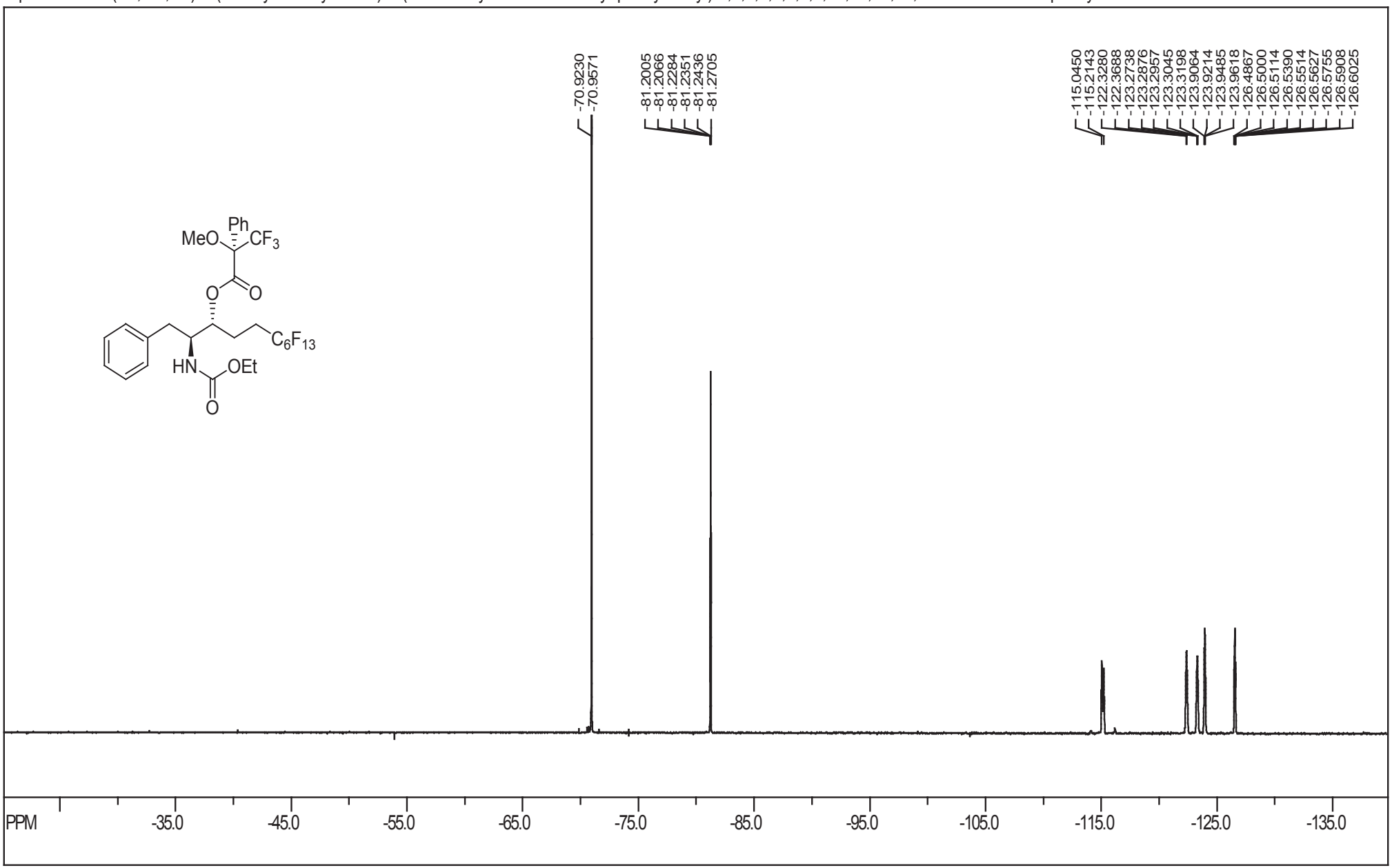

file: C:\NMR\Jason\V\90-100\Jehv_96a\10\fid expt: <zgfhigqn>

freq. of 0 ppm: 282.404481 MHz

SpinWorks 2.4: (2'R,3S,4R)-3-(tert-Butoxycarbonylamino)-4-(2'-methoxy-2'-trifluoromethyl-phenylacetyl)-7,7,8,8,9,9,10,10,11,11,12,12,12-tridecafluoro-2-methyl-dodecan-4-ol

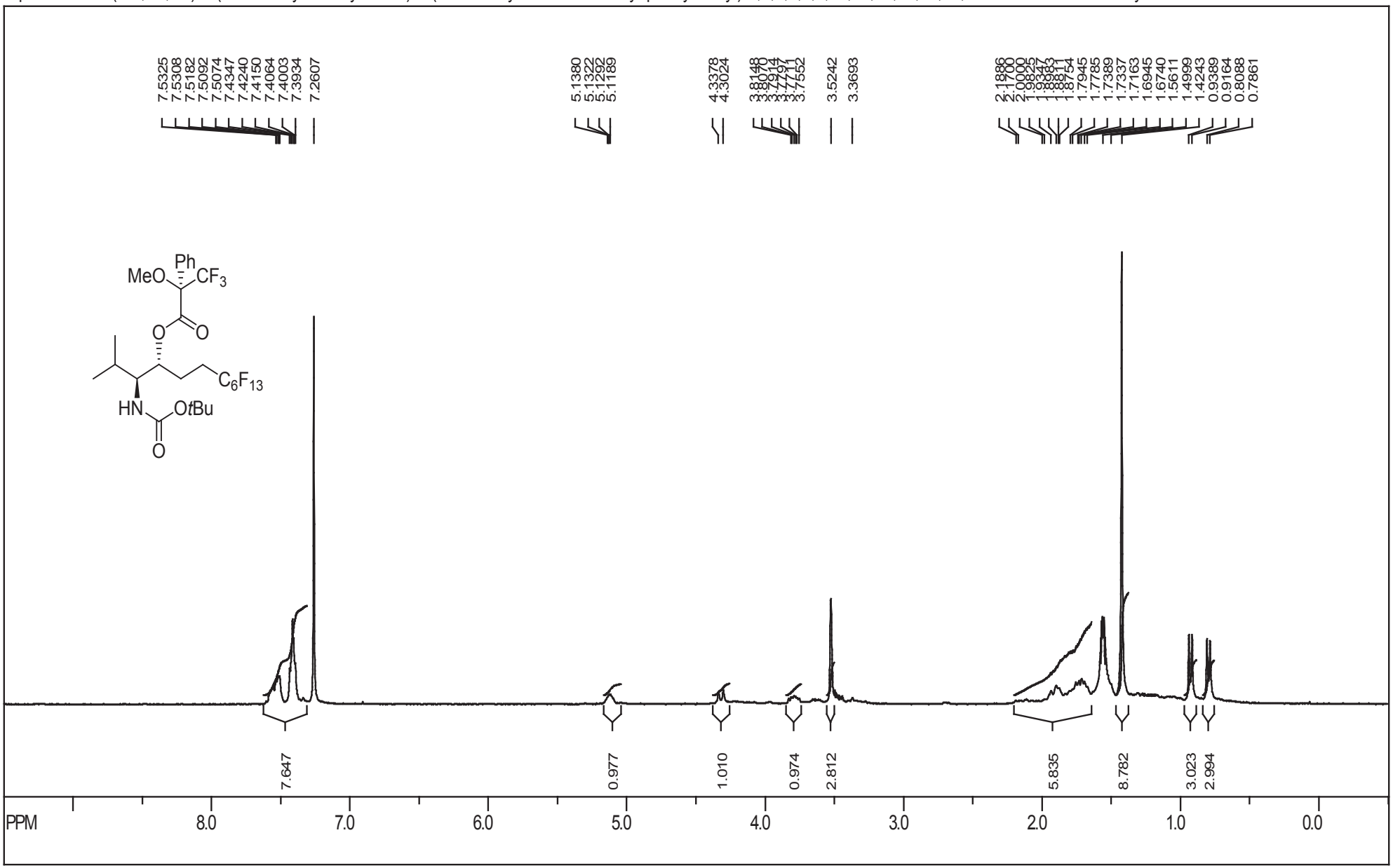

file: C:\NMR\Laina\80-90\lmg84A\3\fid expt: <zg30>

freq. of 0 ppm: 300.130006 MHz

SpinWorks 2.4: (2'R,3S,4R)-3-(tert-Butoxycarbonylamino)-4-(2'-methoxy-2'-trifluoromethyl-phenylacetyl)-7,7,8,8,9,9,10,10,11,11,12,12,12-tridecafluoro-2-methyl-dodecan-4-ol

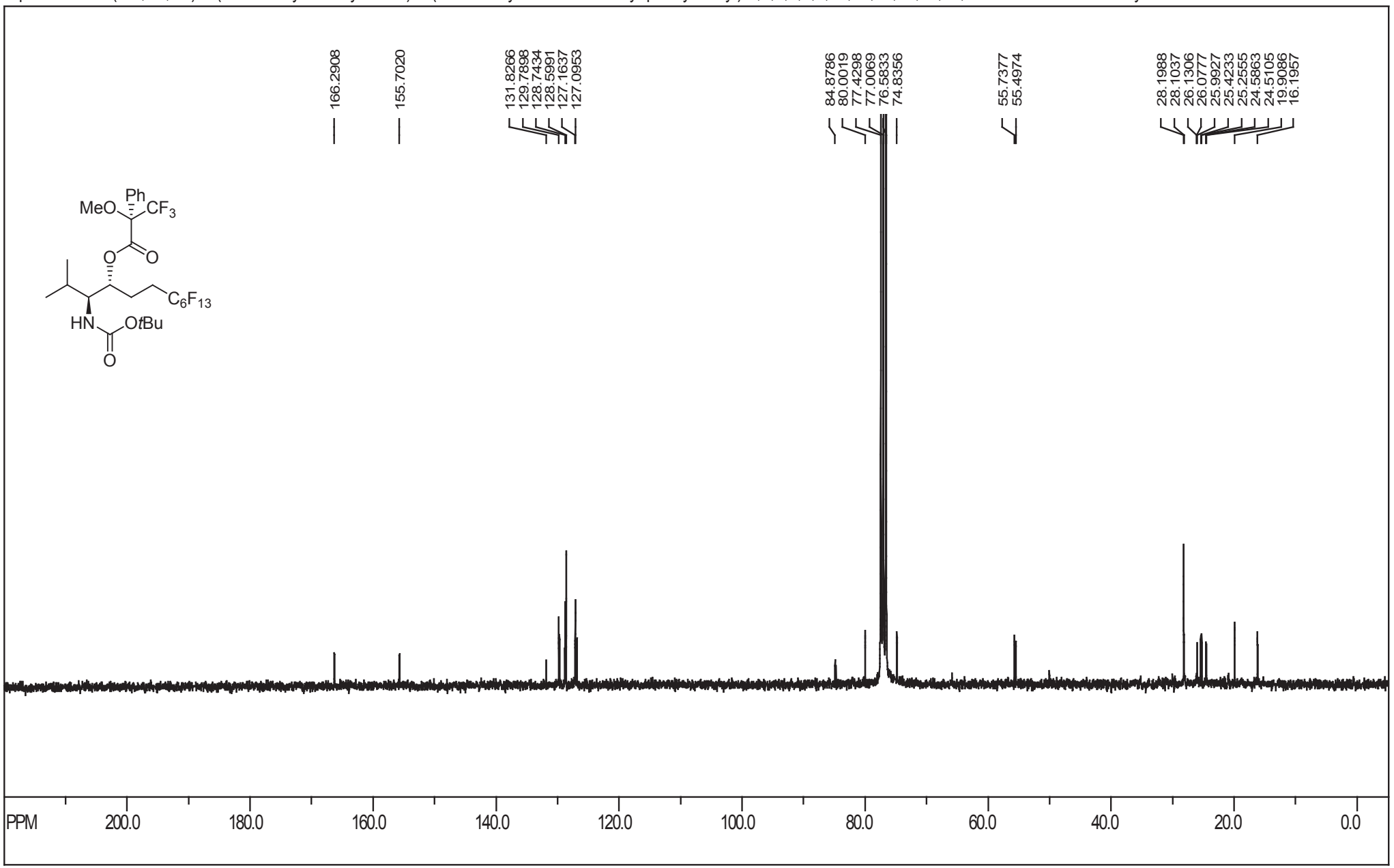

file: C:\NMR\Laina\80-90\lmg84A\9\fid expt: <zgpg30>

freq. of 0 ppm: 75.467749 MHz

SpinWorks 2.4: (2'R,3S,4R)-3-(tert-Butoxycarbonylamino)-4-(2'-methoxy-2'-trifluoromethyl-phenylacetyl)-7,7,8,8,9,9,10,10,11,11,12,12,12-tridecafluoro-2-methyl-dodecan-4-ol

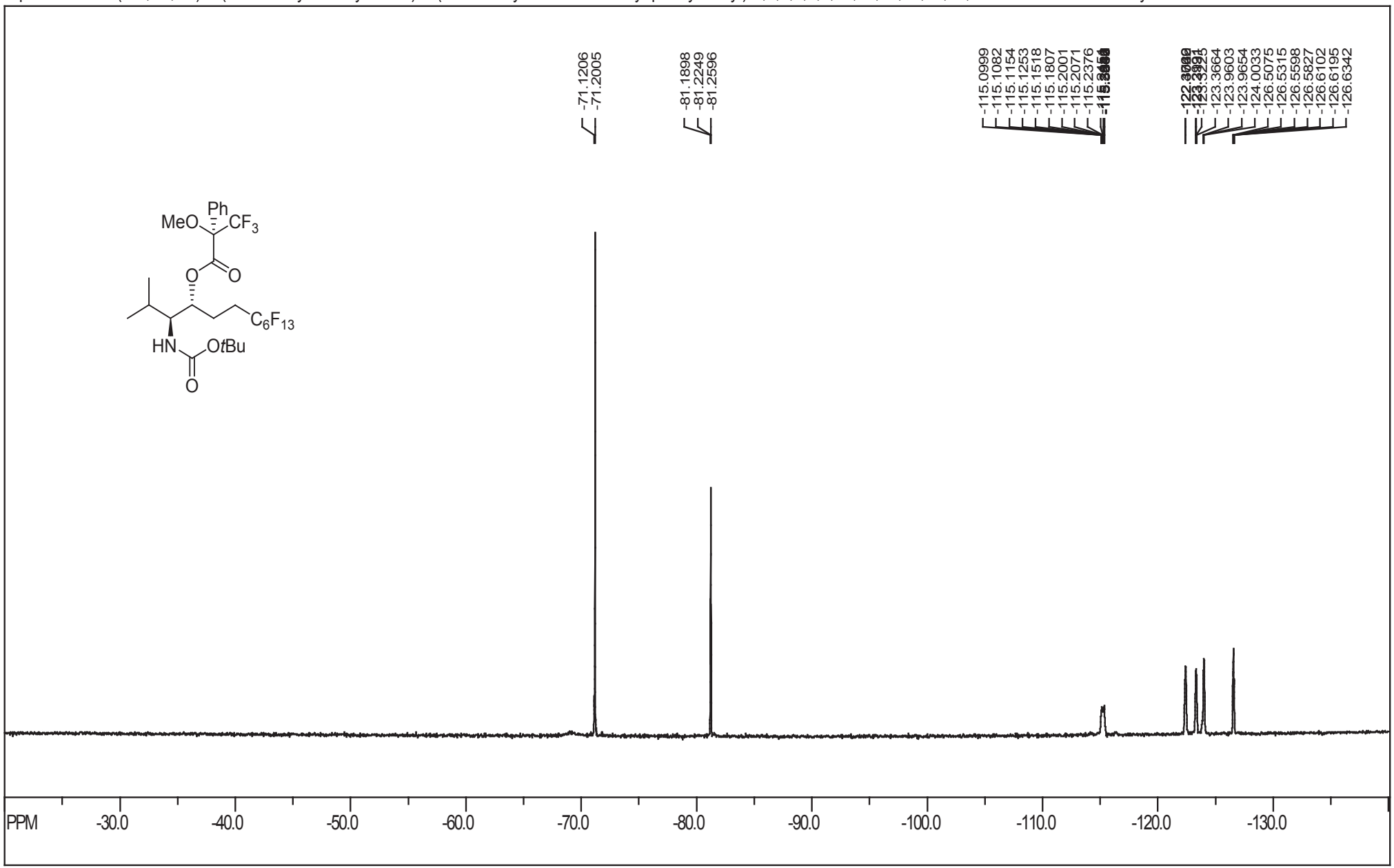

file: C:\NMR\Laina\80-90\lmg84A\8\fid expt: <zgflqn>

freq. of 0 ppm: 282.404481 MHz

SpinWorks 2.4: (2S,2'S,3R)-2-(Ethoxycarbonylamino)-3-(2'-methoxy-2'-trifluoromethyl-phenylacetyl)-6,6,7,7,8,8,9,9,10,10,11,11,11-tridecafluoro-1-phenyl-undecan-3-ol

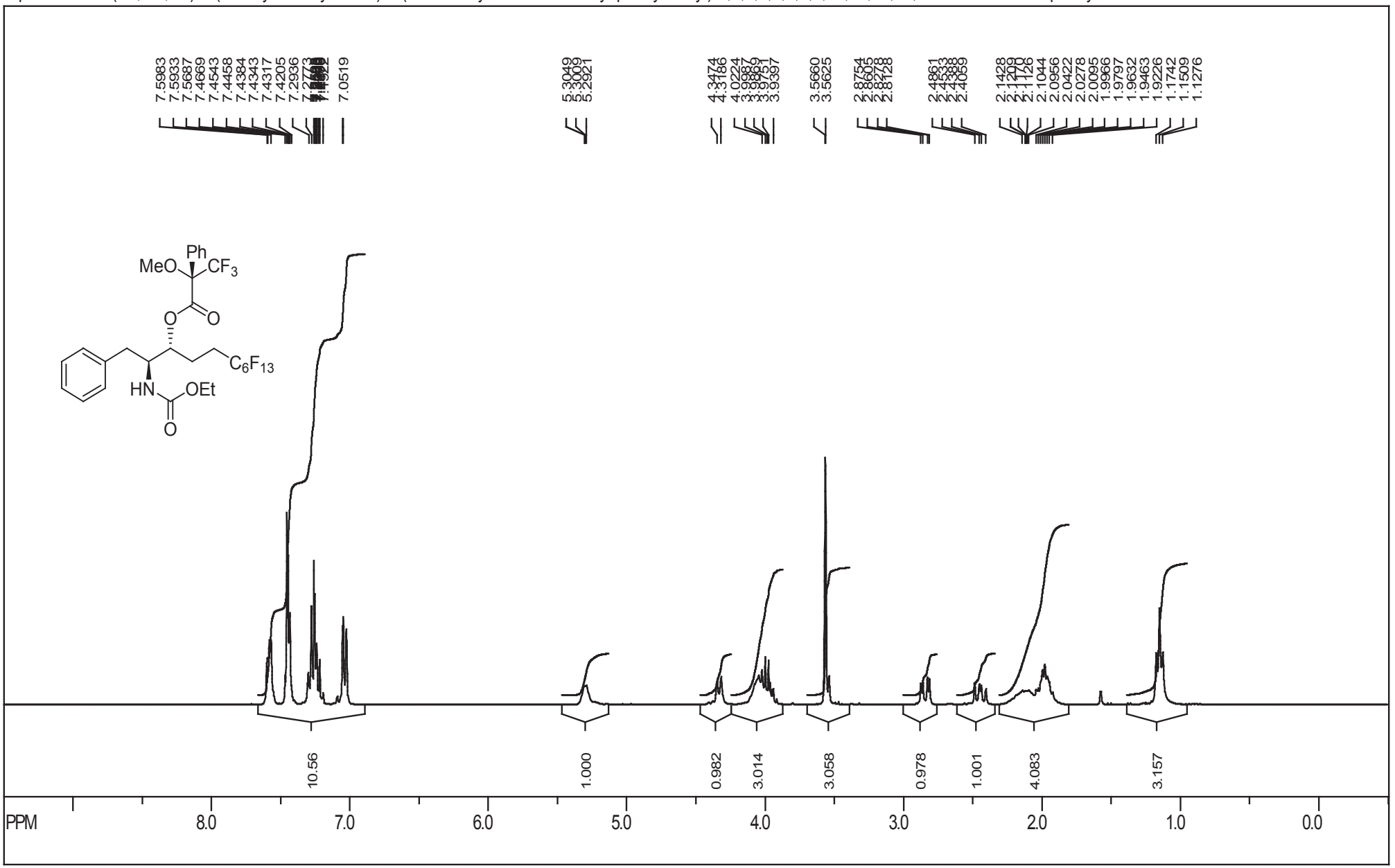

file: C:\NMR\Jason\vi\0-10\Jehvi_9b\1\fid expt: <zg30>

freq. of 0 ppm: 300.130006 MHz

plex points

SpinWorks 2.4: (2S,2'S,3R)-2-(Ethoxycarbonylamino)-3-(2'-methoxy-2'-trifluoromethyl-phenylacetyl)-6,6,7,7,8,8,9,9,10,10,11,11,11-tridecafluoro-1-phenyl-undecan-3-ol

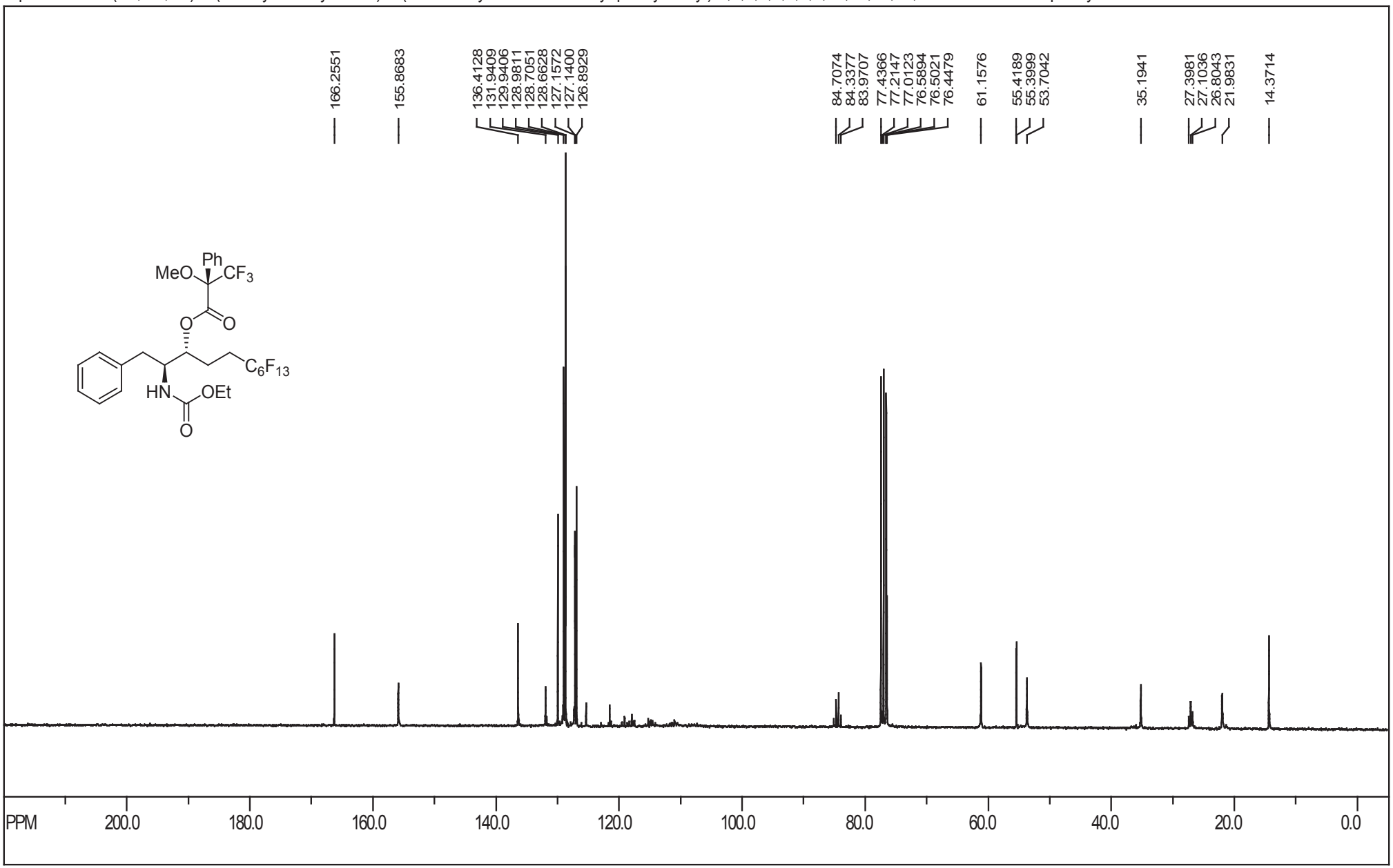

file: C:\NMR\Jason\vi\0-10\Jehvi_9b_char\2\fid expt: <zgpg30>

freq. of 0 ppm: 75.467749 MHz

SpinWorks 2.4: (2S,2'S,3R)-2-(Ethoxycarbonylamino)-3-(2'-methoxy-2'-trifluoromethyl-phenylacetyl)-6,6,7,7,8,8,9,9,10,10,11,11,11-tridecafluoro-1-phenyl-undecan-3-ol

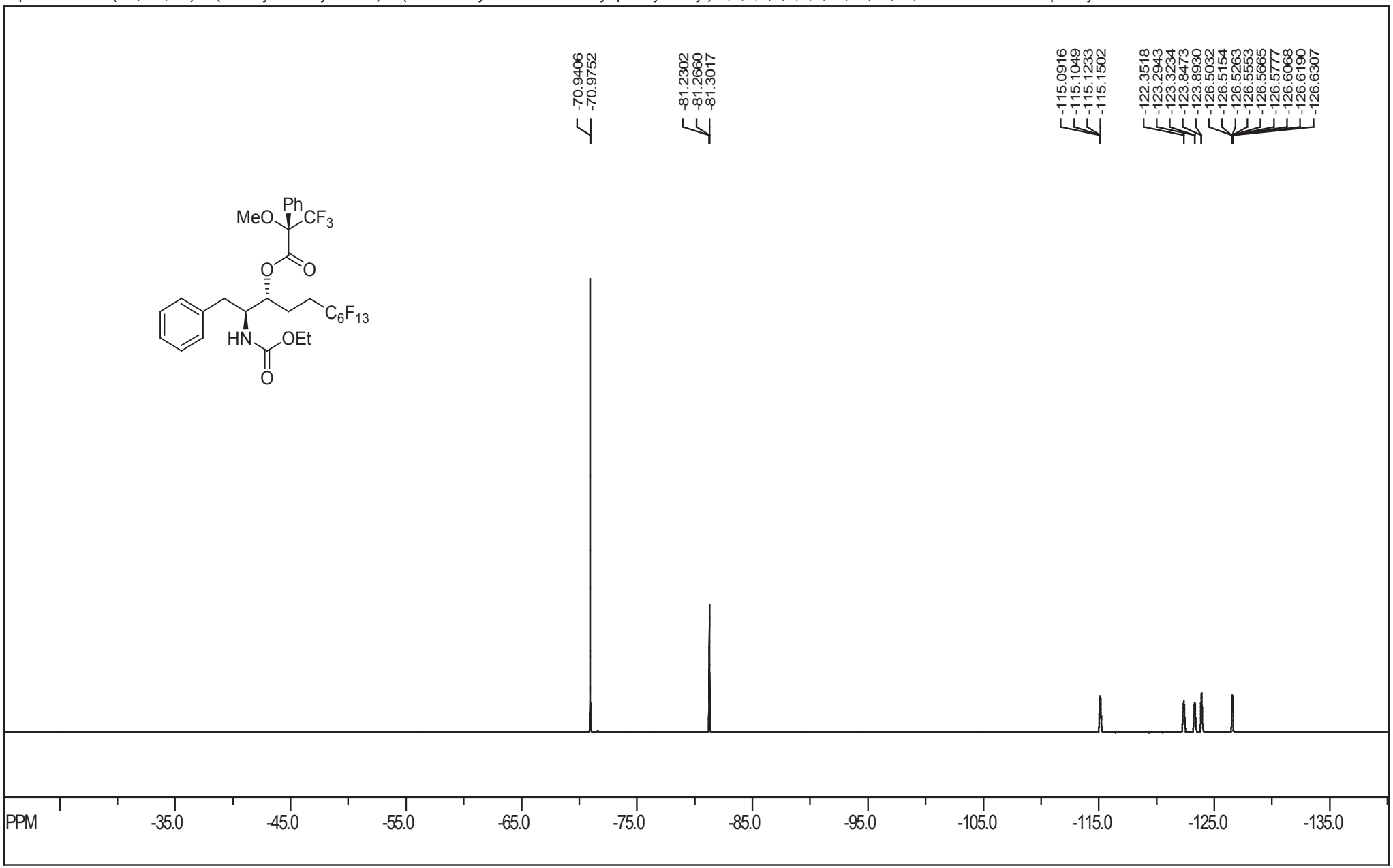

file: C:\NMR\Jason\vi\0-10\Jehvi_9b\4\fid expt: <zgfhigqn>

freq. of 0 ppm: 282.404481 MHz

SpinWorks 2.4: (2'S,3S,4R)-3-(tert-Butoxycarbonylamino)-4-(2'-methoxy-2'-trifluoromethyl-phenylacetyl)-7,7,8,8,9,9,10,10,11,11,12,12,12-tridecafluoro-2-methyl-dodecan-4-ol

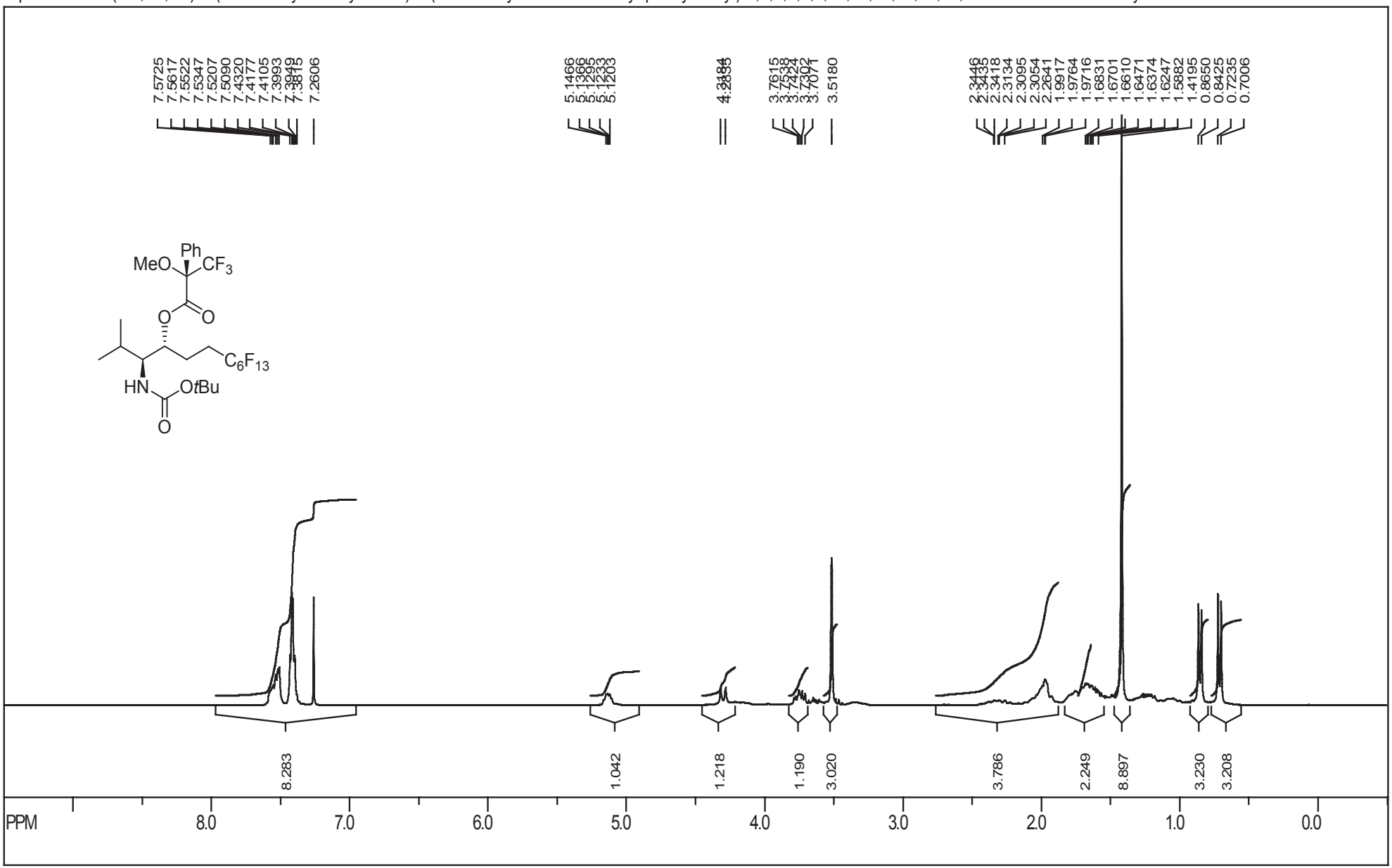

file: C:\NMR\Laina\80-90\lmg84B\1\fid expt: <zg30>

freq. of 0 ppm: 300.130006 MHz

SpinWorks 2.4: (2'S,3S,4R)-3-(tert-Butoxycarbonylamino)-4-(2'-methoxy-2'-trifluoromethyl-phenylacetyl)-7,7,8,8,9,9,10,10,11,11,12,12,12-tridecafluoro-2-methyl-dodecan-4-ol

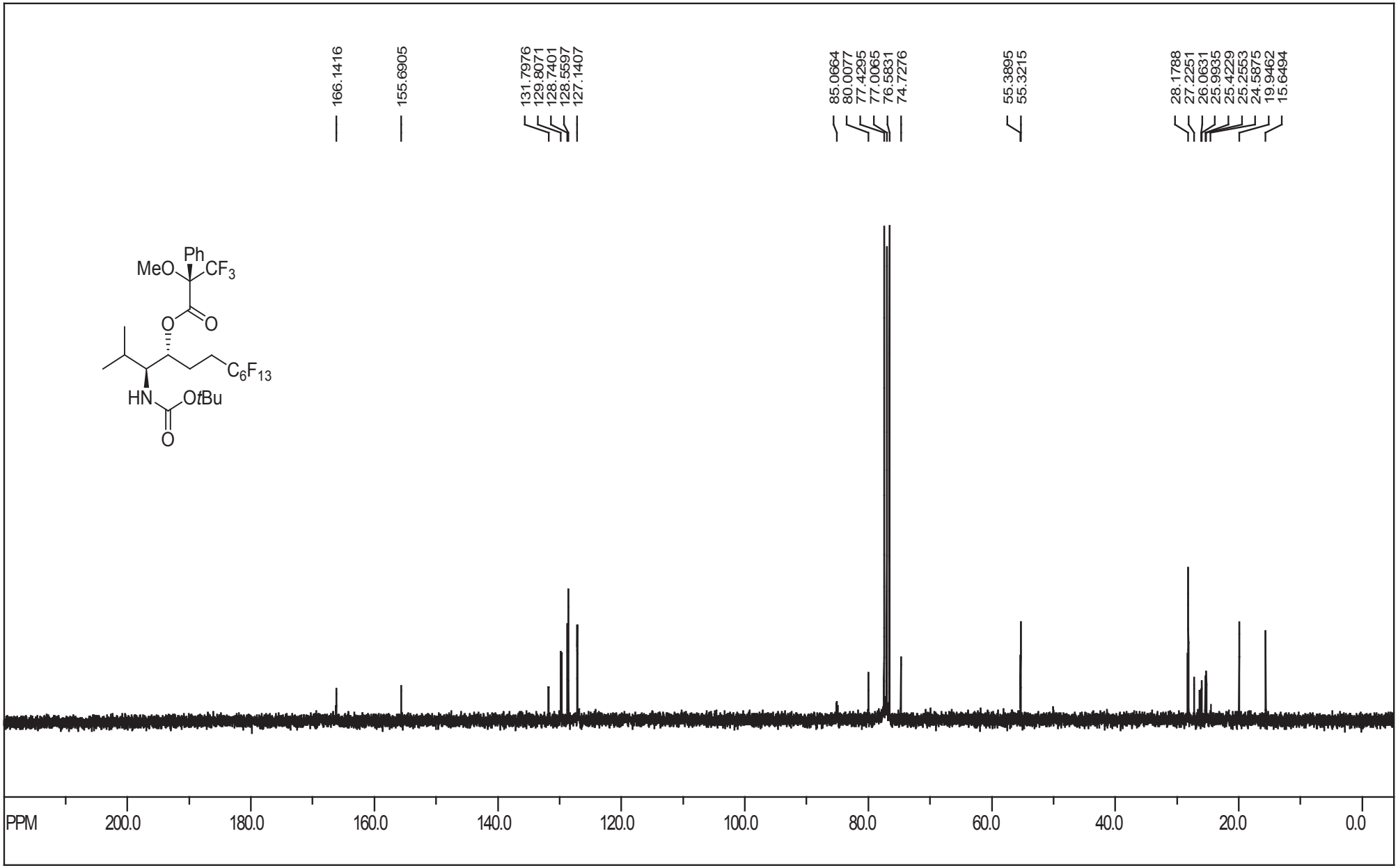

file: C:\NMR\Laina\80-90\lmg84B\2\fid expt: <zgpg30>

freq. of 0 ppm: 75.467749 MHz

SpinWorks 2.4: (2'S,3S,4R)-3-(tert-Butoxycarbonylamino)-4-(2'-methoxy-2'-trifluoromethyl-phenylacetyl)-7,7,8,8,9,9,10,10,11,11,12,12,12-tridecafluoro-2-methyl-dodecan-4-ol

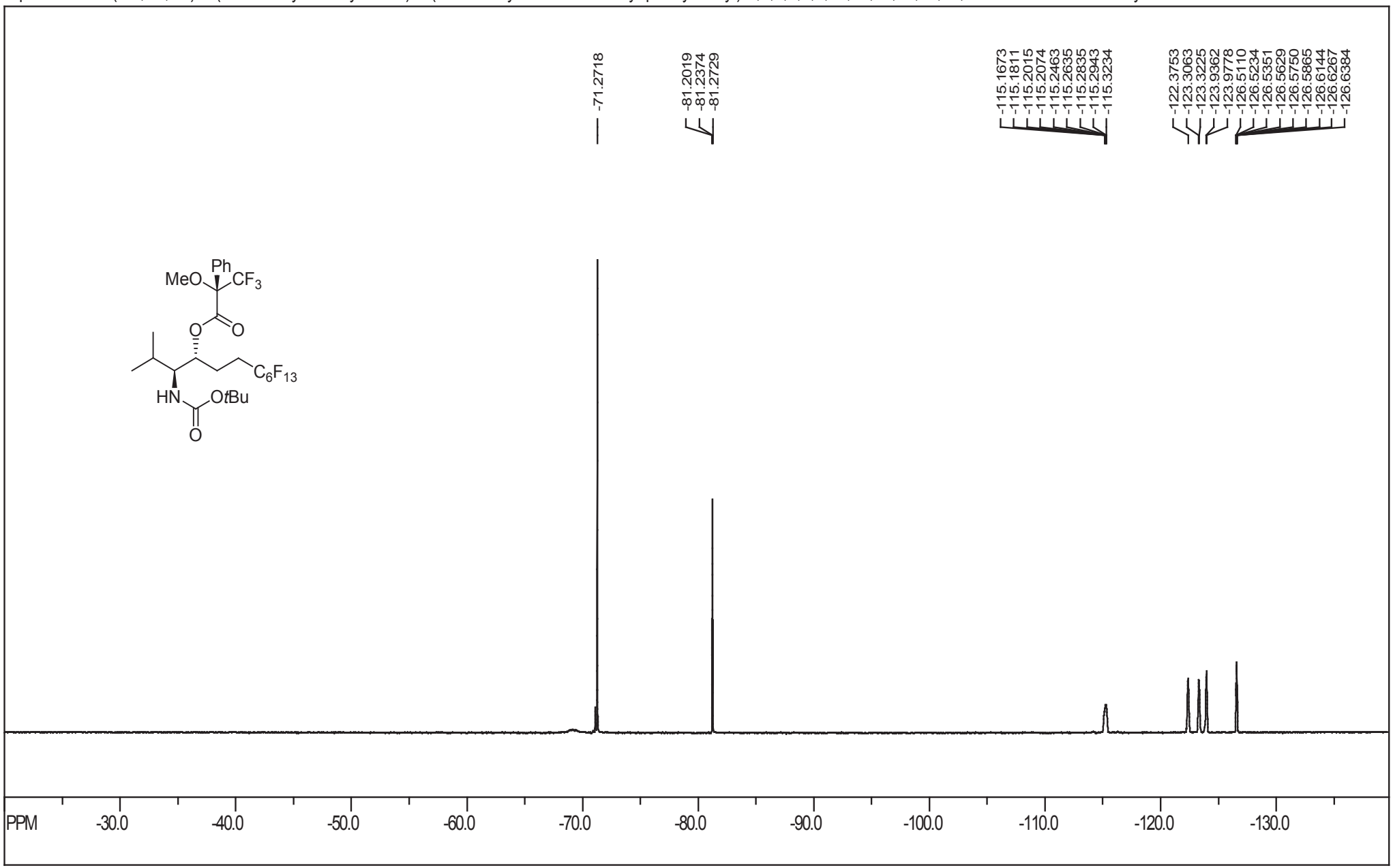

file: C:\NMR\Laina\80-90\lmg84B\5\fid expt: <zgflqn>

freq. of 0 ppm: 282.404481 MHz

SpinWorks 2.4: (1R,2S,2'S)-1-(tert-Butoxycarbonylamino)-2-(2'-methoxy-2'-trifluoromethyl-phenylacetyl)-5,5,6,6,7,7,8,8,9,9,10,10,10-tridecafluoro-1-phenyl-decan-2-ol

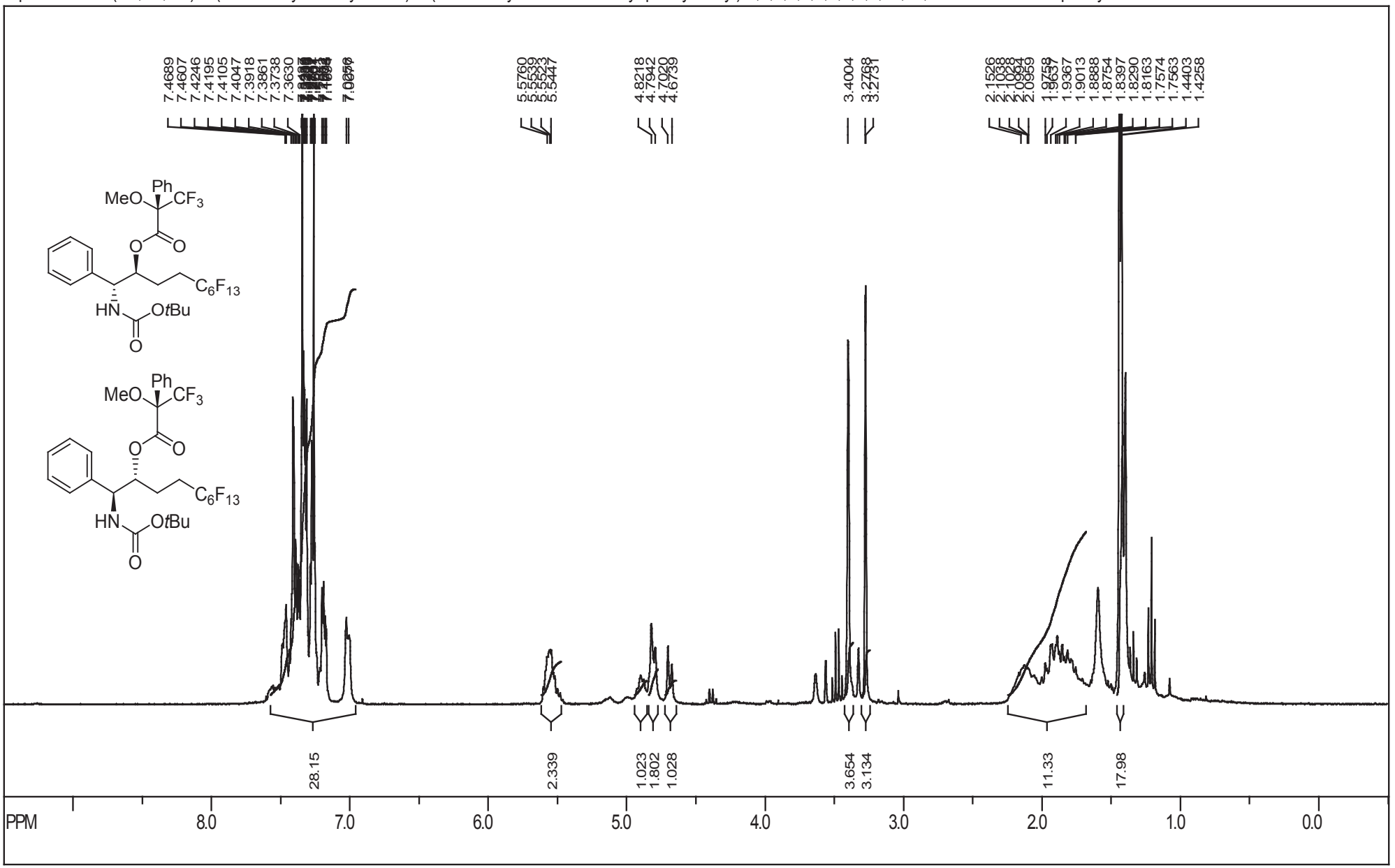

file: C:\NMR\Laina\80-90\lmg82B\3\fid expt: <zg30>

freq. of 0 ppm: 300.130006 MHz

SpinWorks 2.4: (1R,2S,2'S)-1-(tert-Butoxycarbonylamino)-2-(2'-methoxy-2'-trifluoromethyl-phenylacetyl)-5,5,6,6,7,7,8,8,9,9,10,10,10-tridecafluoro-1-phenyl-decan-2-ol

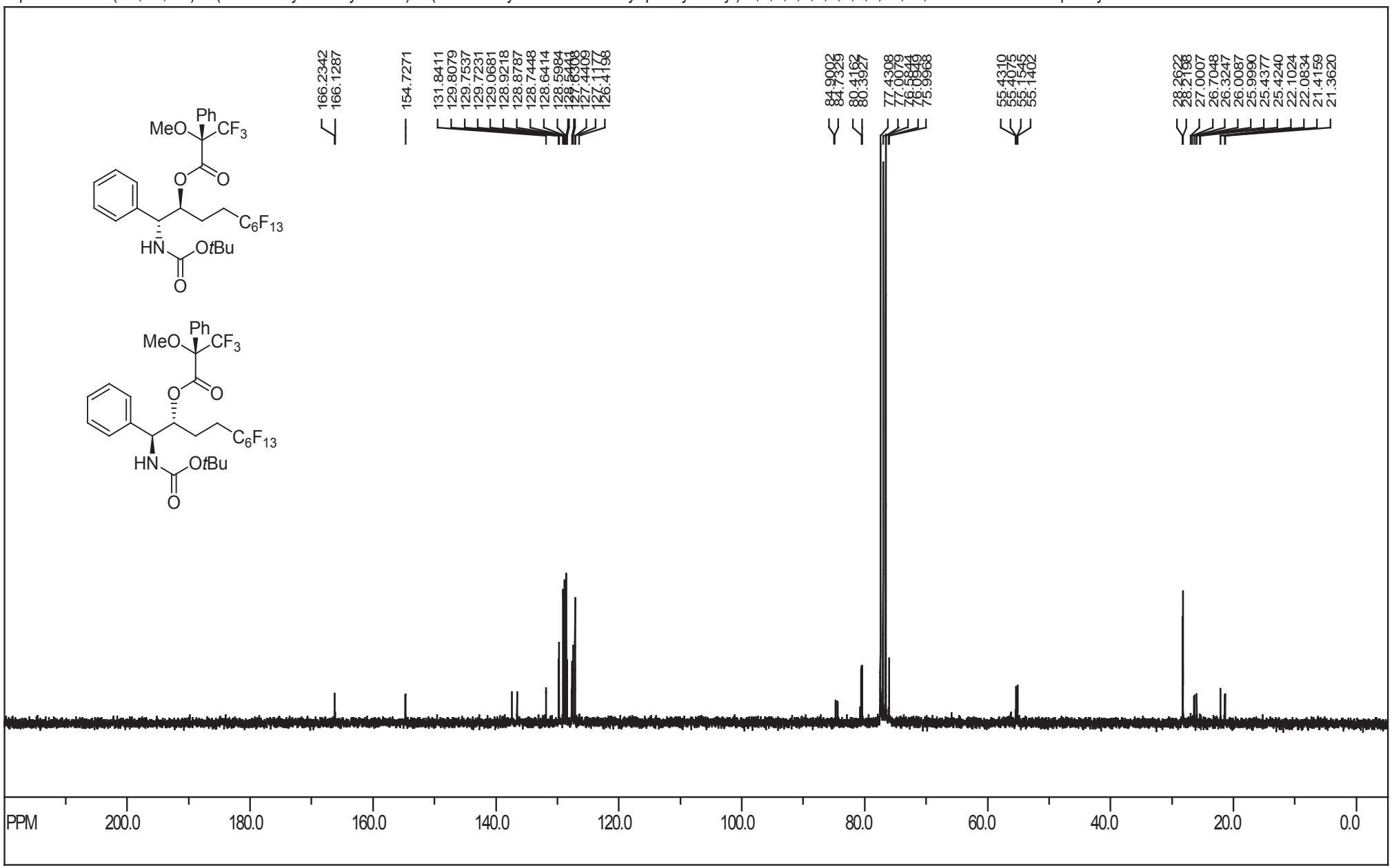

file: C:\NMR\Laina\80-90\Img82B\4\fid expt: <zgpg30>

freq. of 0 ppm: 75.467749 MHz

SpinWorks 2.4: (1R,2S,2'S)-1-(tert-Butoxycarbonylamino)-2-(2'-methoxy-2'-trifluoromethyl-phenylacetyl)-5,5,6,6,7,7,8,8,9,9,10,10,10-tridecafluoro-1-phenyl-decan-2-ol

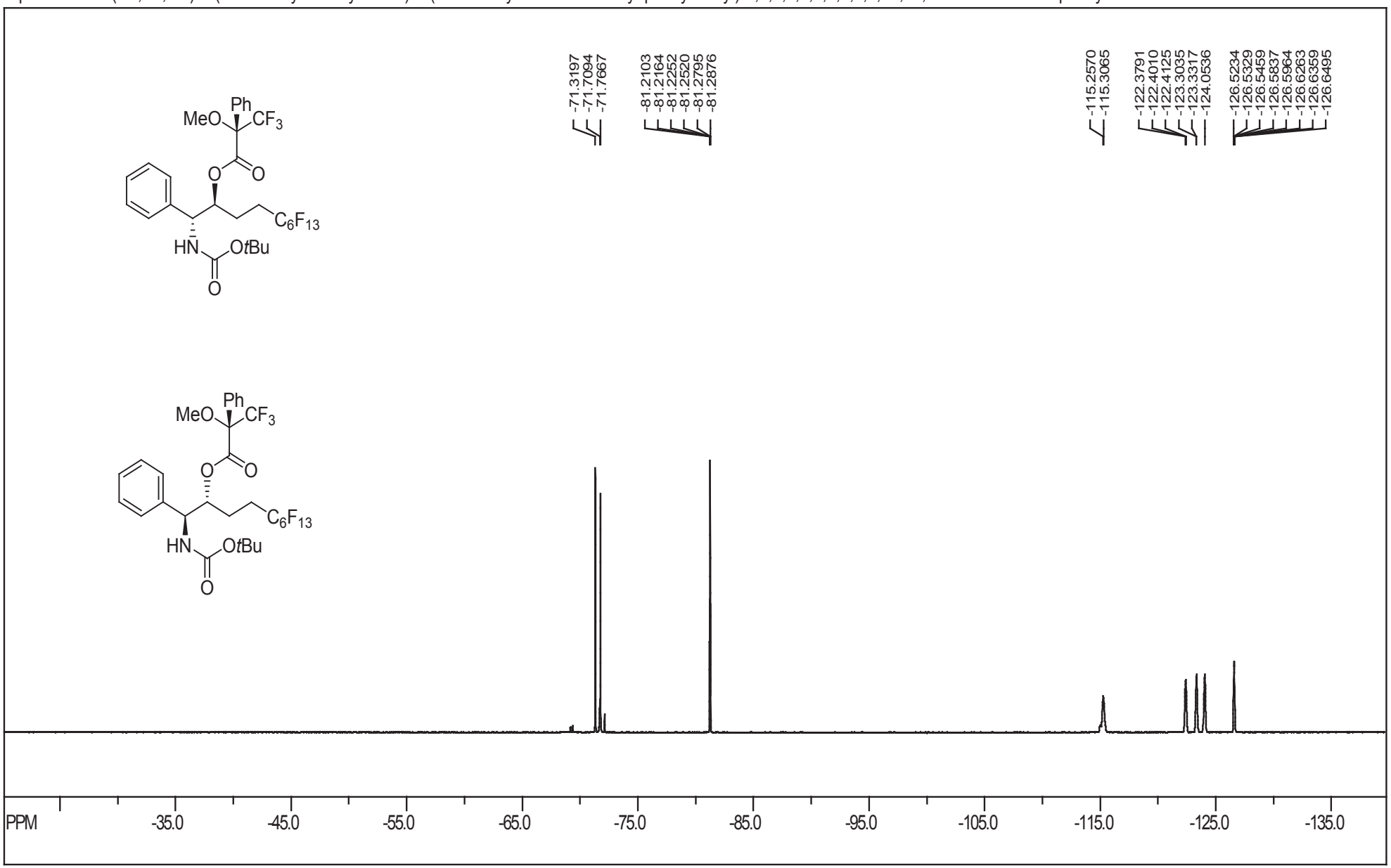

file: C:\NMR\Laina\80-90\img82B\8\fid expt: <zgflqn>

freq. of 0 ppm: 282.404481 MHz

SpinWorks 2.4: (E)-(4S,5R)-4-Benzyl-3-(2'-butenoyl)-5-(1'H,1'H,2'H,2'H-perfluorooctyl)-2-oxazolidinone

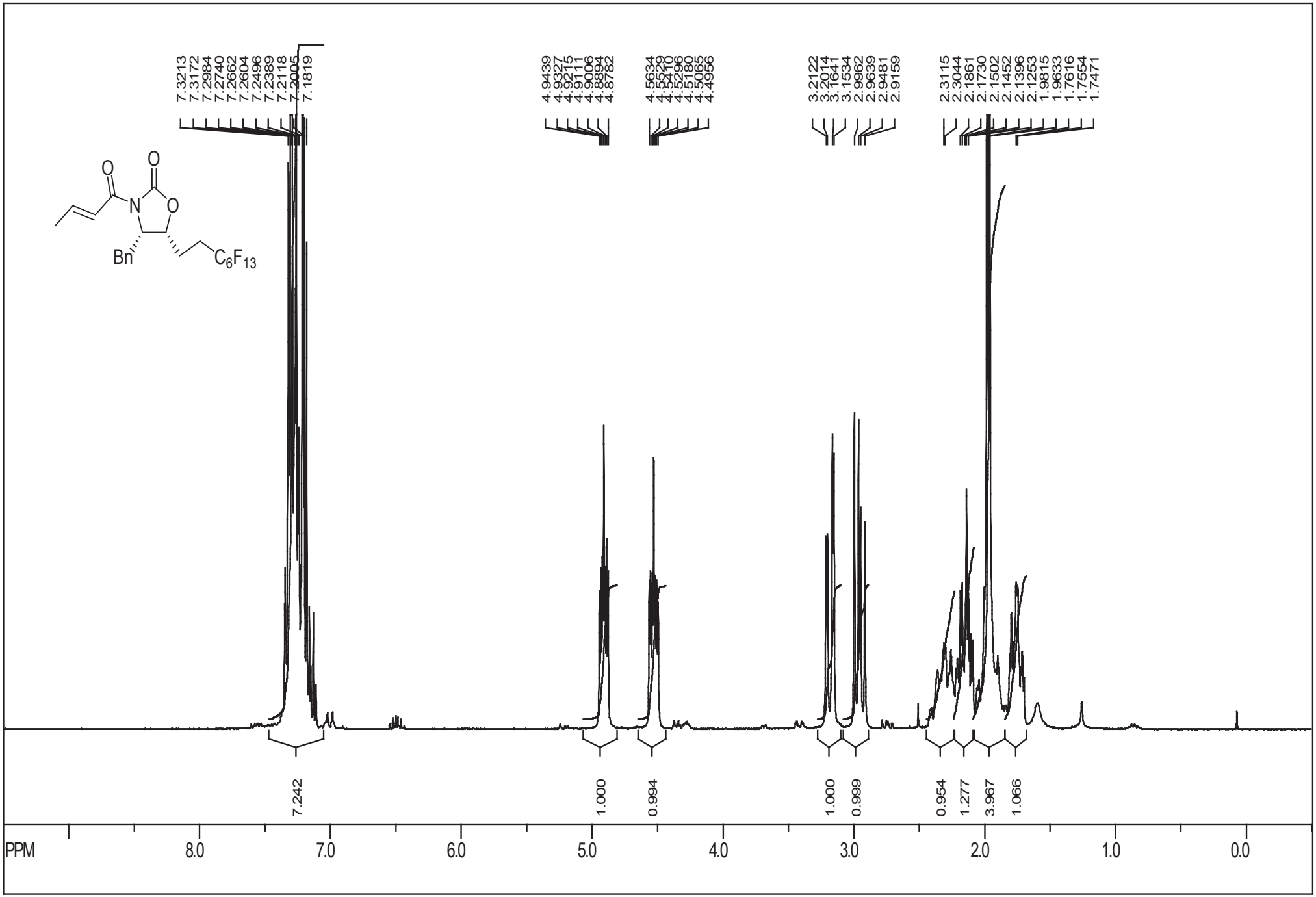

file: C:\NMR\30-40\Jehvi_37_1_tes\1\fid expt: <zg30>

freq. of 0 ppm: 300.130006 MHz

SpinWorks 2.4: (E)-(4S,5R)-4-benzyl-3-(2'-butenoyl)-5-(1'H,1'H,2'H,2'H-perfluorooctyl)-2-oxazolidinone

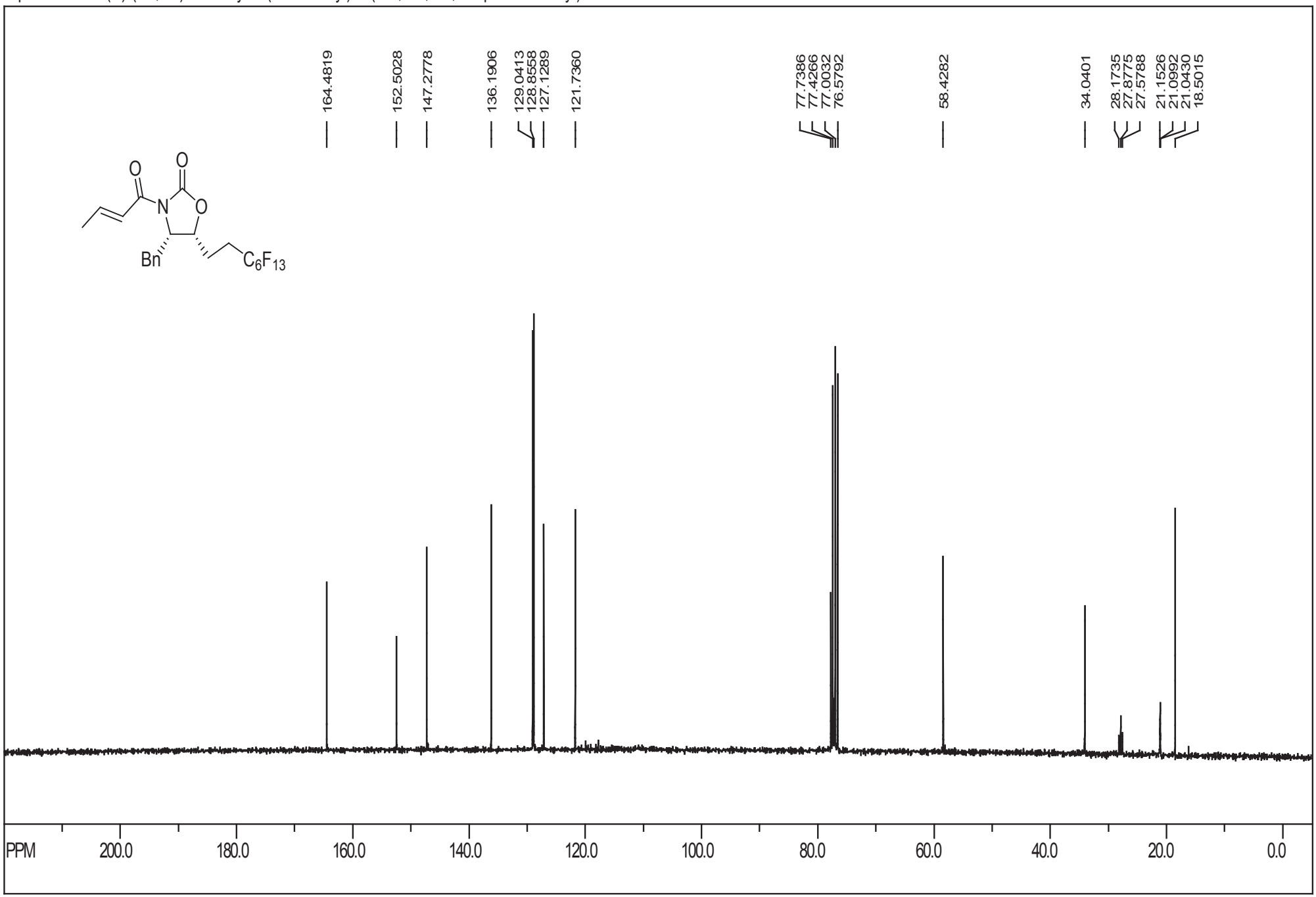

file: C:\NMR\Jehvi_2\7\fid expt: <zgpg30>

freq. of 0 ppm: 75.467749 MHz

SpinWorks 2.4: (E)-(4S,5R)-4-benzyl-3-(3'-phenyl-2'-propenoyl)-5-(1'H,1'H,2'H,2'H-perfluorooctyl)-2-oxazolidinone

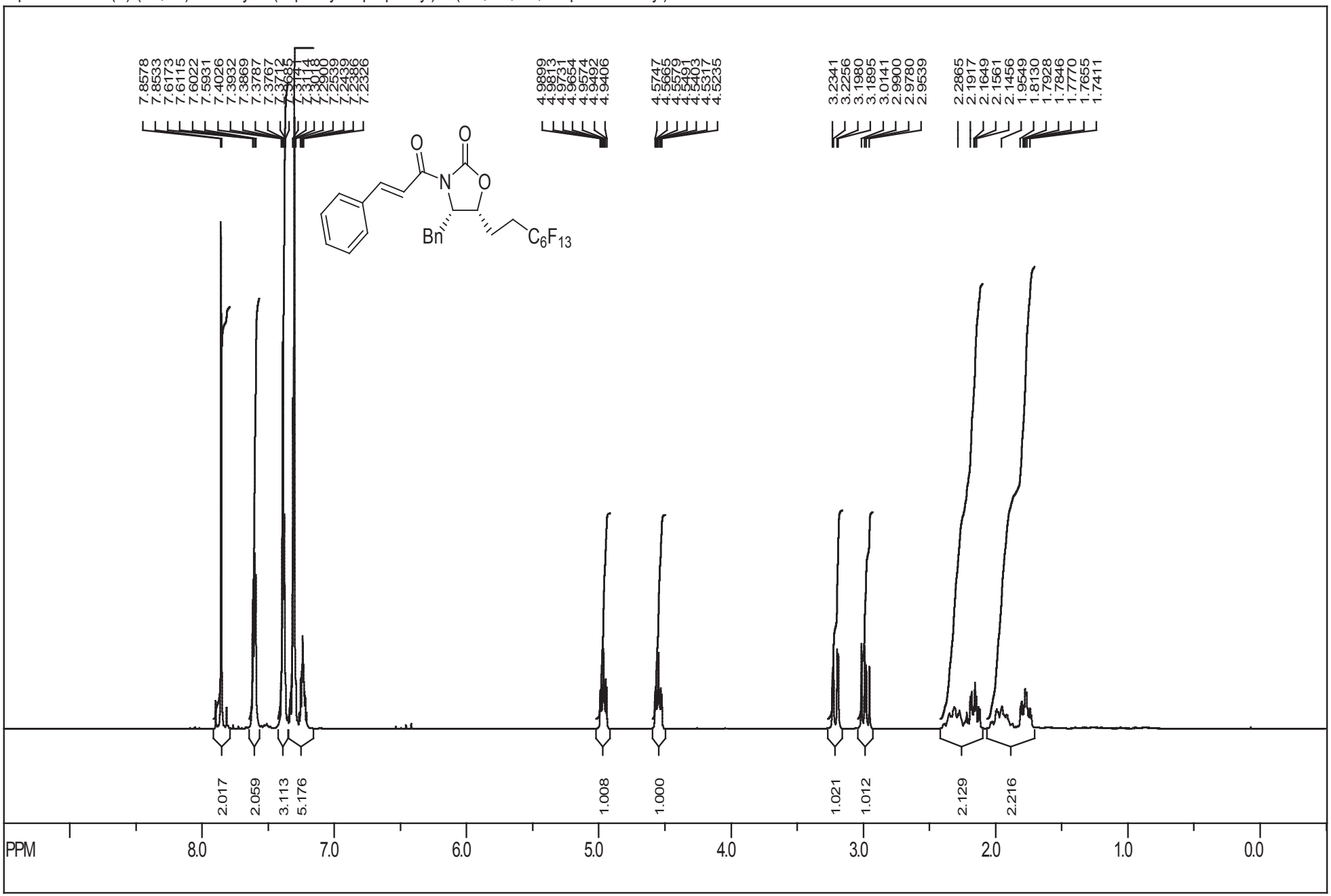

file: C:\NMR\NDSUJEHM_37_2LO.FID\FID block# 1 expt: "s2pul"

freq. of 0 ppm: 399.935650 MHz

SpinWorks 2.4: (E)-(4S,5R)-4-benzyl-3-(3'-phenyl-2'-propenoyl)-5-(1'H,1'H,2'H,2'H-perfluorooctyl)-2-oxazolidinone

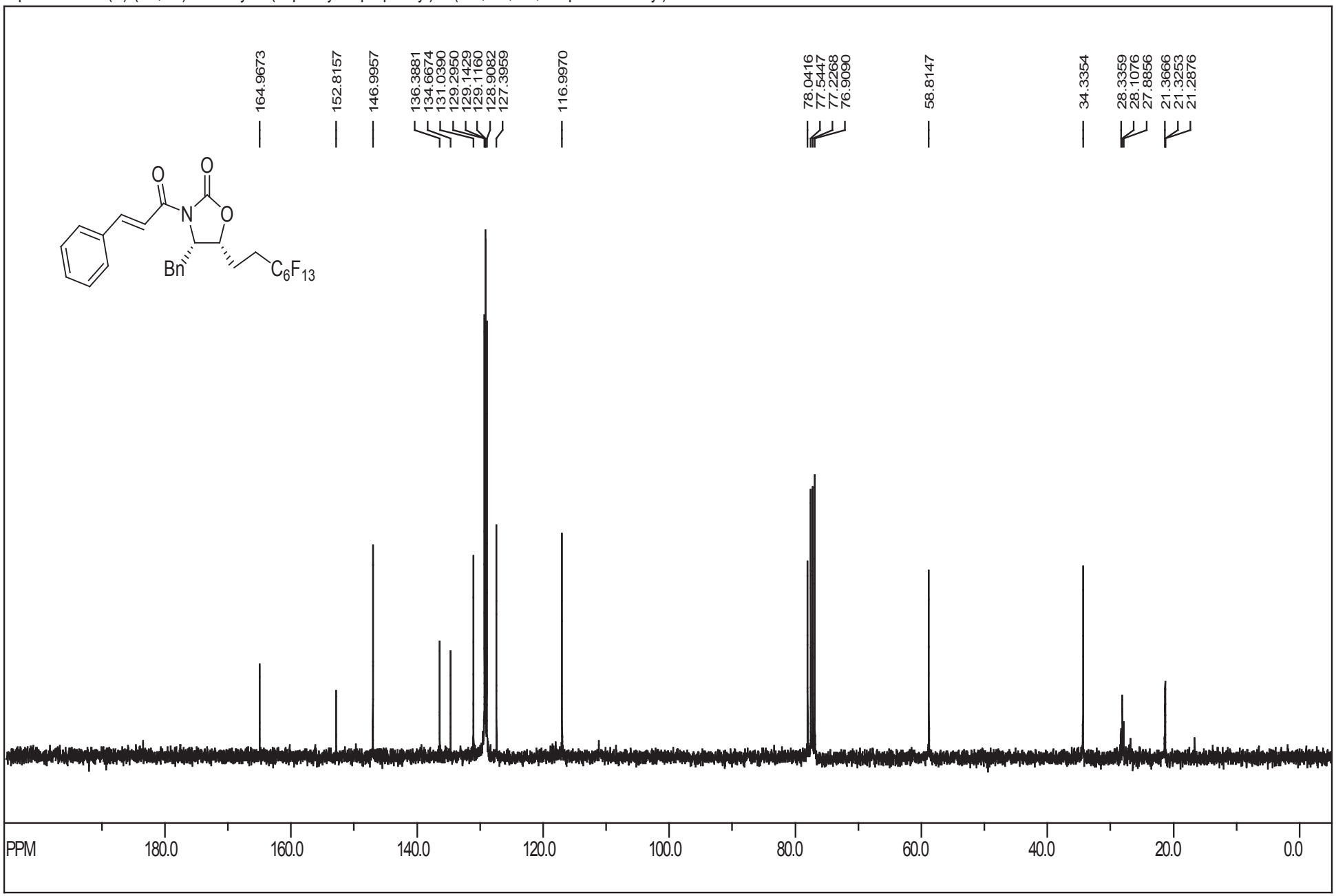

file: C:\NMR\NDSUJEHM_37_2_FSPE_C.FID\FID block# 1 expt: "s2pul"

freq. of 0 ppm: 100.563875 MHz

SpinWorks 2.4: (E)-(4S,5R)-4-benzyl-3-(3'-ethoxycarbonyl-2'-propenoyl)-5-(1'H,1'H,2'H,2'H-perfluorooctyl)-2-oxazolidinone

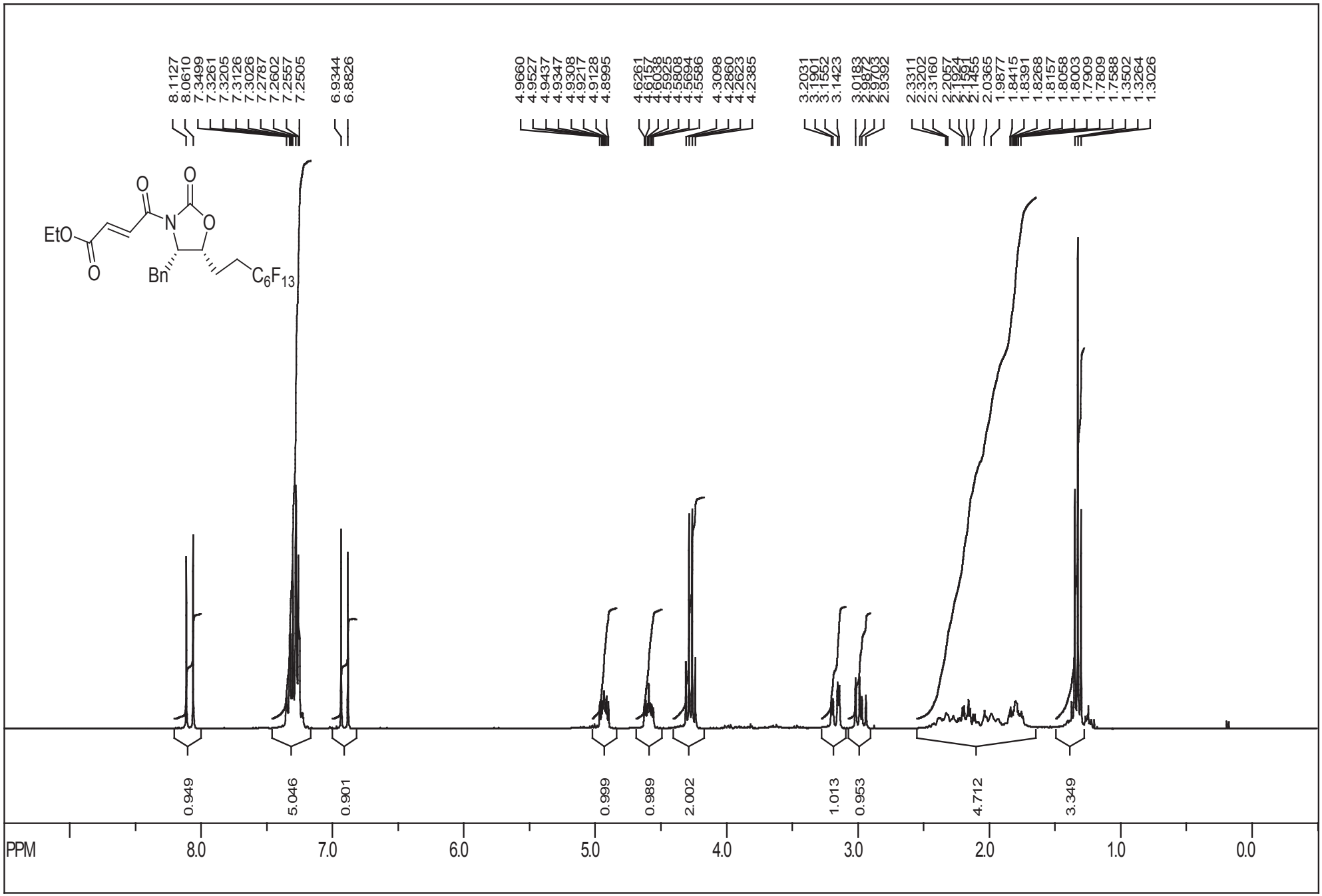

file: C:\NMR\Jehvi_40_c\1\fid expt: <zg30>

freq. of 0 ppm: 300.130006 MHz

SpinWorks 2.4: (E)-(4S,5R)-4-benzyl-3-(3'-ethoxycarbonyl-2'-propenoyl)-5-(1'H,1'H,2'H,2'H-perfluorooctyl)-2-oxazolidinone

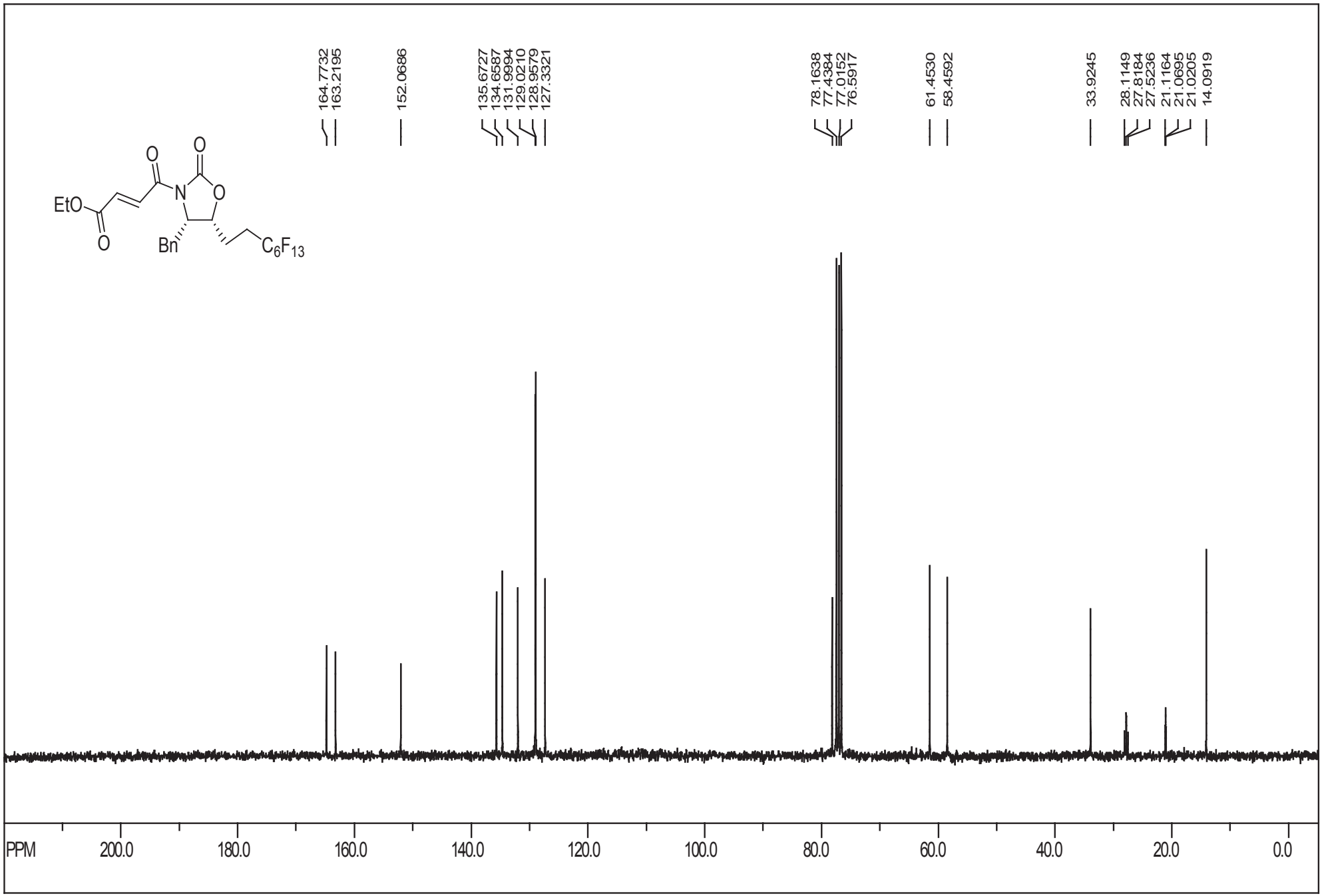

file: C:\NMR\Jehvi_40_c\5\fid expt: <zgpg30>

freq. of 0 ppm: 75.467749 MHz

SpinWorks 2.4: (4S,5R)-4-Benzyl-5-(1'H,1'H,2'H,2'R-perfluorooctyl)-2-oxazolidinone

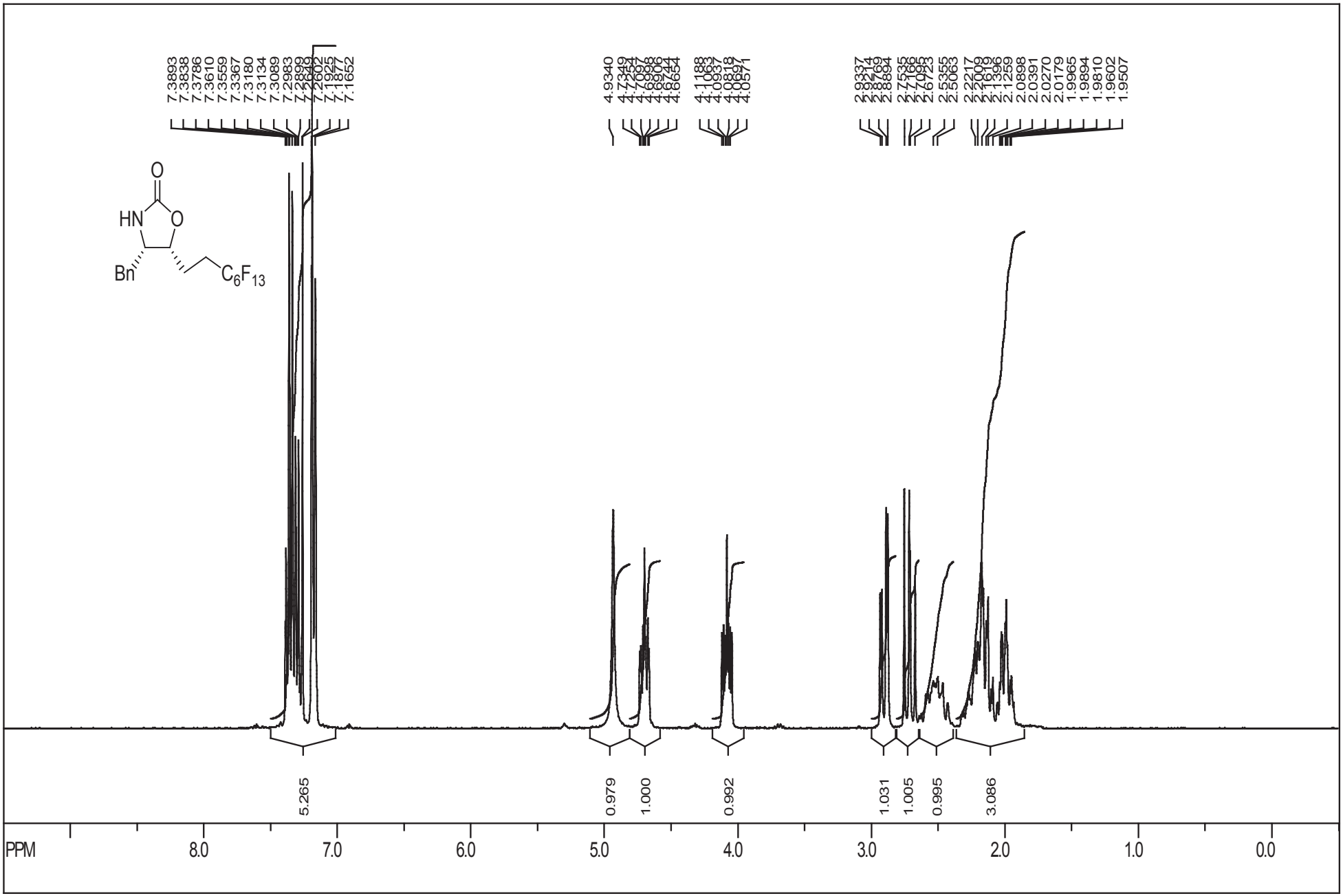

file: C:\NMR\jehv_88c\2\fid expt: <zg30>

SpinWorks 2.4: (4S,5R)-4-Benzyl-5-(1'H,1'H,2'H,2'H-perfluorooctyl)-2-oxazolidinone

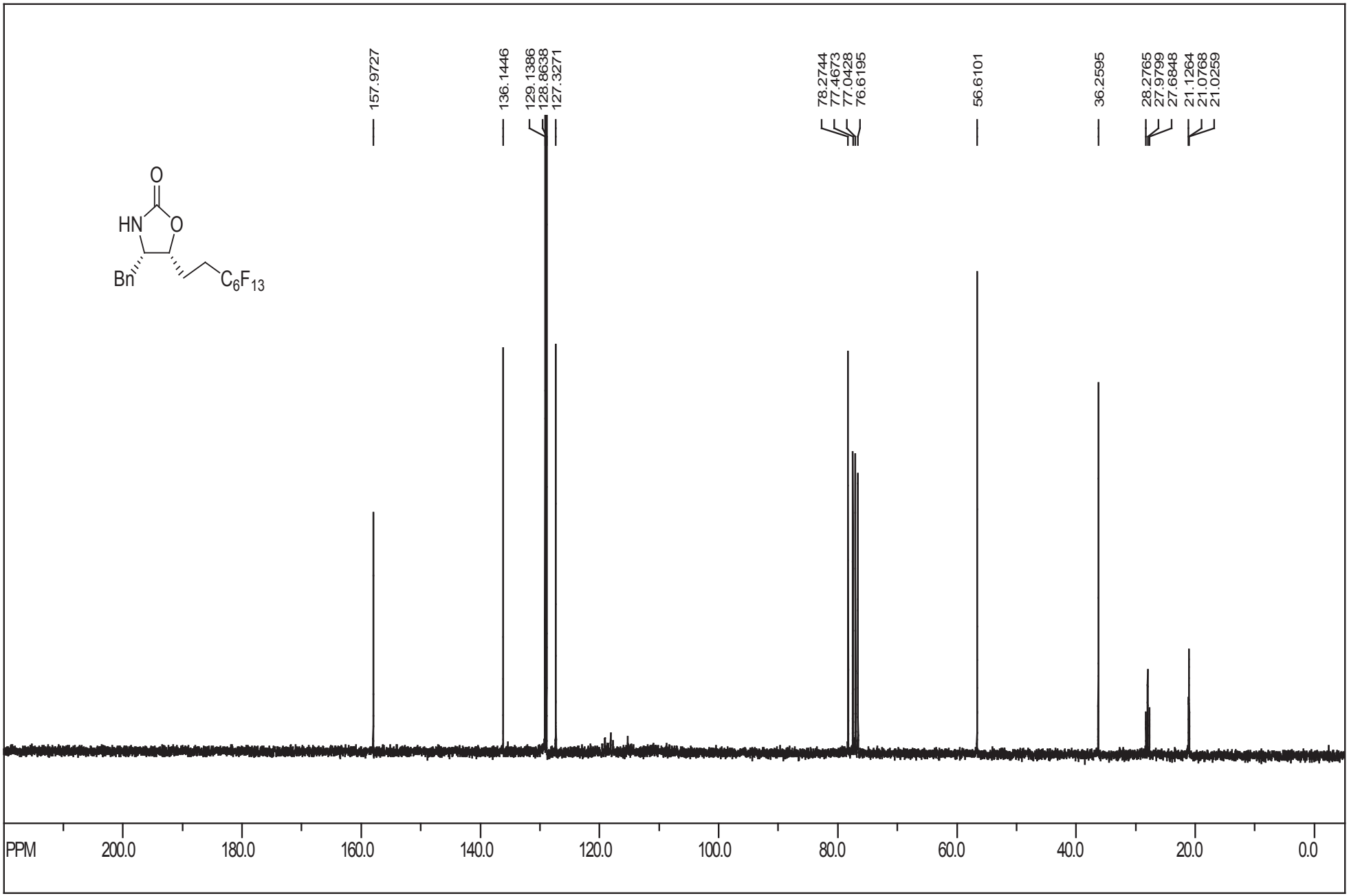

file: C:\NMR\Jehvi_29\5\fid expt: <zgpg30>

SpinWorks 2.4: (E)-(4S,5R)-4-Benzyl-3-(2'-butenoyl)-5-(1'H,1'H,2'H,2'H-perfluorooctyl)-2-oxazolidinone

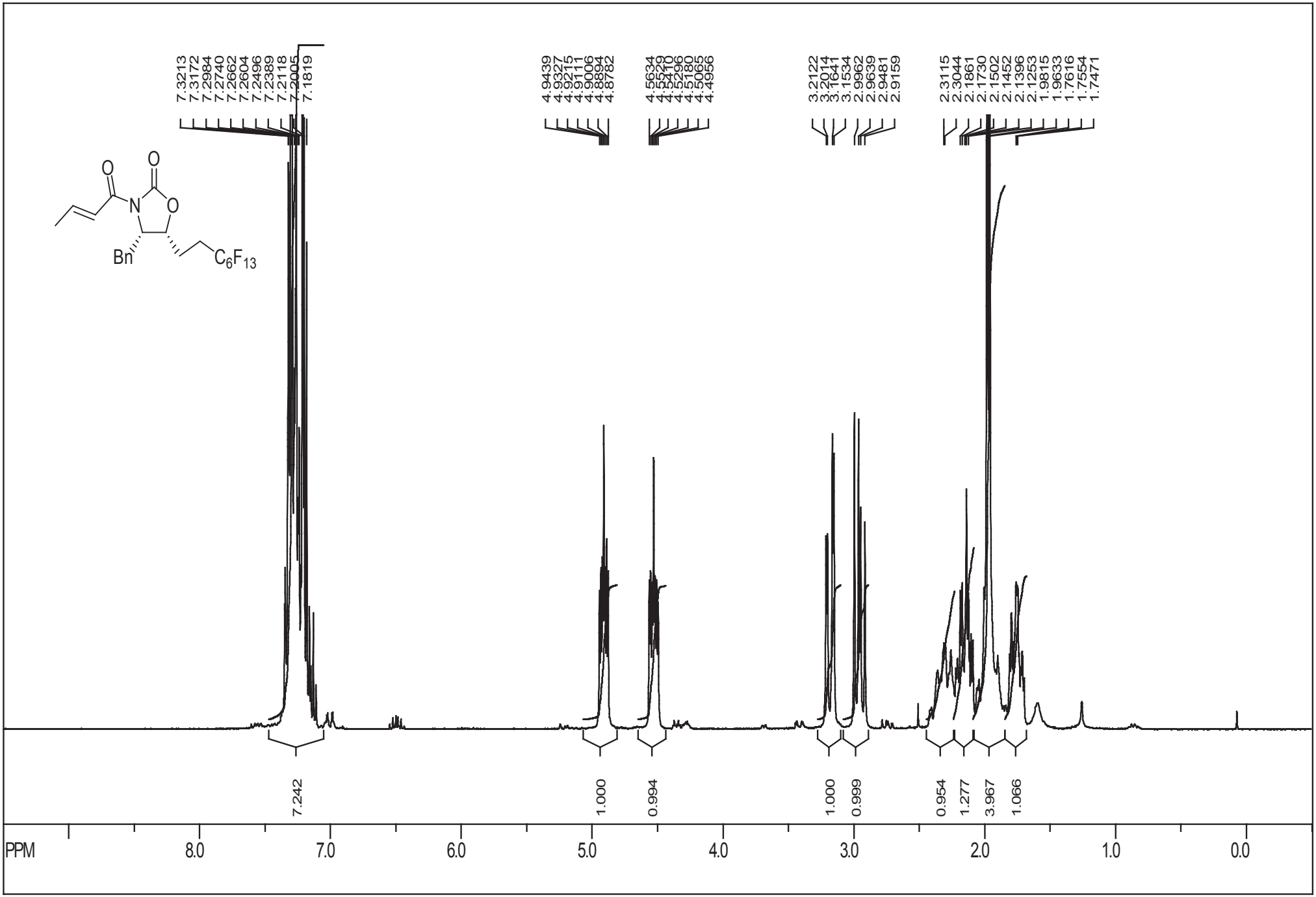

file: C:\NMR\30-40\Jehvi_37_1_tes\1\fid expt: <zg30>

freq. of 0 ppm: 300.130006 MHz

SpinWorks 2.4: (E)-(4S,5R)-4-benzyl-3-(2'-butenoyl)-5-(1'H,1'H,2'H,2'H-perfluorooctyl)-2-oxazolidinone

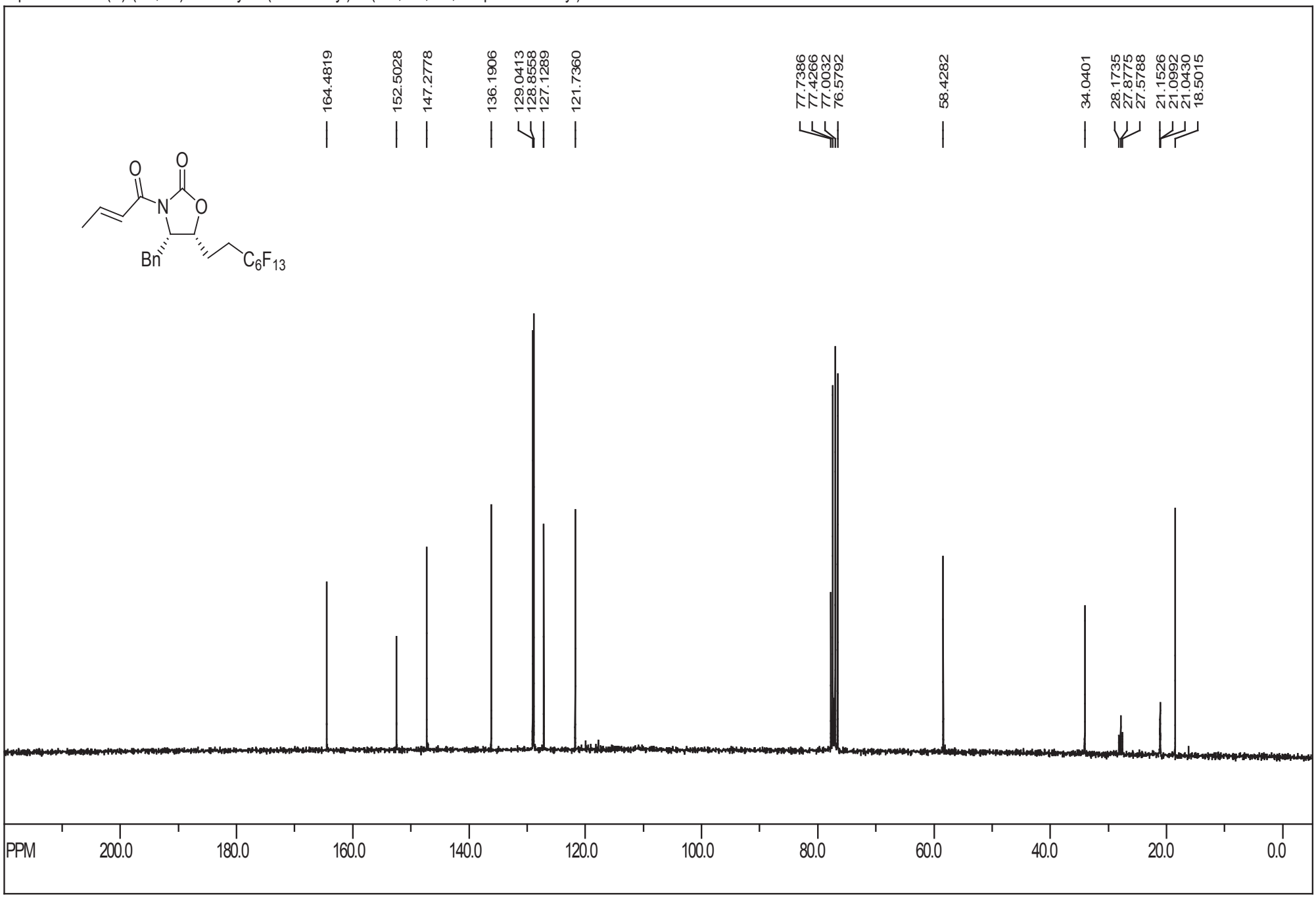

file: C:\NMR\Jehvi_2\7\fid expt: <zgpg30>

freq. of 0 ppm: 75.467749 MHz

SpinWorks 2.4: (E)-(4S,5R)-4-benzyl-3-(3'-phenyl-2'-propenoyl)-5-(1'H,1'H,2'H,2'H-perfluorooctyl)-2-oxazolidinone

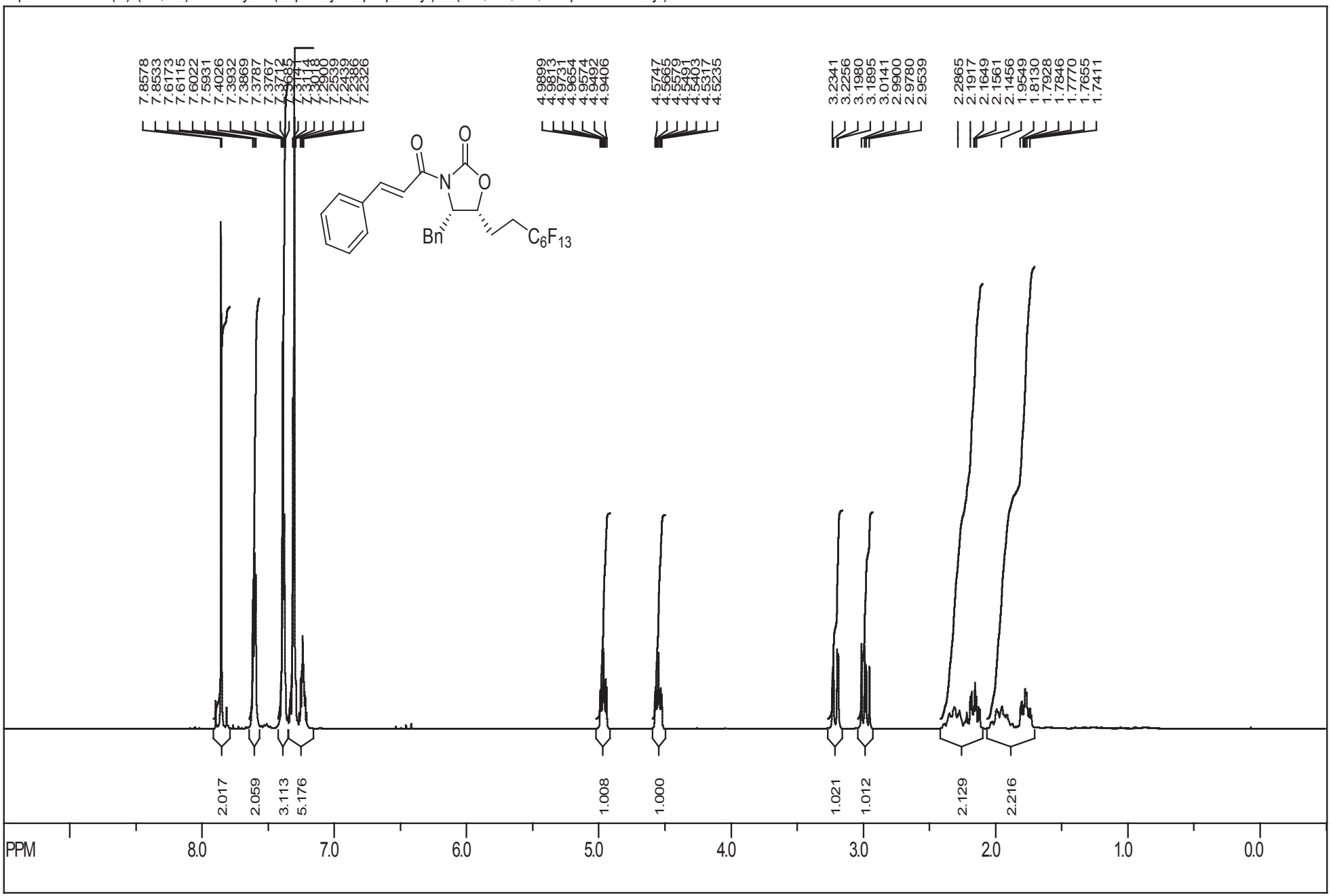

file: C:\NMR\NDSUJEHM_37_2LO.FID\FID block# 1 expt: "s2pul"

freq. of 0 ppm: 399.935650 MHz

SpinWorks 2.4: (E)-(4S,5R)-4-benzyl-3-(3'-phenyl-2'-propenoyl)-5-(1'H,1'H,2'H,2'H-perfluorooctyl)-2-oxazolidinone

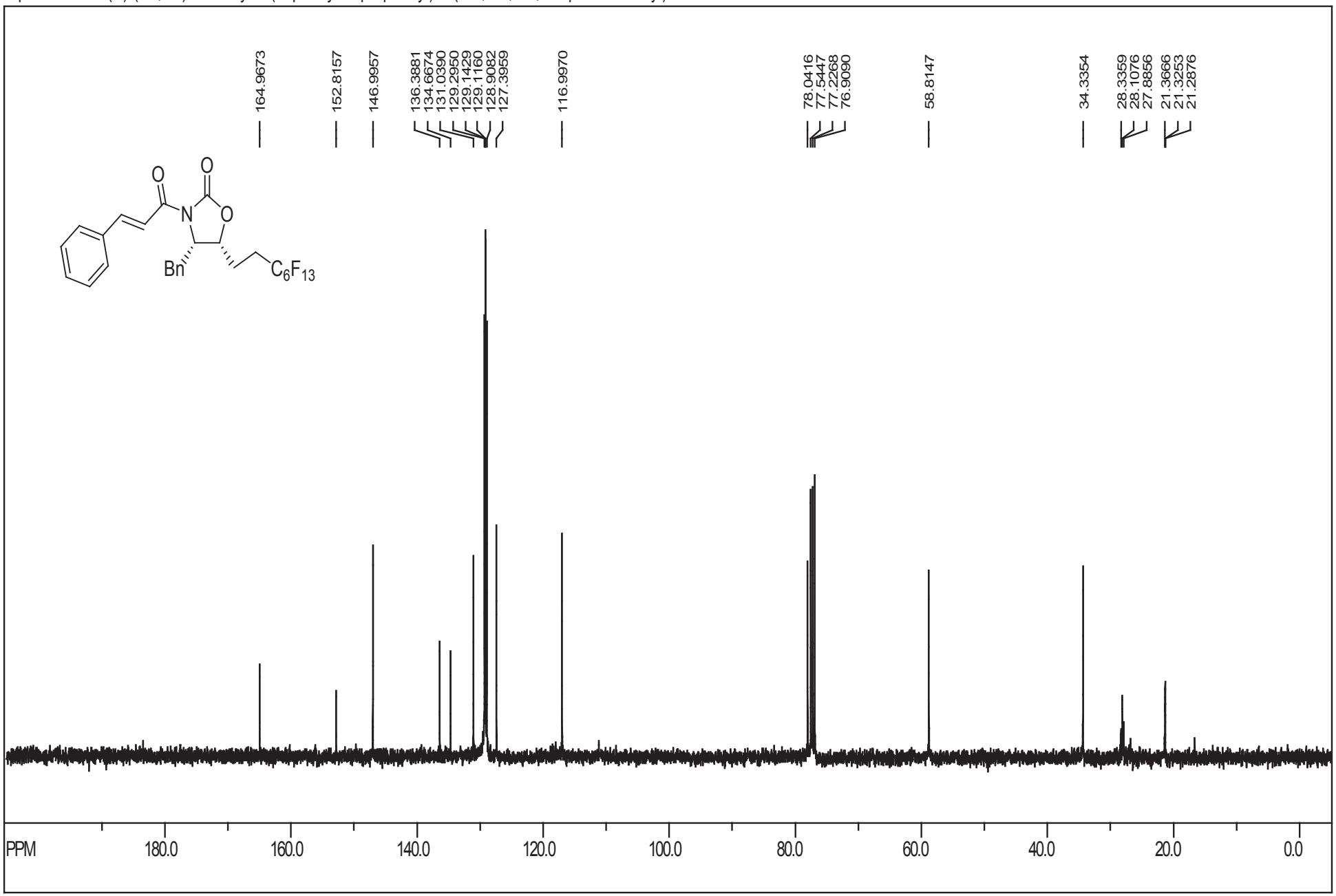

file: C:\NMR\NDSUJEHM_37_2_FSPE_C.FID\FID block# 1 expt: "s2pul"

freq. of 0 ppm: 100.563875 MHz

SpinWorks 2.4: (E)-(4S,5R)-4-benzyl-3-(3'-ethoxycarbonyl-2'-propenoyl)-5-(1'H,1'H,2'H,2'H-perfluorooctyl)-2-oxazolidinone

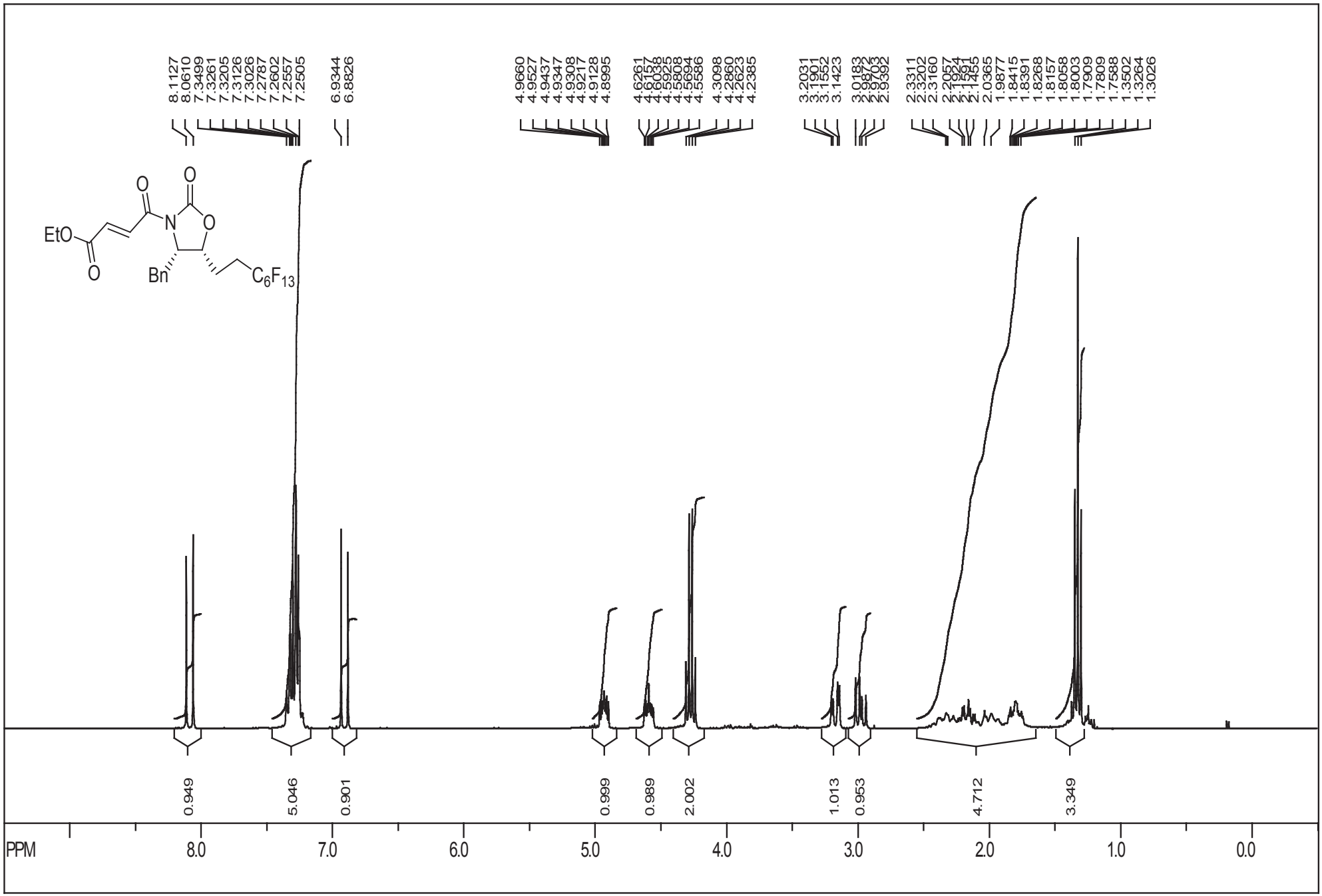

file: C:\NMR\Jehvi_40_c\1\fid expt: <zg30>

freq. of 0 ppm: 300.130006 MHz

SpinWorks 2.4: (E)-(4S,5R)-4-benzyl-3-(3'-ethoxycarbonyl-2'-propenoyl)-5-(1'H,1'H,2'H,2'H-perfluorooctyl)-2-oxazolidinone

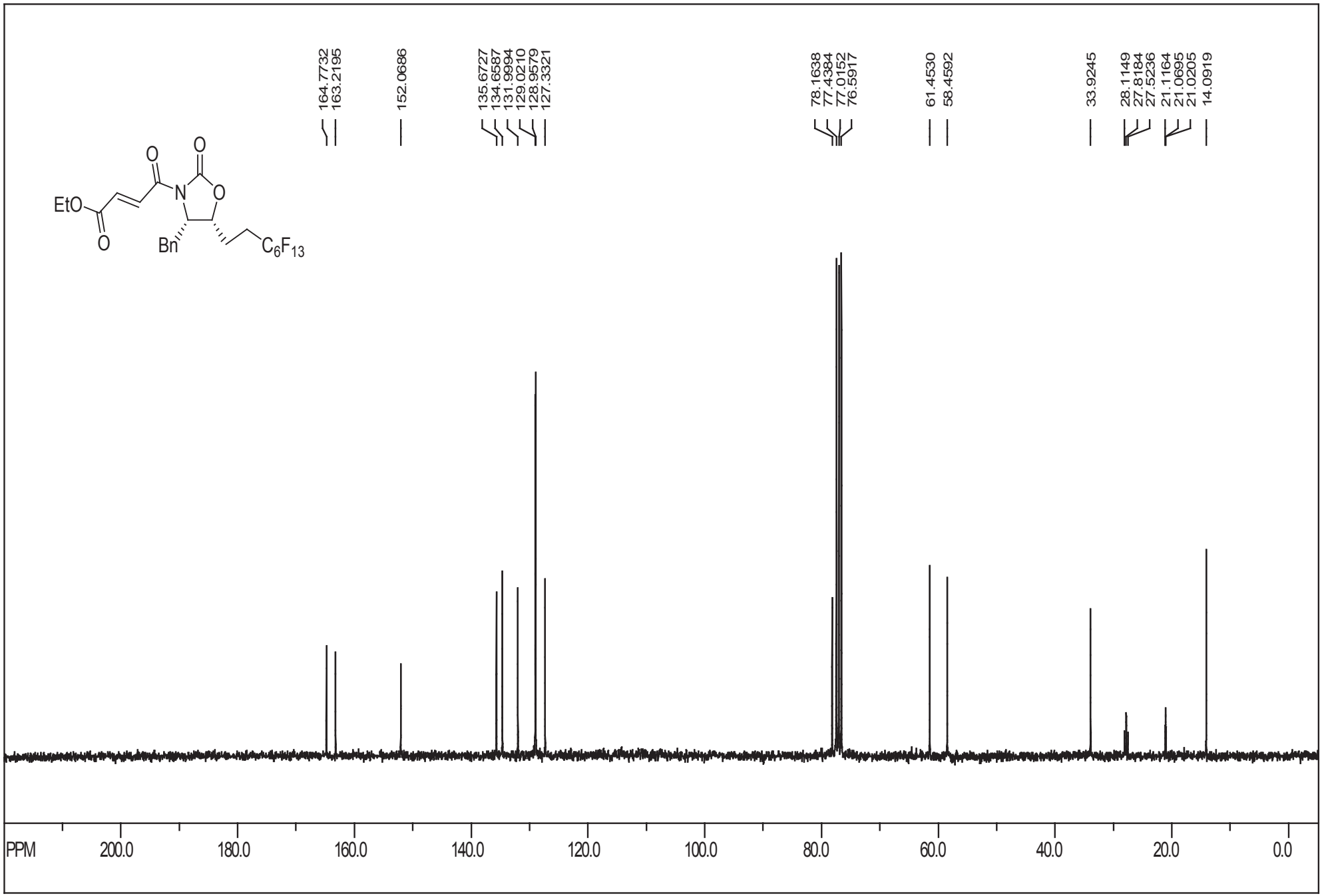

file: C:\NMR\Jehvi_40_c\5\fid expt: <zgpg30>

freq. of 0 ppm: 75.467749 MHz

SpinWorks 2.4: (3'R,4S,5R)-4-benzyl-3-(3',4'-dimethyl-pentanoyl)-5-(1'H,1'H,2'H,2'H-perfluorooctyl)-2-oxazolidinone

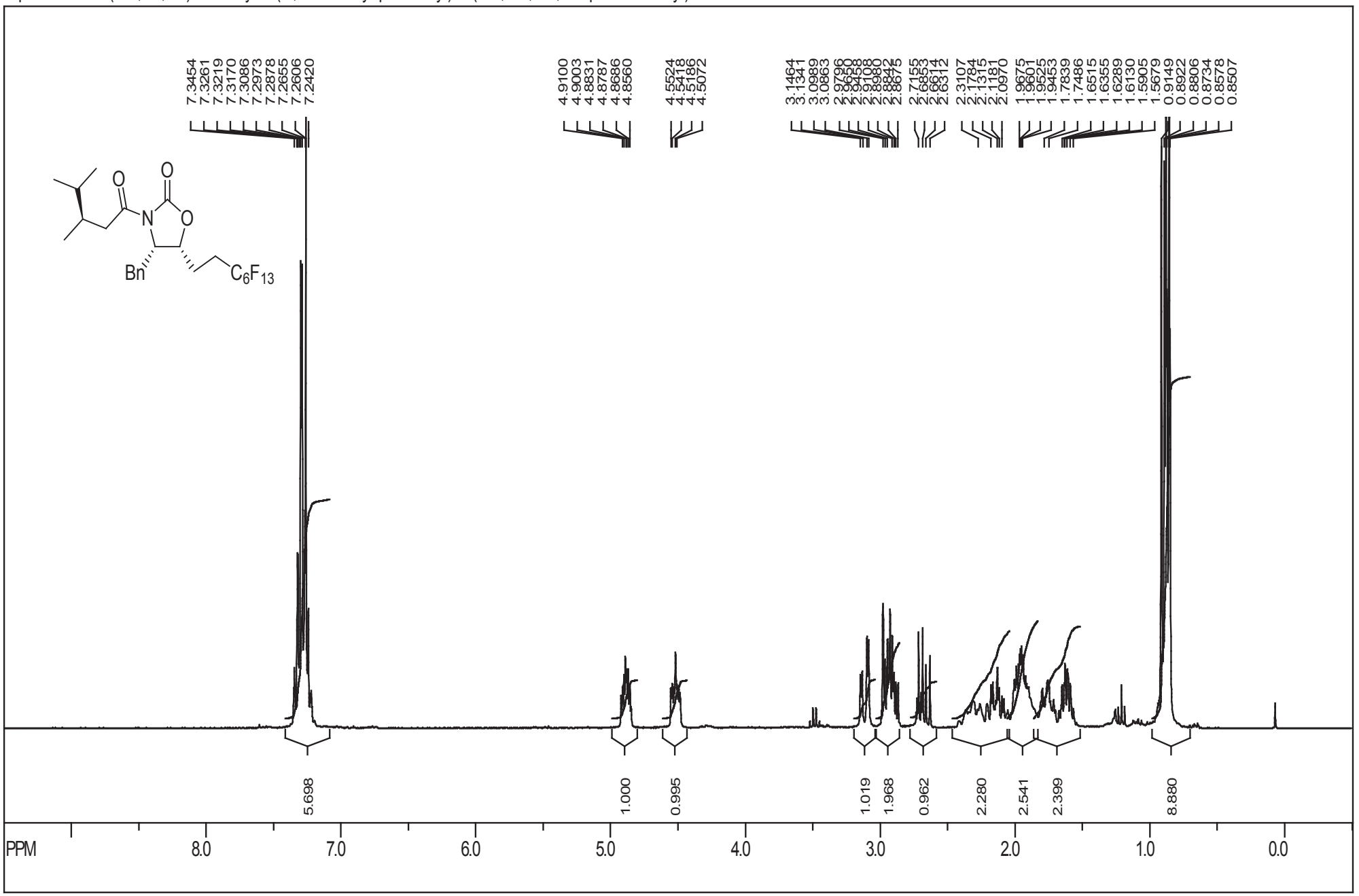

file: C:\NMR\Jehvi_53a_1\1\fid expt: <zg30>

freq. of 0 ppm: 300.130006 MHz

SpinWorks 2.4: (3'R,4S,5R)-4-benzyl-3-(3',4'-dimethyl-pentanoyl)-5-(1'H,1'H,2'H,2'H-perfluorooctyl)-2-oxazolidinone

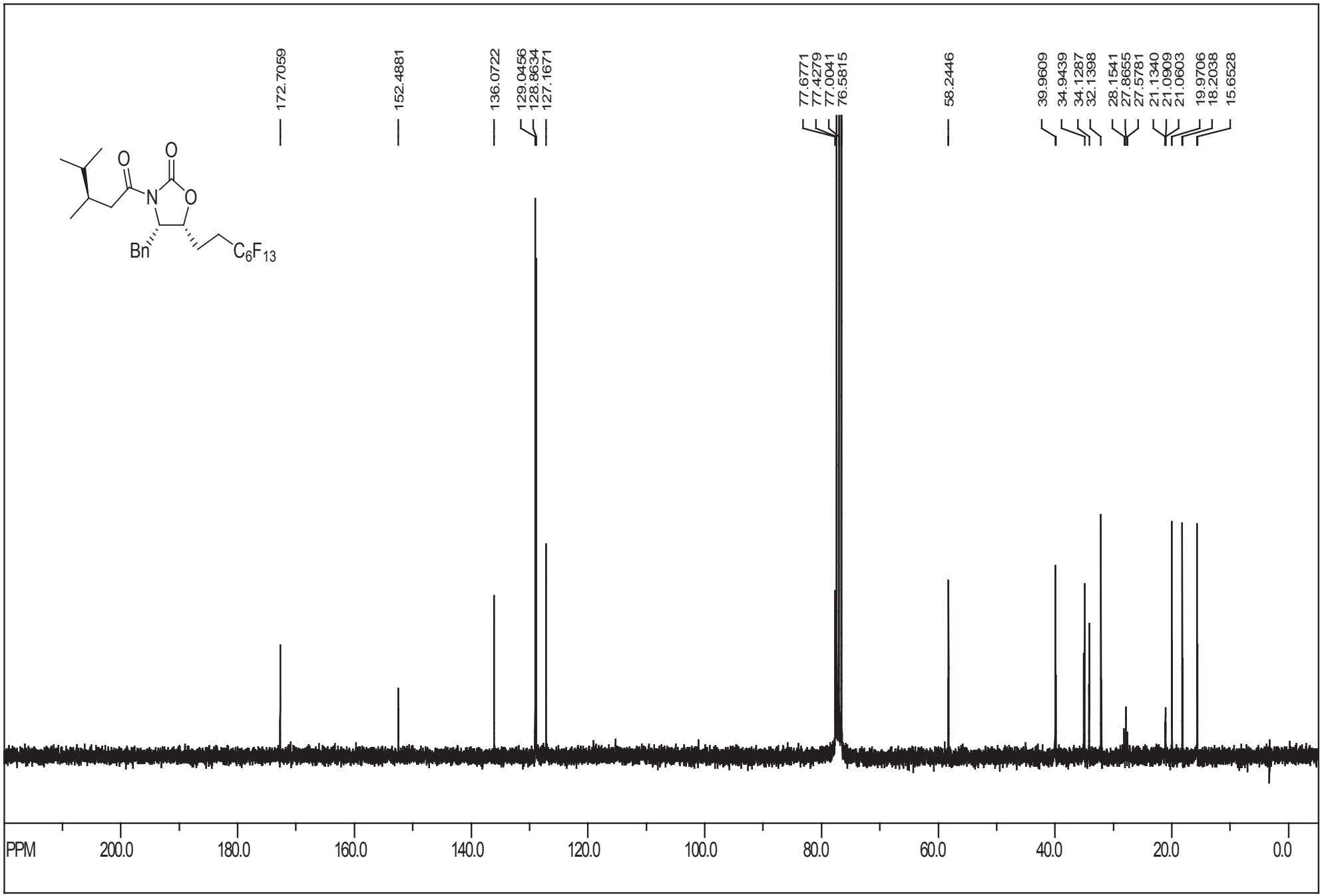

file: C:\NMR\Jehvi_53a_1\4\fid expt: <zgpg30>

freq. of 0 ppm: 75.467749 MHz

SpinWorks 2.4: (3'R,4S,5R)-4-benzyl-3-(4'-methyl-3'-phenyl-pentanoyl)-5-(1'H,1'H,2'H,2'H-perfluorooctyl)-2-oxazolidinone

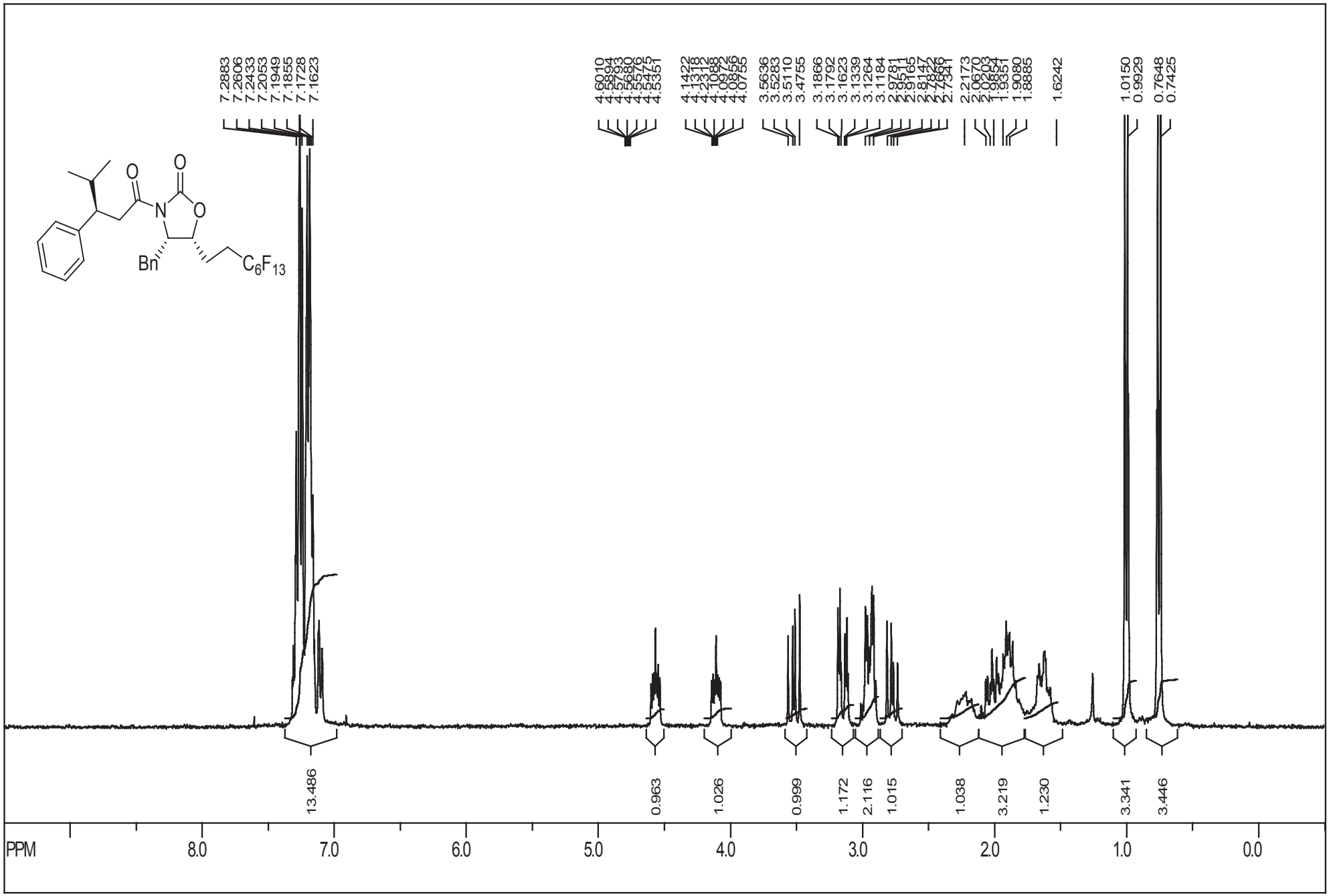

file: C:\NMR\Jehvi_53_h\1\fid expt: <zg30>

freq. of 0 ppm: 300.130006 MHz

SpinWorks 2.4: (3'R,4S,5R)-4-benzyl-3-(4'-methyl-3'-phenyl-pentanoyl)-5-(1'H,1'H,2'H,2'H-perfluorooctyl)-2-oxazolidinone

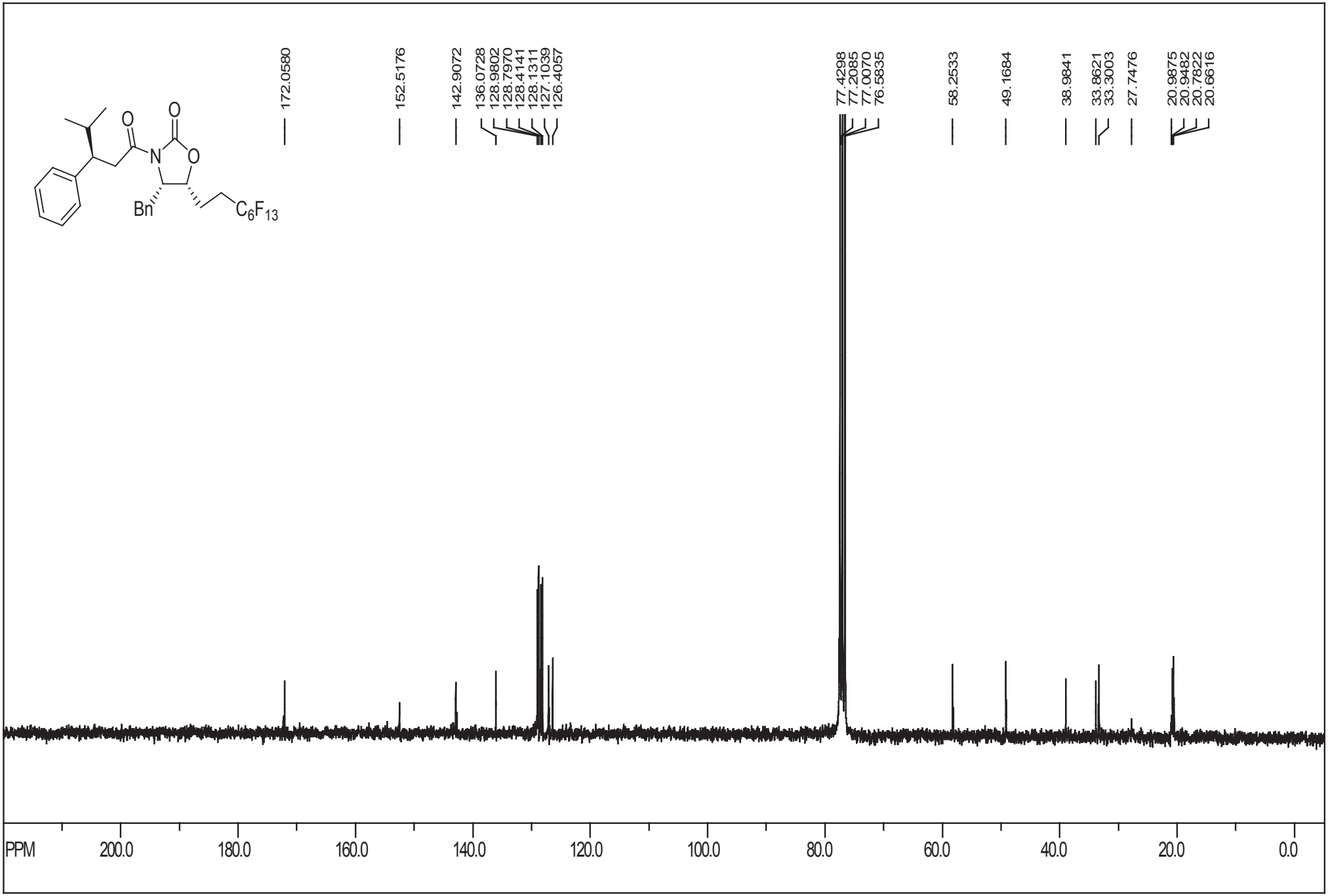

file: C:\NMR\Jehvi_53_h\4\fid expt: <zgpg30>

freq. of 0 ppm: 75.467749 MHz

SpinWorks 2.4: (3'R,4S,5R)-4-benzyl-3-(3'-ethoxycarbonyl-4'-methyl-pentanoyl)-5-(1'H,1'H,2'H,2'H-perfluorooctyl)-2-oxazolidinone

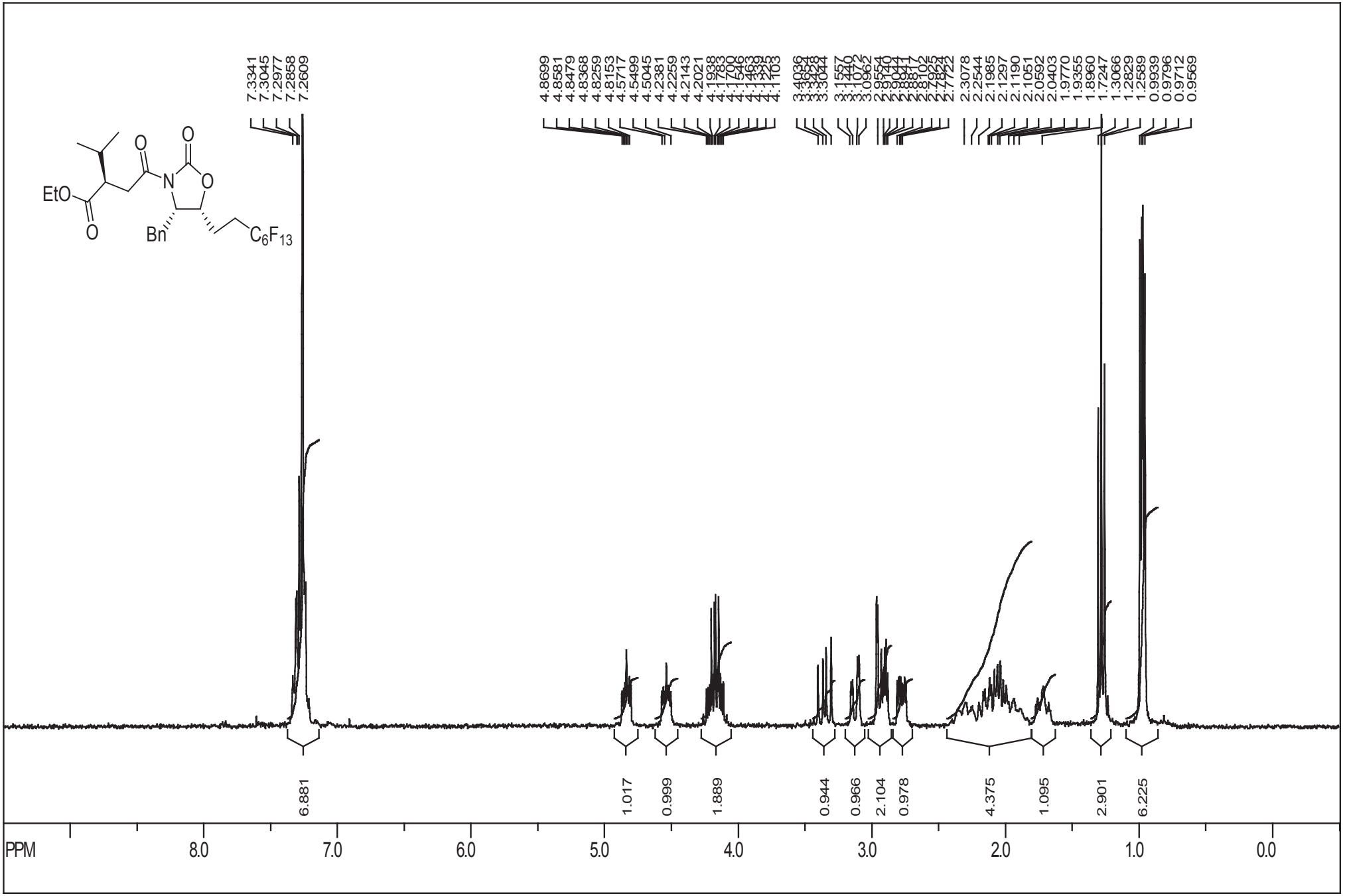

file: C:\NMR\Jehvi_49a_1\1\fid expt: <zg30>

freq. of 0 ppm: 300.130006 MHz

SpinWorks 2.4: (3'R,4S,5R)-4-benzyl-3-(3'-ethoxycarbonyl-4'-methyl-pentanoyl)-5-(1'H,1'H,2'H,2'H-perfluorooctyl)-2-oxazolidinone

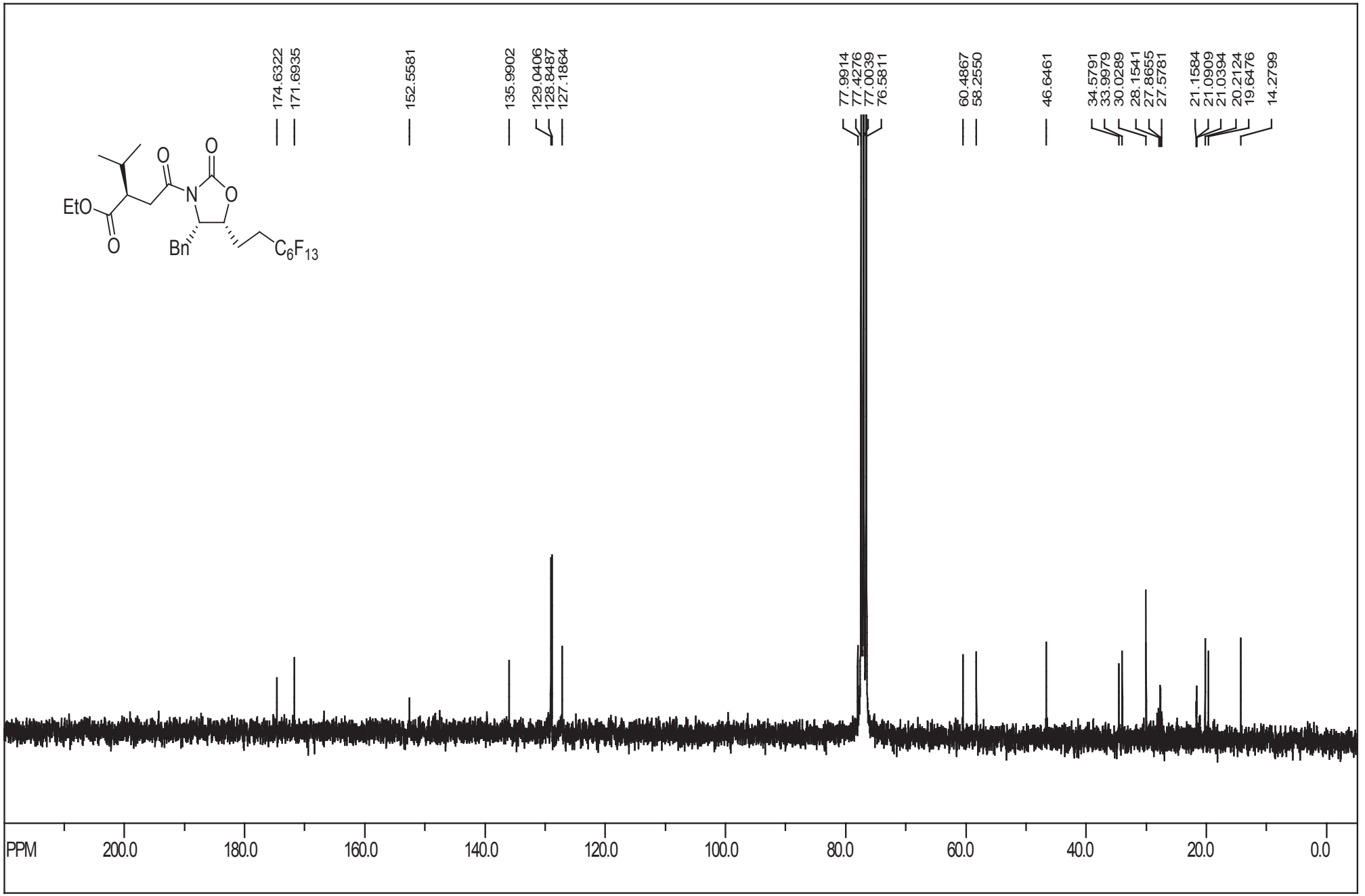

file: C:\NMR\40-50\Jehvi_49a\2\fid expt: <zgpg30>

freq. of 0 ppm: 75.467749 MHz